Use of Enabling Technologies in Combination with Human Pluripotent Stem Cells to Study Neural Differentiation and Neurite Outgrowth

TAMS, DANIEL,MARK

School of Biological and Biomedical Sciences

Use of Enabling Technologies in Combination with Human Pluripotent Stem Cells to Study Neural Differentiation and Neurite Outgrowth

Daniel Mark Tams

A thesis submitted for the degree of Doctor of Philosophy

2013

Abstract

Regeneration of human central nervous system (CNS) neurons is limited due to the inhibitory environment that forms post injury known as the glial scar. Reactive astrocytes within the glial scar produce both inhibitory and permissive extracellular matrix molecules (ECM) into the local environment. Chondroitin sulfate proteoglycans (CSPGs) are a component of the ECM which have been shown *in vitro* and *in vivo* to inhibit neurite regeneration. Physiologically relevant *in vitro* models of the glial scar are essential in developing new therapeutics and understanding the cellular processes that underpin neural regeneration.

In this study human pluripotent stem cells were differentiated using the highly potent and stable synthetic retinoid EC23. A concentration dependent profile of the action of EC23 on stem cell differentiation was determined, furthermore, the mechanisms for the enhanced biological activity of EC23 were investigated.

This study used the well described small molecule EC23 to form aggregates of neural progenitors which were characterised and used in a two dimension (2D) and three dimension (3D) model of neurite outgrowth.

Next, the neurite outgrowth substrate was manipulated to represent the inhibitory ECM of the glial scar using the CSPG Aggrecan. The presence of Aggrecan inhibited neurite development and was used to assess small molecules that could enhance outgrowth in 2D and 3D. Small molecule modulators of; rho-associated protein kinase (ROCK); retinoic acid receptor β2; glycogen synthase kinase 3β and protein tyrosine phosphatase σ were shown to at least partially enhance neurite outgrowth on Aggrecan in 2D and 3D. Furthermore, the bacterial enzyme Chondroitinase ABC was used to cleave chondroitin sulphate glycosaminoglycan side chains (GAG) from Aggrecan to further aid neurite outgrowth in this model. In addition a 2D and 3D co-culture system was developed using the human astroglioma cell line U118MG and human stem cell-derived neural progenitors described previously. This model demonstrated inhibition of neurite outgrowth by U118MG which could be overcome by ROCK inhibition.

This thesis describes the development of a novel model of neurite outgrowth using human stem cell-derived neurons. The model described was used to investigate Aggrecan induced neurite inhibition and to investigate pathways involved in neural regeneration.

List of Contents

List of Contents

CHAPTER 1 INTRODUCTION

CHAPTER 2 MATERIAL AND METHODS

CHAPTER 3 DEVELOPING TOOLS TO DISSECT MOLECULAR PATHWAYS INVOLVED IN NEURAL DEVELOPMENT

CHAPTER 4 INVESTIGATING NEURITE INHIBITION BY HUMAN STEM CELL-DERIVED NEURONS IN CONVENTIONAL 2D CELL CULTURE

CHAPTER 5 INVESTIGATION OF NEURITE INHIBITION USING A NOVEL 3D MODEL OF SPINAL CORD INJURY

CHAPTER 6 DISCUSSION

List of Figures

Chapter 1

Chapter 2

Chapter 3

Chapter 4

Chapter 5

Chapter 6

List of Tables

Acknowledgments

I would like to thank the following for helping me make this thesis possible:

My supervisor Prof S Przyborski for his support, guidance and inspiration over the last four years. Prof A Whiting and Prof T Marder for their Chemistry support and collaboration.

Mrs Bridie Murray for her technical expertise throughout the project, Dr Vikki Maltman for cell culture and flow cytometry training and Dr Dan Maltman for western blot training. Thanks also to Eva Barth for her help on this project during her ERASMUS placement.

All members of both the NRC and SAP group both past and present. Without the beer, curry, cake and tea none of this would have been possible. Also to Sarah for setting up the Touch Rugby team and allowing me to be captain. Matt, Ross, Adam and Arturas for helping me prop up the bar.

I would also like to give special thanks to my immediate family for their continued support throughout my 27 years of education and keeping my beer credits topped up.

Finally to Nicole, Tikka and Rogan for supporting me, putting up with me and confiscating my PS3.

Declaration

The work described herein was carried out in the Department of Chemistry, or the School of Biological and Biomedical Sciences, University of Durham between October 2009 and September 2013. All of the work is my own, except where specifically stated otherwise. No part has previously been submitted for a degree at this or any other university.

Statement of Copyright

List of Abbreviations

2 dimensional	2D
3 dimensional	3D
Alcohol dehydrogenase	ADH
Activation domain	AF
Aggrecan	AGC
All-trans retinol	ATR
All-trans retinoic acid	ATRA
Brain derived neurotrophic factor	BDNF
Bone morphogenic protein	BMP
Cyclic adenosine monophosphate	cAMP
Cerebellar granular neurons	CGN
Cerebral spinal fluid	CSF
Cytokeratin 8	CK8
Central nervous system	CNS
Cellular retinoic acid binding protein	CRABP
Collapsin response mediator protein	CRMP
Chondroitin sulfate proteoglycan	CSPG
Co efficient of variance	CV
4',6-diamidino-2-phenylindole	DAPI
DNA binding domain	DBD
Dulbecco's modified eagles medium	DMEM
Dimethyl sulfoxide	DMSO
Deoxyribonucleic acid	DNA

Dorsal root ganglion	DRG
Dorsal - Ventral	DV
Embryonal carcinoma	EC
Extracellular matrix	ECM
Epidermal growth factor	EGF
Enzyme linked immunosorbant assay	ELISA
Embryonic stem	ES
Fibroblast growth factor	FGF
Glycosaminoglycan	GAG
Glial fibrillary acidic protein	GFAP
Glycogen synthase kinase	GSK
Human embryonal carcinoma	hEC
Human embryonic stem	hES
Horse radish peroxidase	HRP
Insulin gene enhancer protein	ISL1
Keratin sulfate associated glycoprotein	TRA-1-60
Integrin	ITG
Lumbar levels	L1-L5
Leukocyte antigen-related	LAR
Ligand binding pocket	LBP
Myelin associated glycoprotein	MAG
Methyl	Me
Micro gram	µg
Micro meter	µm
Micro molar	µM
Neuron-specific class III beta-tubulin	TUJ-1
Neurite growth factor	NGF

normal human neural progenitor cells	nHNPC
Nano meter	nm
Optical density	OD
Paired box protein	PAX6
Pheochromocytoma	PC12
Poly-D-Lysine	PDL
Paraformaldehyde	PFA
Pico gram	pg
Peri-neuronal net	pnn
Peroxisome proliferator-activated receptor	PPAR
Protein tyrosine phosphatase	PTP
Retinoic acid	RA
Retinaldehyde dehydrogenase	RALDH
Retinoic acid metabolism blocking agent	RAMBA
Retinoic acid receptor	RAR
Retinol binding protein	RBP
Ras homolog gene family member A	RhoA
Rho associated protein kinase	ROCK
Retinol dehydrogenase	RODH
Relative quantity	RQ
Real time polymerase chain reaction	RT-PCR
Retinoic X receptor	RXR
Spinal cord injury	SCI
Sonic hedgehog	Shh
Stage specific embryonic antigen 3	SSEA3
Thoracic levels	T1-T12
Vitamin A deficient	VAD

CHAPTER 1 INTRODUCTION

Combining recent advances in developmental biology, synthetic chemistry and bioengineering will aid the translation of basic biology into potential clinical therapeutics, creating more physiologically relevant models of pathophysiological states. Developmental biology encompasses the understanding of stem cell differentiation and the processes that define cell lineage commitment. There are many advantages of using stem cell-derived tissue over adult tissue, including: human stem cells can produce large numbers of human specific somatic cells; particular stem cells are ethically more acceptable than the use of animals and the manipulation of stem cells *in vitro* allows for more control over the tissue that forms that animal derived cells.

Synthetic chemicals that specifically target key developmental pathways in stem cells are an important tool for investigating the initial steps of stem cell commitment and guiding the cells to form the desired tissue. Finally, stem cell-derived tissues can be combined with enabling technology to create more physiologically relevant models of disease states such as spinal cord injury.

The vitamin A metabolite all-trans retinoic acid (ATRA) is a modulator of cell differentiation *in vivo* and *in vitro*. Understanding the regulation and physiological role of ATRA *in vivo* guides its use during the derivation of stem cell-derived tissue, in particular neural tissue. ATRA induces neural commitment in stem cells both *in vitro* and *in vivo* in a concentration and temporal dependent manner. Understanding the role of these parameters throughout the differentiation process will help produce more physiologically relevant *in vivo* models of neural development.

This study involves the development, characterisation and application of novel technologies to investigate the process of neural differentiation in health and disease. We have investigated the role of synthetic retinoid agonists on modulation of stem cell-derived neural differentiation. We have subsequently applied neural models and have developed to investigate neurite inhibition in the spinal cord glial scar. This Chapter provides a review of the primary literature and work leading up to this project.

1.1 THE CENTRAL NERVOUS SYSTEM

The two major organs that make up the central nervous system (CNS) are the spinal cord and the brain. The role of the CNS is to receive and coordinate information from the peripheral nervous system resulting in a response that is dependant on the stimulus and information recieved. Sensory information received at the level of the spinal cord is sent to and interpreted by the brain via afferent nerve fibres.

Both the spinal cord and the brain are contained within the meninges, which are split into three layers: Dura mater, arachnoid mater and pia mater. The space between the arachnoid and pia mater is filled with cerebral spinal fluid (CSF) produced by the choroid plexus of the brain. The role of the structures that encase the brain is to provide mechanical protection, basic local immunity and help regulate cerebral blood flow.

Spinal Cord

The spinal cord is usually around 40-50 cm in length and 1.5 cm in diameter and extends from the medulla in the brain to the second lumbar vertebrae. The spinal cord is separated into four distinct levels cervical, thoracic, lumbar and sacral. A cross section of the spinal cord reveals distinct areas; white matter at the periphery containing an area of grey matter with a central CSF filled lumen contained by ependymal cells. The grey matter contains cell bodies of neurons and glia in a H like shape and is separated into four main areas: dorsal horn, lateral horn and ventral horn.

Surrounding grey matter are the axons of myelinated and unmeylinated neurons and makes up the white matter. Ascending and descending fibres lie within the white matter. Ascending white matter tracts send this information for higher CNS processing. Descending tracts regulate voluentary movment, posture, balance and nociception. The spinal cord receives information from sensory peripheral neurons that enter the spinal cord via the dorsal root ganglion (DRG). The DRG lying outside the CNS contain cell bodies of peripheral sensory neurons. DRG cells are used throughout developmental and neurobiological research as a model of neurite outgrowth and regeneration [4, 10]. Models of spinal cord development have helped elucidate key mechanisms of regeneration and understanding the anatomy of the spinal cord and associated neural grouping helps functional regeneration in this system [1].

Brain

The brain is the most complex organ in the human body and consists of around 38 billion glia and neuronal cells [11]. The brain has a lot of functional reserve and can adapt remarkably well to insult, but until relatively recently was not thought to regenerate in any way [12]. Recent studies have demonstrated that the function of parts of the brain requires plasticity, which is a type of neural regeneration and strengthens the approach to overcoming neural injury by regeneration [13].

The basic anatomy of the brain is described blow each structure with a different and conserved function. During development this complex organ is under the tight control of cues that define positional identity, neural subtype specificity and hence regenerative capacity.

Forebrain

The forebrain is responsible for many of the higher intellectual functions associated with human life including speech and thought. This part of the brain also controls voluntary movement and sensory integration. Within the forebrain lies the telencephalon containing cerebral hemispheres and the diencephalon which lies within it the thalamus, hypothalamus, epithalmus and subthalmus which are important in endocrine regulation and control many bodily functions such as hunger, thirst, blood pressure/temperature and pleasure. The development of these highly regulatory structures is as influenced by environmental factors as it is genetic and evolutionary indicating at the highly adaptive and complex functions these serve [14].

Midbrain

The midbrain has a variety of very important functions for life. The structure lies between the forebrain and the hindbrain and connects the cerebral hemispheres to the cerebellum. A number of structures within the midbrain influence motor function including the dopaminergic producing cells in the substantia nigra and the reticular formation. Cranial nerves in the midbrain control eye movement, lense shape and pupil diameter. A well-described disease of the midbrain is Parkinson’s disease, which affects the dopamine producing cells in the substantia nigra. Development of this structure is under the regulation of the transcription factor Otx2, regulation of Otx2 in the developing brain is highly regulated and under the influence of multiple gene enhancers and positions the midbrain-hindbrain boundary [15, 16].

Hindbrain

The hindbrain is a highly patterned structure and development is under the regulatory control of multiple transcription factors. As is described later in this Chapter, *HOX* genes regulate hindbrain rhombomere segmentation and development. The Hindbrain is made up of the medulla oblongata and the pons. Information is relayed from the spinal cord to the brain via the medulla oblongata, which is also involved in maintaining heart muscle contractions and breathing rate. The pons has multiple functions including connecting the cerebral cortex with the cerebellum and controlling cranial facial nerve signalling, both sensory and motor.

Tight control and early specification of the distinct areas of the CNS is an important factor during development. Understanding the processes that occur to form these structures and disease pathologies that are related to their development is important in treating congenital disease.

1.1.1 Development of the central nervous system

Folding of the neural plate during early embryonic development results in neural groove formation, which is followed by closure of each of end forming a tube. Failure of neural tube closure results in a number of well-known neural tube defects. Stem cells within the neural tube differentiate into neural and glial progenitors and are under the influence of morphogens produced either by the notochord, ectoderm or flanking somites. The relative concentration of the morphogens; retinoic acid, BMP and SHH to the developing stem cell influences the progenitors and mature cells that develop. As is discussed later in this chapter the anterior-posterior and dorsal-ventral positional identity of developing cells in the neural tube defines their functional identity [17].

Understanding the role of morphogens in neural development has aided or understanding of disease pathologies affecting the CNS and helped elucidate *in vitro* methods of stem cell differentiation for use in developmental and regenerative medicine studies.

Figure 1-1 is a schematic that shows the major structures of the neural tube after closure. The flanking somites produce retinoic acid, which is thought to act via paracrine signalling to regulate neural tissue development. In combination with morphogens from the notochord and ectoderm, retinoic acid guides specific neural development in particular motor neuron subtype specificity.

Retinoic acid is produced by somites flanking the developing neural tube [18]. Paracrine signalling by retinoic acid in developing cells of the neural tube is concentration dependant and regulates anterior-posterior identity. Furthermore, signalling has also been shown to fine tune dorsal-ventral neural subtype and functional activity of mature neurons [19]. Therefore the structures surrounding the neural tube are essential for correct CNS development.

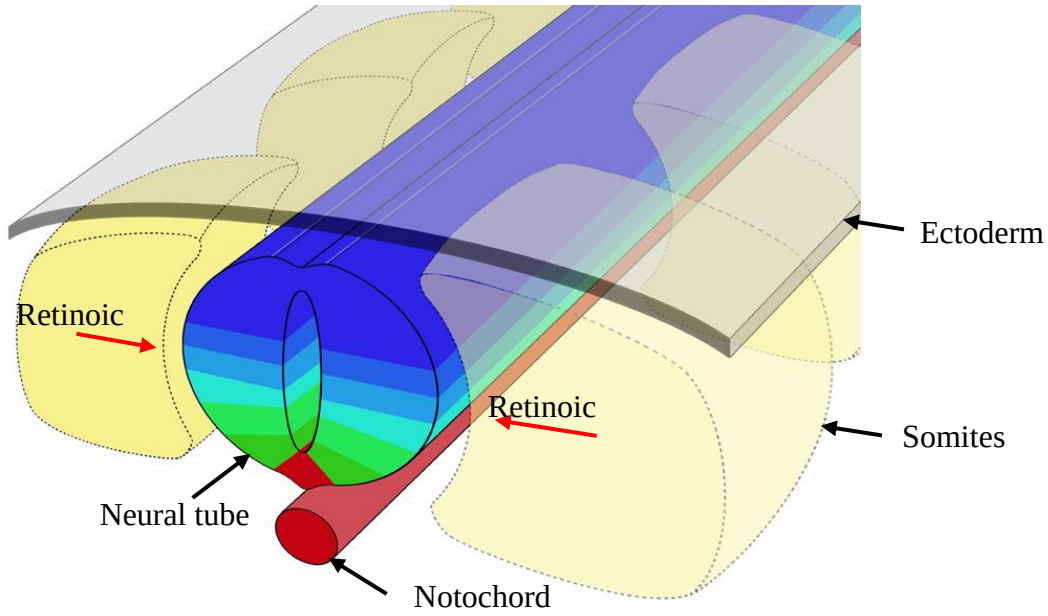

Figure 1-1 Schematic of the developing neural tube. Retinoic acid is produced by the somites shown in yellow. Paracrine activity of retinoid acid acts on developing cells of the CNS to form the anterior-posterior axis and influence neural subtype development via HOX gene expression. The overlying neuro-ectoderm produces the morphogen BMP that acts on the neural tube and the notochord produces Shh which also influences neural subtype development.

Specific genes that control downstream events regulating neural subtype differentiation must also be regulated in a concentration dependant manner to provide tight control over neural development at each level of the developing neural tube. A group of highly conserved genes that are differentially expressed along the anterior-posterior and dorsal-ventral axis and have been associated with neural subtype selectivity are *HOX* genes [20, 21].

HOX genes are discussed in detail later in this chapter, however, *HOX* gene regulation by retinoic acid produced by flanking somites is an important level at which neural progenitors begin to develop and become defined along the anterior-posterior and dorsal ventral axis[22]. Figure 1-2 is a schematic showing relative 5' to 3' *HOX* gene expression

along the gene cluster and its relationship to anterior-posterior development of the neural tube. Note that more 5' HOX genes are expressed in the more posterior developing tissue.

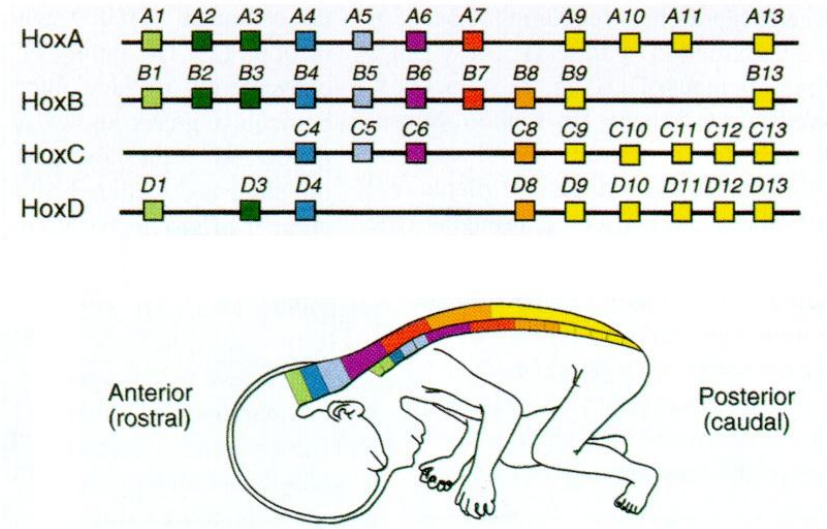

Figure 1-2 Schematic shown the anterior-posterior expression of HOX genes in the developing human embryo. Notice the 3' and 5' anterior-posterior patterning. Retinoic acid produced by the somites shown in figure regulates the expression of HOX genes in the CNS and influences development. Figure adapted from [7].

In addition retinoic acid signalling and *HOX* gene expression profile have been shown to influence developing neural progenitors specifying neural subtype at each level of the developing CNS. In combination with other transcription factors, such as *PAX6, HOX* gene expression and hence, retinoic acid signalling help to tightly define sub populations of neuron. Cross regulation between transcription factors often make it difficult to determine which gene is under the direct influence of retinoic acid one indication is a retinoic acid response element in the coding gene [23].

CNS progenitor cells

In vivo progenitor cells develop in domains that are defined by chemical cues produced by the local embryonic environment. CNS progenitors are an important factor in neural regeneration with the potential of local implantation and repopulation of damaged neural tissue. These cells can also be used to create a permissive environment for neural regeneration and have been demonstrated to aid functional neural tissue regeneration [24].

Understanding the chemical cues and genetic markers of these cell types is important for *in vitro* production of neural progenitors from embryonic or induced pluripotent stem cells for use in regenerative medicine. Two major types of CNS progenitor are described below:

Neural stem cells

Neural stem cells have the potential to develop into neurons, astrocytes and oligodentrocytes, the three main cell types in the CNS. These cells are described further in this Chapter however it is important to note that the majority of cells in the CNS are derived from a small population of neural stem cells. These cells are directed by chemical cues into different lineages with a wide range of functions. In addition a number of precursor cells are maintained in areas of the CNS providing them with plasticity. Another type of neural progenitor cell found within the CNS is the NG2 cell, which has a function in adult neural functionalization and homeostasis.

NG2 glia

These cells are oligodendrocyte precursor cells and a subpopulation of astrocyte, they are evenly distributes throughout the CNS. These cells are defined by expression of the proteoglycan NG2 on their surface membrane. NG2 glia have multiple functions in the CNS and are found in both myelinated and unmyelinated areas of the brain. NG2 cells are closely associated with synapses and the NG2 protein is inhibitory to axonal regeneration indicating at a diverse role of these cells in the CNS. Upon differentiation into oligodendrocytes NG2 precursor cells up regulate myelin associated antigens and down regulate NG2 [25]. These cells seem to descend from ventral CNS domains developing in the presence of Sonic hedgehog (Shh) and that migrate expressing Olig1/2 in the pMN domain and NKX2.2 in the p3 domain (these domains are described later in this Chapter). NG2 begins to be expressed after commitment to these ventral neural progenitors and migration into the spinal cord [26].

Mature CNS cells

Broadly the different type of neural tissue in the CNS can be grouped into: Glia and neurons. Gial cells can be further divided into astrocytes, and oligodendrocytes each with a distinct function and related pathophysiology.

The highly specialised nature of a neuron facilitates the rapid transmission of an electrical signal from neuron to neuron or from a neuron to target tissue. The general function of a neuron is the same between subtypes. Subtype specificity comes from differences in targets for example motor neurons have a highly specialised neuro-muscular junction, whereas other neurons may synapse to post-synaptic membranes as you would expect to see in the brain. Furthermore, the neurotransmitter that is released at the pre-synaptic membrane upon arrival of an electrical impulse also varies. Broadly neurons in the CNS can be classified into either motor or interneurons.

Neurons

Motor neuron

Motor neurons are generally multipolar with a single long axon extending from the cell body that can transmit an impulse either from the cortex to the spinal cord or from the spinal cord to muscle cells. These neurons tend to have multiple dendrites emanating from the cell body allowing for the integration of many input signals.

Sensory and motor neuron connections are extremely specific and act to highly co-ordinate motor output and behaviour. Directed differentiation of motor neurons has been shown to be involved in development of these connections, however, even what is even more regulated is the development of sensory-motor neuron connections via a local environment specific mechanisms. Neural circuit connections and neural regeneration have been shown to be highly regulated by local environmental factors defined by patterning of the CNS [27]. These studies and many more describe how early patterning of the CNS defines neural subtype development and highly specific targeted innervation of tissue. Interestingly the spatial distribution of CNS neuron clusters reflects that of the spatial distribution of the main limb muscle groups [28].

Interneuron

Interneurons are found within the brain and spinal cord of the CNS, this type of neuron are generally short and relay information within the CNS via two axons. They can be both

inhibitory (producing the neurotransmitter GABA) and excitatory (producing glycine or acetylcholine). A number of different types of interneurons are found throughout the brain and spinal cord, each with a unique function and phenotype. It is thought that interneuron diversity is the result of post-mitotic interactions. Furthermore, the genetic profile of each progenitor results in specific migration resulting in experience directed differentiation and functionalization at different areas of the brain and spinal cord. Transcription factor expression and regulation during development of this type of neuron is particularly important and helps specify neural subtype and function. For a review on this topic see Kessaris, N et al (2014) [29] .

Glial cells

Glial cells can be thought of as the support cells of the CNS, they are closely associated with neurons and regulate many functions including: local environment homeostasis, neurotransmitter turnover, neural repair and early neural migration. Neurons rely upon glial cell for a number of functions, however, as is described in later in this Chapter one type of glial cell, the astrocyte can be activated to inhibit neural repair. The two broad type of glial cell are astrocytes and oligodendrocytes their role within the CNS is described below [30].

Astrocytes

Astrocytes are a star shaped cell that is closely associated with neurons in the CNS. Astrocytes express the intermediate filament GFAP and are involved in providing mechanical support, synaptic stability, and nourishment through storage and processing of substrates, regulate neural development and phagocytose debris within the CNS. The microstructure of the CNS is created by astrocytes making them important for correct patterning of the CNS.

Oligodendrocytes

Neurons are myelinated by Oligodendrocytes, myelination allows for rapid signal transduction over relatively large distances. The electrical signal is rapidly passed between gaps in the myelin created by oligodendrocytes called nodes of Ranvier. The myelin sheaths that wrap around axons provide multiple functions to facilitate and optimise signal transduction in the CNS. Multiple pathologies are associated with loss of axon myelination for example multiple sclerosis, indicating at the importance of these cells in the CNS.

Understanding the biology behind myelination of axons by oligodendrocytes and disease pathologies that affect myelination is an important factor when trying to regenerate functional neurons in the CNS.

1.2 RETINOIC ACID AND EMBRYONIC NEURAL DIFFERENTIATION

Indirect evidence for the role of ATRA in CNS development and maturation has come from a number of different experimental methods. Initially ATRA was implicated to have a role in CNS development through vitamin A deprivation studies. Studies on pigs and chickens demonstrated that vitamin A deficiency resulted in signs of motor neuron disease and in some cases loss of eye development [31]. It soon became apparent that a deficiency in vitamin A resulted in a multitude of developmental defects of the spinal cord and CNS, including- Hydrocephalus, Spina bifida and Anopthalmia. Maden, M et al (1996) [32] used a Vitamin A deficient (VAD) quail to investigate developmental defects resulting from VAD, the study demonstrated that RA deficiency caused a reduction in the number of neurons within the neural tube and those that were produced did not show normal neurite outgrowth or correct neurite guidance. Following the elucidation that retinoic acid was the major biologically active metabolite of vitamin A investigation into the presence of retinoic acid in the spinal cord began. McCaffery, P.J et al (1994) [33] demonstrated in mice that retinoic acid was present in the spinal cord and hindbrain of the developing embryo and that the levels of retinoic acid correlated with the amount of RALDH present in the tissue. The expression profiles of both RALDH and CYP26 enzymes were characterised by Reijntjes, S et al (2005) [34] in normal and VAD quail. The expression of RALDH2 was seen in the motor neurons and limb level spinal cord of normal quail, however, this expression was lost in VAD quail, indicating a positive regulatory role of retinoic acid on RALDH2 expression. However, the expression of RALDH2 did not correlate to retinoic acid signalling in the same tissue suggesting a paracrine role of retinoic acid during CNS development.

1.2.1 Dorsal-ventral neural patterning of the spinal cord

There are distinct differences in the type of neuron that form along the dorsal ventral (DV) axis of the spinal cord. Neural subtypes arise through cellular interaction with a multitude of external transcription mediators. One of the main signalling pathways involved in

modulating ventral spinal cord development is Sonic hedgehog (Shh), which acts with retinoic acid to direct neural progenitors into cells with a motor neuron phenotype.

Shh acts as a morphogen to regulate the expression of transcription factors involved in establishing distinct DV neuroprogenitor domains. Shh is produced by the notochord and forms a concentration gradient with high levels ventral and low dorsal. At defined concentrations of Shh, homeodomain-containing transcription factors are either induced or repressed, the combination of transcription factors at each level along the DV axis marks a domain of neuroprogenitor cells. The five progenitor domains are termed vp3, pMN, vp2, vp1, vp0 and pD and are expressed ventral-dorsal respectively [9, 35]. Each progenitor domain gives rise to functionally different neurons e.g. pMN form ventral motor neurons. The pMN progenitor is defined by the combinational expression of the transcription factors *PAX6*, *OLIG2* and *NKX.6* and the motor neurons formed from further differentiation of these progenitors defined by *MNR2* and *Hb9* expression. Figure 1.1 shows the overlapping expression domains of two classes of transcription factors I and II and how these can be used to identify neural progenitor domains along the DV axis [9].

The two groups of transcription factors- class I and class II are under the regulation of Shh signalling. Class I genes are repressed by Shh and class II induced, however, class I and II also cross regulate forming distinct combinations of transcription factors in each progenitor domain. RA is integral to defining distinct progenitors along the DV axis and has an important role in motor neuron differentiation. RA is produced by the somites adjacent to the developing neural tube; furthermore, there is an important interaction between FGF and RA signalling during neural development. For the correct development of ventral neural subclasses RA is required to inhibit FGF8 signalling, failure to do so results in down regulation of markers of ventral neuroprogenitor domains such as Pax6. FGF signalling inhibits the expression of both Class I and Class II transcription factors and has been shown to down regulate RALDH2 expression in paraxial mesoderm. However, RA signalling inhibits FGF expression and subsequently allows Shh regulation over Class I and Class II genes [36]. Furthermore, RA has been shown to induce the expression of Class I transcription factors such as *PAX6* and *NKX*. Interestingly, *PAX6* and *NKX2.2* are required to prevent the expression of transcription factors that inhibit the bHLH containing transcriptional repressor *OLIG2*. *OLIG2* is required for motor neuron differentiation through indirect regulation of Mnx and LIM proteins [37], indicating a role of *PAX6* expression in motor neuron differentiation.

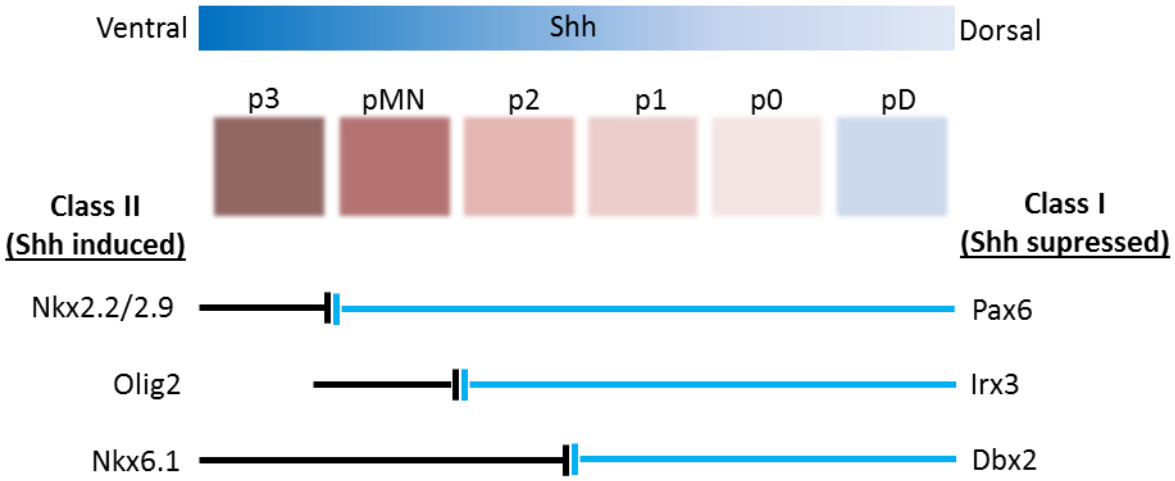

Figure 1-3 Dorsal/ventral transcription factor expression. A diagram representing the transcription factor domains along the DV axis and which class I and class II transcription factors are influenced by Shh. The interplay between opposing transcription factors determines the ventral-dorsal neural progenitor pool that develops, each pool of progenitors along the DV axis is shown as a different colour. . The black lines show genes that are induced by Shh and their influence on each progenitor domain. Blue lines show the expression of genes inhibited by Shh and their DV level of expression. The genes respond differently to different concentrations of Shh. Figure adapted from Lee et al (2001) [9].

Differentiation of each neuroprogenitor into specialised neural tissue is incomplete without directed neurite outgrowth and functional synapse formation with target tissue. Much of the characterisation of functional neurons comes from the neurotransmitters released from the synapse and provides a good link between developmentally discrete neuroprogenitors and their ultimate function in the central nervous system.

Manipulation of stem cells *in vitro* provides important insights into neural development and subtype selectivity, furthermore, the different stages of development can be utilised in disease models of the CNS.

1.3 RETINOIC ACID AND ANTERIOR-POSTERIOR EMBRYONIC PATTERNING

Movement and expansion of the transient epiblast through the primitive groove results in the formation of three germ layers- endoderm, mesoderm and ectoderm, this is the process of gastrulation. Cells during gastrulation are highly migratory and are in constant dynamic flux. Gastrulation is an important stage during development and results in the formation of an anterior-posterior axis (AP)- a process that is directly affected by ATRA signalling [38]. Of the three germ layers the ectoderm gives rise to the neural crest, the neural tube and the epidermis. The mesoderm forms a number of different structures including the notochord and somites which are integral to post gastrulation organogenesis and neurulation. Finally, the endoderm forms the epithelia of the digestive and respiratory systems and some digestive organs. Each of the germ layers and the independent cell niches that arise within them are derived from embryonic stem cells making up the epiblast. Axis formation of the three germ layers is important to ensure proper cellular development and tissue function.

An insight into the role of transcription factors in the process of AP-axis formation came from mutagenesis screens in Drosophila *melanogaster*. Mutations in some of the genes screened revealed ectopic expression of body appendages, such as the ectopic expression of legs in place of antennae or duplication of a wing segment, demonstrating a change in positional identity of cells developing in a particular area of the developing embryo. The genes found to be responsible for these positional changes in Drosophila were termed HOM-C and were found on two clusters; antennapedia and bithorax. The expression of each gene was temporal and spatially restricted along the AP axis and the expression of each gene was determined by its position within the cluster, an effect known as co-linearity [39].

A similar set of evolutionary conserved homeobox-containing transcription factors were discovered in humans, termed *HOX* genes. *HOX* genes are a family of 39 nuclear transcription factors split into four clusters- A, B, C and D [40]. Paralogs of each gene are found between clusters and each paralogue is given a number from 1-13. The temporal expression of each gene is dependent on its spatial arrangement in the cluster, which is directly regulated by retinoic acid [41-43].

HOX genes

Multiple developmental studies have demonstrated that the expression of 3' *HOX* genes is associated with tissue of anterior fate, whereas 5' *HOX* genes provide posteriorisation cues to migrating cells and developing tissue. Formation of the AP axis was hypothesised to involve an external environmental factor; a diffusible morphogen was suggested to regulate the expression of *HOX* genes in a concentration dependent manner. Multiple studies have demonstrated that retinoic acid can alter the expression of *HOX* genes and retinoic acid signalling results in posteriorisation of developing tissue, therefore it is widely accepted that retinoic acid is involved in the expression of many of the *HOX* genes and can act to induce expression through a concentration gradient [42, 44, 45]. Furthermore, many 3' *HOX* genes contain a RARE and are sensitive to low levels of retinoic acid. There are a number of theories about how retinoic acid induces co-linear expression in *HOX* genes, it has been hypothesised that retinoic acid may bind to RARE in the promoter of each *HOX* gene with different affinities and therefore induce each gene with different potencies, however, this require each *HOX* gene promoter to have a RARE, but RARE in many of the *HOX* genes have not been described [23]. A second theory is that the products of 3' *HOX* genes act to regulate later *HOX* genes 5' of the cluster. This is supported by much of the information known about *HOX* genes to date, however, there is still much unknown about the targets of *HOX* genes and how they interact. Figure 1-4 shows diagrammatically the four clusters of *HOX* genes, their associated sensitivity to retinoic acid and their anterior-posterior expression domains.

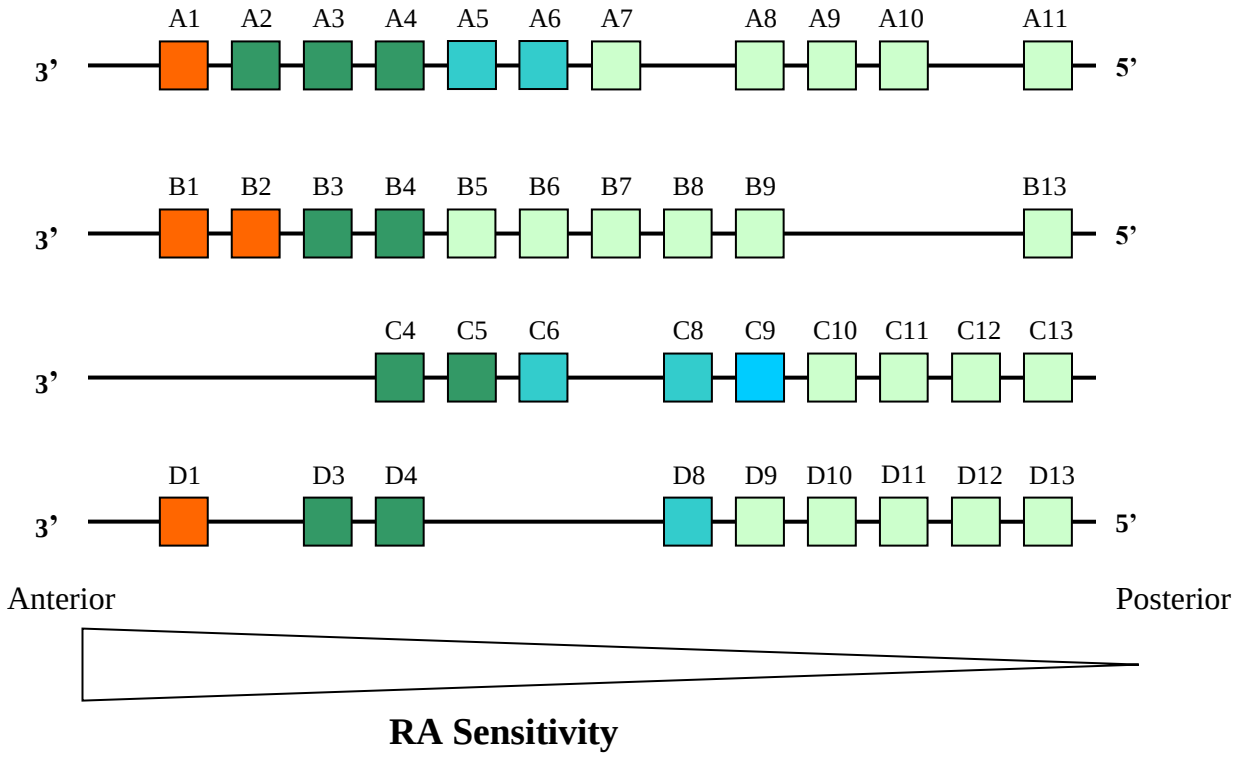

Figure 1-4 *HOX* gene clusters and their relative sensitivity to retinoic acid. The 39 *HOX* genes are arranged into 4 clusters A-D, each cluster contains up to 11 *HOX* genes, with paralogs of genes between clusters. The spatial arrangement of each gene within the cluster determines its temporal expression pattern, which is influenced by retinoic acid signalling.

Further, evidence for the role of retinoic acid in AP patterning came from detailed analysis of rhombomere segmentation and how retinoic acid affects the AP axis within the hindbrain. A normal hindbrain consists of 7 rhombomeres each have a unique positional identity, identified through cell surface and gene expression markers. In the VAD quail expansion of anterior restricted rhombomeres is increased, resulting in an enlargement of the anterior segments, whereas the posterior rhombomeres are truncated [43, 46]. This fits in with the concentration dependent effects of retinoic acid, indicating that retinoic acid signalling results in posteriorisation and without ATRA signalling an anterior fate is adopted. This effect has been shown to be concentration dependent with progressive loss of the posterior hindbrain markers as ATRA is reduced. Models other than VAD have utilised methods of reducing endogenous production of retinoic acid through null mutations in RALDH or through the application of RAR antagonist. RALDH null mutations are essentially equivalent to a VAD phenotype; RAR antagonists require a specific temporal application demonstrating the temporal expression of RAR during development. *HOX* genes have a defined barrier of expression for each of the rhombomeres e.g. *HOXB1*, which is the only *HOX* gene found in rhombomere 4. Vitamin

A treatment results in loss of this defined domain and an expansion of rhombomere 3 indicating posteriorisation, conversely in VAD animals, there is an enlargement of anterior rhombomeres 3 and 4 and a reduction in markers of rhombomere 5 and 6 essentially posterior rhombomeres are lost and replaced by more anterior cells [43], these studies underline the temporal and concentration dependent role of ATRA during development.

HOX genes and differentiation

The ability of *HOX* genes to control axis formation can be used to define areas of the developing embryo, the *HOX* code of any particular developing tissue defines its position within the embryo but it also ultimately determines how the cell will differentiate. The position of the cell within the embryo determines which signalling molecules are present and importantly the concentration they are present at [44]. The teratogenic effects of retinoic acid are partly due to its regulation over *HOX* genes that control AP patterning. *HOX* genes themselves regulate a vast range of transcriptional mediators and genes however, retinoic acid controls initial *HOX* gene expression, hence, aberrant expression of *HOX* genes results in disordered development and differentiation [47].

Human embryonal carcinoma (hEC) stem cells are an efficient and ethically acceptable way of investigating the development of human tissue and the role of retinoic acid in this development (see Section 1.6). *In vitro* experiments demonstrated that in the embryonic carcinoma stem cell line NTER2.cl.D1, a model thought to represent the primitive ectoderm, retinoic acid induced a concentration dependent expression of *HOX* genes from each of the four chromosome clusters in a co-linear manner [48]. A study by Mavilio, F. et al (1988) [49] initially demonstrated that retinoic acid specifically induced differentiation and *HOX* gene expression in NTERA2.cl.D1 EC cells, which was not induced by the compounds hexamethylenebisacetamide or bromodeoxyuridine. Furthermore the effect of retinoic acid was shown to be dependent on the use of the specific EC cell line NTERA2.cl.D1, making this an excellent model for investigating the role of *HOX* genes in cell differentiation. Following on from this study Simeone, A et al (1990) [50] showed that retinoic acid induced a sequential activation of *HOX* genes on cluster 2 *(HOXB*) and activation depended on concentration of and length of exposure to retinoic acid. Further studies exemplified this model to investigate the regulation of *HOX* genes during neural specific development and co-linear expression [41].

The expression of *HOX* genes in this model of differentiation is directly associated with the early stages of differentiation [48, 50]. Furthermore, the induction of *HOX* genes has been implicated in the specific differentiation of human embryonic stem cells, with *HOX* genes serving as markers of cell lineage identity [51]. This suggests that *HOX* genes may be involved in some key aspects of cellular differentiation that are not merely an indirect consequence of AP patterning.

1.4 RETINOIC ACID

1.4.1 Storage and metabolism of retinoic acid

Retinol (vitamin A) is an essential fat soluble nutrient obtained from the mammalian diet in the form of β-carotene or pre-formed retinyl esters [52]. Retinol can be derived from a number of food sources such as meat, vegetables and other Vitamin A fortified foods. Vitamin A and its derivative group of compounds retinoids consist of four isoprenoid units and contain five carbon double bonds. *In vivo* the biological effects of vitamin A are solely due to either the aldehyde or carboxylic acid derivatives, more specifically, 11-*cis* retinal and *all-trans* retinoic acid (ATRA) respectively. Investigation into the ability of ATRA to compensate for rats deficient in vitamin A has shown that although the rats will develop with no obvious defect, they are blind and cannot reproduce. These results indicate that retinoic acid alone cannot completely compensate for vitamin A deficiency and is not the only vitamin A metabolite responsible for its biological actions [53]. Understanding how vitamin A is absorbed, metabolised, stored and transported *in vivo* is important in rationalising treatment of disease relating to the biological activity of vitamin A and its derivatives. Furthermore, elucidating the biologically active components of vitamin A will aid synthetic development of analogues based around these molecules.

Within the intestinal lumen retinyl esters are converted into retinol and along with β-carotene enter the enterocytes via passive diffusion [54]. Once within the enterocytes β carotene is enzymatically converted to retinol. Retinol is then re-esterified by lecithin:retinol acetyltransferase and packaged into chylomicrons for transport within the lymphatics [55]. Hydrolysis of the chylomicron by lipoprotein lipase enzymes bound to epithelial surfaces results in chylomicron remnant formation. The chylomicron remnant associates with APOE, targeting the remnant to hepatic stellate cells for storage as retinyl palmitate, with some remnants associating with lipoprotein receptors on target tissues [56].

Once in the liver release and transport of all-trans retinol (ATR) is though association with serum retinol binding protein (RBP). Quadro, L et al (1999) [57] demonstrated that although RBP is required to mobilise retinol from liver stores it is not needed for accumulation of retinol in the liver. RBP transports ATR to target cells or tissues and associates with a multi-transmembrane domain protein known as STRA6. There is evidence to suggest that the ability of STRA6 to facilitate ATR uptake is dependent upon RBP binding and internalisation, furthermore, tissue expression of STRA6 is in agreement with the developmental, visual, reproductive and CNS roles of retinol derivatives [58]. Once within the cell cytoplasm intracellular control over the biological activity of retinol and its derivatives is essential to prevent unregulated biological activity.

1.4.2 Control over the cellular activity of retinoic acid

Cellular control over the biological effects of all-trans retinoic acid (ATRA) is important to ensure a tissue specific response. Localised production and paracrine activity is controlled by enzymes that regulate production and degradation of retinoic acid at the receptor ligand binding site. Furthermore, transport of intracellular ATRA by the cellular binding proteins can guide the bioactive molecule to either the nuclear receptors or catabolising enzymes, resulting in tight control over activity depending on the regulation of these proteins. This results in the formation of a bioactive gradient of ATRA without the need for a concentration gradient.

Cellular retinoic acid binding protein

Conversion of intracellular retinol to ATRA occurs through a number of oxidation and hydrolysis steps. The first step is rate limiting and results in the formation of all-trans retinal through enzymatic activity of retinol dehydrogenase (RODH or ADH). Retinal is then converted irreversibly to all-trans retinoic acid by a family of retinaldehyde dehydrogenase enzymes (RALDH1, RALDH2 and RALDH3) [59]. Once formed retinoic acid binds one of two proteins found within the cytoplasm, cellular retinoic acid binding protein I or cellular retinoic acid binding protein II (CRABP I and II). The role of CRABP I is to facilitate retinoic acid oxidation. The affinity of CRABP I for RA is higher than CRABP II, however, RA induces the expression of CRABP II resulting in a positive feedback loop and increased binding to CRABP II. CRABP II has been shown to directly influence RAR signalling by actively channelling RA into the ligand binding pocket, indirect evidence for this process came from over expression of CRABP II in a mammary

carcinoma cell line. Over expression resulted in an increased sensitivity of the carcinoma to RA signalling [60]. CRABP II has been detected within the cell nucleus, however, it was found that this was cell type specific and exclusion from the nucleus has also been reported, indicating a possible role of CRABP II in cell specific sensitivity to retinoic acid [61].

CRABP I is a known regulatory protein of retinoic acid signalling and targets RA for metabolism [62]. Metabolism of ATRA is an important step in controlling its biological activity, however, some oxidation products have been shown to have biological activity similar to ATRA. Reijntjes, S et al (2005) [34] demonstrated that the oxidation products 4-oxo-RA, 4-OH-RA and 5,6-epoxy-RA could up-regulate CYP26A1 in the neural tube of quail, probably through RAR α. Furthermore, these products were able to rescue the effects of VAD in quail if provided at the correct stage of development indicating a possible developmental role for these products.

Cytochrome P450 and retinoic acid metabolism

The metabolising enzymes that oxidise retinoic acid are part of cytochrome P450 family 26. Three isomers of CYP26 enzymes that are known to be involved in retinoic acid metabolism are CYP26A1, CYP26B1 and CYP26C1 [63-65]. The expression of each enzyme during development is spatially and temporally distributed, resulting in dramatic variations in retinoic acid concentration throughout the embryo regulating cell development.

Inhibition of this family of enzymes through the use of the imidazole- Liarozole fumarate (R85246) has been shown to increase the bioavailability and enhance the biological activity of ATRA [66-68]. Liarozole is a nonspecific inhibitor of several cytochrome P450 enzymes including CYP26. The group of compounds that are being developed to modulate this pathway are known as retinoic acid metabolism blocking agents (RAMBAs). Work on enhancing retinoic acid potency and action has many applications in stem cell biology and disease treatment. Understanding retinoid metabolism may open up valuable areas of research aimed at enhancing the potency and specificity of its actions. Figure 1-5 shows the oxidation sites on ATRA and the potential bioactive molecules that are produced and may act to bind alternative retinoic acid receptors (RAR) to ATRA.

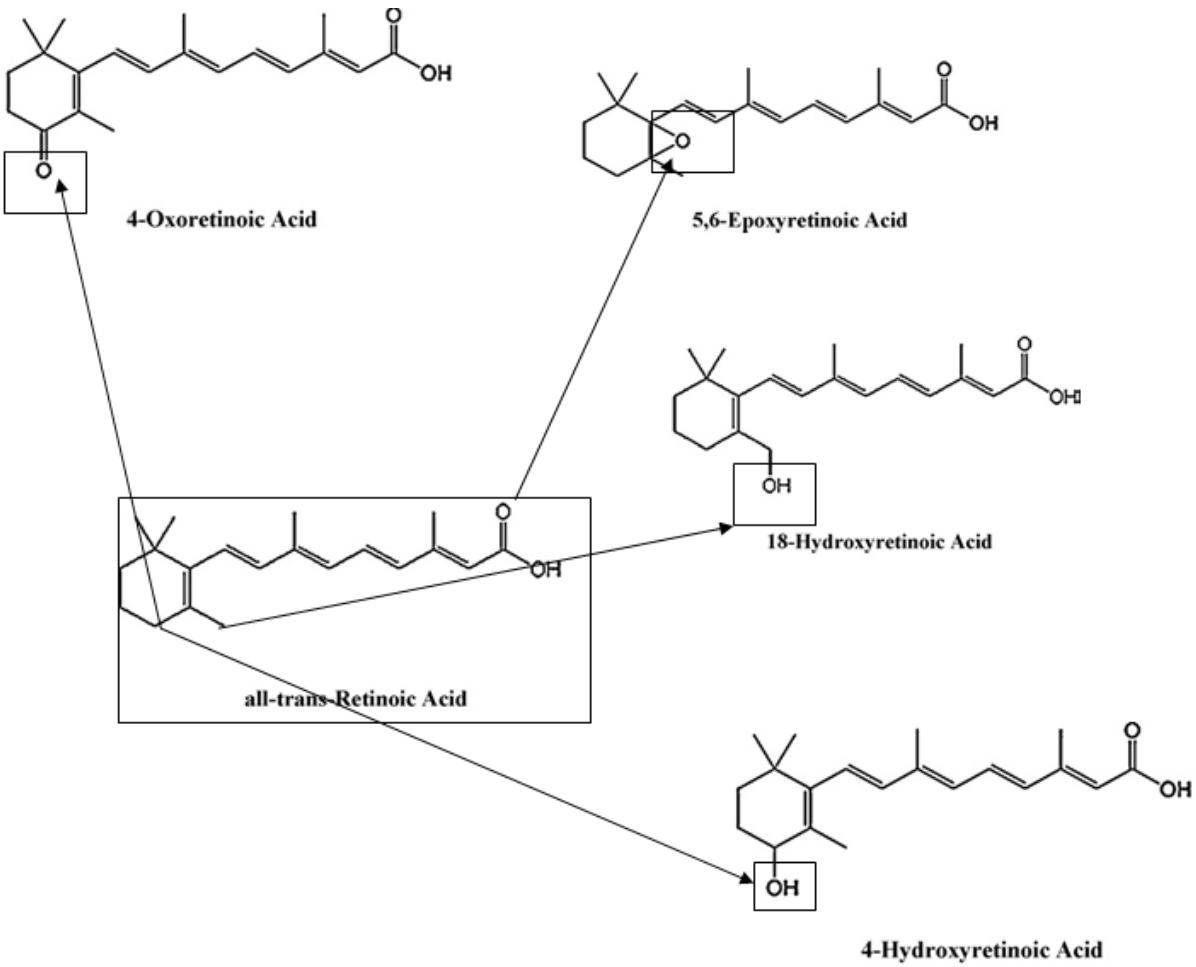

Figure 1-5 Oxidation products of *all*-trans retinoic acid. The cytochrome P450 enzyme family 26 oxidises ATRA to form a number of different products. Some of the products may have the same biological activity as ATRA *in vivo*. It is not well known how biologically relevant each oxidation product is or if their presence is an artefact of *in vitro* culture.

1.4.3 Retinoic acid receptors and signalling

RAR are nuclear-ligand activated transcriptional regulators. The three RAR are: α, β and γ; each RAR group contains isoforms arisen through gene splicing and differential promoter usage and are shown in Figure 1-6. Crystallographic imaging demonstrated that consistent with most other nuclear steroid receptors RAR consist of five distinct regions (A-F), understanding the structure and function of each region is key to receptor binding selectivity. Regions A and B contain the ligand independent activation function (AF1), region C contains the DNA binding domain (DBD) and is composed of two zinc finger

domains, two alpha helices and a COOH terminal extension. The core of the DBD is composed of the two alpha helices crossing at right angles to each other [69]. Region D forms a hinge between regions C and E, where region E contains the ligand binding pocket and the ligand dependent activation function (AF-2). Regions C and E are the most conserved domains between species demonstrating the importance of conserved DNA binding and ligand activation in development and reproduction. Knowledge of the structure of each RAR will aid in the development of subtype selective synthetic retinoids [70].

Gene	Isoforms	Human Chromosome
RAR α	α_1, α_2	17q.21.1
RAR β	$\beta_1, \beta_2, \beta_3, \beta_4$	3p24
RAR γ	γ_1, γ_2	12q13

Figure 1-6 RAR isoforms and their chromosomal locations [71]. Importantly, RARβ1/3 and RARβ2/4 are transcribed via the same promoter, differences in their structure and overall function arise from splice variants of the receptor.

The RARs signal through heterodimerisation with another nuclear receptor; the retinoid X receptor (RXR). As with RAR there are three RXR receptors α, β and γ, however, in contrast to RARs they can regulate gene transcription through homodimerisation or by forming a heterodimer with a nuclear orphan receptor such as receptors from the peroxisome proliferator-activated receptor (PPAR) family. Imaging studies demonstrate that the ligand binding pocket of RAR and RXR are significantly different giving them different ligand specificities. RAR has an I shaped binding pocket and RXR an L shaped pocket. Due to the shape of ATRA it can only bind the I shaped RAR pocket, whereas the ATRA isomer 9-*cis*RA can act as a ligand for both RAR and RXR. The role of 9-*cis*RA signalling *in vivo* is unclear as it has been difficult to isolate endogenous 9-*cis*RA. However, *in vitro* 9-*cis*RA is found and is involved in the retinoid signalling pathway suggesting that 9-*cis*RA is a product of *in vitro* isomerisation of ATRA and not thought to be involved in the biological effect of vitamin A *in vivo* [70]. Understanding the stage specific effect of ATRA signalling *in vivo* will aid its use in *in vitro* developmental studies.

1.5 *IN VITRO* NEURAL DIFFERENTIATION

The process of neural differentiation *in vitro* closely resembles that during neural development *in vivo* as determined by the expression of gene profiles, neural tube-like structures and functional neurites. Producing large numbers of neurons in a defined and reproducible manner is a major advance in neuroscience and has aided high throughput drug screening using human neural progenitors and neurons. To investigate neural development and neurite outgrowth undifferentiated cells capable of forming neuroprogenitors are required, these are often mouse or rat foetal derived brain neural progenitors or embryonic stem cells. The advantage of using pluripotent stem cells as opposed to the more committed foetal progenitors is the enhanced control over the age and specificity of the neurons that develop, furthermore, human stem cells produce human specific tissue, which is directly relevant to human development.

1.5.1 Human embryonic stem cells

Human embryonic stem cells are derived from the inner cell mass of a blastocyst and can be cultured *in vitro* for investigating the molecular processes that direct differentiation, in particular the mechanisms by which human embryonic stem cells can be induced to form specific neural subtypes.

Pluripotent embryonic stem cells are defined by their high expression of the transcription factors *OCT4* and *NANOG*, cell surface expression of the proteins SSEA3/4, TRA-1-60 and high telomerase activity. Under defined conditions these cells are immortal, dividing unrestricted and without morphological change [72].

hES cells can be characterised by their ability to form teratomas in immuno-compromised mice or by functional incorporation into the early inner cell mass of a blastocyst. Both result in complex tissue formation and a multitude of differentiated cells of all three germ layers. Importantly, the teratoma mass formed from implantation of pluripotent stem cells retain a stem cell niche allowing for maintenance of the teratoma through serial transplantation of this sub set of cells [73].

Manipulation of hES cells *in vitro* has helped elucidate the mechanisms behind inducing differentiation, maintenance of pluripotency and cellular development. Many methods of inducing human embryonic stem cells have been described in the literature, most of which

involve the use of small molecules to induce cell signalling that ultimately leads to the stem cells committing to a cell lineage [74, 75]. The stem cell will become an early progenitor. In the case of neurons, stem cells lose the expression of *OCT4* and *NANOG* and begin to express *PAX6* and *NESTIN*, as well as showing characteristic neural rosette morphology. Terminal differentiation of stem cell-derived neurons is characterised by β III Tubulin expression, NF200 and neural subtype markers such as *HB9* for motor neurons [76] and *NKX2.2* for interneurons [77]. Finally functional activity can be determined by synapse formation and electrophysiological measurements [78].

1.5.2 Embryonal carcinoma stem cells

The malignant counterpart of hES is the human embryonal carcinoma stem cell (EC cells) derived from the stem cell niche of a malignant germ cell tumour. EC cells can form complex teratomas when grafted into immune-compromised mice and have the ability to be incorporated into the inner cell mass of a mouse blastocyst. Interestingly these cells do not seem to be cancerous under the conditions found within the inner blastocyst. The use of human embryonic stem cells in developmental research is particularly limited due to ethical and availability constraints; however human EC cells circumnavigate these problems and represent an ideal model of human embryonic development for basic research. There are many similarities between ES and EC cells such as the ability to maintain them in an undifferentiated, self-renewing state. Furthermore, there is a growing body of literature defining the conditions required for directed differentiation of both cell types into functional cells from all three germ layers.

Pioneering studies by Strickland, S et al (1978) [79] demonstrated retinoic acid (RA) induced endodermal differentiation in a murine EC cell line. However, it was later demonstrated that the ability of RA to induce endodermal differentiation was dependent on the EC cell used. *In vivo* many of the murine EC cells were capable of differentiating into cells of all three lineages; however, *in vivo* these cells were more limited in their lineage potential. Studies by Jones-Villenuvive, E.M (1982) [80] demonstrated that the murine P19 EC cell could be induced to differentiate into cells with a neuronal phenotype by treatment with RA. These cells could be purified and were characteristic of ectoderm. The concentration of RA used in these studies was important to ensure a high yield of neurons within the culture. Much of the initial work on directing differentiation of EC cells was done using mouse EC or ES cells; however, it is difficult to say with confidence that

human ES or EC cells would respond in the same way. Therefore to continue using EC cells in research it was important to derive a human cell line. Initially many of the hEC cells derived were unresponsive to retinoic acid and few differentiated into cells with a neuronal phenotype [81]. This may be a consequence of the carcinoma origin of the cells, as it would be evolutionary beneficial if the ability of differentiation was lost in these cells, therefore their ability to differentiate does in many instances not completely reflect that of hES cells.

In 1970 the human EC stem cell TERA2 was derived from the lung metastasis of a male germ cell tumour. In 1984 Andrews, P et al (1984) [82] used a xenograft to form a teratoma in nu/nu mice using the TERA2 cell line and subsequent isolation of single cell clones revealed a subset of cells that expressed high levels of the surface proteins SSEA3/4 and TRA-1-60. Further characterisation of the cells revealed more similarities of the clone to hES cells including high levels of *OCT4* and telomerase expression [83]. It was determined that the TERA2 clone, NTERA2/D1 was induced to differentiate upon retinoic acid treatment. A small proportion of the cells formed were neurons and the rest fibroblast like epithelial cells. Subsequent work on this EC cell line was directed at developmental neuroscience and basic differentiation mechanisms.

Przyborski, S.A (2000) [84] used a modern technique to derive a TERA2 EC stem cell clone that expressed high markers of stem cell specific glycoproteins. Deriving hEC stem cells from different sources has provided scientists with tools that have varying strengths and weaknesses. The application of a modern isolation technique provided a TERA2 clone that would be independent of NTERA2.cl.D1 and likely have a different karyotype and response to retinoids and other small molecules. The method used involved immunomagnetic sorting of cells expressing high levels of the stem cell marker SSEA3 from an early passage of the TERA2 parent lineage, this was unlike NTERA2.cl.D1 that was passed through a nude mouse. SSEA3 specific antibodies were used to separate differentiated cells of the TERA2 from the small stem cell niche. The TERA2.cl.SP12 EC cell was demonstrated to have high levels of SSEA3, TRA-1-60 and was induced to differentiate upon RA treatment. The NTERA2.cl.D1 and TERA2.cl.SP12 EC cells are similar in many respects providing a model of human retinoic acid induced neural differentiation.

TERA2.cl.SP12 hEC stem cells were originally induced to form neurites by retinoic acid in a mono-layer culture. This provided a network of neurites for studying the protein and

genetic regulation of stem cell differentiation by retinoic acid. Aggregates of the cells were also shown to differentiate and express neural and astrocytic markers after 14 days retinoic acid treatment [85, 86]. Recent functional data demonstrated the neurons derived from TERA2.cl.SP12 were electrically active [87] further exemplifying these cells as a model of neural development. Other uses of the cells involve investigating the process of neural differentiation manipulating this process *in vitro* [88-90].

Retinoic acid has been used for many years to induce differentiation of the EC cells described above, however, a major difference between *in vitro* and *in vivo* retinoic acid signalling is the isomerisation of ATRA *in vitro* under ambient conditions. It is unknown exactly how much of an effect the isomerisation of ATRA will have on the results obtained during an experiment; it is known that the actual concentration of ATRA within culture will change as ATRA isomerises. Furthermore, the isomer of ATRA, 9-*cis*RA may have unwanted effects on cellular response. Therefore the reproducibility of ATRA treatment and the concentration dependent effects associated with ATRA will be affected *in vitro* by the instability of the compound [91].

1.6 LIMITATIONS OF RETINOIC ACID *IN VITRO*

Isomerisation and metabolism in cell culture results in the need for high experimental ATRA concentrations. The instability of retinoids is inherent in the five unstable conjugated double bonds, additionally ATRA degrades into a number of other compounds that have an unknown biological activity [90].

The ATRA isomer, 9-*cis*RA may have unwanted effects on cellular response and differentiation. Therefore the reproducibility of ATRA treatment and the concentration dependent effects associated with ATRA will be affected *in vitro* by the instability of the compound, this was highlighted in an article by Murayama, A et al (1997) [91]. A number of small molecule analogues have been designed and synthesised aim at overcoming the inherent instability of ATRA and to probe the biological process regarding retinoic acid signalling *in vitro* and *in vivo*.

1.7 SYNTHETIC RETINOIC ACID ANALOGUES

Advances in the design of small molecules and a better understanding of retinoic acid receptors and their isotype have aided the development of a large range of synthetic analogues. Elucidating the processes regulated by retinoic acid specifically during neural commitment will aid understanding of many disease mechanisms that arise from abnormalities in the signalling pathway.

An understanding of the structure-function relationship of retinoid analogues is important to gain the desired response. It is also necessary to understand the system which the retinoids will be applied to. The biological outcome may be dependent on the expression retinoic acid receptor subtypes. A general retinoid structure is shown in Figure 1-7 the structure consists of a large hydrophobic unit, a linker unit and a polar terminus. Structural modification of the hydrophobic unit has been exemplified by the TTNPB series and leads to alterations in potency. Furthermore, removal of methyl groups from this unit to reduce oxidative metabolism was demonstrated to reduce activity. To bind and activate either the RXR or RAR receptor the polar terminus must be capable of interacting with the bottom of the ligand binding pocket (LBP). This interaction acts to anchor the retinoid to the LBP. Finally, modifications to the linker unit provide selectivity of receptor binding of RXR and RAR as well as RAR isotype selectivity.

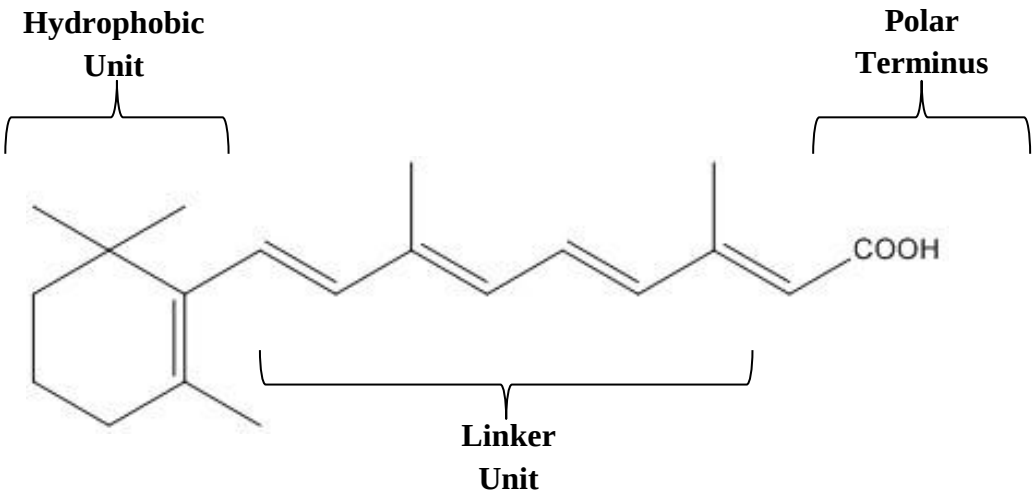

Figure 1-7 General retinoid structure. When designing retinoids three main units are to be considered these are: The hydrophobic unit, the linker unit and the polar terminus.

The synthetic analogue of ATRA – EC23 has been developed to be resistant to oxidation and as such provides a novel model to assess the role of metabolites on stem cell differentiation and the role of metabolising enzymes on the potency of ATRA [89, 90, 92]. EC23 is a highly potent photostable arotinoid which contains active methyl groups on the hydrophobic unit. The active methyl groups provide maximal potency and the presence of a stable linear triple bond ensures RAR selectivity. The aromatic ring prevents oxidative metabolism, all together these modifications account for the enhanced potency of EC23 over ATRA and other retinoid analogues [93].

Structure-function relationship

One specific example of structure activity relationships and the effect on the biological outcome is in the small molecules EC19 and EC23 [89, 94, 95]. These studies describe the differences in biological activity of the retinoid analogues EC19 and EC23. A subtle difference in the position of the carboxylic acid group between EC19 and EC23 did not alter the shape of the molecule but resulted in a large difference in the observed potency. This was possibly a result of reduced receptor binding or differential receptor activation. Figure 1-8 shows the molecular structures of EC19 (*meta* isomer) and EC23 (*para* isomer).

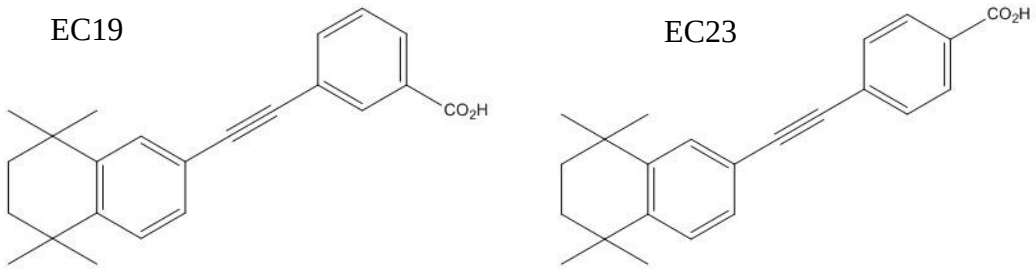

Figure 1-8 Molecular structures of EC19 and EC23.

Recently, data regarding the role of the synthetic retinoid EC23 on stem cell differentiation, neural commitment and receptor subtype activation has shown that the potency of this small molecule is much greater than its natural counterpart – ATRA. Due to its stability in culture, potency and the increasing knowledge of this compound in stem cell differentiation, the use of EC23 to develop neurite outgrowth models is an attractive alternative to ATRA.

1.8 CURRENT MODELS OF NEURITE OUTGROWTH

Assessing neurite outgrowth *in vitro* can be achieved using a number of different models. It is necessary to use the model which best resembles neurons in the natural *in vivo* environment. This is important when investigating neurite regeneration and the role of glial scar proteins in neurite outgrowth. Peripheral and central nervous system neurites will respond differently to extracellular cues [96, 97]. In addition, the developmental age of the neuron is important as studies have demonstrated an ability of some embryonic neurons to overcome the inhibitory environment of the glial scar [98]. Furthermore, species differences when using the models for potential therapeutic drug discovery should be recognised.

1.8.1 Cerebellar Granular Neurons

Cerebellar granular neurons (CGN) are a primary cell representative of CNS neurons and are used to investigate neurite outgrowth *in vitro*. CGN neurons represent a highly homogenous population of brain CNS neurons and are the most abundant neuron in the brain. These neurons are most often isolated from post-natal rat cerebellum [99]. Radio, N et al (2010) [100] used rat CGN in a high throughput screen of compounds that may affect neurite outgrowth. The study showed using a comparison with PC12 neurites that different neural cell models are differentially responsive to chemical treatment and highlighted the fact that reduced cell viability was often associated with a loss in neurite outgrowth – indicating a toxic effect on the neurites, as opposed to a role in neurite outgrowth regulation. Another study that investigated neurite outgrowth from CGN was described in Ahmed, I et al (2006) [101]. This study demonstrated the role of Rho GTPase in neurite outgrowth from CGN. Overall many studies have used this model to investigate neurite outgrowth from primary CNS neurons.

1.8.2 Dorsal Root Ganglia

Another well characterised model of neurite outgrowth is dorsal root ganglia (DRG) derived neurons. DRG are derived from neural crest cells during development and migrate to the periphery. DRG can be isolated from vertebrates of a number of species, including rat, mouse and chicken. DRG neurites have been used to demonstrate the neurite enhancing ability of both retinoic acid and NGF and are ideal for myelination and co-

culture studies. The axons that form spread as a halo around a central aggregate and the length of the neurites is between 1-3 mm, making quantification of neurite length relatively straight forward. The age and method of derivation of DRG determines how the developing neurites will respond to their environment. Furthermore, it is becoming more clear that the age and method of purifying DRG cells determines how the cells will respond to their environment, making the route of isolation particularly important when designing a specific study [102]. More recently, DRG neurons have been used to investigate neural regeneration and models of spinal cord injury [103].

1.8.3 SH-SY5Y

The cell line SH-SY5Y is a human clone of the bone marrow derived neuroblastoma SK-N-SH established in 1970 (ATCC). The cells can be differentiated with retinoic acid, responding more to 9*cis*-RA than *all-trans*-RA, however, this was not likely through RXR homodimer signalling [104, 105]. The cells are mainly used to investigate retinoic acid induced neural differentiation [106] and have been used to investigate GDNF induced peripheral neurite outgrowth [107].

1.8.4 PC12

The PC12 cell line is derived from a rat adrenal medulla neuroendocrine tumour known as a pheochromocytoma. The cells are induced to terminally differentiate upon neurite growth factor (NGF) treatment and become cholinergic-like neurons [108]. The model is used to investigate neural differentiation and neurite outgrowth and to determine the role of NGF and retinoic acid signalling during neural development. Cosgaya, J.M et al (2001) [109] demonstrated the cross regulation between NGF signalling and retinoic acid sensitivity in PC12 cells during neural differentiation via a Ras dependent mechanism. Furthermore, Scheibe, R.J (1992) [110] demonstrated that retinoic acid signalling could increase the sensitivity of PC12 cells to NGF by up-regulating the specific NGF receptor. This demonstrates a fundamental link between NGF, retinoic and neural commitment and neurite outgrowth, making this model good for investigating these links. It is important to realise that this model represents a peripheral neuron and the length of neurites that develop are small making quantification difficult.

1.8.5 Embryonal carcinoma stem cells

The malignant counterpart of embryonic stem cells is the embryonal carcinoma stem cell (hEC) – and has been described earlier. Two hEC stem cell lines have been derived independently and are termed, NTERA2.cl.D1 and TERA2.cl.SP12, both cell lines can be induced to differentiate into neurons by *all-trans* retinoic acid. Models of neurite outgrowth using both cell lines have been described. Initially the stem cells were differentiated and the neural progenitors induced to form neurites on either Poly-D-Lysine (P-D-L) and/or Laminin/Matrigel™ substrates. Tegenege, M.A et al (2011) [111] studied a rapid 14 day aggregate differentiation method to induce human neurite outgrowth from NTERA2.cl.D1. The study demonstrated migration of individual neurites from the differentiated aggregate when placed on P-D-L and Matrigel™. Neurite outgrowth from each neuron could then be measured under different conditions. The neurites expressed the neural specific antigen TUJ-1 and outgrowth was regulated by cAMP dependent signalling. Similar to NTERA2.cl.D1, the TERA2 clone SP12 could be induced to differentiate into neurons with high efficiency. The cell line has been used to investigate neural differentiation and as a model system for investigating neurite outgrowth [112]. Due to the often limited differentiation potential of hEC stem cell the yield of neural progenitors is high. This makes the cells useful for investigating human neurite outgrowth in an efficient and ethically acceptable way.

1.8.6 Embryonic stem cells

Neural differentiation from human embryonic stem (hES) cells offers the ability to produce high numbers of defined neural subtypes for use in neural differentiation and neurite outgrowth studies. Due to the low yield and culture heterogeneity of embryonic stem cell differentiation few studies have used hES cells to investigate neurite outgrowth. Although hES and other species of embryonic stem cells can be induced to form axons, quantification and high throughput screening of compounds using these cells is still in the early stages of research. Ma W et al (2008) [113] measured neurite number and neurite length from differentiated hES cells grown on a variety of extracellular matrix substrates and determined neurite outgrowth differences – neurites grown on Laminin produced the most outgrowth. However, the total length and difference between substrates was very low making the accuracy of this study limited. Laminin induced a maximum outgrowth of 90 µm, whereas Fibronectin and Collagen induced a length of 40 µm. Lin, L et al (2006)

[114] used a mouse embryonic stem cell model to investigate neurite outgrowth, large numbers of neurites were produced from aggregates of neural progenitors, however; again the neurites that formed were short, control cultures extended neurites to around 100 µm. Therefore, although hES cells are an attractive model of human neural development and outgrowth, optimisation of neurite outgrowth must follow the optimisation of neural differentiation for high throughput screening to be beneficial and outcompete other models that are easier to quantify and have less ethical issues.

1.8.7 Induced pluripotent stem cells

A relatively recent advance in the use in stem cells for neural development and neurite outgrowth comes from the ability to derive stem cells from human somatic cells. Inducing somatic cells such as fibroblasts in the skin to become pluripotent and have the ability to form any one of the three germ layers – mesoderm, ectoderm or endoderm, has revolutionised disease modelling and potential therapeutics from stem cells [115].

Induction of pluripotency can be achieved through multiple methods however each method is a different way of inducing the expression of pluripotency genes in non-pluripotent cells. The number and type of pluripotency genes required depends on the starting cells used. Chang, T et al (2011) [116], measured neurite outgrowth from an iPSCs derived from the fibroblasts of a patient suffering with the genetic motor neuron disorder spinal muscular atrophy (SMA). Differentiation of the iPSCs into neurons demonstrated a reduction in motor neuron formation and neurite outgrowth abnormalities. Therefore, the use of iPSCs in this instance may be beneficial at screening for patient specific compounds that can enhance neurite outgrowth in a genetic disease state.

1.8.8 3D models of neurite outgrowth

Using the cells described above multiple studies have focussed on making the models of neurite outgrowth more physiologically relevant. By combining neural progenitors with functionalised or biomimetic scaffolds 3D models of neurite outgrowth can be developed. Numerous methods have been used to produce 3D neurite outgrowth and these usually require the presence of a permissive extracellular matrix protein such as Laminin [117].

Aligning the scaffolds can also achieve directed neurite outgrowth for use as conduits. These models are often used in conjunction with animal spinal cord injury to demonstrate

the ability to enhance outgrowth [118]. The cell line of choice is often DRG explants as they extend long neurites from an aggregate making quantification easier. Multiple studies have used aligned polymers to guide the neurites, however, as with 2D growth only one surface of the developing neurite is exposed to the ECM [119-121]. Furthermore, many of these studies involve co-culture with supportive cells such as Schwann or astrocytic cells that can enhance neurite outgrowth and aid regeneration.

Other 3D neurite outgrowth assays use gels or hydrogels that are composed of ECM molecules that promote outgrowth such as collagen and Laminin [96, 122]. The neurites form inside the gel, these models are difficult to quantify. Small molecule treatment and manipulation of neurite outgrowth often requires functionalization of the scaffold making high throughput screening difficult due to the time required to optimise production [123, 124]. Balgude, A.P et al (2001) [125] investigated the effect of stiffness of an agarose hydrogel on neurite outgrowth from DRG. The study demonstrated that as the % of agarose in the gel increased from 0.75 % to 2 % there was a decrease in neurite outgrowth length. The study also described the change in growth cone from 3D to 2D, where the 3D growth cone was more spherical as opposed to the flattened 2D growth cone seen in many studies.

Other scaffolds made from porous biomaterials provide the most 3D like culture with the neurites in contact with each surface of the scaffold. The scaffold can be functionalised rapidly via coating with ECM proteins and cell media can be supplemented with test compounds. Multiple studies have used this method to induce 3D neurite outgrowth [112, 126]. Hayman, M.W et al (2005) [112], demonstrated using a porous polystyrene scaffold that neurites from differentiated TERA2.cl.SP12 EC cells will grow in 3D, furthermore, coating the scaffold with a combination of Laminin and P-D-L enhanced neurite outgrowth better than coating with P-D-L alone. Interestingly, this study demonstrated that P-D-L coating was required for neurites to attach to the scaffold and Laminin was then used to enhance neurite outgrowth from neuroprogenitors. The study also demonstrated the ability of this scaffold to be coated easily with ECM molecules that regulate neural differentiation.

In vitro models of neurite outgrowth will be useful when investigating disease pathologies that affect neurite development. In addition, by modelling the pathophysiological states *in vitro*, screens of small molecules can be tested for their ability to overcome inhibition of neurite outgrowth. These models important are tools to aid studies into the molecular

processes that occur under different disease conditions or inhibitory environments such as those that develops through spinal cord injury.

1.9 SPINAL CORD INJURY

Traumatic spinal cord injury (SCI) is a life changing and debilitating event that affects approximately 12,000 people every year in the United States, with around 273,000 people living with the disability. The causes of traumatic injury can be the result of a range of events including but not exclusively: Road traffic accidents; sport; violence and falls; with road traffic accidents accounting for 36.5 % of all SCI events [127].

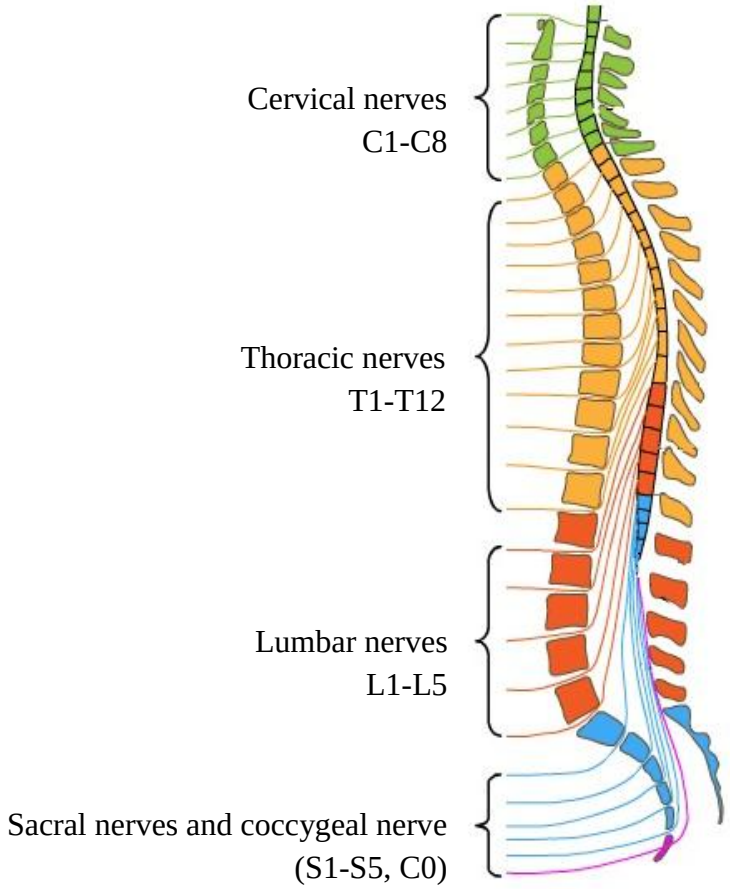

Figure 1-9 Levels of human spinal cord and injury. The level of spinal cord injury determines the extent of paralysis and loss of function for the patient. Injury to cervical nerves results in potential functional loss of all muscles including those that control breathing. Injury to thoracic level nerves (T1-T12) can result in loss of innervation to the legs and/or the trunk. Lumbar level injury (L1-L5) results in loss of sensation in the hip and legs with varying patterns of sensation. Injury to the sacral nerves causes loss of perineum sensation [3]. Figure adapted from Hoa et al (2009) [8].

The level of paralysis caused by traumatic spinal cord injury is determined by the area of the spine that is damaged. Injury to anterior spinal cord cervical level segments often results in full or partial quadriplegia. As the level of spinal cord injury becomes more posterior the resulting paralysis is reduced as the brain receives input from the undamaged neurons. To aid diagnosis and treatment a classification of the level of spinal cord injury is categorised into five levels these are [128]:

Category A: Complete spinal cord injury – no motor or sensory function in the sacral segments S4-S5

Category B: Incomplete spinal cord injury – sensory function is preserved below the level of injury including sacral segments S4-S5 however, motor function is not preserved.

Category C: Incomplete spinal cord injury with preserved motor function below the site of trauma – motor function is defined by more than half of the key muscle s having full range of movement against gravity and an active muscle grade less than 3.

Category D: Incomplete spinal cord injury with preserved motor function below the site of trauma – motor function is defined by at least half of key muscles having full range and active muscle grade 3 or more.

Category E: Normal – motor and sensory function is normal. This does not rule out spinal cord injury.

Traumatic spinal cord injury has had some high profile backing particularly from celebrities most notably the actor Mr C Reeve (1952-2004). Christopher sustained injury to his cervical spinal cord after falling from a horse in 1995, paralysing him from the neck down.

Research into the treatment of traumatic spinal cord injury has taken a number of different approaches recently, including the use of stem cell-based therapies to induce neural regeneration; bio-engineering scaffolds to aid neural growth and technology to facilitate the independence of patients that have suffered the disability. Understanding the glial scar, the mechanisms by which neural regeneration is inhibited and ways of overcoming the inhibition will be necessary for the development of future therapeutics.

1.10 THE GLIAL SCAR

Traumatic spinal cord injury (SCI) as was described in the previous section can result in total or partial paralysis. Although the cause and effect of the disability are well described treatments remain largely incomplete and in the most severe cases aim solely to sustain life.

Hu, R et al (2010) [129], used an *in vivo* rat model of chronic spinal cord injury to demonstrate glial scar and cavity formation by the activation of astrocytes. The resultant scar inhibited axon formation after 4 weeks post-injury. Some regeneration was demonstrated for 1-2 weeks post injury, underlining the regenerative potential of these neurites. These data demonstrate the potential of an ideal time window for therapies to prevent the loss of axonal processes post SCI. Understanding the process of scar formation and the mechanisms behind axon inhibition will directly influence the development of new therapeutics in the area.

1.10.1 Development of the glial scar

The scar that forms after chronic spinal cord trauma is composed of four distinct areas – glial scar, glial limitans, fibrotic scar and the cavity (Figure 1-10). Each area inhibits neurite regeneration either mechanically or biochemically. The cavity of the scar is fluid-filled and the thickness of the scar around the cavity is different rostral and caudally, making the level of neurite inhibition and regeneration heterogeneous [129]. Surrounding the cavity is a fibrotic scar, which comprises fibroblasts and segmented collagen creating a mechanical barrier to neurite outgrowth. Around this zone is a limiting boundary of glial cells that marks the transition into the glial scar – an area that is composed of reactive astrocytes and large deposition of extracellular matrix proteins. The glial scar is highly inhibitory to axonal development and neurite regeneration [130, 131].

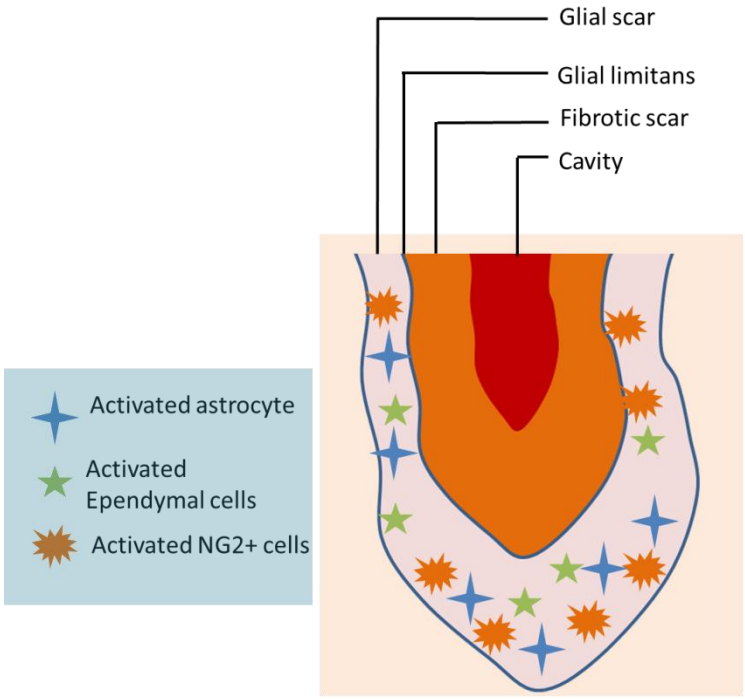

Figure 1-10 Schematic detailing the structure of a chronic traumatic spinal cord injury scar. Four distinct areas of the scar interact with developing neuritis either mechanically or via receptors to inhibit neurite regeneration. These include a cavity, fibrotic scar, the glial limitans and the glial scar. Figure adapted from Yuan et al (2013) [6].

Reactive astrocytes

Chronic damage to the spinal cord results in glial scar and cavity formation predominantly produced by the activated response of astrocytes at the site of injury. Astrocytes are abundant in the CNS and post SCI the local astrocytes are thought to be activated by TGF β undergoing genetic and morphological changes to become reactive [132]. Reactive astrocytes are characterised by high GFAP levels, a star shaped phenotype under histological analysis and the production of ECM into the area of injury – they retain their unique domains upon activation [132]. Since 'reactive astrocytes' compose a large cellular component of the glial scar and are thought to be responsible for producing inhibitory chondroitin sulphate proteoglycans they have been investigated in multiple studies as a potential target for SCI therapies[133-136]. In addition to reactive astrocytes that are proximal to the lesion site, migratory astrocytes and astrocytes derived from stem cells, other cell types also respond to SCI. Cells such as neuron-glial antigen 2 progenitors (NG2), ependymal cells and meningeal cells undergo trans differentiation to become

reactive astrocytes and contribute to scar formation [137-139]. Furthermore, it was demonstrated by Hirsch and Bahr (1999) [140] that the axon inhibitory properties of meningeal cells in the glial scar is much more potent than inhibition by the inhibitory environment produced by reactive astrocytes. This was a likely result of increased keratin sulphate expression and a decrease in expression of the neural cell adhesion molecule (NCAM) in activated meningeal cells.

Scar extracellular matrix

After traumatic SCI TGF β signalling causes reactive gliosis, the astrocytes become reactive and begin producing large amounts of extracellular matrix proteins into the site of injury to form a scar. The large spinal processes of astrocytes create a lattice which bind the ECM proteins together and mechanically inhibit neurite outgrowth and regeneration [132]. It is now largely accepted that the ECM molecules that are excreted by reactive astrocytes are inhibitory to neurite regeneration, induce neurite retraction and growth cone collapse. A major inhibitory ECM protein family that has been widely studied are the Chondroitin sulphate proteoglycans (CSPG) [141], CSPGs have been shown to be up-regulated in the glial scar [142, 143] inhibit neurite outgrowth *in vitro* and their removal *in vivo* results in partial neural regeneration [144] - CSPGs provide an inhibitory environment to neurite regeneration in the chronic injured spinal cord.

Chondroitin sulphate proteoglycans

CSPGs are a family of proteoglycan molecules that have attached negatively charged repeating disaccharide units or glycosaminoglycan (GAG) [135]. CSPGs have varying numbers of GAG chains bound to a protein backbone; the number of side chains affects the biological activity. Chondroitin sulphate regulates CSPG attachment to proteins in the ECM controlling activities such as axonal guidance and path finding. The lectican family of CSPG consist of four glycoproteins -Brevican, Neurocan, Versican and Aggrecan, all of which are expressed in CNS tissue. Aggrecan was thought to be restricted to cartilage expression, where Neurocan, Versican and Brevican regulate neural development and plasticity in the CNS [2]. However, it has been demonstrated that Aggrecan is also an integral structural protein in the CNS making up part of the perineuronal nets in the brain and helping define glial boundaries. All four of the CSPGs are composed of the N-terminal G1 domain and the C-terminal G3 domain, in addition Aggrecan has a short G2

domain near to the C-terminus and some keratin sulphate chains in the N-terminus of the molecule (Figure 1-11).

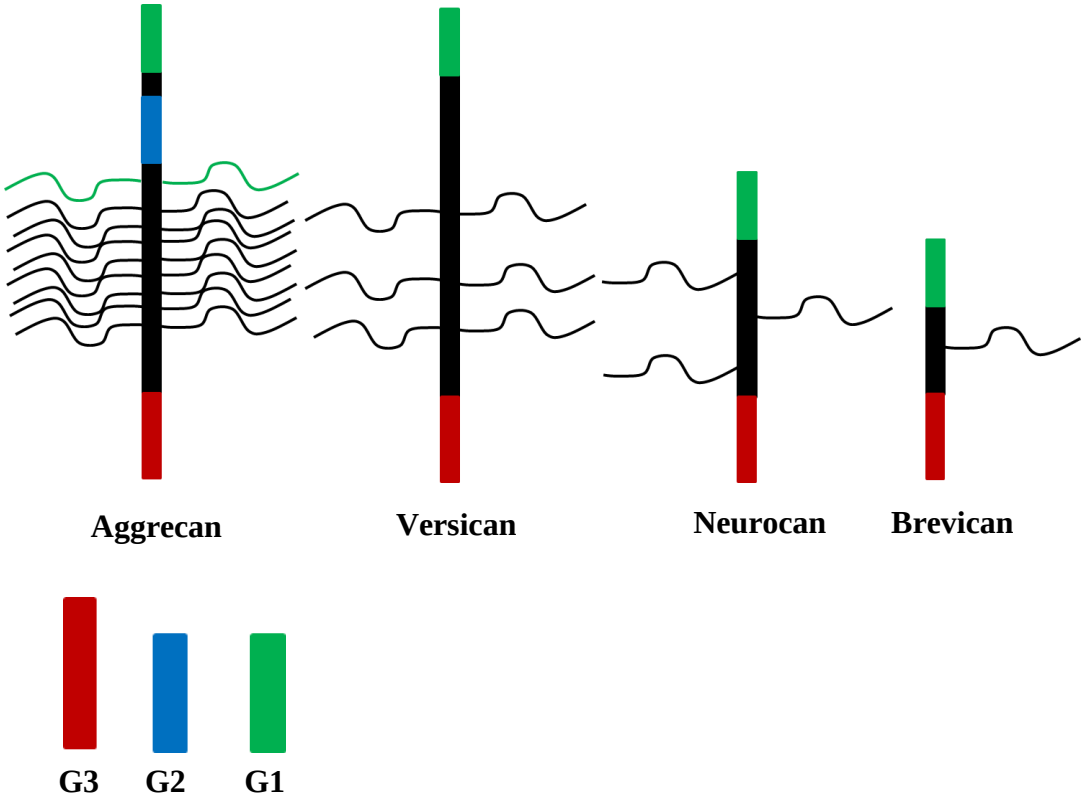

Figure 1-11. Domain structures of the four lecticans – Aggrecan, Versican, Neurocan and Brevican. All four lecticans contain the G1 and G3 domains in addition Aggrecan contains a G2 domain and additional keratin sulphate chains (green). Figure adapted from Yamaguchi, Y (2000) [1, 2].

Up regulation of CSPGs in the glial scar is inhibitory to neurite outgrowth and this is due to the glycosaminoglycan side chains attached to each protein back-bone. The number of potential GAG chains is highest for Aggrecan with around 120 binding sites per molecule which decreases to 20 for Versican, 7 for Neurocan and 3 for Brevican [2]. Therefore, it is likely that the inhibitory potential of Aggrecan is greater than that for the other CSPGs. Evidence for the inhibitory potential of CSPG on neurite outgrowth came from studies on DRG and cerebellar granular neurons [145, 146], which demonstrate a preferential growth on Laminin ECM than on CSPG or keratin sulphate proteoglycan. Aggrecan has been used in multiple models of the glial scar to investigate the role of CSPGs as culturing neural progenitors on an Aggrecan substrate potently inhibits neurite outgrowth [98, 147].

CSPG receptors

Until relatively recently the glial scar and especially the matrix of astrocytic processes were thought to provide mechanical inhibition to neurite outgrowth and regeneration, however, using modern molecular biology it has been possible to establish that two protein tyrosine phosphatase receptors regulate receptor mediated inhibition of neurite outgrowth and regeneration [148].

The two receptors that have been characterised are the protein tyrosine phosphatase (PTP) σ receptor [149] and a leukocyte common antigen related protein tyrosine phosphatase (LAR) [150]. A schematic showing the general structure of both enzymes is described in Figure 1-1-12. Shen, Y et al (2009) [1] demonstrated in a cell free assay the binding of PTPσ receptor to CSPGs, furthermore, the receptor bound to Neurocan on astocytic cells and was shown in a knockout DRG system to significantly reduce neurite outgrowth. Similarly, Fisher, D et al (2011) [148] showed LAR activation by CSPGs in a non-neuronal assay using COS-7 cells and that inhibition of neurite outgrowth in cerebellar granular neurons was by LAR in an AKT and RhoA dependent mechanism. These two studies describe the role of these receptors in the inhibition of neurite regeneration after spinal cord injury.

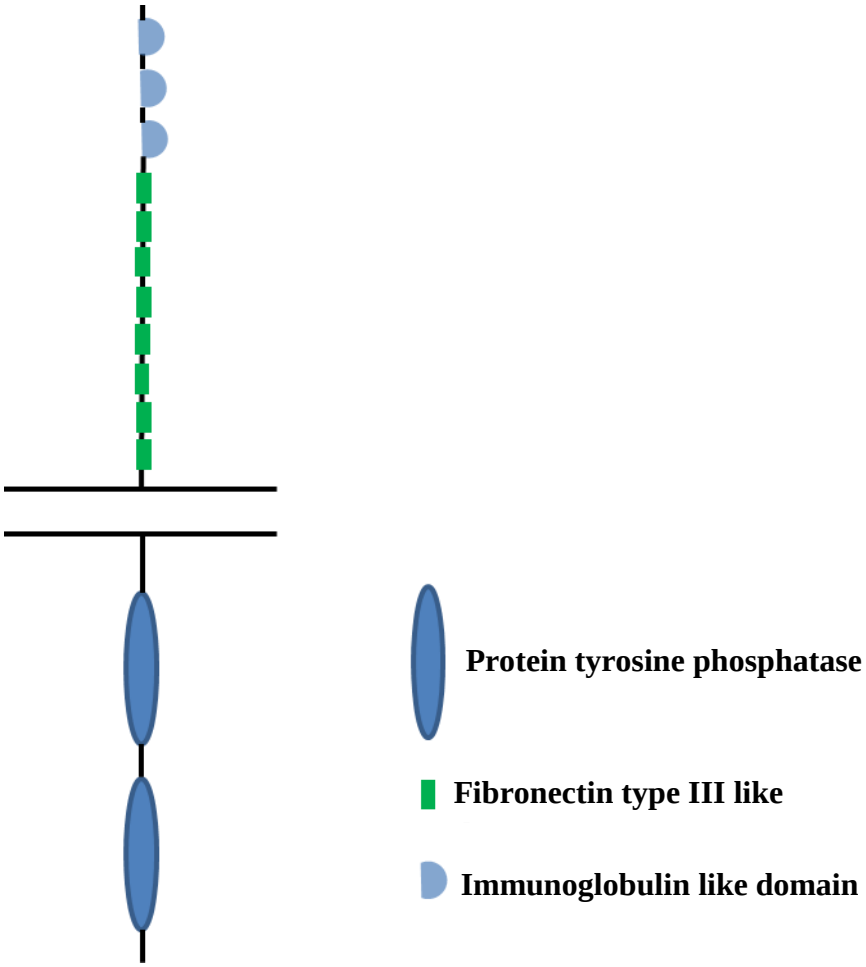

Figure 1-1-12. Structure of protein tyrosine phosphatase receptors. The transmembrane receptor has two intracellular protein tyrosine phosphatases multiple extracellular Fibronectin type III like domains and multiple immunoglobulin like domains.

1.11 MODELLING THE GLIAL SCAR

Modelling the glial scar *in vivo* and *in vitro* have distinct individual advantages however, both aim to either elucidate the mechanisms of CNS injury and neural regeneration with the objective to better understanding targets for regenerative therapies. The glial scar model used will depend on the hypothesis being tested and the complexity of the model should mirror the biological environment required to test the hypothesis. *In vivo* models have much more complexity surrounding the biological response to CNS injury compared to *in vitro* neural models, this allows for whole system dependent hypothesis to be tested. *In vitro* assays provide more specific answers to biological questions and help elucidate key biological mechanisms. One major advantage of using *in vitro* over *in vivo* models is

the potential to test human neural regenerative potential *in vitro*. Some of the current models of the glial scar are discussed below in context with their use in the literature.

1.11.1 Current in vivo models of the glial scar

The majority of *in vivo* spinal cord injury and glial scaring models use either rats or mice with injury to the spinal cord in these models performed under anaesthetic and usually via a transection, hemisection or contusion injury [151]. It is thought that the rat glial scar that forms after injury best recapitulates that seen in the human situation, due to the large cavity that develops as opposed to mouse where the lesion site is composed of a dense accumulation of fibrous connective tissue [152]. An advantage of using mouse models is the ability to knock out whole genes to determine their effect on glial scar formation and neural regeneration. Schreiber, J et al (2013) [153] used a mouse knockout of tenascin-C to investigate the role of this ECM molecule on glial scar formation and neurite regeneration. This model was useful since *in vitro* tenascin-C had both neurite promoting and inhibitory effects. The study demonstrated that this molecule regulated inflammation post-injury; was involved in regulating the composition of the glial scar ECM and resulted in the facilitation of neurite regeneration.

In vivo studies on rats have been used to demonstrate the up-regulation of CSPGs after both cervical and thoracic hemisection, it was shown that chondroitinase ABC could be used to create a permissive environment for DRG transplantation and neurite outgrowth into the scar [154]. Furthermore, Chan, C.C et al (2007) [155] demonstrated that the known small molecule ROCK inhibitor Y-27632 could regulate CSPG production *in vivo*, however, required an *in vitro* model to discern effects on neurite outgrowth. These studies demonstrate in whole systems that the glial scar inhibits neurite outgrowth, furthermore, this inhibitory environment has the potential to be overcome by developing neurites.

Although physiologically these models are relatively close to human neurons and will act in a similar way upon injury, there will be subtle differences that may affect the way the neurons respond to treatment, making translation from *in vivo* models to clinical treatments difficult. Furthermore, using whole animals to study spinal cord injury may make the basic biological mechanism and interactions between cells in the injured spinal cord difficult to elucidate due to the complex interaction between systems. Ethically animal usage is under a lot of pressure to reduce failed experimentation and wastage. This makes it difficult to

complete high throughput screening of potential therapeutic compounds using animal models due to wastage and expense.

1.11.2 Current in vitro models of the glial scar

In vitro modelling of the glial scar utilises the neurite outgrowth model cells described earlier. Neurite outgrowth can be manipulated by altering growth media supplementation or culture substrate. By altering the extracellular matrix the neurites develop on, a model of neurite inhibition can be developed. Through supplementing the culture media or treating the culture substrate methods of enhancing neurite outgrowth and overcoming neurite inhibition can be investigated. The major advantages of *in vitro* models is the ability to perform high throughput screening of test compounds and investigate biological mechanisms between individual proteins or cell types and neurite regeneration.

Manipulating the coating substrate that DRG, CGN and hEC derived neurons are induced to form neurites on is useful for investigating the interaction between neurite development and the ECM. Jin, Y et al (2011) [156] used 1 mm strips of filter paper saturated in CSPGs to investigate the lentiviral expression of Chondroitinase ABC and its ability to induce neurite outgrowth from chick DRG on the inhibitory CSPG substrate. Similar methods have been described using CGN [157, 158] and hEC derived neurites [159]. These models utilise a relatively simple 2D method of coating a substrate and investigating its effect on neurite length and number. Enhancing outgrowth on the 2D inhibitory substrate using small molecules and other compounds are potential therapeutics for spinal cord injury. Using human stem cell-derived neural progenitors is an efficient way to investigate human neurite regeneration in 2D on an inhibitory substrate. Regulation of ROCK activity, integrin stabilisation and enzymatic degradation of CSPGs GAG side chains have all been demonstrated in 2D models of the glial scar [155, 160, 161].

In addition to *in vitro* 2D models of the glial scar, some 3D culture systems are also investigating the interaction between developing/regenerating neurites and molecules that make up the glial scar ECM. The translation to a 3D model is more physiologically relevant to the *in vivo* situation and the use of human stem cell-derived neurons can enhance the physiological relevance. 3D models often utilise ECM coated scaffolds or functionalised scaffold that can be used to either investigate neural regeneration or act as conduits to overcome the inhibitory glial scar environment. It has been demonstrated that

co-culture with other cell types in 3D enhances neural regeneration *in vivo*; furthermore, directed neurite outgrowth by 3D scaffolds will aid functional recovery [120, 162]. Few 3D models have investigated the molecular mechanisms of the neural-glial scar interaction and this is likely a result of the difficulty in quantifying 3D neurite outgrowth.

1.12 PATHWAYS INVOLVED IN NEURITE REGENERATION

1.12.1 Rho associated protein kinase (ROCK) inhibition

As described earlier neuronal signalling through the PTPσ or LAR receptors by CSPG molecules in the CNS results in loss of neurite outgrowth and neurite retraction. The cellular signalling cascade that follows receptor signalling activated mediators such as RhoA and P160 ROCK, which induce changes in gene expression and cytoskeletal architecture [148, 163-165].

Monnier, P.P et al (2003) [158] demonstrated using embryonic day 6 chick retinal explants that CSPGs inhibit neurite growth *in vitro* and this can be overcome by inhibition of ROCK signalling. Inhibition of ROCK was achieved using the synthetic inhibitor Y-27632. This work demonstrated nicely up-regulation of CSPG in the damaged spinal cord and inhibition of neurite outgrowth via ROCK activation. Other studies used human EC derived neurons, DRG neurons, rat cerebellar neurons and optic nerve neurons to demonstrate the same process [159, 166]. ROCK inhibition can be achieved directly by Y-27632 treatment or through up regulation of cAMP and RhoA inhibition using C3 transferase. Either way, inhibition of this signalling cascade at multiple levels was demonstrated to overcome at least partially, neurite outgrowth inhibition induced by CSPGs.

It is thought that ROCK acts by phosphorylating collapsing response mediator protein-2 (CRMP-2), destabilising it and inhibiting its positive effect on neurite outgrowth. CRMP-2 is found at high levels in developing neurites in the CNS. Phosphorylation of CRMP-2 results in growth cone collapse and neurite retraction, whereas overexpression enhances neurite outgrowth [167] making this protein a promising target for neural regeneration.

1.12.2 Retinoic acid receptor β

In the regenerating newt limb a small molecule diffuses from the regenerating limb mass (blastema) to provide guidance and outgrowth signals to neurons in the spinal cord. Dmetrickhuk, J.G (2005) [168] demonstrated that a bead containing retinoic acid could provide similar neuronal outgrowth cues to neurons as that seen *in vitro* with a blastema. Furthermore, this effect is inhibited by the RAR β receptor antagonist LE135 indicating that retinoid signalling within the regenerating limb of a newt may be involved in neurite outgrowth from the spinal cord *in vivo*.

The neurotropic factor NGF β , is used routinely to induce neurite outgrowth in a number of *in vitro* models of neurogenesis from primary cell lines (DRG) and neuroblastoma cells (PC12), providing evidence that neurotrophins may be involved in the initiation, stability and subsequent outgrowth of developing/regenerating axons. Recent studies have implicated retinoic acid (RA) as a downstream target of NGF β signalling. So, P.L et al (2006) [169] demonstrated that DRG from RAR β null mice treated with 0.1 μM RA for 3 days did not form as many NF200 expression neurites than wild type DRG and those that did form were significantly shorter. This implicated RAR β signalling in neurite outgrowth; furthermore, RAR β null DRG cells treated with 20 ng/ml NGF β had a reduction in the average length of neurite compared to wild type DRG, suggesting that NGF β acts at least partially through RAR β. NGF β is known to act upstream of RAR and has been shown to induce expression of RAR β [109] further implicating RAR β in the ability of NGF β to induce neurite outgrowth. The induction of RAR β expression and subsequent neurite outgrowth may be in part due to NGF β inducing the production of enzymes involved in the production of RA.

As described previously retinoids are essential for proper embryonic axis formation and CNS development. The role of retinoid in neurogenesis is complex owing to the three retinoic acid receptors RAR α, RAR β and RAR γ and their respective isoforms. It is known that the receptors have some functional redundancies; however, many of the effects seen in cells treated with retinoic acid are a direct response to activation of a specific RAR subtype. Piu, F et al (2005) [170] treated NTERA2/D1 EC cells with 10 μM RA or one of three RAR β selective agonists for 7 days, the cells were then fixed and stained for Gap43 expression. The author concluded that the cells were differentiating in response to the RAR β selective compounds, however, the undifferentiated control also expressed Gap43

immunostaining and the extensions seen after 7 days in the EC cells were not characteristic of developing neurites and no further maturation of the neurons was performed. It has been recently demonstrated that at least 12 days of continuous ATRA treatment is required for neuronal differentiation in NTERA2.cl.D1 EC cells [171].

In neuroprogenitor cells such as primary DRG and neuroblastoma the RAR β2 isotype has been strongly implicated in neurite outgrowth [169]. Up regulation of rat RAR β2 in DRG has been shown to induce neurite outgrowth and functional regeneration of synapses when co-cultured with spinal cord *in vitro* [172]. Elevated RAR β2 expression has been detected in injured rat cerebral cortex which is further induced in the presence of an RAR β2 agonist [173] indicating that the receptors required for axonal regeneration are present. Corcoran, F et al 2000 [174] utilised receptor specific agonists of RAR β, α and δ to show that NGF and NT-3 dependent DRG neurons require synergistic signalling through RAR β2 and neurotropic factors for maximum neurite outgrowth. Conversely signalling through RAR γ can inhibit neurite outgrowth via down regulation of RAR β2

Studies utilising newly developed RAR β agonists such as CD2019 demonstrate the ability of small lipophilic retinoid analogues to diffuse and affect damaged neurons *in vivo* [173]. Although ATRA acts as an agonist for RAR β2 and will induce neurite outgrowth, gene expression is heterogeneous and nonspecific agonists of the RAR may not be optimum for neuritogenesis as many of the other RAR have been implicated in genes not associated with neuronal differentiation or maturation. Furthermore, RAR β selective agonists have been shown to induce motor neuron lineage commitment in a neuroprogenitor cell line in a concentration dependent manner and induce neurite outgrowth in these cells. However, to maintain mature neuronal differentiation signalling through RARα is required [175].

Investigation into the ability of compounds such as NGF β and RAR selective retinoid to enhance neuritogenesis can be difficult due to the ability of developing neurons to form multiple axons. *In vitro* neurogenesis often results in a spaghetti type structure making it difficult to determine the length or origin of any one neurite (Figure 1.6.2). This makes determining any effect on neuritogenesis almost impossible. Some *in vitro* cell systems are better than others and often rely on a low density of neuroprogenitor cell such as PC12 or rat cerebella granular cell as were described earlier.

1.12.3 Glycogen synthase kinase 3β

The role of AKT inhibition and subsequent GSK3β inhibition has been shown to play at least a partial role in the inhibitory effect of CSPGs on neurite outgrowth [148]. It was demonstrated by Alabed, Y.Z et al (2010) [176] that GSK3β inhibition, inhibited neurite outgrowth from DRG neurons, and this was likely at least an effect of collapsing response mediator protein-4 (CRMP4) inhibition. Furthermore, multiple studies have described the requirement of GSK3β in axonal polarity at the growth cone [177, 178]. These studies demonstrate that GSK3β signalling is required for neurite outgrowth; however, there is some evidence to suggest the opposite effect is true, where GSK3β activation resulted in loss axonal outgrowth. Wang, Y et al (2012) [179] demonstrated in rat cortical neurons that GSK3β signalling induced growth cone collapse and neurite retraction via repulsive guidance molecule-a (RGM-a) dependent pathway. RGM-a signalling caused CRMP-2 phosphorylation ultimately resulting in neurite retraction. The study demonstrated that although there was no evidence for phosphorylation of CRMP-2 by GSK3β, inhibition of GSK3β resulted in loss of RGM-a activity which was shown to be directly responsible for the destabilisation of CRMP-2 and loss of outgrowth.

Due to the pleiotropic effect of signalling effectors such as GSK and the cross regulation between PI3K, AKT and GSK3β it is not surprising that the role of the GSK signalling cascade is dependent on the model used to investigate the relationship. It is likely that both studies are correct and that GSK3β signalling is part of a complex signalling pathway and the outcome on neurite growth depends on other factors as well.

1.12.4 Chondroitinase ABC treatment

Inhibition of neurite outgrowth in human neurites is induced by CSPGs present in the glial scar. The molecular pathway that induces loss of outgrowth is dependent on the binding of glycosaminoglycan (GAG) side chains attached to the proteoglycan backbone, to receptors on the growth cone of regenerating or developing neurites. Molecules or enzymes that prevent binding or activation of this receptor will ultimately prevent down stream signalling of ROCK and as was discussed earlier it is likely neurite outgrowth mediators such as CRMP-2 will not be disrupted.

The bacterial enzyme Chondroitinase ABC is known to cleave chondroitin sulfate GAG from CSPGs and make glial scar explans permissive to neurite outgrowth [141]. Other

evidence came from treating the extracellular matrix produced by reactive astrocytes with Chondoritinase, again making the environment permissive to neurite outgrowth [180]. More recently,Vahidi, B et al (2008) [157] demonstrated using a microfluidic device using strips of the CSPG – Aggrecan, that rat cortical neurons can grow into the inhibitory Aggrecan environment after the Aggrecan strips are treated with chondroitinase ABC for 30 minutes.

It is thought that *in vivo,* Chondroitinase treatment to an injured spinal cord can aid regeneration via a number of mechnaisms, including inhibition of the downstream signalling associated with GAG receptor binding (ROCK etc), freeing up Laminin in the extracellular matrix to allow integrin binding [181], liberating growth factors in the glial scar bound in the CSPG matrix [182] and finally there is some evidence to suggest CSPGs can modulate inflammation in the glial scar [183].

The enzyme is not present in humans, but can be isolated from cultures of Proteus *Vulgaris,* furthermore, lentivirus vectors can be use for targetted expression of the enzyme to developing/regenerating neurites aiding their regeneration in the inhbitory glial scar environment [156].

It is likely that a therapy to aid the regeneration of neurons in the inhibitory glial scar will involve multiple methods described above including Chondroitinase treatment and small molecule modulation of signalling pathways.

1.13 CONCLUSIONS

In conclusion, as our understanding of the glial scar increases, more physiologically relevant models can be developed and used to investigate small molecule modulation and enhancement in the inhibitory environment. Using human stem cell-derived neurons in a model of the glial scar is necessary for enhancing the physiological relevance. This review described the role of retinoids in development and neural differentiation highlighting key signalling pathways and limitations in the use of retinoids. Knowledge of the retinoid pathway and small molecules that can specifically target key receptors involved in retinoid induced neural differentiation will enhance the yield and subtype selectivity of stem cell-derived neurons.

Translating the advancement in stem-cell differentiation protocols and tools into usable, relevant models of the glial scar will require knowledge of the interaction between

components of the scar and the neuron. As 3D models become increasingly important for investigating these interactions combining current advances in biomaterials, stable retinoid analogues and knowledge of the glial scar is necessary for studying human neurite outgrowth in a 3D inhibitory glial scar like environment.

1.13.1 Project Aims

This project aims to build upon current knowledge of small molecule induced stem cell differentiation, investigating the role of structure-function relationships during the induction of stem cell differentiation and neural commitment. Furthermore, this project aims to create a novel model of human neurite outgrowth, by combining small molecule tools with modern bioengineering to produce an efficient model of the glial scar that is physiologically relevant. The model will be used to investigate novel signalling pathways that can enhance neurite outgrowth in the inhibitory environment of the glial scar.

1.13.2 Project Objectives

- Investigate small molecule induced neural differentiation from human pluripotent stem cells.
- Develop a model of human neurite outgrowth in conventional 2D culture and use this model to investigate small molecules that can overcome the glial scar.
- Develop a novel 3D model of the glial scar using human stem cell-derived neurons and use this model to investigate small molecules that can enhance neurite outgrowth in 3D.

CHAPTER 2 MATERIAL AND METHODS

2.1 CELL CULTURE

2.1.1 TERA2.cl.SP12 embryonal carcinoma stem cells

The human embroynal carcinoma stem cell line TERA.cl.SP12 is a subclone isolated from TERA-2 embryonal carcinoma cells by Stefan Przyborski (Durham University) [84]. The TERA-2 cell line was originally isolated from a human lung metastasis of a primary embryonal carcinoma in the testis [184].

Adherent mono-layer culture maintenance and passaging

TERA2.cl.SP12 EC cells were maintained in Dulbecco's modified Eagle's medium (DMEM, high glucose, Lonza BE12 614F) supplemented with 10 % foetal calf serum (Sigma 10270), 2 mM L-glutamine (Lonza BE17 605F) and 100 active units of Penicillin and Streptomycin (Lonza DE17 602F). Cells were incubated at 37 °C in a 5 % CO_2 humidified atmosphere. Cells were propagated in T75 plasma treated tissue culture flasks (NUNC 353136) and passaged every 3-4 days when the cells reached 95 % confluence. Passaging of the cells was by dislodging the cells using x 5 acid washed glass beads (Fisher Scientific G/0300/50) in 3 ml fresh culture media. Cells were then split 1:3 and re-seeded in a T75 cell culture flask in 20 ml fresh media and incubated.

Creating a single cell suspension

A single cell suspension was achieved by the following procedure: Cell culture medium was aspirated and the cells were washed once with 3 ml of sterile PBS to remove excess medium. Cells were then incubated with 3 ml 0.25 % trypsin/2 mM EDTA (Sigma T4049-100 ml) for 2-3 minutes. Detached cells were visualised under a x 10 objective using a light microscope, attached cells were dislodged by short sharp blows to the side of the culture flask. Once all of the cells were detached they were transferred to a 15 ml falcon tube containing 6 ml culture medium to inhibit trypsin. Cells were then pellet by centrifugation at 800 rpm for 3 minutes and the supernatant aspirated. A single cell suspension was then produced by re-suspension of the pellet in 1 ml medium using a 1 ml pipette. Cells could then be counted using a haemocytometer before reseeding at an assay dependent concentration.

Storage of TERA2.cl.SP12

Storage of TERA2.cl.SP12 grown as an adherent monoculture was at -140 °C in FBS supplemented with 10 % DMSO (Sigma D8418). Cells were split 1:3 from a 95 % confluent T75 and re-suspended in freezing medium, cells were then slowly frozen. Thawing of cells was performed rapidly from -140 °C in a 37 °C water bath. Cells were then transferred into a 15 ml falcon tube (Fisher) containing 10 ml of warm TERA2.cl.sp12 maintenance media. Cells were centrifuged at 800 rpm for 3 minutes and the DMSO containing media was removed by careful aspiration into 20 % Trigene. Cells were then re-suspended in 10 ml of fresh media and seeded into a T25 and incubated at 37 °C in a 5 % CO_2 humidified atmosphere for 2-3 days before passaging into a T75 1:1.

Suspension culture maintenance and passaging

For suspension culture 1.5 x 10^6 cells were re-suspended in 20 ml of normal maintenance media and incubated overnight in an untreated 90 mm bacteriological Petri dish (Fisher). Cells were left to aggregate overnight before the addition of any experimental compounds. Replacement of media and passaging of aggregates could be achieved by transferring the suspension into a 50 ml falcon tube and leaving the aggregates to settle for 10 minutes. After 10 minutes the old media was carefully aspirated. Fresh maintenance media was added and the aggregates re-suspended by swirling the media. Aggregates in suspension were then placed in a fresh 90 mm bacteriological Petri dish by gentle pouring and incubated overnight at 37 °C in a 5 % CO_2 humidified atmosphere.

Differentiation of mono-layer TERA2.cl.SP12 EC cells by EC23

Day 1

Confluent cells in a T75 were re-suspended using the previously described procedure, counted using a haemocytometer and seeded onto tissue culture plastic at 12,000 cells/cm^2 in warm (37 °C) Dulbecco's modified Eagle's medium (DMEM, high glucose, Lonza BE12 614F) supplemented with 10 % foetal calf serum (Sigma 10270), 2 mM L-glutamine (Lonza BE17 605F) and 100 active units of Penicillin and Streptomycin (Lonza DE17 602F). Cells were incubated at 37 °C in a 5 % CO_2 humidified atmosphere for 24 hours.

Day 2

Dilute a 10 mM stock of EC23 using DMSO to give a stock of 0.1 mM which can be used in differentiation studies:

MW= 332 g
Known amount= 10 mg
332 g in 1000 ml= 1 M

3.32 g in 1000 ml = 10 mM
0.01/3.32= X/1000
X=3.01 ml of DMSO.

For 0.1 mM to use for stem cell differentiation take 10 µl of 10 mM stock and add this to 990 µl of molecular biology DMSO (mix well using a 1 ml pipette).

To differentiate the mono-layer of TERA2.cl.SP12 use 0.1 µM EC23. Add 50 µl of 0.1 mM stock to 50 ml of maintenance media described on day 1 to get a concentration of 0.1 µl. Carefully aspirate the old media from the cells and replace the new media down the side of the flask ensuring the cells are not washed off by the media.

Maintain the cells at 37 °C in a 5 % CO_2 humidified atmosphere for 21 days changing the media as described above ever 3-4 days.

Differentiation of aggregated TERA2.cl.SP12 EC cells by EC23

Day 1

For suspension differentiation 1.5 x 10^6 cells were re-suspended in 20 ml of Dulbecco's modified Eagle's medium (DMEM, high glucose, Lonza BE12 614F) supplemented with 10 % foetal calf serum (Sigma 10270), 2 mM L-glutamine (Lonza BE17 605F) and 100 active units of Penicillin and Streptomycin (Lonza DE17 602F were incubated at 37 °C in a 5 % CO_2 humidified atmosphere for 24 hours in an untreated 90 mm bacteriological Petri dish (Fisher).

Day 2

After 24 hours to prevent disaggregation EC23 is added directly to the 24 hour old maintenance media added at day 1. Make up a 0.1 mM stock of EC23 as described in the mono-layer differentiation procedure. Using a 200 µl pipette add 20 µl of 0.1 mM EC23 to

the 20 ml of media containing the aggregates. Gently swirl to distribute the compound. Incubate at 37 °C in a 5 % CO_2 humidified atmosphere for a further 21 days changing the media every 4 days by transferring the suspension into a 50 ml falcon tube and leaving the aggregates to settle for 10 minutes. After 10 minutes aspirate the old media being careful to leave the aggregates as sediment. Add 20 ml of fresh maintenance media containing 20 µl of 0.1 mM EC23 to the falcon tube and gently swirl to break up the cell aggregate clump. Pour carefully into a fresh 90 mm Petri dish under sterile conditions.

2.1.2 U-118MG Human Glioblastoma/Astrocytoma cells

U-118MG (ATCC® HTB-15™) cells are an adherent cell line derived from a grade III human brain glioblastoma. Cells have mixed morphology and comprise of astrocytoma and glioblastoma cells. The cells mostly have a characteristic fibroblastic shape and are tumorigenic in nude mice.

Adherent mono-layer maintenance and passaging of U-118MG

U-118MG cell line were maintained in Dulbecco's modified Eagle's medium (DMEM, high glucose, Sigma) supplemented with 10 % foetal calf serum, 2 mM L-glutamine and 100 active units of Penicillin and Streptomycin. Cells were incubated at 37 °C in a 5 % CO_2 humidified atmosphere. Cells were propagated in T75 plasma treated tissue culture flasks (NUNC) and passaged ever 3-4 days when the cells reached 95 % confluence. Passage of the cells was 1:3 – 1:6 and by the following procedure: Aspirate media from the flask and wash cells in 3 ml 0.25 % trypsin/2 mM EDTA briefly, aspirate and replace with 3 ml 0.25 % trypsin/2 mM EDTA for 3 minutes to remove the cells from the plastic. After 3 minutes was any loosely adherent cells with 5 ml of fresh media and place all 8 ml containing the U-118MG in a 15 ml falcon tube. Pellet the cells at 800 rpm for 3 minutes, re-suspend in 3 ml of fresh maintenance media and split the cells into the appropriate T75 flasks containing 15 ml of fresh media making sure the cells are re-suspended.

Storage of U-118MG CELLS

U-118MG cells were stored at -140 °C in complete growth medium 95 %, DMSO 5 %. A single cell suspension of U-118MG was produced as previously described and split 1:3 for storage at -140 °C. Thawing of cells was performed rapidly from -140 °C in a 37 °C water bath. Cells were then transferred into a 15 ml falcon tube (Fisher) containing 10 ml of warm U-118MG growth media. Cells were centrifuged at 800 rpm for 3 minutes and the

DMSO containing media was removed by careful aspiration. Cells were then re-suspended in 10 ml of fresh media and seeded into a T25 and incubated at 37 °C in a 5 % CO_2 humidified atmosphere for 2-3 days before passaging into a T75 1:1.

2.1.3 Small molecules

Throughout this thesis a number of different small molecules have been used to probe cellular processes during differentiation and to manipulate cell signalling pathways.

Stock solutions of each small molecule were aliquot and stored at -80 °C to avoid loss of compound integrity by free/thaw cycling. An example of the calculation used to determine the volume of vehicle required for a 10 mM stock of the small molecule EC23 is shown below. This calculation as then used for all of the other small molecules using in this study by altering the molecular weight, known mass and required concentration.

Stock solutions

Example EC23-

MW= 332 g
Known amount= 10 mg

332 g in 1000 ml= 1 M

3.32 g in 1000 ml = 10 mM
0.01/3.32= X/1000
X=3.01 ml of DMSO.

COMPOUND	STRUCTURE	MOLECULAR WEIGHT (g)	SUPPLIER
EC19	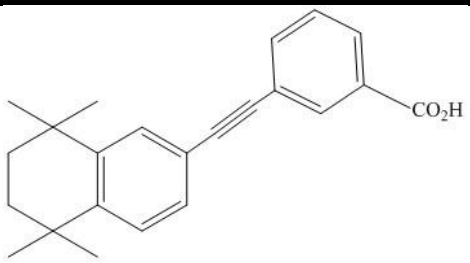	332.44	CHEM DEPT www.dur.ac.uk
EC23	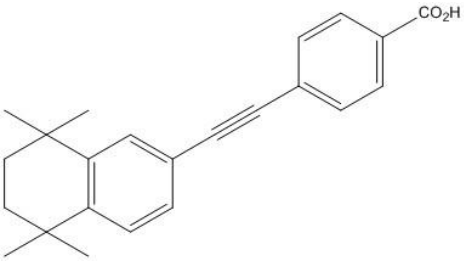	332.44	TOCRIS www.tocris.co.uk 4011
ATRA	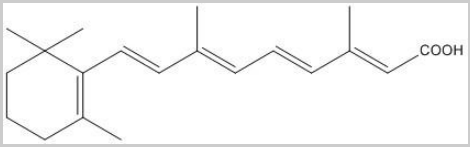	300.44	SIGMA www.sigmaaldrich.com R2625
AH61	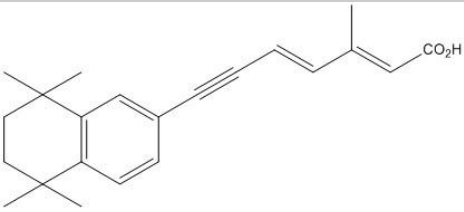	322.19	CHEM DEPT www.dur.ac.uk
Methylated EC19	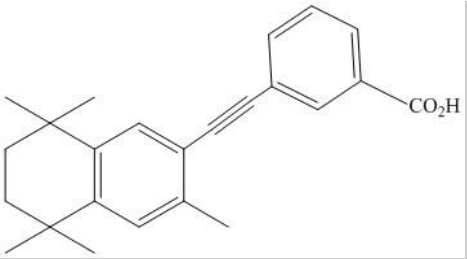	347.44	CHEM DEPT www.dur.ac.uk
Methylated EC23	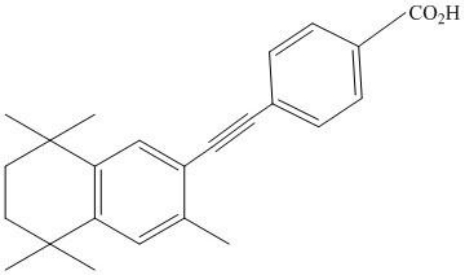	347.44	CHEM DEPT www.dur.ac.uk

AC261066	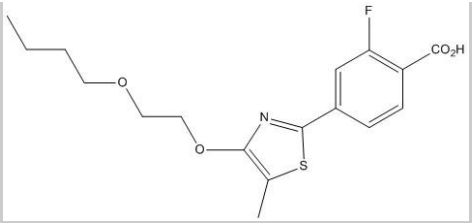	353.41	TOCRIS www.tocris.co.uk 4046
XAV 939	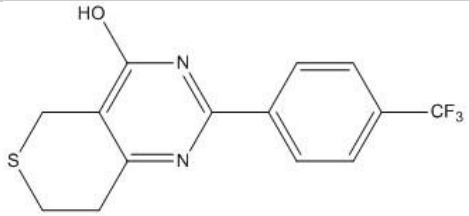	312.31	TOCRIS www.tocris.co.uk 3748
Y-27632 dihydrochloride	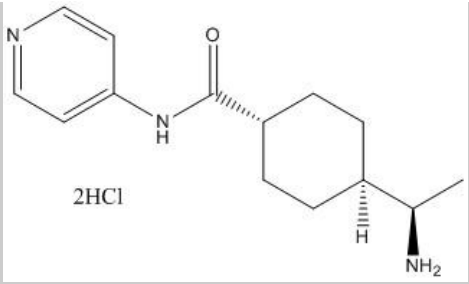	320.26	TOCRIS www.tocris.co.uk 1254
PTP IV inhibitor	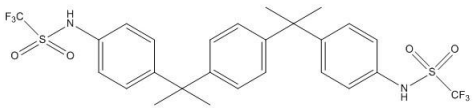	608.6	CALBIOCHEM www.merkmillipore.co.uk 540211
Purmorphamine	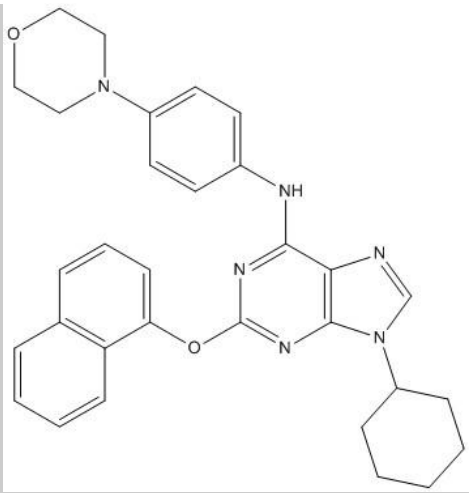	520.6	CALBIOCHEM www.merkmillipore.co.uk 540220

2.2 FLOW CYTOMETRY

Flow cytometry was used to determine the level of cell surface antigens on live cells using fluorescent antibodies. Quantification of fluorescence was used to determine the overall expression of an antigen in a cell population and determine its regulation under different experimental conditions. Use of this technique gave date on the % of positive cells in a population that expressed a particular antigen and the intensity of the positive signal. Quantification using this technique is highly specific and can be used to determine both the up-regulation and down regulation of cellular antigens.

2.2.1 Sample preparation

Cells for flow cytometric analysis were seeded at 300,000 cells in a T25 tissue culture flask. Single cell suspensions of TERA2.cl.sp12 cells for flow cytometry were created as described previously using trypisinsation. Cells were re-suspended in 1 ml blocking buffer (0.1 % Bovine serum albumin in PBS) centrifuged at 800 rpm for 3 minutes and counted using a haemocytometer. A volume of blocking buffer up to 200 µl containing 150,000 cells was added to each well of a flat-bottomed 96 well untreated flow cytometry plate. An example pro-forma is shown in Figure 2.3.1.1. The 96 well plate was then centrifuged at 800rpm for 3 minutes to pellet the cells. Any excess cells not used in the study were lysed in RLT buffer (Lysis buffer, Quiagen – contains Guanidine Isothiocyanate) and stored at -80 °C for real time PCR (see section on RT-PCR).

Cells were re-suspended with 50 µl of the appropriate primary antibody in blocking buffer (0.1 % BSA in PBS) and incubated on ice for 1 hour. The cell pellets were pipette mixed with a 200 µl pipette tip at least 10 times to ensure a single cell suspension. Primary antibodies used and their dilutions are shown in Table **2-1**. Antibodies were diluted from a stock with blocking buffer.

Antibody	Dilution	Supplier
SSEA3	1 in 5	DSHB
TRA-1-60	1 in 10	ABCAM
A2B5	1 in 20	ABCAM
P3X	1 in 10	P.Andrews. University of Sheffield

Table 2-1. Primary antibodies used in flow cytometry.

After incubation 100 µl of blocking buffer was added to each well and the plate centrifuged at 800 rpm for 3 minutes. The supernatant was then removed into the sink and cells washed by re-suspension in 100 µl blocking buffer followed by centrifugation at 800 rpm for 3 minutes, this was repeated a further twice to ensure removal of all excess primary antibody.

The cells were then incubated with an anti-mouse IgM secondary antibody diluted 1:50 (Sigma) in blocking buffer for 1 hour in the dark. After incubation cells were washed 3 times as described above and re-suspended in 200 µl blocking buffer for flow cytometric analysis on the Millipore GuavaCyte Plus Flow cytometer.

(www.millipore.com/flowcytometry)

2.2.2 Flow cytometric analysis

Prior to analysis quality control was performed on the flow cytometer to determine if a calibration was required using Guava Check (Millipore, 4500-0020). The quality control used beads with known size, shape and fluorescence to determine a % coefficient of variance (CV). As with most automated assays the % CV should be less than 5 %.

Debris and clumps of cells were removed from the data set using both forward and side scatter gates. Side scatter gating removed debris and forward scatter clumps of cells, this ensured that the fluorescence detected was from individual cells. An example histogram of the fluorescence detected and data produced by the flow cytometer is shown in Figure 2-1. Using a third gate for intensity the percentage of positive cells can be measured, the gate is shown as a red line on the graph anything within this range is counted as positive, this should be consistant throughout experimental assays. In this example the green line is a negative control, the purple line shows a partial increase in the number of positive cells and the black line is almost completely positive for the antigen being measured.

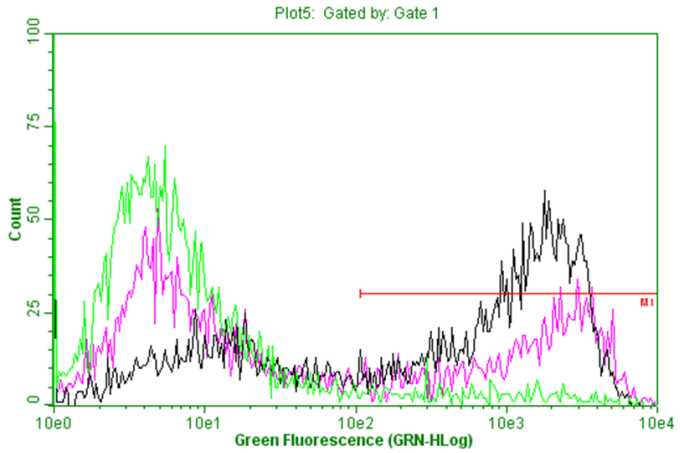

Figure 2-1 A histogram showing cell count number against green fluorescence intensity for three distinct samples using flow cytometry. The red line gates for positive cells and determines the percentage of each population expressing the antigen above this fluorescence threshold.

2.3 REAL-TIME POLYMERASE CHAIN REACTION (RT-PCR)

Relative quantification of cellular mRNA expression can be used to determine the changes that occur under different experimental conditions on the expression of specific genes. Using fluorescence resonance transfer tagged primer probes specific for a gene of interest can be used to give relative fold change in gene expression between two individual cell populations.

2.3.1 RNA extraction (Qiagen kit)

To lyse the cell pellets 350 µl of lysis buffer (RLT) was added and immediately vortex for 30 seconds. Cell membranes were disrupted via aspiration with a 21 G needle 5 times and placed into a new RNase free Eppendorf tube. Cell lysate was then stored at -80°C for a maximum of 2 weeks prior to RNA extraction.

To isolate cell lysate RNA samples were thawed on ice and one volume of 70% molecular biology ethanol was added to each sample. The sample and any precipitate was transferred to a labelled RNeasy spin column and kept on ice. Spin columns were then centrifuged at 10000 pm for 15 seconds and the flow through discarded, samples were kept on ice. The column was then washed with 350 µl RW1 wash buffer, centrifuge at 10,000 rpm for 15 seconds and the flow through discarded. The next step was to remove any genomic DNA within the column.

DNA digestion

From the RNase-free DNase kit (Qiagen 79254) 10 µl of DNase stock was added to 70 µl of RNase-free buffer (RDD) and place directly onto the easy spin column. The column was then left at room temperature for 15 minutes.

After DNA digestion the following wash steps were performed:

Add 350 µl RW1 wash buffer to the column, spun at 10000 rpm for 15 seconds and the flow through discarded. Next 500 µl RPE was buffer (containing molecular biology Ethanol) was added to the column and centrifuged at 10000 rpm for 15 seconds and the flow through discarded finally, complete the wash steps by adding 500 µl RPE and centrifuge at 10000 rpm for 2 min. To remove any excess RPE buffer and importantly

ethanol replace the collection tube and centrifuge at full speed for 2 min. The column now contains purified RNA.

The RNeasy spin column was then placed in a RNA collection tube and 40 µl RNase free water added directly to the column and the water was left to penetrate the easy spin column membrane for 3-5 min. The column was then centrifuged at 10000 rpm for 1 minute to remove dissolving the RNA into solution. The flow through now contains isolated RNA – Do not discard. To increase yield and concentration the flow through was pipette back onto the easy spin column and centrifuged at 10000 rpm for 1 minute. The pellet of RNA can be stored at -80°C prior to analysis.

Purity of RNA

Using the nanodrop measure the absorbance of the RNA at 280, 230 and 260 nm. The ratio 260/280 is an indicator of the level of protein contamination in the sample. The 260/230 ratio is a further measure of purity. The values for both ratios should be between 1.8 and 2.2 for pure RNA. RNA isolated in this study was measured using these parameters.

RNA integrity

Make up 50 x Tris Acetate EDTA using the following protocol:

- To make up 0.5 M EDTA (Sigma EDS) initially add 93.05 g to 400 ml deionized water and pH 8.0. After all of the EDTA powder is dissolved top up the final volume to 500 ml.
- To make a 50 x stock of Tris Acetate EDTA weight out 242 g Tris base (Fisher BP 152-1) and dissolve in 750 ml deionized water.
- Add 57.1 g of glacial acetic acid and 100 ml of 0.5 M EDTA (pH 8.0) and adjust the solution to a final volume of 1 L.

To make up a 1% Agarose gel for electrophoresis dissolve 1 g Agarose (Fisher BP 160-100) into 100 ml and heat for 2 minutes in an 800W microwave or until Agarose in fully dissolved. After the gel begins to cool add 0.5 µg/ml Ethidium Bromide (Sigma E-1510) and gently swirl. Pour the gel into the electrophoresis chamber and allow to set (place the comb in the gel before it sets). Into well 1 add 6 µl of RNA ladder and into the other wells add the test samples (test samples should be diluted with 6 x loading buffer (Promega, C1881) to a total volume of 6 µl and contain around 500 ng RNA).

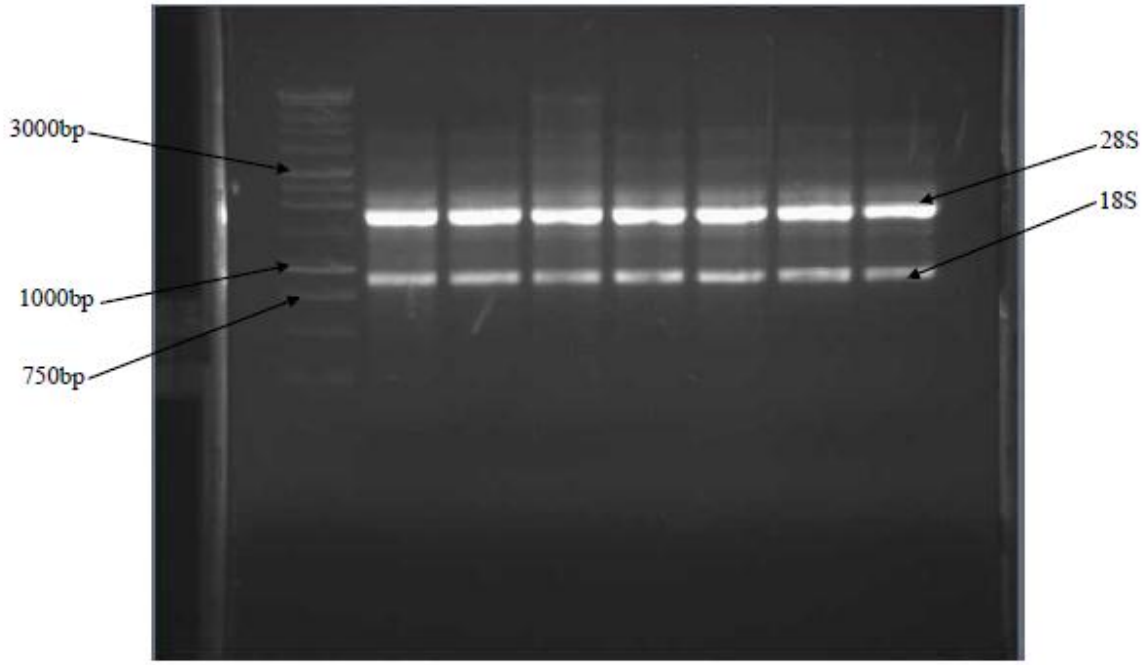

Figure 2-2. Intact ribosomal RNA bands. A 1% TAE agarose EtBr gel separating RNA. 500ng RNA was ran at 100 V. The figure shows intact rRNA, 28S rRNA has around double the staining intensity of 18S, which is another good indicator of intact RNA.

2.3.2 Reverse Transcription

Conversion of isolated mRNA into copy DNA (cDNA) is required for real-time PCR analysis. Each reverse transcription reaction can convert up to 2 µg of mRNA. Quantification of mRNA was done using the Nanodrop and the volume of water containing 2 µg of mRNA was calculated. As the reaction mixture is at 2 x concentration and the reaction reagents make up 10 µl, a total of 2 µg of mRNA in 10 µl molecular biology water was the maximum volume and concentration permissible (lower concentrations of mRNA could be reverse transcribed in the same volume). Make up a stock of reaction mixture for n + 1 where n is the number of reactions.

Figure 2-2 lists the reaction reagents in the reaction mixture and Table 2-3 the heat cycle required for the reaction to proceed using the Biometra Thermocycler. It is assumed that the reaction goes to completion and all 2 µg of mRNA is converted to cDNA.

Component	Volume/reaction µL
10 X RT buffer	2.0
25 X dNTP mix (100mM)	0.8
10 X RT Random primers	2.0
Multiscribe reverse transcriptase	1.0
Nuclease-free H2O	4.2

Table 2-2. Reverse transcription master mix reaction components.

	1	2	3	4
Temperature	25	37	85	4
Time	10 min	120 min	5 sec	∞

Table 2-3 Thermocycle time and temperature settings for reverse transcription

2.3.3 FAST RT-PCR

Real time PCR is a method to determine the relative change of a particular gene of interest under different cellular conditions. The use of fluorescence energy resonance transfer is used to either quench a reported fluorophore or allow detection of its energy. The level of fluorescence changes as the number of gene sequence copies increases giving a stereotypical sigmoidal curve which can be used to determine the starting number of mRNA sequences (Figure 2-3).

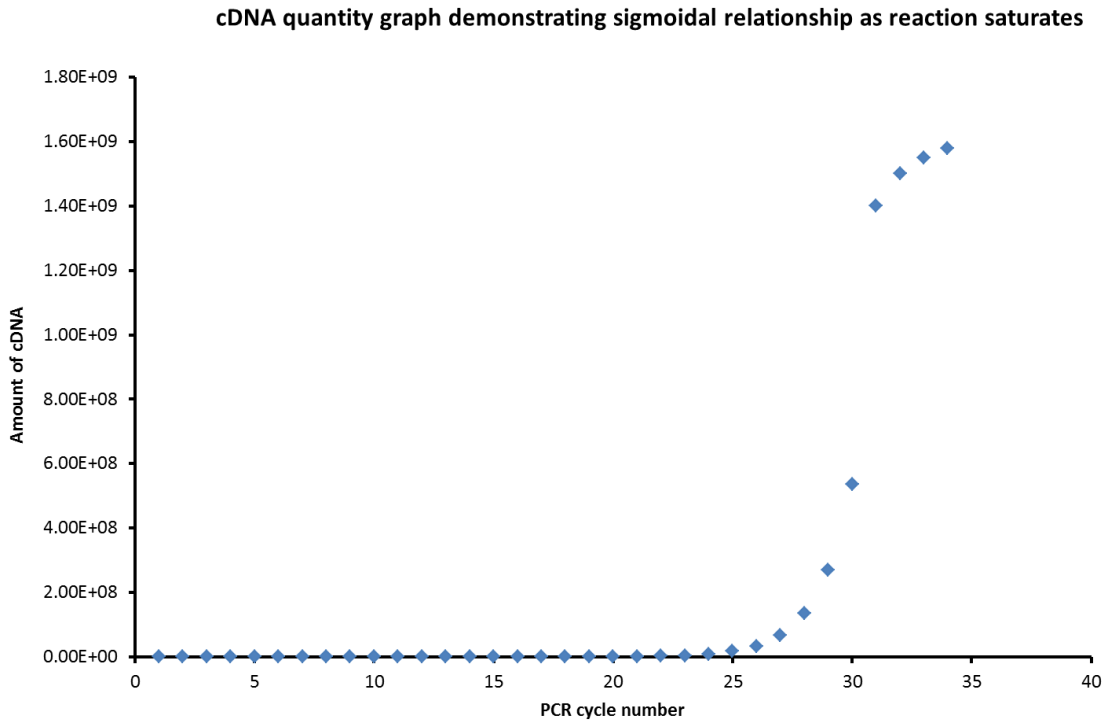

Figure 2-3 Sigmoidal graph representing the relationship between the amount of cDNA produced during a PCR reaction and cycle number. The graph goes through a lag phase, exponential increase, linear relationship and then as the reaction saturates the amount of cDNA tails off. Whereas convention semi-quantitative PCR measures towards the end of the reaction RT-PCR uses the linear phase to extrapolate and determine a relative quantity.

Note: The Applied Biosystems software calculates the relative change in expression and presents this in graphical form.

To set up a real-time PCR reaction using TaqMan master mix and TaqMan primer-probe sets:

The concentration of each stock cDNA sample after reverse transcription was 2000 ng in 20 µl. For RT-PCR each sample was performed in triplicate and each assay contained 50 ng of cDNA (0.5 µl of 2000 ng stock).

All TaqMan gene assays were purchased at 20 x concentration from Applied Biosystems. Upon arrival assays were diluted 1:2 with molecular biology waster aliquot (50 µl) and stored at -20 °C prior to use.

Make up a stock reaction mixture for each gene to be assayed containing the assay (20 x) and the TaqMan mater mix (2 x): For example for 13 assays the stock reaction mixture would contain 13 µl Gene expression assay and 130 µl of 2 x TaqMan Fast Universal Master mix (Invitrogen 4352042). In the bottom of each well 11 µl of reaction mixture was added.

In separate tubes dilute the cDNA samples so that 9 µl of molecular biology water contains 50 ng of DNA. Adding 9 µl of cDNA to the reaction mixture gave a total volume of 20 µl. For example the cDNA stock for 13 samples would contain 7.5 µl cDNA and 110.5 µl Molecular Biology Water, 9 µl of cDNA was then added to the side of each well and kept on ice.

Table 3 shows the components and volume of reagents in each well. An example pro-forma for the 96 well RT-PCR plate can be found at the back of this document.

Each well contained the following constituents:

Reagent	Volume/well (µl)
TaqMan Gene Expression assay (20x)	1
TaqMan Fast Universal Master mix (2x)	10
cDNA	0.5
Water	9
Total	20

A 96 well plate was loaded with each assay and was centrifuged at 2000 rpm for 2 minutes prior to the reaction removing any bubbles in the well. Prior to centrifugation and analysis the plates were kept in a cradle to prevent the bottom of the well being contaminated. A thin film of plastic was used to cover the plate tightly to prevent any evaporation loss during the heating step of the PCR reaction. Fast Real-Time PCR reaction was done using the Applied Biosystems 7500 Fast RT-PCR analyser. The heating steps of the PCR reaction were:

Sample volume: 20 µl per well

Stage 1: Increase temperature of plate to 95 °C

Stage 2: (95 °C for 0:03 seconds then at 65 °C for 0:30 seconds) repeat process for 40 cycles.

Gene	AB code	Interrogated Sequence (gene bank)	Reporter
HOX B1	Hs00157973_m1	X16666.1	FAM
HOX B6	Hs00255831_s1	AK292200.1	FAM
HOX B9	Hs00256886_m1	AK056123.1	FAM
HOX D1	Hs00707081_s1	AF241528.1	FAM
HOX D4	Hs00429605_m1	AK313885.1	FAM
HOX D8	Hs00251905_m1	BQ429720.1	FAM
HOX A1	Hs00939046_m1	AK308067.1	FAM
HOX A5	Hs00430330_m1	BC013682.1	FAM
HOX A6	Hs00430615_m1	BC069497.1	FAM
OCT4	Hs03005111_g1	BC117435.1	FAM
NANOG	Hs02387400_g1	AB093576.1	FAM
RAR β2	Hs00977143_m1	AF157483.1	FAM
GAPDH	4333764F	402869	FAM
NESTIN	Hs00707120_s1	AB073350.1	FAM
PAX6	Hs00240871_m1	AB209177.1	FAM
HB9	Hs00907365_m1	AF107457.1	FAM
ISL1	Hs00158126_m1	AK290742.1	FAM
NKX2.2	Hs00159616_m1	BC075092.2	FAM
NGF	Hs01113193_m1	BC032517.2	FAM
NGFR	Hs00609977_m1	AK303278.1	FAM
PTPΣR	Hs00370080_m1	AB209333.1	FAM
LAR	Hs00892965_m1	AB177857.1	FAM
ITGB1	Hs00559595_m1	AK291697.1	FAM
HOX C4	Hs00205994_m1	X07495.1	FAM
OTX 2	Hs00222238_m1	AB593057.1	FAM

Table 2-4. Fast Real-time PCR primer probe sets. Primer probes are either inventoried from Applied Biosystems or made to order. The AB code provides online information about the assay. Assay details can be found at https://www.invitrogen.com/site/us/en/home/Products-and-Services/Applications/PCR/real-time-pcr/real-time-pcr-assays.html

2.3.4 Sample 96 well pro-forma for real time PCR

Example PCR plate lay out for 3 samples and 4 genes (A-D):

Sample 1: Control

Sample 2: Treatment group 1 (T1)

Sample 3: Treatment group 2 (T2)

No template control (NTC) : No cDNA

	1	**2**	**3**	**4**	**5**	**6**	**7**	**8**	**9**	**10**	**11**	**12**
A	NTC	NTC	NTC	Control	Control	Control	T1	T1	T1	T2	T2	T2
B	NTC	NTC	NTC	Control	Control	Control	T1	T1	T1	T2	T2	T2
C	NTC	NTC	NTC	Control	Control	Control	T1	T1	T1	T2	T2	T2
D	NTC	NTC	NTC	Control	Control	Control	T1	T1	T1	T2	T2	T2
E												
F												
G												
H												

2.4 HISTOLOGY AND IMMUNOSTAINING

Fixation of samples

After treatment cells were washed carefully with PBS and fixed with 4 % paraformaldehyde (PFA) for 30 minutes on ice. Cells were then washed 3 times with PBS to remove excess PFA.

n.b. Fixed cells can be stored in PBS for 2 weeks prior to staining.

Fixation and histological sectioning of wax embedded tissue and 3 dimensional cell culture is a powerful tool for understanding structural changes during 3D development and regulation in a 3D environment. Thin sections of tissue can be used to give a representative sample of 3D culture, with thicker sections used for confocal microscopy and 3D structural imaging.

2.4.1 Preparing wax embedded Alvetex®Scaffold and aggregate sections

Cells grown in Alvetex®Scaffold were fixed in 3.8 % PFA overnight and then washed in PBS three times prior to embedding. The embedding protocol consisted of:

Dehydration through a series of ethanol washes – 30, 50, 70 (containing 1 % crystal violet), 80, 90, 95 and finally 100 % each for 15 minutes. Crystal violet (Sigma C3886) was added to aid sectioning of cells on the scaffold.

After dehydration cells were transferred to histoclear for 15 minutes and then 1:1 wax:histoclear at 60 °C for 30 minutes followed by a final incubation at 60 °C in wax. Embedding into cassettes should be done on half scaffolds and left overnight to solidify. Sections of scaffold can be cut at between 6 and 50 µm for histochemical analysis of the tissue.

2.4.2 Haematoxylin & Eosin(H&E) staining

The following protocol is used for H & E staining of paraffin embedded sections of both Alvetex®Scaffold and fixed cell tissue.

1. Deparaffinise in Histoclear (National diagnostics HS-200) for 5 minutes

2. Transfer into Absolute (100 %) ethanol for 2 minutes
3. Rehydrate in 95 % ethanol, 70 % ethanol and distilled water for 1 minute each
4. Stain in Mayers Haematoxylin (Sigma MH532-1L) for 5 minutes
5. Wash in Distilled water for 30 seconds
6. Blue the nuclei in Alkaline alcohol for 30 seconds
7. Dehydrate in 70 % ethanol and 95 % ethanol for 30 seconds each
8. Stain in Eosin solution (Sigma HT 110232- 1L)
9. Dehydrate in 95 % ethanol twice for 10 seconds each
10. Absolute ethanol for 15 seconds
11. Absolute ethanol for 30 seconds
12. Clear in Histoclear for 3 minutes
13. Clear in Histoclear for 3 minutes
14. Mount in DPX (Fisher D/53 19/05) add glass coverslip and allow to dry

2.4.3 Immunohistological staining

Immunofluorescent staining of paraffin sections may require antigen retrieval, individual antibody requirements were referred to. A general protocol is shown below:

1. Deparaffinise sections in Histoclear for 5 minutes
2. Hydrate through 100, 90 and 70 % ethanol for 2 minutes each
3. Retrieve antigens by placing slides in 200 ml 1 x citrate buffer (pH 6) and microwave (800 W) for 2 x 3 minutes
4. Open the microwave door and leave to stand for 3 minutes
5. Microwave for 3 minutes
6. Leave to stand outside the microwave for 20 minutes
7. Wash in 1 X PBS (3 x 10 minutes)
8. Treat slides with 0.1 % TX-100 for 10 minutes
9. Block slides with 1 % new-born goat serum, 0.1 % Tween-20 in PBS on ice for 1 hour
10. Add primary antibody in blocking buffer at 4 °C in a humidified chamber for 16 hours
11. Wash 3 x 10 minutes in blocking buffer
12. Add secondary antibody + DAPI in blocking buffer and incubate in a dark, humidified chamber for 1 hour

13. Wash in 3 x 10 minutes blocking buffer
14. Mount in Vectashield (Vector labs H-1000) and seal coverslip with nail varnish
15. Store slides in a dark place until visualisation

2.4.4 Immunocytochemistry

Fixed cells were permeabilised with 1 % Triton X-100 in PBS for 10 min and blocked for 30-60 min on ice (Blocking buffer- 1 % goat serum, 0.01 % Tween in PBS). Blocking buffer was then removed and the primary antibody added for 1 hour gently rocking. Antibodies used are shown in Table 2-5 and were diluted in blocking buffer.

Antibody	Dilution	Supplier	Code
Anti β III tubulin Rabbit IgG	1 in 600	Covance	MMS 435P
Anti PAX6	1 in 100	ABCAM	AB 5790
Anti HB9	1 in 50	ABCAM	AB 79541
Anti CSPG	1 in 100	ABCAM	AB 11570
Anti Cytokeratin 8	1 in 500	Ab59400	ABCAM

Table 2-5. Primary antibodies used in immunocytochemistry

Cells were then washed in blocking buffer for 15 minutes gently rocking, this was repeated three times to remove excess primary antibody. The secondary fluorescent antibody was then added, which was specific for the primary antibody used.

Table 2-6 lists the secondary antibodies used in this study and their dilutions. Samples were incubated with secondary antibody for 1 hour which required light protection and gentle rocking.

Antibody	Dilution	Emitted wavelength nm	Selectivity	Code
Alexaflour 488 (Invitrogen)	1 in 600	495	Mouse IgG/Rabbit IgG	R37120/R37116
Anti IgM –FITC (Sigma)	1 in 50	FITC	Mouse IgM	SAB4700348
Cy3 (Jackson Labs)	1 in 600	546	Rabbit IgG	200-162-037
Hoechst 33342 (Invitrogen)	1 in 1000	Blue		H21492

Table 2-6. Secondary antibodies used in immunocytochemistry

2.5 WESTERN BLOT ANALYSIS

2.5.1 Sample collection and protein extraction (Igepal)

Protein was purified from cell pellets for each assay condition using igepal lysis buffer (1 % igepal (Sigma, I8896), 50 mM Tris-HCl [pH 8.0], 150 mM NaCl. 1 mM $MgCl_2$ and a protease inhibitor (Roche Diagnostics). Cell pellets were left on ice in lysis buffer for 30 minutes and then centrifuged at 15000 rpm for 5 minutes. The supernatant containing purified protein was transferred to a fresh tube and stored at -140 °C until required. A Bradford based assay was used to determine protein concentration using spectroscopy (see below):

Standard curve:

Make up 1 mg/ml BSA (Sigma, A2153) stock solution.

Dilute the required concentration of BSA to 1 ml molecular biology water. For example: 0 µg/ml (1 ml water), 1 µg/ml (1 µl BSA stock and 999 µl water), 5 µg/ml (5 µl BSA stock and 995 µl water), 10 µg/ml (10 µl BSA stock and 990 µl water), 20 µg/ml (20 µl BSA stock and 980 µl water) and 50 µg/ml (50 µl BSA stock and 950 µl water) as shown in **Figure 2-4**.

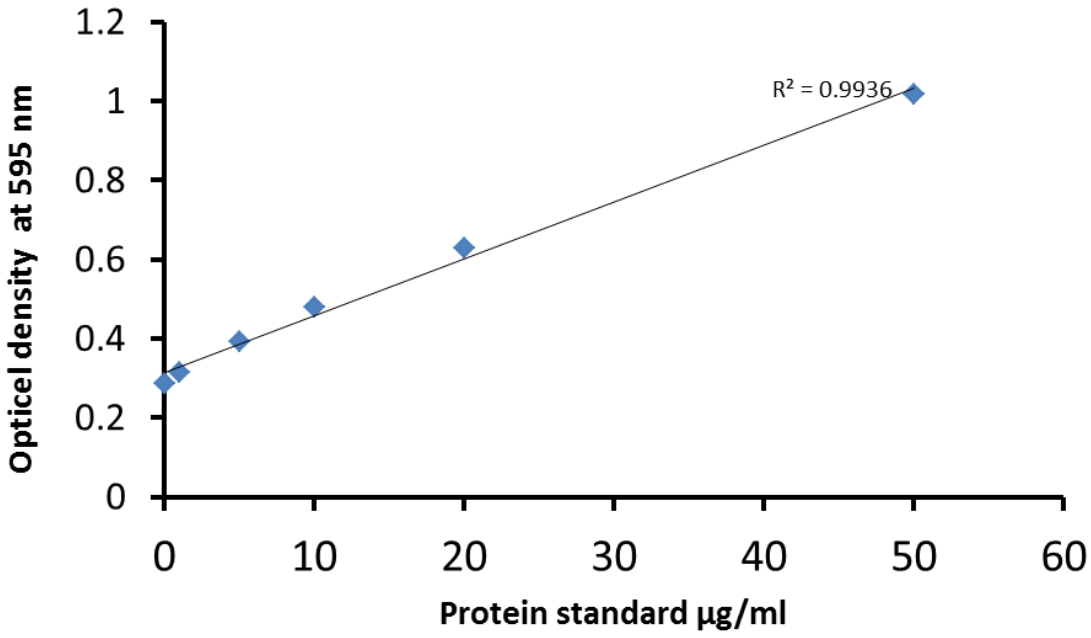

Figure 2-4 Standard curve for protein quantification using a Bradford assay. The R^2 values demonstrates the correlation between the two parameters, the closer to 1.0 the more correlated the parameters are.

Bradford Assay:

Add 2 µl of protein sample to 998 µl molecular biology water and add 250 µl Bradford Reagent (Sigma, B6916). Leave for 10 minutes and then measure absorbance 595 nm. Compare your absorbance value to a standard curve to provide protein quantification for your sample. To get a protein quantification of sample per µl the quantity measured is divided by 2.

2.5.2 SDS-Polyacrylamide Gel Electrophoresis

Samples were loaded on to a 12-well, 1 mm thick NuPage 4-12 % Bis-Tris pre-cast gel (Invitrogen) and ran at 100 V in Invitrogen's XCell SureLock Mini-Cell and system.

Samples comprised on 75 µg/µl protein per sample in a total volume of 20 µl. Sample comprised – 4 µl 4x Gel Loading Dye + 2 µl Reducing Agent + H2O.

2.5.3 Western Blot

Electrophoresed samples were blot on Hybond – LFP membrane (GE Healthcare) at 30 V for 1 hour. Blots were then blocked overnight in 5 % dried milk powder and 0.1 % Tween-20 in Tris-Buffered Saline at 4 °C.

Primary antibody solution consisted of: 1 in 5000 mouse beta-actin Ab (Sigma) and 1/2500 rabbit TUJ-1 Ab in 5 ml blocking buffer. The blots were incubated for 1 hour at room temperature on a roller.

Following incubation with primary antibody a 2 x rinse with 0.1 % Tween-20 in PBS was performed followed by a 2 x 5 minutes wash.

Secondary antibody solution consisted: 2 µl CY3-labelled anti mouse secondary and 2 µl CY5-labelled anti rabbit secondary. Blots were incubated in the dark for 1 hour at room temperature on a roller.

Following incubation samples were rinsed 3 x in 0.1% Tween 20 in PBS followed by 4 x 5 min washes and 3 x rinse with PBS.

Blots were left to dry in the dark at room temperature overnight between two sheets of blotting paper and imaged on the FLA-3000 Fluorescent Image Analyser. The CY3 label was detected via 532 nm laser excitation and the CY5 detected by 633 nm laser excitation.

2.6 SUMMARY OF ANTIBODIES USED

Antibody	Dilution	Code	Supplier
SSEA3	1 in 5	MC-631	DSHB
TRA-1-60	1 in 10	Ab16288	ABCAM
A2B5	1 in 20	Ab53521	ABCAM
P3X	1 in 10		P.Andrews University of Sheffield
Anti β III tubulin Rabbit IgG	1 in 600	MMS 435P	Covance
Anti PAX6	1 in 100	AB 5790	ABCAM
Anti HB9	1 in 50	AB 79541	ABCAM
Anti CSPG	1 in 100	AB 11570	ABCAM
Alexaflour 488	1 in 600	R37120/R37116	Invitrogen
Anti IgM –FITC	1 in 50	SAB4700348	Sigma
Cy3	1 in 600	200-162-037	Jackson Labs
Anti Cytokeratin 8	1 in 500	Ab59400	ABCAM

Table 2.7. Details of the antibodies used throughout this thesis. Antibodies and their suppliers are shown alongside recommended dilutions for applications detailed earlier in the thesis.

2.7 STATISTICAL ANALYSIS

Paired samples were assessed for statistical differences using students paired T-test.

Comparison between the mean of two groups of multiple samples was performed using ANOVA.

Error between samples was assessed by standard error mean values except for real time PCR where error is shown as standard deviation from the mean.

2.8 MICROSCOPY

2.8.1 Light microscope

Leica ICC50 High definition camera mounted onto a Leica microscope with objectives: x5, x10, x20 and x40

2.8.2 Fluorescence Microscopy

Leica DFC 310FX with digital camera DMI 3000B. Objectives x5, x10, x20, x40. Filters: DAPI and 488 nm

Nikon DIAPHOT 300 fluorescence microscope with camera DMX 1200. Objectives x4, x10, x20, x40. Filters DAPI, 488 nm and 650 nm

Leica SP5 Confocal Laser Scanning Microscope SP5

For confocal microscopy on Alvetex®Scaffold: Follow the immunocytochemical staining procedure on whole scaffold, ensuring the secondary antibodies used are compatible with the lasers of the confocal microscope.

After staining place the scaffold on a glass slide and add a drop of VectaShield (Vector labs H-1000) and mount with a glass cover slip ensuring the side to be imaged is against the coverslip. Seal using nail varnish.

Laser Lines (nm) excitatory: 405/458/478/488/494/514/543/594/633

Filters (emission): Fully tuneable

Lenses: 10x HCX PL APO CS, 20x HCX PL APO oil UV, 40x HCX PL APO Oil UV, 63x HCX PL APO Oil UV

Images were taken at a 100 Hz laser rate with a resolution of 1500/1500 and Z-stack slices of 1 µm.

2.9 EQUIPMENT USED

Water- Milli-Q 0.22 µm filtered de-ionised water

Slide dryer – Thermo Scientific

Centrifuge- Eppendorf 5412R, 5810R

Pipette tips--1-10 µl RNase/DNase free tips, 10-100 µl RNase/DNase free tips, 20-200 µl RNase/DNase free tips, 100-1000 µl RNase/DNase free tips, glass pastettes.

Imaging- Digital camera DXM1200, Leica ICC50 High definition camera, Leica DFC 310FX with digital camera DMI 3000B

Balance- AND EK-200g d=0.01g

Thermocycler- Biometra thermocycler

Spectrophotometer- Nanodrop 1000

pH meter- HANNA instruments H12210

Water Bath-Grant (J B Aqua 12 plus)

Orbital Shaker- Stuarts Scientific (SSM1)

Tissue culture plastic- NUNC, BD (T25, T75)

Trans-illuminator- Bio-Rad

PCR machine- Applied Biosystems FAST 7500 PCR

CO_2 Incubator- SANYO MCO – 18A1C (UV)

Florescent imager - FLA-3000 Fluorescent Image Analyser

Flow cytometer - Millipore GuavaCyte Plus Flow cytometer

Microtome – LEICA RM2125

Wax embedded – LEICA EG1120

CHAPTER 3 DEVELOPING TOOLS TO DISSECT MOLECULAR PATHWAYS INVOLVED IN NEURAL DEVELOPMENT

3.1 INTRODUCTION

3.1.1 Retinoic acid and embryonic development

Control over the precise patterning of the central nervous system during embryonic development is essential for correct differentiation of neural subtypes [185, 186]. Many types of neuron develop at precise locations along the anterior-posterior axis. A two-step mechanism of directing neural cells along the AP axis is responsible for guiding cells to develop into the correct neural progenitor at the right position. The two-step mechanisms responsible for this comprise an activating signal that induces cells to become anterior neuroectoderm and a posteriorisation of areas to become the CNS and hindbrain. The posteriorising signal that cells in the CNS and hindbrain are sensitive to has been shown to be retinoic acid. The action of retinoic acid along this axis occurs in a concentration dependent manner, either through control over metabolism and the biological availability of RA or via paracrine secretion [187].

Many genes associated with loss of pluripotency such as *OCT4* and *NANOG* or genes associated with specific neural progenitors such as *PAX6* contain a RARE in their promoter regions and are under the direct transcriptional control of retinoic acid receptors. Retinoids can regulate the cell cycle arrest and differentiation in stem cells; furthermore, due to the regulation of key neural genes, retinoic acid treatment induces neural commitment. Control over the gene processes that regulate embryonic patterning will in part be responsible for the subtype selectivity provided to developing neural cells by RA. Part of the role of RA signalling during development is to provide anterior-posterior positional identity during neurulation, providing cells with position specific gene expression through *HOX* gene regulation.

Work into embryonic patterning has been advanced by investigating the developmental patterning of the hindbrain [188]; the hindbrain shows very discrete segments along its AP axis regulated by genetic ques. *HOX* genes have been implicated in the regulation of hindbrain segments since their expression is often located at the boundaries between segments. Ectopic expression of *HOX* genes associated with posterior identity to anterior

cells resulted in posteriorisation of anterior hindbrain segments (see Chapter 1 for a review of *HOX* genes). Posteriorisation of anterior hindbrain and developing embryonic tissue can be achieved through the application of retinoic acid indicating a link between retinoic acid, *HOX* genes and AP axis development. It has been demonstrated recently that many of the 3' *HOX* genes associated with an anterior fate contain RAREs.

In a study by Simeone, A et al (2009) [50] retinoic acid (RA) was demonstrated to induce the expression of *HOX* gene mRNA in the human embryonal carcinoma stem cell NT2/D1. Regulation of *HOX* genes by retinoic acid in this model was shown to be time and concentration dependent. Expression of genes on the *HOX B* cluster was dependent on the length of time the cells had been exposed to RA for. *HOX* genes at the 3' end of the cluster would were the most sensitive and expression occurred soon after RA treatment (0-20 hours), as exposure time increased more 5' genes became expressed. Indicating a co-linear expression pattern of *HOX B* genes Furthermore, expression of the genes investigated were shown to be regulated in a concentration dependent manner by RA. Other work went on to demonstrate the co-linear, temporal expression of *HOX* genes on the other three clusters [189]. These studies demonstrated the effectiveness of using hEC cells and described some fundamental gene regulation by retinoic acid during stem cell differentiation and neural lineage commitment.

As well as control over the anterior-posterior identity of the developing neuroectoderm retinoic acid is highly implicated in specific neural subtype commitment and development within the spinal cord, specifically along the dorsal-ventral axis. One way retinoic acid affects the developing spinal cord through paracrine secretion from flanking somites. Transduction of the retinoic acid signal is controlled by a number of different mechanisms, including cellular retinoic acid binding proteins, metabolising enzymes and retinoic acid receptor number and isotype.

Furthermore, retinoic acid has been implicated as necessary for mature neural differentiation, axon guidance and neural regeneration. Therefore, when investigating the role of retinoic acid in each of these processes it is important to have a model that represents the stage of differentiation at which the process is occurring.

3.1.2 Retinoic acid and stem cell differentiation

Stem cells have been used for many years to investigate the role of retinoic acid in cell differentiation, and in particular neural differentiation. Human stem cells represent a model of early development in man that can be induced to undergo lineage commitment and maturation for investigations into later developmental processes. Studying the biological mechanisms that underlie initiation of stem cell differentiation; specific lineage commitment of stem cells; cellular maturation and finally regeneration after injury, will all prove to be useful for many aspects of medicine and cellular biology.

The use of retinoic acid in stem cell differentiation and development has come from many years of work using a variety of *in vitro* and *in vivo* models. There is a close link between the role of retinoic acid in the developing embryo and that demonstrated *in vitro* using stem cell models. Retinoic acid is used in animal and cell models to induce posterior identity to the developing tissue [190]. It is well documented that retinoic acid acts in a temporal and concentration dependent manner in both *in vivo* and *in vitro* systems. Elucidating the developmental mechanisms behind the role of retinoic acid using animal models is difficult due to its pleiotropic action. Through the use of stem cells, specific developmental processes can be investigated in depth using molecular approaches, providing a good model for investigating the role of retinoic acid in development.

Pluripotent embryonal carcinoma stem cells can be derived by multiple methods from teratocarinomas [84, 191]. Clones that are derived from the different teratocarcinomas exhibit different lineage potential and some require feeder layers for survival [192], never the less stem cells derived from teratocarcinomas are recognised as good models for investigating stem cell differentiation and embryonic development [193].

The stem cells used in this study are the human embryonal carcinoma stem cell line, TERA2.cl.SP12, isolated from the TERA2 parent lineage, using direct immunomagnetic sorting for high expression of the stem cell marker SSEA3. The stem cells express high levels of *OCT4* and *NANOG;* do not require a feeder layer; are immortal and importantly can be induced to differentiate into neural and glial tissue upon retinoid treatment. Accordingly, this model cell system is useful for investigating neural tissue development *in vitro* [84, 86, 194] and has been used extensively throughout this thesis.

3.1.3 Limitations of all-trans retinoic acid in cell culture

Most stem cell protocols that require retinoic acid use *all trans* retinoic acid (ATRA) which acts through heterodimersiation of RAR-RXR receptors to induce gene transcription [56]. As described earlier it is known that the concentration of ATRA in culture is a key determinant of the genes that are transcribed. One limitation of the use of ATRA is that it is isomerised at ambient temperature and in natural light; isomers of ATRA such as 9-*cis*-RA can induce gene transcription by homodimerisation of RXR which affects the overall concentration of ATRA in culture and induces heterogeneity and inconsistency into the stem cell differentiation protocol [195]. Therefore, when handling ATRA in the laboratory, great care must be taken to prevent isomerisation. However, this is difficult in practice due to the nature of cell culture.

The response of stem cells to retinoic acid induced signalling is dependent on concentration both *in vitro* and *in vivo* [64, 196]. The cellular concentration of retinoic acid in developing neurons determines neural lineage subtype. Furthermore, retinoic acid signalling also regulates anterior-posterior patterning in a concentration dependent manner [48, 197], providing positional cues to developing cells. Variable concentrations of RA due to isomerisation and metabolism make investigating these effects difficult *in vitro*. Due to the instability of RA in the laboratory its exact concentration is unknown throughout the investigation, adding variability to the assay. It is also unknown what effect the isomerisation products of RA have on stem cell development. It is required to use RA in a dark environment; however, this adds risk to any laboratory procedure and is often overlooked. The replacement of RA with a stable analogue would overcome many of the problems associated with RA metabolism.

The small molecule, EC23, has been developed to overcome the variability introduced by ATRA by isomerisation and add consistency and reproducibility to the concentration and induction of retinoic acid responsive genes in culture. EC23 is a stable synthetic analogue of ATRA and is not isomerised under normal cell culture conditions. Work has described the ability of EC23 to replace ATRA in stem cell differentiation protocols [95]. Furthermore, recent evidence demonstrates that EC23 is a pan RAR agonist that is much more potent than ATRA and other synthetic analogues of ATRA such as TTNPB [93]. EC23 exemplifies the ability to design small molecules to use as tools to investigate key molecular pathways.

3.1.4 Synthetic modulation of signalling pathways

Multiple studies describe work involving the modulation of signalling pathways using synthetic small molecules to replace the less consistent natural analogues that are either unstable, non-specific or subject to batch variability [198]. EC23 has been described here as one example of the use of synthetic molecules, however many differentiation protocols utilise a wide range of different small molecules to induce specific neural commitment. Sonic hedgehog (Shh) is used in stem cell differentiation protocols to provide ventralisation cues to the cells for motor neuron specific differentiation. As with many natural small molecules, Shh is a protein and is subject to large batch variations during production, therefore, there are inconsistencies of its activity in culture. The small molecule Purmorphamine is a synthetic modulator of the Shh pathway and has been used in many differentiation protocols as a replacement of Shh as it induces more consistent Shh activation and has a very narrow range of activity giving a high level of reproducibility [199, 200]. Although EC23 has been used in protocols to induce neural differentiation in replacement of ATRA, and Purmorphamine has been used in motor neuron differentiation protocols to replace Shh, both have not been used in conjunction to induce specific neural commitment. The use of multiple synthetic small molecules may increase the yield and reproducibility of stem cell differentiation, however, more research is required to understand these compounds and how they affect the cell compared to their natural counterparts.

Aims

This Chapter aims to use synthetic small molecules to investigate the molecular pathways involved in retinoic acid induced stem cell differentiation and neural commitment. It has been demonstrated by previous studies that the synthetic retinoid EC23 can induce neural differentiation of stem cells in a similar way to ATRA [95]; furthermore, some model systems report that EC23 can induce more neurogenic lineage commitment than ATRA [95]. EC23 was designed to overcome the practical limitations of ATRA when used in cell culture and has provided a model for retinoic acid receptor activation without loss through isomerisation; furthermore, it is hypothesised that EC23 will not be metabolised by many of the cytochrome enzymes that oxidise ATRA due to its stable structure. Therefore, EC23 removes many of the heterogeneous side effects resulting from ATRA instability providing a stable and reproducible tool to investigate retinoid activity and consistently induce neurogenesis.

Retinoid concentration, which is a key modulator of human cellular development, was modelled *in vitro* and the key metabolic, genetic and phenotypical differences of EC23 and ATRA activity in stem cells investigated. In addition, the role of subtle structural changes of EC23 and its analogue EC19 on stem cell differentiation were assessed through a small screen of small molecules aimed at controlling cell fate during differentiation. Throughout this Chapter, retinoid structure, potency and concentration will be discussed and related to early neural commitment and late neural phenotype development using the human stem cell TERA2.cl.SP12 model of neurogenesis.

Specific Objectives

- Use TERA2.cl.SP12 EC cells to determine the role of small molecule concentration on neural commitment between ATRA and EC23.
- Use Liarozole to determine the influence of metabolism on the ability of ATRA and EC23 to induce stem cell differentiation. Data can then be used to relate *HOX* expression to potency and determine a minimum concentration for neural commitment.
- Concentration dependent and temporal differences between 9 *HOX* genes located at both 3' and 5' on three clusters was used to investigate the differences between ATRA and EC23 during early neural commitment.
- Determine the role of subtle structural differences of EC23 and EC19 on neural commitment. Specifically methylation of each small molecule.
- Develop a reproducible method of neural differentiation from stem cells using synthetic small molecules.
- Determine the differentiation of specific neural subtype differences between EC23 and ATRA in human TERA2.cl.SP12 cells using gene expression profiles and synthetic ventralisation by Purmorphamine.

3.2 RESULTS

3.2.1 Investigating the induction of differentiation of human pluripotent stem cells by the synthetic retinoid EC23

To investigate the concentration dependent effects of retinoid induced differentiation on human pluripotent stem cells, the cell line TERA2.cl.SP12 was treated with serial concentrations of EC23 or ATRA from 10 µM – 0.001 µM for a period of 3 or 6 days prior to analysis. Due to the enhanced photo-stability of EC23 it was hypothesised that the concentration dependent regulation of retinoic acid receptors would be less heterogeneous and represents true signalling through these receptors, without side effects from isomers that could arise from compound isomerisation during handling of ATRA in cell culture. Furthermore, understanding the potency differences between EC23 and ATRA will aid the design of future compounds and is useful when planning investigations that require a specific response from a narrow retinoid concentration.

To determine loss of pluripotency by TERA2.cl.SP12 human stem cells a number of cell surface phenotype and genetic markers were quantitatively measured after treatment with EC23 or ATRA. Figure 3-1 demonstrates by light microscopy the characteristic shape of cells treated with EC23 or ATRA. Note that following retinoid treatment, cells stop proliferating, look less dense and tend not to overgrow in the culture in contrast to undifferentiated cultures and DMSO treated control-cells.

To assess this change quantitatively the percentage of cells that expressed the glycolipid stem cell markers SSEA3 and TRA-1-60 was determined on the membrane of the cells by flow cytometery in each condition (Figure 3-2). After 3 days treatment only small changes in the expression of SSEA3 or TRA-1-60 were demonstrated by treatment with either EC23 or ATRA, with the exception of SSEA3 levels after 10 µM ATRA treatment which showed a large decrease in expression. Loss of SSEA3 expression after 3 days under these conditions indicates very early changes occur on the surface of the cells after treatment with ATRA, however, no loss of surface antigens were induced by EC23 after just 3 days treatment. After 6 days ATRA induced an almost complete loss of SSEA3 expression at 10 µM and 1 µM and a substantial loss of TRA-1-60 expression at these concentrations. Only small changes in expression were measured below these concentrations. In contrast EC23 induced an almost complete loss of SSEA3 expression after 6 days treatment at

concentrations of 10-0.01 µM and this was mirrored by a substantial decrease in TRA-1-60 expression at these concentrations indicating a higher potency of EC23.

To further investigate early changes of pluripotency induced by EC23 or ATRA the relative mRNA expression of the genes *OCT4* and *NANOG* were measured in the same cells that were analysed by flow cytometry (Figure 3-3) after 6 days. The levels of both *OCT4* and *NANOG* correlated well with flow cytometry data indicating a loss of gene expression induced by 10-1 µM ATRA and 10-0.01 µM EC23. The relative expression of *OCT4* and *NANOG* was more sensitive at measuring the effect of retinoid treatment than cell surface glycoprotein expression. At 0.001 µM EC23/ATRA loss of both *NANOG* and *OCT4* was measurable. However, at this concentration little or no expressional change of the cell surface glycoproteins SSEA3/ TRA-1-60 was detected.

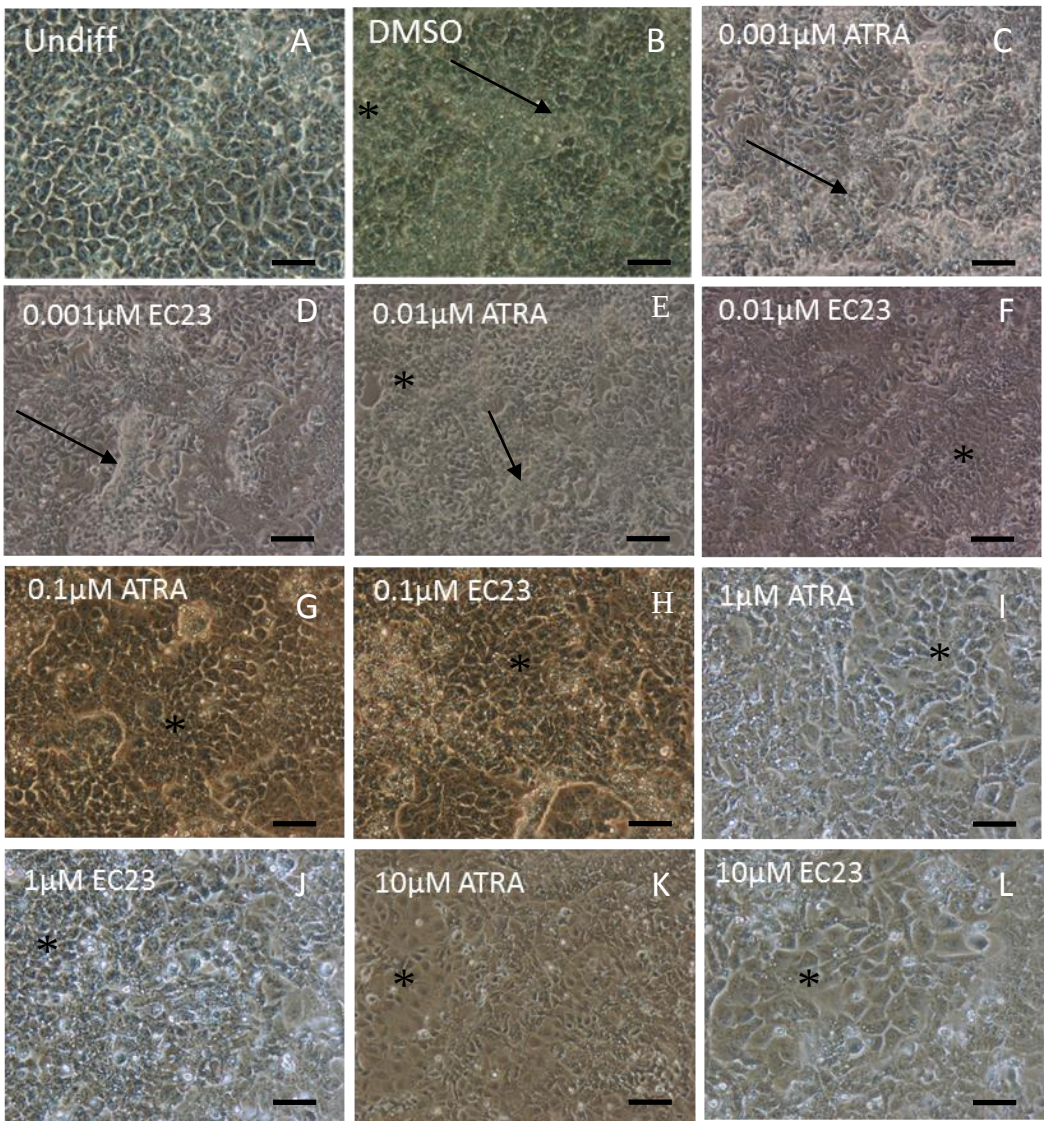

Figure 3-1 Phase microscopy of TERA2.cl.SP12 cells differentiated with EC23 or ATRA for 21 days. Cells were cultured with either ATRA or EC23 at 0.001 µM-10 µM for 21 days prior to imaging. Notice the overgrowth that occurs in cultures that do not contain retinoid Undifferentiated (A) and DMSO (B). DMSO was added at 0.1% v/v. Cultures were treated with ATRA at 0.001 µM (C), 0.01 µM (E), 0.1 µM (G), 1 µM (I), 10 µM (K) or EC23 at 0.001 µM (D), 0.01 µM (F), 0.1 µM (H), 1 µM (J), 10 µM (L). Arrows show high density cell areas asterisk marks low density cells. Note the heterogeneity within the cultures which is more prominent at low retinoid concentrations. Scale bars: 100 µm. n=3.

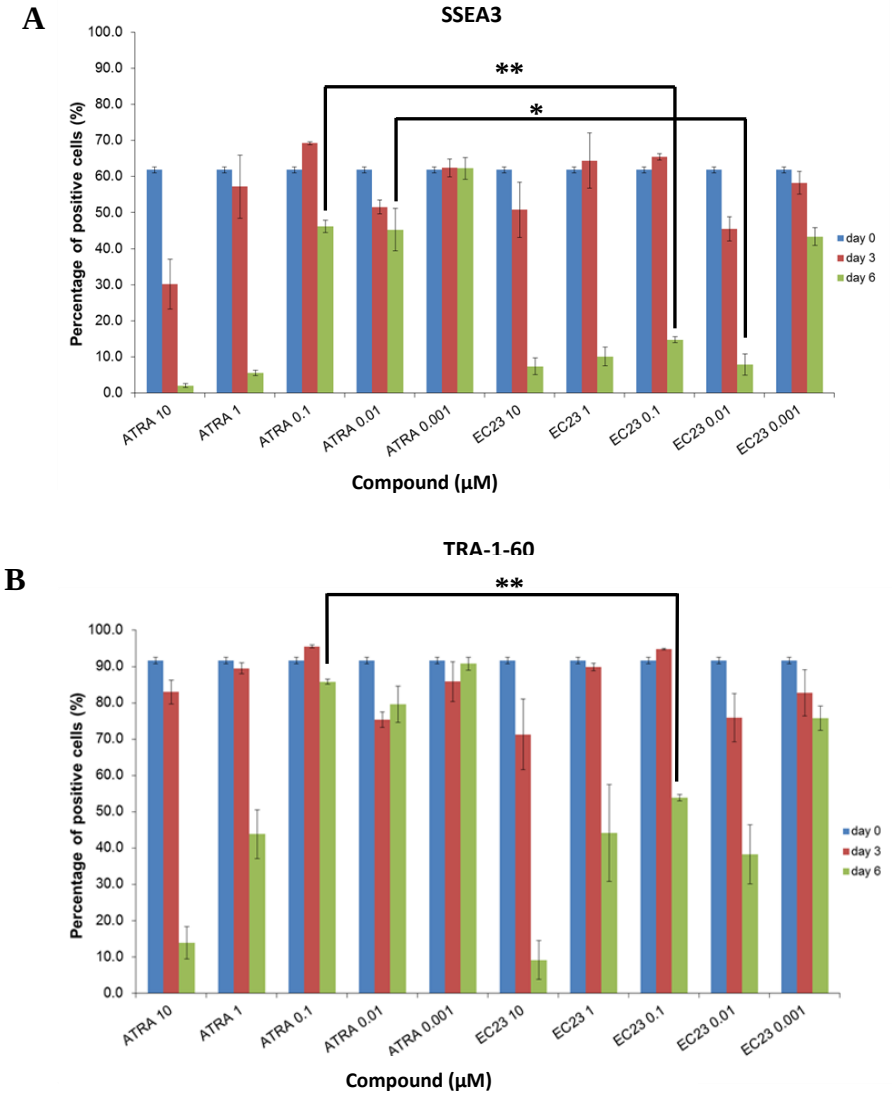

Figure 3-2 Regulation of stem cell markers during treatment with retinoids. Cell membrane expression of SSEA3 and TRA-1-60 in TERA2.cl.SP12 stem cells treated with either EC23 or ATRA. Cells were treated with 0.001, 0.01, 0.1,1 or 10 µM EC23 or ATRA, for 0, 3 or 6 days. Live cell flow cytometry was used to measure the percentage of the cell population that expressed either SSEA3 (A) or TRA-1-60 (B) under each condition. Loss of expression was induced by both ATRA and EC23. Expression changes were detected after just 3 days with ATRA, however, this was not demonstrated by EC23. Since, EC23 showed significant activity at 0.1 µM – 0.01 µM compared to ATRA after 6 days, it appeared that EC23 was active at 100 times lower concentration than ATRA. Data represent mean ± SEM, n=3. * $p \leq 0.005$** $p \leq 0.0005$. Student's t-test corrected for multiple testing between compared sample poulations using the Bonifferoni correction.

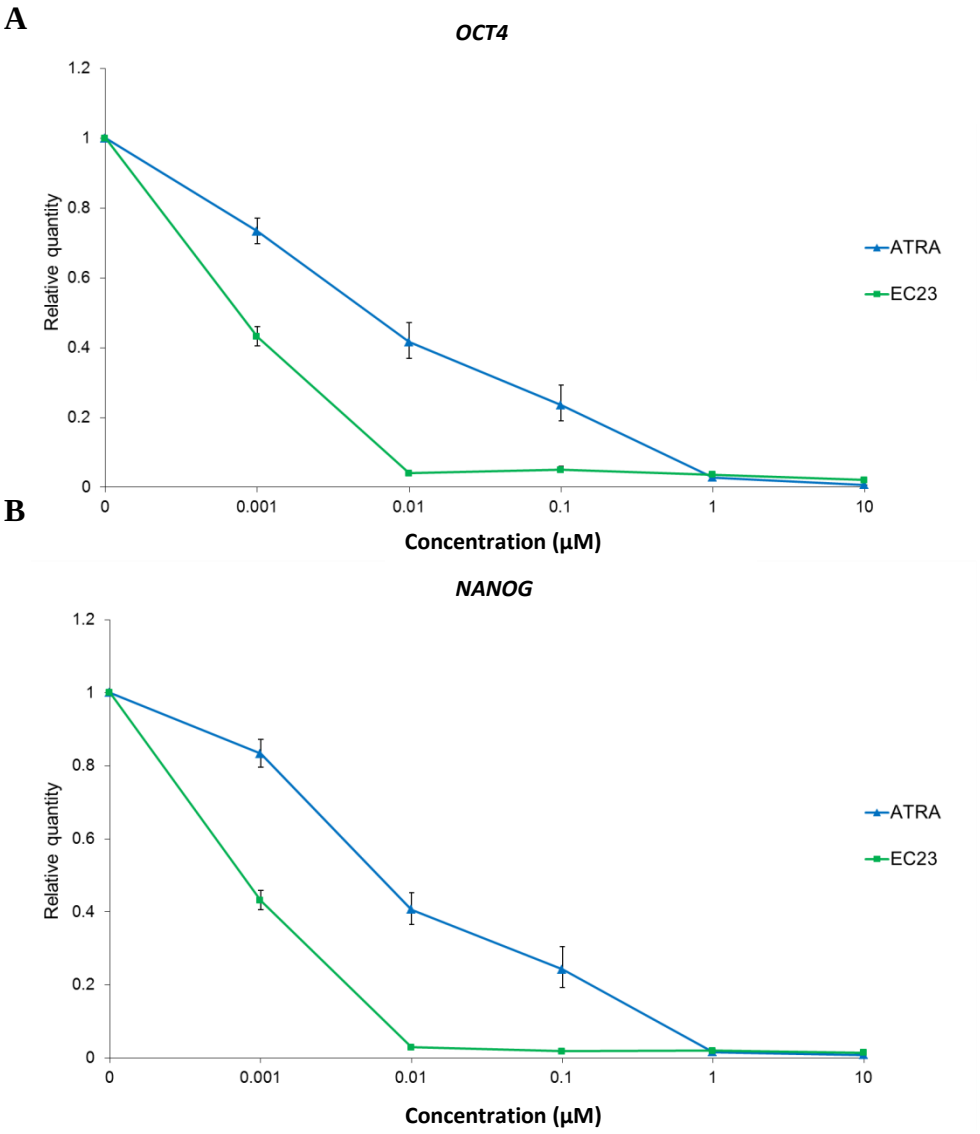

Figure 3-3 Differential regulation of pluripotent stem cell markers in response to retinoids. Real time PCR expression of the pluripotency genes *OCT4* (A) and *NANOG* (B). TERA2.cl.SP12 cells were exposed to 0.001 µM, 0.01 µM, 0.1 µM, 1 µM and 10 µM EC23 or ATRA for 6 days in monoculture. Increasing concentrations of ATRA resulted in a gradual loss of expression of both genes with maximal loss associated with 1 µM and 10 µM. EC23 showed a similar gene expression profile, however, almost complete loss of expression was demonstrated at 0.01 µM, a 100 times lower concentration to ATRA. Gene profile quantification is relative to the level of gene expression in undifferentiated TERA2.cl.SP12 cultured for 6 days. Data represent mean ± SEM, n=3.

3.2.2 Investigating the induction of neural commitment of human pluripotent stem cells by the synthetic retinoid EC23

To determine the role of concentration and potency of EC23 at inducing neural commitment, the neural specific cell surface glycoprotein A2B5 was measured using flow cytometry under the same experimental conditions as previously described. Cells were treated with 10-0.001 μM EC23 or ATRA for 3 and 6 days prior to flow cytometric analysis. An increase in A2B5 expression is indicative of early neural commitment and a percentage population of cells expressing the surface glycoprotein is a good indicator of the differentiation inducing potential of the small molecules being investigated. Figure 3-4 shows that as with loss of pluripotency ATRA induces neural commitment at 10 μM and 1 μM after 6 days, any concentrations below this did not induce a significant amount of neural commitment indicated by A2B5 expression. EC23 induced an increase in A2B5 expression at concentrations from 10 μM - 0.01μM after 6 days. Note that after 3 days only changes in the highest ATRA concentration was measured indicating that EC23 acts slower than ATRA even though it as a higher overall potency.

To determine the genomic level neural commitment induced by EC23 under these conditions and assess more sensitively the early changes that are occurring during induction of differentiation, the mRNA level of *PAX6,* a transcription factor associated with neural commitment, was measured using real time PCR. *PAX6* contains a RARE in its promoter this is an ideal candidate to investigate any differences between the retinoids. Data on gene transcription events that occur during differentiation was used to determine similarities and differences between ATRA and EC23 at the genetic level (Figure 3-5). Figure 3-5 shows data from day 3 and day 6 of retinoid treatment of the relative change in quantity of *PAX6* mRNA compared to the undifferentiated control.

As with the induction of A2B5 expression, EC23 does not induce a measurable *PAX6* response in the cells after 3 days treatment. In contrast, as was demonstrated by A2B5, treatment with a high concentration of ATRA induced neural commitment and this is seen at the genomic level by high levels of *PAX6* expression after 3 days of 10 μM ATRA treatment.

After 6 days continuous treatment a peak of *PAX6* expression was demonstrated at 0.1 μM EC23 which tails off either side of this concentration, indicating an optimal dosage for inducing *PAX6* in this model by EC23 and potential optimal concentration for specific neural subtypes. ATRA induced a peak of *PAX6* expression at 10 μM which reduced with concentration in a dose dependent manner.

Immunocytochemical staining of Pax6 protein demonstrates high levels at 0.1 μM EC23 or 10 μM ATRA only (Figure 3-6). Note that Pax6 seems to be located in areas of high cell density indicating heterogeneity within the cultures which may result in sub-optimal neural differentiation and variation in the cell population across the culture dish.

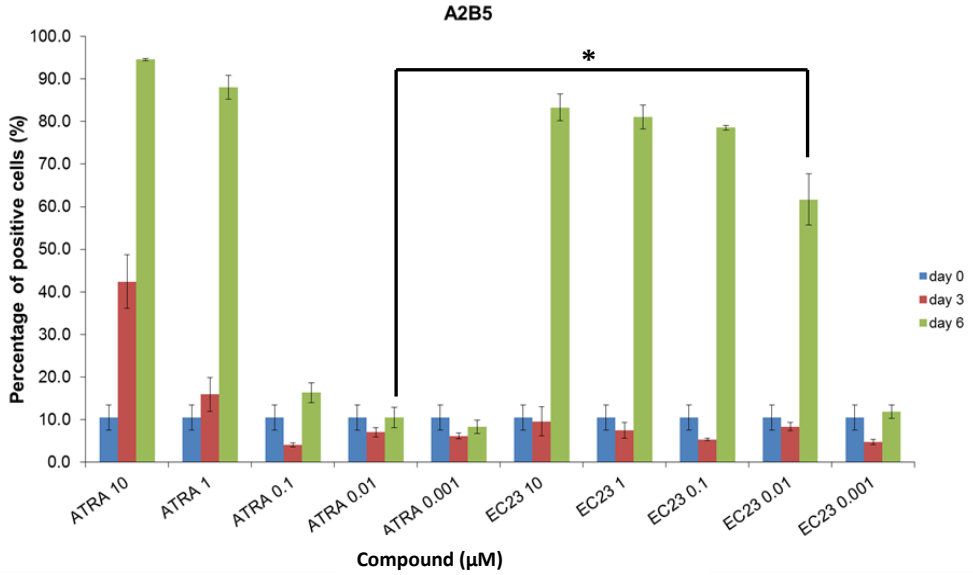

Figure 3-4 Regulation of neuronal marker A2B5 during treatment with retinoid. Cells were treated with 0.001, 0.01, 0.1,1 or 10 µM EC23 or ATRA, for 0, 3 or 6 days. Live cell flow cytomery was used to measure the percentage of the cell population that expressed A2B5 under each condition. Loss of expression was induced by both ATRA and EC23, however, EC23 was active at 100 times lower concentration than ATRA. Expression changes were detected after just 3 days with ATRA, however, this was not demonstrated by EC23. High levels of A2B5 are indicative of commitment to the neural lineage by differentiating stem cells. Data represent mean ± SEM, n=3. *$p \leq 0.005$ Student's t-test corrected for multiple testing between compared sample poulations using the Bonifferoni correction.

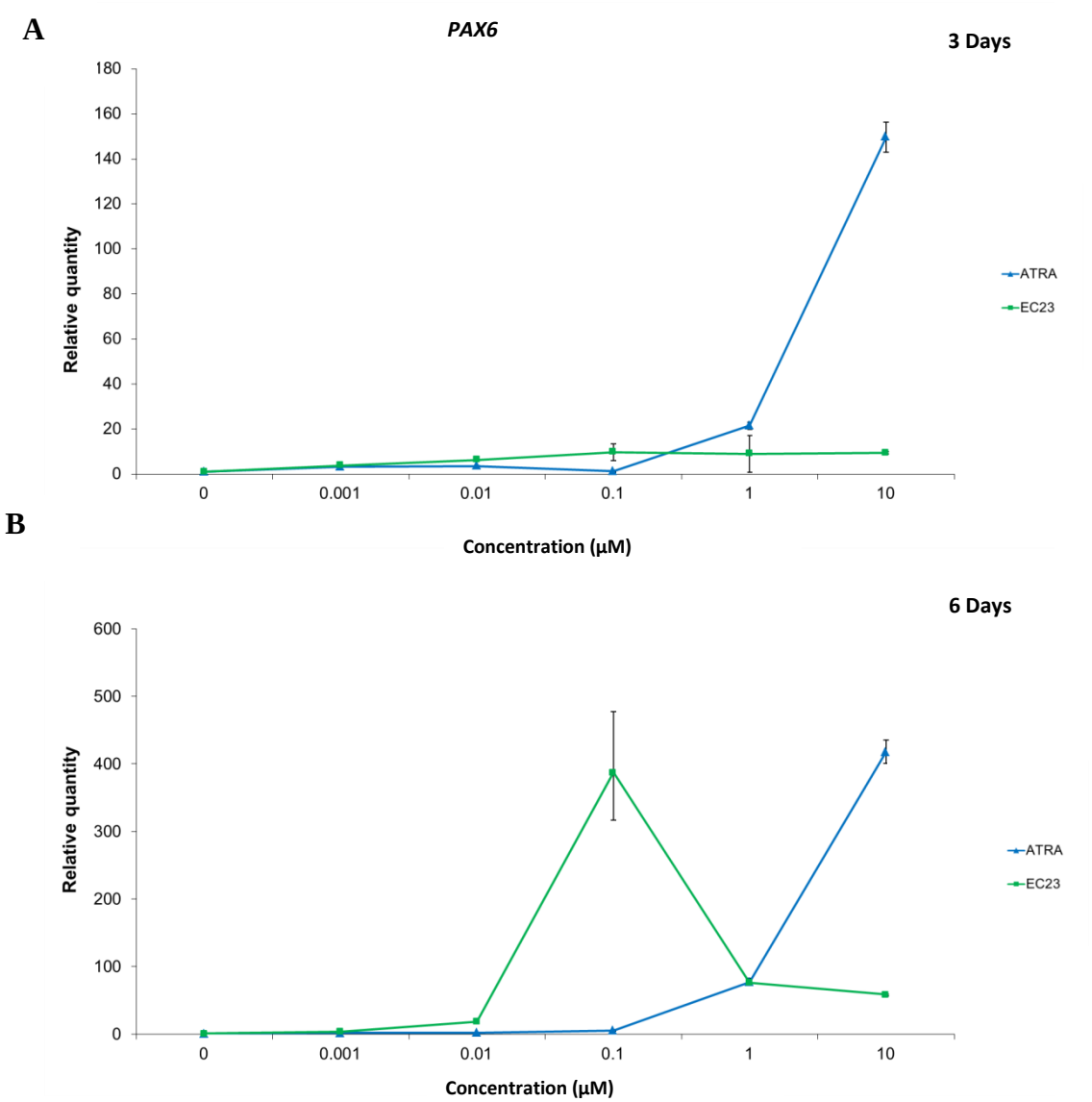

Figure 3-5 Differential regulation of *PAX6* expression demonstrating concentration dependent neural commitment by exposure of human pluripotent stem cells to retinoids. TERA2.cl.SP12 cells in monoculture were exposed to 0.001 µM, 0.01 µM, 0.1 µM, 1 µM or 10 µM for 3 days (A) or 6 days (B) respectively and *PAX6* gene expression was measured by real time PCR. Expression at day 3 for both compounds was low, except for 10 µM ATRA which indicated an early response at this concentration. Each concentration of EC23 induced a small increases in expression after 3 days, indicating a lag in the induction of neural differentiation compared to ATRA at high concentrations. This correlated with flow data for A2B5 (Figure 3.4) and SSEA3 (Figure 3.2) at day 3 where similarly high concentrations of ATRA induced changes in expression not seen by EC23. After 6 days treatment ATRA induced a concentration dependent response in gene expression as concentration increased so did *PAX6* expression; in contrast maximal expression in cells treated with EC23 was at 0.1 µM which reduced as concentration either side of this concentration, indicating a potential regulatory feedback effect on *PAX6* expression not seen by ATRA due to the toxic when a higher than 10 µM concentration is used. Data represent mean ± SEM, n=3.

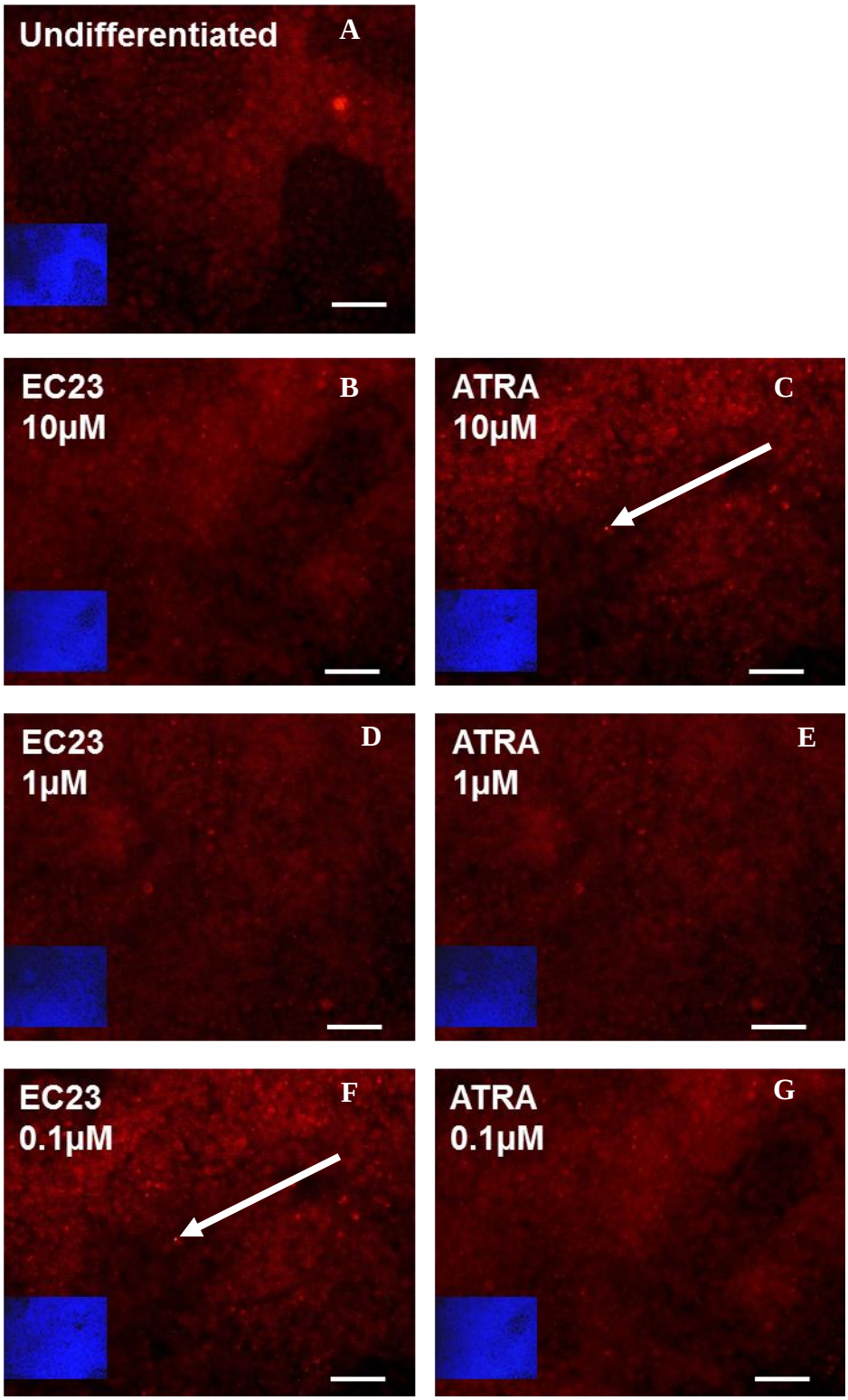

Figure 3-6 Differential regulation of nuclear protein Pax6 in response to retinoids. Immunocytochemistry demonstrates concentration dependent expression of Pax6 by EC23 and ATRA. TERA2.cl.SP12 cells were exposed to 0.1 µM, 1 µM and 10 µM EC23 (B,D,F) or ATRA (C,E,G) for 6 days in mono layer culture. Nuclear staining of Pax6 was seen in all cultures in areas of high density (DAPI shown in blue). Maximum expression of Pax6 was shown at 10 µM ATRA (C) and 0.1 µM EC23 (F) which correlated with real time PCR data shown in Figure 3.5. The low level nuclear staining at high concentrations of EC23 and the low expression at 0.1 µM ATRA also correlate with gene expression data. Pax6 indicates commitment to neural differentiation and is specific for more ventral neural subtypes. Notice Pax6 is expressed highly in high density areas of cell nuclei. Arrows indicate areas of nuclear Pax6 staining Scale bars: 50 µm. n=3.

In a more extensive commitment of retinoid-induced cell differentiation, cells were cultured for 21 days in the continued presence of 10-0.001 μM EC23 or ATRA. After 21 days the cells were fixed in 4 % PFA and stained for the neuronal cytoskeletal protein β III Tubulin and the non-neuronal protein Cytokeratin 8. Figure 3-7 shows immunocytochemical staining of the neural specific cytoskeletal protein, β III Tubulin, at three concentrations of ATRA: 0.1 μM, 1 μM and 10 μM. This data demonstrates neural differentiation at all three concentrations. However, at 0.1 μM ATRA the amount of neural differentiation is visibly reduced. Comparing gene expression data, flow cytometric data and immunocytochemical morphology and protein expression data it is evident that 0.1 μM ATRA was sufficient to induce neural commitment in a sub set of the stem cells. It is important to note that SSEA3, TRA-1-60 and A2B5 expression was not changed at this concentration, however, *OCT4* and *NANOG* mRNA expression was reduced. This indicates a possible advantage of mRNA analysis over cell surface glycoprotein expression measurement when screening for compounds that induce differentiation of stem cells.

Stem cells treated with EC23 for 21 days produced cells with a characteristic neural phenotype from (10-0.01 μM EC23). To quantify the level of neural protein in each culture and a western blot was performed on the highest expressing cultures. Figure 3-8 shows protein quantification of β III Tubulin on protein from cells treated with 10, 1 or 0.1 μM EC23 or ATRA from 21 days. Notice the low level of protein expression in both the untreated control and low concentration of ATRA treated cultures. Co-staining for the non-neuronal protein Cytokeratin 8 (Figure 3-9) demonstrated a heterogeneous culture of neuronal and non-neuronal cells in the 0.1 μM ATRA treated cells as demonstrated by the large flat epithelial like cells. In contrast very few large epithelial like cells were seen in EC23 treated cultures. Undifferentiated and DMSO treated controls became over confluent and cells died indicating they continued to proliferate and did not differentiate. Furthermore, cells treated with 0.01 μM ATRA or 0.001 μM EC23 did not survive to 21 days culture, the cells that became over confluent, lifted off the cell culture plastic substrate and such cultures were terminated.

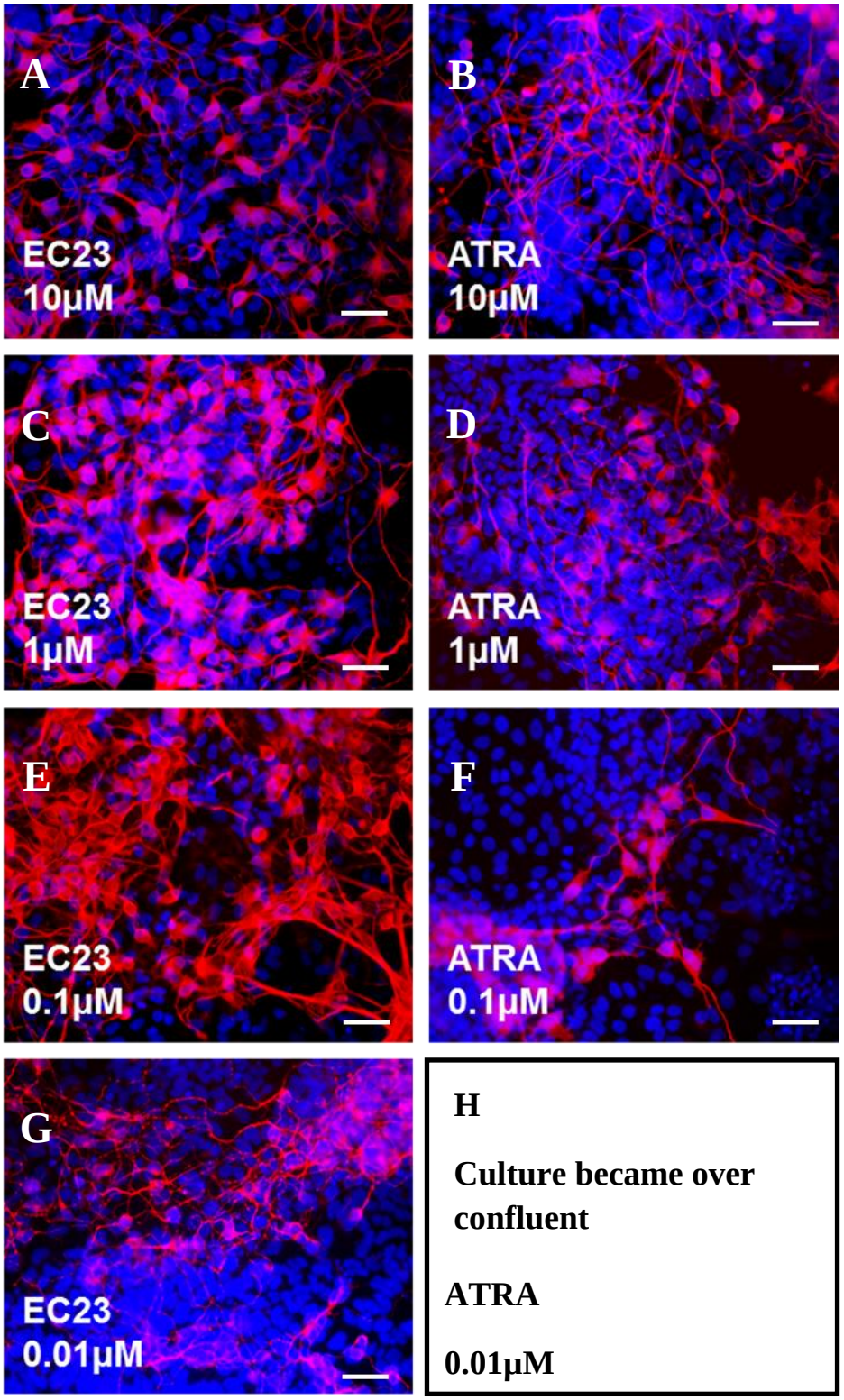

Figure 3-7 Neural differentiation of cells treated with EC23 and ATRA. Cells were treated with 10 µM, 1 µM, 0.1 µM and 0.01 µM EC23 (A,C,E,G) or ATRA (B,D,F). Cells treated with 0.001 µM EC23, 0.001 µM ATRA and 0.01 µM ATRA died by over proliferation (H). Due to the nature of the cells decreasing the starting density to prevent cells becoming over confluent was not possible. The stem cell phenotype of the cells are density dependent and at low densities spontaneously differentiate into epithelial like cells. In the presence of retinoid the cells stop proliferating and express neuronal markers. Cells were exposed to each concentration for 21 days, fixed in 4 % PFA and stained for the pan-neural epitope TUJ-1(Red) and DAPI (Blue). Neural differentiation was demonstrated at each concentration of EC23, ATRA induced neurite differentiation to a concentration of 0.1 µM. Note the reduction in neural development in cultures exposed to low levels of ATRA compared to EC23. Scale bars: 50 µm. n=3.

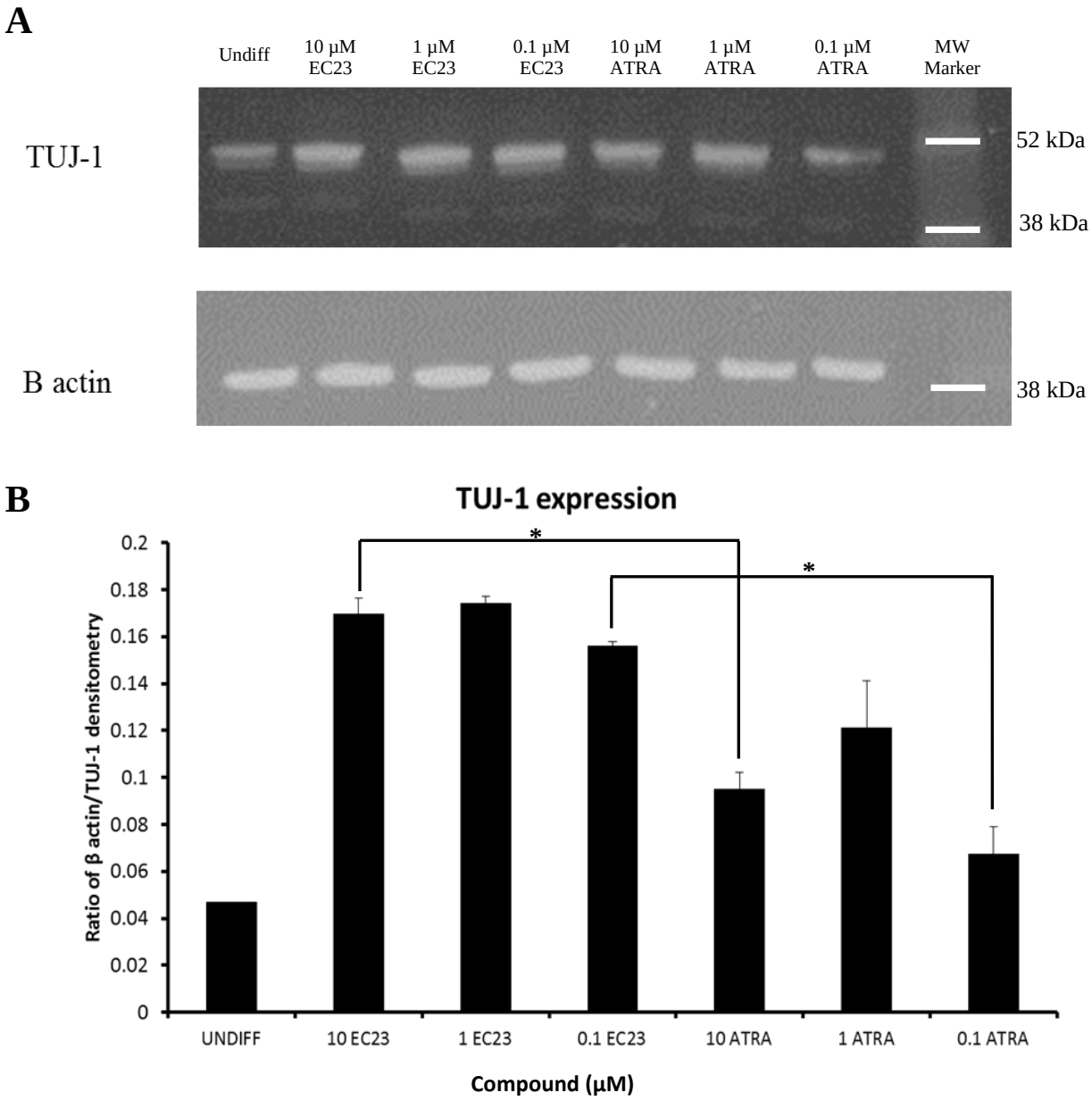

Figure 3-8 Regulation of neural proteins by retinoid treatment. Western blot analysis was used to quantify the protein expression of β III Tubulin in TERA2.cl.SP12 (A) cells treated with 10, 1 or 0.1 µM EC23 or ATRA for 21 days. Densitometry measurement of protein expression (B). Significantly higher levels were seen in retinoid treated groups than the undifferentiated controls. Levels were higher consistently in EC23 treated cultures. Data represent mean ± SEM, n=3.* $p \leq 0.005$ Student's t-test corrected for multiple testing between compared sample poulations using the Bonifferoni correction.

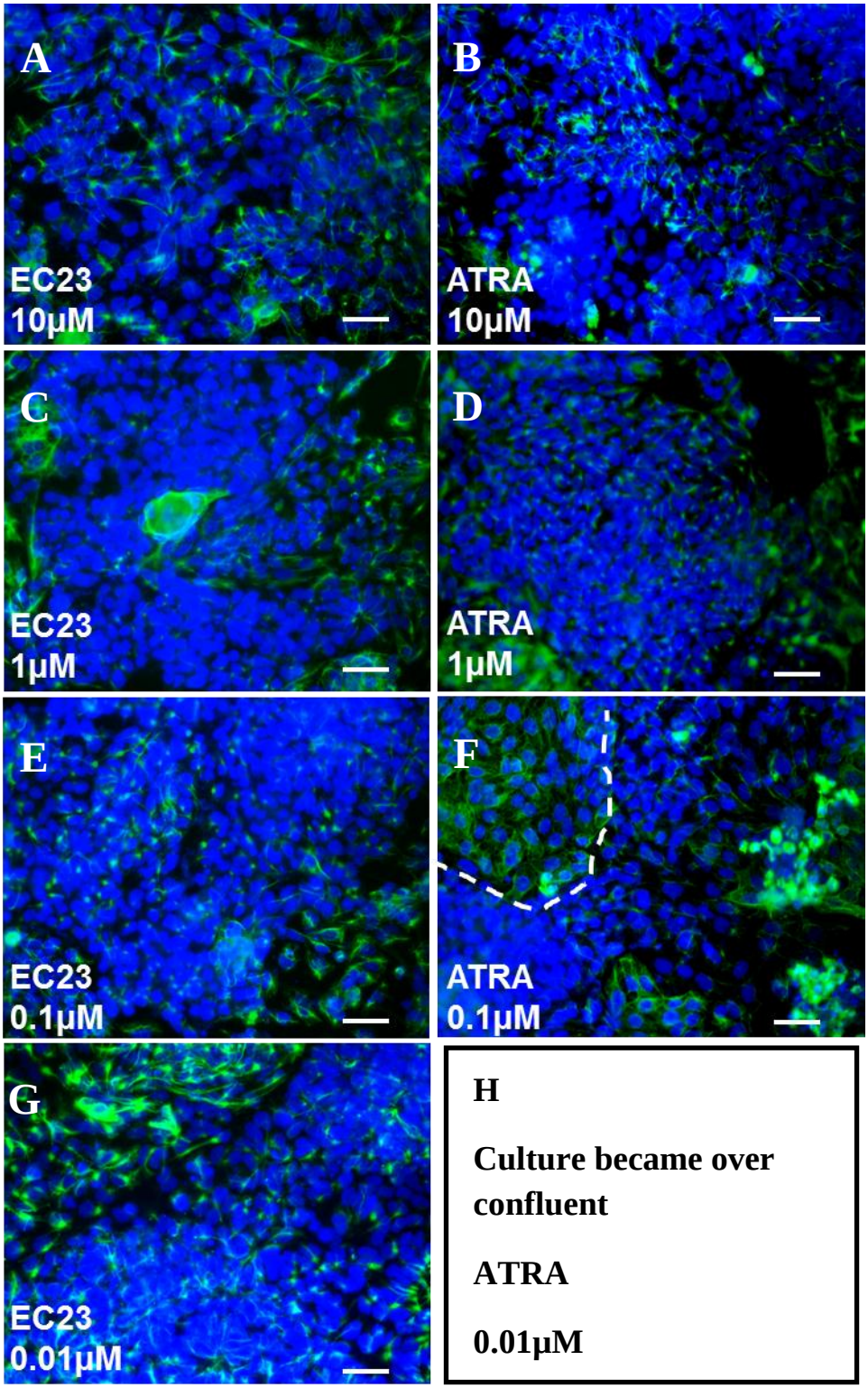

Figure 3-9 Non-neural differentiation of cells by EC23 or ATRA. Cells were treated with 0.001 µM, 0.01 µM, 0.1 µM. 1 µM or 10 µM EC23 (A,C,E,G) or ATRA (B,D,F) for 21 days. Cells treated with 0.001 µM EC23, 0.001 µM ATRA and 0.01 µM ATRA died by over proliferation (H). Due to the nature of the cells decreasing the starting density to prevent cells becoming over confluent was not possible. The stem cell phenotype of the cells are density dependent. After treatment cells were fixed in 4 % PFA and stained for the cytoskeletal protein cytokeratin 8 (Green) and DAPI (Blue). Non-neural differentiation indicated by cytokeratin 8 positive areas of large flat epithelial like cells was demonstrated at 0.1 µM ATRA. Note the higher expression of cytokeratin 8 staining and plaque formation in cultures exposed to low levels of retinoid (dashed lines). Scale bars: 50 µm.n=3.

3.2.3 Determining the role of metabolism on the potency of EC23 and neural commitment of human pluripotent stem cells.

Cytochrome P450 inhibiting compounds, known clinically as retinoic acid metabolism blocking agents or RAMBA's, are used to enhance the biological potency of endogenous retinoic acid. The use of RAMBA agents is predominantly for increasing the endogenous activity of retinoic acid in skin disease [62]. One relatively recently developed RAMBA is Liarozole hydrochloride [62]. In this section it was hypothesised that the enhanced potency of EC23 seen over ATRA is due to EC23 not being metabolised and hence is available to bind receptors constantly even at low concentrations. In contrast, ATRA would be metabolised by a group of cytochrome P450 enzymes family 26, and lose the ability to induce gene transcription by retinoic acid receptors.

Due to the presence of low levels of endogenous retinoic acid in FBS, an initial screen to determine if incubation with Liarozole alone was sufficient to enhance the biological effect of endogenous retinoic acid resulting in stem cell differentiation (Figure 3-10). In addition it is known that DMSO can induce differentiation if at high enough concentration (around 1 %) therefore it was important to determine the effect of Liarozole on the potency of DMSO in this model. Figure 3-10 demonstrates that the addition of 10 µM Liarozole dissolved in DMSO 0.1 % v/v did not induce any changes in SSEA3, TRA-1-60 or A2B5 expression compared to the undifferentiated control, furthermore, no change in cell expression of SSEA3, TRA-1-60 or A2B5 was measured in cells treated with Liarozole in DMSO 0.2 % v/v (control). The higher percentage of DMSO in the control (0.2 % v/v) accounts for the DMSO used to dissolve EC23 or ATRA as well as Liarozole.

To assess the role of retinoid metabolism on potency of retinoids to induce stem cell differentiation, TERA2.cl.SP12 cells were treated with three concentrations of ATRA that did not induce differentiation, 0.001 µM, 0.01 µM and 0.1 µM for 6 days with and without 10 µM Liarozole (Figure 3-11). After 6 days a significant and large change in the expression of SSEA3, TRA-1-60 and A2B5 was seen in cells treated with 0.01 µM and 0.1 µM ATRA with the addition of Liarozole, indicating loss of pluripotency and neural commitment with higher potency than ATRA alone. There was some enhancement of biological activity at 0.001 µM ATRA plus Liarozole compared to the ATRA only control. To determine if the enhanced potency demonstrated by EC23 was due to its resistance to metabolism TERA2.cl.SP2 stem cells were treated with 0.001 µM (an inactive concentration of EC23), 0.01 µM and 0.1 µM EC23 with and without Liarozole. Markers

of pluripotency and neural commitment were then assessed by flow cytometry (Figure 3-12). The levels of each of the markers assessed, SSEA3, TRA-1-60 and A2B5 were not altered by the presence of Liarozole, indicating that the potency of EC23 was not affected by inhibition of metabolising enzymes.

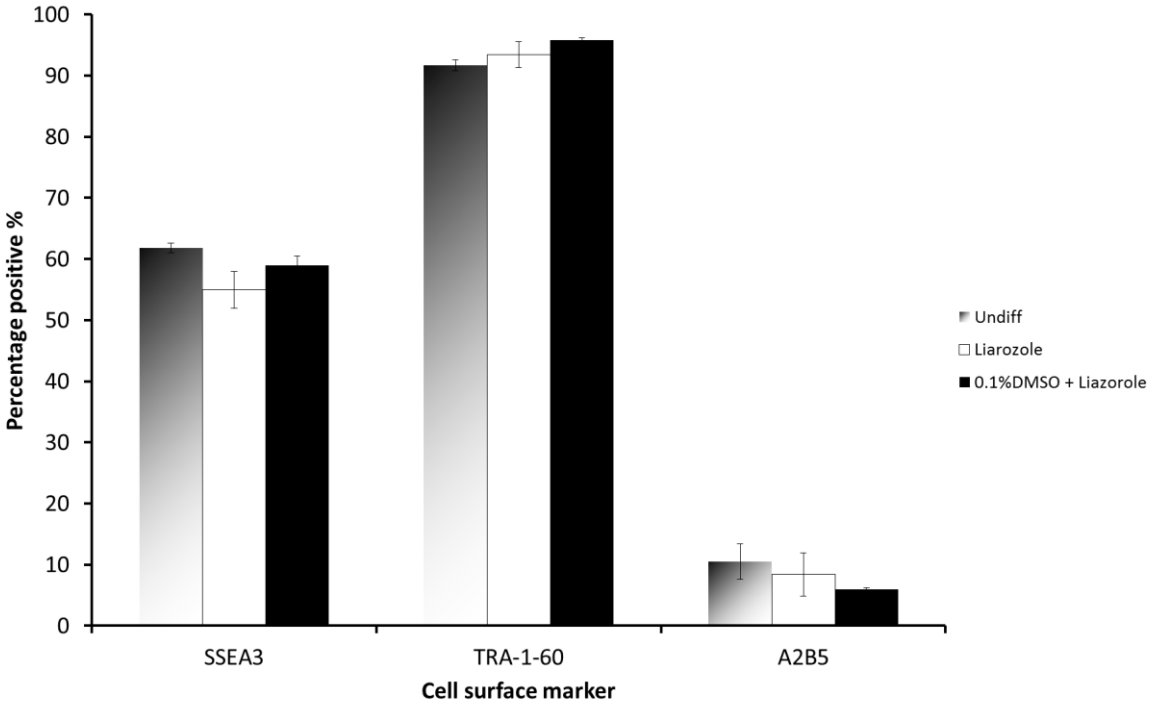

Figure 3-10 Application of Liarozole alone does not influence cell phenotype. TERA2.cl.SP12 cells were exposed to Liarozole and Liarozole plus 0.1 % DMSO as a control for subsequent experiments using Liarozole. Expression of the cell surface markers SSEA3, TRA-1-60 and A2B5 did not change with the addition of Liarozole or Liarozole plus 0.1 % DMSO compared to untreated controls. This demonstrates the inability of any endogenous ATRA in the cell culture media at inducing differentiation with the addition of Liarozole. Data represent mean ± SEM, n=3.

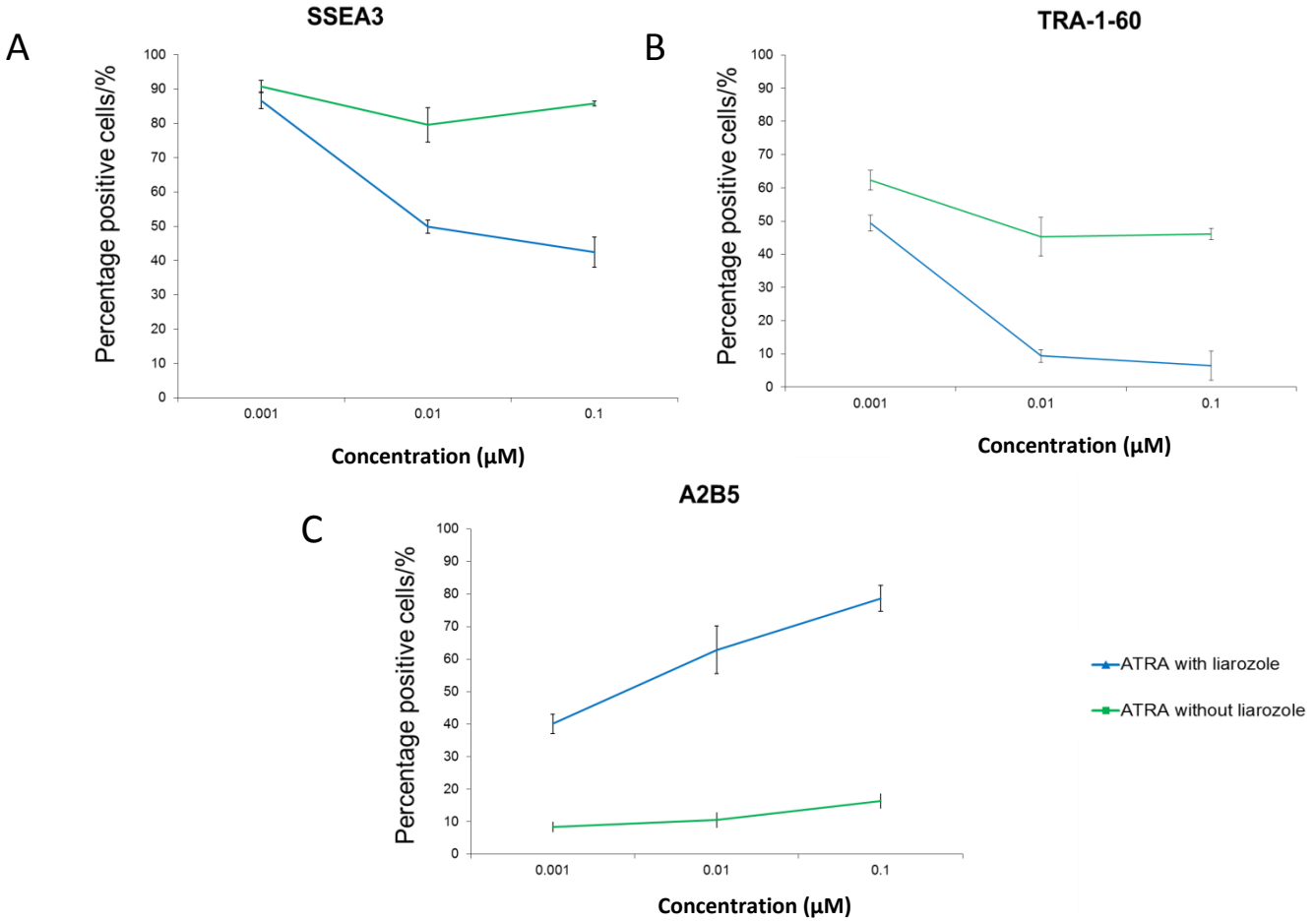

Figure 3-11 Addition of Liarozole enhances the activity of ATRA. Flow cytometric analysis of the stem cell markers SSEA3 (A), TRA-1-60 (B) and the pan-neural marker A2B5 (C).TERA2.cl.SP12 cells were exposed to ATRA at concentrations of 0.001 µM, 0.01 µM or 0.1 µM with and without the presence of 10 µM Liarozole hydrochloride for 6 days. At 0.001 µM and 0.01 µM ATRA no change in the expression of each cell surface marker was measured, with only small changes at 0.1 µM. The addition of Liarozole hydrochloride resulted in an almost complete loss of SSEA3, a much reduced expression of TRA-1-60 and high levels of A2B5 expression at 0.01 µM and 0.1 µM, indicating enhancement of potency. Only small changes in expression were seen at 0.001 µM with Liarozole. These data suggest the role cytochrome P450 enzymes in the regulation of ATRA in this system. Data represent mean ± SEM, n=3.

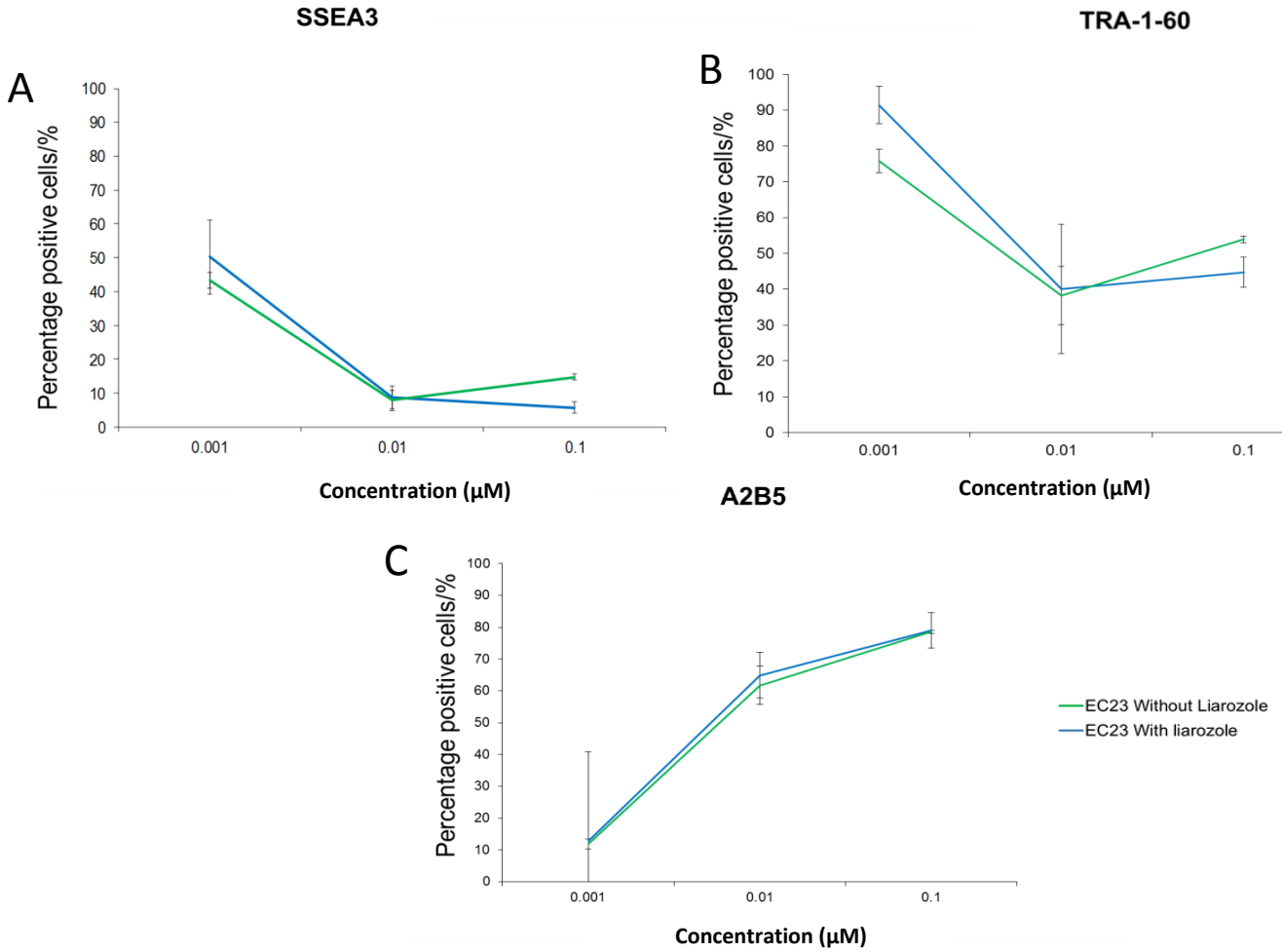

Figure 3-12 Addition of Liarozole does not change the activity of EC23. Flow cytometric analysis of the pluripotency markers SSEA3 (A), TRA-1-60 (B) and the pan-neural marker A2B5 (C).TERA2.cl.SP12 cells were exposed to EC23 at concentrations of 0.001 µM, 0.01 µM or 0.1 µM for 6 days with and without the presence of 10 µM Liarozole hydrochloride. Differentiation was demonstrated at 10 µM by loss of SSEA3, TRA-1-60 and expression of A2B5, no change in the number of cell surface markers were seen at 1 µM and 0.1 µM. Data suggest that EC23 is not metabolised by enzymes from the CYP 450 family, specifically EC23 is unlikely to be metabolised by CYP 26 enzymes. No statistically significant differences were shown between groups. Data represent mean ± SEM, n=3.

To further investigate the role of metabolism on the activity of ATRA and EC23, and to determine if metabolites of ATRA have a role in inducing neural differentiation a pulse and refresh experiment was performed. In this experiment, cells were pulsed with either 0.1 µM EC23 or ATRA (Figure 3-13) or 1 µM EC23 or ATRA (Figure 3-14) for 1 minute, 1 hour, 1 day or added continuously. After pulsing with the compound the cells were washed in PBS and fresh media without retinoid was added, cells were then incubated to 6 days prior to flow cytometry of SSEA3, TRA-1-60 and A2B5.

EC23 induced differentiation in the stem cells after just 1 minute incubation at 0.1 µM, the level of differentiation increased with incubation time. Only small changes in differentiated were demonstrated by 0.1 µM ATRA. At 1 µM EC23 induced an almost complete loss of SSEA3 and TRA-1-60 expression by the cells at each of the incubation times and this was accompanied by high levels of A2B5 expression. In contrast only continuous exposure to 1 µM ATRA induced the same level of changes in the cell surface markers as EC23. Finally Liarozole was added to a pulse of ATRA or EC23 to determine if a pulse of ATRA or EC23 that was previously inactive could be enhanced (Figure 3-15). No change in potency of EC23 was observed at 0.1 µM pulsed for 1 hour in the presence of 10 µM Liarozole, however, pulsing for 1 hour with 1 µM ATRA in the presence of Liarozole did result in an enhanced activity.

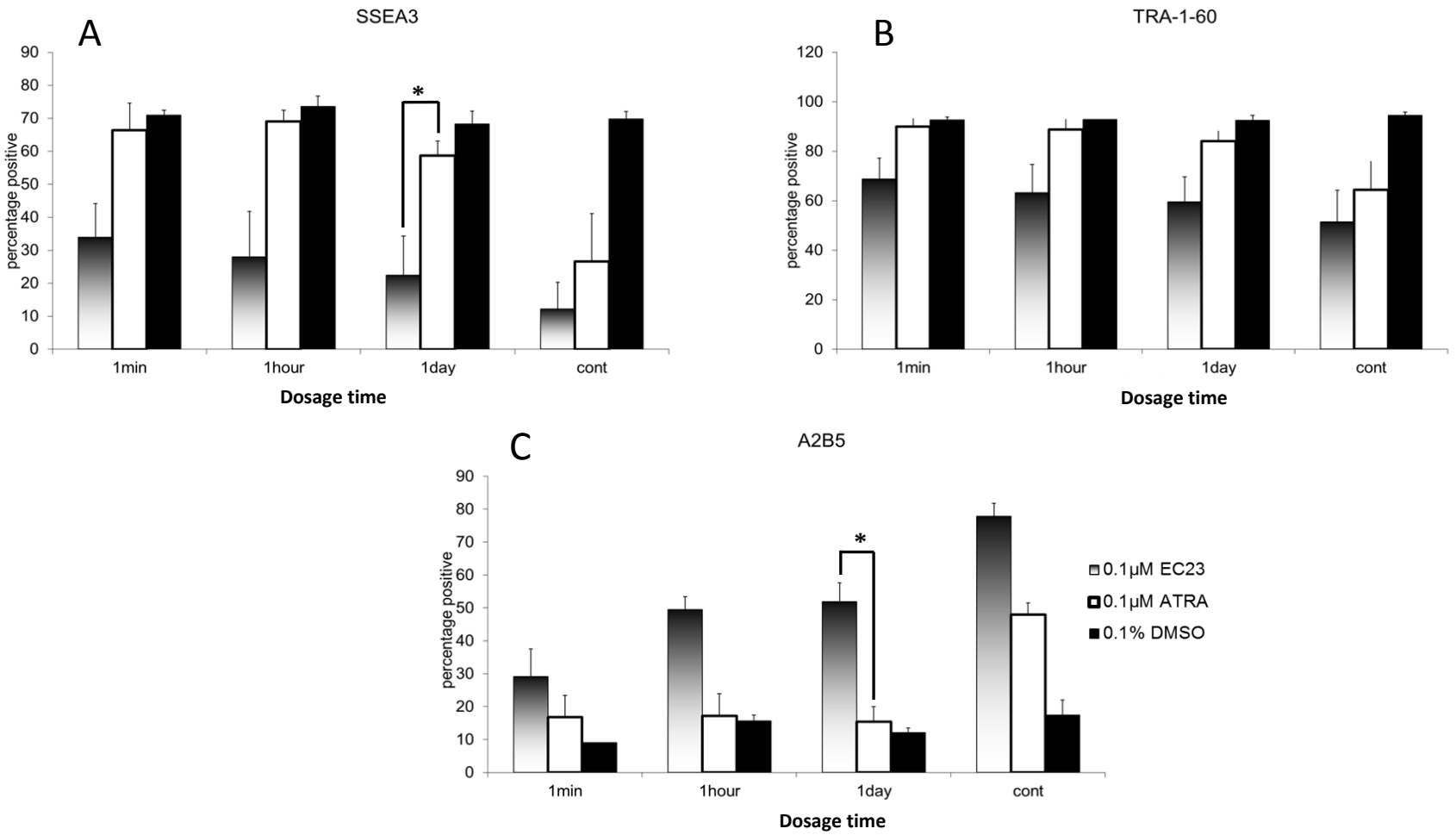

Figure 3-13 A single pulse of 0.1 µM EC23 is sufficient to induce differentiation. TERA2.cl.SP12 cells were treated with 0.1 µM EC23, 0.1 µM ATRA or 0.1 % DMSO for 1 minute, 1 hour, 1 day or continuously. After treatment cultures were maintained for 6 days in fresh media. Quantification of the stem cells surface proteins SSEA3 (A) and TRA-1-60 (B) as well as the neural marker A2B5 (C) by flow cytometry showed if the cells were differentiating. In all cases EC23 induced a loss of SSEA3 and TRA-1-60 expression and an increased expression of A2B5. The change in cell surface markers induced by EC23 at this concentration was lower in the pulsed experiments than in continuous exposure. Data represent mean ± SEM, n=3. * $p \leq 0.05$ using Student's paried t-test.

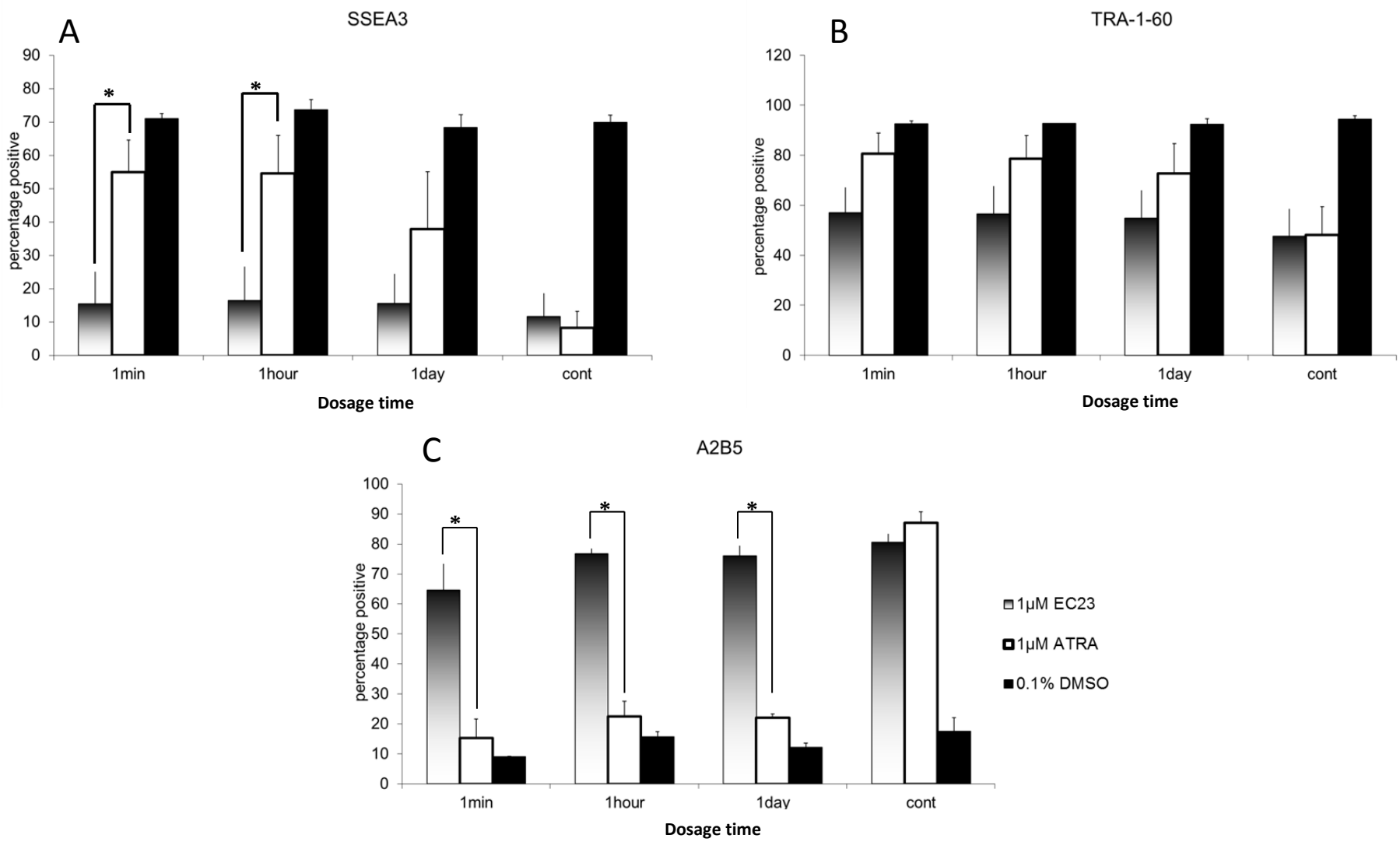

Figure 3-14 A single pulse of 1 µM EC23 is sufficient to induce differentiation. TERA2.cl.SP12 cells were treated with either 1 µM EC23, 1 µM ATRA or 0.1 % DMSO for 1 minute, 1 hour, 1 day or continuously. After treatment cultures were maintained for 6 days in fresh media. Quantification of the stem cells surface proteins SSEA3 (A) and TRA-1-60 (B) as well as the neural marker A2B5 (C) by flow cytometry showed if the cells were differentiating. In all cases EC23 induced a loss of SSEA3 and TRA-1-60 expression and an increased expression of A2B5. The affect seen by ATRA was much less pronounced at any of the pulsed times indicating metabolism and loss of activity in these cultures. Data represent mean ± SEM, n=3. * $p \leq 0.05$ using Student's paired t-test.

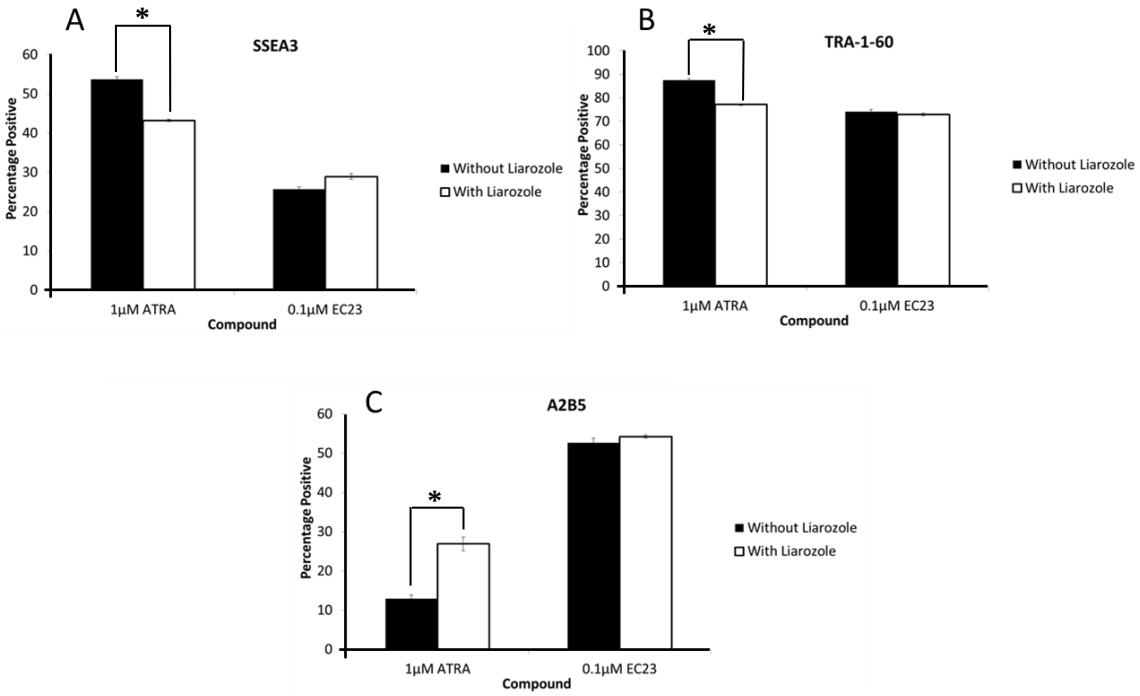

Figure 3-15 An ineffective pulse treatment of ATRA can be enhanced by Liarozole treatment. TERA2.cl.SP12 cells were treated with 1 µM ATRA or 0.1 µM EC23 for 1 hour with and without 10 µM Liarozole. The cells were then maintained in fresh cell culture media for 6 days. Flow cytometric analysis of the cell surface markers SSEA3 (A), TRA-1-60 (B) and A2B5 (C) was used to determine if the cells were differentiating. There was a significant enhancement of the activity of ATRA with the addition of Liarozole, however this was not demonstrated with EC23. Data demonstrates the effect of metabolism on the potency of ATRA. Data represent mean ± SEM, n=3. * ≤0.05 using Students paired t-test.

3.2.4 Enhancing the potency of synthetic retinoids by incorporation of a methyl group

The small molecule EC23 was developed alongside the small molecule, EC19. EC19 and EC23 have a similar structure; however the carboxyl group on EC19 is at the *meta*-position, compared with EC23 where it is in the *para*-position (Figure 3-16).

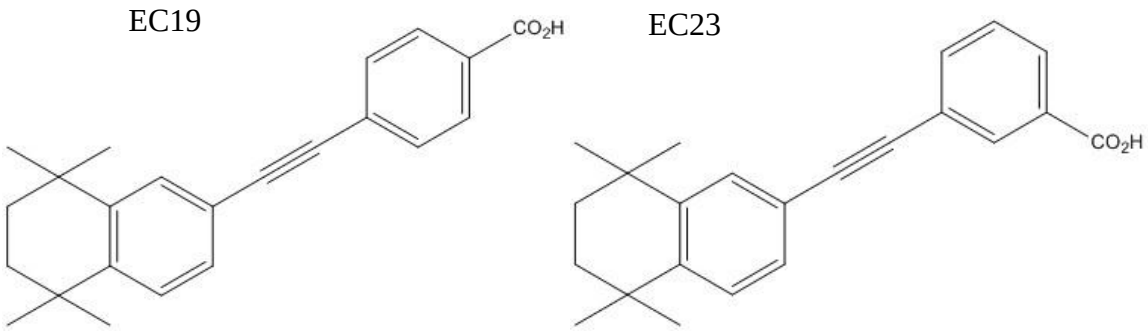

Figure 3-16 Molecular structures of EC19 and EC23. Both EC19 and EC23 contain a highly stabilising triple bond and no oxidation sites.

EC23 can induce consistent neural differentiation in human stem cells, whereas EC19 treatment resulted in large flat epithelial like cells with very few neurons [95]. The differential response between EC19 and EC23 may suggest activation of alternative receptors in this model. The structure activity relationship between retinoids has been studies extensively and is apparent naturally. The *cis* configuration of at the 9 carbon position in 9-*cis*-RA confers a differential response in neuroblastoma cells compared to *all-trans* RA. Another analogue of ATRA, TTNPB is very similar to the structure of EC23 and contains a *cis*-bond isomerisation and can induce enhanced apoptosis in some cell models. TTNPB is similar in potency to EC23; however, EC23 has been shown recently to result in higher RAR binding [93].

As with EC23, TTNPB is not metabolised demonstrated by Liarozole models [201]. In this section it was hypothesised that 3-methylation of EC19 and EC23 may affect their biological activity. The addition of a 3-methyl group to TTNPB resulted in a decrease in RAR activity and increased RXR activity suggesting either a possible increase in TTNPB metabolism [202] or a change in ligand binding to the receptor. Investigating the role of carbon 3 methylation on change in receptor selectivity/metabolism and stem-cell differentiation will provide useful insights when designing synthetic compounds in the future to induce specific receptor activity. In this section biological activity of 3-carbon

methylated EC19 and EC23 was investigated in TERA2.cl.SP12. The structures of methylated EC19 and EC23 are shown in Figure 3-17, due to the rigidity of the triple bond in EC19 and EC23, addition of the methyl group should not interfere with the conformation and thus not affect interaction with the ligand binding pocket (LBP) of the RARs and hence, biological activity.

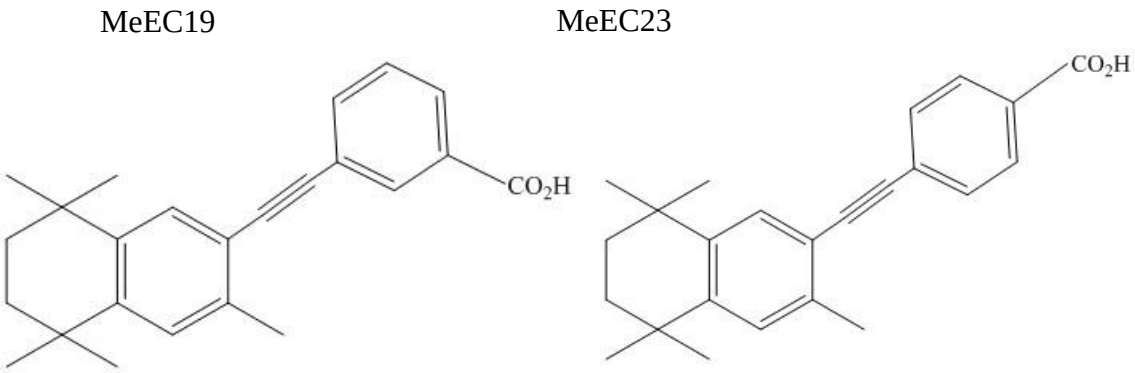

Figure 3-17 Chemical structure of methylated EC19 and EC23. Compounds are identical to EC19 and EC23, however, contain a methylated 3 carbon which will not affect the shape of the molecule.

Figure 3-18 shows flow cytometric data of TERA2.cl.SP12 cells treated with either EC19 or methyl-EC19 (MeEC19). As has been demonstrated previously that EC19 did not induce a marked change of SSEA3, TRA-1-60 or A2B5 at 10, 1 or 0.1 µM, indicating a low activity in this system. Methylation of EC19 resulted in a marked increase in biological activity at 10 µM, as indicated by a loss of SSEA3 and TRA-1-60 expression and an increase in A2B5 positive cells. At the lower concentrations 1 µM and 0.1 µM no significant difference was shown.

To assess if methylation of EC23 resulted in a change of the potency of the molecule, active and inactive concentrations of EC23 were investigated using flow cytometry. There was no change in potency at either the active concentrations 0.1 µM or 0.01 µM or the inactive concentration tested 0.001 µM (Figure 3-19), suggesting EC23 already induced a maximal response regardless of the methyl group.

Real time PCR was used to determine if the enhanced activity demonstrated by methyl EC19 at 10 µM was also demonstrated in an enhanced neural progenitor commitment through the gene expression analysis of *PAX6*. Figure 3-20 demonstrates that 10 µM

ATRA, EC23, MeEC23 and MeEC19 induce expression of *PAX6*, ATRA induced the highest expression and MeEC19 the lowest. No expression was detected in EC19 treated cells, indicating an enhancement of EC19 activity by addition of the methyl group.

To assess if the addition of a methyl group to either EC19 or EC23 resulted in an increased metabolism of either of the compounds 10 µM Liarozole hydrochloride was added to concentrations of EC19 (Figure 3-21), MeEC19 (Figure 3-22) and MeEC23 (Figure 3-23) that were ineffective at inducing changes in expression of SSEA3, TRA-1-60 and A2B5. As was shown previously, ATRA can be enhanced though synergistic activity with Liarozole (Figure 3-11), any metabolism as a result of the addition of the methyl group will be inhibited by Liarozole. The data demonstrated that methylation of EC19 and EC23 did not appear to change its metabolism in this model. Furthermore, EC19 was not enhanced by Liarozole, suggesting it also is not metabolised similar to EC23 and its lower potency may be due to sequestering effects or poor receptor binding affinity/alternative receptor binding.

Understanding the structure activity relationship of retinoic acid analogues is important for compound design directed at control of cell differentiation. The large array of RAR and RXR receptor isotypes and growing knowledge of the role different heterodimers during development makes designing small molecules capable of specific RAR or RXR subtype selectivity important for future research into retinoids and their biological activity.

In summary this study has described how subtle chemical modifications can alter the biological activity of synthetic retinoids without affecting the overall conformation of the molecule. Hence, the addition of a methyl group to EC19 resulted in a small increase in RAR LBP affinity.

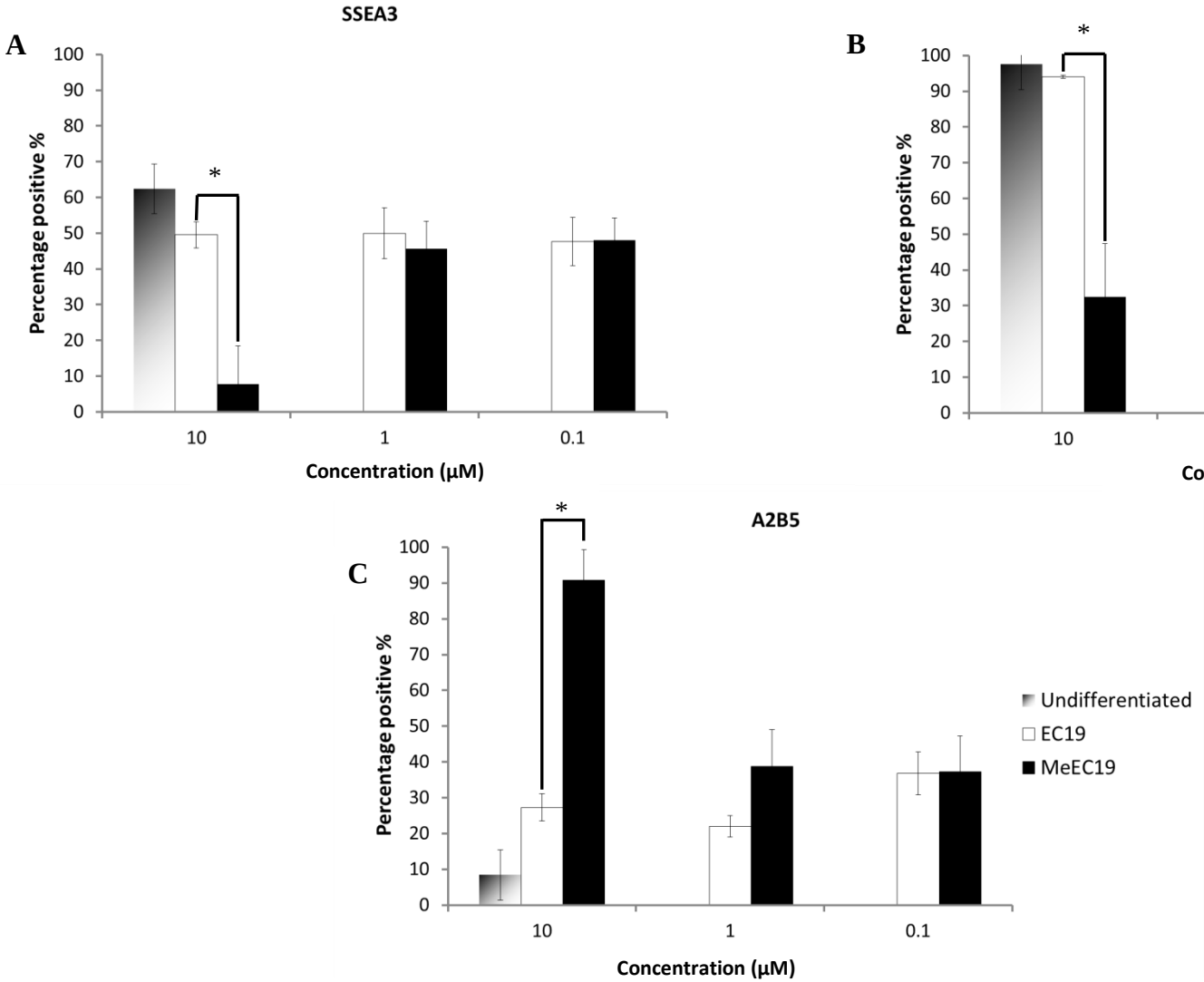

Figure 3-18 Concentration dependent differentiation of TERA2.cl.SP12 cells by 3-Methyl EC19 (MeEC19) and EC19. Cells were treated with either 10 µM, 1 µM or 0.1 µM MeEC19 or EC19 for 6 days. Using flow cytometric analysis the number of cells expressing the cell surface markers SSEA3 (A), TRA-1-60 (B) or A2B5 (C) were quantified. No change in expression was seen at 0.1 µM or 1 µM of both EC19 and MeEC19 compared to an untreated control. There was no change of the cell surface markers demonstrated by 10 µM EC19. However, MeEC19 induced differentiation of the cells at 10 µM as demonstrated by a loss of SSEA3 and TRA-1-60 expression and an increase in A2B5 expression. These data indicate that methyl EC19 shows enhanced biological activity over EC19. Data represent mean ± SEM, n=3. * $p \leq 0.01$ Students t-test.

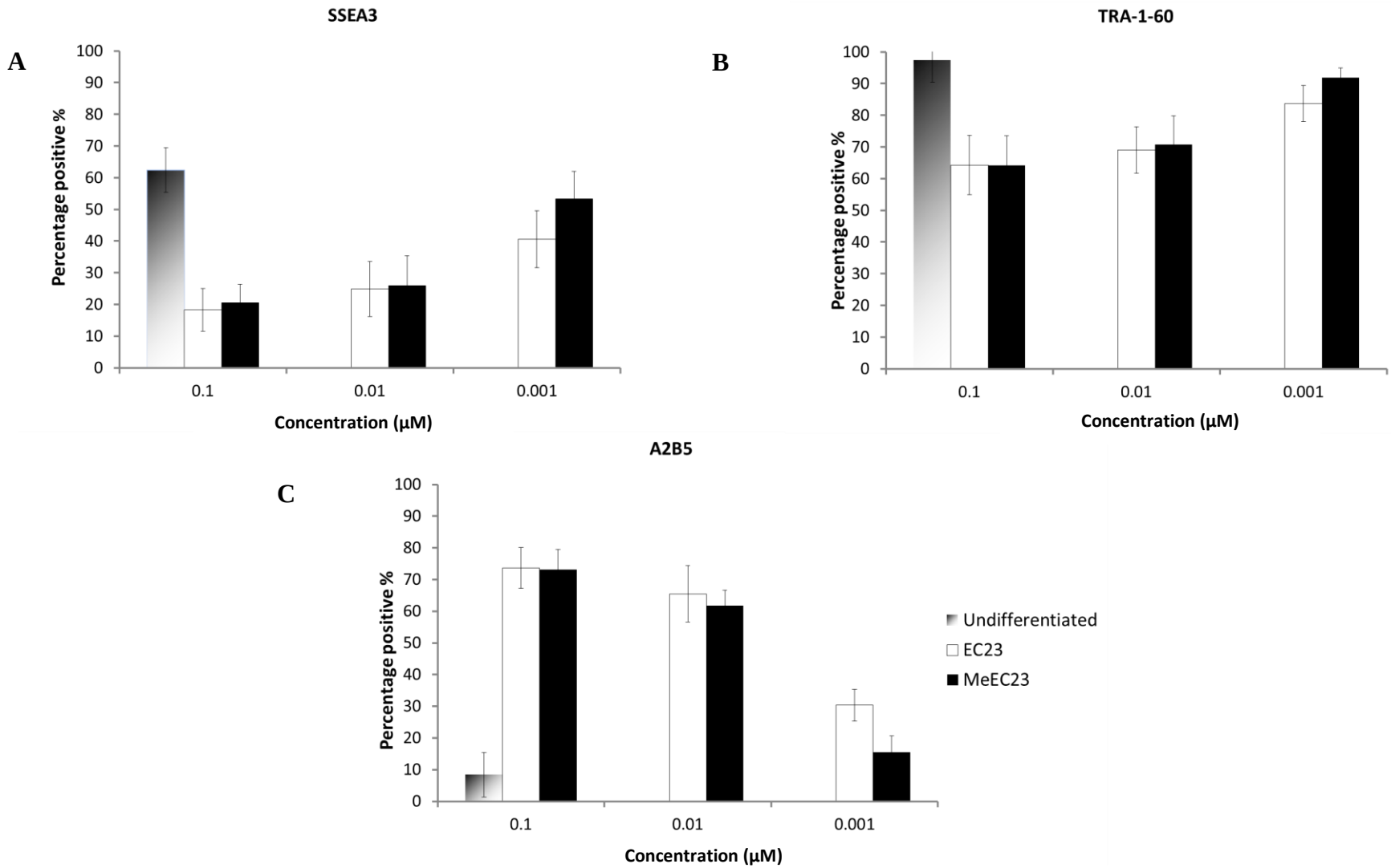

Figure 3-19 Concentration dependent differentiation of TERA2.cl.SP12 cells by Methyl EC23 (MeEC19) and EC23. Cells were treated with either 0.1 µM, 0.01 µM or 0.001 µM MeEC23 or EC23 for 6 days. Using flow cytometric analysis the number of cells expressing the cell surface markers SSEA3 (A), TRA-1-60 (B) or A2B5 (C) were quantified. Very little change in expression was seen at 0.001 µM of both EC23 and MeEC23 compared to an untreated control. At the higher concentrations 0.01 µM and 0.1 µM both MeEC23 and EC23 induced differentiation as demonstrated by a loss of SSEA3 and TRA-1-60 expression and an increase in A2B5 expression. These data show that addition of a methyl group to EC23 does not appear to influence its biological activity. Data represent mean ± SEM, n=3.

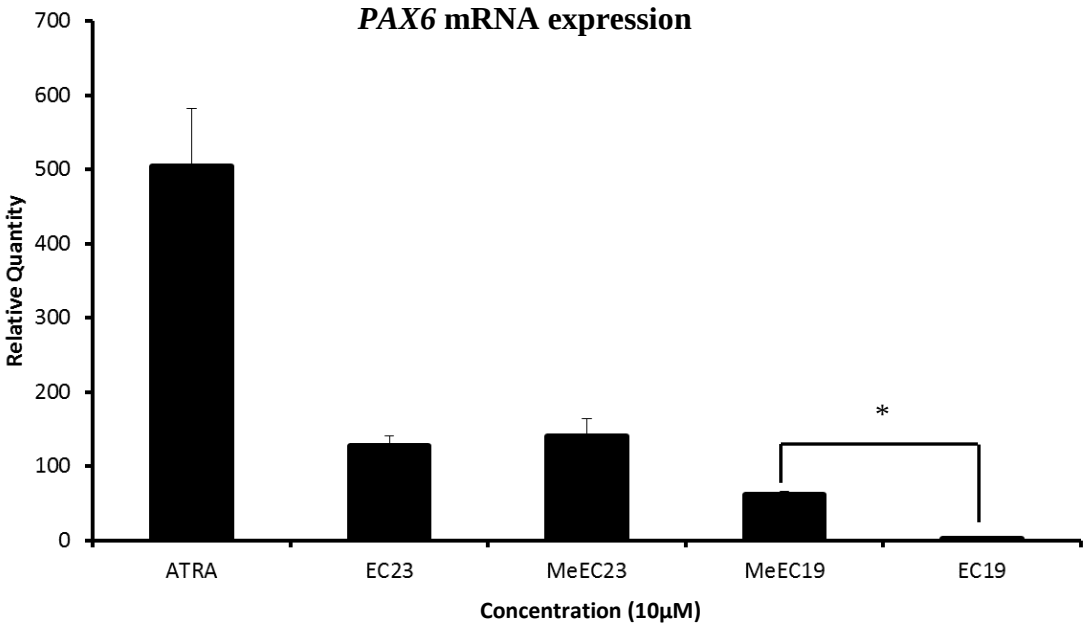

Figure 3-20 *PAX6* expression is enhanced by methylation of EC19. TERA2.cl.SP12 cells were treated with 10 μM ATRA, EC23, methyl EC23 (MeEC23), methyl EC19 (MeEC19) and EC19 for 6days. The mRNA expression of *PAX6* was measured using real-time PCR and gave a representation of any enhancment of potency after methylation. Methylation of EC19 induced a 24 times significant increase in *PAX6* expression in this model compared to EC19. No change in activity was seen by EC23. Data represent mean ± SEM, n=3. * $p \leq 0.05$ Students t-test.

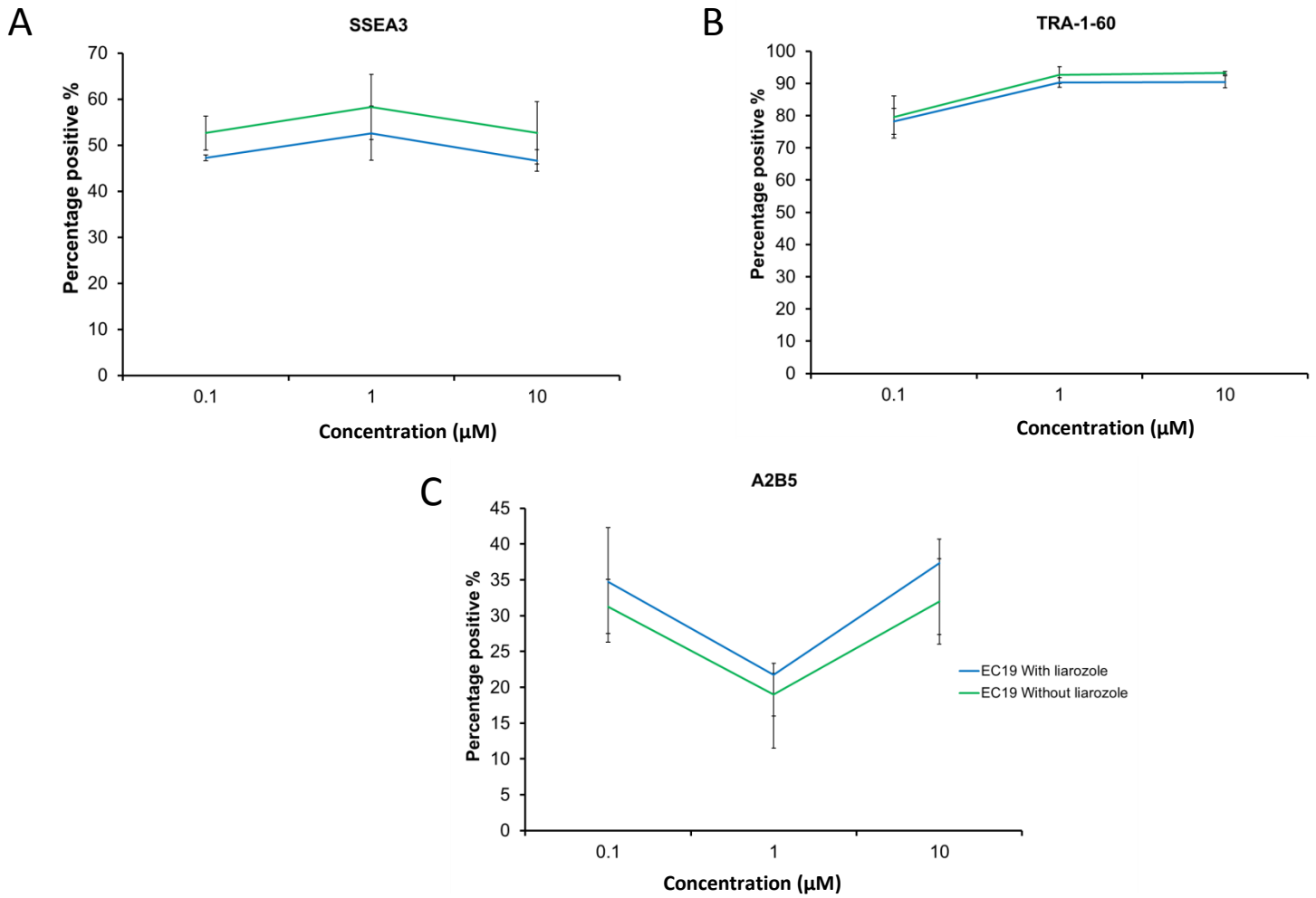

Figure 3-21 Addition of Liarozole to cells treated with EC19 does not appear to change the activity of EC19. Flow cytometric analysis of the pluripotency markers SSEA3 (A), TRA-1-60 (B) and the pan-neural marker A2B5 (C). TERA2.cl.SP12 cells were exposed to EC19 at concentrations of 0.1 µM, 1 µM or 10 µM for 6 days with and without the presence of 10µM Liarozole hydrochloride. The addition of Liarozole to each concentration did not enhance the potency of EC19. No statistically significant differences were shown between groups Data represent mean ± SEM, n=3.

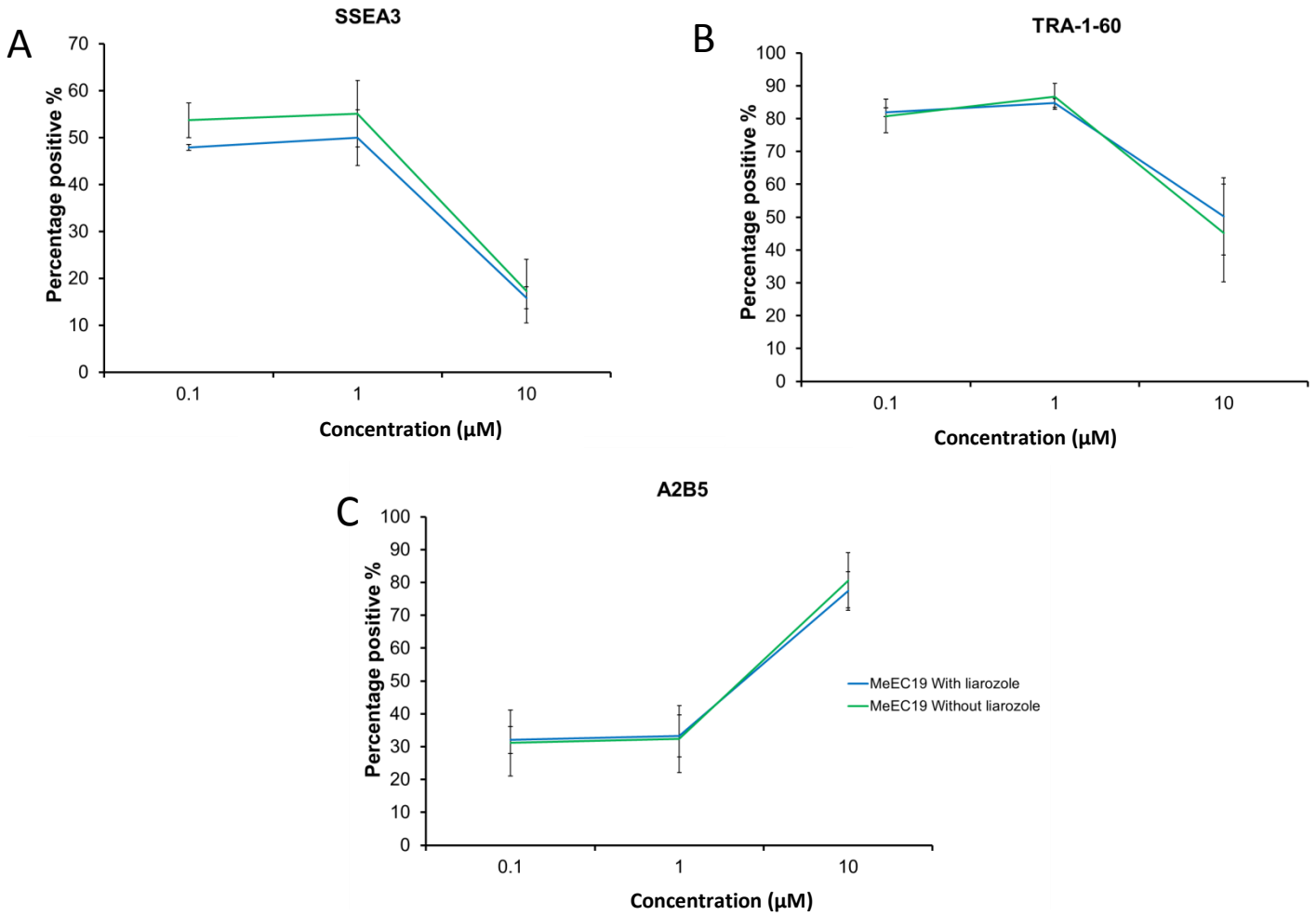

Figure 3-22 Addition of Liarozole to cells treated with MeEC19 does not appear to change the activity of MeEC19. Flow cytometric analysis of the pluripotency markers SSEA3 (A), TRA-1-60 (B) and the pan-neural marker A2B5 (C). TERA2.cl.SP12 cells were exposed to MeEC19 at concentrations of 0.1 µM, 1 µM or 10 µM for 6 days with and without the presence of 10 µM Liarozole hydrochloride. Differentiation was demonstrated at 10 µM, no change in the number of cell surface markers were seen at 1 µM and 0.1 µM. The addition of Liarozole to each concentration did not enhance the potency of MeEC19. No statistically significant differences were shown between groups. Data represent mean ± SEM, n=3.

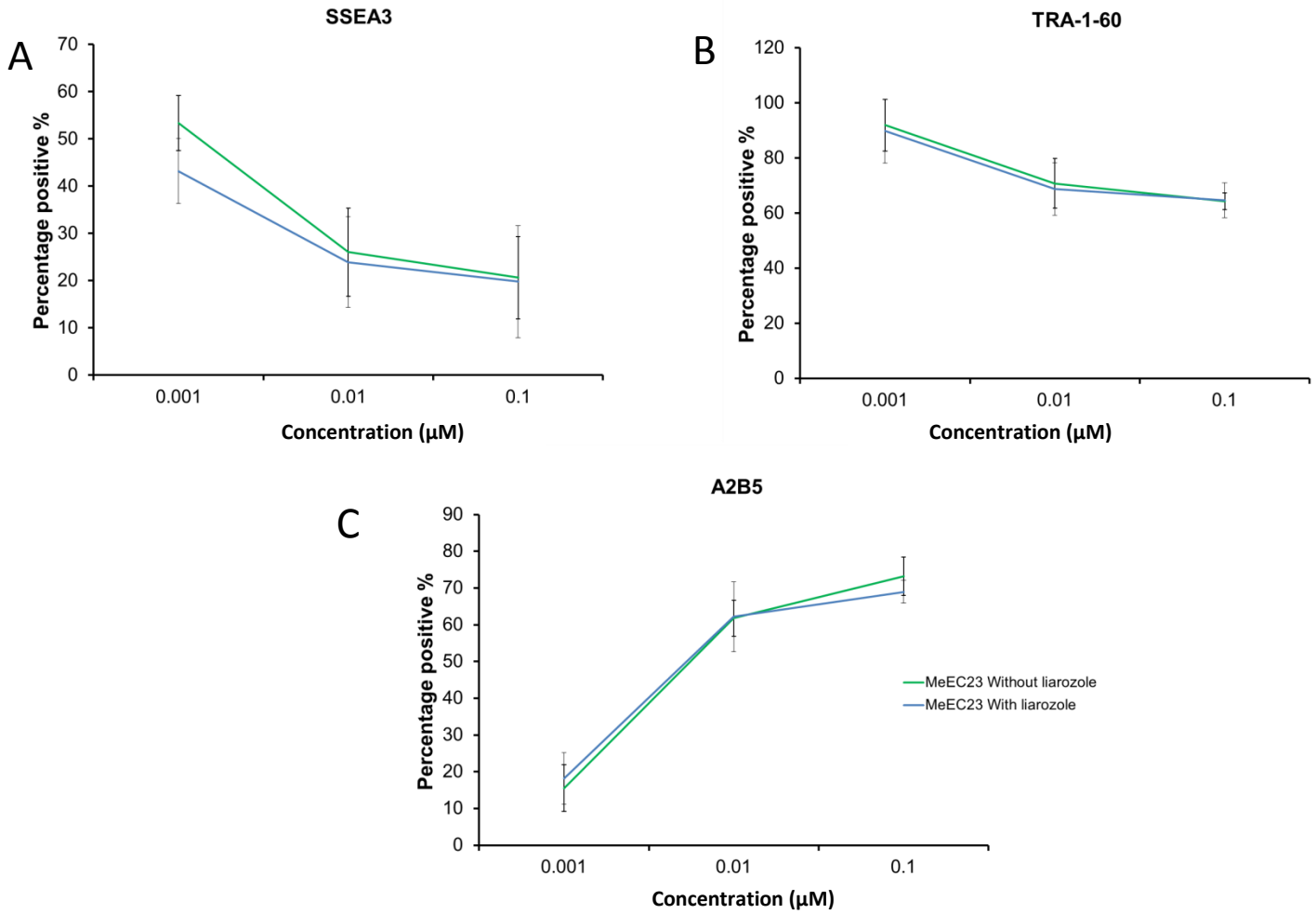

Figure 3-23 Addition of Liarozole to cells treated with MeEC23 does not appear to change the activity of MeEC23. Flow cytometric analysis of the pluripotency markers SSEA3 (A), TRA-1-60 (B) and the pan-neural marker A2B5 (C). TERA2.cl.SP12 cells were exposed to MeEC23 at concentrations of 0.001 µM, 0.01 µM or 0.1 µM for 6 days with and without the presence of 10 µM Liarozole hydrochloride. Differentiation was demonstrated at 0.1 µM and 0.01 µM, however no change in the number of cell surface markers were seen at 0.001 µM. No statistically significant differences were shown between groups .The addition of Liarozole to each concentration did not enhance the potency of MeEC23. Data represent mean ± SEM, n=3.

3.2.5 Modulation of embryonic anterior-posterior patterning genes during stem cell differentiation using synthetic small molecules

Regulation of developmental patterning by a group of genes known as *HOX* genes is key to the correct differentiation of neural subtypes through environmental cues. *HOX* genes contain a DNA binding homeobox which is conserved among different species. Human *HOX* genes are located on four different chromosomes and consist of 39 genes clustered into four distinct regions; A, B, C and D. Regulation of *HOX* genes is developmentally conserved and requires a morphogenic stimulus. Mammalian *HOX* genes are thought to pattern the anterior-posterior axis via co-linear expression; co-linear expression means that due to the proximity of the *HOX* genes on each cluster the expression of each gene along the A-P axis is determined by its position in the cluster i.e. *HOX* genes 3' in the cluster are expressed in the anterior developing embryo, whereas 5' *HOX* genes are only expressed in the posterior developing embryo. The hypothesis behind the ability of these genes to be expressed in this way is due to a concentration gradient of retinoic acid. Many of the 3' *HOX* genes are able to induce the expression of *HOX* genes more 5'. In addition 3' *HOX* genes usually contain a RARE, therefore retinoic acid is thought to regulate *HOX* gene expression directly and hence, anterior-posterior patterning and differentiation. It was demonstrated *in vitro* that retinoic acid can induce temporal and concentration dependent co-linear expression of *HOX* genes. For a detailed review see Chapter 1.

This section is aimed to investigate the regulation of *HOX* genes in a temporal and concentration dependent manner by ATRA. Furthermore, using the synthetic ATRA analogue EC23, it was hypothesised a more consistent, reproducible and accurate concentration/activity could be achieved and give a better understanding as to the regulation of *HOX* genes by RARE activation.

Initially 9 genes were chosen to be investigated, including *HOX* A1, 5, 6 B1, 6, 9 and D1, 4, 8. These represent *HOX* genes at both the 3' and 5' ends of three clusters of genes. It is known that *HOX* A1, B1, D1 and D4 all contain RARE. Relative expression of each gene to the untreated control was measured by real time PCR at 72 and 144 hours treatment to assess temporal regulation. To determine concentration dependent regulation and co-linearity in our model, TERA2.cl.SP12 cells were treated for 72 and 144 hours with five different concentrations of both EC23 and ATRA. The concentrations used were: 0.001 µM, 0.01 µM, 0.1 µM, 1 µM and 10 µM. Furthermore, it was demonstrated earlier in this Chapter using real time PCR and flow cytometry which of the retinoid

concentrations induce neural differentiation. (Figure 3-24 - Figure 3-29).

The expression of *HOX* genes induced in our stem cell model by each concentration of EC23 or ATRA for 72 hours is shown for cluster A in Figure 3-24, cluster B in Figure 3-25 and cluster D in Figure 3-26. The *HOX* genes on cluster A after 72 hours of induction by EC23 or ATRA demonstrated concentration dependent expression. ATRA did not induce the expression of *HOXA1*, *A5* or *A6* to high levels in cultures treated with 0.001 µM, 0.01 µM or 0.1 µM. High levels of *HOXA1* and *HOXA5* were demonstrated at both 1 µM and 10 µM treatment; however, *HOXA6* even at 10 µM did not induce a large increase in relative expression, indicating a co-linear relationship between these genes. In contrast the expression of all genes A1, A5 and A6 were induced by EC23 at 0.001 µM - 10 µM in a concentration dependent manner. The level of maximal expression was lower than that of ATRA treated cultures, however, EC23 induced more expression at the lower concentrations investigated. The low expression levels seen are typical of EC23 after 72 hours.

Regulation of *HOX* genes on cluster B demonstrated less fold change in the 3' genes compared to that of *HOXA*. However, in contrast to *HOXA1*, the 3' gene *HOXB1* was induced maximally after 72 hours by a low concentration of EC23 – 0.01 µM. Expression was demonstrated at 0.001 µM, peaked at 0.01 µM and reduced with EC23 concentration. *HOXB1* increased with dose in cells treated with ATRA indicating a differential response of *HOXB1* to EC23 and ATRA. Very little change in expression of *HOXB6* was demonstrated after 72 hours induction by EC23 or ATRA. However, *HOXB9* was induced maximally by 1 µM EC23 and ATRA and remained at high levels to 10 µM of each compound; little or no change in expression was demonstrated at the low concentrations tested for *HOXB9* (Figure 3-25).

The three *HOX* genes from cluster D measured were *D1*, *D4* and *D8*. The genes analysed on cluster D were demonstrated to be regulated in a concentration dependent manner. Data in Figure 3-26 demonstrates that EC23 induced maximal *HOXD1* expression at 0.1 µM which decreased either side on this concentration a similar pattern was produced with *PAX6* expression. Regulation of *HOXD4* and *HOXD8* by EC23 after 72 hours was minimal. With only a small peak demonstrated at 1 µM for both *HOXD4* and *HOXD8*. In contrast ATRA induced a direct increase of *HOXD1* with concentration; however expression levels did not reach that of 0.1 µM EC23. High levels of both *HOXD4* and *HOXD8* were induced in similar pattern; the transcript was almost completely absent from

0.001 µM – 0.1 µM. A steep increase of expression was demonstrated at 1-10 µM in ATRA treated cultures.

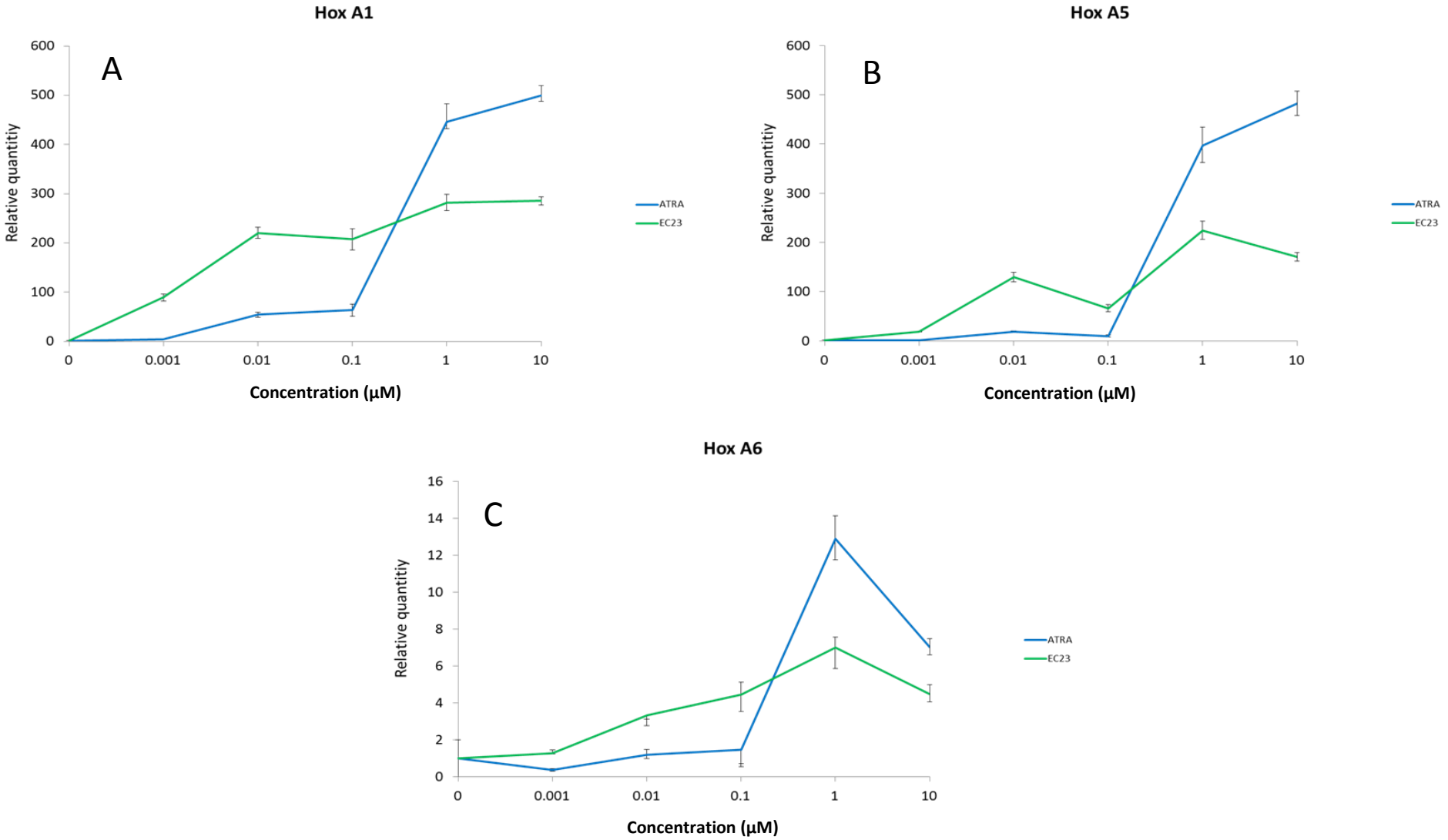

Figure 3-24 Regulation of *HOXA1, A5* and *A6* concentration dependent expression induced by EC23 or ATRA. TERA2.cl.SP12 cells were treated with 0.001 µM, 0.01 µM, 0.1 µM, 1 µM or 10 µM for 3 days. RNA was extracted and purified and using real time PCR the relative expression change of *HOXA1* (A), *HOXA5* (B) and *HOXA6* (C) was measured. Data demonstrates a similar dose response at each concentration for each gene assayed for the individual compounds. EC23 induces changes in expression at a lower concentration, however, does not reach the level of change demonstrated by high concentrations of ATRA. The relative changes measured were highest in the more 3' genes assayed –*HOXA1* and *A5*. Data represent mean ± SEM, n=3.

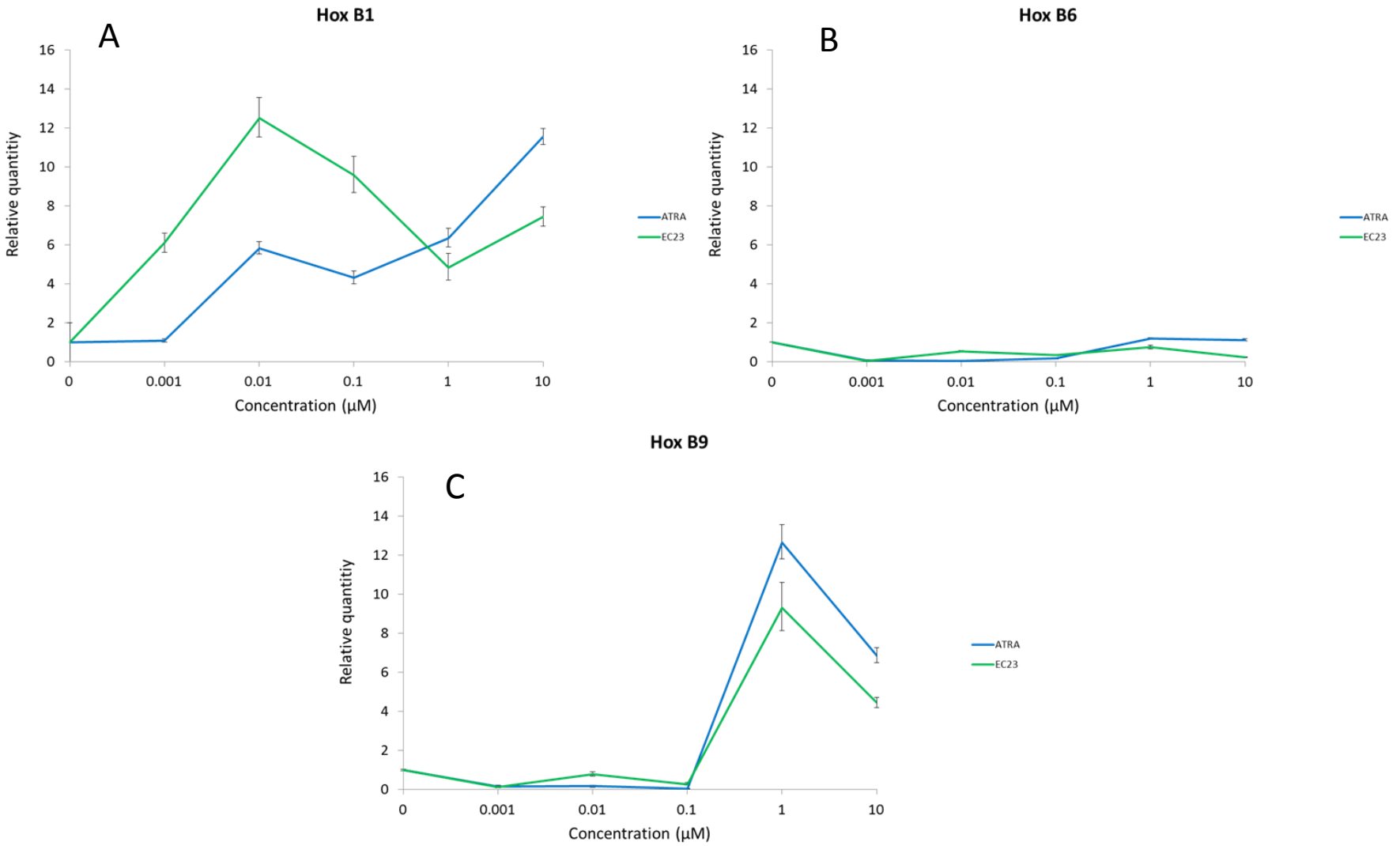

Figure 3-25 Regulation of *HOXB1*, *B6* and *B9* concentration dependent expression induced by EC23 or ATRA. TERA2.cl.SP12 cells were treated with 0.001 µM, 0.01 µM, 0.1 µM, 1 µM or 10 µM for 3 days. RNA was extracted and purified and using real time PCR the relative expression change of *HOXB1* (A), *HOXB6* (B) and *HOXB9* (C) was measured. Data demonstrates a peak of *HOXB1* expression by both EC23 and ATRA at low concentrations, however, the relative change is more pronounced with EC23, negligible changes in expression are demonstrated in *HOXB6* with both compounds. A comparable increase in expression of *HOXB9* is demonstrated between EC23 and ATRA at high concentrations. There seems to be a concentration dependent co-linearity between *HOXB1* and *HOXB9* at this time point. Data represent mean ± SEM, n=3.

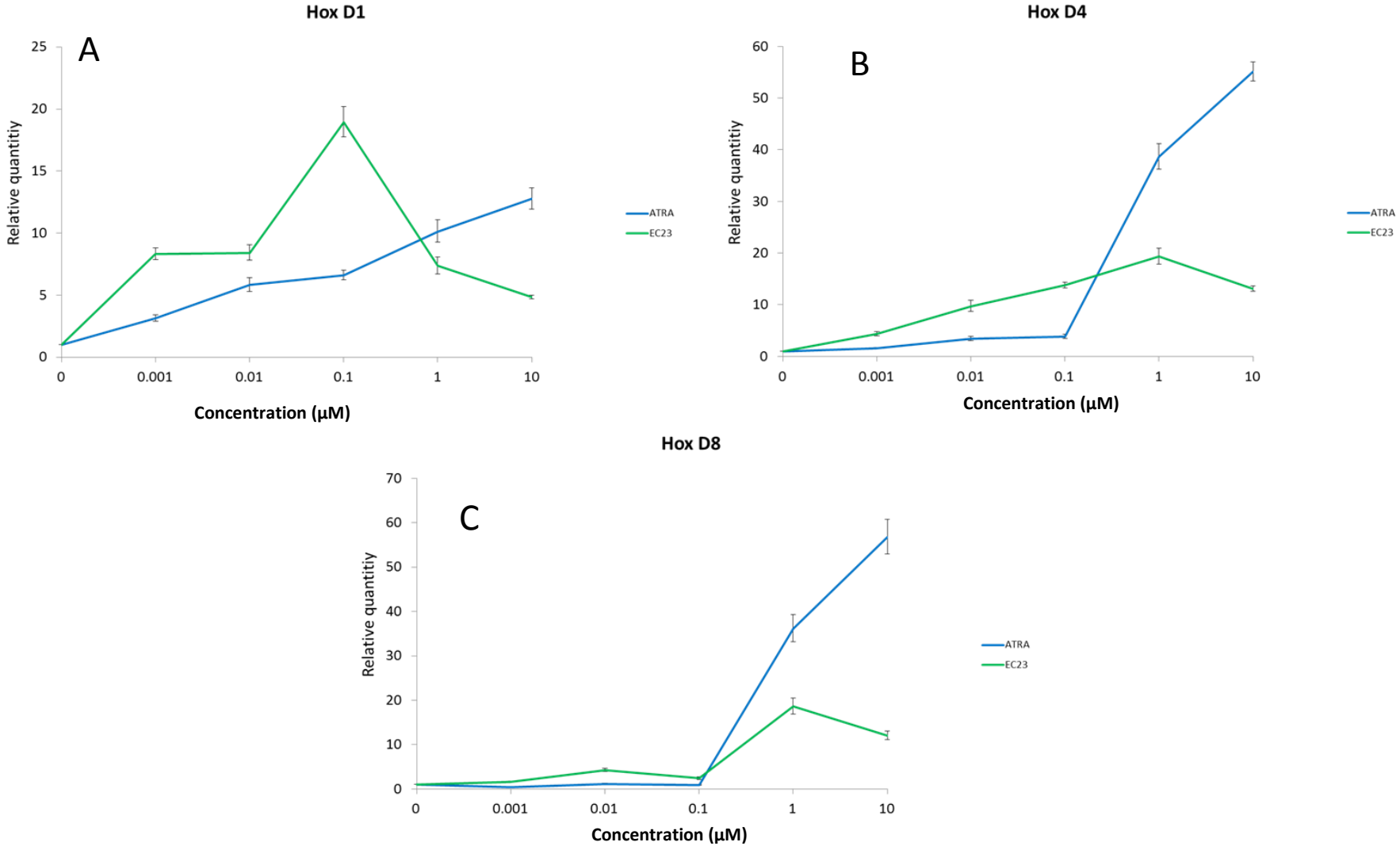

Figure 3-26 Regulation of *HOXD1, D4* and *D8* by EC23 and ATRA is concentration dependent. TERA2.cl.SP12 cells were treated with 0.001 µM, 0.01 µM, 0.1 µM, 1 µM or 10 µM for 3 days. RNA was extracted and purified and using real time PCR the relative expression change of *HOXD1* (A), *HOXD4* (B) and *HOXD8* (C) was measured. Data demonstrates a peak of *HOX*D1 expression by 0.1 µM EC23, however ATRA induces a linear dose response. ATRA induced a large increase in the relative expression of *HOXD4* and *HOXD8* at 1 µM and 10 µM. In comparison *HOXD4* was induced by EC23 at each concentration tested, however to a much lower level increase than the maximum induced by ATRA. EC23 induced *HOXD8* expression at 1 µM and 10 µM but levels were much lower than ATRA. Similar expression patterns were demonstrated between *HOXD4* and *HOXD8* possibly indicating a link between their regulation. Data represent mean ± SEM, n=3.

After a further 72 hours of treatment with EC23 or ATRA at 0.001 µM - 10 µM mRNA expression was determined of the 9 *HOX* mRNA transcripts described previously. Again the genes were from three *HOX* gene clusters A, B and D, and represented 3' and 5' genes within each cluster.

The expression of *HOXA1* was induced at the lowest concentration of both EC23 and ATRA (Figure 3-27). EC23 induced much more expression in the cells at low concentrations than ATRA, however, ATRA induced similar levels at 1 µM to EC23 but higher levels at 10 µM then EC23. Although relative to ATRA *HOXA5* was induced to low levels by EC23, the overall relative change from base line was high, indicating some level of regulation, however, much higher levels of *HOXA5* were induced by 10 µM ATRA in comparison to EC23. The same pattern as *HOXA5* was seen with *HOXA6* and however, the relative increase in transcript number was much less. This may be due to the downstream regulation of *HOXA6* by *HOXA5* indicating co-linear expression. Increasing the time of treatment may well induce much higher levels of 5' *HOXA6*.

Genes on the *HOXB* cluster measured were *HOXB1*, *HOXB6* and *HOXB9* which are spread from 3' to 5' along the cluster. Data demonstrate that this cluster is highly regulated by the concentration of both EC23 and ATRA (Figure 3-28). *HOXB1* was expressed highest at 0.001 µM and 0.1 µM EC23 and ATRA, indicating a highly sensitive RARE within the promoters, since increasing the concentration further resulted in a decrease in expression a negative feedback mechanisms may be in place. *HOX B6* was induced by 0.01 µM-10 µM EC23 with peak expression at 0.1 µM and ATRA induced expression maximally at 1-10 µM. The 5' *HOXB9* gene which would be expected to be least responsive to retinoic acid stimulation was expressed at high levels by 1-10 µM EC23 and ATRA, with little or no expression at lower concentrations. The three genes investigated on *HOXB* are induced by EC23 by concentration dependent regulatory mechanisms. Finally, the regulation of genes *HOXD1*, *D4* and *D8* from the *HOXD* cluster, after 6 days treatment demonstrated a pattern similar to that after 3 days treatment, with both EC23 and ATRA. However, the level of relative expression was much higher after 6 days. This indicated that the number of transcripts increases in a temporal manner; however, the relative change is not greater in 3' genes than 5' genes. This may be since there is a low level of 3' *HOX* gene expression in undifferentiated cells making any relative change from base line less pronounced. Due to the concentration effects on *HOX* genes by retinoids described here it is likely that regulation of *HOX* genes is through concentration dependent regulation, in addition to a co-linear temporal response.

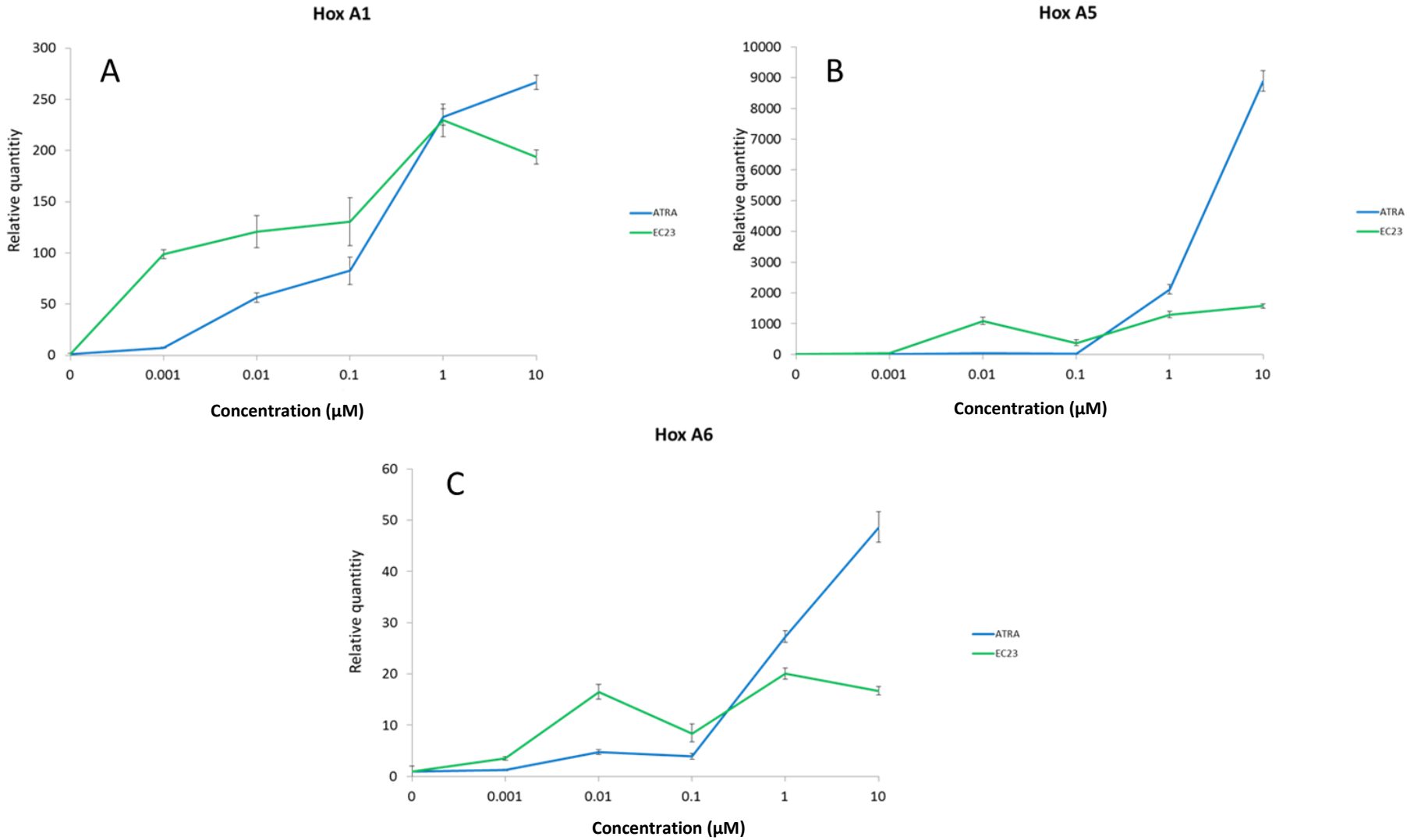

Figure 3-27 Regulation of *HOXA1, A5* and *A6* concentration dependent expression induced by EC23 or ATRA. TERA2.cl.SP12 cells were treated with 0.001 µM, 0.01 µM, 0.1 µM, 1 µM or 10 µM for 6 days. RNA was extracted and purified and using real time PCR the relative expression change of *HOXA1* (A), *HOXA5* (B) and *HOXA6* (C) was measured. Increased expression of *HOXA1* was seen at all concentrations of ATRA and EC23 with a gradual increase with concentration, higher levels were induced at concentrations of 0.001 µM, 0.01 µM and 0.1 µM EC23 than ATRA. *HOXA5* and *HOXA6* showed a similar pattern of expression at each concentration of ATRA and EC23, however the expression of both was induced much higher with ATRA than EC23 at 1 µM and 10 µM. Data represent mean ± SEM, n=3.

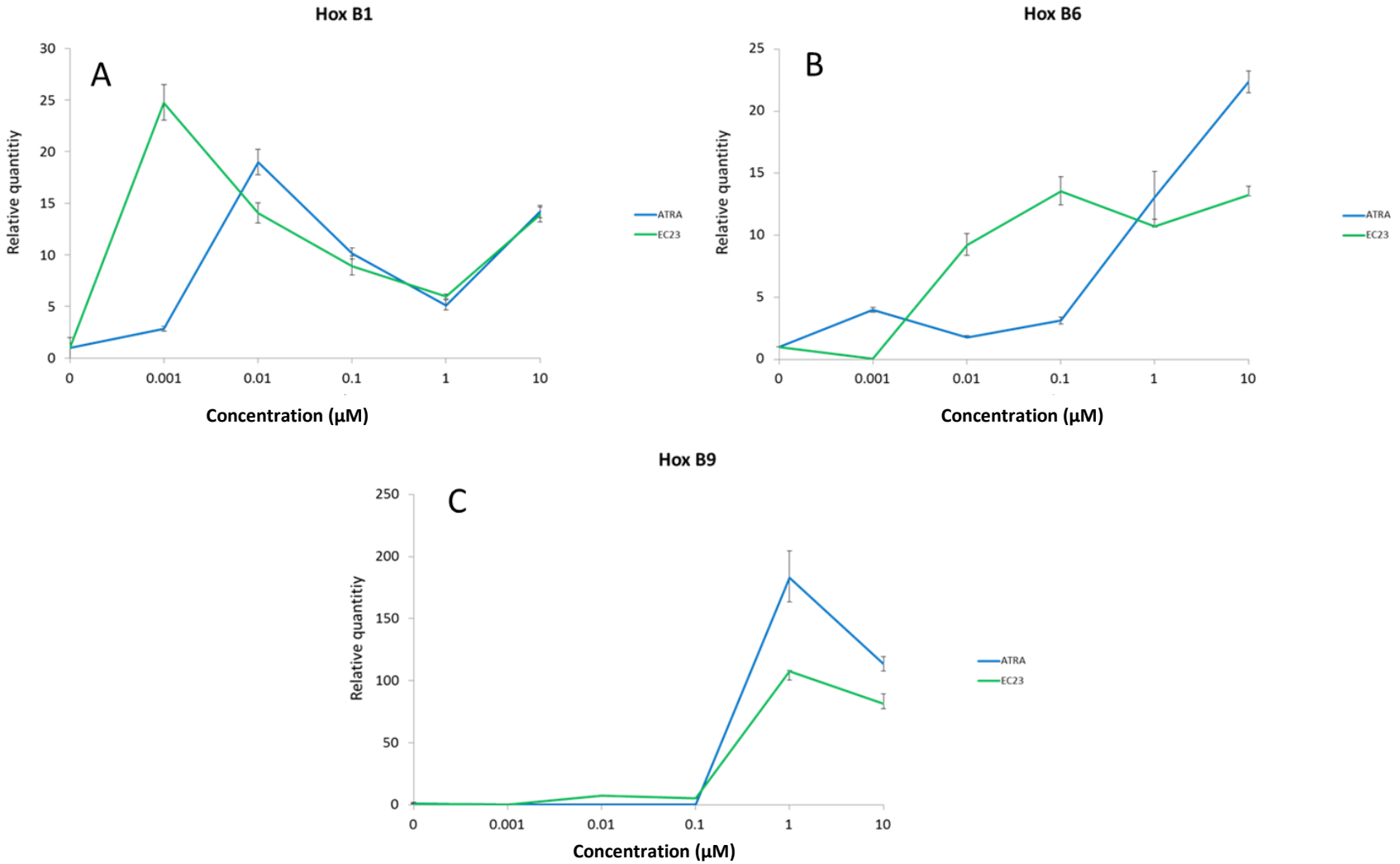

Figure 3-28 Regulation of *HOXB1, B6* and *B9* concentration dependent expression induced by EC23 or ATRA. TERA2.cl.SP12 cells were treated with 0.001 µM, 0.01 µM, 0.1 µM, 1 µM or 10 µM for 6 days. RNA was extracted and purified and using real time PCR the relative expression change of *HOXB1* (A), *HOXB6* (B) and *HOXB9* (C) was measured. Both EC23 and ATRA induced a shift in expression between 3' *HOXB1* to more 5' *HOXB6* and *HOXB9*. Similar patterns of expression were seen between EC23 and ATRA for *HOXB1* with high levels induced at the lowest concentrations. Some differences were observed between EC23 and ATRA at inducing *HOXB6* expression, EC23 induced much higher levels than ATRA at 0.01 µM and 0.1 µM. The 5' *HOXB9* gene was only expressed at 1 µM and 10 µM of both ATRA and EC23, similar pattern of expression was demonstrated between ATRA and EC23. These data clearly demonstrate a difference in concentration induced expression from 3' to 5' *HOX* genes on cluster B. Data represent mean ± SEM, n=3.

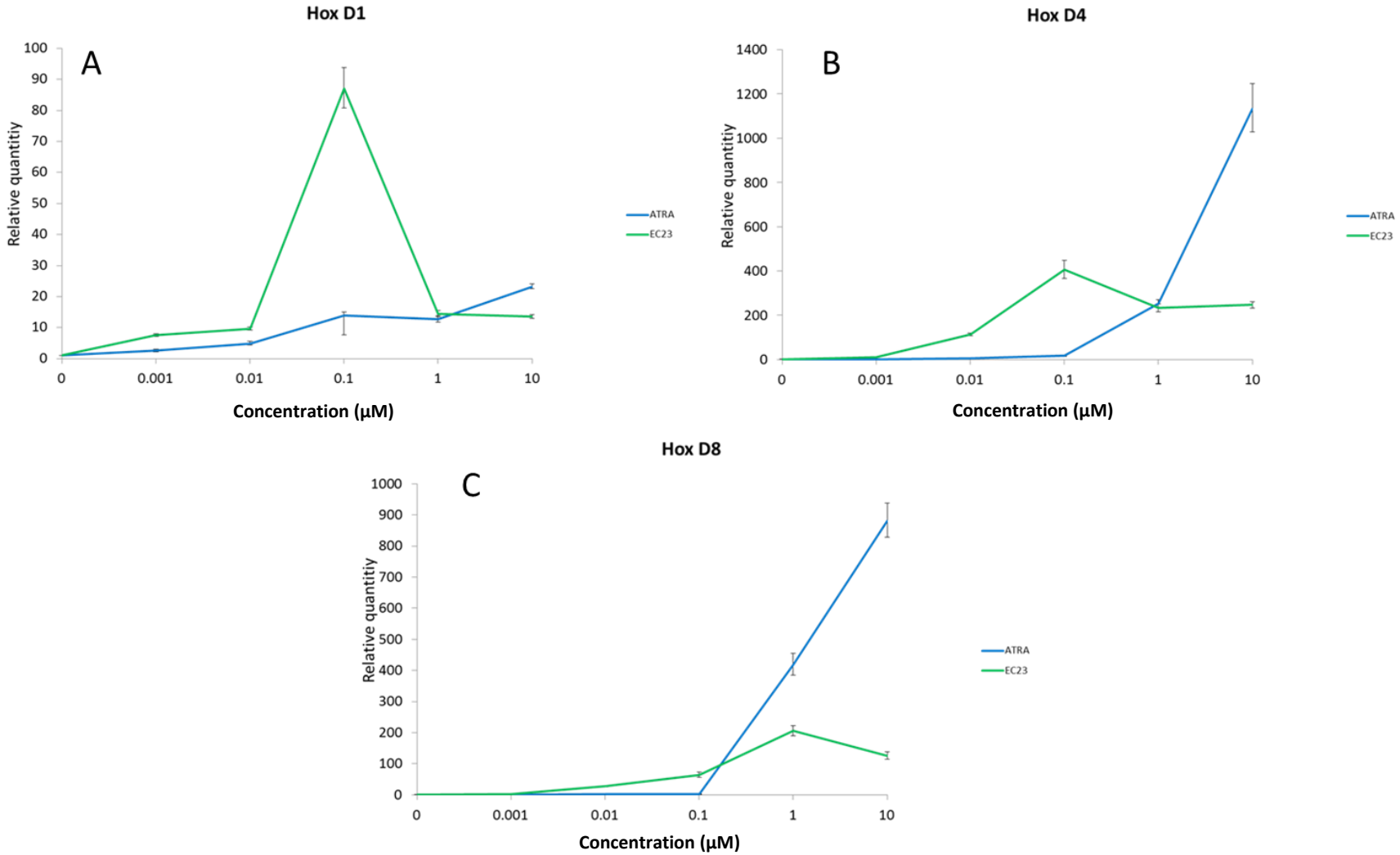

Figure 3-29 Regulation of *HOX D1, D4* and *D8* by EC23 and ATRA is concentration dependent. TERA2.cl.SP12 cells were treated with 0.001 µM, 0.01 µM, 0.1 µM, 1 µM or 10 µM for 6 days. RNA was extracted and purified and using real time PCR the relative expression change of *HOXD1* (A), *HOXD4* (B) and *HOXD8* (C) was measured. Data demonstrates a large peak of *HOXD1* expression by 0.1 µM EC23, however ATRA induces a linear dose response with much a much lower fold increase. ATRA induced large a large increase in the relative expression of *HOXD4* and *HOXD8* at 1 µM and 10 µM. In comparison *HOXD4* was induced by EC23 at each concentration tested excluding 0.001 µM, however to a much lower level increase than the maximum induced by ATRA. EC23 induced *HOXD8* expression at 0.1 µM, 1 µM and 10 µM but levels were much lower than ATRA. Similar expression patterns were demonstrated between *HOXD4* and *HOXD8* possibly indicating a link between their regulation. Data represent mean ± SEM, n=3.

3.2.6 Synthetic modulation of the dorsal-ventral axis during neural differentiation

The homeodomain containing gene *PAX6* has been demonstrated to be involved in neural subtype specification of hindbrain, spinal cord V1 interneuron and somatic motor neurons. Interneuron and motor neurons develop in the ventral part of the CNS [203, 204], therefore morphogens that provide ventral position identity to developing neural stem cells will express markers of interneuron or motor neurons. As described earlier EC23 and ATRA induce the expression of *PAX6* mRNA in stem cells that differentiate into neurons, furthermore, the concentration of each retinoid appears to influence the level of *PAX6* expression in the cell population. It is unknown how retinoic acid concentration affects ventral neural subtype identity.

In this model ventral specification signals are provided to cells via the morphogen sonic hedgehog (Shh). Sonic Hedgehog is produced by the notochord in the developing neural tube and acts in a concentration dependent way to specify either *NKX2.2* interneuron fate or *ISL1*+ motor neuron identity.

This study aimed to use a single concentration of the synthetic Shh agonist Purmorphamine (1 µM) from day 6 to induce ventralisation of differentiating TERA2.cl.SP12 stem cells. Using the neural subtype specific markers *ISL1*, *HB9* and *NKX2.2* to monitor specific ventral neural commitment varying concentrations of retinoid were investigated for their influence on ventral subtype identity.

Initially cells were treated with either 0.1 µM, 1 µM or 10 µM EC23 or ATRA for 6 days. At day 6 a single 1 µM concentration of Purmorphamine was added to the culture to ventralise the cells. Cultures were maintained for a further 8-22 days. The expression profile of *PAX6* mRNA (Figure 3-30) was typical of that expected during differentiation. As before, EC23 induced a peak expression of *PAX6* at 0.1 µM at day 6, but reduced from day 14-21 to levels similar to that induced maximally by 1 µM EC23. Only low levels of *PAX6* expression were induced throughout by 10 µM EC23. ATRA induced *PAX6* expression maximally after 6 days in cells treated with 1 µM and 10 µM but by day 14-21 expression reduced to levels induced by 0.1 µM ATRA. These data suggest for neural differentiation a reduction in *PAX6* is necessary. It may be however, that those concentrations of EC23 that maintain a higher level after 14-21 days induce commitment of different neural subtypes than the lower levels of expression.

Low mRNA levels of the motor neuron marker *HB9* were detected throughout the culture period up to 28 days at each concentration. EC23 demonstrated very little variability in expression between concentrations, whereas ATRA induced maximal expression at 10 µM (Figure 3-31). After 14 days 0.1 µM and 10 µM treated cells were stained for *HB9* protein (Figure 3-32) only low nuclear expression was detected, however, more immune-reactivity was seen in cells treated with retinoid and Purmorphamine than Purmorphamine alone.

Since *HB9*+ cells can give rise to both interneuron and motor neurons the relative mRNA expression of two more markers specific for either motor neuron identity (*ISL1*) or V1 interneuron (*NKX2.2*) was measured at each 0.1-10 µM EC23 or ATRA treated cells after 21 days.

Data demonstrates a differential expression of both *NKX2.2* and *ISL1* expression dependent on the concentration (Figure 3-33). Only high concentrations of ATRA and EC23 induced *ISL1* expression in the cells, this is in contrast to *NKX2.2* where cells treated with 0.1 µM of EC23 or ATRA induced a higher level of expression than at 10 µM. A similar pattern was also demonstrated at 1 µM EC23, indicating that retinoid signalling may influence interneuron and motor neuron fate.

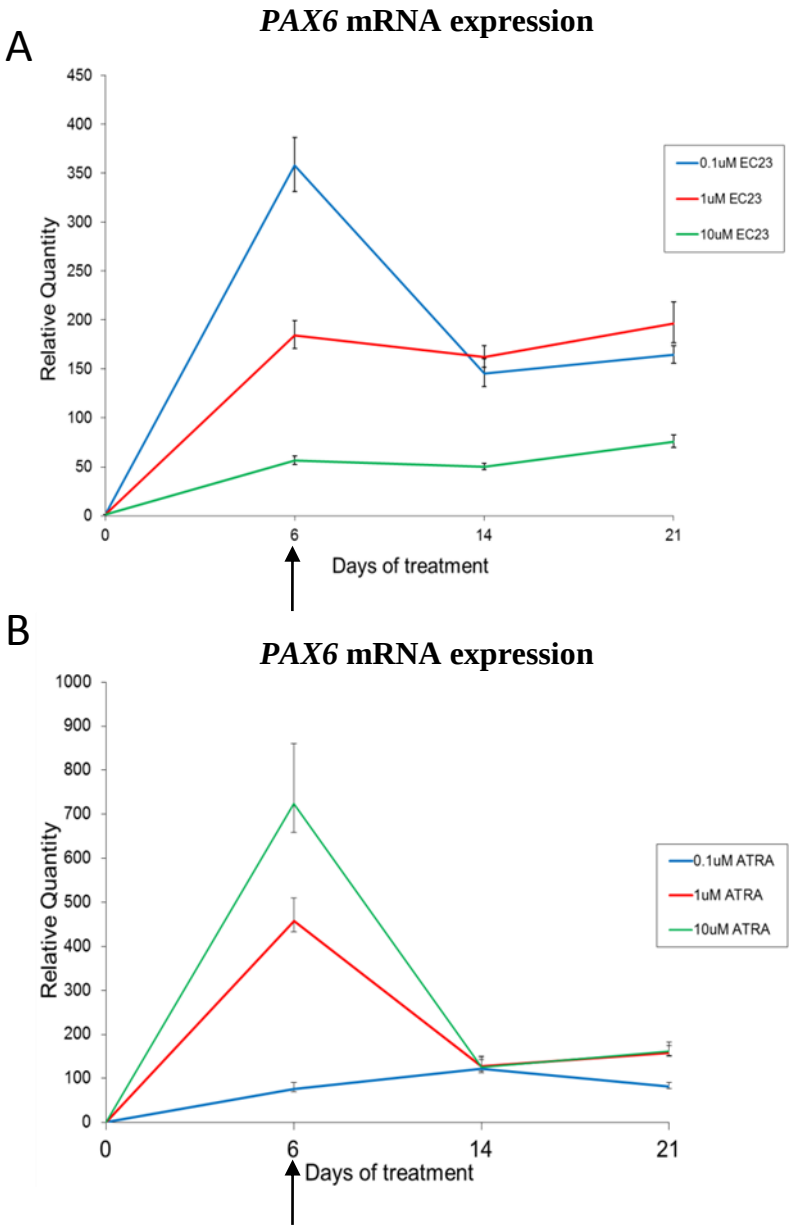

Figure 3-30 Regulation of *PAX6* gene expression during TERA2.cl.SP12 cell differentiation with EC23/ATRA and Purmorphamine. Monolayer cultures of TERA2.cl.SP12 cells were treated with 0.1 µM, 1 µM and 10 µM EC23 (A) or ATRA (B) for 21 days. At day 6 Purmorphamine was added to the culture media and continued to day 21. Arrows mark point at which Purmorphamine is added to the culture media. mRNA expression was measured at day 0, 6, 14 and 21. Data demonstrate the loss of *PAX6* expression as the cells differentiate past day 6. Data represent mean ± SEM, n=3.

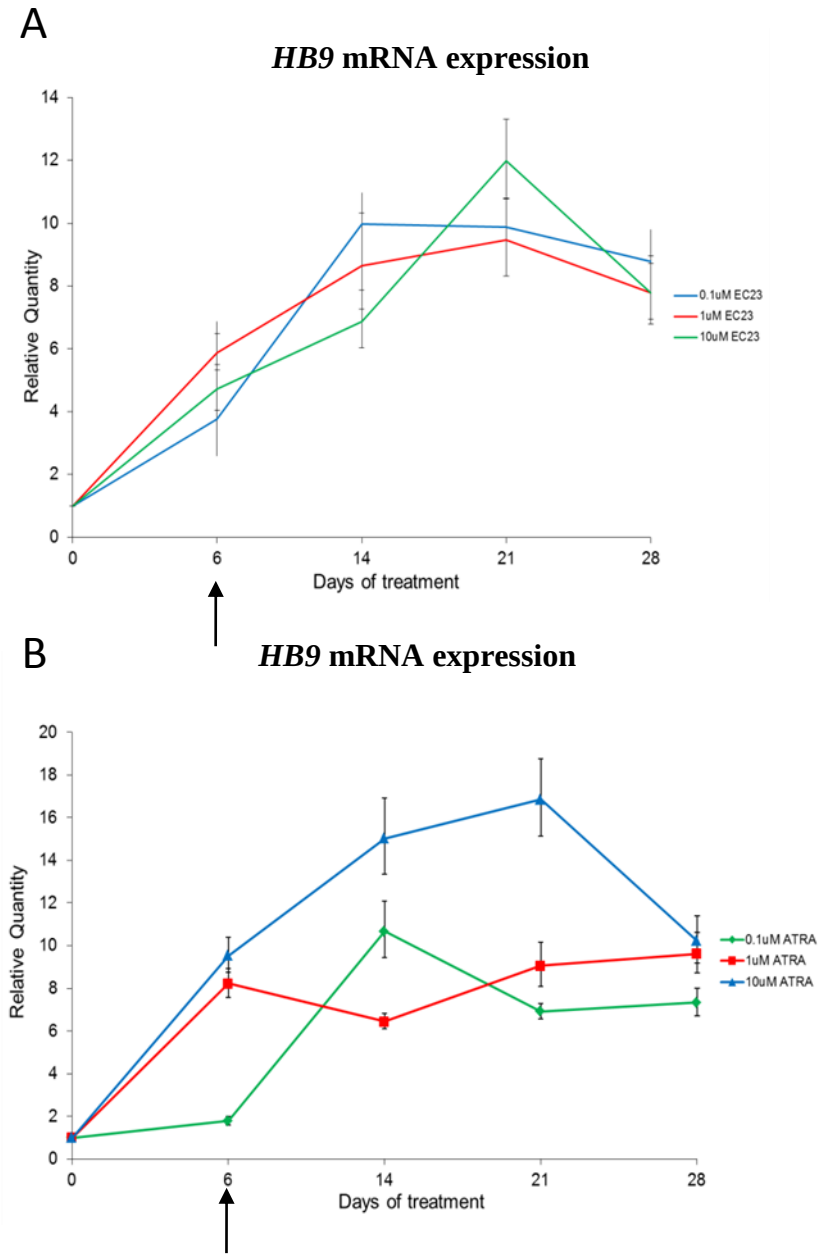

Figure 3-31 Regulation of *HB9* gene expression by real-time PCR during TERA2.cl.SP12 differentiation by EC23/ATRA and Purmorphamine. Monolayer cultures of TERA2.cl.SP12 cells were treated with 0.1 µM, 1 µM and 10 µM EC23 (A) or ATRA (B) for 28 days. At day 6 Purmorphamine was added to the culture media and continued to day 28. mRNA expression was measured at day 0, 6, 14, 21 and 28. Arrows mark point at which Purmorphamine is added to the culture media. Data demonstrate increasing level of *HB9* expression throughout differentiation indicating a ventral phenotype of the differentiating neurons. Data represent mean ± SEM, n=3.

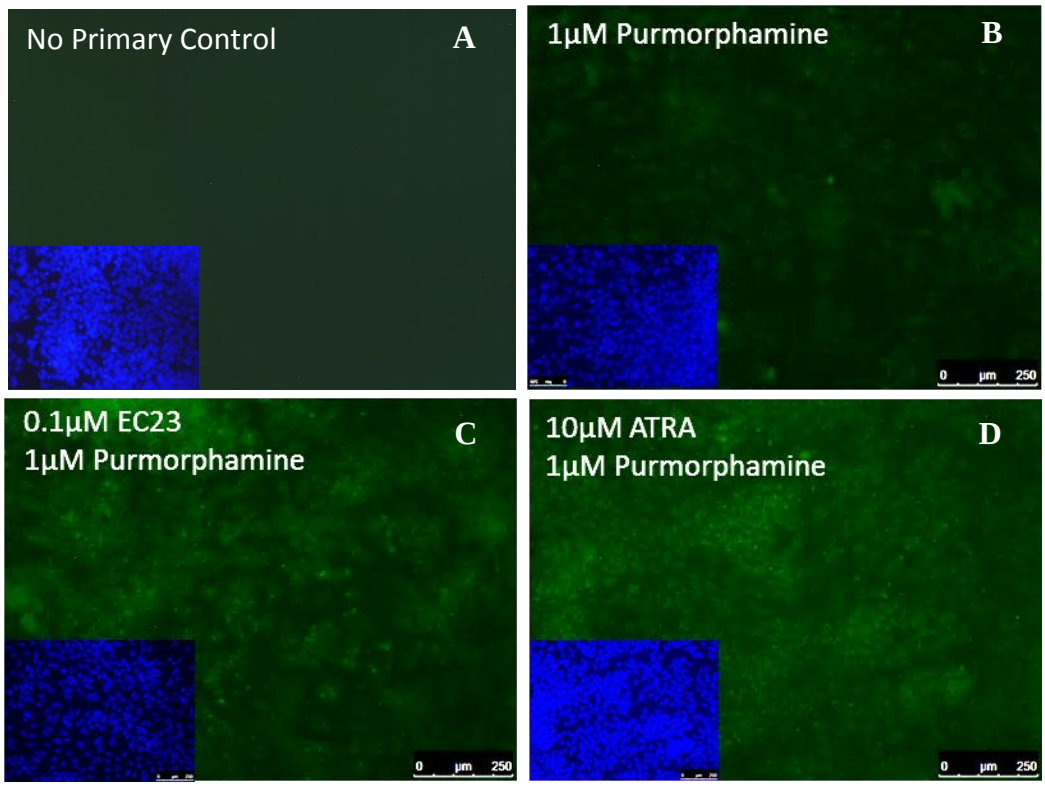

Figure 3-32 *HB9* expression in TERA2.cl.SP12 cells during differentiation. Cells were treated for 14 days with 1 µM Purmorphamine (B) or EC23 (C)/ATRA (D) for 6 days followed by the addition of 1 µM Purmorphamine for a further 8 days. Cells were stained with a *HB9* specific antibody. Some nuclear staining for *HB9* was detected in the cultures containing either ATRA or EC23 however not in the Purmorphamine only control. n=3.

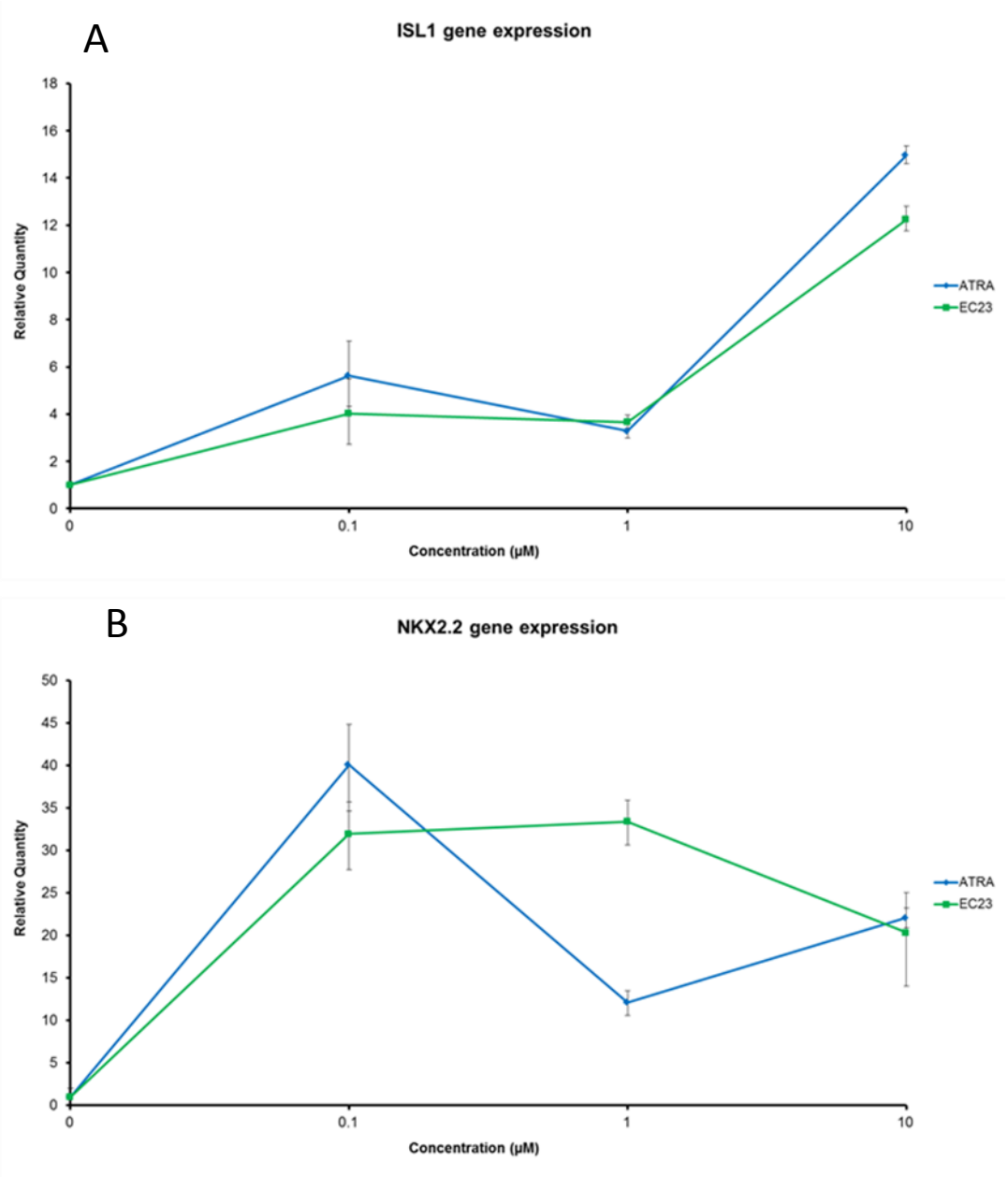

Figure 3-33 Concentration dependent regulation of gene expression associated with ventral neural progenitors in TERA2.cl.SP12 cells differentiated with EC23/ATRA and Purmorphamine. TERA2.cl.SP12 cells were treated with 0.1 µM, 1 µM and 10 µM EC23 or ATRA for 21 days. At day 0 the undifferentiated cells were given a relative quantity of 1.0. From day 6, 1 µM Purmorphamine was included in the culture media. Expression of *ISL1*, a motor neuron associated gene was maximally expressed at 10 µM of both EC23 and ATRA. In comparison the ventral interneuron marker *NKX2.2* was expressed maximally at 0.1 µM by both compounds and decreased as concentration was increased. Data represent mean ± SEM, n=3.

3.3 DISCUSSION

Directed differentiation of pluripotent stem cells is necessary to advance areas of cell biology and regenerative medicine. As the understanding of how external signals affect stem cell fate the focus of using the stem cell-derived neurons for investigating disease and developmental pathways becomes more physiologically relevant. Furthermore, there is scope for direct implantation of specific neural subtype progenitors to treat disease such as Parkinson's. Differentiating human stem cells into a neural progenitor fate using small lipophilic molecules is an attractive method of achieving a high yield of neural progenitors and mature neurons from stem cells for use in such application.

Modulation of know developmental pathways can influence cell fate decisions, synthetic small molecules that engage with these pathways can be designed to be more potent, stable and more specific, guiding cells more efficiently and accurately. Designing small molecules that affect biological signalling pathways in this way requires knowledge of the compound and its effects in multiple stem cell systems. In addition the combination of small molecules both temporally and synergistically will no doubt be required to facilitate the most specific and optimum neural differentiation of human stem cells for regenerative medicine.

3.3.1 Induction of differentiation and neural commitment by EC23 and ATRA

Loss of pluripotency induced by EC23 and ATRA

The cell surface antigens globoseries stage specific embryonic antigen 3 (SSEA3) and Keratin-sulfate-associated-glycoprotein surface marker (TRA-1-60) have been demonstrated to be specific for an undifferentiated cell phenotype in both hES and hEC cells [82, 205-207]. Furthermore, SSEA3 has been used to separate the undifferentiated hES and hEC stem cell niche from a population of differentiated heterogeneous cells, indicating the specificity of this cell surface antigen for pluripotency [84, 207]. As well as cell surface markers, expression of certain genes have also been used to separate pluripotent and committed cells – both *OCT3/4* and *NANOG* are well documented for their ability to determine pluripotency.

The results from this study demonstrate that as published previously, ATRA induces down regulation of both SSEA3 and TRA-1-60 in the EC cell TERA2.cl.SP12 at concentrations

of 10 μM and 1 μM over 6 days of treatment [95], however, at concentrations of 0.1-0.001 μM the differentiation capability of ATRA is significantly reduced (Figure 3-2).

The cell surface antigens SSEA3 and TRA-1-60 are good overall markers of an undifferentiated phenotype, however, due to the post-translational processing required prior to expression of these proteins at the cell surface, small changes in pluripotency induced by low levels of retinoid may not be detected until after 6 days. Therefore, to assess more accurately the effect of low concentrations of ATRA and EC23 on TERA2.cl.SP12 differentiation the relative mRNA levels of transcription factors *OCT4* and *NANOG* was determined using RT-PCR (Figure 3-3). *OCT4* and *NANOG* are well described in the literature as 'gate keepers' of the pluripotency phenotype, their expression is required to maintain and induce pluripotency therefore a suppression of their expression is indicative of differentiation [208]. The results from this study demonstrate that both EC23 and ATRA induce suppression of the transcription factors *OCT4* and *NANOG* at 10 μM and 1 μM, however, below these concentrations ATRA induces only moderate suppression, whereas, EC23 induces a high level of suppression up to 0.01 μM, indicative of its high potency.

The data in this section agree with published data on EC23 and ATRA. Both can induce neural differentiation of stem cells. Both ATRA and EC23 have been shown to induce differentiation of TERA2.cl.SP12 EC cells and Human embryonic stem cells [90, 92]. This study investigated the concentration dependent role of EC23 and ATRA during differentiation of TERA2.cl.SP12 and although EC23 has not been demonstrated to be active at the concentrations used in this study below 1 μM there was a differential effect observed with concentration. It is well documented in the literature that retinoic acid signalling *in vivo* acts via concentration dependent mechanisms [31, 34], therefore understanding these effects *in vitro* with the synthetic analogue of ATRA, EC23 was important for its characterisation. It has been shown recently that EC23 induces RAR activation in a concentration dependent manner which is different to ATRA and other molecules. Firstly, EC23 induces a much higher activation than many other retinoids including similar synthetic analogues of ATRA such as TTNPB and secondly, EC23 has maximal receptor activation at 0.1 μM, fitting in well with data described in this thesis [93].

Neural differentiation induced by EC23 and ATRA

The EC cell TERA2.cl.SP12 is a well characterised model of *in vitro* neural differentiation and has been shown in multiple studies to differentiate into mature neurons through treatment with ATRA. The cell line is thought to represent pluripotent cells of the early ectoderm, hence, differentiates into CNS neurons, Glial cells and neural-epithelia [84]. To determine the effect of concentration on neural lineage commitment the percentage expression of a cell surface antigen, A2B5 was determined in cells treated with concentrations 0.001-10 μM ATRA for 3 and 6 days.

Monoclonal antibodies raised against the glycoside antigen A2B5 has been described in many models as a marker of early neural commitment and is thought to be a marker of neural progenitor cells [85, 209]. High levels of A2B5 expression is demonstrated on the cell surface membrane of Oligodendrocyte progenitors and neural stem cells, furthermore, A2B5 antibodies can be used to isolate neural stem cells from animal tissue. In this study expression of A2B5 was indicative of neural commitment and was used to determine the activity of small molecules aimed at inducing neural lineage differentiation. As with what was seen with the loss of pluripotency markers, ATRA induced the highest percentage expression of A2B5 at 10 μM and this decreased with concentration (Figure 3-4). In contrast EC23 induced high levels of A2B5 expression at concentrations from 0.01 μM-10 μM, again exemplifying the enhanced potency of EC23. These data are in broad agreement with previously published data on EC23 [89, 90].

PAX6 is a pan-neuronal marker, expression of *PAX6 in vivo* is found throughout the spinal cord [210] and during retinal neural progenitor development [211]. *PAX6* expression is found in discrete areas of the CNS and provides ventral positional cues to developing neural cells induced through controlled feedback between SHH and BMP signalling [203, 212]. In combination with other transcription factors such as *OLIG2* and *ISL1*, *PAX6* can be used to distinguish neuroprogenitor cells and their potential differentiation fate [213, 214].

In this study *PAX6* mRNA levels were measured in the same cells used for flow cytometry at day 3 and 6 of EC23 or ATRA supplementation. As expected a concentration dependent increase was observed in cells treated with ATRA after 6 days, a 5 times increase in expression was measured between 10 μM and 1 μM indicating that ATRA induced neural commitment in the TERA2.cl.SP12 EC cells as described in previous publications. The

concentration-activity relationship demonstrated by ATRA linear, indicating as more receptors were activated the more *PAX6* mRNA was transcribed.

In contrast to the relationship of concentration observed with EC23 expression with the antigens SSEA3, TRA-1-60 and the transcription factors *OCT4* and *NANOG*, the expression of *PAX6* gene transcription was optimum at 0.1 μM. This may reflect a negative feedback loop that occurs with high concentrations of retinoid signalling, however, due to the effect of high concentrations of ATRA on cell survival it is not possible to demonstrate this with ATRA. Protein levels of *PAX6* observed by immunocytochemical staining after 6 days treatment with 10, 1, or 0.1 μM, EC23 or ATRA demonstrated high expression at 0.1 μM EC23 and 10 μM ATRA (Figure 3-6). Furthermore, the expression of translational products was located at areas of high cell density, representing areas most likely to become neuronal, this effect of cell density has been observed recently [171]. High levels of *PAX6* mRNA are indicative of good neural commitment during the early stages of differentiation. Maintaining high levels provides positional cues to developing neural progenitors to form ventral neural subtypes. Although it is difficult to determine that the observed differences in *PAX6* expression at each of the retinoid concentrations will result in a different phenotype it does suggest that the cells with high *PAX6* expression would be more likely to become motor neurons than cells with an initially low *PAX6* mRNA level [215, 216].

This section described how EC23 and ATRA induce a similar response in TERA2.cl.SP12 EC cells at 10 μM and 1 μM. The response indicates neural differentiation of the cells that has been described by Christie, V.B et al (2008) [95]. The biological effect of EC23 remains high at the concentrations of ATRA which showed limited biological activity. Furthermore, EC23 can induce mature neuronal differentiation at much lower concentrations than ATRA demonstrating a correlation between potency during initiation of differentiation and maturation of the neural progenitor cells into neurons. Whether or not EC23 signalling is required throughout the complete neural differentiation protocol is unknown; however, it is likely that as with ATRA a minimum of 12 days treatment is required [171]. In addition these results suggest that treatment with concentrations of 10 μM and 1 μM EC23 may not be optimum in TERA2.cl.SP12 for inducing neural lineage commitment, this is supported by flow cytometry data published by Christie V,B et al (2008) [95] demonstrating an enhanced effect of EC23 at 1 μM compared to 10 μM (0.1 μM was not tested). The expression of *PAX6* mRNA in this study demonstrates the most striking increase at an individual concentration. The decrease in *PAX6* mRNA expression

at concentrations above 0.1 μM may be a result of negative feedback pathway not normally seen with ATRA.

Neurite formation and the morphology of differentiated neurons were assessed after 21 days culture in TERA2.cl.SP12 EC cells treated with 0.01, 0.1, 1 and 10 μM EC23 or ATRA. Staining fixed cells for the cytoskeletal protein, β III Tubulin demonstrated neurite formation by cells differentiated with 0.01-10 μM EC23 and 0.1-10 μM ATRA (Figure 3-7). Cells treated with 0.01 μM ATRA and 0.001 μM EC23 and ATRA became over confluent and were disposed. To visually assess the heterogeneity between concentrations and compounds a non-neuronal cytoskeletal protein was also stained for, cytokeratin 8 staining demonstrated that at low concentration of ATRA there was in increase in epithelial like plaques (Figure 3-9). Quantification of β III Tubulin protein using western blot from cells treated with 0.1, 1 and 10 μM EC23 or ATRA for 21 days demonstrated a higher level of neural protein in EC23 treated cultures. A robust and reproducible method for inducing neural differentiation from TERA2.cl.SP12 cells by EC23 is included in Chapter 2 (Methods) and can be used to investigate many of the molecular processes that occur during stem cell differentiation *in vitro*.

In summary this section demonstrated the ability of EC23 to induce neural differentiation of human stem cells with greater potency than its natural analogue ATRA. Therefore, the use of this stable synthetic molecule is useful as a replacement for ATRA, however, the concentration that it is used should be considered if used for comparative studies with ATRA.

3.3.2 Testing the role of metabolism as a mechanism to explain the apparent increased potency of EC23 during EC cell differentiation

ATRA is oxidised by the cytochrome P450 family 26 group of enzymes, the oxidisation products are either excreted, have less biological activity or are further metabolised. Therefore, this process reduces the bioavailability of ATRA and hence, reduces the effects of low concentrations. This section aims to investigate the role of retinoic acid oxidation on the increased potency of EC23 and determine if the loss of biological activity demonstrated in Section 3.1 with low concentrations of ATRA can be rescued by inhibiting this process.

To investigate the role of retinoid metabolising enzymes on EC23 induced differentiation the cytochrome P450 enzyme (CYP) family 26 (CYP26), was inhibited using the pan CYP

inhibitor, Liarozole Fumarate. Studies have demonstrated that Liarozole can enhance the effects of low concentration of retinoid in mouse EC and mouse limb bud cells, presumably through inhibition of ATRA metabolism [66, 217]. ATRA is oxidised by the family of CYP26 enzymes into the products of metabolism shown in Figure 1.3, therefore, inhibition of this process should increase the amount of ATRA available to bind the RAR. Many of the ATRA oxidation products have been shown to have biological effects [218], however, there has been no data relating to treatment of human EC cells with Liarozole and the effect of Liarozole on increasing the ability of low concentrations of ATRA to induce neural differentiation.

Figure 3-9 demonstrates the effect of Liarozole on TERA2.cl.SP12 differentiation through flow cytometric analysis of SSEA3, TRA-1-60 and A2B5. Cells were treated with 10 μM Liarozole for 6 days with and without 0.1 % DMSO v/v, to assess the effect of Liarozole alone on the stem cells. There was no change in expression of the cell surface glycoproteins after 6 days compared to the undifferentiated control. Preliminary studies demonstrated that consistent with Liarozole concentrations used in the mouse F9 teratocarcinoma cell line. In the study 1-10 μM Liarozole inhibited CYP26 activity sufficient to demonstrate increased ATRA response [66], importantly Liarozole was not shown to have any retinoid like properties.

The effect of Liarozole on the potency of ATRA and EC23

In Figure 3-11, 10 μM of Liarozole induced an enhancement of EC cell differentiation at concentrations of ATRA that were shown previously to have little or no effect on pluripotency. Flow cytometry of EC cells treated with 0.01 μM and 0.1 μM ATRA demonstrated suppression of SSEA3 and TRA-1-60. Furthermore, at these concentrations expression of A2B5 was enhanced, indicating neural lineage commitment in these cells. Treatment with Liarozole enhances the activity of ATRA at these concentrations and the enhancement results in similar activity (as assessed by these markers) to EC23, alone. These data also indicates that metabolites of ATRA are unlikely to contribute to the differentiation inducing potential of ATRA, since prevention of oxidation products results in an enhanced potency of ATRA. As has been described by the use of clinically and in models of ATRA potency, the addition of Liarozole results in enhancement of the biological activity of ATRA [62, 66]. This is the first time Liarozole has been shown to enhance the biological activity of ATRA in human stem cells. This model can be used to assess other retinoid analogues for the effect of metabolism on their biological activity.

This model was therefore also used to assess the role of metabolism on the biological activity of EC23. Stem cells were treated with 0.01, 0.1 and 0.001 μM EC23 for 6 days. The cells were then analysed as described previously for cell surface glycoproteins indicative of loss of pluripotency and neural commitment. As was known previously treatment with EC23 induced differentiation at concentrations 0.01 and 0.1 μM and this was the same with and without Liarozole (Figure 3-12). However at 0.001 μM a concentration that did not induce differentiation in these cells, no enhancement was detected in the presence of Liarozole. This may suggest that EC23 is not oxidised by CYP26 and hence, inhibiting this group of enzymes did not contribute to any elevated intracellular binding of receptors. This correlated with structural data since the compound structure of EC23 is predicated not to have any of the oxidation sites found in ATRA.

The synthetic retinoid TTNPB has been demonstrated to have 1000 fold greater potency than ATRA and this increased potency is in part due to its resistance to metabolism and greater availability to bind RAR [201]. Therefore, it is likely that the increased potency of EC23 is due to its resistance to metabolism in this cell model. These data also suggest that the oxidation products of ATRA are not involved in the initiation of differentiation of hEC cells, as inhibition of their production enhances this process.

This section demonstrated that EC23 was not metabolised by cytochrome P450 enzymes, however, the biological activity of ATRA was enhanced by Liarozole indicating metabolism, as expected. Since inhibition of ATRA metabolism in the stem cells resulted in an enhancement of neural differentiation, it can be deduced that metabolites of ATRA do not contribute to the differentiation process. Furthermore, these data suggest the potency of EC23 may be due in part to its resistance to metabolism.

Pulsing of EC23 and ATRA

Since EC23 was demonstrated not to be metabolised by CYP enzymes it was hypothesised that a single dose pulse of EC23 would be sufficient to induce differentiation in the TERA2.cl.SP12 stem cells. A pulse of EC23 would remain within the cell cytoplasm, bound to cellular retinoic acid binding proteins and be constantly activating the retinoic acid receptors in the nucleus. It was unknown if the sequestering proteins, namely cellular retinoic acid binding protein (CRABP I) I would be in high enough concentration to prevent differentiation. Induction of the CRABP I, II and the cellular retinol binding protein I (CRBP I) by 10 μM EC23 has been demonstrated by Maltman, D et al (2009) [219], other proteins that were shown to be up-regulated by EC23 by neural specific

differentiation were Profilin and phosphorylated Stathmin which was similar to levels induced by 10 µM ATRA. Tongue, J.R. et al (2012) [171] indicated that a single dose of ATRA for ≤ 3 days in a similar EC cell line NTERA2.cl.D1 (a different TERA2 clone) was in-sufficient to induce large expressional change in the mRNA of the neuronal markers *PAX6* and *NEUROD1* – cells were maintained to 12 days after the initial ATRA dose. Data from this study also showed that *OCT4* and *NANOG* were still highly expressed in cells treated with ATRA for 1 day, furthermore, up-regulation of Endomesodermin a trophoblast and endoderm marker was detected in cells pulsed for ≤ 3 days indicating a differential lineage commitment in these cells similar to treatment with the small molecule EC19. Maximal A2B5 and *PAX6* expression was induced after a 12 day pulse of 10 µM ATRA treatment in NTERA2 EC cells which resulted in a high yield of neurons after 21 days similar to continuous supplementation with ATRA. Significantly lower neuronal yield of neuron was detected after a pulse of 6 days ATRA, even though stem cell markers were highly decreased and neural specific mRNA expression was increased significantly.

In this study cells were pulsed for 1 minute, 1 hour and 1 day or continuously by 0.1 µM or 1 µM, EC23 or ATRA. Cells were exposed to the compounds in cell culture media for the time required, washed in PBS once and cultured to 6 days in fresh media. As has been described earlier, cells were then analysed using live cell flow cytometry for the cell surface glycoprotein, SSEA3, TRA-1-60 and A2B5 (Figure 3-13 and Figure 3-14). The data from this section demonstrated that at 0.1 µM or 1 µM ATRA, continuous treatment was required for cell glycoprotein changes after 6 days which correlates well with published data [171]. In contrast EC23 induce significant expressional changes in SSEA3, TRA-1-60 and A2B5 after just 1 minute exposure to 1 µM and 1 hour exposure to 0.1 µM. Providing further evidence that EC23 is not metabolised in these cells and constitutively activates RAR signalling inducing cell differentiation.

The solvent DMSO is used to dissolve synthetic small molecules for transport across the cellular membrane, however, may affect cellular differentiation of both hES and hEC cells affecting the overall outcome when investigating specific small molecules and concentrations. Smith, S.C. et al 1987 [220] demonstrated that aggregation of the embryonic carcinoma stem cell line P19 and treatment with 1 % DMSO for 5-6 days results in endodermal differentiation into epithelial and cardiac tissue. A comparison between the effect of 1 % DMSO treatment and retinoic acid treatment in hES aggregates demonstrated a differential regulation of haematopoietic markers through Wnt dependent

signalling [221]. Although in these studies on hEC and hES cells the concentration of DMSO is around 10 x higher than that used throughout this thesis it may be that even small levels of DMSO can reduce the level of neural differentiation in TERA2.cl.SP12. The pulse effect of EC23 would be a suitable method for decreasing DMSO exposure; however, data showing terminal neural differentiation after 1 minute pulse would be required.

In this section the resistance of EC23 to metabolism was utilised to reduce the exposure of stem cells being differentiated to DMSO. Pulsing the cells with EC23 for one minute was sufficient to induce neural differentiation in this model. This was not demonstrated for ATRA. A minimum concentration and time of exposure was required for EC23 to induce differentiation. With further phenotypical data the pulse effect of EC23 may lead to an additional improvement to the optimised protocol in both hEC and hES cells.

3.3.3 Enhancing the potency of synthetic retinoids by incorporating a methyl group

The relationship between retinoid structure and biological activity is exemplified by the differential regulation of stem cell differentiation by the small molecules EC19 and EC23 [95]. The small change in chemical structure between EC19 and EC23 seemed to affect the receptor specificity of the molecules, making EC19 apparently less active than EC23. Development of panels of retinoid analogues has aided research and discovery into the retinoic structure-activity relationship, however, the model system use to investigate the cellular effects of each retinoid analogue is important [70]. For example, although EC19 is relatively inactive in TERA.2.cl.SP12 EC cells its receptor specificity and activity may be highly potent at inducing – for instance P19 endodermal differentiation. Recent insights have been available from receptor binding assays of retinoid analogues and provide a standardised method of investigating structure-activity relationships for RAR activity [93, 222].

Previous studies have demonstrated that methylation of the synthetic retinoid analogue TTNPB results in a 90° twist in conformation (Durham University, Chemistry Dept-Unpublished data); the twist allows the retinoid to access the L-shaped retinoid X receptor (RXR) which is not possible with the native TTNPB compound. Methyl-TTNPB takes on a more 9cis-RA conformation and activates biological signalling characteristic of RXR signalling [223]. In this part of the study a methyl group was added to the 3-Carbon position of both EC19 and EC23. Due to the inherent stability of the structure of EC19 and EC23 methylation would not change the conformation of the structures. Data in this

Chapter demonstrate that methylation of EC23 does not alter its activity; however, methylation of EC19 seems to increase its activity at high concentrations, inducing both genetic and cell surface expression of neuronal markers. The observed enhancement in EC19 activity after methylation may be the result of enhanced RAR binding.

3.3.4 Regulation of anterior-posterior patterning genes

The role of retinoids in establishing the anterior-posterior axis has been hypothesised to involve a gradient of retinoic acid activity such that genes responsible for conferring anterior positional identity are highly sensitive to retinoic acid signalling and hence, respond to low levels of retinoic acid. The converse is true for genes that confer posterior identity; hence retinoic acid treatment is generally used to induce posterior identity during cellular development. In the case of *HOX* genes there exists a concentration dependent and co-linear expression of the 39 genes in response to retinoic acid.

Aberrant expression of *HOX* genes has been shown to be induced by retinoic acid and leads to alterations in the anterior-posterior axis of the developing embryo, which inevitably results in altered differentiation of cells relating to their position along the AP axis. Alterations in *HOX* gene expression is one cause of the teratogenic effects seen with retinoic acid signalling and emphasises the importance of correct RA signalling during development [47].

Simeone A et al (1991) [48, 50] demonstrated through semi-quantitative analysis, that retinoic acid could induce co-linear and concentration dependent expression of *HOX* genes in the embryonic carcinoma stem cell NTERA2.cl.D1. The study detailed the time dependent regulation of *HOX* signalling in stem cells treated with retinoic acid. This provided a unique model to investigate the effect of retinoic acid on the expression of these genes and their role in embryogenesis. Little is known about how synthetic retinoids affect the expression of *HOX* genes and the role of concentration on *HOX* gene regulation.

In addition to *in vitro* modelling of *HOX* gene regulation, numerous animal models have utilised modern labelling techniques to investigate the barrier of *HOX* gene expression during development. Amirthalingam, G. et al (2009) [224] used whole-mount chick embryo *in-situ* hybridization to establish that flanking somites can up-regulate HoxB4, regulating the anterior patterning of the neural tube through a retinoic acid dependent mechanism. Furthermore, HoxB4 is associated with dorsalisation of neural tube via BMP4 signalling. This study demonstrate the regulation of one *HOX* gene by retinoic acid *in vivo*

and its ability to regulate-at least in part the developmental patterning of the chick neural tube [224].

Regulation of HOX genes by EC23 and ATRA

This study aimed to investigate the ability of the synthetic retinoid EC23 to regulate the co-linear, concentration dependent and temporal expression of *HOX* genes in the EC cell TERA2.cl.SP12 and compare the expression profiles to that of ATRA. Of the 39 *HOX* genes present on four clusters, 9 genes were assayed, the *HOX* genes chosen were from throughout the clusters of A, B and D, representing 3' and 5' genes some with known RARE and some without direct retinoic acid transcriptional regulation.

Cells were treated for 72 and 144 hours with either EC23 or ATRA. After 72 hours many of the genes were only expressed at low levels relative to the undifferentiated control. The concentration dependent changes that occurred after 72 hours were mirrored at 144 hours but at higher fold change indicating a temporal induction. The small increased in *HOX* gene expression after 72 hours may have only been measured due to the highly sensitive nature of the assay. In less sensitive assays many of the 5' *HOX* genes that demonstrated some expression after 72 hours may have not shown any expression and be assumed un-responsive at that time point or retinoid concentration [41, 48, 50]. This may detract from the overall picture as to how ATRA regulates *HOX* gene expression, since many of the small changes in *HOX* gene mRNA may be due to biological variation and not represent retinoid acid signalling. Furthermore, the pattern of expression at 72 hours and 144 hours were similar in each of the genes investigated and did not clearly demonstrate temporal co-linear expression. This may have been a result of the time points used, since after 72 hours many of the genes were being expressed making it hard to determine if any one gene was induced before the other. Therefore, a much early time point would be required to determine if, for instance the 3' *HOXB1* gene at 0.01 μM was expressed before the more 5' *HOXB6* gene at the same concentration.

Due to the increased potency of EC23 signalling and the high yield of neural cells formed from differentiating TERA2.cl.SP12 EC cells with EC23, elevated levels of expression of any of the *HOX* genes may relate to increased neurogenesis

As the concentration of ATRA decreased its apparent biological activity also decreased when measuring *HOX* gene levels. Relative expression of 3' and 5' *HOX* gene mRNA reduced, with only *HOXA1* being expressed greater than 50 times the undifferentiated

control at 0.1 μM and 0.01 μM ATRA. In comparison five *HOX* genes were induced by 0.1 μM EC23 to greater than 50 times the control. The genes that are consistently elevated during the concentrations of EC23 and ATRA that are capable to induce highly efficient neural differentiation in this model are: *HOXA1*, *D4*, *D8* and *A5*. Each is known to contain a RARE in their promoter sequence and so their expression is directly induced by retinoic acid signalling. Furthermore, there is evidence to suggest some of the *HOX* genes are directly involved in the process of cellular differentiation.

HOXA1

It has been demonstrated that *HOXA1* mRNA expression in mouse EC cells, requires RARγ signalling, however, there is also a reduction in expression when *RARβ2* is knocked out, interestingly RAR α knockouts have no change in *HOXA1* expression [225, 226]. Therefore, the higher RQ of *HOXA1* induced by EC23 at 10 μM, 1 μM and 0.1 μM may be due to increased signalling through RAR γ or RAR β2. As described earlier *HOXA1* has been shown to be required for neural differentiation in mouse ES cells.

HOXD4

As was seen with *PAX6* the maximum expression of *HOXD4* induced by EC23 was at 0.1 μM and interestingly *PAX6* has been implicated in regulation of *HOXD4* through binding to its neural enhancer. Therefore, the peak of *PAX6* mRNA at 0.1 μM EC23 may explain the increase of *HOXD4* mRNA at this concentration [227], and could be involved in differentiation of the hEC cells into neural progenitors.

HOXA5

At even lower concentration i.e. 0.01 μM EC23 induced the expression of *HOXA5* to levels much higher than that at 0.1 μM, the levels of expression were similar to that seen at 10 μM and 1 μM. It has been demonstrated that RAR β is required for the expression of *HOXA5* and *HOXA5* is implicated in growth inhibition and apoptosis of breast cancer cells [228]. The same property of growth inhibition is demonstrated in hEC cells since treatment with retinoic acid results in loss of cell proliferation; however, this may not be a result of *HOXA5* transcription.

HOXD8

Little is known about *HOXD8*, however, the results shown in this study suggest that it is likely involved in maintaining neural lineage commitment. Furthermore, *HOXD8* has been demonstrated to be induced by retinoid acid during neuroblastoma differentiation. Further suggesting its involvement in neurogenesis [229].

The induction of neurogenesis induced by retinoic acid and the high relative expression of *HOXA1*, *A5*, *D4* and *D8* in this model suggest that these transcription factors, at least in part are involved in the initial process of differentiation.

The schematic in Figure 3-34 demonstrates the concentration of EC23 required to induce a maximal response in most of the *HOX* genes tested in this study. With the exception of *HOXD1* and *HOXD4* expression as this was maximal at 0.1 µM and may represent activation via an alternative RARE to that of the other *HOX* genes. It was interesting to demonstrate the concentration dependent and temporal associated with *HOX* gene expression and these data demonstrate that both the concentration of retinoic acid and the exposure time is important to determine the extent of expression.

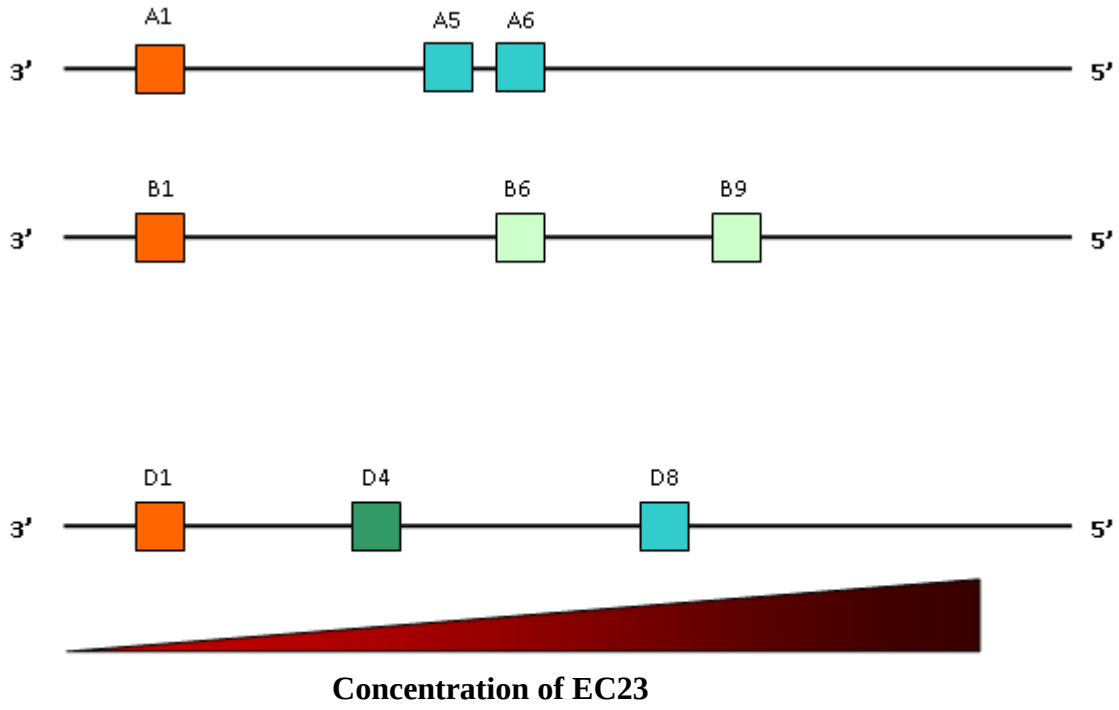

Figure 3-34 Concentration of EC23 required to induce *HOX* gene expression. Schematic demonstrates visually the position of each *HOX* gene used in this study in each chromosome cluster. The concentration required of EC23 to induce expression of each gene is also depicted. Note the sensitivity of each *HOX* gene to EC23 decreases as the genes become more 5' providing a regulatory role of EC23 in *HOX* gene expression and AP patterning. Low concentrations of EC23 induced the expression of more 3' genes as concentration increased the expression of 5' genes were induced. Schematic describes day 6 *HOX* gene expression data.

Regulation of the anterior-posterior developmental axis is complex and requires numerous mechanisms to ensure correct positional identity of developing cells. It is known that *HOX* genes are directly involved in regulating such positional identity and control both A-P axis and in some cases D-V axis development. The role of retinoic acid in inducing the co-linear expression of *HOX* genes is still being investigated.

Temporal regulation of *HOX* genes was through to be a result on co-linearity, where activation of 3' *HOX* genes can, via a positive feedback loop induce the expression of more 5' genes on the same cluster; hence, a domino like effect would ensue. Data from this Chapter suggest that although *HOX* gene expression does increase with time i.e. from 0-72 and 72-144 hours, differential regulation is due to retinoid sensitivity and retinoid concentration and not an effect of co-linear activation. It may be that earlier time points would be more likely to demonstrate co-linear activation of *HOX* genes in this model and may be more evident after a single pulse of EC23/ATRA.

HOX regulation of mature neural differentiation

The role of *HOX* genes and retinoic acid concentration in stem cell and neural differentiation is complex and the outcome of multiple signals working in positive and negative feedback loops. There are, however, some key regulatory pathways that link *HOX* gene expression, retinoic acid and neural differentiation. Neuronal column organisation is responsible for motor neuron organisation which regulates differential peripheral muscle innervation. The mechanisms that give rise to the different motor column groups involve numerous signalling pathways and specific gene expression profiles. Distinct *HOX*-C homeodomain protein clusters are expressed at different levels of the developing motor neuron columns. The lateral motor column (LMC) neurons can be distinguished from other groups by their expression of the retinoic acid producing enzyme Retinaldehyde dehydrogenase 2 (RALDH), implicating a role for retinoic acid (RA) in the development of LMC, or a paracrine effect of RA on surrounding developing tissue [230]. Furthermore, the co-expression of multiple *HOX* genes is associated with the development of specific LMC specification and is likely to offer some functional redundancy [231]. A recent study has implicated the expression of the 3' *HOXB1* gene with inducing a more dorsal neural phenotype, as measured by a decrease in *NKX2.2* expression in embryonic stem cells forced to express *HOXB1*. Data from this Chapter suggests that *NKX2.2* does in fact negatively follow the expression of *HOXB1*. No *NKX2.2* expression was detected at the lowest concentrations of EC23 or ATRA tested, however, since these provided the

highest up-regulation of *HOXB1* it is likely very low levels of *NKX2.2* would be detected [232].

The data presented in this thesis suggest a concentration dependent regulation of *HOX* gene expression with little emphasis on temporal expression. Furthermore, *HOX* genes are regulated in a retinoic acid receptor subtype specific manner, this is apparent since EC23 induced differences in the expression of the *HOX* genes investigated compared to ATRA, suggesting simple RARE activation is not sufficient to induce a co-linear cascade response. These data further exemplify EC23 as a replacement for ATRA, removing much of the heterogeneity in the use of ATRA and provide insights into *HOX* gene regulation during neural differentiation in TERA2.cl.SP12 EC cells. Furthermore, *HOXB1* has been shown to regulate CRABP I and II expression in mouse ES cells controlling hindbrain neural differentiation and patterning [51].

3.3.5 Synthetic modulation of the dorsal-ventral axis during neural differentiation

Neural subtype differentiation can be enhanced using specific small molecules for key molecular signalling pathways. As has been discussed in this Chapter the replacement of ATRA with EC23 enhances neurogenesis in our model. Other small molecules can be used as replacements for proteins that affect other signalling pathways associated with neural differentiation for example, Purmorphamine. Purmorphamine is a synthetic Shh pathway agonist that can be used as a replacement for the recombinant Shh protein in stem cell differentiation protocols for motor neuron differentiation [213]. In this study the addition of Purmorphamine to the cell culture media was used to investigate the concentration dependent role of retinoic acid on the motor neuron markers *HB9* and *ISL1,* and the interneuron marker *NKX2.2*. As with previous studies, Purmorphamine treated cultures expressed transcriptional markers characteristic of ventral spinal cord neural progenitors [77, 213]; however, the relative expression of *NKX2.2*, *ISL1* and *HB9* was dependent on the concentration of either EC23 or ATRA when used in conjunction with Purmorphamine. Data demonstrated that retinoic acid concentration regulated the expression of the motor neuron marker *ISL1* and the ventral interneuron marker *NKX2.2*, indicating the ability of retinoic acid to determine neural subtype. The role of retinoic acid in motor neuron specificity and spatial regulation along the dorsal ventral neural tube was demonstrated by Wilson, L. et al (2004) [233] using VAD quail model.

These data showed in an *in vitro* model of neural differentiation that not only is retinoid concentration an important factor for inducing differentiation, but it is also involved in

directing the neural progenitor cells into specific ventral neural subtypes. Used in combination with an optimal ventralisation signal from Purmorphamine directing neural subtypes will benefit from the use of stable retinoic acid analogues such as EC23. Further work on the role of retinoic acid in neural subtype selectivity should look at the functional development of the mature neuron and any differences observed.

3.3.6 Conclusion

This Chapter has described a model of human neurite differentiation using the synthetic small molecule EC23. EC23 was used alongside its natural analogue ATRA and a concentration dependent regulation of stem cell differentiation was demonstrated. Due to the inherent instability of ATRA, the need for a more robust and reproducible protocol for stem cell differentiation is advantageous. This has been evidenced throughout this Chapter by the concentration dependent role of RAR activation was discussed in relation to neural differentiation. Stable and potent retinoid analogues are necessary for the controlled regulation of RAR activation by refined concentrations. A method for inducing mono-layer neural differentiation using EC23 can be found in Chapter 2 (Methods) and uses concentration data obtained from the work in this thesis to determine optimal conditions of differentiation.

EC23 is around 100 times more potent than ATRA and was shown using a novel method with the CYP26 inhibitor Liarozole to be resistant to metabolism. Differentiation protocols require the continuous exposure of ATRA currently; this means that the vehicle DMSO is also present continuously. Since EC23 is resistant to metabolism it was shown that a single pulse of EC23 was sufficient to induce loss of pluripotency markers.

The structure activity relationship between synthetic small molecules was then investigated further. Previous studies demonstrated the addition of a methyl group resulted in a 90° change in angle and enhanced biological activity in a synthetic analogue of ATRA. To investigate this, a 3Methyl group was added to EC23 and the relatively inactive EC19. Addition of this group resulted in enhancement of EC19 however; no increase in activity was demonstrated by EC23, as it is likely inducing the maximal response. Furthermore, 3methylation did not increase the metabolism of each small molecule.

To investigate the regulation of anterior-posterior patterning in a concentration dependent manner by EC23 9 *HOX* genes were assayed at 5 concentrations of both EC23 and ATRA. EC23 was used as a tool to probe the specific concentration dependent effect of RARE

activation, since it will not be metabolised or isomerised *in vitro* and thus have a constant concentration within the cell cytoplasm. Data demonstrated a concentration dependent response to retinoic acid and the response was dependent on the position of each *HOX* gene on the chromosome cluster.

There has been evidence to suggest that retinoic acid is not only required for neural development and anterior-posterior patterning but is also necessary for correct dorsal-ventral patterning in the neural tube. To investigate the ventralising molecule, Purmorphamine was added to the neural differentiation protocol. Three concentrations of ATRA and EC23 were then investigated for changes in the ventral markers *NKX2.2*, *HB9* and *ISL1*. Data demonstrated that retinoid concentration was important for the subtype selectivity of motor neurons determined by either *ISL1* or *NKX2.2* expression.

Controlling the subtype identity of neurons is important for relating *in vitro* models to the *in vivo* cell. The neural subtypes that can be formed by stem cells interact with different targets and are functionally different. For instance motor neurons target muscle tissue and utilise acetylcholine as the neurotransmitter whereas neurons in the mesencephalon are likely dopaminergic and are associated with multiple actions.

Robustly controlling neural subtype differentiation will aid the development of specific *in vitro* models of disease which can be used in a reproducible mode for drug discovery. Utilising potent, selective and stable small molecules will aid the development of these robust, reproducible and efficient human neural models.

The next Chapter of this thesis will build upon the use of small molecules in neural differentiation and investigate the role of retinoid signalling in neurite outgrowth.

CHAPTER 4 INVESTIGATING NEURITE INHIBITION BY HUMAN STEM CELL-DERIVED NEURONS IN CONVENTIONAL 2D CELL CULTURE

4.1 INTRODUCTION

4.1.1 Application of a stem cell model of human neuritogenesis

Using stem cells to produce large amounts of human neurons in a reproducible and consistent manner is beneficial for studying the process of human neurite outgrowth *in vitro*. Human stem cell-derived neurons are an important source of human specific tissue. As was demonstrated in Chapter 3 differentiation of the human EC stem cell line TERA2.cl.SP12 using synthetic small molecule analogues of ATRA can result in highly neurogenic differentiation of TERA2.cl.SP12. Using human neural tissue derived in this way is both ethically and biologically efficient; differentiation of the stem cells can be controlled using defined protocols and specific receptor agonists. In this Chapter the stem cell-derived neurons discussed in Chapter 3 will be used as a human *in vitro* model of neurite outgrowth.

Modelling neurite outgrowth and investigating the processes that result in loss of neurite regeneration in the damaged central nervous system (CNS) is important for discovering key molecular and biochemical processes that can be targeted for therapeutics. The glial scar that forms after CNS injury is the result of a dynamic response termed "reactive gliosis" [135]. This process is initiated by loss of tissue architecture in the CNS and normal tissue boundaries ultimately resulting in the formation of a glial scar.

4.1.2 Glial Scar

Traumatic injury to the central nervous system (CNS) and spinal cord results in the development of a structure known as the glial scar. The glial scar comprises of both cellular and extracellular matrix components (ECM) and consists of molecules that are permissive or inhibitory to neurite regeneration. The ratio between inhibitory and permissive components of the scar determines to what extent regeneration occurs, towards the centre of the scar inhibitory molecules dominate over the permissive ECM which

results in neurite retraction and an environment inhibitory to neurite growth [234]. Overcoming this inhibitory environment is a major focus for regenerative therapeutics aimed at CNS regeneration. The evolutionary advantage of rapid scar formation is through repair of the blood-brain barrier and infection prevention [235], however, due to medical advances scaring is to an unnecessary extent. A major cellular component of the glial scar is the reactive astrocyte, astrocytes become activated by TGF-β signalling post-injury [236]. Activation results in a morphological change to the astrocyte and an increase in the secretion of extracellular matrix proteins such as Laminin, Collagen IV and Fibronectin which are permissive to neurite regeneration and act as a matrix for neurite outgrowth. In addition to the secretion of permissive molecules chondroitin sulphate proteoglycans (CSPG) which are strongly inhibitory to neurite outgrowth and regeneration are produced and make up a large part of the scar. The dynamic process of astrocyte activation and glial scar formation is known as "reactive gliosis" [134].

Until recently it was thought that CSPGs represented a physical barrier to neurite regeneration however, recent studies have shown that CSPGs act through at least two protein tyrosine phosphatase (PTP) receptors PTPσ and LAR [150]. Activation of PTPσ and LAR on the growth cone has been shown to induce neurite retraction and inhibit regeneration of damaged axons [150]. The three main CSPG's that activate these receptors and are present within the glial scar include: Aggrecan, Neurocan, Brevican, Phosphocan and Versican which make up the lectican family of hyaluronan-binding CSPG's.

The major ligand for the LAR and PTPσ receptors is the glycosaminoglycan (GAG) side chain that is found attached to the protein backbone of CSPG's [237]. Removal of the GAG side chains through enzymatic cleavage demonstrates a loss of CSPG induced neurite retraction both *in vivo* and *in vitro* [141]. Furthermore inhibition of downstream signalling elements involved in the signal transduction of PTPσ or LAR transduction has been demonstrated to be sufficient to overcome neurite outgrowth inhibition by CSPG. ROCK inhibitors and cAMP analogues were shown to overcome both CSPG and Myelin associated neurite retraction; there is also evidence to suggest that activation of the *RAR β2* receptor can result in neural regeneration [238]. Due to the non-specific effects of these modulators it is important to determine new ways of overcoming receptor mediated neurite retraction and inhibition of neurite outgrowth for use in treatments of acute and chronic CNS damage.

One focus of neural regeneration research is the role of the CSPG- Aggrecan in the glial scar. Aggrecan is normally associated with avascular cartilage but is up-regulated after traumatic injury to the CNS. Aggrecan inhibits axon regeneration through a number of mechanisms, including activation of ROCK [239] and inhibition of integrin receptor activation – a key receptor for Laminin binding and initiation of axon formation [240]. The effect of Aggrecan can be overcome by chondroitinase ABC treatment, ROCK inhibition and integrin stabilisation [160, 240]. The key mechanisms of how human neurites respond to Aggrecan and the molecular pathways involved in neurite retraction are still relatively unknown. Basic models of neurite outgrowth and regeneration will help pinpoint the role of Aggrecan in the glial scar and help determine new ways of enhancing neural regeneration.

4.1.3 Models of Neurite outgrowth and Regeneration

The most utilised models of neurite outgrowth for *in vitro* research of neural regeneration currently are rat dorsal root ganglion cells (rDRG) [4] or embryonic cortical cultures [241]. These models can be induced to form long neurites which are relatively simple to quantify. Other models such as PC12 rat pheochromocytoma [242] or N1E-115 [243] cells also form neurites and have been developed into commercial neurite outgrowth kits, however the length of the neurites that form are relatively short making it difficult to assess any changes in length accurately. DRG neurons are heterogeneous and their activity not only depends on the way they were isolated, but the growth factors and morphogens present during the experiment [174, 244]. Although rDRG is a good model of neurite outgrowth, it is of peripheral sensory nervous system origin [245] and therefore represents a different neural subtype to that found within the CNS. The major disadvantage of all of these models is their non-human origin; furthermore, the exact stage of the neural progenitor is unknown making it difficult to relate the regenerative potential of the neurons to the developmental stage, which is a key advantage of human stem cell-derived neurons.

Human neural progenitors are commercially available; however, as with many models of neurite outgrowth the ability to accurately quantify any change in neurite length or number is difficult due to the heterogeneity of the cells that develop and the network of neurites that forms. Alternative methods of producing human neurons for use in neurite outgrowth studies have been developed using human embryonal carcinoma stem cells [159]. hEC stem cells can be differentiated using the same techniques as hES cells, however their use

in research is less restricted. Furthermore, many hEC stem cells are limited in their lineage potential resulting in a highly reproducible, defined method of producing different cell types. Current models for studying neurite outgrowth are reviewed in Chapter 1.

4.1.4 Small molecule regulation of stem cell differentiation

Protocols to induce neural differentiation of human stem cells often include the morphogen ATRA and as discussed earlier there are many limitations of the use of ATRA. Synthetic analogues of ATRA have been demonstrated to overcome many of these limitations and enhance the consistency of both the molecule in culture and its concentration [89, 95].

The small molecule analogues of ATRA, EC23 and AH61 were chosen to investigate the advantage of using synthetic retinoid that are more stable and potent when ATRA in the neural differentiation protocol to produce neurons for use in neurite outgrowth models. As discussed earlier EC23 is well defined in its genetic and phenotype effect on stem cells and this has also been demonstrated for AH61 [246].

Aim

This Chapter aims to develop a unique, highly reproducible, highly neurogenic model of human neurite outgrowth using stem cells differentiated using the potent synthetic retinoids, AH61 and EC23. This model will be optimised alongside ATRA and used to investigate the molecular mechanisms that undergo CSPG-induced neurite inhibition and regeneration. Recent studies have implicated the CSPG- Aggrecan in neural growth cone collapse and neurite retraction in the glial scar [247] the effect of Aggrecan in this model will be investigated.

In this section a 2 dimensional (2D) approach for assessing human neurite outgrowth and modulation of neurite outgrowth by CSPGs has been used. The 2D model utilises conventional tissue plastic to grow neurites from aggregates of differentiated human stem cells. Neurites form on a single plain as a halo around the aggregate meaning only one membrane surface of the neurite is in contact with the tissue culture plastic substrate.

Specific Objectives

- Develop a reproducible model of human neurite outgrowth using the synthetic small molecules AH61 and EC23 and compare neurite outgrowth with cells differentiated with conventional ATRA.

- Using this defined model of human neurite outgrowth investigate CSPG induced neurite inhibition

- Investigate small molecules that can overcome neurite inhibition in response to the CSPG-Aggrecan

- Investigate neurite inhibition in a neural/glial co-culture model.

4.2 METHODS

4.2.1 2 Neurite outgrowth assay: performed on 2D conventional cell culture plastic.

TERA2.cl.SP12 embryonal carcinoma stem cells passage < 35 were cultured as described in Chapter 2.

Prior to starting the differentiation procedure ensure:

- Good stocks of untreated 90 mm Petri Dishes (Fisher Scientific FB51504)
- At least 200 µl of 0.1 mM EC23(Reinnervate) in molecular biology grade DMSO (Sigma Aldrich D8418)
- 1 x 500 ml bottle of DMEM (Lonza BE12-614F) containing 10 % FBS(Sigma Aldrich), 5 mM L-glutamine(Lonza BE17-605F) and penicillin/streptomycin (Lonza DE17 602F) (DMEMFGP)
- Access to a class I laminar flow microbiological safety cabinet
- 0.25% trypsin/2 mM EDTA (Sigma Aldrich T4049)

To begin the differentiation procedure a single cell suspension of TERA2.cl.SP12 EC cells is needed. A single cell suspension was achieved as described in Chapter 2. Cells were counted using a haemocytometer as described in Chapter 2.

For differentiation of cells as aggregate follow the steps below:

1. Add 1.5 x 10^6 TERA2.cl.SP12 EC cells to 20 ml DMEMFGP and leave overnight to initiate cell aggregation
2. After 24 hours aggregation add 20 µl of a 0.1 mM EC23 stock directly to the media and gently swirl
3. After 4 days treatment with a final concentration of 0.1 µM EC23 place the media containing aggregates into a 50 ml Falcon tube for 15 minutes allowing the aggregates to settle – this must be done in a sterile environment
4. Using an aspirator, supernatant leaving the pellet of aggregates in the bottom of the Falcon tube.
5. Add 20 ml of DMEMFGP and 20 µl of 0.1 mM EC23.
6. Gently swirl and place in to a fresh 90 mm untreated bacteriological Petri dish
7. Repeat steps 3-7 every 3-4 days or when required
8. After 21 days aggregates are differentiated and capable of forming neurites

4.2.2 Coating conventional 2D tissue culture plastic for neurite outgrowth studies

Materials required:

1 mg/ml Engelberth-Holm-Swarm murine sarcoma membrane (Sigma Aldrich L2020)

5 mg Poly-D-lysine (Sigma Aldrich P7405)

500 ml PBS without calcium and magnesium (Lonza 13E17-512F)

Coating procedure:

1. Add 5 ml of PBS without Ca^{++}, Mg^{++} to 5 mg of Poly-D-lysine in a sterile environment and gently swirl to dissolve.
2. Dilute 500 µl of 1mg/ml P-D-L solution and 500 µl of 1 mg/ml Engelberth-Holm-Swarm murine sarcoma membrane into 49 ml of PBS. To create 50 ml of 10 µg/ml Laminin/P-D-L solution working stock.
3. Add 150 µl to each well of 48 well tissue culture treated plastic and seal lid with Parafilm.
4. Leave coating at room temperature overnight.
5. After 24 hours remove excess coating solution and wash 3 x with PBS and store in PBS prior to use – use within 12 hours.

4.2.3 To induce neurite outgrowth from cell aggregates differentiated with 0.1 µM EC23 for 21 days

Materials required:

Laminin/P-D-L coated 48 well tissue culture plastic (Beckton Dickinson 353078)

10 mM 5'fluoro 2' deoxyuridine (Sigma Aldrich F0503)

10 mM Uridine (Sigma Aldrich U3003)

1 mM Cytosine β-D arabinofuranoside (Sigma Aldrich C1768)

DMEMFGP

Paraformaldehyde (Sigma Aldrich P6148)

100 µm tissue culture filter (Fisher Scientific 22363549)

Neurite outgrowth procedure:

1. Filter differentiated aggregates through a 100 μM filter and rinse with fresh DMEMFGP do not discard neurospheres in filter.
2. Backwash aggregates in filter (>100 μm in size) with 10 ml fresh media w/o EC23 into a new 90 mm bacteriological Petri dish, swirl to distribute.
3. Make up 50 ml of DMEMFGP containing 1 μM Cytosine Arabinosine, 10 μM 5'Fluoro 2' Deoxyuridine and 10 μM Uridine.
4. Remove PBS from Laminin/P-D-L coated tissue culture plastic
5. Using a 200 μl pipette take up 30 μl of media containing 1-2 neurospheres and expel into a Laminin/P-D-L coated tissue culture plastic well and repeat for each well
6. Add 500 μl of DMEMFGP containing mitotic inhibitors and culture at 37 °C, 5 % CO_2 in a humidified atmosphere for 10 days (do not change the media during this time, as this affects neurite growth).
7. For cell fixation, after 10 days remove all culture media and add 200 μl of 4 % PFA for 1 hour. After fixation wash once with PBS and store at 4 °C prior to analysis

4.2.4 Aggrecan coating

For neurite outgrowth inhibition studies follow the procedure as above, however, when coating perform the following additional steps:

1. Dissolve 1 mg Aggrecan from bovine cartilage (Sigma Aldrich) in 1ml PBS w/o Ca^{++}, Mg^{++}.
2. To make up the inhibitor coating solution place 19 ml of 10 μg/ml Laminin/P-D-L solution (made as described above) into a new 50 ml Falcon tube and add 1 ml of 1 mg/ml Aggrecan solution.
3. Add 150 μl of solution containing: 50 μg/ml Aggrecan, 10 μg/ml Laminin and 10 μg/ml P-D-L to each well of 48 well tissue culture plastic and seal with Parafilm for 24 hours.
4. Follow the above procedure for neurite outgrowth studies involving Aggrecan

4.2.5 Chondroitinase ABC pre-treatment in 2D

Chondroitinase ABC enzyme buffer and dilution:

Chondroitinase ABC (Sigma Aldrich C3667), from Proteus vulgaris was reconstituted with 1 ml 0.1 % BSA (Sigma Aldrich A7906) giving a concentration of 5 units/ml. Stock solution was diluted in enzyme buffer to 0.15units per well in. Enzyme buffer consisted of:

- 0.02 % BSA
- 50 mM TRIS pH8
- 60 mM Sodium acetate (Sigma Aldrich)
- PBS w/o Ca^{++}, Mg^{++}

Treatment of Aggrecan coated plastic with Chondroitinase ABC:

1. Tissue cultured plastic was coated with Aggrecan, P-D-L and Laminin as described above
2. Wash coated plastic with PBS x 3
3. Add 150 µl of either Chondroitinase buffer (control) or buffer containing 5units/ml enzyme
4. Incubate for 1 hour at 37 °C, 5 % CO_2
5. After 1 hour incubation wash 3 x with PBS and follow the above procedure for neurite outgrowth from differentiated TERA2.cl.SP12 aggregates.

4.2.6 2D U118MG astroglioma/neural co-culture

1. For neural/glial co-culture at day 14 aggregate differentiation begin culture of U118MG cells in 2D as described in Chapter 2.
2. Coat 48 well tissue culture plastic with 10 µg/ml Laminin/P-D-L as described above
3. Filter and backwash neurospheres as described above for neurite outgrowth study at day 21
4. For co-culture add 5,000 U118MG cells in 500 µl DMEMFGP containing mitotic inhibitors to each test well
5. Take 1 neurosphere in 30 µl media and add to each well as necessary
6. Add 500 µl of DMEMFGP containing mitotic inhibitors and culture at 37 °C, 5 % CO_2 in a humidified atmosphere for 10 days (do not change the media during this time, as this affects neurite growth).

7. Fix cells for 1 hour in 4% PFA and wash 3 x in DPBS.

4.2.7 Aggrecan ELISA

Protein was purified and quantified as described in Chapter 2. Briefly, protein from 1 x 10^6 U118MG cells were purified using an IGEPAL method and quantified using the Bradford assay (for details see Chapter 2).

For the Aggrecan ELISA the following method was followed:

BlueGene Human Aggrecan (AGC) Elisa Kit (AMSBIO, AMS.E01A0413) utilised a sandwich enzyme immunoassay technique to quantify AGC in total protein samples. The kit used a microtiter plate pre-coated with a monoclonal antibody specific for AGC. A polyclonal anti-ACG antibody conjugated to horseradish peroxidase (HRP) was used to report any binding to the monoclonal antibody in the microtitre plate. A colour change was detected using a 450 nm microplate reader.

Sample preparation

- Bring all kit components and samples to room temperature
- Dilute 10 mL of wash solution (100 x) with 990 ml of deionized or distilled water to prepare 1000 mL of 1 x wash solution.

Assay procedure:

1. Add 50 µL of standards or samples to the appropriate well in the antibody pre-coated Microtitre Plate. Add 50 µL PBS in the blank control well. Standards used were 0, 2.5, 5.0, 10, 25 and 50 ng/ml Aggrecan. For the sample under investigation 50 ng of purified U118MG protein were added to the test well.
2. Dispense 5 µL of Balance Solution into 50 µL specimens, mix well.
3. Add 100 µL of Conjugate to each well (but do not add to blank control well). Pipette up and down 10 x to mix. (n.b Mixing well in this step is important). Cover and incubate the plate for 1 hour at 37 °C
4. Wash the micro titre plate using manual washing technique. This must be repeated five x and blot dried by short sharp downward movements onto a

thick piece of tissue paper (n.b. blot dry until no liquid is left on the tissue paper).

5. Add 50 µL Substrate A and 50 µL Substrate B to each well including blank control well, subsequently. Cover and incubate for 10-15 minutes at 37 °C (Avoid sunlight)
6. Add 50 µL of Stop Solution to each well including blank control well. Mix well.
7. Determine the Optical Density (OD) at 450 nm using a microplate reader (BioTek, ELx800) immediately.

4.2.8 Neurite quantification

Neurite number

Digital images (Tiff files) of neurite outgrowth to be counted were opened using Image-J (http://rsbweb.nih.gov/ij/). Using the magnification option in Image-J a section of neurites stained for β III Tubulin (TUJ-1) (Green) were magnified. Using the multiple count option individual neurites were marked at the growth cone. To move to another area of the aggregate the scroll option in Image-J was used. Each mark had a number assigned the last neurite to be marked gave the number of neurites around the aggregate. **Figure 4-1** shows an example of magnified neurites being counted using Image-J software.

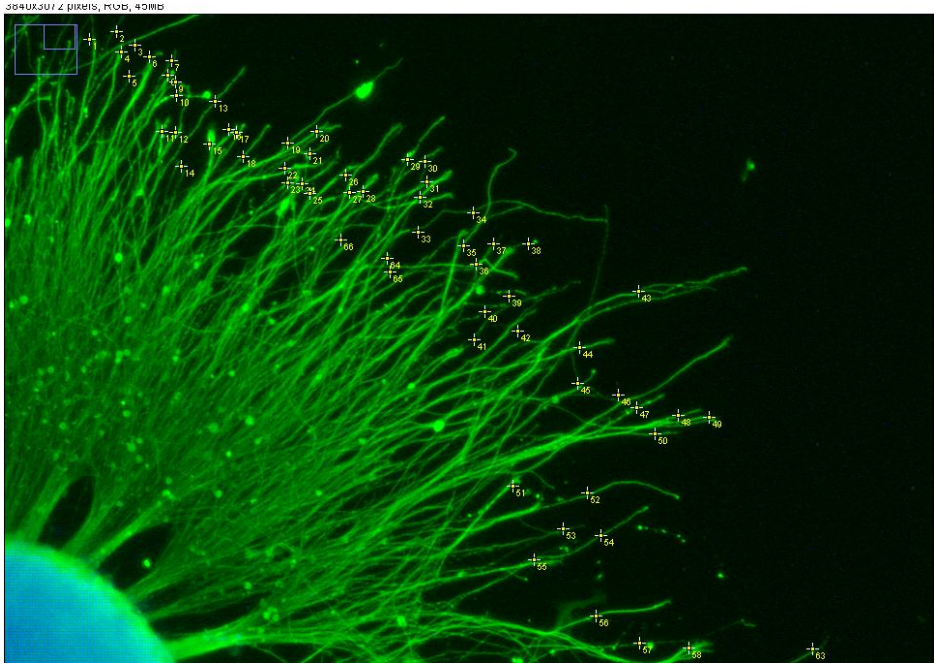

Figure 4-1 Quantification of the number of neurites using Image-J. Image- J was used to magnify the individual neurites and count neurite growth cone/ends of neurites for quantification.

Neurite length quantification

Using the Leica advanced fluorescence software (hhtp://www.leica-microsystems.com/products/microscope-software/life-sciences/las-af-advanced-flourescence/) traces of individual neurites could be drawn. Using the statistical option exportation of data into Microsoft Excel could be achieved. The length of each free drawn line could then be averaged in Microsoft Excel. Note: It is important to ensure the correct magnification is chosen when taking the image in this software to ensure the correct neurite length is calculated. Figure 4-2 shows an example of neurite length quantification using Leica AF software. Image A shows un-traced neurites stained for TUJ-1 (Green), Image B shows traced neurites using Leica AF software.

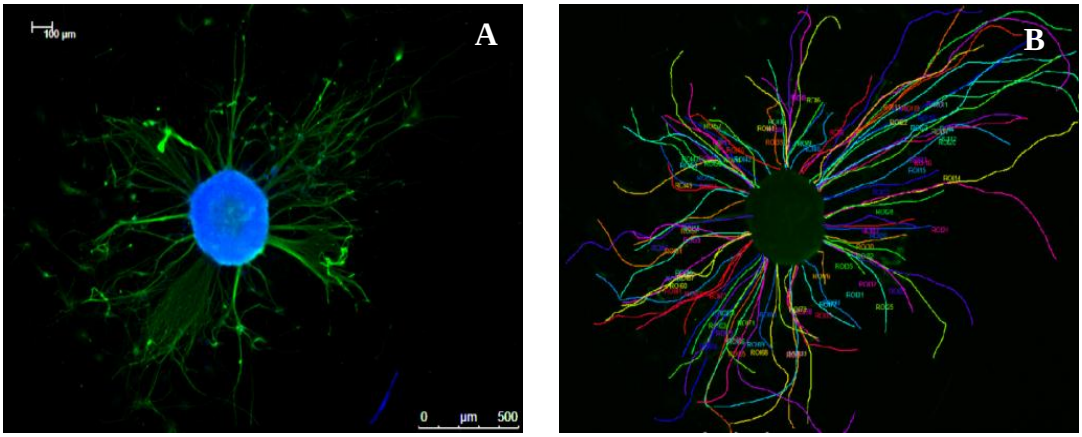

Figure 4-2 Neurite length quantification using Leica AF software. Image A shows un-traced neurites stained for β III Tubulin (TUJ-1) (Green), Image B shows traced neurites using Leica AF software. Numbers on traces can be used to identify individual neurite length and the number of neurites measured.

4.3 RESULTS

4.3.1 Induction of neurogenesis in cell aggregates by synthetic small molecule

As described in the previous Chapter, to study human neurite outgrowth and differentiation a 2D monolayer protocol was developed. The technique resulted in high levels of neurite outgrowth and neural tissue development as demonstrated in Chapter 3, Figure 3.2. Using this highly neurogenic model would prove difficult to determine any subtle length or number changes in neurite under experimental conditions, due to the complete network of neurites that form. Accordingly this was not an appropriate method of differentiation to assess neurite outgrowth.

An alternative differentiation protocol utilised suspension aggregates of TERA2.cl.SP12 cells and has been shown previously to be neurogenic [85]. It has been reported that the incorporation of a high concentration of retinoic acid into the differentiation protocol of human stem cells can result in an enhancement of neurite outgrowth from differentiated embryoid bodies [248]. However, the consistency and reproducibility of neurite outgrowth from each aggregate was low and often resulted in complex neural networks that were difficult to quantify for change in length or number. Figure 4-3 shows in a simple schematic the difference between 2D monolayer neurite outgrowth and development of neurite from an aggregate in 2D.

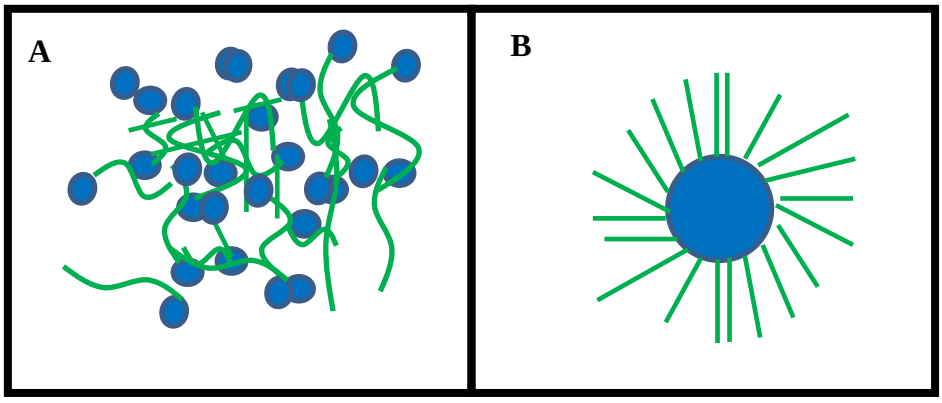

Figure 4-3. Neurite outgrowth from mono-layer or aggregate derived differentiation protocols. Schematic depicting the difference between a mono-layer network of neurites (A) and a central focal point of neural origin derived from aggregate neural progenitors (B). Neurites are depicted in green and nuclei in blue.

The commercial synthetic retinoid EC23 and the novel retinoid analogue AH61 both induce highly potent neural commitment in a variety of cell models and have been shown to be significantly more potent than ATRA [246] [95]. EC23 has been described throughout Chapter 3, however, the synthetic retinoid AH61 has not been used so far. AH61 was discovered to potently induce neural differentiation of TERA2.cl.SP12 in a screen of compounds performed as part of a PhD thesis [246]. Data from this thesis indicated that AH61 was very similar to EC23 in potency in mono-layer cultures, however, no data was described about its effect on aggregates of TERA2.cl.SP12 hEC stem cells.

In this study the enhanced activity of these compounds was exploited to induce neural differentiation from stem cell aggregates and assess the potential for neurite outgrowth. Initially TERA2.cl.SP12 hEC stem cells were grown and maintained as a monolayer to no more than passage 30. Aggregates were formed by transferring a single cell suspension of the cells into an untreated bacteriological Petri-dish in normal growth media. After 24 hours ATRA or synthetic retinoid was added to the media.

Figure 4-4 shows the difference in cell contact between monolayer and aggregate culture. Notice that the aggregate method results in a 3D-like spherical structure. The concentration of any small molecule within the culture media would have to diffuse throughout the aggregate to gain access to the cells in the centre. It is therefore important that small lipophilic molecules such as retinoids are used and aggregates are not allowed to become too large to ensure differentiation is complete throughout the aggregate

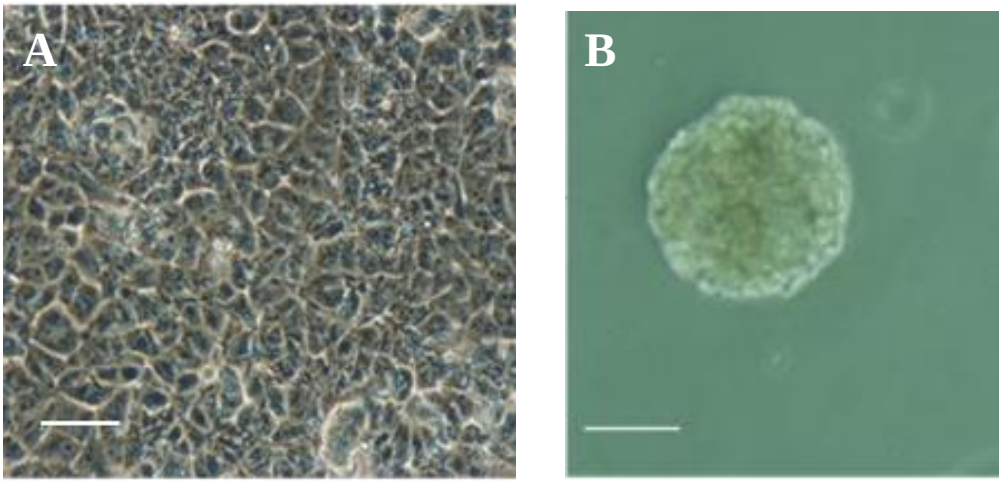

Figure 4-4 Monolayer and aggregate culture of the human EC cell TERA2.cl.SP12. Cells were maintained in a monolayer (A) and differentiated as an aggregate (B). The close cell contact demonstrated in culture (A) is necessary to maintain the TERA2.cl.SP12 stem cell phenotype. Cells were transferred to form cultures as aggregates (B) when the differentiation protocol was followed. Cells were left to aggregate overnight on non-adherent plastic (B) prior to retinoid treatment. Image (B) demonstrates the typical structure of an aggregate differentiated for 21 days with 0.1 µM EC23. Scale bars: (A) 50 µM (B) 250 µM.

Aggregates of TERA2.cl.SP12 cells were initially differentiated for 14 days by media supplementation with AH61, ATRA or EC23 at 10, 1 or 0.1µM. To investigate structural differences between aggregates treated by each compound and concentration, H & E stained histological sections of day 14 neurospheres were imaged (Figure 4-5). High concentrations of each small molecule resulted in the formation of neural rosettes and the development of structures within the aggregate. Aggregates were relatively small in size which may be a consequence of the dehydration process during wax embedding. Interestingly the aggregates differentiated by AH61 were much larger than those treated with ATRA or EC23.

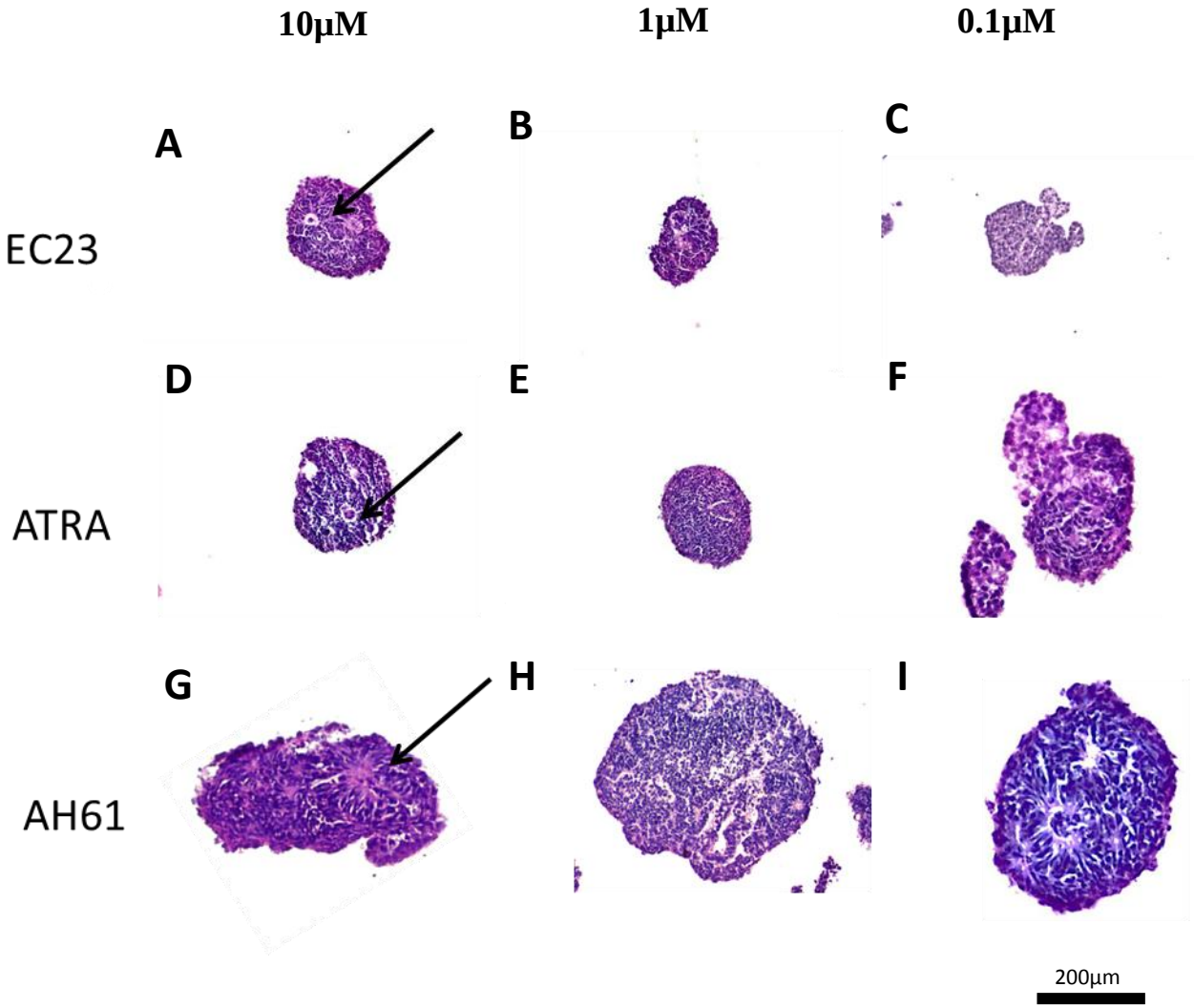

Figure 4-5 Internal aggregate structure demonstrates neural rosette formation and heterogeneous cell patterning after 14 days differentiation. Aggregates were differentiated with EC23 (A,B,C), ATRA (D,E,F) or AH61(G,H,I) at 10 µM, 1 µM or 0.1 µM respectively, for 14 days. Differentiated aggregates were then fixed, embedded, sectioned and stained with Haematoxylin & Eosin. Staining demonstrates structural similarities between each compound, after 14 days neural rosettes have developed in the highest concentrations used, however these structures are not seen at the lower concentration used. Large structures can be seen within the aggregates many representing neural rosettes (arrows).

Sections of cell aggregates differentiated for 14 days were analysed to determine how the concentration of each small molecule influences neural commitment. Sections of each aggregate for each treatment group were immuno-stained for Nestin, TUJ-1 and nuclei. Nestin is indicative of neural progenitor formation and represents early neural commitment. Cells that express Nestin are usually proliferating neuroprogenitor cells; in contrast TUJ-1 expression in neural tissue indicates a more committed neural phenotype, representative of later stages of neural development. Figure 4-6 shows aggregates stained and sectioned after 14 days treatment with EC23. A high concentration of EC23 induced the highest level of TUJ-1 expression, as would be expected, at the lowest concentration of EC23 high levels of Nestin and low expression of TUJ-1 was visualised, indicating early neural commitment characteristic of the lag time prior to EC23 eliciting a cellular response. In contrast ATRA induced low levels of both Nestin and TUJ-1 expression at each concentration, with the highest levels of Nestin and TUJ-1 expression at 10 µM (Figure 4-7).

The ATRA analogue AH61 was shown to be highly potent at inducing neural commitment in 2D monolayer cultures of TERA2.cl.SP12 [246]. Neural protein expression after 14 days indicated that AH61 induced TUJ-1 and Nestin to high levels at 10 µM and 1 µM, poor expression of Nestin and TUJ-1 was seen at 0.1 µM. These results so far indicate that differentiation of aggregates for 14 days induced both TUJ-1 and Nestin expression in TERA2.cl.SP12 human stem cell, the level and proteins expressed were determined by the type of small molecule used and its concentration.

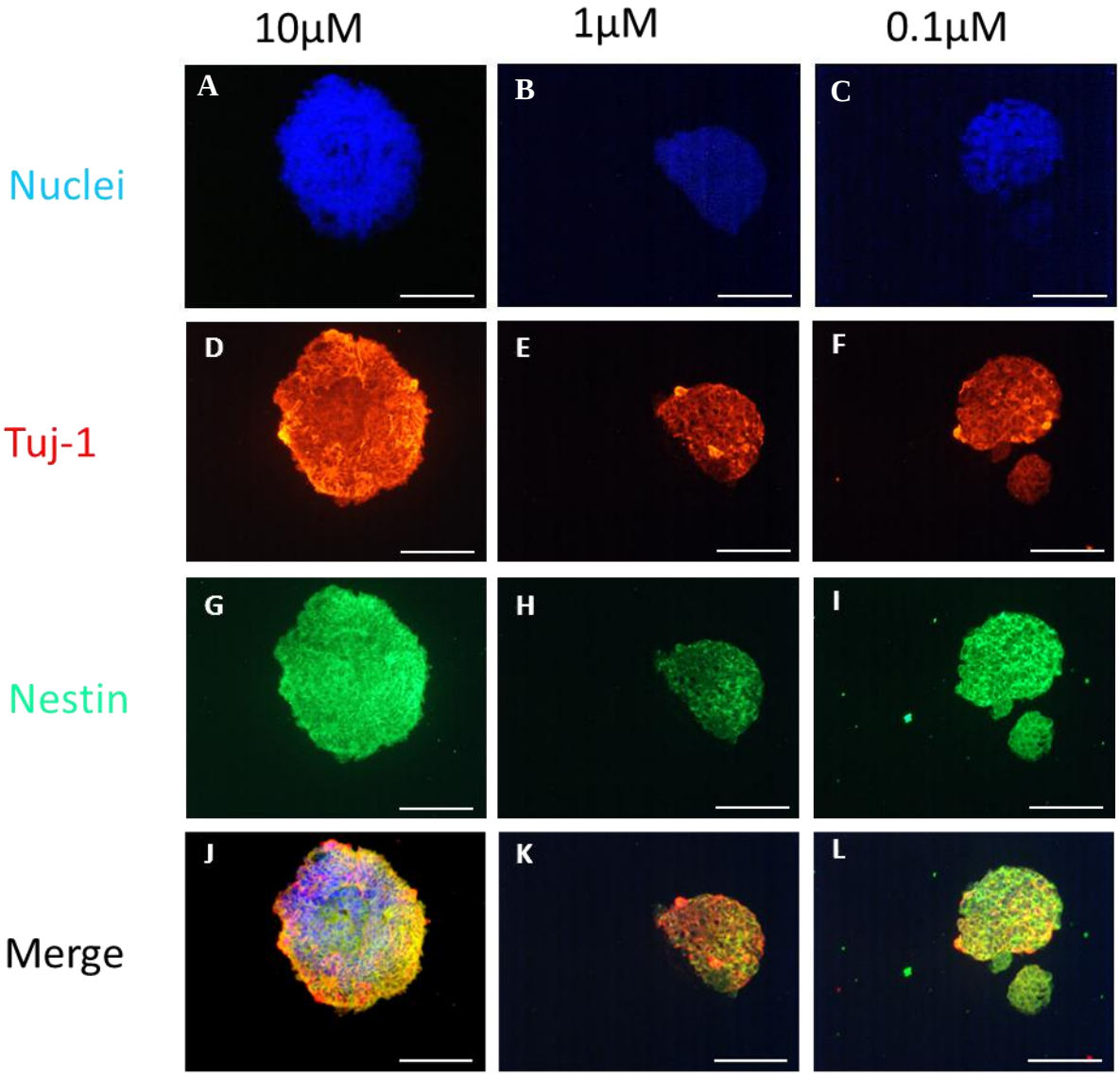

Figure 4-6 Expression of neural proteins in TERA2.cl.SP12 aggregates after differentiation for 14 days with EC23. Differentiated aggregates were fixed and embedded prior to sectioning and staining for the neural proteins, Nestin (Green) and β III Tubulin (TUJ-1) (Red). The data shown is DAPI (A,B,C), Tuj-1 (D,E,F), Nestin (G,H,I) and merged flourescence (J,K.L) at 10 µM, 1 µM and 0.1 µM. Nuclei were stained with DAPI (Blue). Aggregates were positive for both Nestin and β III Tubulin (TUJ-1). Higher β III Tubulin (TUJ-1) expression was visible in aggregates differentiated at 10 µM. The lowest concentration of EC23 0.1 µM had visibly higher levels of Nestin expression than β III Tubulin (TUJ-1) indicating that the cells represent early neural progenitors. Scale bars = 250 µm. n=3

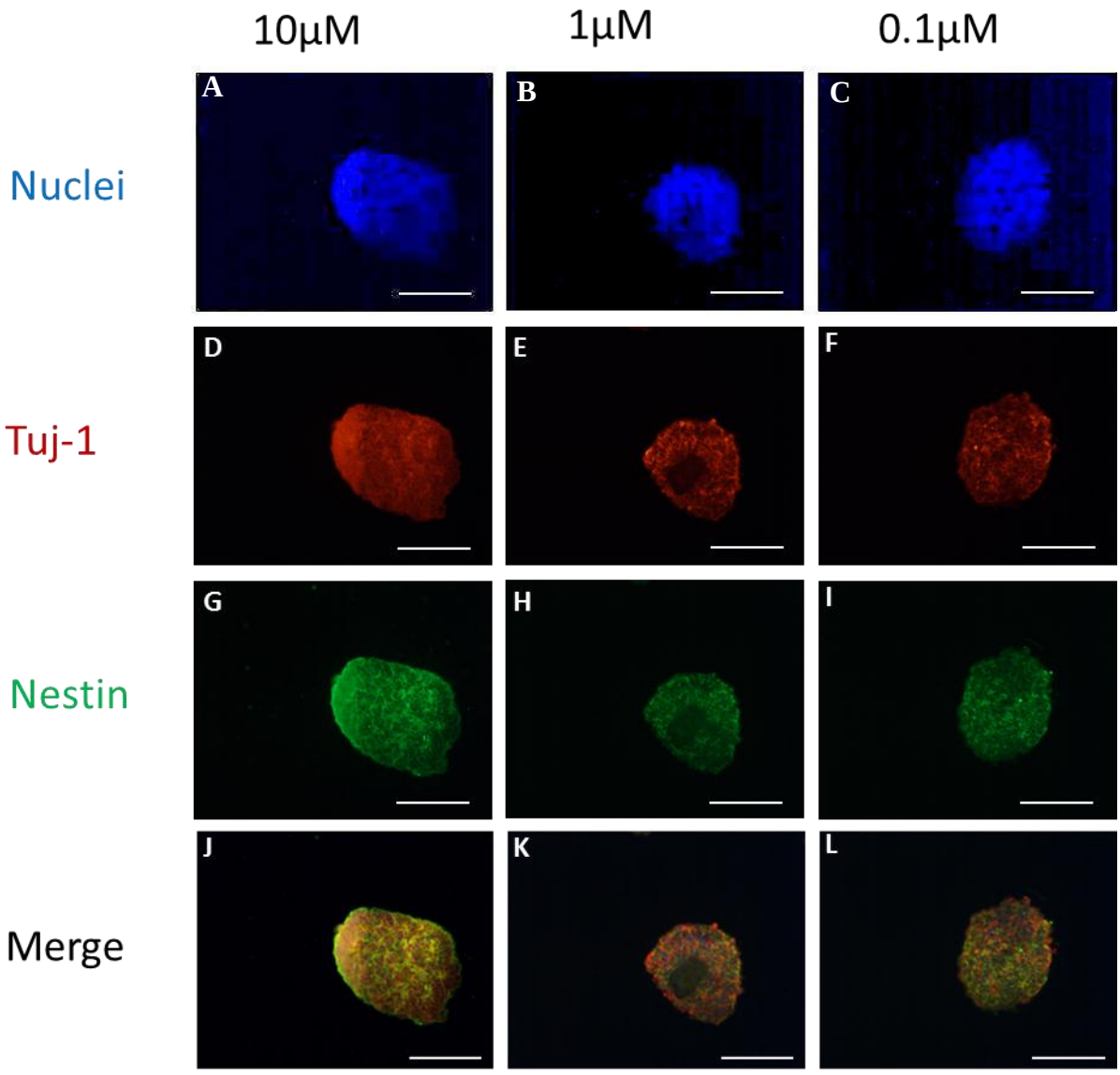

Figure 4-7 Expression of neural proteins in TERA2.cl.SP12 aggregates after differentiation for 14 days with ATRA. Differentiated aggregates were fixed and embedded prior to sectioning and staining for the neural proteins, Nestin (Green) and β III Tubulin (TUJ-1) (Red). The data shown is DAPI (A,B,C), Tuj-1 (D,E,F), Nestin (G,H,I) and merged flourescence (J,K.L) at 10 µM, 1 µM and 0.1 µM. Nuclei were stained with DAPI (Blue). Aggregates were positive for both Nestin and β III Tubulin (TUJ-1). High levels of Nestin were present at 10 µM EC23. Low levels of β III Tubulin (TUJ-1) was expressed throughout all three concentrations. These cells were in the early stages of neural commitment. Notice the central area of aggregates E, and H do not express typical neruonal markers. This is likely due to non-neuronal lineage commitment or cell death. Scale bars = 250 µm. n=3

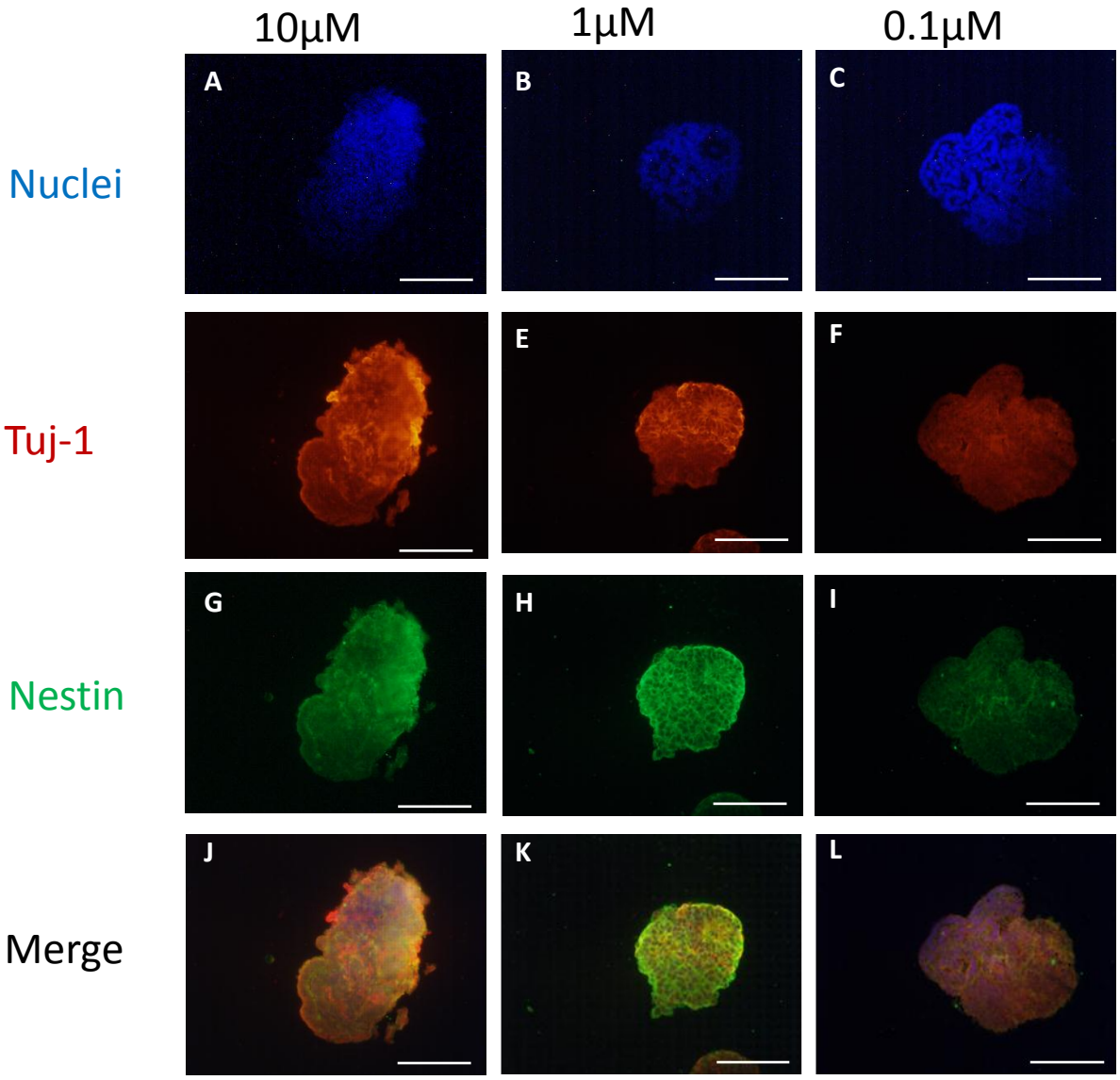

Figure 4-8 Expression of neural proteins in TERA2.cl.SP12 aggregates after differentiation for 14 days with AH61. Differentiated aggregates were fixed and embedded prior to sectioning and staining for the neural proteins, Nestin (Green) and β III Tubulin (TUJ-1) (Red). The data shown is DAPI (A,B,C), Tuj-1 (D,E,F), Nestin (G,H,I) and merged flourescence (J,K.L) at 10 µM, 1 µM and 0.1 µM. Nuclei were stained with DAPI (Blue). Aggregates were positive for both Nestin and β III Tubulin (TUJ-1). High levels of β III Tubulin (TUJ-1) were present at 1 and 10 µM AH61. Very high levels of Nestin are observed at 1 µM. Low expression of β III Tubulin (TUJ-1) and Nestin was observed at 0.1 µM, indicating a direct developmental response in the cells depending on the concentration of AH61 used. Scale bars: 250 µm. n=3

It was hypothesised that increasing the differentiation of TERA2.cl.SP12 with each of the compounds from 14 to 21 days would result in an aggregate that contained more mature neural progeny than at 14 days. Increasing the time period of cell differentiation appears to result in a more mature neural phenotype. Under such conditions it would be predicted that cell aggregates may express more β III tubulin and a reduced level of Nestin. Furthermore, cells may act differently when encouraged to form neurites. Initially the internal structural differences of each aggregate under each condition were assessed. Figure 4-9 provides evidence to suggest a differential response between the length of differentiation and the potency of the retinoid used to induce differentiation. Each aggregate was approximately the same size after 21 days. Furthermore, the perimeter and spherical nature of each aggregate was more clearly defined than that at 14 days. In some cases aggregates contained large internal structures with a characteristic neural rosette shape indicative of an early neural progenitor phenotype. The neural rosette structures were mainly seen in aggregates treated with the least potent retinoid or concentration i.e. 0.1 μM AH61 and ATRA, and the higher concentrations of EC23 10 μM and 1 μM. Interestingly, the internal structure of aggregates differentiated with each concentration of EC23 was much more heterogeneous than the high concentrations of ATRA or AH61, indicating a differential effect across the aggregate by EC23.

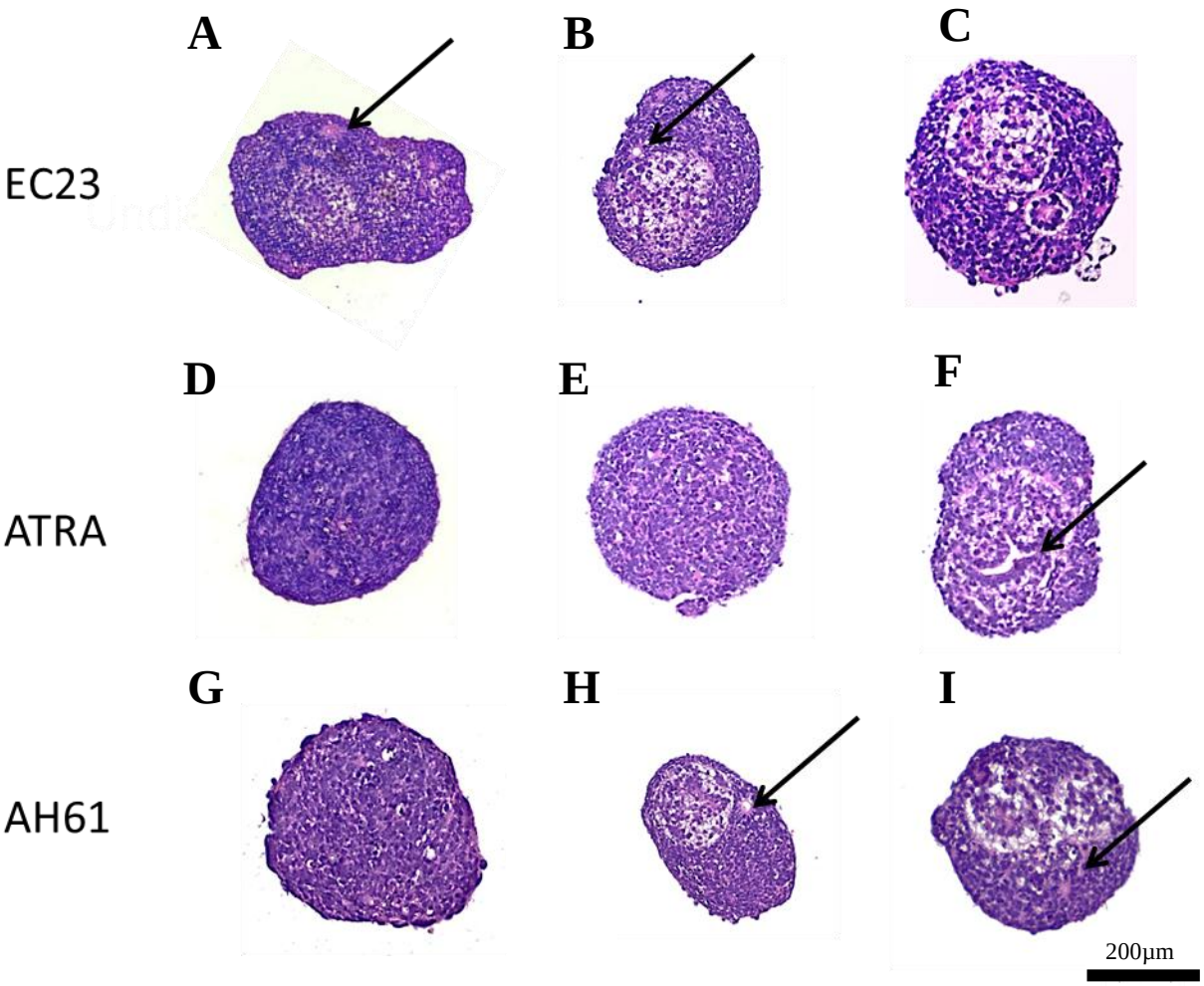

Figure 4-9 Internal aggregate structure demonstrates neural rosette formation and differential cell patterning after 21 days differentiation. H & E staining of aggregates differentiated with EC23(A,B,C), ATRA (D,E,F) or AH61(G,H,I) at 10 µM, 1 µM or 0.1 µM respectivly for 21 days. Histological analysis demonstrate structural similarities between each compound, after 21 days neural rosettes have developed in many of the lower concentrations used. Some non-rosette like structures also formed in the synthetic compounds 0.1 µM EC23 and 1 µM and 0.1 µM AH61. The overall shape and size of the aggregates are more consistent between compounds indicating structural limitations of the aggregates. Arrows show internal neural rosette structures. n=3.

The neural rosette structure observed within some of the differentiated cell aggregates is characteristic of neural progenitor formation [5]. The progenitors are generally able to develop into the three main types of neural cell – oligodendrocyte, neuron and astrocyte however this was not tested.

Neural rosettes have a characteristic radial-columnar structure and express neural specific cytoskeletal proteins such as Nestin and β III Tubulin. H & E staining so far has demonstrated the presence of neural rosettes in some aggregates, suggesting neural progenitor formation, aggregates without rosettes may be non-neuronal or more developed neural tissue. Figure 4-10 demonstrates a high magnification image of a neural rosette from TER2.cl.SP12 EC cells differentiated by 1 µM EC23 for 21 days.

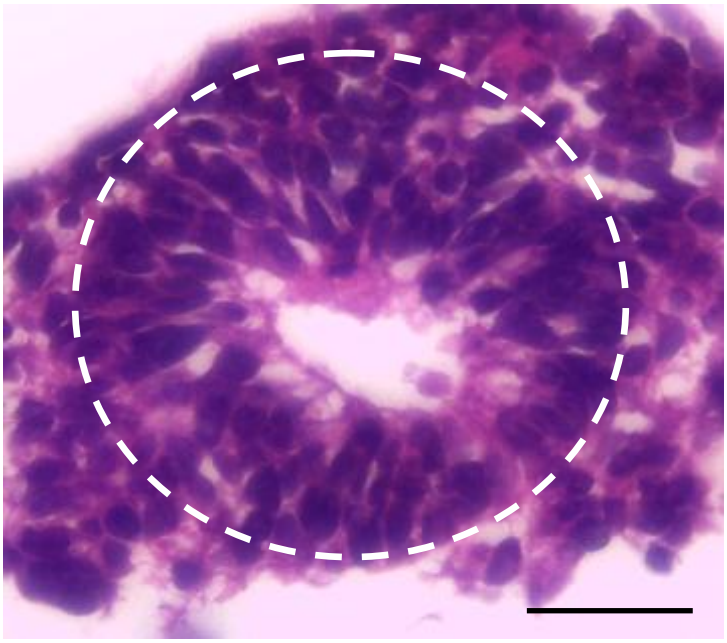

Figure 4-10 Neural rosette structure characteristic of neuroprogenitors differentiation from stem cells. Development of neural rosettes are characteristic of neuroprogenitor formation. Rosettes have a radial arrangement of columnar cells and express proteins associated with neural development [5]. TERA2.cl.SP12 EC cells were differentiated for 21 days by 1µM EC23 and stained with H& E. The white line marks the approximate outer edge of the neural rosette. Scale bar: 50 µm.

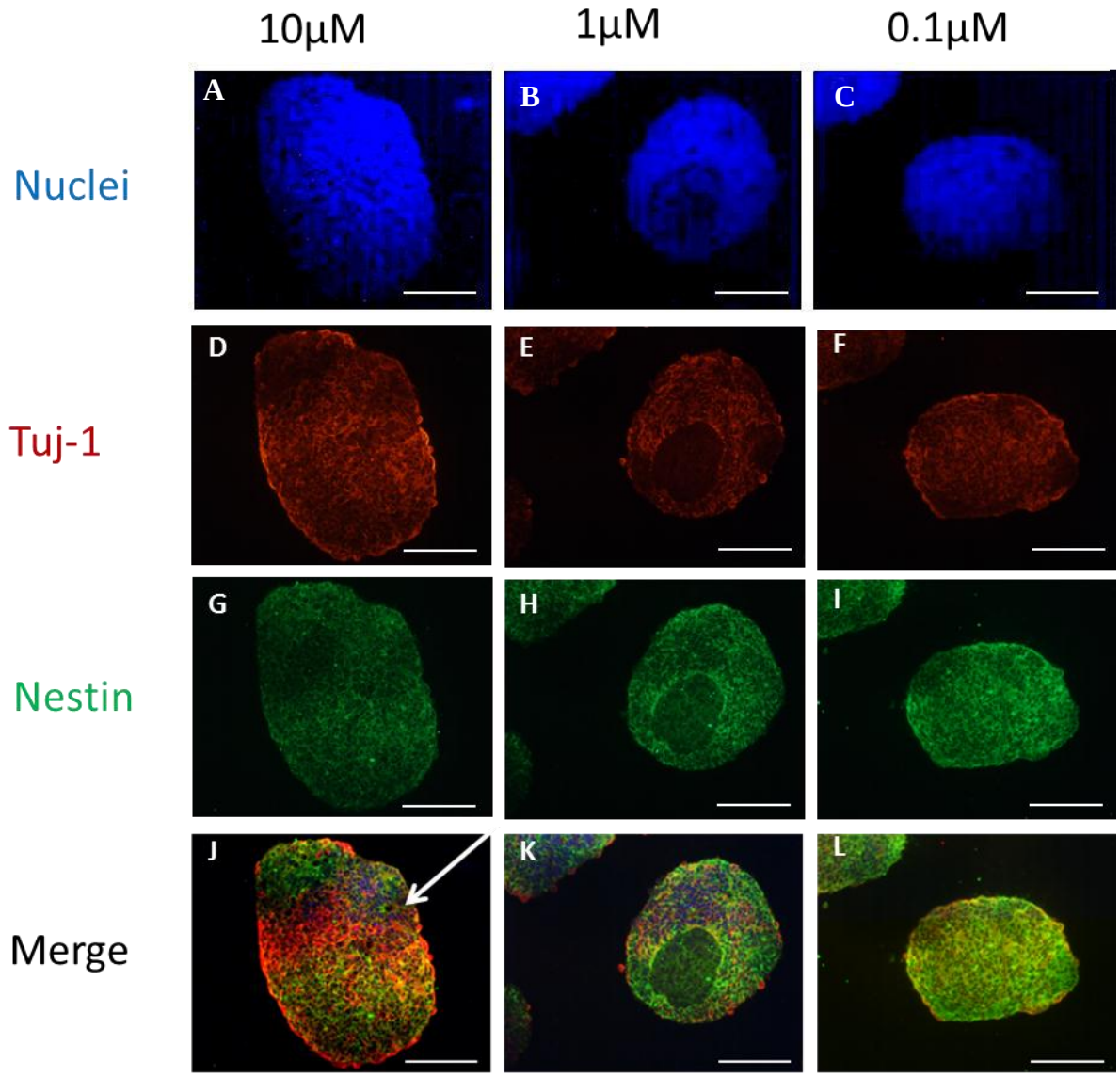

Figure 4-11 Expression of neural proteins in TERA2.cl.SP12 aggregates after differentiation for 21 days with EC23. Differentiated aggregates were fixed and embedded prior to sectioning and staining for the neural proteins, Nestin (Green) and β III Tubulin (TUJ-1) (Red). The data shown is DAPI (A,B,C), Tuj-1 (D,E,F), Nestin (G,H,I) and merged flourescence (J,K.L) at 10 µM, 1 µM and 0.1 µM. Nuclei were stained with DAPI (Blue). Aggregates were positive for both Nestin and β III Tubulin (TUJ-1). Higher β III Tubulin (TUJ-1) expression was visible in aggregates differentiated at 10 µM. The lowest concentration of EC23 0.1 µM had visibly higher levels of Nestin expression than β III Tubulin (TUJ-1) indicating that the cells represent early neural progenitors. Notice the central area of aggregates E, and H do not express typical neruonal markers. This is likely due to non-neuronal lineage commitment or cell death. Scale bars : 250 µm. n=3

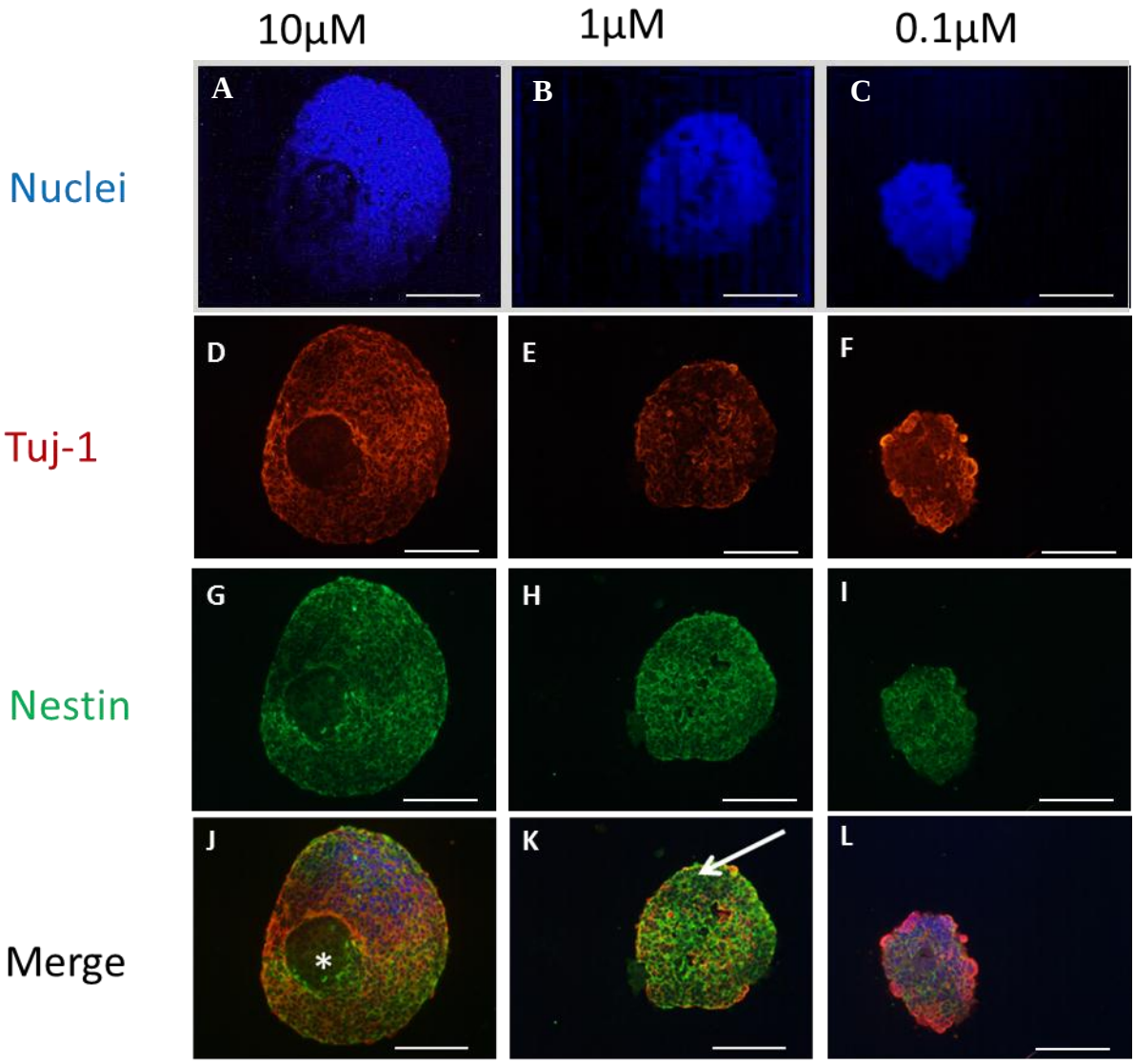

Figure 4-12 Expression of neural proteins in TERA2.cl.SP12 aggregates after differentiation for 21 days with ATRA. Differentiated aggregates were fixed and embedded prior to sectioning and staining for the neural proteins, Nestin (Green) and β III Tubulin (TUJ-1) (Red). The data shown is DAPI (A,B,C), Tuj-1 (D,E,F), Nestin (G,H,I) and merged flourescence (J,K.L) at 10 µM, 1 µM and 0.1 µM. Nuclei were stained with DAPI (Blue). Aggregates were positive for both Nestin and β III Tubulin (TUJ-1). High levels of Nestin were present at 10 µM ATRA. Low levels of β III Tubulin (TUJ-1) was expressed throughout all three concentrations. These cells were in the early stages of neural commitment. Notice the central area of aggregates D, and G do not express typical neruonal markers. This is likely due to non-neuronal lineage commitment or cell death. Scale bars : 250 µm. n=3.

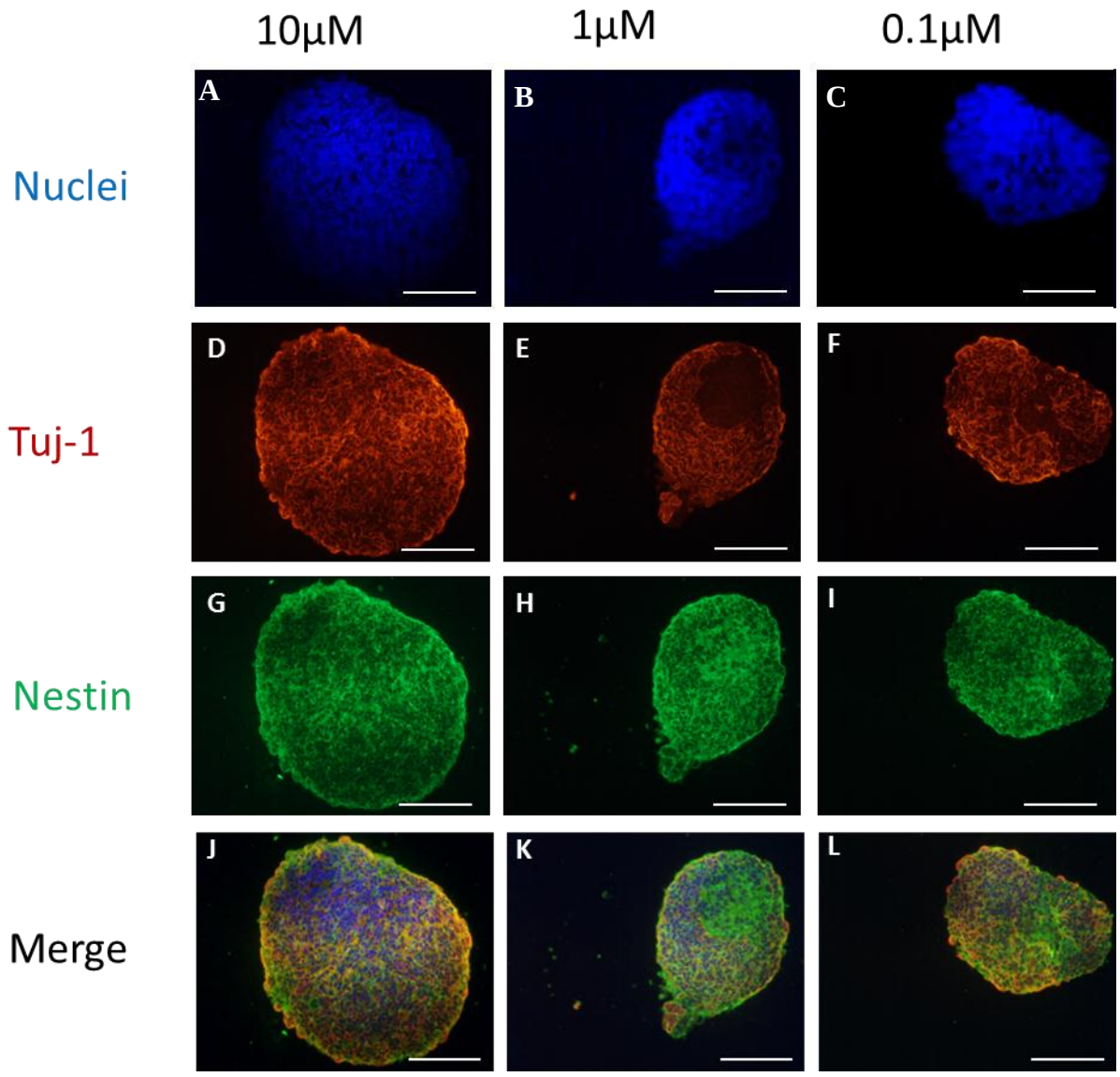

Figure 4-13 Expression of neural proteins in TERA2.cl.SP12 aggregates after differentiation for 21 days with AH61. Differentiated aggregates were fixed and embedded prior to sectioning and staining for the neural proteins, Nestin (Green) and β III Tubulin (TUJ-1) (Red). The data shown is DAPI (A,B,C), Tuj-1 (D,E,F), Nestin (G,H,I) and merged flourescence (J,K.L) at 10 µM, 1 µM and 0.1 µM. Nuclei were stained with DAPI (Blue). Aggregates were positive for both Nestin and β III Tubulin (TUJ-1). High levels of β III Tubulin (TUJ-1) were present at 1 and 10 µM AH61. Very high levels of Nestin were expressed at 1µM, low expression of β III Tubulin (TUJ-1) and Nestin was observed at 0.1 µM, indicating a direct developmental response in the cells depending on the concentration of AH61 used. Notice the central area of aggregate D does not express TUJ-1 however, nestin is expressed indicating a proliferative neural progenitor. Scale bars : 250 µm. n=3

4.3.2 Neurite Outgrowth from differentiated neurospheres using synthetic retinoids

Evidence suggests that the cell aggregates are neurogenic and clearly resemble the structure typical of a neurosphere. Aggregates of cells differentiated in suspension for 14 or 21 days expressed a combination of Nestin and TUJ-1 indicating neural commitment, however, the apparent stage of differentiation depended on the compound, concentration and length of time used to differentiate the cells. To further differentiate the cells and induce neurite formation the aggregates from each treatment group were placed onto a Laminin and P-D-L coated substrate. Each of the aggregates adhered to the substrate and neurites developed from the central sphere. In this part of the differentiation process retinoid was not included in the media; however, to control any excess cell by proliferation, mitotic inhibitors were added throughout this part of the protocol.

Aggregates differentiated for 14 days regardless of the concentration or compound used lost the integrity and smooth border of the aggregate (Figure 4-14). Many cell nuclei migrated away from the aggregate and formed individual neurites. More cells remained in the central aggregate when differentiated with AH61, however, the aggregate began to disperse. Such cell migration and loss of aggregate integrity resulted in difficulty of quantification of any change in length or number of neurites, as with 2D mono-layer differentiation. The migratory ability of the cells may be in part the result of early neural commitment and high Nestin levels typical of neuroprogenitors. Although most of the treatment groups resulted in such cell dispersal, this was more pronounced when using lower concentrations of ATRA. In contrast many more cells were maintained as a central sphere when differentiated with synthetic retinoids EC23 or AH61.

Increasing the length of the differentiation period from 14 to 21 days resulted in a more consistent aggregate structure and size. Furthermore, an apparent increase in TUJ-1 staining indicated the formation of more mature, differentiated neural cells. Transfer of the aggregates differentiated under each condition for 21 days to a Laminin/P-D-L substrate for 10 days resulted in a distinct halo of individual neurites projecting from a central sphere of cell nuclei (Figure 4-15). Quantification of the number of neurites that developed from the aggregate under each condition revealed differences between the potency of compound and the number of neurites that developed. The highest number of neurites developed from aggregates that were differentiated with 10 µM and 1 µM ATRA, AH61 or 0.1 and 1 µM, EC23. The lowest number of neurites that formed was from 0.1 µM ATRA

and 10 µM EC23 differentiated cells. It became apparent that for a consistent model of neurite outgrowth that can be quantified consistently the cells would need 21 days differentiation with a potent or concentrated level of retinoid.

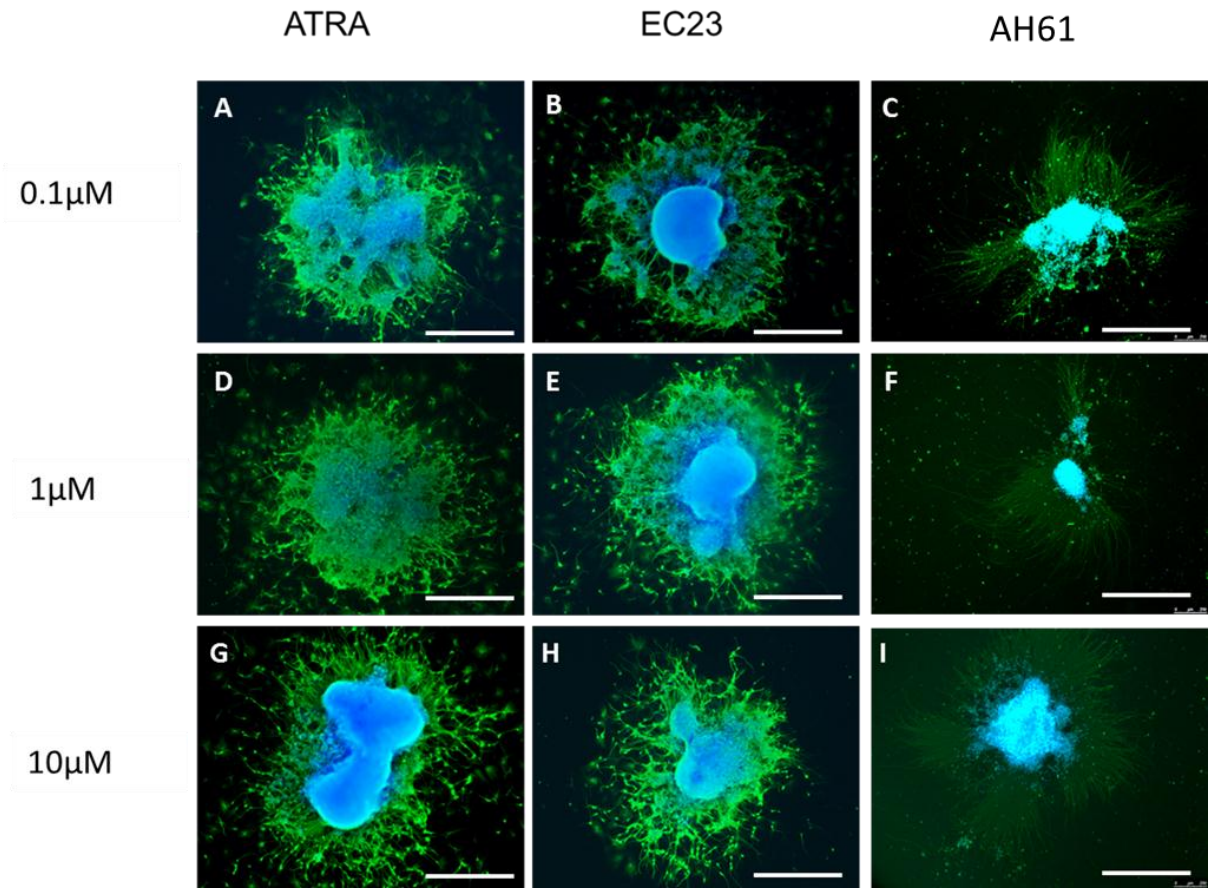

Figure 4-14 Neurite outgrowth from aggregates differentiated for 14 days. Aggregates of TERA2.cl.SP12 EC cells were differentiated for 14 days in the presence of ATRA (A,D,G), EC23 (B,E,H) or AH61 (C,F,I) at 10, 1 or 0.1 µM respectively. After 14 days the aggregates were placed onto tissue culture plastic coated with 10 µg/ml Laminin/P-D-L for 10 days in the presence of mitotic inhibitors. After 10 days aggregates were fixed in 4% PFA and stained for β III Tubulin (TUJ-1) (Green) and DAPI (Blue). The structural integrity of the aggregate was not maintained as many cells migrated away from the neurosphere. Migrating cells formed individual neurites on the Laminin/P-D-L substrate. More migration from the central spehre was seen by low levels of ATRA than the same concentration of AH61 or EC23. This indicated a more mature 14 day differentiated neural progenitor or a different type of progentiro has developed. Some non-tuj-1 expressing cells also migrated from the aggregate. Scale bars: 500 µm. n=3.

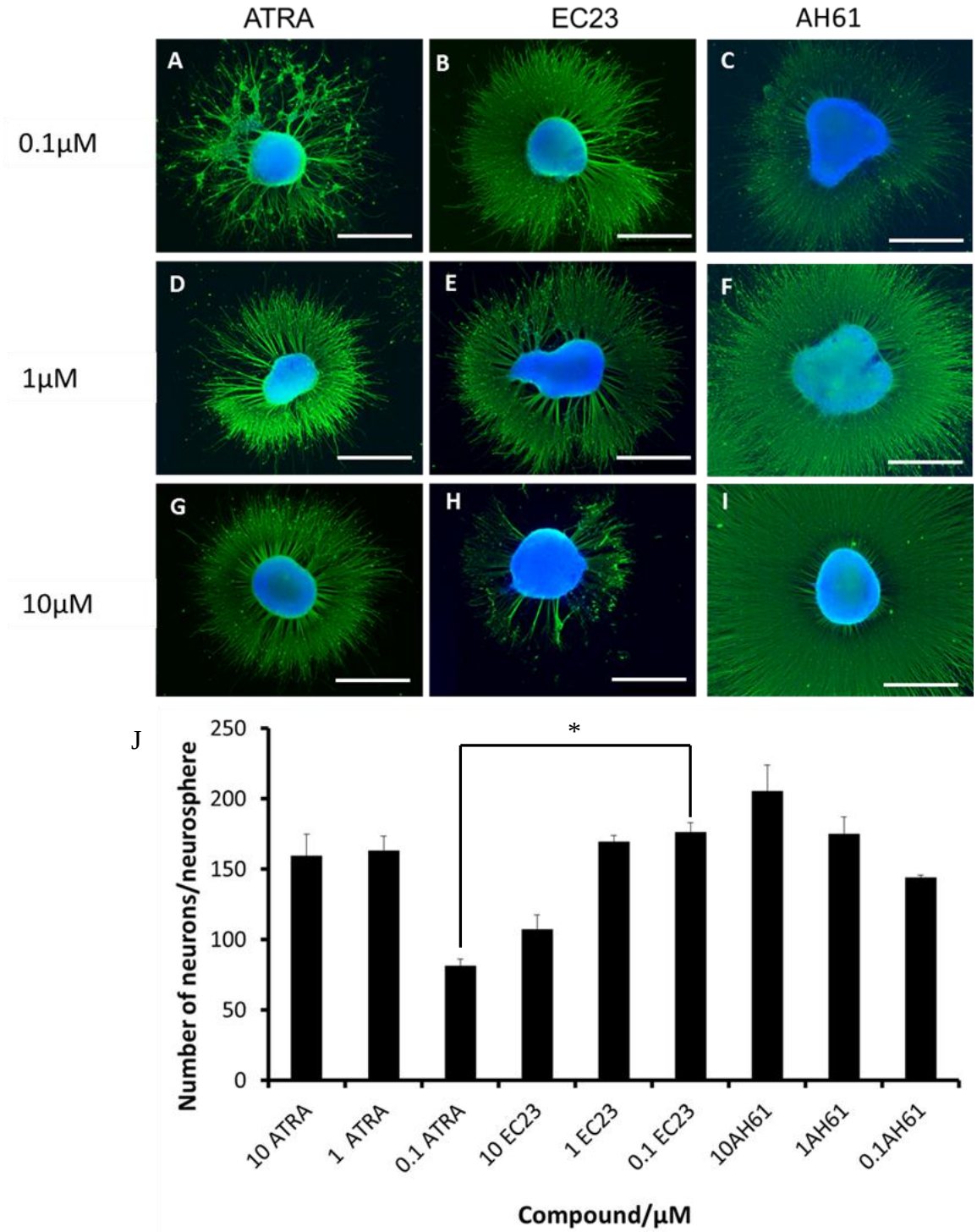

Figure 4-15 Induction and quantification of neurite outgrowth from human pluripotent stem cells after 21 days treatment with ATRA, EC23 or AH61. Aggregates of TERA2.cl.SP12 were incubated with either ATRA (A,D,G), EC23 (B,E,H) or AH61 (C,F,I) at 0.1 µM, 1 µM or 10 µM respectively for 21 days. Aggregates were plated onto Laminin/P-D-L for 10 days and stained for the pan neuronal antigen β III Tubulin (TUJ-1). The number of neurites that developed from each aggregate depended on the concentration of compound used. Neurites were quantified by magnification and counting using Image-J software. Interestingly an increase in differentiation time to 21 days resulted in a loss of cell migration from the aggregate, maintaining a tight sphere. Scales Bars: 500 µm. Data represent mean ± SEM, n≥3. * p≤0.005 Student's t-test corrected for multiple testing between compared sample poulations using the Bonifferoni correction.

It was decided not to take AH61 any further into the study, since much less was known about its biological effect on TERA2.cl.SP12 and due to constraints on production, AH61 was less available than EC23 which was purchased having undergone quality control procedures, making the compound more reliable and consistent for large scale studies. Furthermore, due to its highly neurogenic activity, stability and the genetic profiles known about its mode of action, EC23 was selected to be used in this model of neurite outgrowth. Since 0.1 µM EC23 induced the optimum level of neural differentiation this was chosen as the concentration to use throughout the rest of this thesis.

To further characterise the neural cell types that develop from treatment with 0.1 µM EC23 a number of genetic CNS markers were assessed. Figure 4-16 shows the gene profiles of developing aggregates treated with 0.1 µM EC23 for 0, 7, 14 and 21 days. The relative quantity of the gene *PAX6*, indicative of neural commitment [203], *OTX2* a gene associated with anterior forebrain CNS development [249] and *HOXC4* which is associated with posterior CNS development, were measured [250]. The profiles expressed by the cells represented neural commitment into ventral posterior CNS. *OTX2* levels decreased with time and this was concomitant with an increase in *HOX*C4. As expected there was an initial peak of *PAX6* and this was maintained at a high level throughout differentiation indicating potential ventral progenitor development as observed previously (Chapter 3).

A

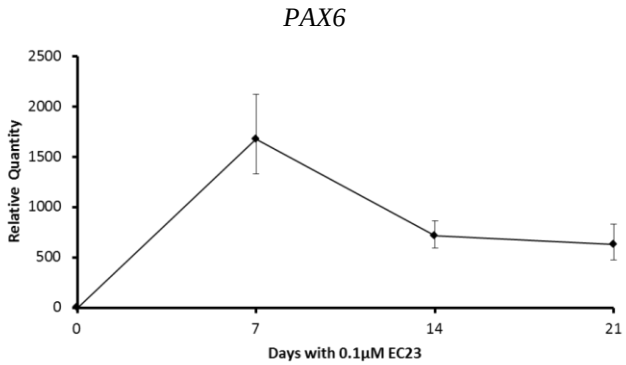

B

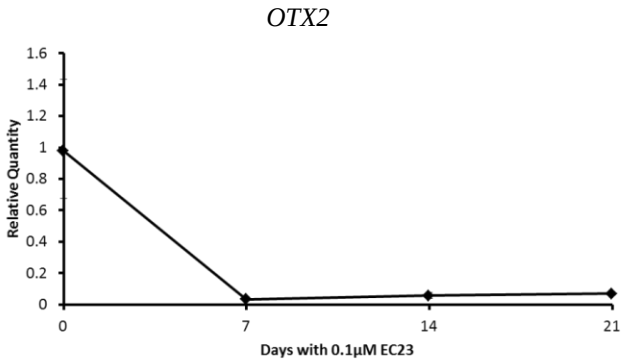

C

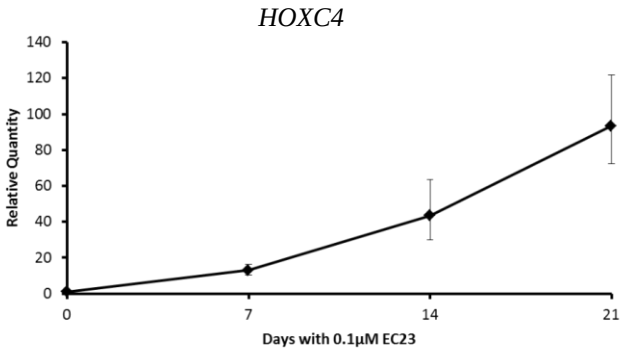

Figure 4-16 Transcriptional profiling of genes associated with neural commitment, forebrain development and caudal CNS development. Data shows relative real time PCR expression of the genes *PAX6* (A), *OTX2* (B) and *HOXC4* (C). Aggregates of TERA2.cl.SP12 cells were exposed to 0.1 µM EC23 for 0, 7, 14 and 21 days. A peak of *PAX6* expression was seen at day 7 this was reduced at day 14 and the lower level maintained to day 21, indicating neural commitment. Expression of the CNS forebrain marker *OTX2* decreased to almost undetectable levels after treatment with EC23, however the posterior CNS gene marker *HOX*C4 gradually increased to around 90 fold compared to the undifferentiated control. Suggesting aggregates develop into posterior CNS neural progenitors. Data represent mean ± SEM, n=3.

4.3.3 Regulation of retinoid receptors during induction of stem cell differentiation

The regulation and modulation of receptors involved in neural commitment and development is important for determining the responsiveness of cells to particular extracellular ligands and ultimately for directing neural specificity.

The retinoic acid receptor β2 has been demonstrated to be involved in numerous developmental stages of neurogenesis, including neural commitment [251], neurite outgrowth [174, 252] and neural differentiation [238]. Since our model of neurite outgrowth will be assessing the role of *RAR* β2 in key molecular pathways involved in neurite regeneration it was important that the receptor was expressed in the differentiated cells. Figure 4-17 demonstrates the rapid up regulation of *RAR* β2 mRNA induced by EC23 treatment. Furthermore, the expression was sustained throughout the differentiation process. These data provide information as to the predicted responsiveness of the cells to agonists of this receptor, of which EC23 is thought to be one [93]. The rapid up-regulation of *RAR* β2 mRNA is likely to be in part a positive feedback response induced by EC23.

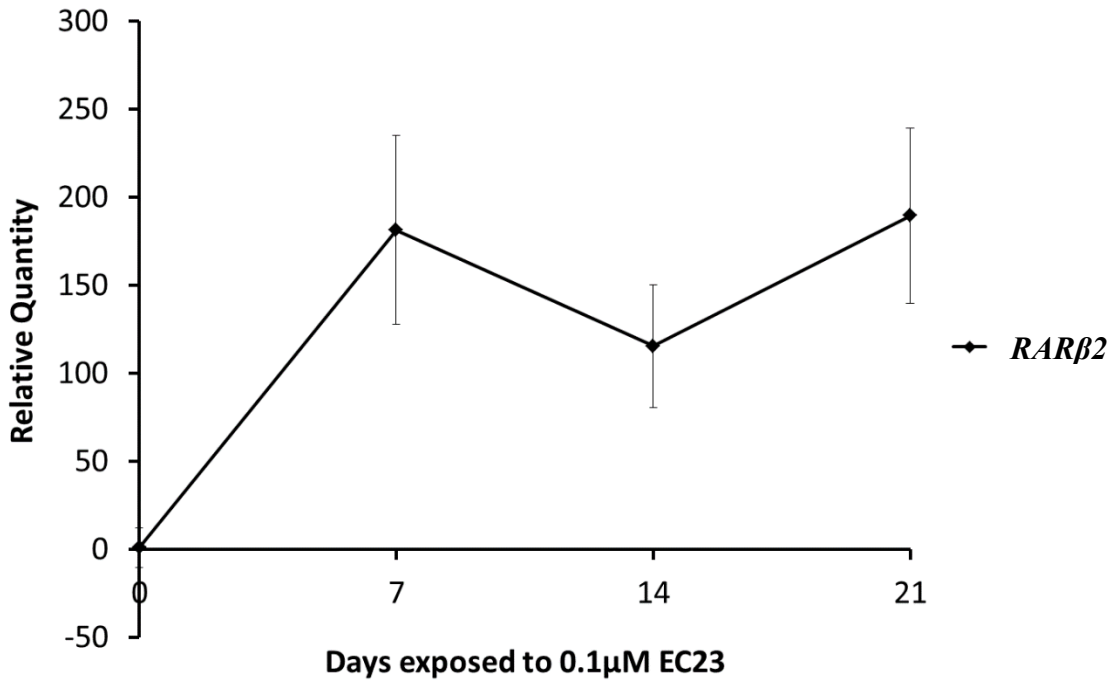

Figure 4-17 Regulation of gene expression profile of the retinoic acid receptor β2 during induction of stem cell differentiation. Aggregates of TERA2.cl.SP12 cells treated with 0.1 µM EC23 were lysed after 0, 7, 14 and 21 days for gene expression analysis by real time PCR. High levels of the receptor was induced and maintained throughout the differentiation protocol. This indicates a link between neural differentation and neural maintenance with the retinoic acid receptor. Data represent mean ± SEM, n=3

The NGF receptor is a trans-membrane receptor often referred to as $p75^{NTR}$ and transmits the signal for neurotropic factors from the neurotrophin family of molecule such as nerve growth factor β (NGF β) and brain-derived neurotropic factor (BDNF) [253].

NGFR receptor or p75 is involved in neural differentiation in a number of cell models such as SH-SY5Y [254], PC12 [255] and rat DRG [256]. Furthermore, NGF expression is associated with development of CNS neurons, commitment to neural tissue, regeneration and sustained adult nervous system function [253]. The stages of development, regenerative potential and neural subtype are important in discerning the expression of the NGF receptor [257-259].

NGFR signalling directly affects *RAR* β expression and hence many of the downstream affects associated with this signalling [109]. Treating cell aggregates with a *NGFR* receptor agonist did not affect neurite outgrowth, however, understanding the temporal expression of this receptor may give insight into the type of neuron that will develop.

To further assess the expression of receptors involved in neural differentiation and commitment, the relative mRNA expression level of nerve growth factor receptor (*NGFR*) and its ligand *NGFR* β were measured in the aggregates at 0, 7 14 and 21 days after treatment with 0.1 µM EC23.

The expression of *NGFR* β mRNA increased with time as the stem cells differentiated, indicating a possible response to ligands of the receptor. The expression in the neuroprogenitors may not correspond to that in the neurons and requires further analysis. There was an initial peak in *NGF β* mRNA which may be responsible for the increased receptor expression however, there was no sustained production of *NGF β* mRNA suggesting supplementing the media of developing aggregates may induce a response.

These data suggest a developmental role of *NGFR β* in the stem cell aggregates which may be exploited to further direct the neuroprogenitors, or prime them for neurite outgrowth.

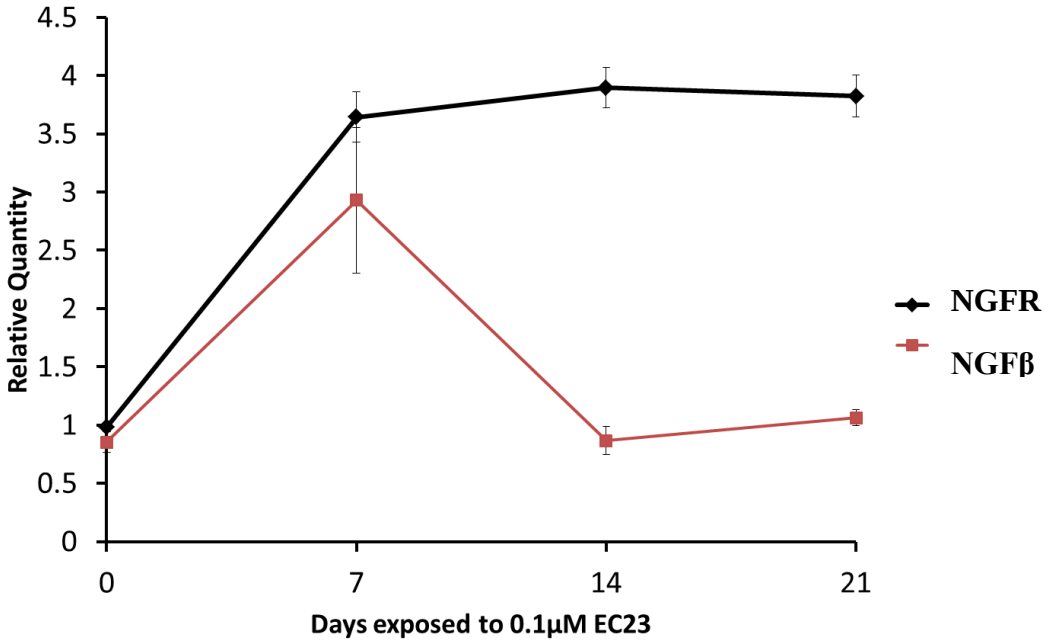

Figure 4-18 Regulation of *NGFR* receptor and *NGFR* β mRNA expression in aggregates treated with EC23. TERA2.cl.SP12 cells were treated with 0.1µM EC23 for 0,7,14 and 21 days. At each time point the mRNA expression of *NGFR* and *NGFβ* was determined relative to the undifferentiated aggregate. The mRNA expression of *NGFR* increased rapidly to around 3.5 fold the undifferentiated control and was miantained throughout the differentiation protocol. The mRNA expression of the *NGFR* ligand *NGFβ* peaked initially, however, rapidly reduced to basal levels indicating no sustained release of this protein from the cells. Data represent mean ± SEM, n=3.

4.3.4 Application of stem cell derived neurogenic culture model

In the previous Sections a defined model of neural progenitor development and neurite outgrowth has been described. This model utilises a well described cell line used in neurobiological research and a highly stable well characterised small molecule that is analogous to natural ATRA. Using these tools a robust and reproducible model of human neurite outgrowth has been developed that is highly neurogenic and neurite outgrowth is easy quantifiable.

This model can now be applied to investigate human neurogenesis in health and disease specifically in regard to robust neurite outgrowth; however, there are differences to be aware of. The neurites that form from the differentiated aggregate on Laminin and P-D-L have not undergone damage as would have occurred in neurons after traumatic CNS injury and represent neurite outgrowth similar to that which may be seen during embryogenesis. It is known that as a consequence of CNS injury, genes associated with early embryonic neurite outgrowth are up regulated [260]. Some regeneration is demonstrated in the CNS post-injury which is characterised by growth cone formation and extension of the neurite, however, much of the outgrowth is perpendicular to the direction of the damaged spinal nerves, indicating an inhibitory environment within the glial scar. Growth cone formation is indicative of embryonic development and neural regeneration after injury.

Developmental programmes that are switched off in the mature neuron become activated once more in an effort to recover the lost neuronal tissue. It is important to understand why these neurites do not fully re-innervate the CNS and work out ways of enhancing the regeneration to aid recovery. The model developed herein represents an early stage of neural development that recapitulates many aspects of neurons post-CNS injury, thus making the model useful for basic research into enhancing neural regeneration and restoration after CNS injury.

4.3.4 Inhibition of human neurite outgrowth by the CSPG - Aggrecan

Recently direct receptor activation on the membrane of neurites has been associated with neurite retraction and inhibition of regeneration induced by chondroitin sulphate proteoglycans within the glial scar. Two of these receptors are protein tyrosine phosphatase σ (PTPσ) and the leukocyte common antigen receptor (LAR) also a protein tyrosine phosphatase [1, 261].

To use our human model neurite outgrowth to assess neural regeneration when grown in an Aggrecan rich environment it is essential that these receptors are present in the aggregates and developing neurites.

Figure 4-19 shows the expression of both LAR and PTP σ in the developing aggregates, although the fold change is only small, reaching around 2 fold increase from baseline mRNA levels, the receptors are expressed at the gene transcription level. This is encouraging since, the next part of this study assessed the effect of ligand interaction of each of these receptors on neurite outgrowth.

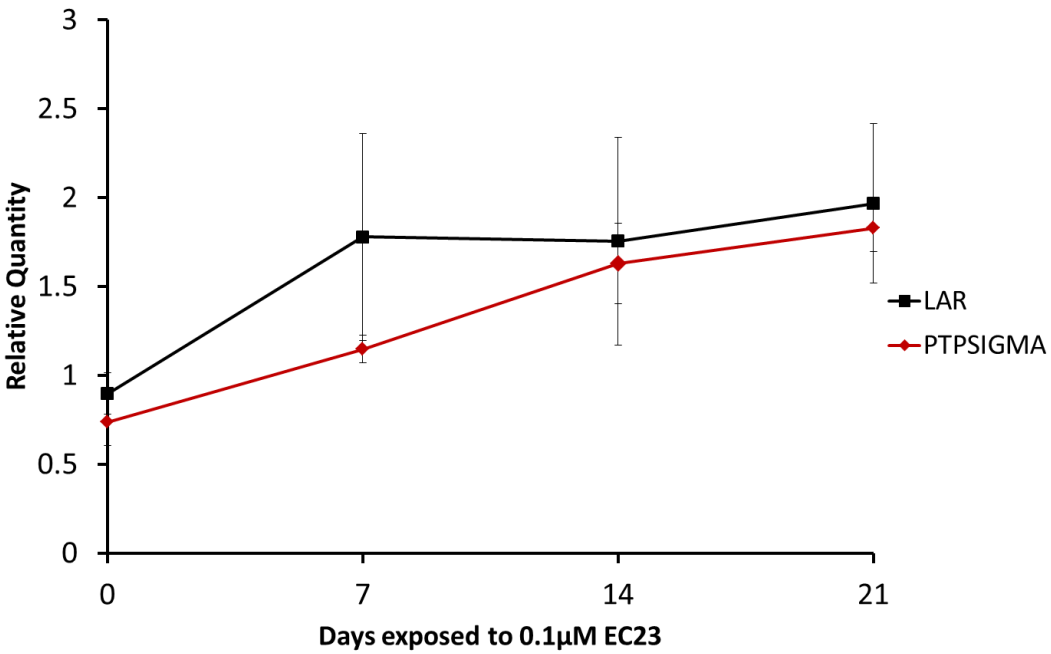

Figure 4-19 LAR and PTPSIGMA receptor mRNA expression in TERA2.cl.SP12 EC cells. The mRNA of both LAR and PTPSIGMA were expressed in the developing aggregates. High basal mRNA level resulted in only small relative changes over the 21 day differentiation period. High basal levels in the aggregates may be indicative of the neural propensity of the cells, or the receptors may have an alternative role in undifferentiated stem cells relating to pluripotency. Data represent mean ± SEM, n=3.

This part of the study aimed to develop a model of the glial scar to simulate neurite inhibition. This will be achieved by altering the substrate of neurite outgrowth by adding Aggrecan, an ECM protein up regulated in the glial scar and highly inhibitory to neural regeneration. Initially to assess the effect of concentration, Aggrecan was added to the Laminin/P-D-L coating substrate at four concentrations 0 µg/ml, 1 µg/ml, 25 µg/ml, and 50 µg/ml (Figure 4-20). Data demonstrates that the addition of Aggrecan reduces the length of neurites that form and also the number of neurites in a concentration dependent manner. Maximum loss was demonstrated from neurites grown on a 50 µg/ml Aggrecan substrate. Throughout the rest of this Chapter Aggrecan was used at a concentration of 50 µg/ml which gave the greatest inhibition of neurite outgrowth from the cells and is similar to published concentrations used in DRG neurons.

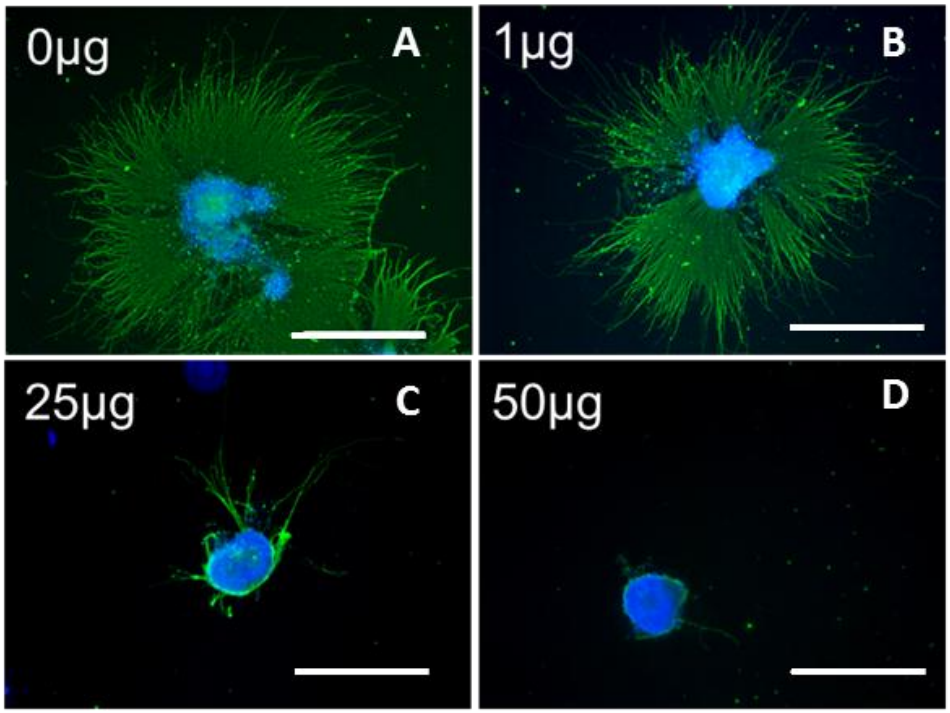

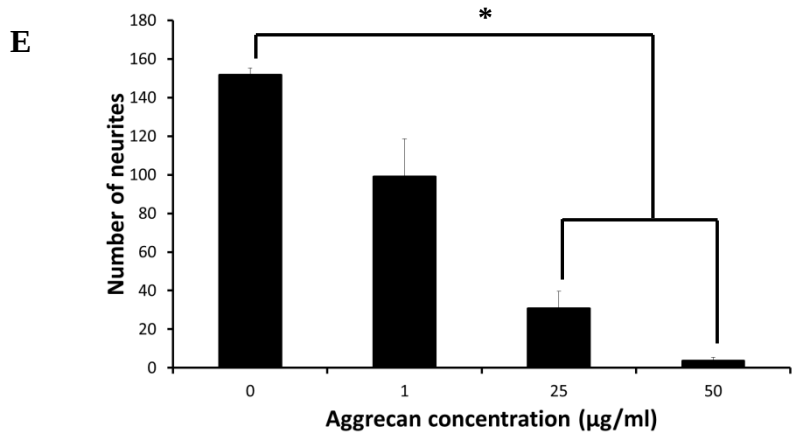

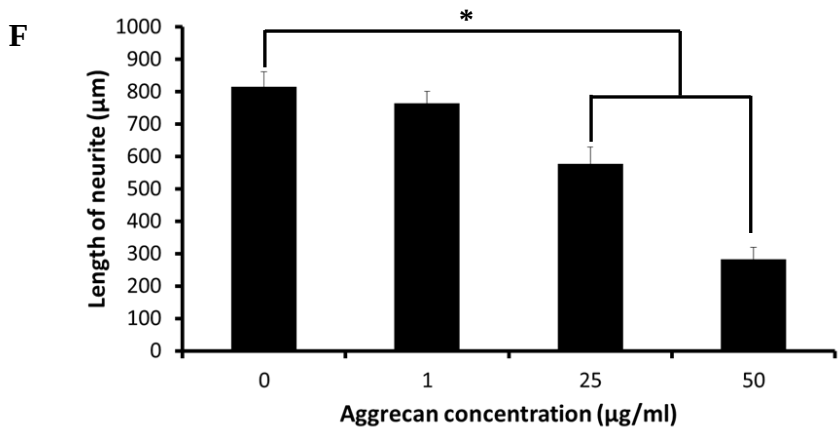

Figure 4-20 Loss of neurite outgrowth from differentiated human pluripotent stem cells by the addition of Aggrecan to the ECM. Aggregates of neural-progenitors developed from TERA2.cl.SP12 cells exposed to 0.1 µM EC23 for 21 days were placed onto a Laminin, P-D-L and Aggrecan substrate. Laminin and P-D-L concentration was kept constant at 10 µg/ml. Aggrecan was added at a concentration of 0 µg/ml (A), 1 µg/ml (B), 25 µg/ml (C) or 50 µg/ml (D) to the coating solution as described in the methods. Aggregates were placed on the different substrates for 10 days prior to staining with β III Tubulin (TUJ-1) for quantification. Measurement of the number of neurites in each condition (E) and length of neurites (F) were taken. Data demonstrated that incorporation of Aggrecan reduced the number of neurites developing from the aggregate and an almost complete loss of neurite outgrowth at 50 µg/ml. Scale Bars: 500 µm. * $p \leq 0.005$ Student's t-test corrected for multiple testing between compared sample poulations using the Bonifferoni correction.

4.3.5 Restoration of neurite outgrowth using small molecules

Small molecule analogues of receptor ligands and synthetic mediators of specific signalling pathways provide a reproducible method of inducing specific responses in cells and are often more potent or induce fewer non-specific side effects due to their enhanced specificity for particular pathways. This section focuses on the synthetic modulation of signalling pathways involved in the Aggrecan mediated inhibition of neurite outgrowth. The experiments performed aimed to investigate known and novel small molecules for their ability to overcome Aggrecan-induced neurite inhibition. Using our human model of neurite outgrowth and Aggrecan-induced neural inhibition small molecules representing four individual receptor mediated pathways were tested for their ability to revive neurite outgrowth when cultured on an unfavourable substrate. Details concerning work performed with the compounds tested are described below.

4.3.6 ROCK Inhibition and recovery of neurite outgrowth

The commercially available Rho associated protein kinase (ROCK) inhibitor, Y-27632 has many applications in stem cell biology and neurobiology. The small molecule is highly specific for p160 ROCK and has a Ki value of 0.14 (TOCRIS Bioscience). The enzyme ROCK activates a downstream modulator RhoA which then affects actin organisation and processes such as cell motility, contraction and apoptosis [262, 263]. Furthermore, ROCK activation has been implicated in the inhibition of CRMP2 by phosphorylation [167]. CRMP2 and CRMP4 are known to promote axon formation and inhibition induces growth cone collapse in developing neurites. The inhibition of ROCK and subsequently RhoA has been shown to overcome CSPG and Myelin Associated Glycoprotein (MAG) induced loss of neurite outgrowth in rat DRG neurons possibly through a CRMP2/4 mechanism [167, 245].

Y-27632

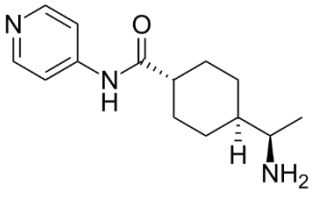

To investigate how ROCK inhibition affects neurite outgrowth from neurons in our model grown on an inhibitory Aggrecan substrate Y-27632 was added to the culture media at 0 µM, 0.5 µM, 10 µM and 15 µM (Figure 4-22). Treating the cultures for 10 days with Y-27632 resulted in recovery of neurite outgrowth from the aggregates on a substrate coated with Aggrecan, Laminin and P-D-L. The number of neurites that developed in cultures treated with 15 µM Y-27632 was similar to the control; however there was an enhanced length induced on the inhibitory substrate by 15 µM Y-27632. At lower concentrations Y-26732 induced a reduced enhancement of neurite outgrowth but the effects were apparent with just 0.5 µM Y-27632. In this study an Aggrecan negative control demonstrated good neurite outgrowth and an Aggrecan positive culture without Y-27632 supplementation had inhibited neurite outgrowth both in neurite length and number. Figure 4-21 shows schematically the level at which the small molecule Y-27632 inhibits the signalling cascade induced by Aggrecan.

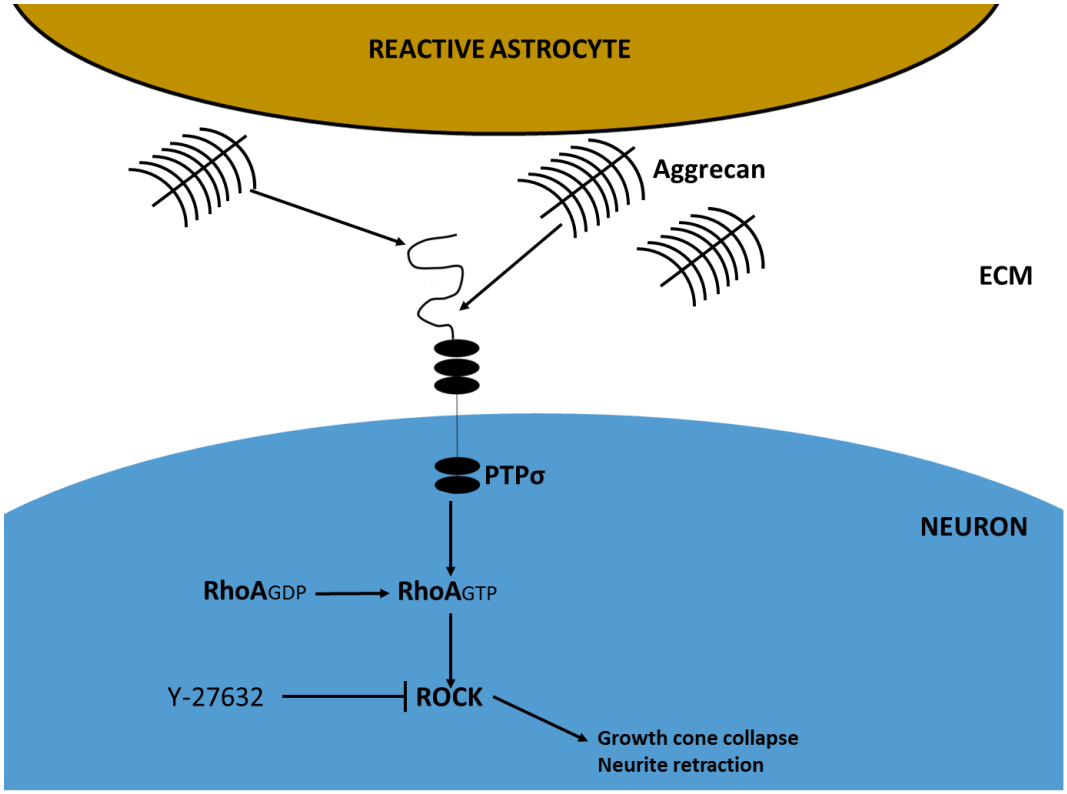

Figure 4-21. The small molecule Y-27632 enhances neurite outgrowth in human stem-cell derived neurons grown on Aggrecan. Activation of Rho Associated Protein Kinase (ROCK) by Aggrecan results in growth cone collapse and neurite retraction in developing axons. Inhibition of ROCK by Y-27632 overcomes the effect of Aggrecan by preventing the loss of cytoskeletal architecture by ROCK. The schematic demonstrates where in the signalling cascade Y-27632 acts.

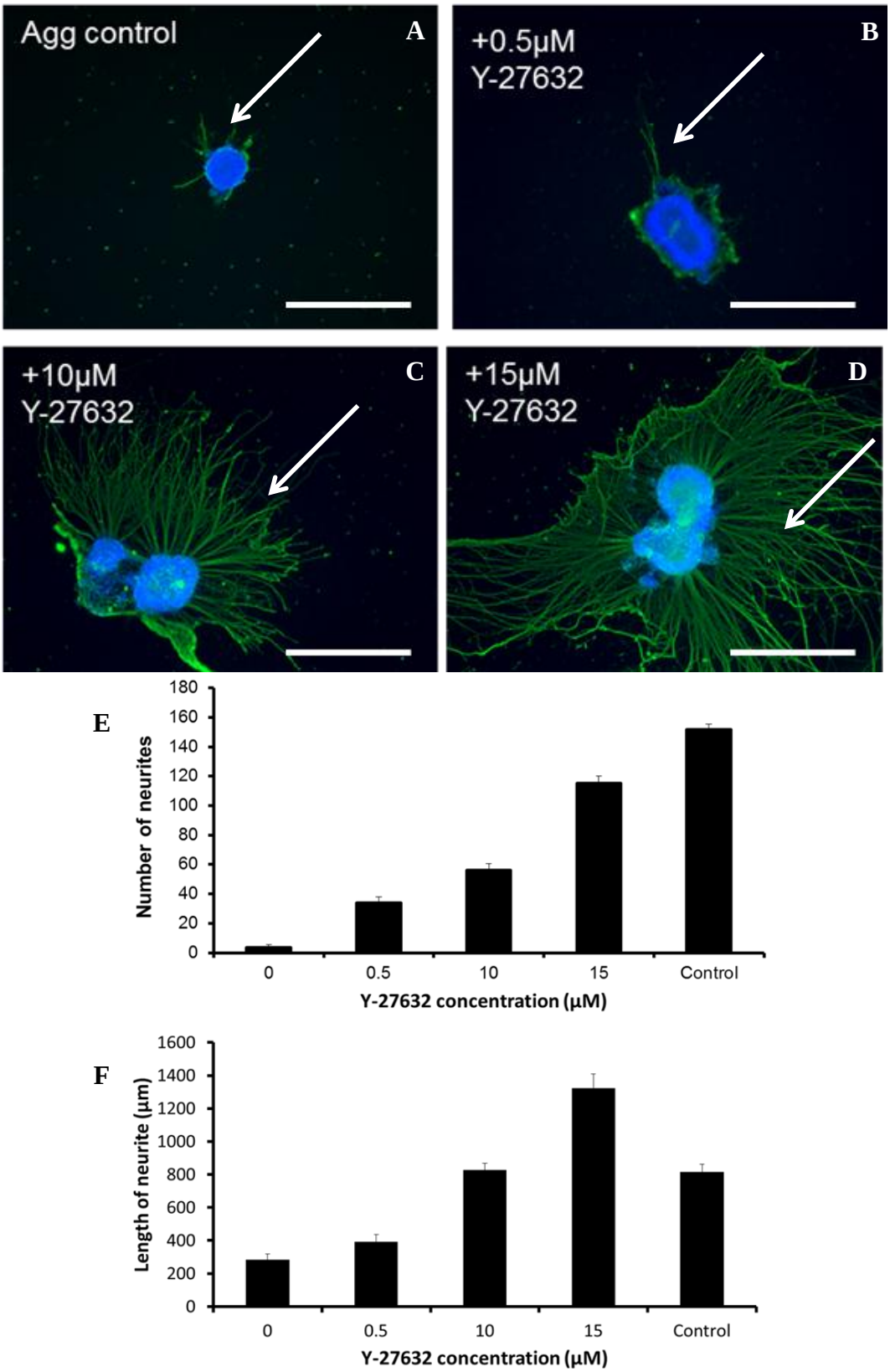

Figure 4-22 Rescue of Aggrecan-induced neurite inhibition by ROCK inhibition. Aggregates of TERA2.cl.SP12 EC cells were differentiated with 0.1 μM EC23 for 21 days and then placed onto a 10 μg/ml Laminin and P-D-L substrate supplemented with 50 μg/ml Aggrecan. The no Aggrecan control aggregates were grown on Laminin and P-D-L only substrate. Aggregate media was conditioned with the small molecule Y-27632 (TOCRIS), a ROCK –P160 inhibitor to investigate the enzymes role in neurite outgrowth under these conditions. Y-27632 was added to the media at 0.5 μM (B), 10 μM (C) or 15 μM (D) for 10 days. Measurement of the number of neurites in each condition (E) and length of neurites (F) were taken. Arrows highlight neurite outgrowth. Recovery of neurite outgrowth was concentration dependent with maximal enhancment at 15 μM. Both neurite length and number were increase by Y-27632 treatment. Scale bars: 500 μm. Data represent mean ± SEM, n=3.

4.3.7 Neurite outgrowth recovery by retinoid agonist – AC261066

A well described receptor *RAR*β2, that has been implicated in neural regeneration has been discussed earlier. Agonists of this receptor have been shown enhance neurite outgrowth in explants of rat DRG and cortical neurons. Furthermore, the small molecule *RAR* β agonist CD2019 could overcome MAG induced inhibition of rat cerebellar neurons and regeneration of lesioned rat spinal cord via PI3K. It was also demonstrated that in the regenerating spinal cord *RAR*β2 was up regulated. Relatively recently a highly potent *RAR*β2 synthetic agonist, AC261066 was developed and is commercially available [238].

AC261066

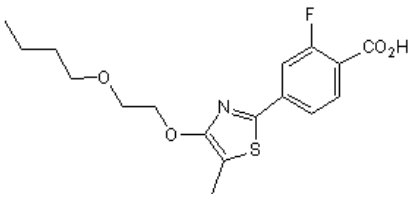

The small molecule AC261066 is a potent and selective *RAR*β2 agonist the pEC_{50} = 8.1 compared to the *RAR*β1 isotype where pEC_{50} = 6.4 (TOCRIS Bioscience). The specificity of this small molecule is important when designing drugs since activation of other receptors may result in unwanted side affects and in our model may shadow the true action of *RAR*β2. Although this small molecule has not been used in neural regeneration models other less potent and less selective agonists have been used and demonstrated receovery or enhancment of neurite outgrowth [238] [252].

Figure 4-24 demonstrates the treatment of our model of neurite regeneration with AC261066 on an inhibitory Aggrecan substrate. Aggregates were treated with 0 µM, 1 µM, 5 µM and 10 µM for 10 days. Treatment resulted in a partial recovery of neurite length and number compared to the control culture grown on a Laminin and P-D-L permissive substrate. The optimum concentration of AC261066 for enhancing length and number was 5 µM. Neurons in control Aggrecan cultures were inhibited as was described earlier in this Chapter. These data demonstrate for the first time that *RAR*β2 agonists may be a possible treatment for CSPG induced human neurite inhibition in the glial scar. Figure 4-23 shows schematically the level at which the small molecule AC261066 inhibits the signalling cascade induced by Aggrecan. This small molecule activates RAR β2 and likely acts through more than one mechanism, still yet to be elucidated.

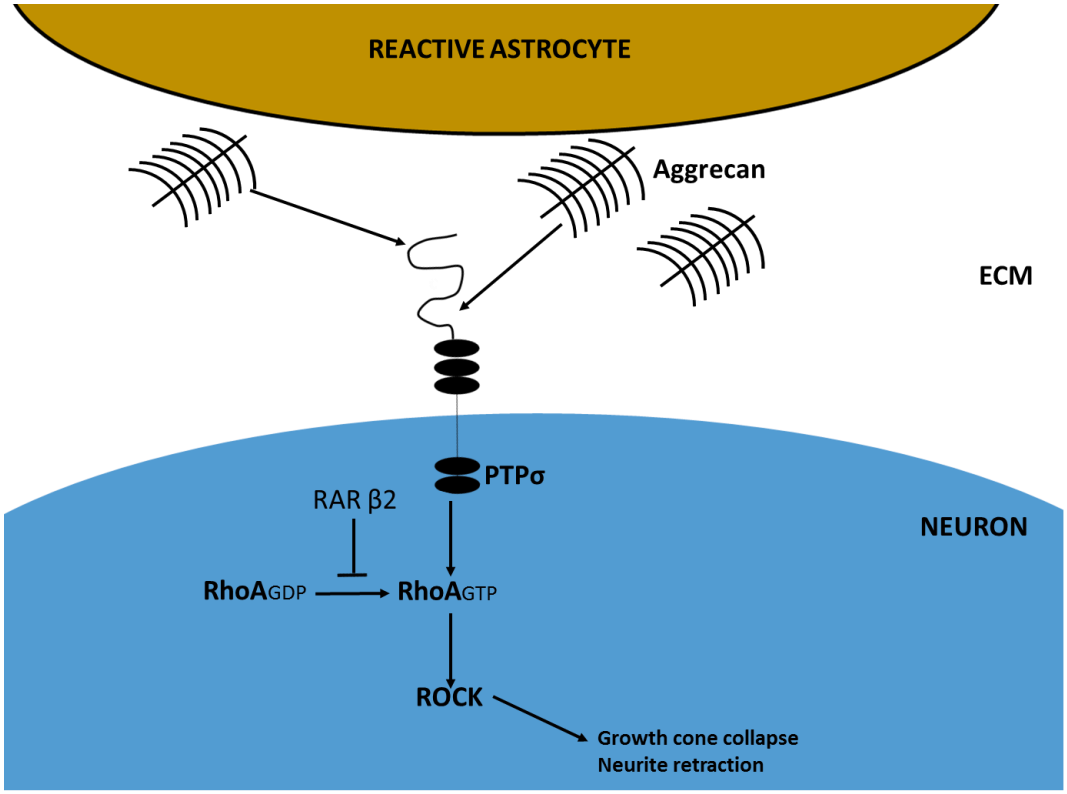

Figure 4-23. The small molecule AC261066 partially recovers neurite outgrowth in human stem-cell derived neurons grown on Aggrecan. The small molecule AC261066 is a potent and specific RARβ2 agonist and is thought to inhibit ROCK activation by acting to supress RhoA through a cAMP mechanism [4]. This small molecule acts up-stream of ROCK and so may be a more specific modulator of regeneration that ROCK inhibitors.

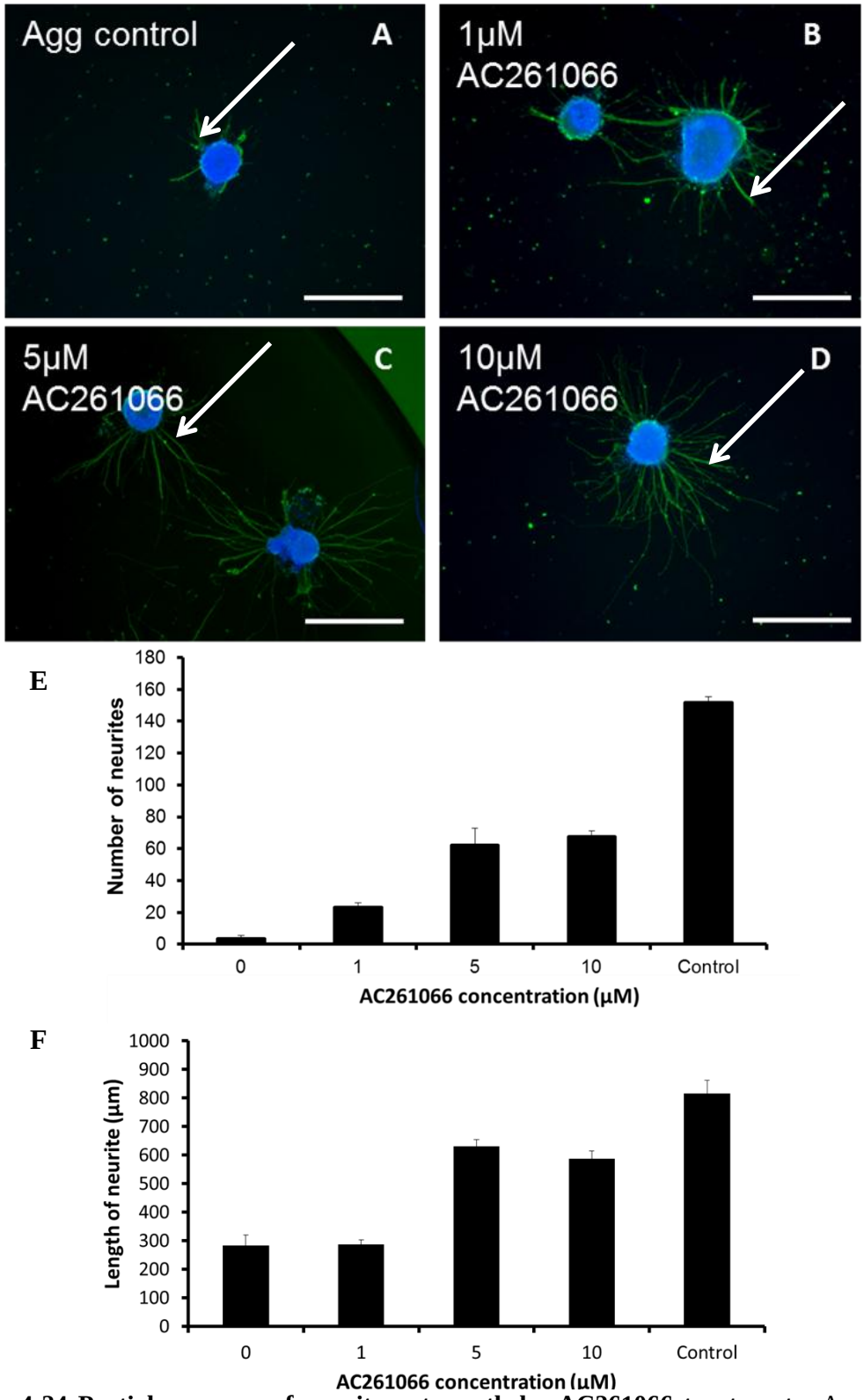

Figure 4-24 Partial recovery of neurite outgrowth by AC261066 treatment. Aggregates of TERA.2.cl.SP12 EC cells were differentiated with 0.1 μM EC23 for 21 days were placed onto a 10 μg/ml Laminin and P-D-L substrate supplemented with 50 μg/ml Aggrecan. The no Aggrecan control aggregates were grown on 10 μg/ml Laminin and P-D-L only substrate. Aggregate media was conditioned with the small molecule AC261066 (TOCRIS), a potent RAR β2 agonist. AC261066 was added to the media at either 0 μM (A) 1 μM (B), 5 μM (C) or 10 μM (D) for 10 days. The number of neurites (E) and length of neurites (F) were measured. Recovery of neurite outgrowth was concentration dependent with maximal recovery at 10 μM. Only partial recovery was demonstrated. Arrows mark out typical neurites that develop from each aggregate Scale bars: 500 μm. Data represent mean ± SEM, n=3.

4.3.8 Wnt activation and recovery of neurite outgrowth

Signalling through the Wnt pathway controls a wide range of biological processes. It is not surprising that published research has described the role of modulators of Wnt signalling on neurite outgrowth and regeneration [167, 176, 245, 264]. What is surprising is that research has provided conflicting evidence to suggest that this pathway can both enhance neurite outgrowth and inhibit outgrowth under different conditions. This may be in part to the small molecules used to regulate this pathway and their non-specific nature, or more likely, due to heterogeneity in many key factors that affect how neurites respond to their external environment. The developmental age of explanted neural tissue, the amount of neural damage and the type of neuron/position within the CNS are often unknown and affect the regenerative potential of neurons. The model described in this thesis thus far is robust and well characterised. The age of neurites that develop from stem cells is known. Furthermore, processes which are occurring in the neurites that correspond with their stage of development are predictable, making this model ideal for comparison between small molecule modulators of signalling pathways. In addition the nature and composition of the controlled substrate proteins can be used giving rise to specific effects on the neurites and investigating neurite outgrowth under either a permissive or inhibitory environment.

GSK3 α and β inhibition

The small molecule CHIR 99021 is a highly selective inhibitor of the enzyme GSK3 (TOCRIS Bioscience). Inhibition of GSK3 results in loss of Wnt activated signalling and a build-up of β catenin a gene transcription regulator. It is thought that the outcome of GSK3 signalling is dependent on the amount of GSK3 activity in the developing neurons.

In this part of the study our model of neurite outgrowth was used to assess the role of GSK3 signalling inhibition on neurite outgrowth. The small molecule was added to the neurite outgrowth culture media described in Methods at concentrations of 0.01, 0.1, 1 and 10 µM for 10 days and the length of neurites measured. The results demonstrate that addition of 1-10 µM CHIR 99021 inhibited neurite outgrowth on a permissive Laminin/P-D-L substrate (Figure 4-26).

To investigate the mechanisms by which CHIR 99021 induced loss of neurite outgrowth and if activation of P160 ROCK was involved in the inhibition demonstrated by 1 µM, 15 µM of the small molecule Y-27632 was added to a culture containing 1 µM CHIR 99021. Results demonstrate no enhancement of neurite length when cultures were supplemented

with Y-27632, possibly indicating loss of neurite outgrowth via a non-ROCK activating signalling pathway (Figure 4-27). Control culture without CHIR 99021 had good neurite outgrowth as has been described previously. Figure 4-25 shows schematically the inhibition of GSK 3β by the small molecule CHIR 99021 which ultimately resulted in loss of neurite outgrowth on a permissive substrate.

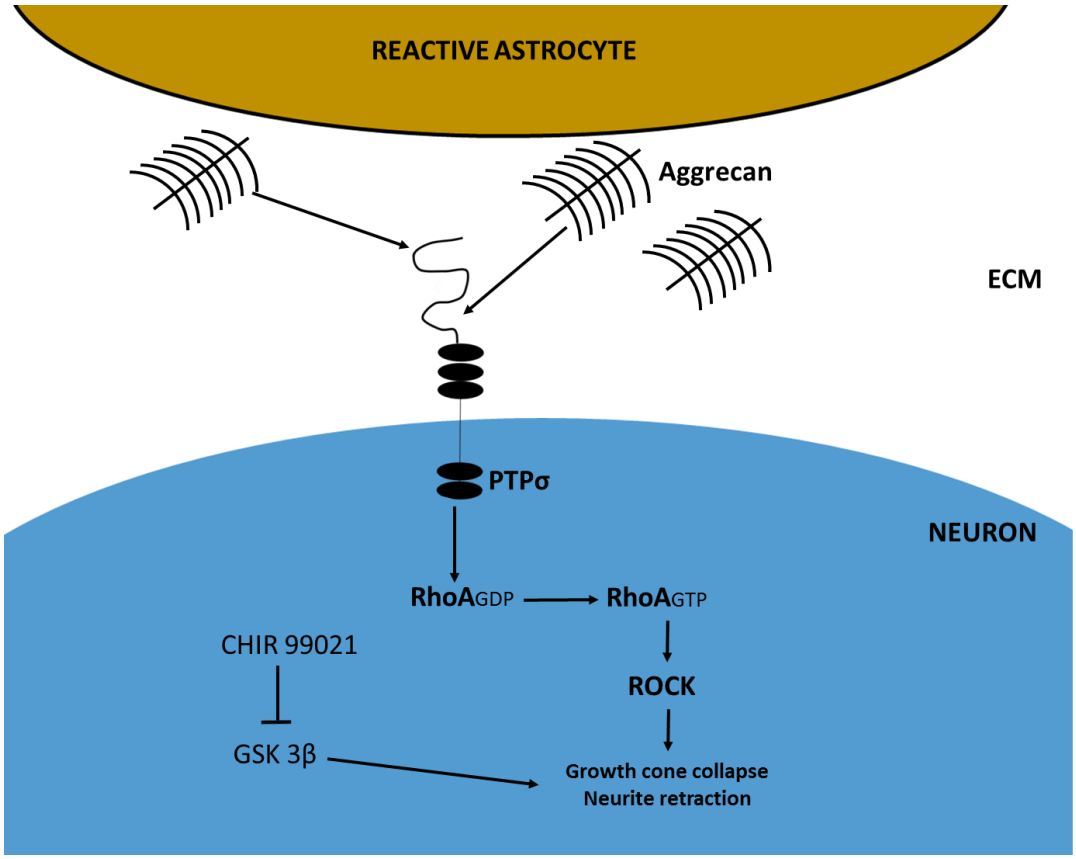

Figure 4-25 CHIR99021 inhibits neurite outgrowth of human stem-cell derived neurites on a permissive substrate. The small molecule CHIR 99021 inhibits GSK 3β and induces loss of neurite outgrowth in our model.

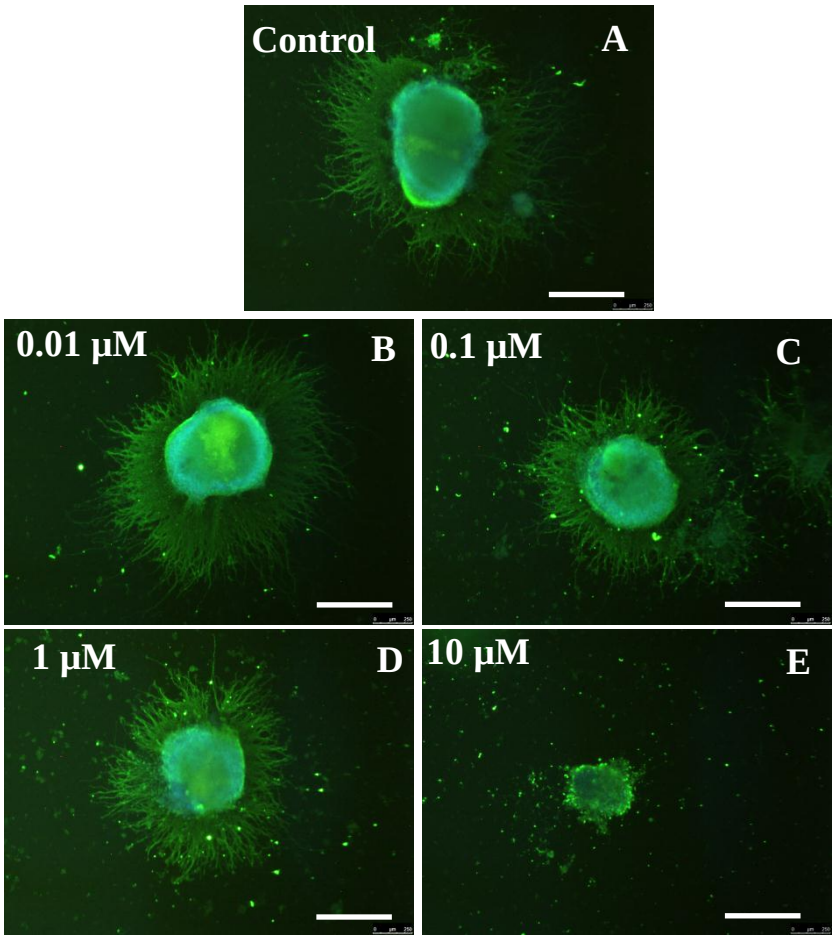

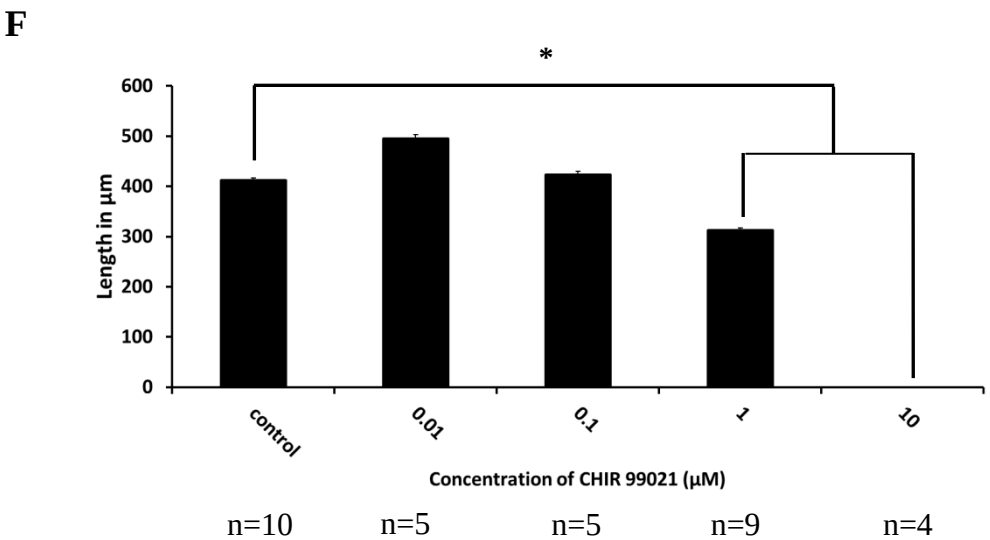

Figure 4-26 Inhibition of GSK3 results in loss of neurite outgrowth on a permissive substrate. Aggregates of the human pluripotent stem cell (TERA2.cl.SP12) were differentiated with 0.1 µM EC23 for 21 days. Aggregates were then grown on a permissive Laminin/P-D-L substrate in the presence of mitotic inhibitions (as described in Methods). The no Aggrecan control aggregates were grown on Laminin and P-D-L only substrate. Cultures were treated with CHIR 99021 from day 1 at a concentration of 0 µM (A), 0.01 µM (B), 0.1 µM (C), 1 µM (D) or 10 µM (E). Using LEICA AF software neurite length was measured from the neurospheres (F). Data demonstrate a loss of neurite outgrowth from aggregates treated with 1 and 10 µM CHIR99021. Data represent mean ± SEM. * $p \leq 0.05$ compared to the control by Students T-test. Scale bars: 500 µm.

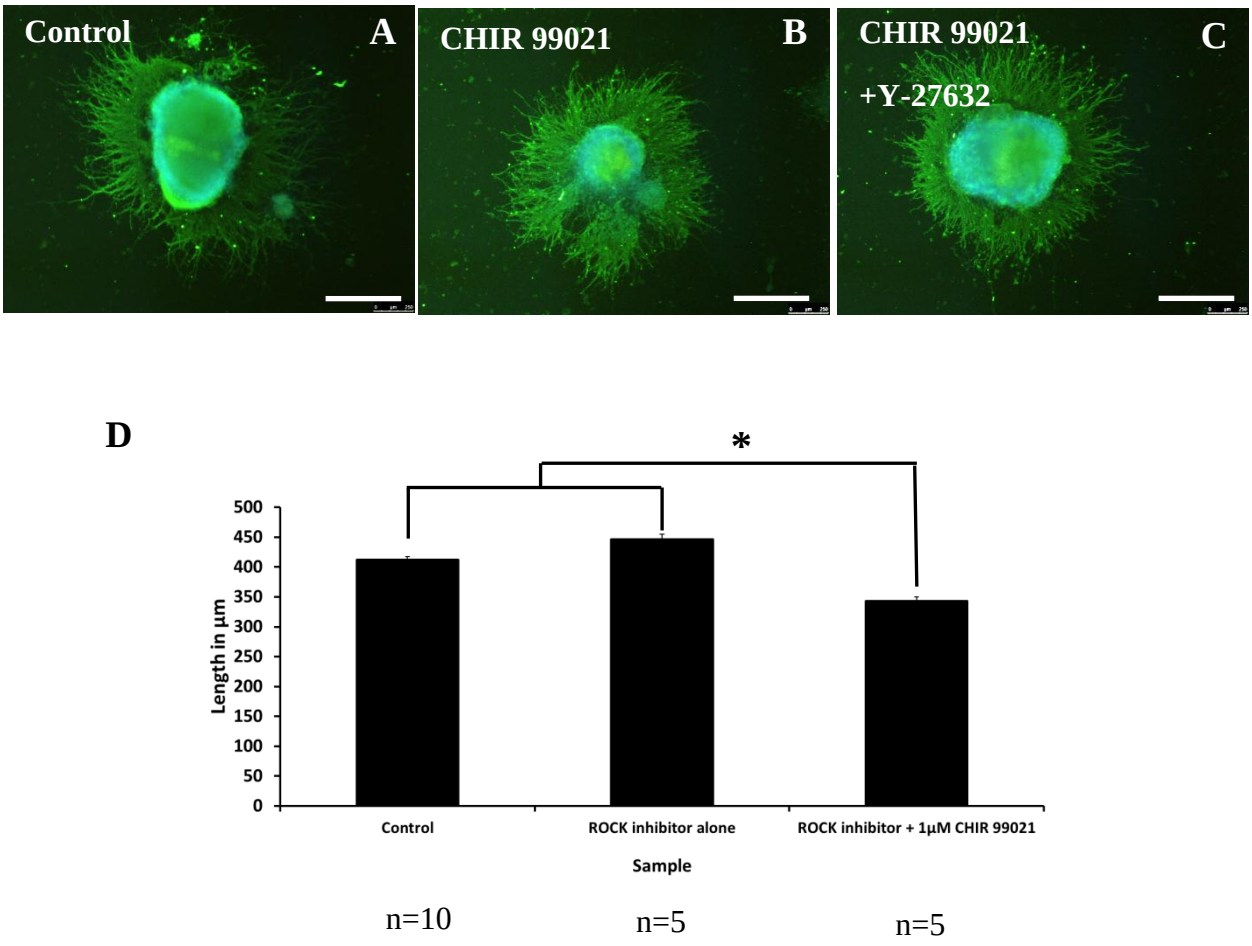

Figure 4-27 Inhibition of neurite outgrowth by CHIR 99021 is not overcome by ROCK inhibition. Aggregates of the human pluripotent stem cell (TERA2.cl.SP12) were differentiated with 0.1µM EC23 for 21 days. Aggregates were then grown on a permissive Laminin/P-D-L substrate in the prese of mitotic inhibitions (as described in Methods). To assess if ROCK inhibition can overcome the affects of CHIR99021 15 µM Y-27632 was added to cultures treated with 1 µM CHIR99021 (C). Control cultures without Y-27632 (A) and with Y-27632 (B) had normal neurite length formation. LEICA AF software was used to measure neurite length from >5 neurospheres (D). Data demonstrate a loss of neurite outgrowth from aggregates treated with 1 µM CHIR99021 and Y-27632 were inhibited compared to control cultures. Data represent mean ± SEM. * $p<0.05$ Students T-test. Scale bars: 500 µm.

The small molecule - XAV 939 is an Axin stabiliser and acts to enhance GSK3β activity resulting in β-catenin degradation and increased Wnt signalling. This small molecule has been used in various studies to investigate the role of Wnt signalling. The effect of this small molecule would be opposite to that of CHIR 99021 and so would not be expected to inhibited neurite outgrowth.

XAV 939

The small molecule was XAV 939 was used to investigate the role of Wnt enhancement on neurite outgrowth in our model of Aggrecan induced inhibition. XAV 939 which is a commercially available small molecule from TOCRIS. In our system XAV 939 was added at three concentrations 0.1, 1 and 10 µM to the neurite outgrowth culture media for 10 days, on an Aggrecan/Laminin/P-D-L substrate.

Figure 4-29 demonstrates the effect of XAV 939 supplementation on neurite outgrowth on an Aggrecan substrate. Neurite number and length was measured under each condition. Addition of XAV 939 resulted in a recovery of neurite length and number. Furthermore, at 0.1 µM and 1 µM an increase in the migration of cells from the aggregate was observed. This may be a non-specific effect of this small molecule resulting in increased cell motility an observation that would require further analysis to determine the cells that were migrating. Figure 4-28 shows schematically the level at which the small molecule XAV939 inhibits the signalling cascade induced by Aggrecan.

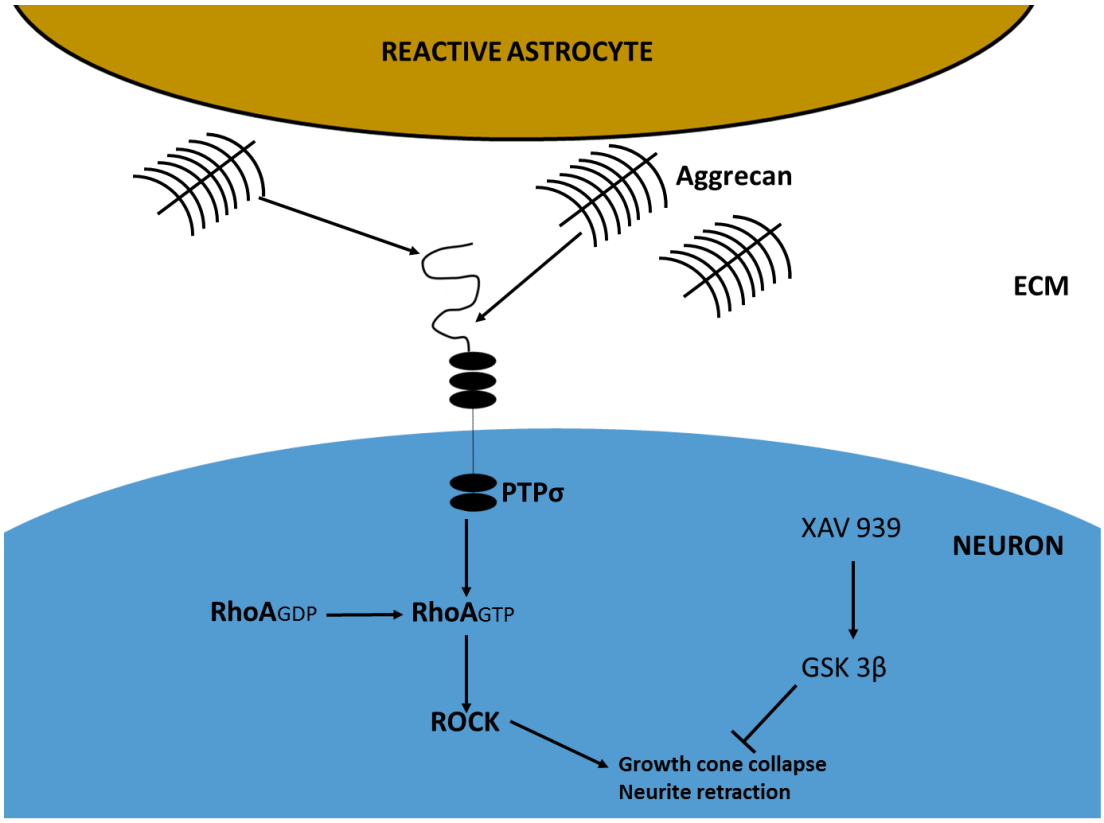

Figure 4-28. The small molecule XAV 939 enhances neurite outgrowth in human stem cell-derived neurons grown on Aggrecan. XAV 939 stabilises the GSK 3β enzyme complex which prevents growth cone collapse and neurite retraction on Aggrecan.

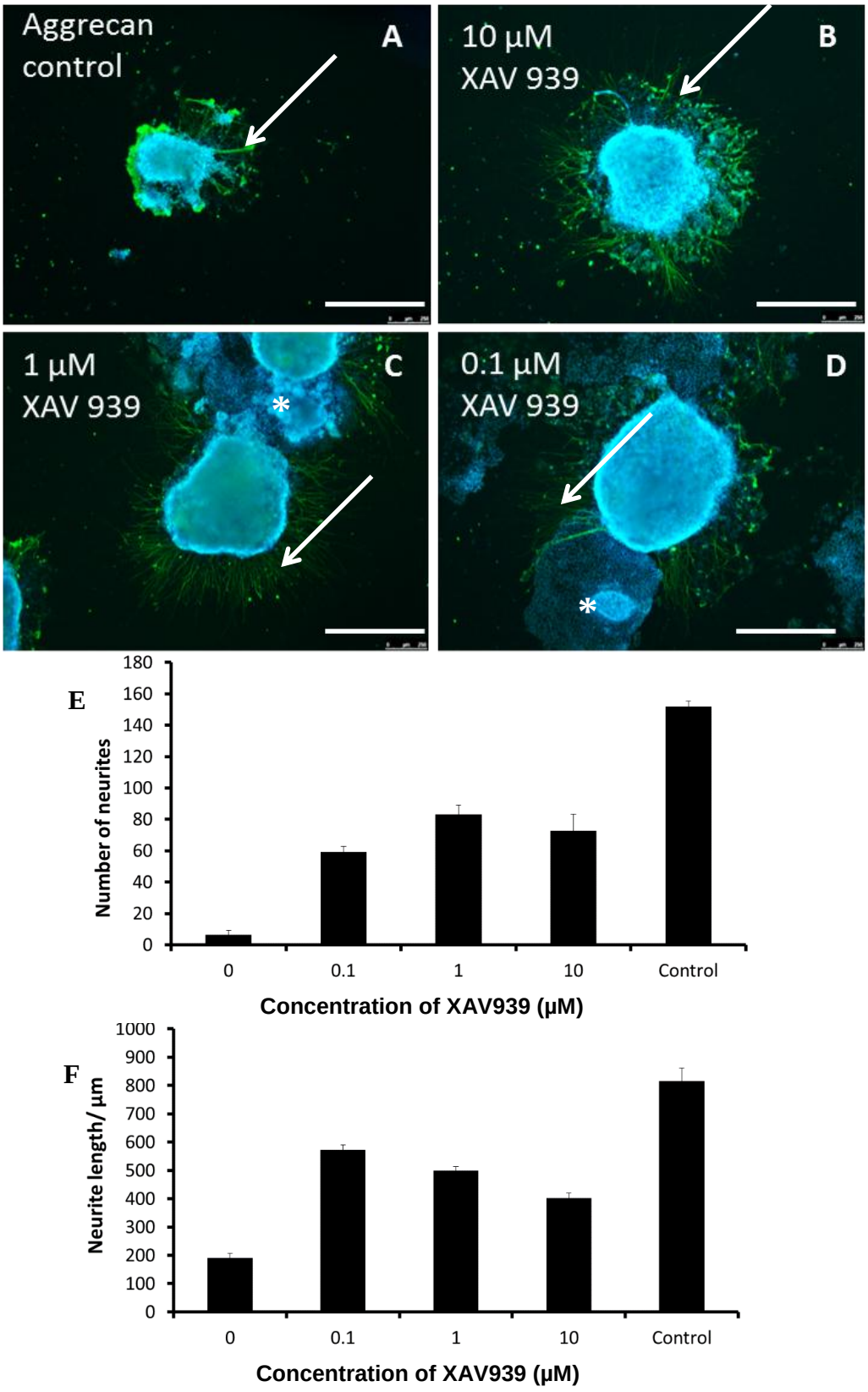

Figure 4-29 GSK3β stabilisation by XAV 939 can potentially overcome Aggrecan-induced neurite outgrowth inhibition. Aggregates differentiated with 0.1 µM EC23 for 21 days were placed onto a Laminin and P-D-L substrate supplemented with 50 µg/ml Aggrecan. The no Aggrecan control aggregates were grown on Laminin and P-D-L only substrate. Aggregate media was conditioned with the small molecule XAV 939, a Tankyrase inhibitor. XAV 939 was added to the media at either 0 µM (A), 0.1 µM (B), 1 µM (C) or 10 µM (D) for 10 days and subsequently fixed in 4 % PFA. Neurite number (E) and neurite length (F) were measured for quantification. Recovery of neurite length was concentration dependent with maximal recovery at 0.1 µM, however, the number of neurites that developed was maximal at 1 µM. Large colonies of non-neural cells migrated from the central sphere at 0.1 µM and 1 µM XAV 939. Arrows show neurites. Asterisk marks migrating cells. Scale bars: 500 µm. Data represent mean ± SEM, n=3.

4.3.9 PTP IV Inhibition and recovery of neurite outgrowth

The small molecule modulators that enhance neurite outgrowth on an inhibitory Aggrecan substrate described so far affect the key signalling pathways involving ROCK, GSK3β and *RAR*β2. Due to the large biological role of each of these modulators it is likely that *in vivo* applications would result in non-specific side effects that are likely detrimental to the organism. More specific modulators of the receptor-ligand interaction inducing the downstream response of Aggrecan may be more suitable for *in vivo* and clinical applications in the future. One method of influencing the effect of Aggrecan on neurite retraction is to inhibit protein tyrosine phosphatase receptor activation [149]. Furthermore, it is known that PTPσR signalling regulates NGF by dephosphorylating its receptor TrkA, and does so without causing enhanced cell death, ectopically increasing PTPσR also resulted in reduced neurite outgrowth, indicating inhibition of PTPσR a key target for enhancing neurite outgrowth [265]. It is known that reducing the activation of PTPσR in mouse DRG sensory neurons can overcome CSPG induced neurite inhibition [1]. Inhibition of PTPσR by the small molecule PTP IV inhibitor has the potential to prevent Aggrecan induced neurite inhibition. [266].

PTPIV Inhibitor

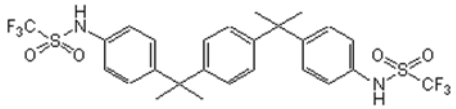

The PTP IV inhibitor is a selective non-competitive, reversible, active site directed inhibitor of PTPσ, the intracellular protein tyrosine phosphatase of the PTPσ receptor. The IC_{50} of this inhibitor for PTP σ is 20 μM (TOCRIS Bioscience). Since the GAG side chains on Aggrecan bind PTPσR and activate the second messenger system, inhibiting the intracellular enzymes of this system will prevent signalling and hence many of the downstream responses such as ROCK and RhoA activation which lead to CRMP2 phosphorylation and growth cone collapse [149].

Using our model of neurite outgrowth on an Aggrecan substrate, five concentrations of the PTPIV inhibitor were tested (0 μM, 0.1 μM, 1 μM, 5 μM and 10 μM). Cell media was supplemented with the compound for 10 days prior to fixation and analysis. Figure 4-31 demonstrates that both the number and length of neurites were significantly decreased in

cultures grown on Aggrecan alone. However, the addition of PTP IV to the cultures recovered the length of neurites to that of the control at 1 µM and partially enhanced neurite number at each concentration. The fold increase in neurite length was 3 fold for both 10 and 0.1 µM PTP IV inhibition compared to the Aggrecan control length. Maximal increase in neurite length was demonstrated by 1 µM with a 4 fold increase. These data indicate that this small molecule can be used for overcoming Aggrecan induced neurite inhibition in human neurons. This is the first known report detailing the role of PTP IV inhibition on human neurite outgrowth and its potential role in regenerative neurons. Figure 4-30 shows schematically the level at which the small molecule PTP IV inhibitor, inhibits the signalling cascade induced by Aggrecan, and does so by preventing PTPσR activation and downstream signalling.

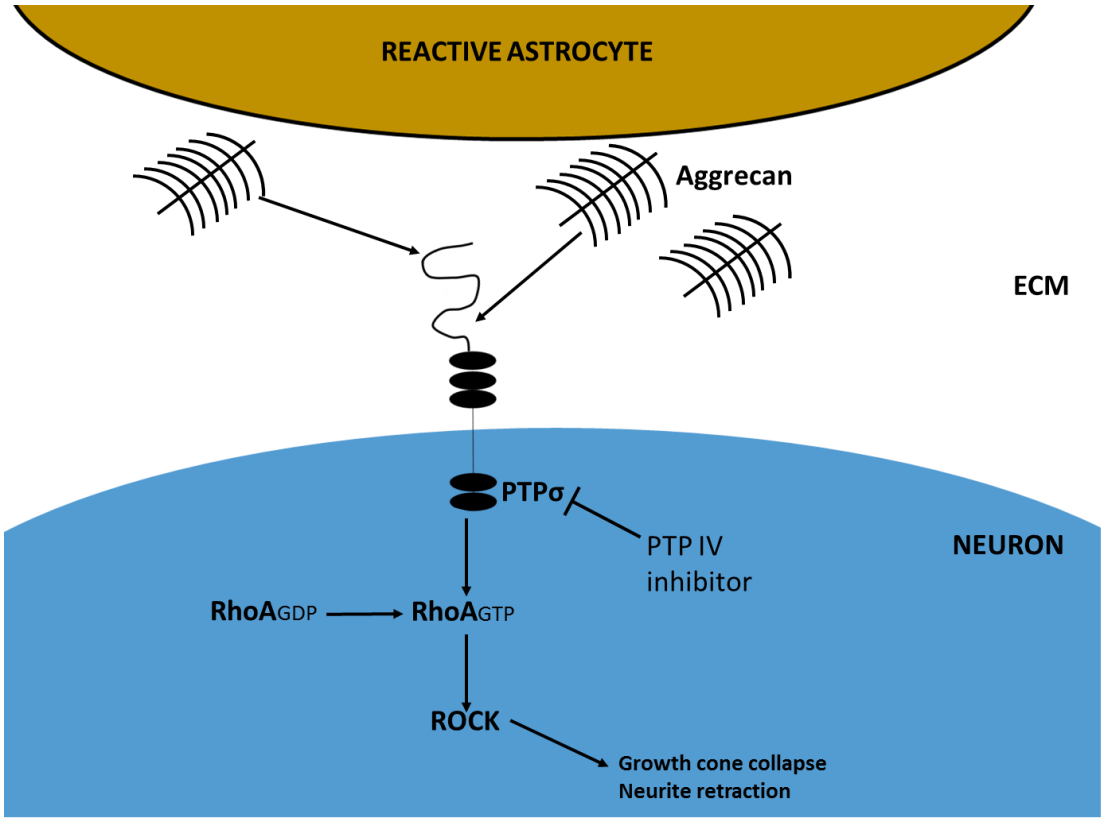

Figure 4-30 The small molecule PTP IV inhibitor enhances neurite outgrowth in human stem cell-derived neurons on Aggrecan. The small molecule inhibits activation of the Aggrecan receptor enzyme PTPσ on the neurite membrane. Inhibition of the receptor prevents downstream activation of the Rho A and ROCK second messengers.

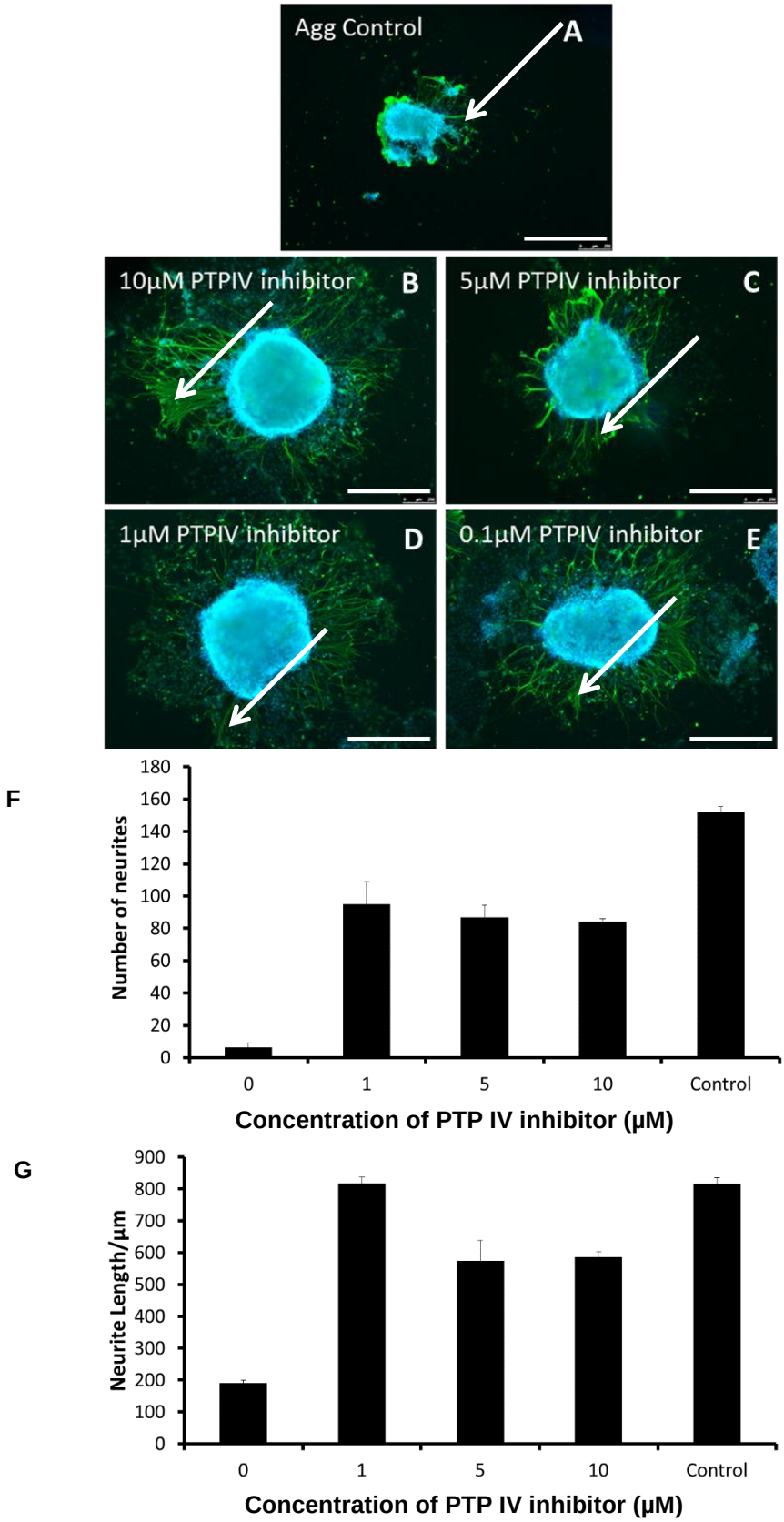

Figure 4-31 Inhibition of protein tyrosine phosphatase σ receptor using the synthetic PTP IV inhibitor results in enhanced neuritogenesis. Aggregates of TERA2.cl.SP12 cells were differentiated for 21 days by 0.1 µM EC23. Aggregates were then placed on tissue culture plastic coated with 10 µg/ml Laminin and P-D-L and 50 µg/ml Aggrecan. Loss of neurite outgrowth was demonstrated on Aggrecan coated plastic as described earlier. Cell culture media was supplemented with 0 µM (A) 0.1 µM (B), 1 µM (C), 5 µM (D) or 10 µM (E) PTP IV inhibitor. After 10 days of outgrowth the aggregates were fixed in 4 % PFA, stained for DAPI (Blue) and β III Tubulin (TUJ-1) (Green) and the neurite length was measured using the Leica AF quantification and tracing software. Neurites were counted (F) using Image-J as described in Methods Section. Recovery of neurite outgrowth was demonstrated at each concentration of PTP IV inhibition with maximum recovery at 1 µM (G). Arrows show neurites. Scale bars: 500 µm. Data represent mean ± SEM, n=3.

4.3.10 Chondroitinase pre-treatment and recovery of neurite outgrowth

Another way of targeting PTPσ receptor activation by Aggrecan is to remove the glycosaminoglycan side chain from the core Aggrecan protein [267]. The GAG side chain as discussed previously is the ligand that interacts and modulates the PTPσ receptor [261]. Removal of this side chain can be achieved by treating Aggrecan with the bacterial enzyme chondroitinase ABC. Chondroitinase ABC or chondroitin-sulfate (ABC) endolyase can be isolated and purified from *Proteus vulgaris*. The enzyme has been demonstrated extensively in chick DRG and mouse models to enhance CNS regeneration after traumatic injury [156, 268]. It is unknown if the enhanced regeneration demonstrated by chondroitinase treatment is the direct response of GAG cleavage or if cleavage results in a secondary immune or vascularisation of the tissue enhancing recovery. In our robust model of neurite differentiation any neurite outgrowth from neurites achieved by the pre-treatment of Aggrecan by chondroitinase ABC is potentially the direct effect of loss of ligand epitope i.e. GAG cleavage. Furthermore, it is unknown if cleavage of GAG on Aggrecan by chondroitinase affects human neurites in a similar way to that seen in rodent neurons.

Prior to seeding the differentiated aggregates onto the Aggrecan substrate 0.15 active units of enzyme in buffer or enzyme buffer alone was added to the appropriate Aggrecan coated test well for 1 hour at 37 °C and then washed x 3 in PBS. After treatment, differentiated aggregates were added to each well and cultured for 10 days as described previously. Data in Figure 4-33 and Figure 4-34 demonstrate the enhancement of neurite outgrowth from aggregates on Aggrecan substrates treated with chondroitinase. Both the number and length of neurites were increased compared to the wells treated with enzyme buffer alone. The length of neurites that formed were similar to that seen in control Laminin/P-D-L cultures reaching around 700 µm and the number of neurites that developed was around 50 % that of the control cultures. This indicates that there may be an incomplete digestion of GAG side chains, resulting in some inhibition of neurite development. Incomplete digestion of GAG side chains may be the result of enzyme saturation; this may be compensated by increasing the number of active enzyme units used or by raising the incubation time from 1 hour. Furthermore, it is unknown if free GAG cleaved by Chondroitinase can affect these neurites and so an additional PBS wash may overcome the incomplete recovery seen in this model. Figure 4-32 demonstrates schematically the level

at which Chondroitinase inhibits the ligand-receptor interaction of Aggrecan and PTPσR, note that other receptors including LAR will also be inhibited by this method.

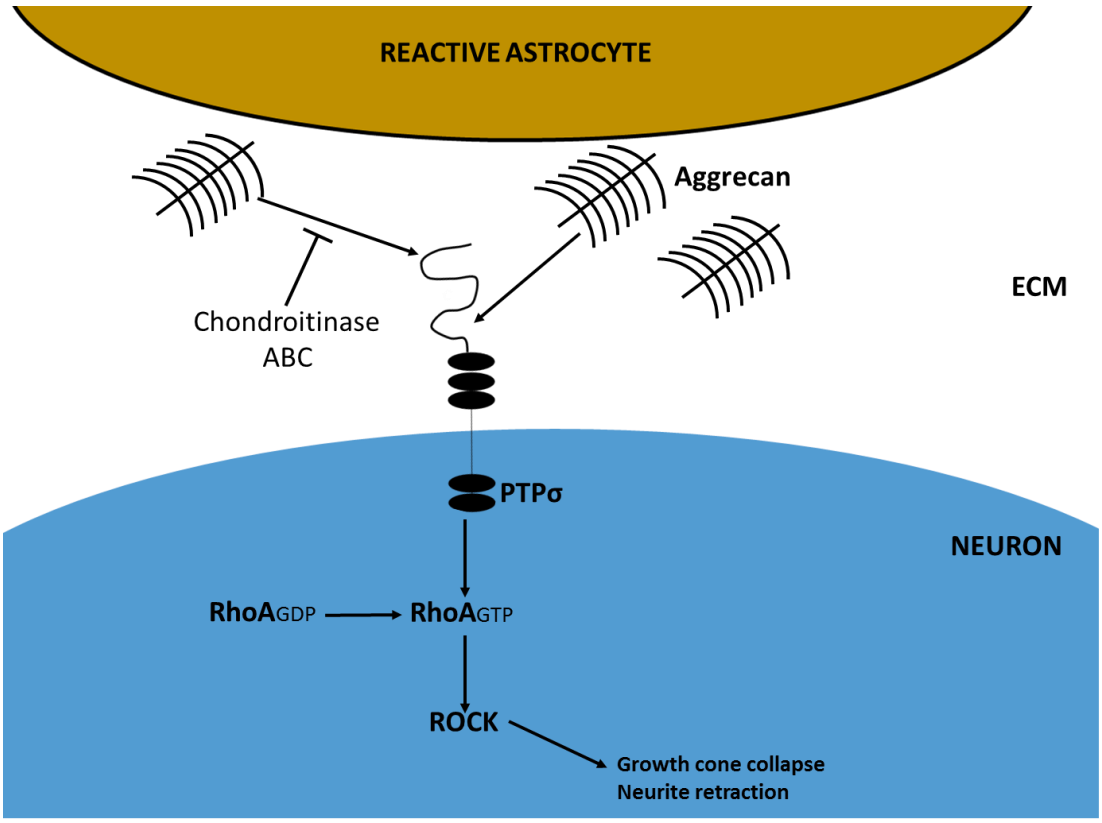

Figure 4-32. The bacterial enzyme Chondroitinase ABC inhibits Aggrecan signalling and creates a permissive substrate for neurite outgrowth. Pre-treatment of the Aggrecan coated substrate with Chondroitinase ABC resulted in cleavage of glycosaminoglycan (GAG) side chains and decreased PTPσ activation. The resulting effect was decreased ROCK activation and neurite outgrowth was permissible.

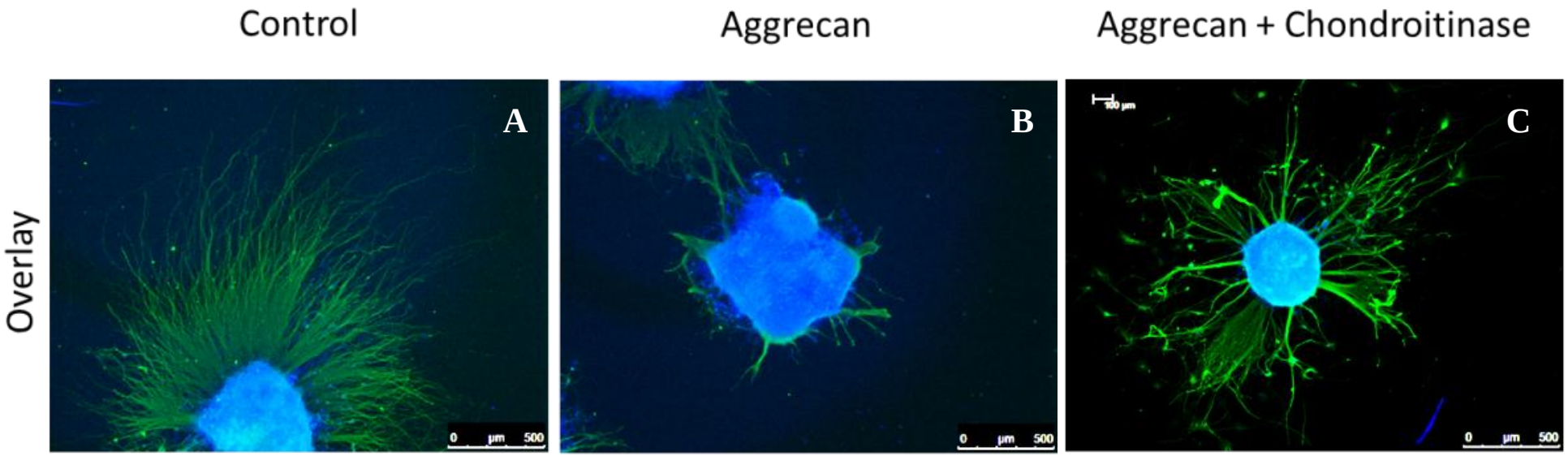

Figure 4-33 Overcoming neurite outgrowth induced by Aggrecan using Chondroitinase ABC pre-treatment. Negative control neurons were grown on Laminin/P-D-L only substrates washed for 1 hour with enzyme buffer and formed large numbers of long neurites, Control (A). Positive control neurons were grown on Laminin/P-D-L plus Aggrecan as described in the Methods Section and were also washed with enzyme buffer (B). Chondroitinase was added to the enzyme buffer and resulted in neurite outgrowth recovery on Laminin/P-D-L plus Aggrecan substrate (C). Scale bars: 500 µm. n=3.

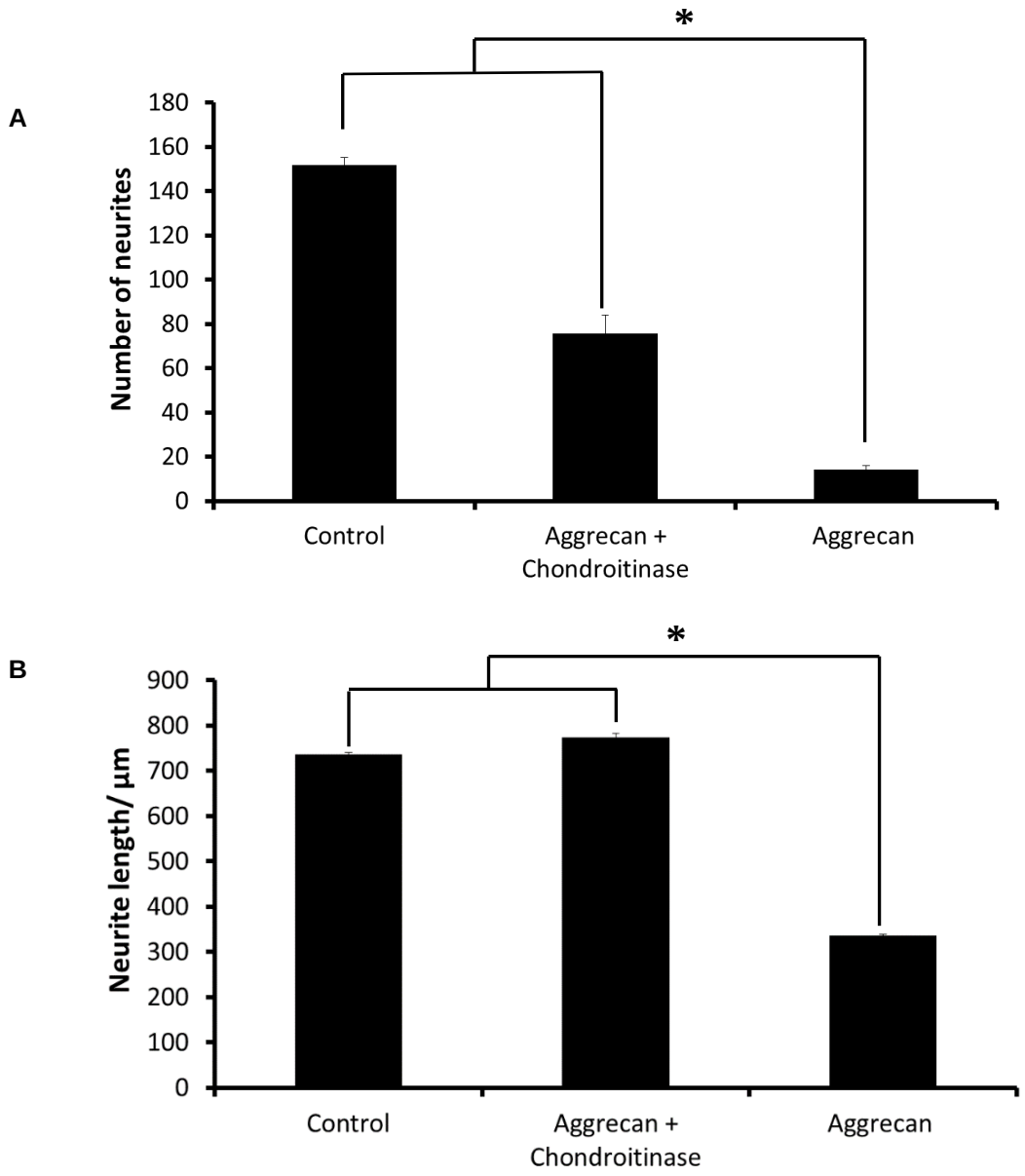

Figure 4-34 Recovery of neurite outgrowth on Aggrecan treated with chondroitinase ABC. Tissue culture plastic was coated with 10 µg/ml Laminin and P-D-L in PBS, which is permissive to neurite outgrowth. For inhibition of outgrowth 50 µg/ml Aggrecan was added to the Laminin-P-D-L coating substrate overnight. The cultures were then treated with chondroitinase in enzyme buffer or enzyme buffer alone, for 1 hour at 37 °C. The plates were then washed thoroughly to remove an excess enzyme or buffer and aggregates differentiated for 21 days by 0.1 µM EC23 were placed onto each substrate for 10 days. Pre-treatment with chondroitinase ABC resulted in recovery of neurite outgrowth on an inhibitory Aggrecan substrate. Neurites were counted using Image-J software (A). Using LEICA AF software the length of neurites were traced and measured (B). Pre-treatment of chondroitinase ovefcame the inhibitory effect of Aggrecan on neurite length and partially restored neurite number. Data represent mean ± SEM, n=3. * $p \leq 0.05$ compared to the Aggrecan only control by Students *t*-test.

4.3.11 Modelling neuronal/glial interactions in co-culture using conventional 2D substrates

The dynamic structure of the glial scar that develops post CNS injury contains both extra cellular matrix proteins that modulate regeneration and a cellular component which influences the composition of the scar and hence neurite outgrowth. Post-CNS injury an increase in TGF β signalling results in reactive gliosis [6]. Astrocytes in the CNS become activated and begin to produce ECM proteins such as Laminin, Fibronectin and some of the CSPG's such as Aggrecan, Brevican and Neurocan [269]. In this part of the study a 2D co-culture method was developed to determine the effect of the astroglioma cell line U118MG on human neurite outgrowth.

U118MG is derived from a human brain glioblastoma, for the purpose of this study it is used as a model of the reactive astrocyte. However, like most models this is not perfect due to its lack of GFAP expression and cancerous origin, it cannot be directly related to the glial scar.

In Figure 4-35 human U118MG astroglioma cells were seeded at a density of 6000 cells/cm^2 along with 1 neurosphere in each well of a conventional 48 well culture plate. The presence of the astroglioma cells prevented neurite outgrowth over 10 days from the cell aggregates. Image A in Figure 4-35 shows the surrounding U118MG nuclei with DAPI staining (Blue) and the neurites stained for TUJ-1 (Red). When the cultures were grown in the presence of the ROCK inhibitor – Y-27632, neurites formed from the aggregate and developed over the U118MG cells. Therefore, it was determined that the U118MG cells induce a receptor mediated inhibition of neurite outgrowth, possibly from a cell membrane molecule. It is known that in the brain glial cells and astrocytes express CSPGs, therefore it was hypothesised that the inhibition of neurite outgrowth was due to the expression of membrane bound CSPGs.

To determine if Aggrecan was expressed by the astroglioma cells a total protein ELISA was performed for human Aggrecan. However, no expression was detected in purified protein from U118MG lysate (Figure 4-36). Another CSPG that has been associated with glial cells in the brain is Brevican. Brevican is tightly regulated in the brain and is associated with boundaries of neural/glial processes. It was hypothesised that the U118MG may express Brevican on their surface resulting in neurite retraction.

Figure 4-37 demonstrates the cell membrane expression and up regulation of Brevican by U118MG grown on Laminin and P-D-L in 2D. The addition of Y-27632 or AC261066 resulted in an increased the level of Brevican membrane expression. This was backed up further by the relative mRNA expression of human Brevican by the cells under the different conditions (Figure 4-38).

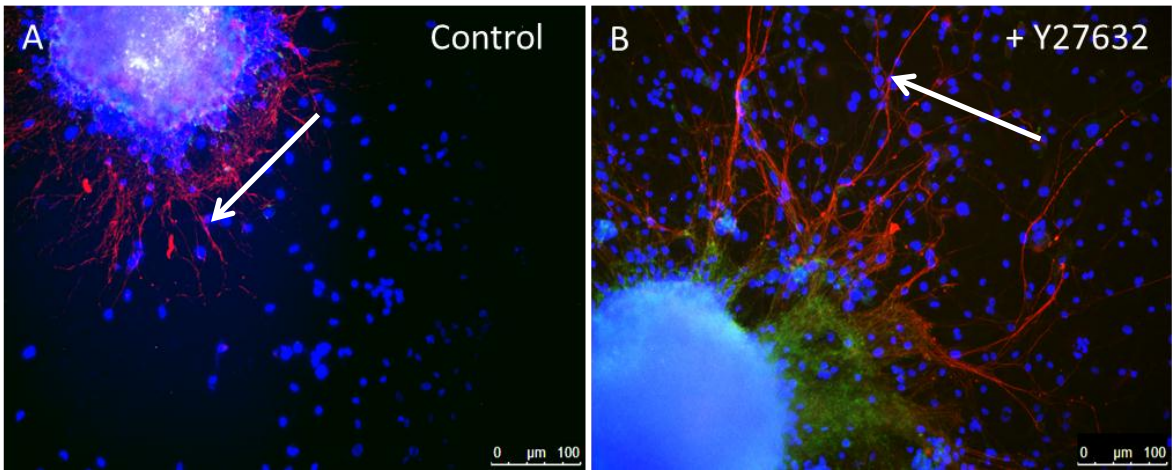

Figure 4-35 Co-culture of human glioblastoma and human neuronal tissue on 2D plastic. The glioblastoma cell line U118MG and differentiated TERA2.cl.SP12 aggregates were seeded at the same time onto Laminin/P-D-L coated tissue culture plastic. Approximatly 5,000 U118MG cells were seeded in a 48 well plate along with 1-2 aggregates. Cells were maintained for 10 days in maintenance media supplemented with mitotic inhibitors. Fixed cells were then stained for β III Tubulin (TUJ-1) (red) and DAPI (Blue). Image A shows inhibition of neurite outgrowth in the presence of U118MG (shown as nuclei-Blue). Image B demonstrates the recovery of neurite outgrowth over U118MG cells with the incorporation of 15 µM Y-27632. Arrows show presence of growing neurites. Scal Bars: 100 µm. n=3.

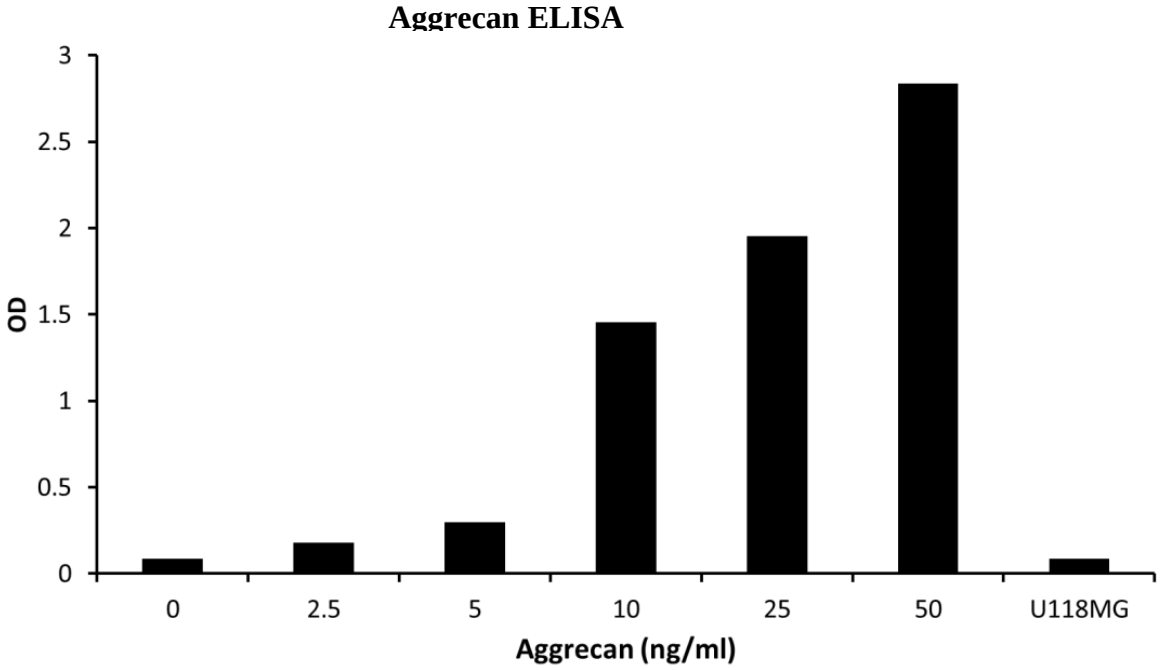

Figure 4-36 Aggrecan ELISA standard measurements. Standard concentrations of Aggrecan were measured by ELISA. The graph demonstrates concentration of Aggrecan ng/ml against optical density (OD). Data demonstrates an increase in OD with concentration of Aggrecan. Note the OD from 50 ng of purified U118MG protein was the same as the OD of 0 ng/ml Aggrecan standard indicating that the protein extract from U118MG does not contain Aggrecan. n=1.

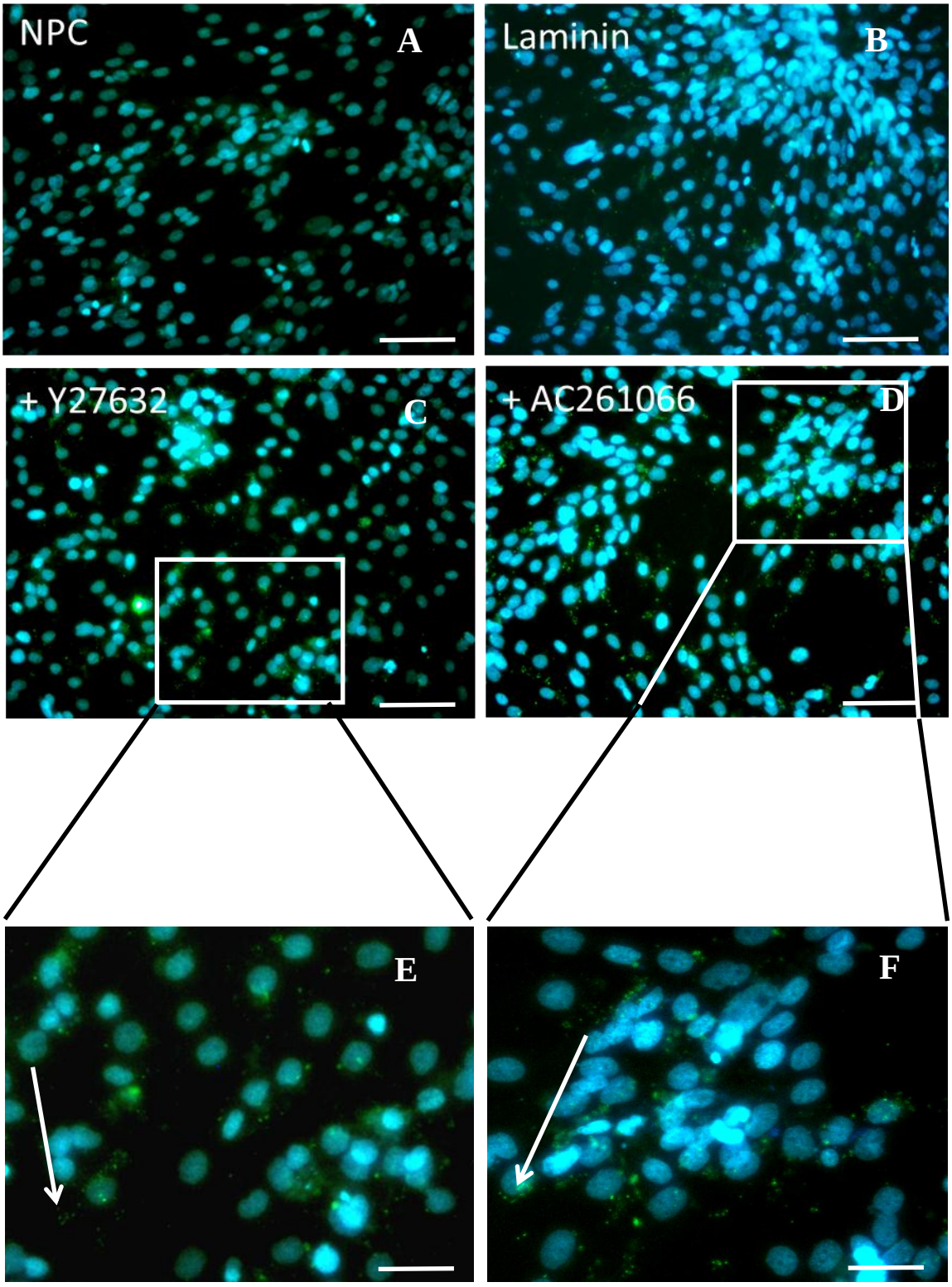

Figure 4-37 Brevican immunostaining of U118MG cells grown in 2D. No primary antibody control (A) and untreated cells (B) did not demonstrate any Brevican staining (green). Points of Brevican staining can be seen on cultures treated with 15 µM Y-27632 (C,E) or 10 µM AC261066 (D,F) which are located on the membrane of the cell. Indicating a possible mechanism for inhibition of neurite outgrowth induced by the presence of these cells. Arrows show neurites. Scale bars: 100 µm (A-D), 20 µm (E,F). n=3.

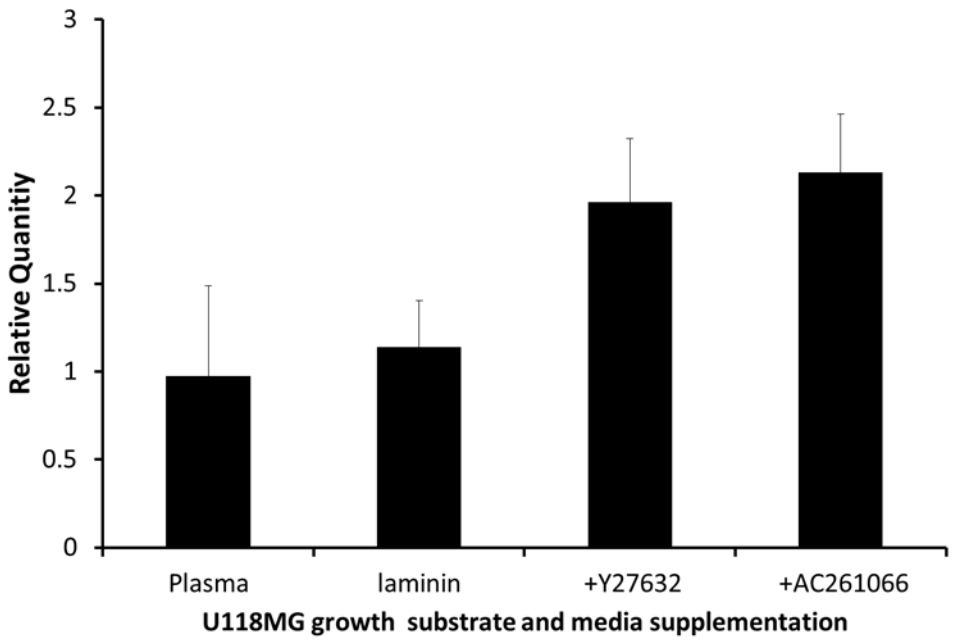

Figure 4-38 Relative quantitation of Brevican mRNA in U118MG astroglioma cells. Cells were grown on plasma treated only, Laminin coated or Laminin coated plus 15 µM Y-27632 or 10 µM AC261066. The mRNA expression of Brevican was measured relative to cells grown on plasma treated only substrate using real time PCR. Data demonstrates the presence of Brevican mRNA in the cells and an enhancement of Brevican mRNA in cells grown on Laminin and treated with either Y-27632 of AC261066. Data represent mean ± SEM, n=3.

4.4 DISCUSSION

4.4.1 Differentiation of human stem cells into neurons using an aggregate – based method

Differentiation of human embryonal carcinoma (hEC) stem cells using the aggregate based method has been demonstrated to be an alternative approach to mono-layer differentiation for neural tissue development *in vitro*. hEC stem cell derived aggregates are very similar to the embryoid body that forms from aggregates of human embryonic stem cells.

The cells in this study were TERA2.cl.SP12 human EC cells which are known to differentiate into neurons following retinoic acid treatment. Differentiating these cells with ATRA in 2D mono-layer culture results in around 10-15 % neural cell differentiation, the purity and yield of neural tissue can be enhanced by the aggregate-based differentiation method [85].

Early stages of retinoic acid treatment results in the up-regulation of Nestin and the formation of proliferative neural rosettes. The intermediate filament Nestin was first discovered in 1985 from antibodies produced by immunizing mouse with spinal cord extract of 15 day old rat embryos. Nestin forms heterodimers with other intermediate filaments such as α Vimentin. The primary role of Nestin is thought to be in regulating the intracellular environment and stabilising cell structure, necessary for cell division and migration. Nestin is associated with many areas of the nervous system particularly early stages of development both *in vitro* and *in vivo*. Furthermore, Nestin is associated with the regeneration of damaged brain and regenerating/proliferating neural progenitors. As development progresses Nestin is replaced with either GFAP expression in glial cells or Neurofillaments such as β III Tubulin in neuronal cells. It is therefore suggested for the purpose of this study that Nestin is representative of an early neural phenotype. The Neurofillament β III Tubulin is strongly expressed throughout the mature central nervous system. In this study aggregates of EC23 treated TERA2.cl.SP12 EC cells expressed the cytoskeletal proteins Nestin, an early neural progenitor marker and β III Tubulin a later marker of neural commitment. High levels of β III Tubulin from aggregates induced to form neurites was indicative of late neural commitment, however, in aggregate sections both high levels of Nestin and β III Tubulin were seen indicating a mixed population. It would be interesting to use flow cytometry to quantify the number of Nestin positive and β III Tubulin positive cells in aggregates under each retinoid condition, however,

disaggregation is difficult due to complex structures and ECM proteins within the aggregate.

In this study aggregates of TERA2.cl.SP12 cells were differentiated with either EC23, AH61 or ATRA. The temporal and concentration dependent effects of each small molecule were assessed for their ability to induce differentiation. The small molecule EC23 a synthetic analogue of ATRA was described in Chapter 4 as a potent inducer of neural differentiation in TERA2.cl.SP12. This is most likely due to its stability in culture and EC23 induces a more sustained single concentration effect than ATRA. AH61 is another novel synthetic analogue of ATRA described in detail by A.Henderson's (2013) [246] thesis which induces neural differentiation in TERA2.cl.SP12 EC cells grown as a mono-layer. In this Chapter the use of stable synthetic small molecules to induce robust and consistent differentiation of human stem-cells was investigated as an alternative to ATRA

Aggregates were differentiated with 10, 1 or 0.1 μM, EC23, ATRA or AH61 for 14 or 21 days. The aggregates were then fixed, sectioned and stained with H&E for structural imaging or for the neural antigens Nestin and TUJ-1. The results indicate that as with previous studies each of the retinoids induced neural rosette formation and neural differentiation after 14 days. Aggregates of TERA2.cl.SP12 differentiated with ATRA for 14 days has been shown previously to result in neural differentiation [270], agreeing with data from this section, furthermore, hES embryoid bodies are also known to form neural progenitors after just 14 days [271]. There was a visible decrease in neural rosette formation and Nestin expression in the most potent small molecules after 21 days. Furthermore, the aggregates looked more homogeneous in structure after 21 days, longer differentiation protocols from 21-28 days have been published in the literature and suggests that increasing the length of differentiation results in more mature progenitor formation [272]. Some areas in the aggregate did not express TUJ-1 or Nestin indicating they may be non-neuronal or represent a heterogeneous population of starting cells. The induction of cytoskeletal proteins associated with neural progenitor formation and structures that resemble neural development demonstrates the high neural activity of each of these compounds, allowing determination of an optimal concentration and compound to be used.

4.4.2 Development of a robust and reproducible model of neurite outgrowth

Neurite outgrowth from each of the aggregates differentiated using 10, 1 or 0.1 μM, EC23, ATRA or AH61 for 14 or 21 days were assessed. Neuroprogenitors within the aggregates

were induced to form axons on a Laminin and P-D-L substrate for 10 days. Induction of neurite outgrowth by Laminin is common among many neural progenitor cells and is regulated through the Integrin α1β1 receptor heterodimer. In addition, to prevent the division of proliferative cells in the aggregate and loss of the neurosphere mitotic inhibitors were added as described in Horrocks, G et al (2003) [85]. Aggregates differentiated for 14 days in each of the concentration and retinoid groups demonstrate migration of cell bodies from the central aggregate. In addition a vast network of neurites formed from each aggregate with the exception of 10 μM EC23 where only a few neurites developed. Migration of cell bodies from the aggregate is likely due to the early developmental stage of the progenitors as would be seen in neural progenitor of the early developing neural tube. Migration of developing neuroprogenitors is essential for correct AP and DV patterning [35]. High Nestin levels in some of the 14 day aggregates may indicate a high migratory potential of the cells, since neural progenitors are known to be migratory [273].

The formation of neural progenitors after 14 days differentiation has been published previously [85]. The time used to differentiate the aggregates was increased from 14 to 21 days to investigate the temporal dependent effects on neurite outgrowth and any differences between the aggregates that may have developed. In this section our data demonstrated that there was a reduction in migration of cell bodies form the central aggregate when cells were differentiated for 21 days as opposed to the previous 14 days. Furthermore, the length and number of neurites was much easier to quantify as a halo of individual neurites formed around a central point of origin. Staining of DAPI (Blue) and neurons (TUJ-1, Green) clearly separated the two primary structural aspects of the neuron. There was also a clear effect of retinoid concentration on neurite number, high concentrations of EC23 and low concentrations of ATRA induced fewer neurites than the converse. This concentration affect is likely due to the initiation of neural development within the aggregate. Retinoid concentration has been demonstrated to be highly regulatory over the differentiation of mouse ES cells; low concentrations of ATRA around 0.001 μM and 0.01 μM were associated with an increased level of mesoderm and epidermal markers [196]. In our aggregate-based model concentration had a similar differential effect, the low concentrations of ATRA induce poor neural commitment and neurite outgrowth suggesting an alternative germ layer developed, however, the high concentration of EC23 also induced a similar low level neural commitment and neurite outgrowth, possibly due to complex feedback mechanisms involving Pax6 as was discussed in Chapter 3.

In light of the published data and research described so far in Chapters 3 and 4 the most optimised and described method of neurite outgrowth for studying neural development would involve the differentiation of TERA2.cl.SP12 EC cells with 0.1 µM EC23. This concentration and cell line were chosen to be taken forward in this study to investigate the molecular mechanisms involved in neurite regeneration (see Methods Section for the standard operating procedure). To further classify the neurons that were developing in this model a number of anterior-posterior gene markers and receptors were also assessed.

Anterior-posterior axis specification of neural tissue in the CNS is regulated by morphogens from the Wnt, BMP, FGF and RA family of small molecules [213, 274-276]. The morphogen that signals to the cells and ultimately determines their fate depends on their anatomical location in the CNS. Initially the anterior-posterior axis of the neural tube is formed and results in the development of distinct forebrain, midbrain, hindbrain and spinal cord structures. The development of each structure is regulated by a distinct pattern of genes induced by combinations of the morphogens described earlier. *In vitro* development of neural tissue from embryonic stem cells utilises combinations of these morphogens and induction of gene markers can be used to determine the subtype of cell that will develop [277]. The use of markers to determine the which region of the CNS differentiating stem cells are developing into is important for translating *in vitro* data into hypothesis that can be tested *in vivo* – for instance, small molecule that enhance spinal cord regeneration may not have the same effect on neurons in the forebrain.

To determine genetically the area of CNS cells treated with 0.1 µM EC23 most represented a marker of forebrain development, *OTX2* which is expressed during development and the hindbrain/spinal cord marker *HOXC4* were measured using real time PCR. The results indicate a loss of *OTX2* mRNA expression in the cells and a temporal dependent increase in *HOXC4* mRNA expression which indicated a thoracic identity of these cells. *HOXC* regulation is related to spinal cord development, since *HOXC4* is an anterior *HOX* gene it is likely that these cells represent a more hindbrain/anterior spinal cord neuroprogenitor cells type [196]. In addition *PAX6* mRNA expression was also determined over the 21 days, this indicated a peak in *PAX6* mRNA after 7 days which remained high, *PAX6* is indicative of ventral neural spinal cord development, *PAX6* is also found within the forebrain, however, due to the high level of *HOXC4* it is likely that the *PAX6* expression in these cells is representative of a motor neuron or V1 interneuron phenotype [278].

The data from Figure 4-17 shows that *RARβ2* mRNA is sustained at a high level after 7 days in cells treated with 0.1 µM EC23, after 21 days treatment high mRNA levels likely

indicate that the neurites that form from the neurospheres will be responsive to agonists of *RAR*β2.

The *RARβ2* receptor is a common regulator in many neurobiological processes, including initiation and sustained neural differentiation of stem cells [251], neurite outgrowth[252], axon formation and neurite regeneration [4]. *RAR*β2 has been demonstrated to be involved in anterior-posterior axis formation through the regulation of *HOX* genes such as *HOXD4*, *HOXB4* [279] and *HOXA5* [228]. Cross regulation between *PAX6*, *HOXD4* and *RARβ2* are likely key modulators of the response of cells to retinoic acid during the early stages of AP axis patterning, since *PAX6* has been demonstrated to be highly involved in the initiation and maintenance of neural differentiation [280], furthermore both *PAX6* and *RARβ2* are closely involved in the regulation of *HOXD4* and various other *HOX* genes [227, 279].

In addition to the cross-regulation between *RARβ2* and the patterning genes described above the neurotropic factor, nerve growth factor and the neurotropic receptor (*NGFR*R) or TrkA are also closely involved in the activation of *RARβ2* and hence the downstream events that occur [109]. Basal stimulation of *RAR*β2 expression by *NGFR* was through a Ras dependent mechanism which could be enhanced by retinoic acid treatment in PC12 cells. *NGFR*R is expressed both in the CNS and PNS, up-regulation of *NGFR*R by ATRA is associated with cell survival and in some neurons neurite outgrowth is enhanced.

It has been shown by Maden, M et al (2000) [174], that primary rat DRG neurons are induced to form neurites by *NGFR* treatment express both the *RAR*β2 receptor and *RAR*γ1 retinoic acid receptors. In contrast DRG neurons that do not require *NGFR* treatment for neurite outgrowth which were isolated from a BDNF responsive population express *RARβ2* but not *RAR*γ1 [174]. Since the neurons in this study extend axons without *NGFR* treatment and express *RARβ2* it would be interesting to determine the expression level of *RAR*γ1 in our model. Data from Figure 4-18 demonstrates that although the receptor mRNA is expressed and increases possibly through retinoic acid dependent mechanisms the production of *NGFR* decreases in expression and therefore *NGFR* signalling is unlikely to affect the development of these cells.

The neurite outgrowth model described so far has been optimised to produce a high yield of neurons in a defined and controlled way; furthermore, the neurites that develop have been characterised using gene expression techniques to determine the likely neural subtype that they represent in the spinal cord. The model will now be applied to investigate the

inhibition of human neurite outgrowth by the CSPG, Aggrecan and determine small molecules that can modulate the process of neurite outgrowth and development.

4.4.3 Inhibition of human neurite outgrowth by the CSPG Aggrecan

Chondroitin sulphate proteoglycans (CSPGs) are a family of extracellular matrix molecules that comprise a core protein with variable numbers of glycosaminoglycan (GAG) side chains [281].

CSPGs are sulphate lecticans which include Neurocan, Versican, Brevican and Aggrecan. The C-terminal of the lecticans consists of a C-type lectin, epidermal growth factor and regulators of the complement pathway. The C-type lectin domain of these CSPGs is involved in protein-protein interactions, such as binding Fibronectin. Many of the CSPGs found within the central nervous system regulating many neural processes such as plasticity and development. Since the CSPGs have a physiological role in neural plasticity and development it is not surprising that their dis-regulation both during embryonic development and in the adult CNS is associated with neural pathophysiology.

CSPG are known to be strongly inhibitory of neural regeneration in CNS neurons. CSPGs are deposited and bind to collagen IV [282] in the glial scar during reactive gliosis, deposition of CSPGs and other extracellular matrix proteins is predominantly the role of activated astrocytes, characterised by high GFAP expression. CSPGs exert their affect through binding to the protein tyrosine phosphatase receptors σ and F, which are expressed on the surface of developing and regenerating neurites. Receptor activation is through binding of CSPG GAG side chains which results in an intracellular signalling cascade [1]. Signalling through PTP receptors activates RhoA which in turn phosphorylates and activates P160 ROCK. Activation of P160 ROCK results in growth cone collapse and axon retraction in neurites through effector molecules such as collapsing response mediator protein 2 (CRMP2) [283]. Mixed extracts and *in vivo* models of spinal cord injury has associated CSPGs with neurite inhibition, however, very few studies have investigated the effect of individual CSPG subtypes on neurite outgrowth.

The CSPG, Aggrecan is strongly up regulated in the glial scar post CNS injury. Few studies have directly investigated Aggrecan and neurite outgrowth. However, Aggrecan has been demonstrated to induce loss of neurite outgrowth and regeneration in both *in vitro* and *in vivo* studies. Animal models and cells were utilised to investigate the role of Aggrecan in this process. The majority of studies on Aggrecan have involved the use of

rat DRG and are focussed on integrin receptor regulation [98] or ROCK inhibition to recover outgrowth [284].

In this study Aggrecan was added to a permissive Laminin and P-D-L substrate to determine its effect on human synthetically derived neuroprogenitor cells and their ability to form neurites. Aggrecan induced a concentration dependent decrease in neurite length and number in this model (Figure 4-20). A high level of compensation can be achieved by neurites on a mixture of Laminin and Aggrecan since up regulation of integrin receptors can overcome CSPG induced neurite inhibition. This affect is similar to what is demonstrated in DRG models of neural regeneration on Aggrecan [98]. Furthermore, the presence of Aggrecan or any other CSPG is not sufficient to cause neurite retraction and loss of axon regeneration when Laminin is in excess, the ratio between Laminin concentration and CSPG concentration which is important and is directly linked to the number of integrin receptors on the neurite [234], making recovery of outgrowth possible by increasing integrin receptor clustering [160]. High levels of CSPG are required for loss of neurite outgrowth which in a glial scar is normally associated closely with origin of the scar (epicentre). Snow, D.M et al (1995) [285] demonstrated that when grown on a Laminin substrate, neurites are not affected by soluble CSPG, however, bound CSPG inhibited DRG neurite outgrowth. In contrast there was significant decrease in the rate of DRG neurite elongation when Fibronectin was used instead of Laminin. The ability to investigate these processes using Human neurons will provide insight into early regeneration and the requirement of permissive ECM proteins in neural regeneration [285].

The molecular mechanisms involved in the inhibition of neurite regeneration by Aggrecan are well known and as described before act through recently discovered protein tyrosine phosphatase receptors. Manipulation of the pathways involved in transmitting the Aggrecan signal to a morphological change in cell architecture is currently of interest in neural regenerative research.

4.4.4 Small molecule recovery of Aggrecan induced inhibition of neurite outgrowth

The CSPG, Aggrecan is up-regulated in the glial scar by activated astrocytes that infiltrate and attempt to limit further damage by infection. The scar that forms consists of a network of different ECM proteins some permissive and some inhibitory to neurite outgrowth such as Laminin and Aggrecan respectively. Damage and scar formation results in loss of neural processes and subsequent paralysis of the injured animal. Using small molecule modulation of the inhibitory signalling pathways that are activated in neurons by the glial

scar is an attractive approach enhances recovery of the damaged neurites and aid functional recovery. Multiple small molecules have been investigated in this Chapter, targeting known signalling pathways involved in neurite outgrowth.

Y-27632

The CSPG Aggrecan has been shown to induce neurite retraction and inhibition of regeneration in our model of neurite outgrowth and post-traumatic spinal cord injury *in vivo*. Aggrecan acts through receptors on the neurite membrane to activate downstream signalling by ROCK subsequently resulting in neurite retraction and loss of neurite outgrowth. Activation of the same signalling cascade is known to occur *in vivo,* providing potential targets for inhibitors that can overcome activation of this cascade.

Recent studies have focussed on inhibiting p160 ROCK using small molecules such as Y-27632 [155, 164]. Inhibition of ROCK resulted in recovery of neurite outgrowth and allowed the neurties to develop on and through inhibitory CSPG substrates. To determine if in our model ROCK inhibition by Y-27632 can overcome Aggrecan induced neurite outgrowth inhibition as has been published previously [155]; a concentration profile of Y-27632 and an assessment of neurite length and number were performed. The data from this study demonstrated that incorporation of Y-27632 to neurites that are inhibited by Aggrecan results in enhanced neurite outgrowth both in the length and number of neurites (Figure 4-22). This is similar to published data and demonstrates consistency in our model and with current literature. Chan, C.C et al (2008) [155] demonstrated that both Aggrecan aggregates and monomer inhibited neurite outgrowth from E9 chick DRG cells and Lingor, P et al (2007) [159] used an embyonal carcinoma (hEC) stem cell model of human neurite outgrowth to demonstrate inhibition by a mixture of CSPG proteins. The hEC cells were NTERA2.cl.D1 and were differentiated for 21 days by 10 µM ATRA. Data from this study demonstrated 20 % neurite outgrowth from aggregates grown on a 20 µg/ml CSPG substrate (with poly-lysine and 20 µg/ml Laminin). Unlike work in this Chapter, NTERA2.cl.D1 cells were differentiated as a monolayer and allowed to aggregate after differentiation, however, poor neurite outgrowth was observed in the control cultures, partly due to the use of Phalloidin to stain and quantify neurite outgrowth. Furthermore, using this model the group demonstrated recovery of neurite outgrowth on CSPG by the treatment of 10 µM Y-27632. The optimised protocol in this Thesis and the use of stable small molecules provided a unique method for producing human neurites which demonstrated loss of neurite outgrowth specifically induced by Aggrecan and recovery by the ROCK inhibitor Y-27632.

AC261066

Multiple articles have demonstrated the role of *RAR β2* in developing axons and regenerating neurites. Different methods have been used to enhance or investigate this receptor in developing axons including small molecule agonists [238], viral vectors containing the gene for *RAR β2* [172] and receptor knock out models [286]. Puttagunta, R et al (2011) [286] demonstrated in mouse cerebellar granular neurons *RAR* β2 up-regulation and retinoid treatment could overcome a specific myelin induced neurite inhibition, and this was not seen when the neurites were grown on CSPG. The reason up-regulation of this receptor did not overcome CSPG induced neurite inhibition in this study may be neuron specific or require a more specific activation of the receptor by small molecules that only act on the *RAR β2* receptor. In our study the highly potent *RAR β2* agonist AC261066 was used to enhance neurite outgrowth in our model of Aggrecan induced inhibition. Data demonstrated that the application of AC261066 enhanced neurite length and number in our human model (Figure 4-24). Another way this receptor pathway may overcome neurite inhibition by proteins such as Aggrecan is through up regulation of the Laminin receptor. It has been demonstrated that in retinoic acid and nerve growth factor responsive neurites that neurite outgrowth is enhanced on Laminin through up regulation of α1β1 [255, 287], which can be determined in future studies using the model described in this Chapter.

CHIR 99021 and XAV 939

Since it has been shown that *RAR β2* activation acts to activate AKT [238], and it is known that AKT can inhibit GSK3β modulating multiple downstream molecules associated with neurite outgrowth and cytoskeletal integrity [264] regulation of the GSK, AKT pathway was investigated. Literature suggests that inhibition of GSK3β may enhance neurite outgrowth [177, 288], however, there is also evidence to suggest that activating GSK 3β pathway/ the WNT pathway can overcome neurite inhibition and enhance regeneration [163, 289]. Kawakami, Y et al (2006) [289] demonstrated that Wnt signalling is necessary for regeneration axolotl, *Xenopus* and Zebrafish, furthermore, signalling of this pathway can enhance regeneration in these model systems. There is conflicting data as to the role of this signalling pathway in neurite regeneration and these will likely be due to differences in the models and methods used to investigate the pathway.

In this study, stabilisation of the GSK 3β enzyme complex via Tankyrase inhibition using the small molecule XAV 939 resulted in enhancement of neurite outgrowth on an Aggrecan substrate (Figure 4-29). This small molecule has been shown to enhance the rate of myelination after CNS demyelinating injury in mouse spinal cord, indicating at its

biological activity and potency, further associating GSK 3β enhancement with regeneration [290]. In addition, inhibition of GSK3β post treatment with the small molecule CHIR99021 resulted in loss of outgrowth on a Laminin only substrate Figure 4-26, this could not be overcome by ROCK inhibition Figure 4-27. These data agree with multiple studies that Wnt signalling is important for enhancing neurite outgrowth and it does so via a non-ROCK associated pathway. Therefore these data suggest in human stem cell derived neurons; activation of GSK3beta can overcome Aggrecan induced neurite retraction.

PTP IV inhibition

The neural protein tyrosine phosphatase receptor σ for Aggrecan was discussed earlier and is known to be one example of how CSPGs influence neurite outgrowth. Binding of the GAG side chain attached to the core protein of Aggrecan to this receptor results in activation of a second messenger system involving RhoA and ROCK as described previously [1, 149]. It was hypothesised that inhibition of the enzyme PTPσ by the small molecule inhibitor PTP IV could prevent the downstream activation of the second messenger that result in growth cone collapse and neurite retraction. Studies recently have associated ROCK inhibition with an increase in astrocyte production of CSPG, thus raising the question if the effect of ROCK inhibition on neurite regeneration would be overcome by the increased CSPG production *in vivo* [155]. Using our described model of Aggrecan induced neurite inhibition a concentration dependent recovery of neurite length and number was demonstrated in the presence of PTP IV inhibition. Although the PTP IV inhibitor inhibits the PTP σ receptor, its selectivity for this specific receptor and potency is limited and for therapeutic application would need to be more potent and much more selective.

Chondroitinase ABC

In addition to small molecule manipulation of receptor signalling pathways initiated by Aggrecan, work has recently focussed on utilising a bacterial enzyme that cleaves the GAG side chains of CSPGs [267]. Cleavage of GAG results in loss of ligand binding to receptors on neurite, facilitating neural regeneration and development. Most studies have utilised animal models of spinal cord injury to investigate the ability of the enzyme chondroitinase ABC to overcome inhibition of neurite outgrowth by the glial scar, for example Hunanyan, A.S et al (2010) [291] used chronic unilateral hemisection of adult rat spinal cord to investigate the rescue of axonal conduction by Chondroitinase ABC injections, the enzyme did indeed rescue neurite function in this model. However, due to the many physiological processes that occur during reactive gliosis and neurite regeneration it is unknown if the enzyme acts to prevent the biological activity of CSPGs

on neurites or if cleavage of GAG from CSPGs induces a secondary response such as angiogenesis, which may facilitate removal of CSPG aiding neural regeneration. Other studies have described regeneration of neurites in injured spinal cord after Chondroitinase ABC treatment [292], furthermore, since the full effects of CSPGs in the glial scar are not fully elucidated it may be that intervention at this level will provide the most regenerative therapies. In the model described in this Chapter, although some survival factors will be in the serum in the culture medium the model simplifies the investigation of Aggrecan on neurite outgrowth. Enhanced neurite outgrowth in this model is through a direct effect on either Aggrecan or the signalling cascade induced by Aggrecan. Data from this Chapter demonstrated that pre-treatment of Aggrecan coated plastic with chondroitinase ABC overcame a significant level of neurite outgrowth inhibition induced by Aggrecan (Figure 4-33). These data suggest that the role of chondroitinase ABC in regeneration of the spinal cord is to prevent CSPG signalling via GAG cleavage, these data do not rule out further effects from increased angiogenesis or immune cell chemo taxis. These results agree with previous *in vivo* studies that demonstrate recovery of neurite outgrowth post-CNS trauma by Chondroitinase treatment [267, 269, 293].

The study so far has demonstrated how small molecules can be used to interact with different parts of the signalling cascade that occurs when neurons are grown on an Aggrecan substrate. By inhibiting or activating different mediators of the cascade a reduction of inhibition of the effect of Aggrecan is achieved. This provides useful data into the role of Aggrecan in human neurons after traumatic spinal cord injury. Figure 4-39 is a schematic describing the interaction of small molecules and the signalling cascade that occurs after during Aggrecan induced neurite inhibition.

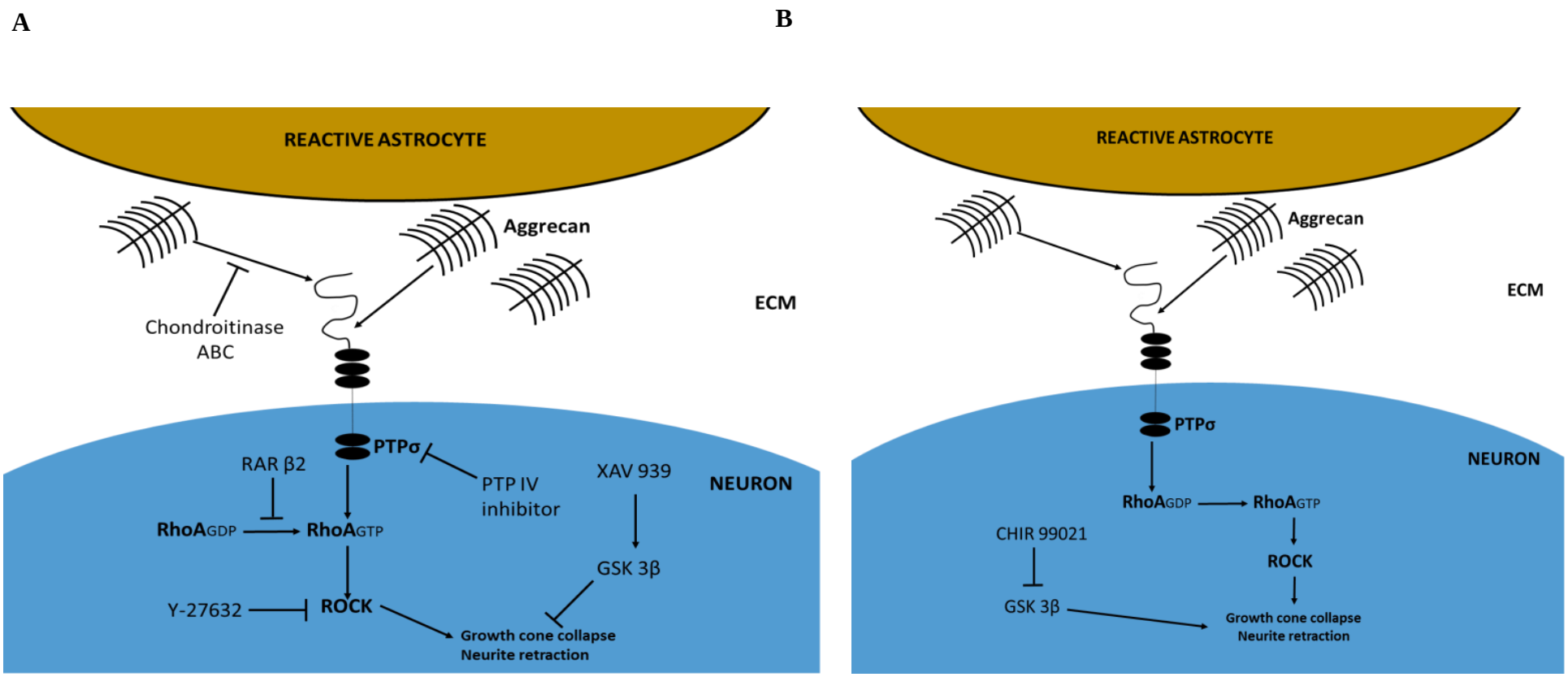

Figure 4-39 A schematic of Aggrecan induced neurite inhibition and small molecule modulators of the signalling cascade induced. The artificial ECM produced by the reactive astrocyte can be simulated using purified protein. In this schematic different levels of the signalling cascade can be inhibited using enzymes and small molecule modulators. Inhibition of the RhoA-ROCK signalling cascade can be achieved through a number of mechanisms such as RAR β2 agonists, ROCK inhibitors, Chondroitinase pre-treatment and PTPσ inhibition. Enhancing GSK 3β signalling using the small molecule XAV 939 also resulted in neurite outgrowth on Aggrecan (A), in contrast inhibition of GSK 3β by CHIR 99021 resulted in loss of neurite outgrowth on a permissive Laminin substrate (B). Regulation of different parts of the Aggrecan induced signalling cascade by small molecules is a potential therapeutic for spinal cord injury, and may require multiple targets to act in synergy depending on the extent of injury.

4.4.5 Neural-glial co-culture and neurite inhibition

In vitro co-culture between neural and other cells of the CNS is important for elucidate key molecular interactions including enchantment of neural survival and neurite outgrowth or inhibitory consequences on neurite development from other cells. The interaction between two cell types may be through contact such as cell membrane associated proteins, or through the excretion of proteins/chemical mediators into the matrix surrounding the cells. In the case of the 'reactive astrocyte', excretion of ECM proteins inhibitory to neurite regeneration and survival results an interaction between the two cell types and results in sustained damage to the organism. Model systems to investigate cell-cell interactions after often limited by the availability of the cells, media requirements (which must be the same for co-culture) an ability to distinguish the cell types and growth rate.

To model the neural-glial interaction in conventional 2D culture the astroglioma cell line U118MG was used in co-culture with the human stem cell-derived neurons. U118MG is a human astroglioma and represents a model of human astroglioma cells. This cell line was chosen due to the adherent nature and good growth on Laminin/P-D-L, furthermore, the media requirements for both the neural and U118MG cells was the same.

The astroglioma cell line U118MG was co-cultured with human stem cell derived neurons as described in this Chapter. The presence of U118MG was sufficient to visually inhibit neurite outgrowth from human stem cell derived neuroprogenitors, indicating either a mechanical barrier to neurite outgrowth or a receptor mediated response; it may be that the presence of U118MG mask Laminin epitopes for integrin binding. It was demonstrated that by addition of Y-27632 an observable amount of neurite outgrowth was recovered. These data indicate a possible receptor mediated inhibitory affect by U118MG on the stem cell-derived human-neural cells. It may be that U118MG cells are representative of a 'reactive astrocyte' like phenotype, this could be demonstrated by determining the protein composition of the ECM surrounding U118MG. It is known that 'reactive astrocytes' inhibit neurite outgrowth and induce neurite retraction by the production of CSPG's and other ECM proteins [141], if this was also shown in U118MG it would suggest a similar mechanisms of neurite inhibition. Furthermore, it was shown by Chan, C.C et al (2007) [155] that ROCK inhibition induced a change in CSPG processing resulting in an increase in production of chondroitin sulphate proteoglycans and further loss of neurite outgrowth, these affects were overcome by Chondroitinase ABC treatment. Data from this work

demonstrated that ROCK inhibition resulted in a decrease in CSPGs in cell culture media or cerebrospinal fluid [155]. Results in this thesis demonstrate that it is likely the U118MG cells have CSPGs on their membrane surface, as has been suggested in studies on other glial cell lines such as the expression of the CSPG Vesican by U87MG and A172 [294]. Furthermore, it is known that the proteoglycan Endocan is expressed by U118MG and may be responsible for some of the neurite inhibition demonstrated in the co-culture model [295]. In this Chapter an increase in CSPG immunoreactivity was demonstrated after Y-27632 or AC261066 treatment and this correlated with an increase in Brevican mRNA expression. It is likely that combinations of multiple proteoglycans were expressed by U118MG, Brevican, has been shown to be produced by high grade astrocytoma cells and is involved in invasion of the tumour. Furthermore, Brevican was expressed on the membrane of astrocytoma and was excreted into the ECM [296].

A visible increase in CSPG was shown after treatment with Y-27632, but Y-27632 was sufficient to stabilise the neuronal cytoskeleton and overcome inhibition of neurite outgrowth to some extent even in this highly inhibitory environment. Up-regulation of CSPG protection by Y-28632 is a known phenomenon but does not hinder the neurite forming effects of ROCK inhibition [155]. There was no detection of Aggrecan expression in protein lysate from U118MG as measured by a specific and quantitative ELISA. This is interesting, however, consistent with the cartilage [297] and peri-neuronal net [298] restricted expression of Aggrecan, but it would be expected that 'reactive astrocytes' express this protein at least to some level consistent with its presence in the glial scar.

The data from this section demonstrates the co-culture of two individual cell lines; however the quantification of this was made difficult due to the presence of the second cell line and increased network formation/neurite crossover close to the neural aggregate. As this is a model of co-culture it is suggested that more suitable cell types can be used in conjunction with our human neurite outgrowth model. Primary glial/astrocytes cells can be derived from animal tissue; however, the species differences may be apparent. Recently Guo, Y et al (2013) [299] used primary rat hippocampal astrocytes in a co-culture model with neural stem cells and Shi, M et al (2013) [300] co-cultured rat brain derived glial cells with rat hippocampal neurons. It is also possible to compare astrocytic cells from a glial scar and those in a normal physiological environment, however, human tissue is difficult to obtain and so the ability to derive neural tissue from stem cells will provide a consistent and reliable source of human tissue.

4.5 CONCLUSION

This Chapter has described the development of a robust and reliable human neurite outgrowth model using human stem cells and synthetic retinoids. The Chapter exemplified the use of EC23 over ATRA and described in detail the neural progenitors that developed from using EC23. The temporal and concentration dependent use of these small molecules was an important factor throughout this Chapter.

The defined model of human neurite outgrowth was used to investigate neurite inhibition in response to key characteristics of the glial scar that forms post CNS injury. In this model the glial scar CSPG proteins demonstrated inhibition of human neurite outgrowth. Furthermore, utilising this system to investigate small molecule modulation of the inhibitory effect of the CSPG Aggrecan revealed a number of compounds capable of enhancing neurite outgrowth. Specifically, the inhibition of PTP IV inhibition was found to be a novel way of inducing regeneration in this environment.

Finally, a simple co-culture method was described using human stem cell derived neural progenitors and a human astroglioma cell line (U118MG). Data demonstrated the inhibition of neurite outgrowth in the presence of U118MG, which could be partially recovered by p160 ROCK inhibition.

Future work involving the use of this aggregate model of synthetic stem cell differentiation will include translation into a more physiologically relevant 3 dimensional (3D) method of neurite outgrowth and 3D co-culture, which is discussed in Chapter 5.

CHAPTER 5 INVESTIGATION OF NEURITE INHIBITION USING A NOVEL 3D MODEL OF SPINAL CORD INJURY

5.1 INTRODUCTION

5.1.1 The developing glial scar

The dynamic structure that develops through a process of reactive gliosis post CNS injury and comprises the glial scar has been demonstrated to induce growth cone collapse and neurite retraction from CNS neurons. Furthermore, the physical presence of the scar and the inhibitor signals in the extracellular matrix (ECM) results in an environment not permissible to neurite regeneration [301] . The scar that forms is made up of a few key areas, including the lesion cavity, levels of increasing proteoglycans and the glial limitans composed of Reactive Astrocytes and Fibroblasts [302]. The reactive astrocytes produce a range of supportive ECM proteins that are both permissive and inhibitory to neurite survival and regeneration making the dynamic interplay between the local environment and damaged neurons key in neural regeneration studies. It is the ratio between permissive and inhibitory ECM molecules that determines the response of the neurite to its environment and ultimately regulates neurite regeneration and functional recovery. Furthermore, death of the neurite results in an immune response leading to inflammation, secondary destruction and further neurite degeneration induced by myelin fragments such as myelin associated glycoprotein (MAG) [260, 303, 304].

Although some regeneration can occur in the CNS giving rise to the hypothesis that neurons in the CNS have the ability to regenerate, overall the regenerative capability of damaged CNS is inhibited by the glial scar [305]. Degeneration of neural tissue results in loss of innervation and depending on the level of the CNS at which injury occurs a grade of paralysis is likely in the patient. The regenerative capability of damaged neurons is dependent on the local microenvironment. It is thought that unlike in the PNS the essential growth enhancing molecules required to induce the gene profile required for regeneration are not present in the CNS [306]. Small molecule modulators of cell signalling may offer an attractive method of inducing these genetic responses or can inhibit the inhibitory signals provided by the glial scar [307]. The 3D microenvironment surrounding each regenerating and degenerating neurite is pivotal to how the neurite responds after injury.

Understanding the interaction of developing neurites in this 3D environment may lead to advances in treatment at an early stage of injury.

5.1.2 Stem cells and human neurite outgrowth studies

With the growing knowledge of stem cell biology and enhancements in the manipulation of stem cells to form tissue of interest, the ability to use human neurons derived from stem cells has made *in vitro* neurobiology much more relevant to humans. Furthermore, as understanding of neural subtype selectivity, functional neurobiology and neural/non-neural interactions develop, more complex assays are available that can answer questions directed at specific areas of the nervous system. Stem cell derived neural progenitors can be produced to specifically investigate one neural subtype; furthermore, the age of neuron can also be manipulated. Combining stem-cell differentiated neurons and biomaterials that express specific ECM proteins relevant to a particular disease or pathology will result in the ability to ask very specific questions in neurobiology. Although conventional 2D culture has been able to elucidate some key pathways of the *in vivo* system a more physiological 3D model system may provide a closer match to that experienced by cells *in vivo.*

5.1.3 Physiologically relevant neurite outgrowth assays

Development of physiologically relevant model cell systems for investigating small molecule modulation of neurite outgrowth and regeneration is necessary to bridge the gap between basic biology, therapeutics and clinical treatment. Utilising relevant and specific *in vitro* cultures that closely represent the *in vivo* environment is important for reducing unnecessary animal usage in research and limiting the number of failures that occur at each stage of a clinical trial. 2D stem cell culture has been utilised as a first step in the research of small molecules with potential therapeutic application [308]. However, studies have suggested that the response of 2D tissue to its environment is far removed from the physiological 3D matrix. There are many limitations of 2D cell culture model systems, including a difficulty to co-culture with other cell types, limited 3D structure formation and the extra cellular matrix (ECM) is only affective on one linear plane resulting in cytoskeletal and architecture changes which would not be representative of the *in vivo* cell shape or function [309-311].

The advantage of growing cells in a 3D environment has been exemplified for multiple cell systems. Advantages of 3D over 2D culture include; more physiologically relevant protein

and gene expression profiles; robust stem cell differentiation protocols; regulation over 3D ECM protein coating and co-culture of different interacting cell types.

3D cell culture and neurite development models often use gel-based systems such as hydrogel and Matrigel™ to create an artificial extracellular matrix microenvironment which often utilises Collagen I fibres or mixtures of Laminin, P-D-L and Collagen. These cultures are permissive to neurite outgrowth and allow for the development of neurites. Cultures using these models tend to utilise peripheral nervous system neurons such as DRG [96] and PC12 cells, as well as neuroblastoma (SH-SY-5Y) [123]. These neural models do not recapitulate the *in vivo* development of CNS neurons. Few studies have used stem cell-derived neuroprogenitors for neurite outgrowth studies in 3D due to the complexity of the assay. In this study the combined use of small molecules, 3D scaffolds and stem cells has allowed for a defined, reproducible, physiologically relevant model of human neurite outgrowth.

The scaffold using in this study well described for culturing cells in 3D. Alvetex®Scaffold, a 200 µm thick porous polymer made from styrene monomers. The scaffold can be treated as conventional 2D plastic making 2D/3D cell culture comparisons routine. (see Chapter 1 for a review of literature on 3D neurite outgrowth models) .

Aims

This Chapter aims to translate the 2D neurite outgrowth model described in Chapter IV to 3D using Alvetex®Scaffold and use this 3D model to investigate inhibition of neurite outgrowth by Aggrecan. Furthermore, this study aims to translate the small molecule effectors described in Chapter IV into the more physiologically relevant 3D model. The study will utilise the 3D environment to assess the effect of co-culturing human stem cell derived neurons and glial cells. Based on previous reports/review of literature it is hypothesised that neurite inhibition by the glial scar observed *in vivo* can be replicated in a novel neuro-glial *in vitro* model.

5.1.5 Specific objectives

- Develop a more physiologically relevant model of neurite outgrowth using a 3D scaffold.
- Create a cell-based assay to investigate the interaction of neurons and glia in 3D.
- Investigate the small molecule modulation of neurite outgrowth in 3D.

5.2 METHODS

5.2.1 Aligned Scaffold

In collaboration with Dr R Shah, Durham University, Chemistry Dept an Aligned Scaffold was produced by the following procedure:

Polymer solutions for electrospinning were prepared by dissolving polystyrene (Aldrich Chemical Inc, USA; Typical M_n -170,000, Typical Mw -170,000, Melt index 2.00 – 4.00 g/10 min (200°C/5.0 kg, ASTM D1238) in a 3:1 ratio of THF: DMF at a concentration of 30 % (w/v). The polymer solution was placed in a 10 ml syringe with a blunt metal needle (30 Gauge) attached. The syringe was connected to a syringe infusion pump (KDS 100, KD Scientific Inc, Holliston, MA01746, USA) which controlled the flow rate (2 ml/hour) of the polymer solution and a positive voltage was applied to the needle tip. A high voltage power supply (Gamma High Voltage ES 30P, Gamma High Voltage Research, Florida, USA) was used to generate the potential difference from 18 kV. The fibres were collected on aluminium foil covering the rotating drum collector. The uniform poly(styrene) based uniform electrospun scaffold for cell culture was synthesised by layer by layer collection method on the rotating drum collector at a speed of 1165 rpm (rotation per minute) at tip-to-collector distance of 30 cm with total continuous collection time of 40 minutes.

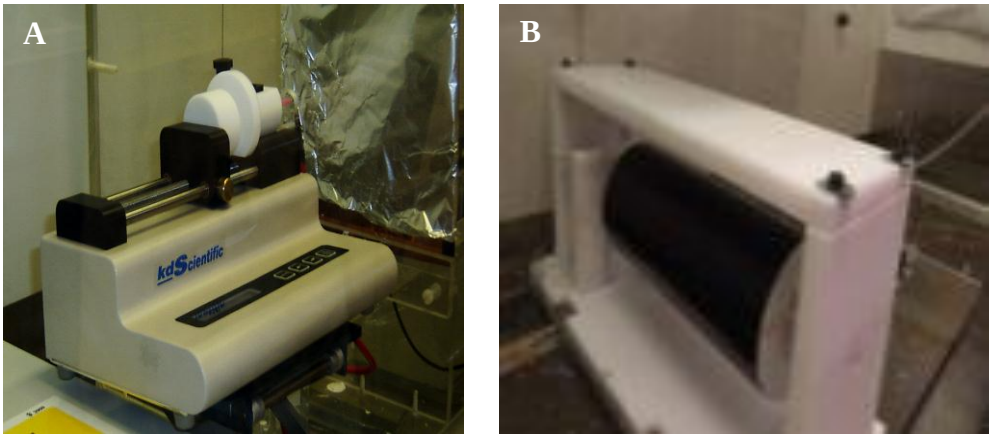

Figure 5-1 Electrospinning rig for producing aligned scaffolds.

5.2.2 Coating of aligned electrospun polymer

Aligned electrospun scaffolds were carefully peeled off the conductive aluminium mat and washed 3 x in 70 % ethanol. Scaffolds were then coated overnight with 10 µg/ml Laminin/P-D-L in PBS. After 24 hours coating with Laminin and P-D-L scaffolds were washed 3 x in PBS and remained in PBS until they were required.

5.2.3 Neurite outgrowth on Aligned electrospun scaffolds

Differentiated aggregates were 100 µm filtered and back washed into a fresh Petri dish with fresh media prior to seeding onto the Laminin/P-D-L coated scaffold. Aggregates were seeded at a density of 10-20 per aligned scaffold and cultured for 10 days in DMEM with 10 % foetal calf serum, 2 mM L-glutamine (Sigma,G3126), 100 active units of Penicillin and Streptomycin (Invitrogen, 15070-063) and the mitotic inhibitors : 10 µM 5'fluoro'2'deoxyuridine, 10 µM Uridine and 1 µM Cytosine-arabinoside. Media was not changed. After 10 days cells were fixed with 4 % PFA for 1 day and then washed 3 x in PBS and imaged using confocal microscopy.

5.2.4 Co-culture using Aligned electrospun scaffolds

1. For neural/glial co-culture at day 14 aggregate differentiation begin culture of U118MG cells in 2D as described in Chapter 2. One confluent flask contains around 6 x 10^6 U118MG cells and takes around 3-4 days to become confluent.
2. Plasma treat and coat Aligned electrospun scaffold as described above with 10 µg/ml Laminin/P-D-L
3. Filter and backwash neurospheres as described above for neurite outgrowth study at day 21
4. Prior to seeding the differentiated aggregates 1x10^6 U118MG cells in suspension were seeded in 100 µl DMEM:FBS on top of the scaffold and allowed to settle for 15 minutes at 37 °C .
5. Take 5-10 neurospheres in 100 µl media and add to each well as necessary
6. Add 2 ml of DMEMFGP containing mitotic inhibitors (10 µM 5'fluoro'2'deoxyuridine, 10 µM Uridine and 1 µM Cytosine-arabinoside) to each well and culture at 37 °C, 5 % CO_2 in a humidified atmosphere for 10 days (do not change the media during this time, as this affects neurite growth).
7. Fix cells for 1 hour in 4 % PFA and wash 3 x in DPBS.

5.2.2 3D neurite outgrowth Alvetex®Scaffold assay

The 3D neurite outgrowth assay utilised plasma treated and extracellular matrix (ECM) coated Alvetex®Scaffold to create a 3D environment permissible of neurite outgrowth. Prior to ECM coating the scaffold plasma treatment was necessary to prime the Scaffold making it hydrophilic.

5.2.3 Plasma treatment of polystyrene scaffolds

Plasma treatment of Polystyrene scaffolds is used to coat the polymer with a layer of highly charged oxygen plasma. Coating is used as a procedure to remove fungal contamination and to create a hydrophilic surface for cell adhesion.

On day 20 aggregate differentiation 12 well inserts of Alvetex®Scaffold were plasma treated using the Emitech K1050X Plasma Asher with the following parameters using the up and down buttons on the front of the Plasma treater (circled):

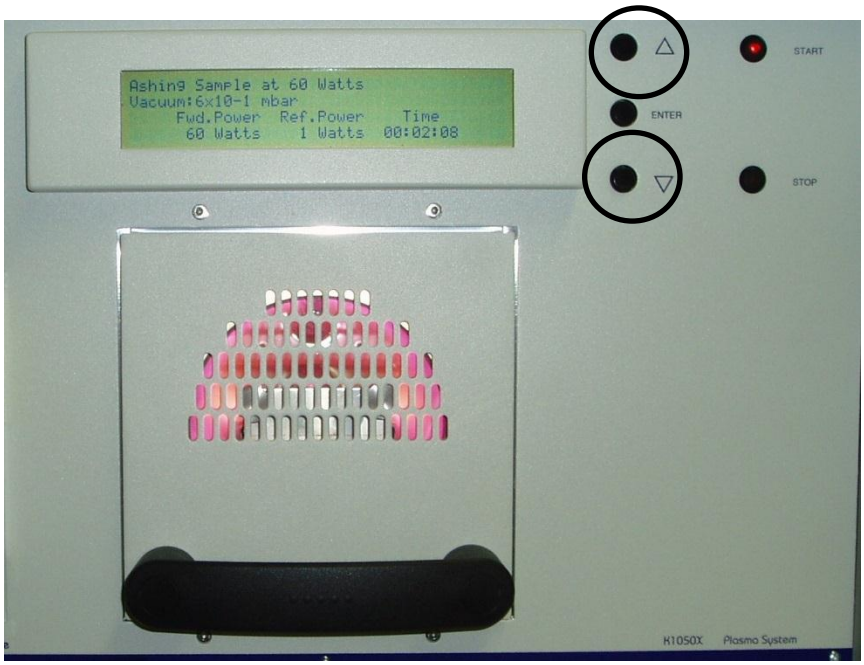

- RF power level-40 Watts
- Ashing time-5 minutes
- Bleed delay-15 seconds
- Process Gas-as appropriate
- Vent valve -Unrestricted
- Restrict vent time-120 Seconds
- Pump spin down time -15 Seconds

- Vent hold time -0 Seconds
- Gas shutoff time- 10 Seconds
- Turbo pumping enabled-0

After setting the parameters load your plate containing Scaffolds without the lid on and press start.

5.2.4 ECM coating and cell culture

After plasma treatment Alvetex®Scaffold was completely submersed in 10 µg/ml Laminin and P-D-L in PBS for 24 hours and then washed 3 x in PBS. This procedure coated the Scaffold in the ECM proteins making the hydrophilic scaffold permissive and stimulatory of neurite outgrowth.

5.2.5 Aggrecan coating Alvetex®Scaffold

To make up a 50 µg/ml Aggrecan coating solution, 1 mg of Aggrecan was dissolved in 1 ml PBS and added to 19 ml of 10 µg/ml (Laminin and P-D-L). This solution was then stored at -20 °C prior to use.

To coat Alvetex®Scaffold with the above solution follow the steps above but replace the submersion step with the Aggrecan coating solution.

5.2.6 Neurite outgrowth in 3D using Alvetex®Scaffold

Differentiated aggregates were 100 µm filtered and back washed with fresh media prior to seeding onto the Laminin/P-D-L coated plastic. Aggregates were seeded at a density of 10-20 per scaffold and cultured for 10 days in DMEM with 10 % foetal calf serum, 2 mM L-glutamine (Sigma), 100 active units of Penicillin and Streptomycin (Invitrogen) and the mitotic inhibitors: 10 µM 5'fluoro'2'deoxyuridine, 10 µM uridine and 1 µM cytosine-arabinoside. Media was not changed. After 10 days cells were fixed with 4 % PFA for 1 day and then washed 3 x in PBS. Neurons within and on top of the scaffold were stained for TUJ-1 and DAPI and then the whole scaffold imaged using confocal microscopy (488 and 405 nm excitation) or the scaffold was wax embedded, sectioned and then stained as described in Chapter 2. Sections can then be imaged using a fluorescence or confocal microscope.

5.2.7 3D glial-neural co-culture assay

8. For neural/glial co-culture at day 14 aggregate differentiation begin culture of U118MG cells in 2D as described in Chapter 2. One confluent flask contains around 6 x 10^6 U118MG cells and takes around 3-4 days to become confluent.
9. Plasma treat and coat Alvetex®Scaffold as described above with 10 µg/ml Laminin/P-D-L
10. Filter and backwash neurospheres as described above for neurite outgrowth study at day 21
11. Prior to seeding the differentiated aggregates 1x10^6 U118MG cells in suspension were seeded in 100 µl DMEM:FBS on top of the scaffold and allowed to settle for 15 minutes at 37 °C .
12. Take 5-10 neurospheres in 100 µl media and add to each well as necessary
13. Add 2 ml of DMEMFGP containing mitotic inhibitors (10 µM 5'fluoro'2'deoxyuridine, 10 µM Uridine and 1 µM Cytosine-arabinoside) to each well and culture at 37 °C, 5 % CO_2 in a humidified atmosphere for 10 days (do not change the media during this time, as this affects neurite growth).
14. Fix cells for 1 hour in 4 % PFA and wash 3 x in DPBS.

5.2.8 Chondroitinase ABC enzyme buffer and dilution

Chondroitinase ABC (Sigma Aldrich C3667), from Proteus Vulgaris was reconstituted with 1 ml of 0.1 % BSA (Sigma Aldrich A7906) giving a concentration of 5 units/ml. Stock solution was diluted in enzyme buffer to 0.15 units/ml by adding 30 µl stock to 970 µl buffer, a total of 1 ml was added to each well being treated.

Enzyme buffer consisted of:

- 0.02 % BSA
- 50 mM TRIS pH8
- 60 mM Sodium acetate (Sigma Aldrich)
- PBS w/o Ca^{++}, Mg^{++}

Treatment of Aggrecan coated plastic with Chondroitinase ABC:

1. Alvetex®Scaffold was plasma treated and coated with Aggrecan, P-D-L and Laminin as described above
2. Wash Alvetex®Scaffold with PBS x 3 after ECM coating
3. Add 1 ml of either Chondroitinase buffer (control) or buffer containing 0.15 units/ml enzyme to each well ensuring scaffold is completely submerged
4. Incubate for 1 hour at 37 °C, 5 % CO_2
5. After 1 hour incubation wash 3 x with PBS and follow the procedure for neurite outgrowth from differentiated TERA2.cl.SP12 aggregates.

5.2.9 Primary embryonic mouse cultures

As a collaboration with the University of Reading (Dr B Whalley and Dr I Smith) human and mouse neurons grown in 3D using Alvetex®Scaffold coated with Aggrecan.

Brain dissection from 14-16 day old Swiss mouse embryos

Recuperation of the Vitellin bag (membrane that surrounds the individual mouse embryos)

- Soak the abdomen of the mouse with ethanol to sterilize
- Hold up the skin with the forceps and cut/open the abdominal cavity with scissors
- Recover the vitellin bag that contains the embryos by cutting away the membrane
- Place the vitellin bag in a 50 ml falcon tube containing PBS/Glucose 33 mM

Recuperation of embryos

- Hold the embryos by the placenta and open the bag with scissors
- Place the embryos in a petri dish containing PBS/Glucose 33mM

Decapitation of the embryos

- Hold the embryos in the middle with forceps, decapitate the embryos by cutting behind the head
- Place the heads in a Petri dish containing a solution of PBS/Glucose 33 mM and wash
- Transfer heads into a new Petri dish containing PBS/Glucose 33 mM

Stabilisation of the heads under microscopes

- Using fine forceps, put an embryo head under the microscope with its eyes facing towards the left, so the back of the brain is on the right
- Stabilize the head by planting the two points of the forceps in the embryo's eyes, do not squeeze too hard

Liberation of the brain

- To release the brain, carry out three incisions using fine scissors: one lateral incision across the back of the head, about 2 cm of the way up, and one either side of that first incision.
- Release the brain by placing the scissors behind the cortices and gently push towards the incision.
- Place the brain in a new petri dish containing a solution of PBS /Glucose 33 mM

Dissociation of the cortices

- Cut out the cerebellum and separate the two hemispheres
- Remove the striatum
- Remove meninges with forceps. If needed, use fine scissors to remove them

Mechanical dissociation of cells

- Smooth a Pasteur pipette using fire and coat the pipette with sterile Heat inactivated FBS
- Place cortices in a 15 ml sterile falcon tube and add 5 ml PBS/Glucose 33 mM
- Dissociate cells by slowly and gently pipetting up and down 30-40 times
- Add PBS/Glucose 33 mM to a final volume of 12 ml
- Dissociate the cells in this volume
- Wait a few minutes for the non-dissociated elements form a deposit
- Centrifuge at 950 rpm (200 g) for 5 min at room temperature
- Aspirate supernatant carefully so that the pellet is not disturbed
- Alvetex®Scaffold in either 48 well or 96 well discs were ethanol wet using 2 x 70 % ethanol washes and 1x PBS wash.
- Scaffolds were coated with Aggrecan as described before prior to serum coating.
- After coating/ethanol wetting the discs were washed in 3 x PBS and 1 x DMEM:F12 .
- Scaffolds were left overnight in DMEM:F12 + 10 % FBS

- Freshly dissociated mouse cortical neuroprogenitors were seeded on to Alvetex®Scaffold at a concentration of 200,000 cells/cm^2

Freshly dissociated mouse cortical neuroprogenitors were seeded on to Alvetex®Scaffold at a concentration of 200,000 cells/cm^2

5.2.10 Primary human neuronal cultures

- 0.5 cm Alvetex®Scaffold discs were ethanol wet using 2 x 70 % ethanol washes and 3 x HBSS washes. Circles were not allowed to dry.
- Scaffolds were the coated with either 1 ng/ml or 10 µg/ml Aggrecan as described previously.
- The scaffolds were then washed 3 x in HBSS (Lonza, BE10-508F) and coated with 1 x DMEM:F12 (Lonza, BE12-719F).
- Scaffolds were then incubated at 37 °C until cell seeding, in 10 % Human AB donor serum (Labtech, male - HU-490, female - HU-463) made up as 10 % v/v in DMEM-F12 with 10 µg/mL gentamicin sulphate (Lonza, BE02-012E).
- Prior to cell seeding 50 µl NPMM (Lonza kit CC-3329 + 20 ng/ml rh EGF (Preprotech AF-100-15) and bFGF (Preprotech 100-18B) was added to each well and incubated to equilibrate.
- P8 human normal mesencephalon neuroprogenitors (originally P1 Lonza, PT-2599) were seeded at 15,000 cells/cm^2 (96 W) in NPMM. Media was exchanged 50 % the next day and every other day for the next 5 days.
- Human neurons were differentiated by exchanging 50 % media containing BDNF (Preprotech, 450-02) instead of EGF and bFGF. Cells were maintained for 25-35 days before electrical activity was measured using MEA.

5.2.11 Multi electrode array (MEA)

- Primary cells were maintained and differentiated as described in 5.2.12 and 5.2.13.
- Cells were rested on the MEA for 10 minutes
- Basal MEA recordings were for 10 minutes
- Drugs were added directly to the MEA for 5 minutes individually with 5 minutes rest and 10 minutes basal recording between each drug.

- The drugs used were: 20 μM CNQX and 100 μM DLAP5 10 μM tetrodotoxin citrate (TTX, ABCAM). TTX was stored at -20 °C in the appropriate solvent at manufacturer's recommendations.
- Data was analysed in 300 second blocks and compared for a mean firing rate (Hz).

5.3 RESULTS

5.3.1 Neurite outgrowth in 3D

An advantage over other 3D Scaffolds and hydrogels is the ease at which the Alvetex®Scaffold matrix can be manipulated. The scaffold can be coated to contain extracellular matrix proteins through the coating procedure described in the Methods section. Coating the scaffold was used to investigate the 3D development of neurite outgrowth from stem cell-derived neural progenitor aggregates. The scaffold was used to assess the 3D growth and differentiation potential of neuroprogenitors derived from TERA2.cl.SP12 cells treated with 0.1 µM EC23 for 21 days. Differentiated aggregates were placed on a 200 µm thick Alvetex®Scaffold and cultured for 10 days in the presence of mitotic inhibitors. The cells were then fixed in 4 % PFA, wax embedded, sectioned and stained by H & E to determine the level of penetration of cells into the Scaffold. H & E stained slides also gave an indication to if any neural tissue was present either within the aggregate or in the Scaffold. Neural tissue can be distinguished in these cultures by the structures that develop such as neural rosettes or highly fibrous cytoplasmic areas.

Data in Figure 5-2 demonstrates the need for ECM coating Alvetex®Scaffold to ensure good cellular penetration and 3D growth. The Scaffold in Image (A) was plasma treated and therefore represented a hydrophilic scaffold, growth of aggregates on the scaffold after 10 days demonstrated very few cells in 3D and no structural evidence of developing neural tissue; there was also loss of aggregate from the surface indicating poor attachment to the scaffold. Therefore further functionalization of the scaffold was necessary to induce 3D neurite outgrowth form the neural progenitor aggregates.

To assess the role of Laminin/P-D-L in 3D neurite outgrowth and maintenance the Alvetex®Scaffold was coated in 10 µg/ml Laminin/P-D-L for 24 hours. Laminin has been demonstrated to stimulate neurite outgrowth [287, 312] and P-D-L is often the coating choice for enhancing cell adhesion, a combination of both would provide a good ECM within the scaffold to support neurite outgrowth and development and has been demonstrated to be the optimal coating procedure for neurite outgrowth from embryonic stem cells [113]. Coating resulted in an increase of cytoplasmic staining within the polymer seen after H & E staining of paraffin embedded sections Figure 5-2 (B). Cytoplasmic staining and fibrous development is indicative of neural tissue development, a higher magnification image of fibres within the scaffold further indicated at neurite

outgrowth in 3D Figure 5-2 (C). It is known that neural tissue on 2D surface is promoted by Laminin coating; this was also indicated from 3D tissue.

Although cytoplasmic staining of filaments developing from neural progenitors is indicative of neurite outgrowth it is possible that these outgrowths were non-neural and so to further determine if neurites were developing in 3D using Alvetex®Scaffold when coated with Laminin/P-D-L, sections of differentiated aggregates were stained for the pan-neuronal cytoskeletal antigen TUJ-1. This antigen is specific for the cytoskeletal protein β III Tubulin and is specific for early neurite development.

Figure 5-3 demonstrates the large amount of neural tissue that forms within the scaffold after 10 days (TUJ-1, Green) (D & E). The large number of neurites in the 10 µm section indicated high levels of neurite outgrowth from the aggregates in 3D. Furthermore, notice that the aggregate nuclei stained blue remains on top of the scaffold; this is the effect of the mitotic inhibitors which disrupt mitosis preventing cell division which would result in loss of the aggregate integrity and dispersal of the cells into the scaffold. A contained aggregates makes the assay predominantly focussed on neurite outgrowth with minimal cell migration into 3D. Confocal microscopy was used to image the aggregate developing on top of the scaffold and the neurites that transit the scaffold and grow on the bottom elevation. Neurite that developed horizontally from the cell aggregate were much shorter than in 2D however, these neurite then grew through the scaffold weaving through the pores making the total length of neurites around the same as that in 2D. A large number of neurites projected and were imaged on the bottom elevation. These neurites had woven through the scaffold interacting with the scaffold in a 3D manner.

These data indicate that human neurites can develop in a 3D scaffold when coated in the extracellular matrix proteins Laminin and P-D-L. This model can be used to manipulate proteins within the extracellular matrix and determine their influence on 3D human neurite outgrowth.

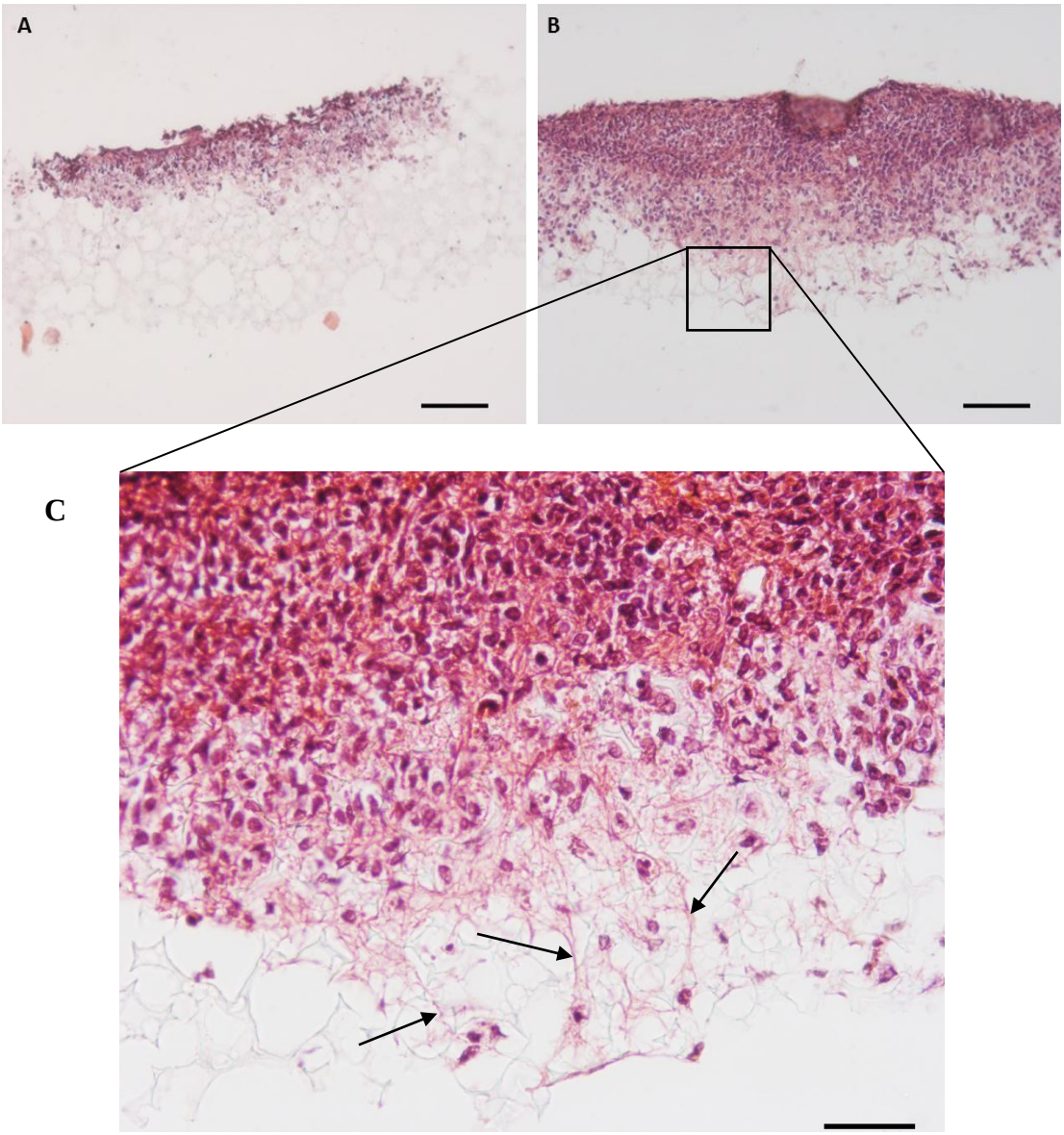

Figure 5-2 Attachment of neural aggregates to Alvetex®Scaffold. TERA2.cl.SP12 cells were differentiated with 0.1 µM EC23 for 21 days and placed on an uncoated scaffold, few cells attached and there was little evidence of cell penetration and a loss of aggregate was observed. (A). Scaffold coated with 10 µg/ml Laminin and P-D-L. Coating scaffold provided a permissive substrate for neurite outgrowth. There is significant evidence of cell attachment, excellent cellular penetration and neurite extension into the scaffold (B). High magnification image of image B demonstrates areas of long filaments of cytoskeletal staining indicative of neural processes (light purple) (arrow) (C). The processes emanated from areas of high nuclear staining (dark purple) further indicating at the presence of neurites. Data demonstrates the advantage of coating the scaffold with the ECM protein Laminin and P-D-L over uncoated Alvetex®Scaffold. Scale bars: (A,B,)100 µm, (C) 50 µm. n=2.

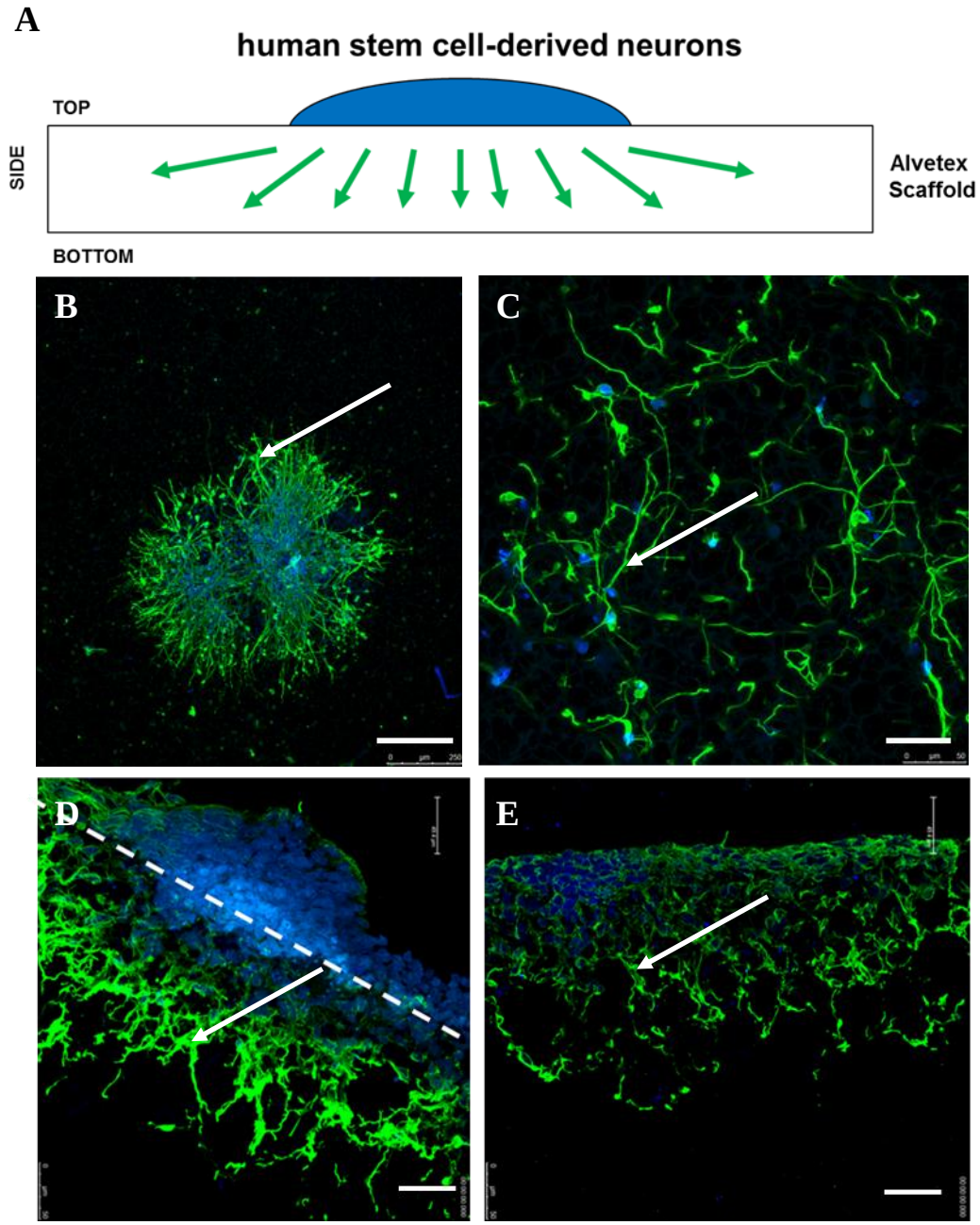

Figure 5-3 Extensive neurite outgrowth from neuroprogenitors derived from human stem cells grown in Alvetex®Scaffold. The scaffold was coated with 10 µg/ml Laminin and P-D-L TERA2.cl.SP12 aggregates were differentiated with 0.1 µM EC23 for 21 days. Differentiated aggregates were then placed on the scaffold in the presence of mitotic inhibitors for a further 10 days. During this time neurites formed within the scaffold, whereas the cell bodies remained on top of the scaffold in an aggregate. This is shown diagrammatically (A). Sections of wax embedded scaffold were stained with TUJ-1(Green) and DAPI (Blue) (D, E) followed by confocal microscopy (B, C). Notice that the cell bodies (Blue) remain outside the scaffold (asterisk). Dashed line indicated approximate top interface of Alvetex®. Arrows mark neurites within the scaffold. Scale Bars : (C, D, E)= 50 µm (B)= 250 µm. n=3.

5.3.2 Inhibition of neurite outgrowth by Aggrecan

Coating a 3D substrate with ECM proteins provides a more physiologically relevant environment for cellular development. In particular the development of neurites *in vivo* is dependent on extracellular cues that regulate gene expression and neurite migration. Guidance of growth cones and neurite outgrowth helps to regulate synapse formation and correct tissue innervation [313]. As described previously the ECM proteins Laminin/P-D-L are highly inductive of neurite outgrowth and can act to regulate neurite development. Coating Alvetex®Scaffold with Laminin and P-D-L resulted in a permissive 3D extracellular matrix environment for neurite outgrowth. Human neurites grow into the scaffold when coated with a permissive substrate however; this is not demonstrated when the proteins are not present, indicating specific interaction of the neuron with the 3D environment. By changing the proteins that coat Alvetex®Scaffold manipulation of the 3D growth substrate of human neurites can be achieved, allowing for both permissive and inhibitory environments to be investigated.

As was discussed in Chapter IV, the CSPG – Aggrecan is inhibitory to human neurite outgrowth. Inhibition of neurite outgrowth and subsequent neural regeneration depends on the balance between permissive and inhibitory proteins in the glial scar and this is dependent on the stage of the scar, the size of the injury and the distance from the scar epicentre. Chapter IV described the concentration dependent effect of Aggrecan on neurite outgrowth in 2D. Almost complete loss of neurite outgrowth was demonstrated in our conventional 2D model when 50 µg/ml of Aggrecan was added to 10 µg/ml Laminin/P-D-L substrate. In this section Aggrecan was added to the Alvetex®Scaffold coating substrate to determine the effect of Aggrecan on 3D neurite outgrowth. Data in Figure 5-4 demonstrates that the incorporation of 50 µg/ml Aggrecan to 10 µg/ml Laminin/P-D-L resulted in a loss of neurite penetration into the scaffold. Thin sections of the scaffold revealed poor neurite outgrowth (D, E) and this was accompanied by a loss of neurites on the bottom elevation of the scaffold from neurites that penetrated the whole scaffold. Interestingly, the top elevation did not show much loss of outgrowth compared to the control, this may be due to the porous nature of the scaffold (B), allowing neurites to develop in areas of low Aggrecan concentration, the growth of some neurites through the scaffold in (C) may be indicative of heterogeneous coating and reflects the concentration dependent nature of the effect of Aggrecan on neurite outgrowth. These data indicate that the use of stem cell-derived human neuroprogenitor aggregates in a 3D model of neurite outgrowth can be used to investigate the role of Aggrecan in the inhibition of neurite

outgrowth and subsequent enhancement of neurite outgrowth in this microenvironment. Furthermore, the model can facilitate the pre-clinical drug discovery of small molecules which overcome loss of neurite outgrowth specifically induced by Aggrecan in human neurites.

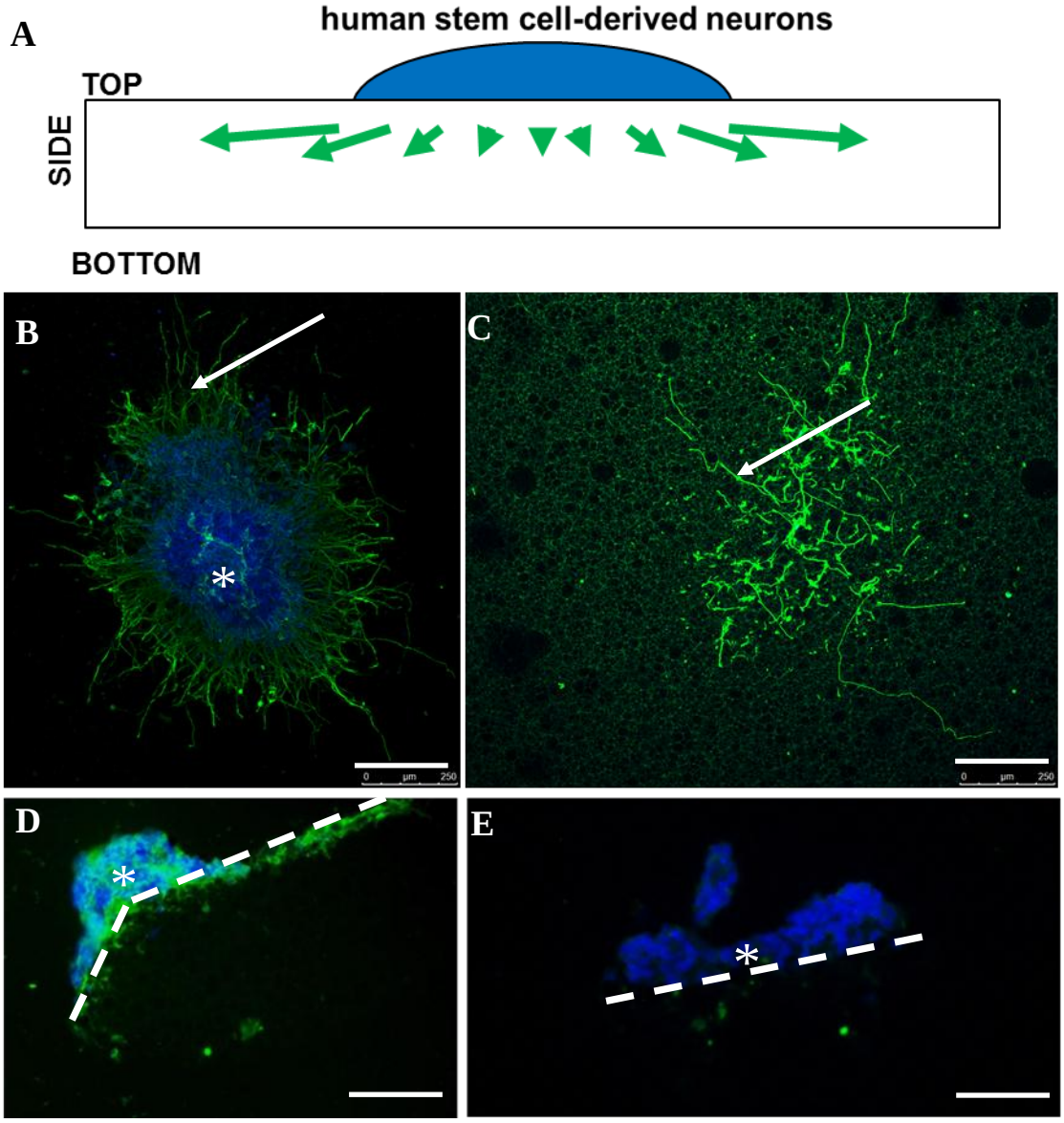

Figure 5-4 Inhibition of neurite outgrowth from neuroprogenitors derived from human stem cells grown in Alvetex®Scaffold. The scaffold was coated with 10 µg/ml Laminin and P-D-L and 50 µg/ml Aggrecan. TERA2.cl.SP12 aggregates were differentiated with 0.1 µM EC23 for 21 days. Differentiated aggregates were then placed on the scaffold in the presence of mitotic inhibitors for a further 10 days, shown schematically in A. During this time neurites failed formed within the scaffold the neural cell bodies remained on top of the scaffold in an aggregate and were immuno-positive for TUJ-1. Confocal imaging from the top elevation of Alvetex® (B) demonstrated neurite outgrowth on the horizontal plain. The bottom elevation (C) shows neurite outgrowth penetrating the scaffold, this is reduced compared to the control (Figure 5-3 C). Sections (10 µm) of wax embedded scaffold were stained with TUJ-1(Green) and DAPI (Blue). Sections of Alvetex® scaffold demonstrated poor 3D neurite outgrowth into Aggrecan coated Alvetex® (D, E). Dashed line indicated approximate top interface of Alvetex®. Asterisk marks aggregate cell bodies. Arrors point to neurites. Scale bars: (B,C) 250 µm, (D,E) 100 µm. n=3.

5.3.3 Rescue of neurite inhibition by Aggrecan using small molecules

It is known that manipulation of cell signalling pathways using small molecules can control the response of cells to the external environment. One way cells respond to the extracellular environment is via receptor mediated signalling. Proteins in the ECM can bind receptors on the surface of cells such as neurons and activate a conformational change in the receptor protein. The conformational change then activates a signalling cascade within the cell resulting in a number of downstream responses such as changes in cytoskeletal architecture and regulation of gene expression. One example of this is the positive effect of Laminin on neurite outgrowth and neural development, Laminin is known to act through heterodimers of integrin receptors and specifically required Integrin β1 [287].

In the 2D environment ECM proteins bind receptors on a single plain in contact with the tissue culture plastic, this results in cells having a differential response to the environment between the attached surface and the un-attached surface. Since only one surface of the cell is in contact with the ECM there is reduced receptor activation compared to a 3D environment. Therefore, small molecules and proteins that can regulate the signal in 2D may be insufficient to do so in 3D due to stronger receptor activation from the 3D ECM. In addition compensatory mechanisms which may occur to overcome inhibitory proteins affect by the external environment will only be affective on one side in 2D. Neurites that develop in 3D have a number of different responses to their environment. These responses affect the structure of the neuron and growth cone making it more rounded, gene expression profiles are different as the environment is more consistent and cells behave more like those that would be seen *in vivo.* The more true-like physiology of neurons that develop in 3D makes investigating signalling pathways more relevant when using 3D models than traditional 2D culture.

This section utilises a 3D ECM model of neurite outgrowth to determine how small molecule modulators of the signalling cascade induced by Aggrecan can overcome neurite inhibition, as was demonstrated in Chapter IV. The main difference between 2D and 3D in this model is the surrounding ECM that neurons in 3D will be responding to which may alter the concentration of each small molecule required to induce neurite outgrowth.

Figure 5-5 is a schematic of the assay used to investigate small molecule modulation of Aggrecan induced inhibition of neurite outgrowth in 3D. Note the descriptions of each imaging angle – top elevation is imaged via confocal microscopy on a complete scaffold

and will visibly show the aggregate, this is the same for bottom elevation however imagining will be of neurites projecting through the scaffold. Sections of the scaffold embedded in paraffin wax were imaged using a fluorescence microscope.

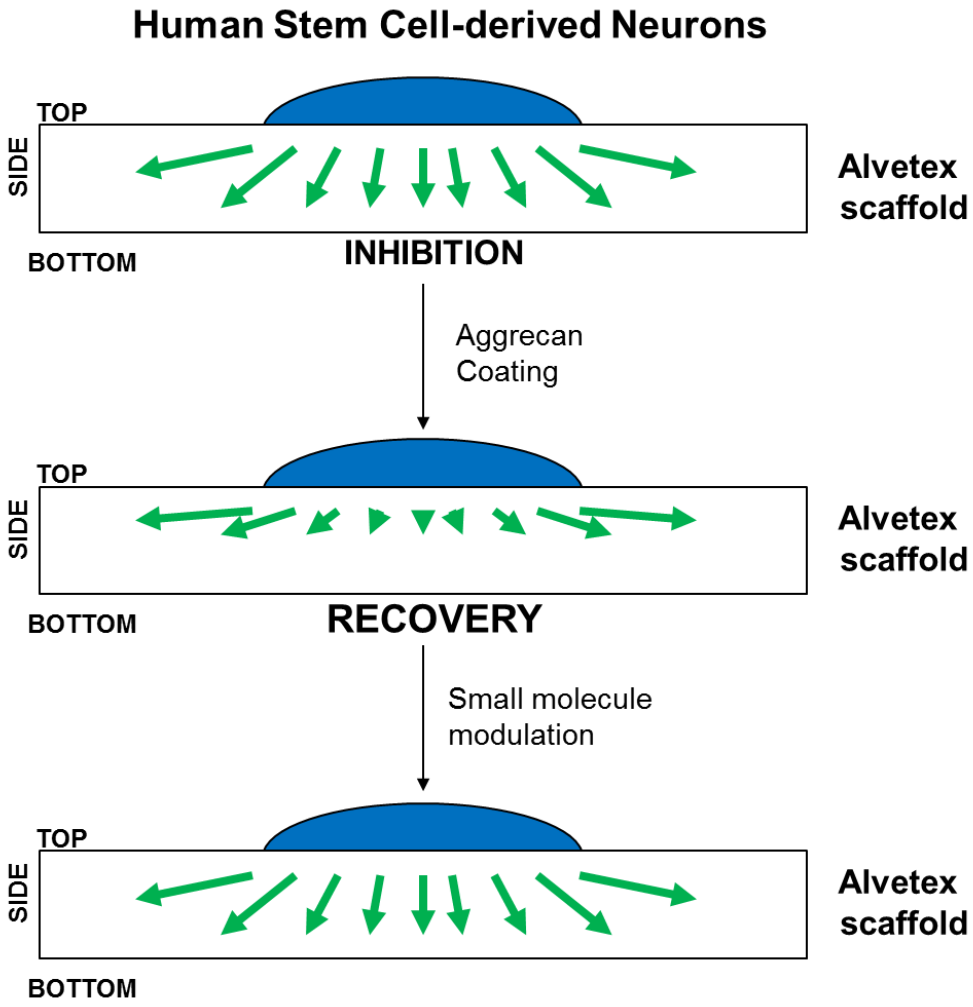

Figure 5-5 Schematic of the experimental approach used to investigate the small molecule modulation of Aggrecan induced human neurite outgrowth inhibition. Neurite outgrowth into the scaffold can be inhibited by coating adding 50 µg/ml Aggrecan to the permissive Laminin/P-D-L coating solution. This model can be used to investigate recovery of neurite outgrowth from inhibited neurites via the addition of bio-active small molecules targeting key cellular pathways involved in the modulation of neuritogenesis.

As described in Chapter IV the application of 15 µM Y-27632 or 10 µM AC261066 to neurites inhibited by Aggrecan resulted in recovery of neurite outgrowth. These compounds acted through modulation of known cell signalling pathways. It was unknown how the human neurites would respond to Aggrecan if the ECM surface was in 3D around the neurites, and if the application of these small molecules to the cell culture media was sufficient to recover neurite outgrowth.

In this section human neurites were grown in 3D using Alvetex®Scaffold coated with 10 µg/ml Laminin/P-D-L with and without 50 µg/ml Aggrecan. 3D neurite outgrowth was demonstrated with the permissive Laminin/P-D-L only substrate; however, the addition of Aggrecan significantly reduced the number of neurites that completely penetrated the scaffold (Figure 5-6). As was described in Chapter IV the small molecules Y-27632 and AC261066 rescue the inhibitory response to Aggrecan. To investigate this in our 3D model Y-27632 and AC261066 were subsequently added to the cell culture media. Application of the small molecules to this system resulted in recovery of neurite outgrowth to 3D Aggrecan inhibited neurites (Figure 5-6). The number of neurites that projected through the scaffold were imaged by confocal microscopy and given a depth code to make individual neurons easier to distinguish. A depth code gives a different false colour to each Z-stack section taken by the confocal microscope. This makes it easier to follow neurites to their origin as the lowest and highest levels of the neurite are easily distinguishable. Neurons were counted on the bottom elevation under each condition and demonstrated the recovery of neurite outgrowth in 3D by both AC261066 and Y-27632.

In Chapter IV, two other small molecule modulators of neurite outgrowth were assessed; these were XAV 939 and PTP IV inhibitor. Aggregates grown in 3D with and without Aggrecan treated with XAV 939 did not attach to the Alvetex®Scaffold/were loosely attached and lost during processing making any imaging analysis/ processing incomplete. The small molecule PTP IV, however, did induce some neurite outgrowth recovery from neurites grown on an Aggrecan rich ECM (Figure 5-7). 3D neurite outgrowth into the inhibitory Aggrecan environment was demonstrated after treatment with 1 µM PTP IV for 10 days. Neurite outgrowth did not penetrate the complete scaffold, as demonstrated by confocal microscopy. However outgrowth was apparent by sectioning the scaffold, no outgrowth into the scaffold seen in untreated cultures. Incomplete recovery of neurite outgrowth by PTP IV treatment may be due to differences in the optimal concentration of between 2D and 3D. Although 1 µM was optimal in 2D, a concentration-response study

may demonstrate a shift in the optimal concentration in 3D due to the increase in activated PTPσ receptors from the 3D ECM.

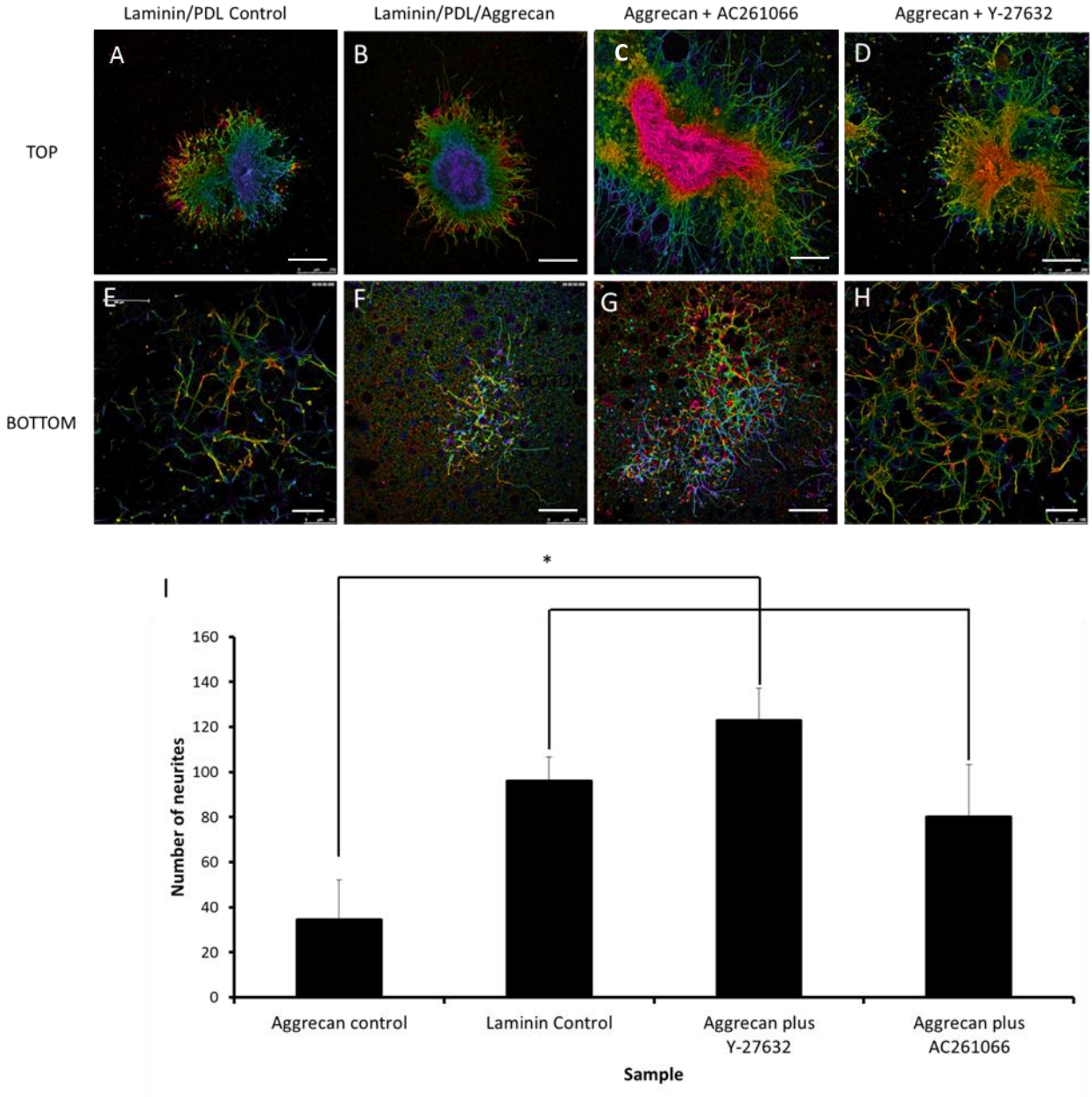

Figure 5-6 Neurite outgrowth inhibited by Aggrecan can be overcome by Y-27632 or AC261066 treatment. Alvetex®Scaffold was coated with Laminin and P-D-L (A, E) or Laminin, P-D-L and Aggrecan (B, C, D, F, G, H). Addition of Aggrecan resulted in a significant decrease in the number of neurites growing through the scaffold. Addition of 10 µM Y-27632 (D, H) or AC261066 (C, G) resulted in enhanced neurite outgrowth and differentiation on an Aggrecan substrate. A Z-stack by confocal microscopy was used to image TUJ-1 stained neurites and aggregates. The images were modified using depth coding which provides a different false colour to each section of the Z-Stack. Through depth coding individual neurites could be distinguished on the bottom elevation of Alvetex®Scaffold for quantification (E-H). Quantification Demonstrated enhanced neurite outgrowth in the presence of Y-27632 and AC261066 (I). Data represent mean ± SEM, n=3. Scale Bar: (A-D, F, G) 250 µm, (E, H) 100 µm * $p \leq 0.05$ Students paired t-test.

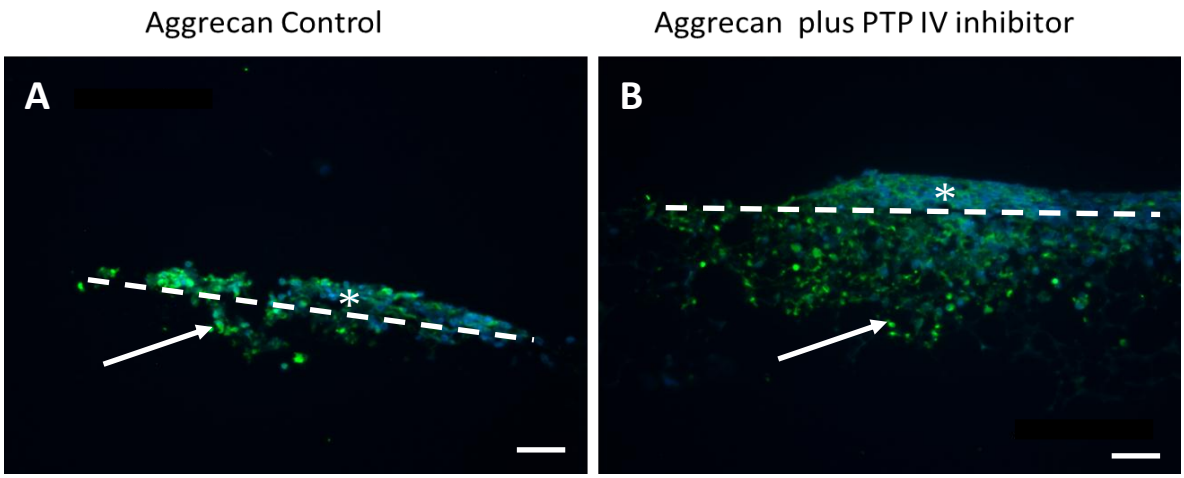

Figure 5-7 Neurite outgrowth inhibition by Aggrecan coated Alvetex®Scaffold can be partially overcome by PTPIV inhibition. Aggregates of TERA2.cl.SP12 cells differentiated for 21 days by 0.1 µM EC23 were placed onto Alvetex®Scaffold coated with 10 µg/ml Laminin, P-D-L and 50 µg/ml Aggrecan untreated (A) or with the addition of 1 µM PTP IV inhibitor (B) for 10 days. Transverse sections of Alvetex®Scaffold were taken from each condition. Condition (A) was not permissive for neurite outgrowth and resulted in no neural projections in to the scaffold. However, condition (B) was permissive to partial neurite outgrowth demonstrating recovery of neuritogenesis into a previously inhibitory environment. Arrow marks neurite outgrowth into Scaffold. Dashed line indicated approximate top interface of Alvetex®. Asterisk marks aggregate cell bodies Scale bars: 50 µm. n=3.

5.3.4 Recovery of neurite inhibition by chondroitinase ABC treatment of Aggrecan coated Alvetex®Scaffold

The enzyme chondroitinase ABC, a bacterial enzyme, is known to cleave glycosaminoglycan (GAG) chains from proteoglycans such as CSPGs [161]. It has been shown that the major active component of CSPG signalling in neurons is via GAG which is a ligand for protein tyrosine phosphatase receptors on the neural membrane [314]. CSPGs are produced in the spinal cord post injury by activated astrocytes and activate PTP receptors [1]. Activation results in growth cone collapse and neurite retraction at the neural level and loss of function at the whole animal level due to loss of innervation. Sustained loss of innervation results in loss of synapse at the tissue target making speed of treatment a major obstacle for neural regeneration [315]. Removal of GAG from Aggrecan in our 2D model of neurite outgrowth resulted in recovery axon elongation. It has been demonstrated in published literature that chondroitinase treatment to areas of damaged spinal cord can aid neural regeneration and functional recovery.

In this Chapter a 3D model of Aggrecan induced human neurite inhibition was used to assess the basic mechanism by which Chondroitinase ABC treatment may work. This is the first study to utilise synthetically differentiated stem cell derived human neurons and a 3D model of spinal cord ECM with specific protein composition to assess Chondroitinase treatment. The advantage of this model over animal models is the defined human neural process that is occurring and the defined ECM coating of the 3D scaffold.

In this section Alvetex®Scaffold was coated as described previously with and without Aggrecan. Prior to seeding the differentiated neurospheres, Chondroitinase was added for 1 hour at 37 °C as described in the methods section. To control for any effect of the buffer used to dissolve the active enzyme on neurite outgrowth controls using the enzyme buffer alone were performed. Figure 5-8 demonstrates pan-CSPG staining (Green) on sections of Alvetex®Scaffold coated with and without Aggrecan. These data demonstrate that there is no staining for pan-CSPG in Laminin/P-D-L only coated scaffold (A), however, in both the Aggrecan coated and Aggrecan coated plus enzyme buffer a layer of CSPG - in this case Aggrecan, is visible (B,C). Note some areas of the scaffold have a higher intensity staining than others indicating a non-homogenous coating procedure, which may account for some neurites developing on Aggrecan coated Alvetex®Scaffold, seen previously. Finally, treating the Aggrecan coated scaffold with Chondroitinase ABC resulted in points of high

intensity fluorescence (D), where much of the scaffold was negatively stained, this may indicate trapping of the GAG side chains in the scaffold after enzymatic cleavage.

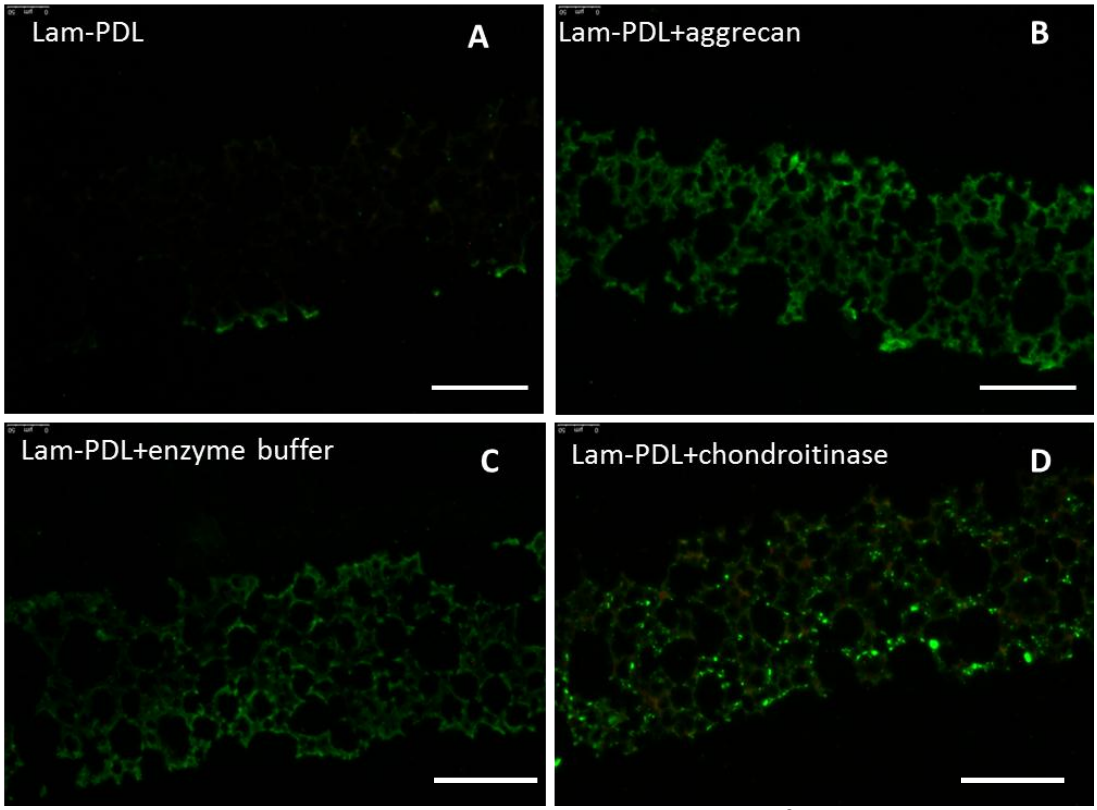

Figure 5-8 Chondroitinase digests Aggrecan coated on Alvetex®Scaffold. Transverse sections of Alvetex®Scaffold were stained for a pan-CSPG epitope (Green). Control staining with Laminin and P-D-L only (A), Alvetex®Scaffold coated with Aggrecan (B), Alvetex®Scaffold coated with Aggrecan and washed with the chondroitinase enzyme buffer for 1 hour (C), coated with Aggrecan and washed with chondroitinase in buffer for 1 hour (D). Positive staining was demonstrated in each of the Aggrecan coated scaffolds; however, the addition of chondroitinase resulted in less homogenous coating of the scaffold and areas of highly concentrated staining. Scale bars: 100 µm. n=2.

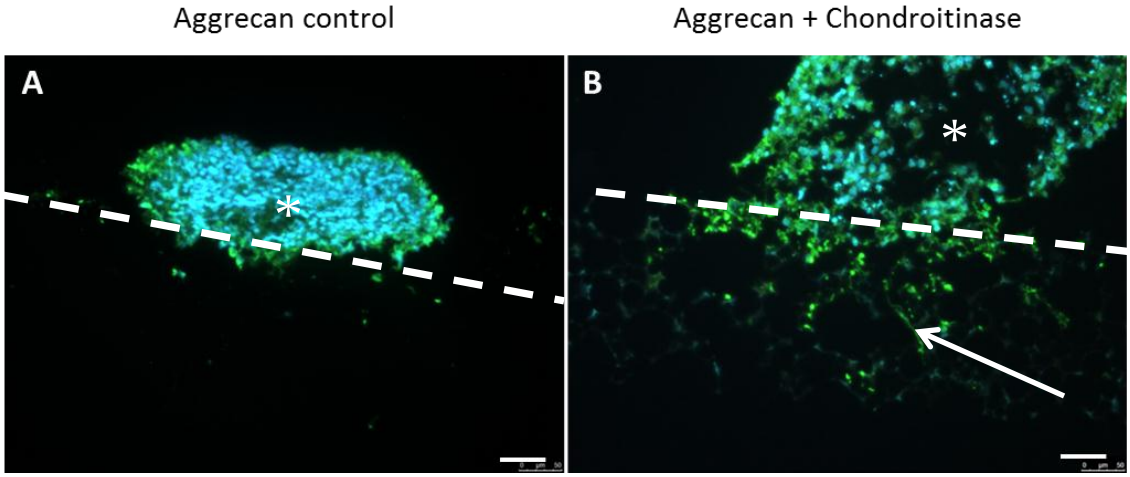

Figure 5-9 Neurite outgrowth inhibition by Aggrecan coated Alvetex®Scaffold can be overcome by chondroitinase pre-treatment. Alvetex®Scaffold was coated with 10 µg/ml Laminin, P-D-L and 50 µg/ml Aggrecan, creating a 3D environment for neurite outgrowth to be investigated. Scaffolds were then either washed for 1 hour with enzyme buffer (A) or buffer containing the enzyme chondroitinase (B). Aggregates of TERA2.cl.SP12 cells were differentiated for 21 days by 0.1 µM EC23 prior to coating the scaffold, after coating and treatment the aggregates were placed onto the scaffold. Aggregates were maintained for 10 days under each condition. Transverse sections of Alvetex®Scaffold were taken and stained for TUJ-1 (green) and DAPI (blue). Condition A was not permissive for neurite outgrowth and resulted in no neural projections in to the scaffold. Condition B was permissive to partial neurite outgrowth demonstrating recovery of neuritogenesis into a previously inhibitory environment. Dashed line indicated approximate top interface of Alvetex®. Arrow marks neurite outgrowth into Scaffold. Asterisk marks aggregate cell bodies. Scale bars: 50 µm. n=3.

5.3.5 Investigating the effect of Aggrecan on primary neural progenitor differentiation in 3D

The neural progenitor cells used so far in this study have been derived from the human pluripotent stem cells TERA2.cl.SP12 grown in an aggregate and treated with the synthetic retinoid EC23. The neural progenitors that form express a variety of markers specific to CNS cells and go through key developmental step to form differentiated neural progenitors. Although this represents a defined model of neurite development the cells are derived from a cancer stem-cell line that has some genetic abnormalities, therefore throughout this study it has been assumed that they would respond to the various ECM and small molecules in a normal way as would be demonstrated *in vivo*. Since the neural developmental process shows normal changes and the neurites that form are electrophysiological active the response of the neurites to the environment demonstrated is likely physiologically relevant. The next part of this study was to investigate the effect of Aggrecan on the 3D growth of primary mouse and human neural progenitor development to determine if the response seen in the stem cell-derived neural progenitors is similar to that of primary cells.

Note that, as was described earlier, one benefit of the stem cell-derived 3D neurite outgrowth method was the quantification of neurite outgrowth, the use of primary neurons makes quantification of neurite outgrowth much more difficult due to the individual neural processes that develop in networks and the lack of directional growth observed. Again this study utilised Alvetex®Scaffold as a scaffold for 3D neurite growth.

Mouse embryonic cortical cultures

Embryonic mouse cortical cultures were isolated and cultured in 3D as described in the methods section. Differentiation of the mouse cultures in 3D resulted in aggregates consisting of both neural and glial cells as defined by either TUJ-1 expression for axons and GFAP for glia. Figure 5-10 shows images of the differentiated aggregates with the Alvetex®Scaffold visible in the background. The cells formed discrete aggregates visible on the scaffold (A); the neural tissue could be seen clearly within the aggregate at high magnification (B). In this figure the scaffold was ethanol wet and coated protein coated with FBS. In Figure 5-11 the addition of an Aggrecan coating stem resulted in a visible reduction in the number of embryonic mouse cortical cell aggregates. It is unknown the mechanism by which cell aggregates are reduced, however it is likely a toxic effect. In this figure only cell bodies stained with DAPI (Blue) and neural processes stained for TUJ-1 (green) were imaged. Although this primary model may represent more physiologically

relevant cells the biological information that is gained from culturing these cells on Aggrecan coated Alvetex® is limited. Note: It was not possible to perform sectioning of the scaffold since the scaffold did not contain a sufficient number of cells for processing. Furthermore, due to species differences primary human neural progenitor differentiation would be more relevant.

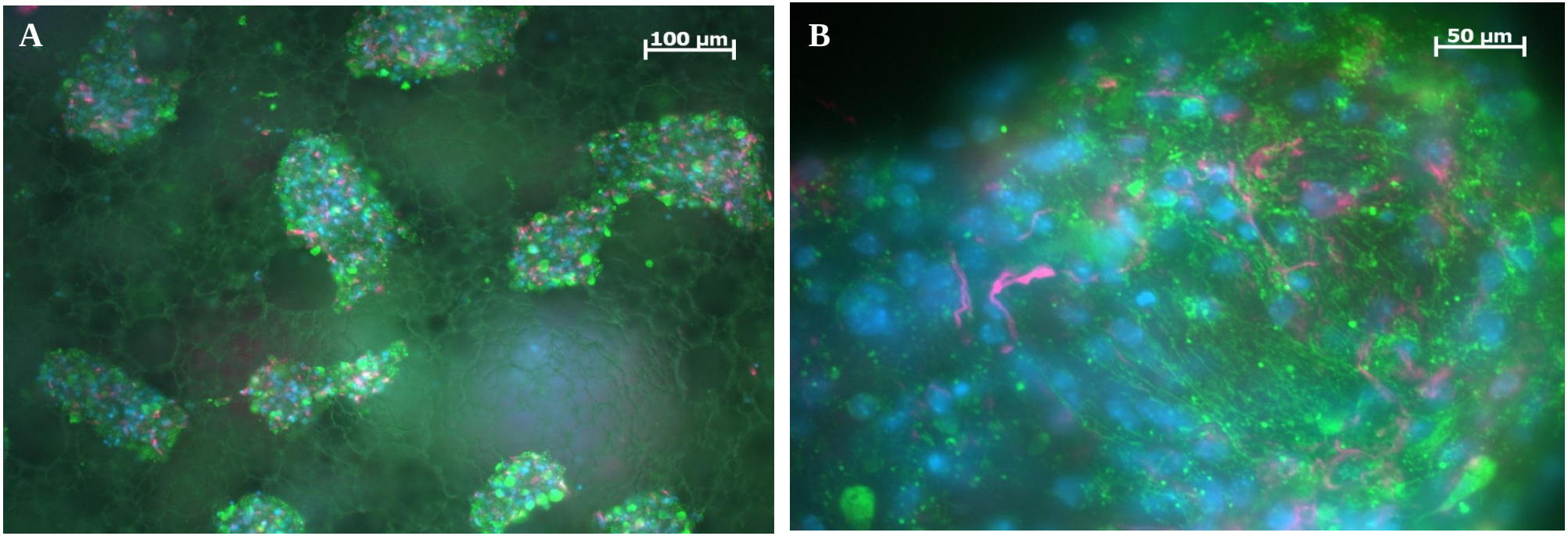

Figure 5-10 Embryonic mouse cortical cultures differentiated on Alvetex®Scaffold. Day 14-16 embryonic mouse brains were dissociated and differentiated on Alvetex® as described in the Methods section. The cultures formed aggregates of cells containing axons (TUJ-1, Green) and Glial (GFAP, Red). Cell nuclei were stained with DAPI (Blue). Alvetex® was serum coated prior to cells seeding giving the scaffold a hydrophilic surface. Low magnification image shows aggregates of cells (A). High magnification image (B) demonstrates the filamentous TUJ-1 staining and associated GFAP positive cells. These data demonstrate the 3D differentiation of primary mouse neuroprogenitors in to neurons and glial. These images were taken on an Epi-flourescence microscope (Data generated in collaboration with Dr I Smith and Dr B Whalley Reading University). n=3.

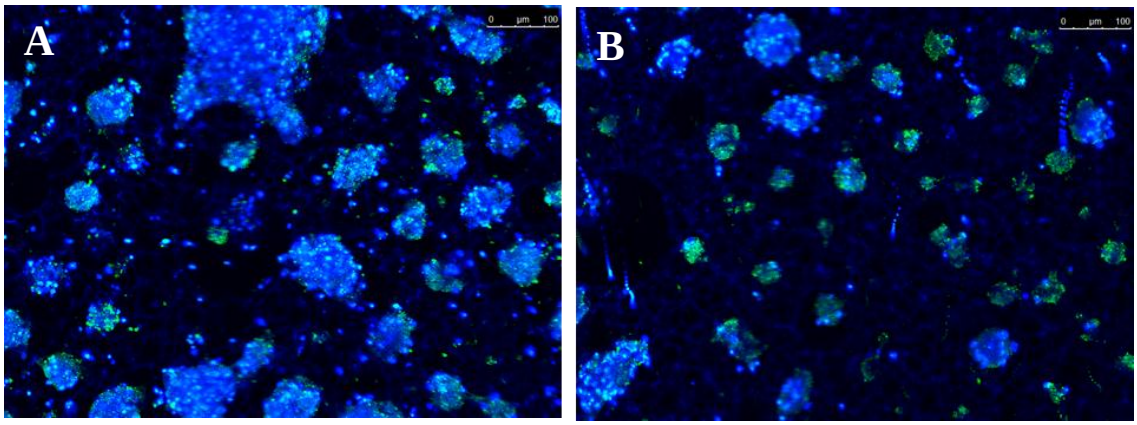

Figure 5-11 Growth of embryonic mouse primary cortical neuroprogenitors on Aggrecan coated Alvetex®Scaffold. Primary mouse cortical neurons were seeded on 96 well Alvetex®Scaffold coated with DMEM: F12 + 10 % FBS ± 10 µg/ml Aggrecan. Neurons were stained for TUJ-1 (Green) and DAPI (Blue). Images were taken using a confocal microscope (488 nm and 405 nm). Cells aggregated on both uncoated scaffolds (A) and Aggrecan coated (B) scaffolds, however, there was notably less aggregates of cells in the Aggrecan coated Scaffold, possibly indicating toxicity of Aggrecan to the cells. Scale bars: 100 µm. n=3.

Normal human neural progenitor culture

Normal human neural progenitor cells (nHNPC) derived from human brain mesencephalon were acquired from LONZA (PT-2599). The cells are cryopreserved and shipped as neurospheres, the neurospheres differentiate upon treatment with BDNF into neural and glial lineages. Although the nHNPC are commercial and cryopreserved they are a primary human model and can be used for drug toxicology, CNS function and electrophysiology studies. The cells are derived from a single donor reducing heterogeneity and are at a concentration of 1.2 x 106 cells / vial. Treatment with BDNF in 2D results in differentiation of the progenitors into neural and glial cells (Figure 5-12) for use in the above studies.

To differentiate the nHNP cells in 3D they were seeded onto human serum coated Alvetex®Scaffold as described in Section 5.2.13 and maintained in neural maintenance media containing FGF and EGF for 5 days. After 5 days FGF and EGF treatment was stopped and the cells were differentiated by treatment with BDNF. Cells were maintained in the 3D environment for 25 days prior to fixation, staining (TUJ-1 and GFAP) and imaging using confocal microscopy. Figure 5-13 shows the 3D differentiation of nHNPC in Alvetex®. Neural processes were demonstrated by TUJ-1 staining (Green) and associated GFAP staining demonstrated the presence of Glial cells (Red). Multi-electrode array (MEA) data of the complete Alvetex®Scaffold demonstrated good firing potentials on 258 electrodes from the human neurons; note that in 2D human neurons do not induce any action potentials measurable by MEA. The addition of tetrodotoxin toxin (TTX), a voltage gated, fast sodium channel blocker and CNQX/DLAP5 AMPA/NDMA antagonists, to the control cultures, caused an almost complete inhibition of firing potential validating the action potential of the neurons grown in 3D in this model (Figure 5-14).

To assess the effect of Aggrecan coating on nHNPC differentiation in 3D the scaffold was coated with 1 ng/ml or 10 µg/ml Aggrecan overnight prior to human serum coating and cell seeding – cells were then differentiated with BDNF for 35 days. Cultures were fixed in 4 % PFA and stained with TUJ-1. Confocal imaging demonstrates the effect of Aggrecan on the cultures (Figure 5-15). The control culture demonstrated good neural differentiation and neurite outgrowth (A), the addition of 1 ng/ml Aggrecan coating did not result in loss of neurite outgrowth and the neurons looked healthy (B).

Using a MEA to measure the action potential of neurons grown in the presence of 1 ng/ml Aggrecan revealed a significant decrease in firing rate compared to the control (Figure 5-15). Since TUJ-1 staining demonstrated good neurite growth on both control and 1 ng/ml Aggrecan coated Alvetex® the effect of Aggrecan on the action potential of human neurons grown in 3D was not related to neurite outgrowth. Furthermore, there was a significantly higher number of firing events in Aggrecan coated cultures compared to the TTX treated control, indicating that although these neurites were not firing they had the potential to fire.

Coating Alvetex® in 10 µg/ml Aggrecan resulted in aggregation and loss of neurite outgrowth; the cells had a defined periphery and looked more like mouse cortical cultures in Figure 5-11 (C). No action potential was measured from neurons differentiated in the presence of 10 µg/ml Aggrecan using MEA.

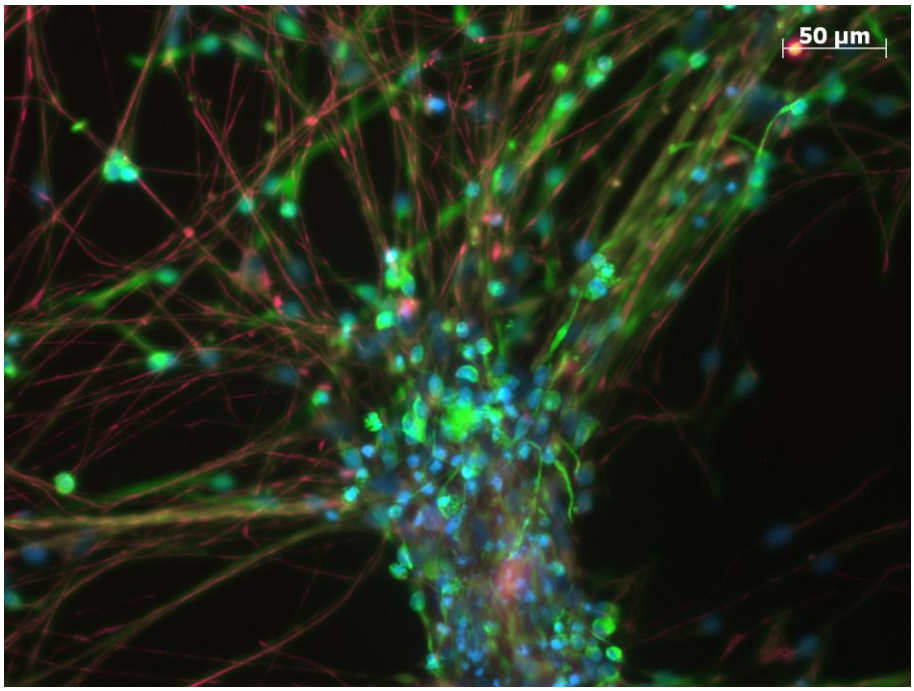

Figure 5-12 Normal human neural progenitors grown on a 2D MEA. Tuj-1 positive neurites (green), GFAP positive glial cells (red) and cell nuclei (DAPI, blue) form after nHNP are induced to differentiate with BDNF. No action potential is measurable in by MEA from these cultures. (Data generated in collaboration Dr I Smith and Dr B Whalley, Reading University). n=3.

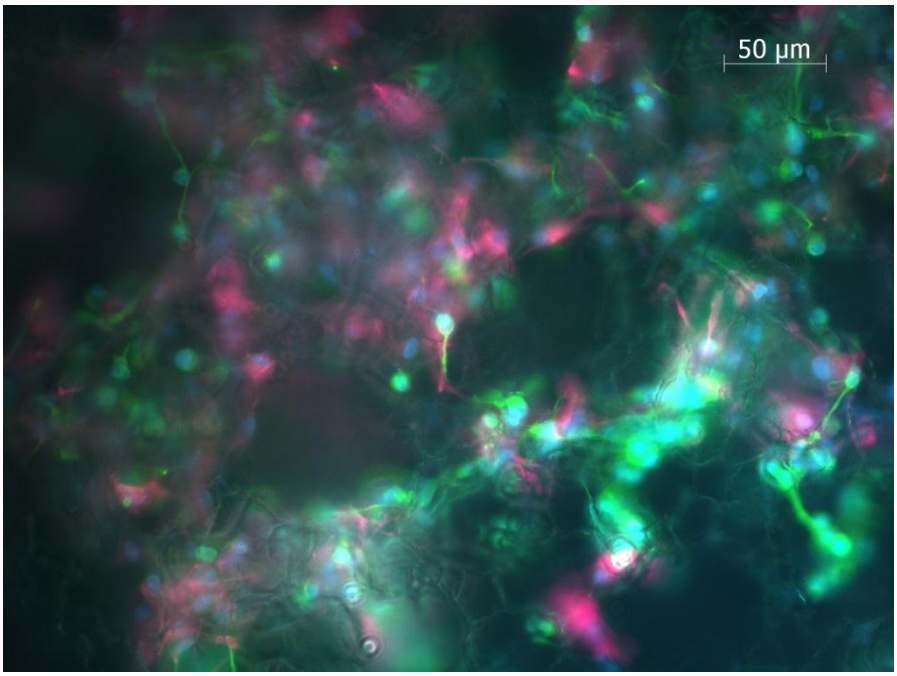

Figure 5-13 Normal human neural progenitors differentiation in 3D using Alvetex®Scaffold. Human neural progenitor cells were induced to differentiate in 3D by the addition of BDNF. The cells were cultured as described in the Methods section and expressed TUJ-1 (Green), GFAP (Red) and DAPI (Blue) after 25 days culture. Notice that compared to mouse cortical cultures the neurites form more in a network that as an aggregate. This image was taken using Epi-fluorescence, (Data generated in collaboration Dr I Smith and Dr B Whalley, Reading University). n=3.

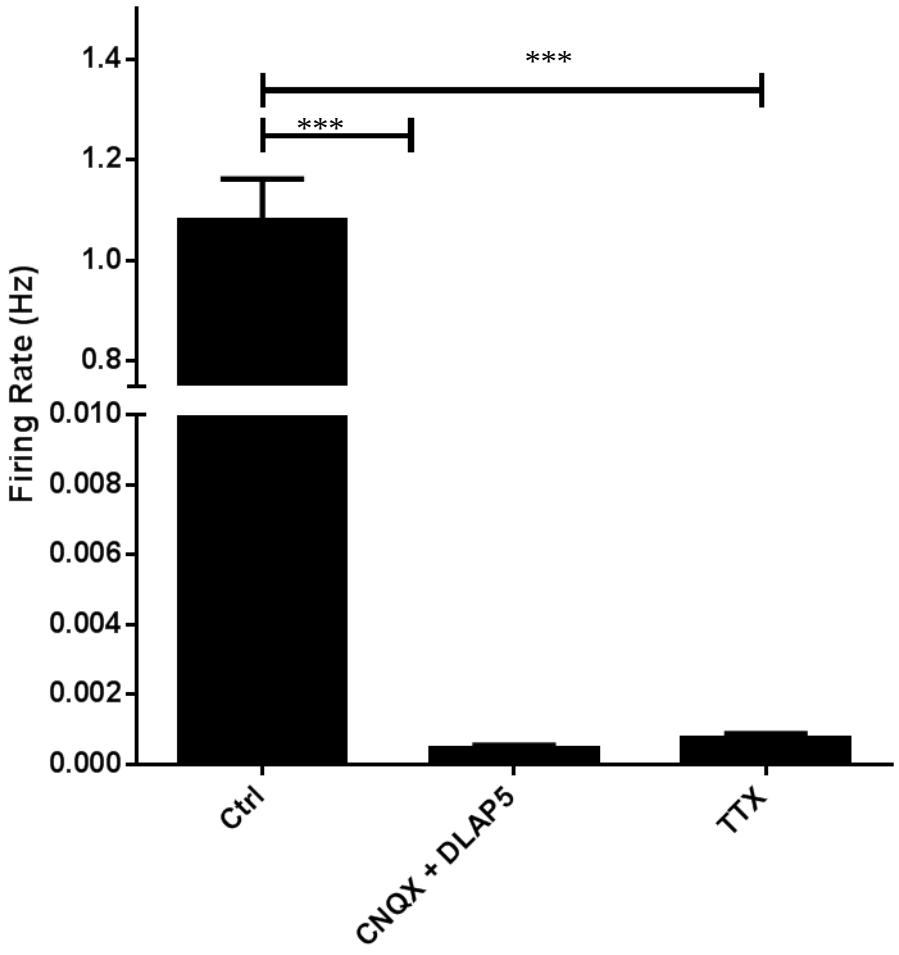

Figure 5-14 Action potential of human neural progenitor neurons differentiated in 3D. Normal human neural progenitors were differentiated on Alvetex® in the presence of BDNF. Using MEA the action potential from 258 electrodes was recorded. The firing rate of control neurons was 1.1 Hz and this could be significantly reduced by the addition of 10 μM TTX. These data demonstrate that the firing that was observed by MEA was the result of a sodium pump in the neural membrane. Paired students *t*-test ***P<0.0001 n=258 electrodes. Error= ±SEM.

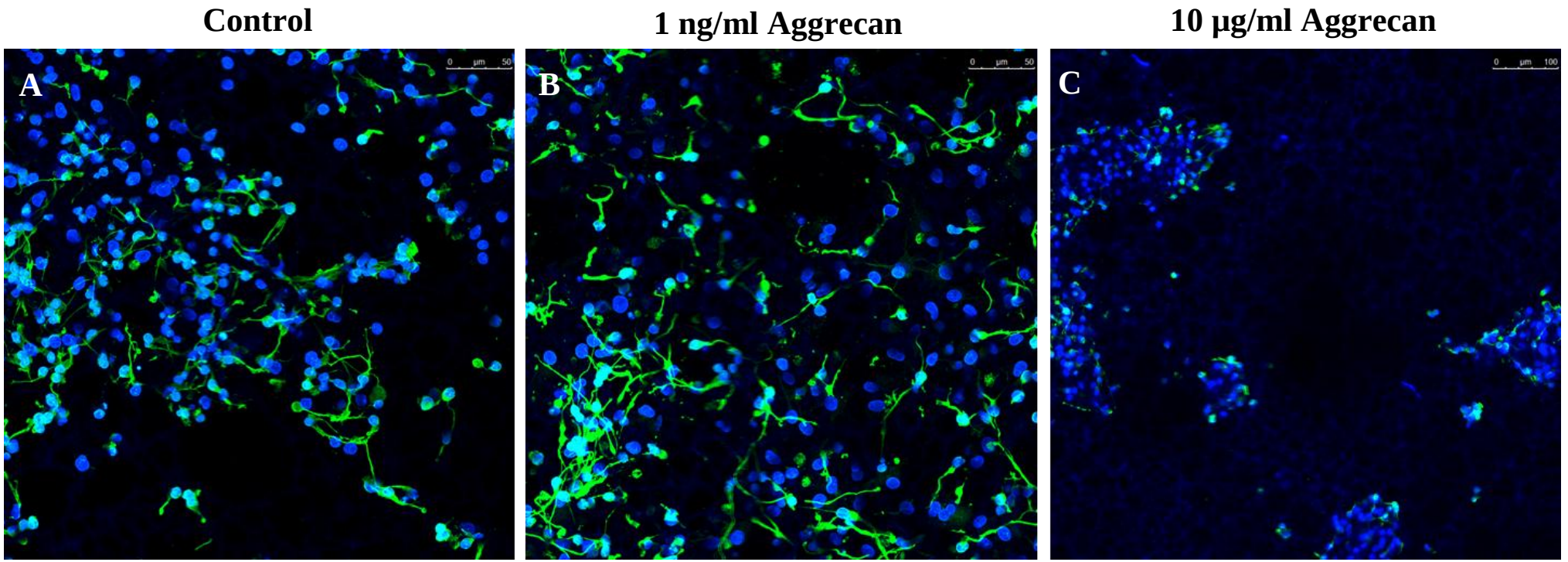

Figure 5-15 Normal human neural progenitors differentiated in 3D on Aggrecan coated Alvetex®Scaffold. Normal human neural progenitors were seeded onto Alvetex®Scaffold in 96 well plates as described in Methods. Scaffolds were treated with DMEM: F12 + 10% Ab –ve human serum overnight. Aggrecan scaffolds were coated with either 1 ng/ml or 10 µg/ml Aggrecan overnight prior to DMEM: F12 serum treatment. Neurons were stained for TUJ-1 (Green) and DAPI (Blue). Images were taken using a confocal microscope (488 nm and 405 nm). Low concentrations of Aggrecan (1 ng/ml) coating did not have an effect visibly on neurite formation (B), however, at much higher concentration (10 µg/ml) coating resulted in an apparent loss of neurite formation and aggregation of neurons. This demonstrates the regulatory ability of Aggrecan on primary human neural progenitor differentiation. Scale bars: (A,B) =50 µm, C=100 µm. n=3.

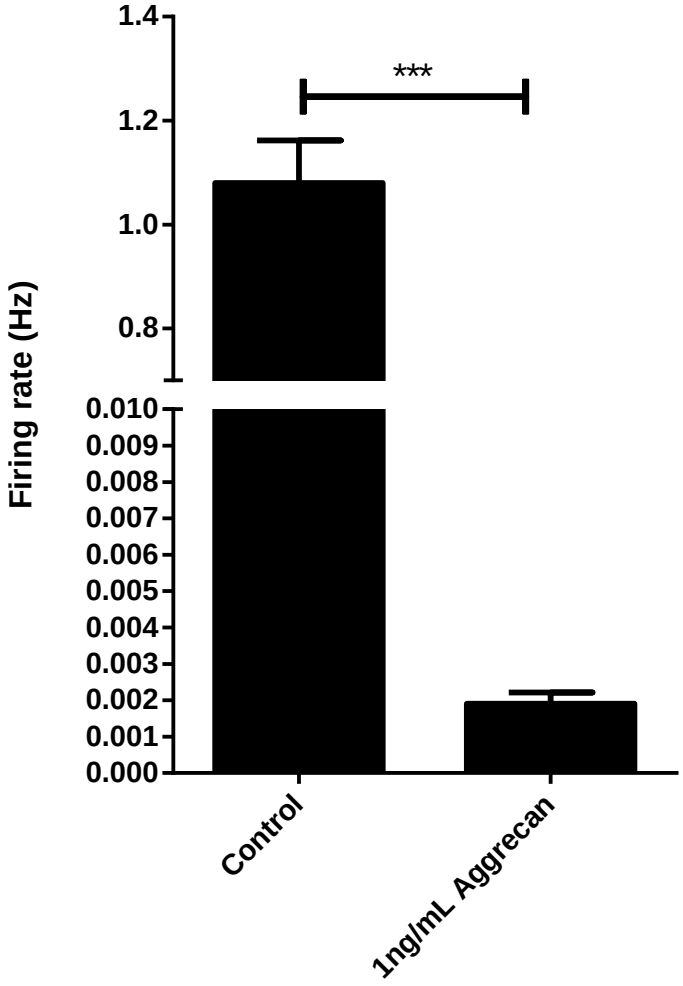

Figure 5-16 Inhibition of the 3D neural action potential by Aggrecan. Multi electrode array (MEA) analysis was used to measure the action potential in neurons grown in 3D. The assay determined the electrical signal from multiple electrodes in contact with the scaffold. Addition of 1 ng/ml Aggrecan to the scaffold resulted in an almost complete loss of firing from the neurites. Control n=258 electrodes, Aggrecan n=63 electrodes. Error bars= ±SEM. Unpaired student's *t*-test with Welch's correction ***P<0.0001.

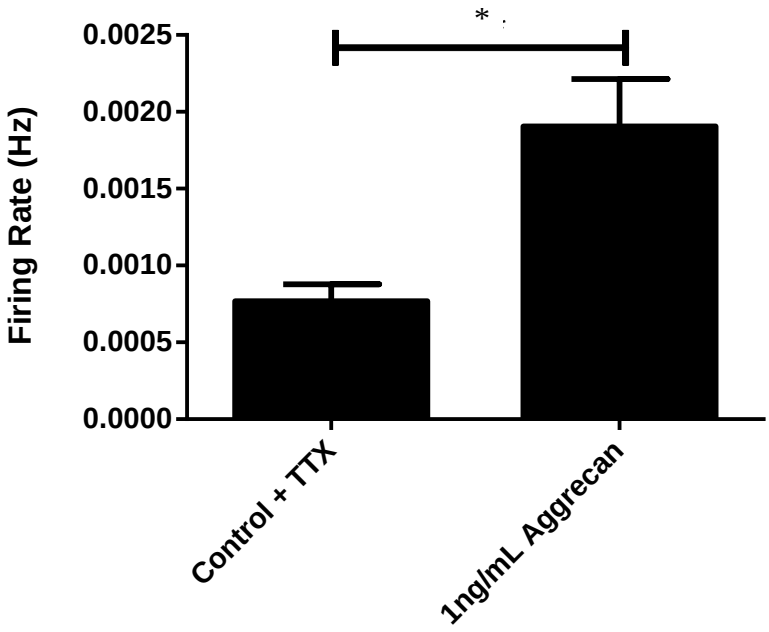

Figure 5-17 Control cultures treated with tetrodotoxin (TTX) had a lower firing potential than neurons grown on Aggrecan in 3D. Multi electrode array (MEA) analysis was used to measure the action potential in neurons grown in 3D. The assay determined the electrical signal from multiple electrodes in contact with the scaffold. Addition of 1 ng/ml Aggrecan to the scaffold resulted in an almost complete loss of firing from the neurites, however, the firing rate was around double that of control cultures treated with TTX, indicating potential firing of neurite on Aggrecan treated scaffolds. Control n=258 electrodes, Aggrecan n=63 electrodes. Error bars= ±SEM. Unpaired student's *t*-test with Welch's correction * $P<0.05$.

5.3.6 Enhancing Physiological Relevance: Co-culture of human stem cell derived neurons and U118MG astroglioma cell to investigate neurite outgrowth

Within the central nervous system glial cells provide support and protection of neurons during embryonic development and adult homeostasis. The supporting cells of the CNS consist of Astrocytes, Oligodendrocytes and Microglia and act to sustain and myelinate CNS neurons including the synaptic support and plasticity [316]. The interaction between glial and neuronal cells is complex and pathology involving glia often results in loss of neural function [317].

Activation of astrocytes post-CNS injury results in the formation of an ECM that is inhibitory to neurite outgrowth. Post-CNS injury, astrocytes are activated by the production of high levels of TGF-β and begin to express glial fibrillary acidic protein (GFAP) the cells also change shape becoming star-like which are good indicators of reactive gliosis post CNS trauma [318]. One of the first indications that astrocytes, specifically reactive astrocytes are involved in propagation of the glial scar was through their specific location to the injury site after injury forming a visible barrier and periphery to the scar. Further studies revealed that the reactive astrocytes produce ECM proteins that help compose the glial scar [319].

In this section a 3D model of CNS neural/astrocyte co-culture was developed using the human astroglioma cell line U118MG and our human neurite outgrowth mode, as described in Chapter IV in 2D.

Figure 5-18 demonstrates the H & E staining of U118MG cells grown within the scaffold. Sections of the scaffold show good cell penetration. Cells appeared viable with large areas of cytoplasm characteristic of U118MG cells (A). Co-culture with human stem cell derived neural progenitor aggregates and U118MG cells (B) demonstrated that the aggregate remains on top of the scaffold allowing for the potential of axonal projections into the scaffold in co-culture with U118MG. Due to the high cytoplasmic content of U118MG culture in 3D it was not possible to determine if neurite outgrowth was present at this stage.

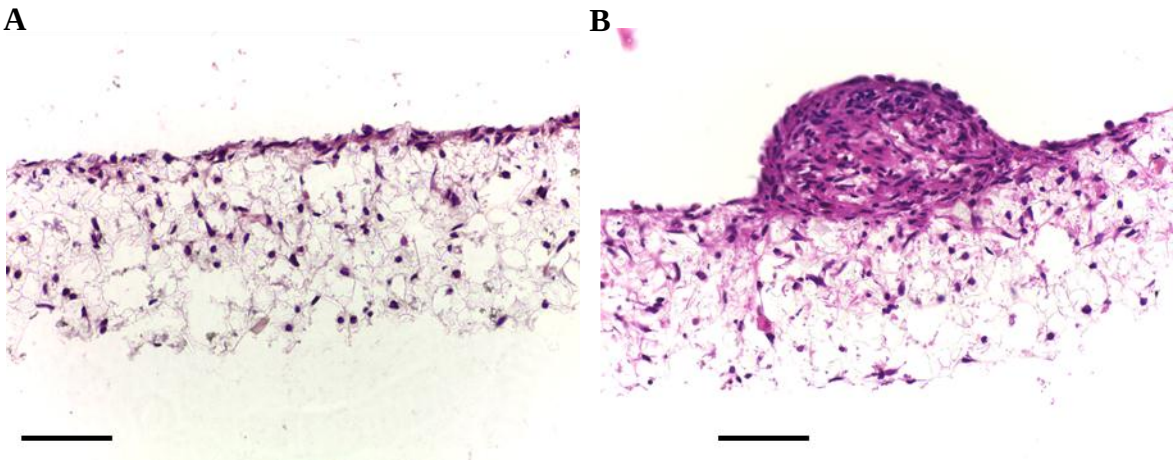

Figure 5-18 Co-culture of U118-MG and human stem cell derived neurons using Alvetex®Scaffold. U118MG cells were grown in Alvetex®Scaffold coated with Laminin and P-D-L. Cells were grown for 10 days in the presence of mitotic inhibitors; wax embedded sectioned (10 µm) and stained with H & E (A). For co-culture U118MG were allowed to settle for 15 minutes at 37 °C prior to an aggregate being added to the top of the scaffold (B). Note that the presence of mitotic inhibitors or Laminin/P-D-L does not result in loss of U118MG culture. Scale bars: 100 µm. n=3.

To assess the neurite outgrowth potential of human neurons that develop from aggregates of neural progenitors when co-cultured with astroglioma cells, sections of Alvetex®Scaffold were taken and stained for the neural specific antigen TUJ-1 and DAPI (showing U118MG nuclei within the scaffold). Figure 5-19 demonstrates that no neurites developed into the scaffold when co-cultured with U118MG cells, as would be expected from the preliminary data described in Chapter IV.

The physical influence of U118MG cells in 3D would be much greater than in 2D. In 2D neurites can develop between gaps in U118MG cells, however, in 3D a 200 µm confluent block of U118MG tissue would make the development of growing neurites much more difficult. Interestingly, the physical barrier of 3D U118MG cells was overcome by ROCK inhibition demonstrating a receptor mediated inhibition on neurite outgrowth by U118MG. Enhancement of neurite outgrowth was demonstrated in co-culture when the cells were treated with the ROCK inhibitor Y-27632, as was described in 2D in Chapter IV.

It was suggested that ROCK inhibition may induced neural development over U118MG and through the scaffold to quantify the enhanced 3D neurite outgrowth neurites would be required to develop through the scaffold and to the bottom elevation. Complete penetration would allow for accurate neurite counting on the bottom elevation of Alvetex®. As described in Chapter IV that inhibition of neurite outgrowth was likely to be the result of the presence of CSPGs on the membrane of U118MG cells. Figure 5-20, demonstrates the top elevation of human neurites alone (A) and co-cultured with U118MG (B), notice co-culturing resulted in loss of any horizontal outgrowth from the neural aggregate. Neurites in co-culture tended to rap around the aggregate, suggesting inhibition by the astroglioma cells. To quantify the extent of neurite inhibition bottom elevation of projecting neurites were counted; Figure 5-20 (C) demonstrates good growth of neurites through the scaffold when U118MG cells are not present. Co-culture with U118MG cells resulted in loss of projecting neurites demonstrated by only DAPI staining on the bottom elevation (D), as described in Chapter IV neurite outgrowth can be recovered with the addition of the ROCK inhibitor of Y-27632, Figure 5-20 (E) indicating a receptor mediated interaction between U118MG and neural progenitor development that can be overcome by cytoskeletal stabilisation and inhibition of downstream ROCK activation. These data agree with what was demonstrated in Chapter IV.

To investigate if U118MG cells expressed GAG motifs on their surface which may account for inhibition of neurite outgrowth 10 µM sectioned scaffolds were immuno-stained by an anti-CSPG antibody specific for a GAG epitope. Immuno-staining demonstrated high levels of CSPG expression indicative of membrane associated CSPG, the expression of such molecules may be a feature of the tumorous nature of the cells since the CSPG Brevican a CNS restricted CSPG is known to enhance the invasiveness of glioma [296]. Interestingly there was an apparent increase in staining intensity when U118MG cells were treated with Y-27632, this has been observed in previous studies in similar cells and may be representative of the non-selective nature of Y-27632 treatment. Enhancement of neurite outgrowth in the presence of Y-27632 and U118MG cells suggests the effect of cytoskeletal stabilisation in developing neurons is sufficient to overcome any amount of CSPG induced inhibition.

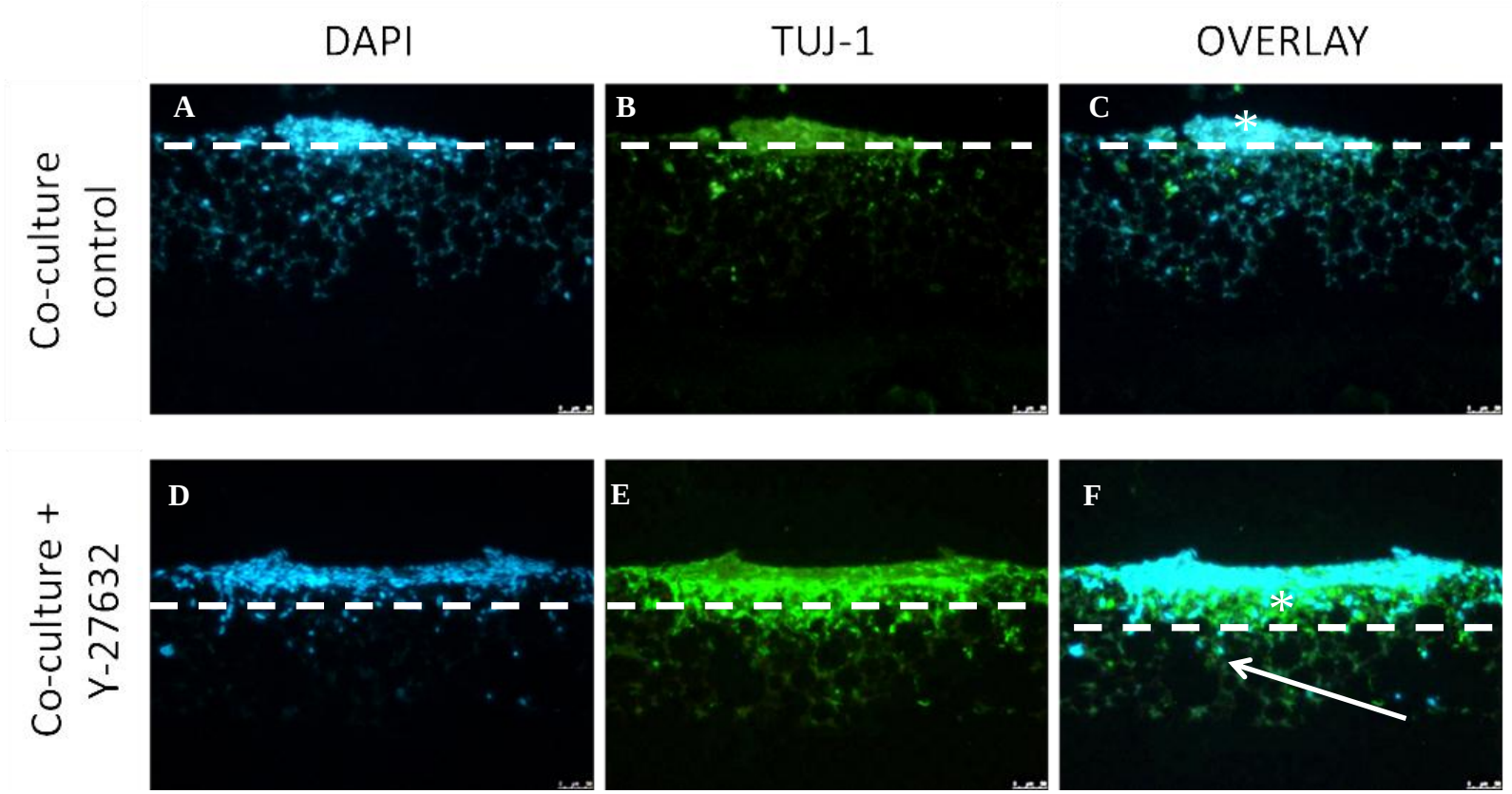

Figure 5-19 Inhibition of neurite outgrowth by U118MG co-culture can be overcome by ROCK inhibition. The scaffold was coated in a 10 µg/ml Laminin and P-D-L solution. U118MG cells colonised Alvetex®Scaffold, after colonisation a TERA2.cl.SP12 cell aggregate differentiated for 21 days with 0.1 µM EC23 was placed on top. Cells were then cultured for 10 days either with 15 µM Y-27632 or as an untreated control prior to fixation with 4 % PFA. Alvetex®Scaffold was dehydrated, wax embed , sectioned to 10 µm and stained for TUJ-1 (Green) indicating neural tissue (B,E) or DAPI (Blue) indicating U118MG inside the scaffold and the aggregate neural cell bodies on top (A,D). Overlay of DAPI and TUJ-1 indicate neurite outgrowth into the Scaffold (C, F). Note an increase in TUJ-1 staining within the scaffold in the Y-27632 treated culture. Dashed lines indicate the approximate top side of the Scaffold. Arrow marks neurite formation inside the scaffold. Asterisk marks the aggregate on top of Alvetex®. Scale bars: 100 µm. n=3.

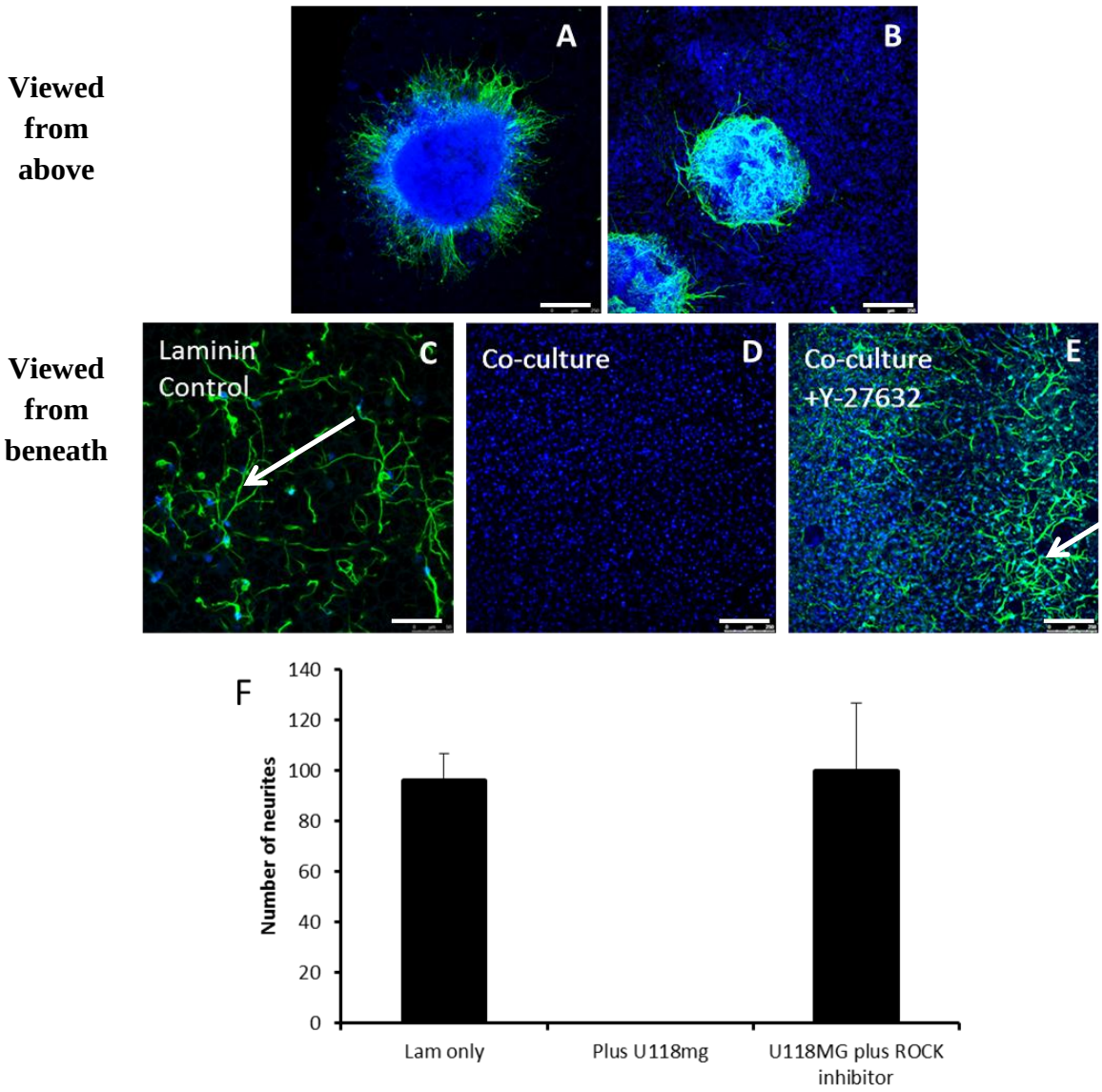

Figure 5-20 Inhibition of neurite outgrowth by U118MG co-culture can be overcome by ROCK inhibition. Co-culture with U118MG astroglioma cells resulted in loss of neurite outgrowth from the stem cell derived neural progenitors (B and D). In the absence of U118MG cells (A and C) or with the addition of the ROCK inhibitor Y-27632 (E) neurites projected through the scaffold. Neurites and neurospheres were stained with TUJ-1 (Green) and U118MG nuclei were stained with DAPI (Blue). In the presence of U118MG cells, neurites did not extend from the neural aggregate (B). Quantification of the number of neurites that project through the Alvetex®Scaffold (F). Arrows mark neurites that developed through the scaffold. Data represent mean ± SEM, n=3. Scale Bar: 250 µm.

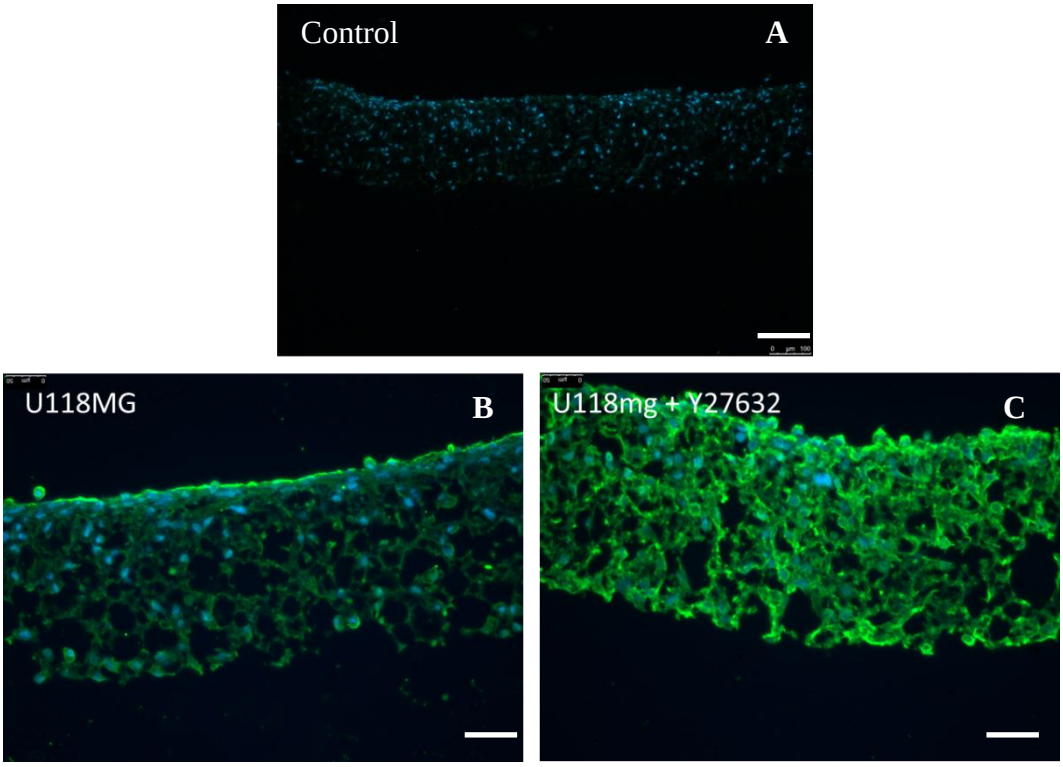

Figure 5-21 Chondroitin sulphate proteoglycan expression by U118MG cells. Sections of Alvetex®Scaffold contain U118MG cells were stained using an anti-CSPG antibody (Green) and DAPI (Blue). No evidence of none specific staining of the secondary antibody was demonstrated in the no primary antibody control (A). Some low level CSPG positive staining was detected by U118MG cells grown on Laminin/P-D-L (B). High levels of positive staining was demonstrated when U118MG cells were treated with 15 µM Y-27632 (C). Scale bars: (A) = 100 µm, (B,C) = 50 µm. n=3.

5.3.7 Guidance of neurite outgrowth using physical conduits

The use of nerve conduits to guide axon formation is used in treatments of PNS injury allowing for a short length of nerve to regenerate when autograft tissue is not sufficient [320]. The use of nerve conduits to guide CNS axon growth is not as feasible for CNS injury due to the lack of axonal regenerative potential in the CNS [306]. One treatment for CNS injury is a peripheral nerve grafts which can be grown in conduits spanning the glial scar in the CNS offering some functional regeneration to the patient, however, due to the increased invasive nature of the procedure this is not ideal. Enhancing the neurite outgrowth potential of CNS neurons is an attractive replacement for graft tissue. Guidance of regenerating axons will be important for treatment of CNS injury and will likely involve a number of stimulatory cues of neurite outgrowth. Directed neurite outgrowth for use in neural graft tissue is a major obstacle for human neural regeneration. The random direction of developing axons may result in incorrect innervation or death of neural tissue [96]. The use of chemo attractants, guidance proteins and nerve conduits can facilitate the growth of axons in the CNS.

Multiple studies have demonstrated the use of aligned polymer scaffolds to direct neurite outgrowth [118, 121, 321]. In this section polystyrene electrospun scaffolds were used to direct human neurite outgrowth from stem cell-derived neuroprogenitor aggregates. The aligned scaffold used is not naturally permissive to neurite outgrowth as it does not contain any guidance molecules or ECM proteins. To ensure the scaffold was permissive to neurite outgrowth the scaffold was coated in a high concentration of Laminin and P-D-L, as described in the methods section of this Chapter. After coating the scaffold with ECM protein it was permissive of neurite outgrowth from the human stem cell derived neuroprogenitors. Furthermore, the presence of Laminin induced the axon elongation along the aligned fibres. Induction of neurite outgrowth by Laminin is through an Integrin receptor binding mechanism [312].

Figure 5-22 demonstrates the guidance of human neurites developing from aggregates of differentiated stem cells. The neurites developed along the electrospun fibres in both directions; no neurites tended to develop perpendicular to the aligned fibres indicating either guidance by the ECM proteins Laminin/P-D-L or a stimulatory cue provided by the protein coated scaffold [312, 322]. This model can be used to assess the guidance of neurites along fibres using different coating ECM proteins.

Design of nerve conduits for peripheral nerve regeneration demonstrate that co-culture with support cells such as Schwann cells produces more robust axon growth and direction. Georgiou M et al (2013) [323], demonstrated using rat DRG that aligned Schwann cells can induce directed neurite outgrowth and the conduit can be used to treat a rat sciatic nerve injury model. The use of supporting cells in this way could be beneficial for CNS regeneration. Other studies have used electrospun scaffolds to co-culture and align Swann cells/Glial cells supporting and guiding the development of rat DRG neurons [324]. Although these studies utilise peripheral nerves some insight as to how CNS neurons may develop can be taken from the work.

Figure 5-23 demonstrates the effect of co-culturing stem cell-derived human neuroprogenitor aggregates (production described in Methods section) with astroglioma U118MG cells on Laminin/P-D-L coated aligned scaffold. Initially 1 x 10^6 U118MG cells were seeded onto the electrospun scaffold and left to adhere for 15 minutes. After 15 minutes incubation 5-10 stem cell-derived neural-progenitor aggregates were placed on the scaffold in the presence of mitotic inhibitors. The scaffold was the incubated as described in the Methods Section, for 10 days before fixation in 4 % PFA and immunostaining for TUJ-1 and DAPI. The presence of U118MG cells resulted in loss of directed outgrowth from neurites growing along the aligned fibres, indicating either a physical or biochemical effect from the U118MG cells; however, the presence of the aligned fibres did tend to allow for some outgrowth to occur between the U118MG cells but not in any particular direction. The U118MG cells did not line along the scaffold fibres but spanned them in a non-polarised manner; this may be due to the tumorous nature of the cells. More physiologically relevant astrocytic cells would likely have a positive effect on neurite outgrowth, the opposite to what has been demonstrated in this section.

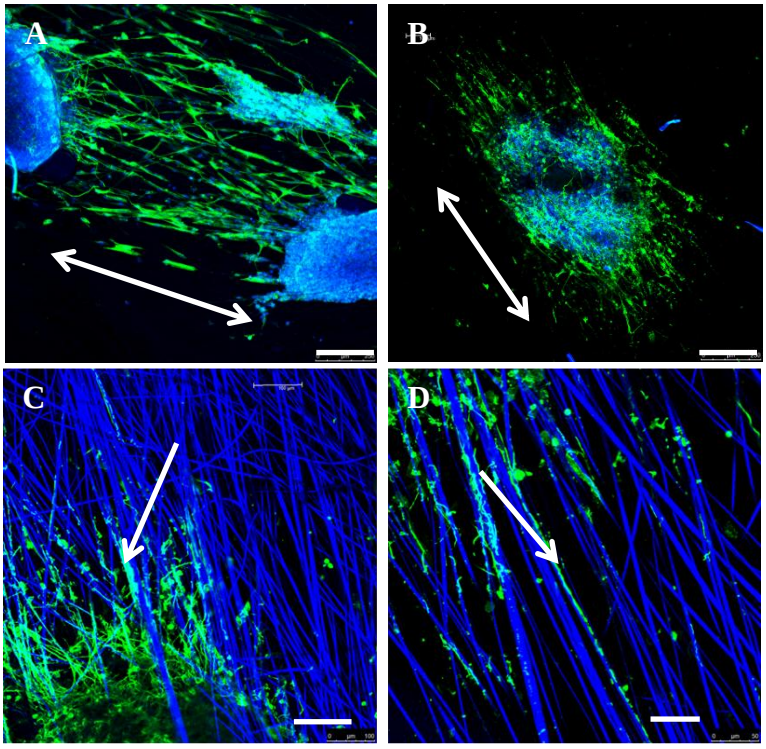

Figure 5-22 Human neurons grow along aligned electrospun fibres. Electrospun fibres were coated with 10 µg/ml Laminin and P-D-L overnight. Aggregates of TERA2.cl.SP12 cells treated with 0.1 µM EC23 for 21 days were placed on the fibres, in cell culture media containing mitotic inhibitors for 10 days. The cultures were fixed in 4 % PFA and stained for TUJ-1 (Green). DAPI (Blue) (A, B), Aligned Fibres (Blue) (C, D). Imaging through confocal microscopy demonstrates neurites growing along the fibres (arrows). Fibres fluoresced blue when excited with 458 nm light by the confocal microscope. Double ended arrow indicates direction of fibres. These data indicate the directed neurite outgrowth of human neurons along an electrospun scaffold. Scale bars: (A, B) = 250 µM, (C) = 100 µM, (D) = 50 µM. n=3.

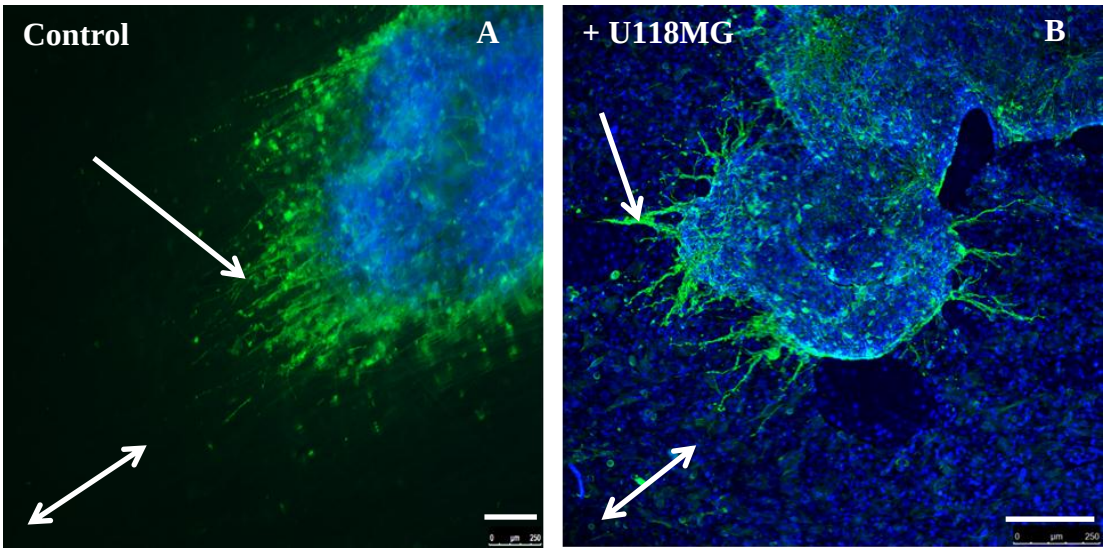

Figure 5-23 Co culture of human neurons and human astrocytoma cells using electrospun scaffold. Aggregates of TERA2.cl.SP12 cells treated with 0.1 µM EC23 for 21 days were placed onto aligned electrospun scaffolds coated with 10 µg/ml Laminin/P-D-L. Neurites formed along the fibres away from the aggregate TUJ-1 (Green) (A). The addition of 100,000 U118MG to the media resulted in loss of directed outgrowth (B). Arrows demonstrate direction of fibre alignment. TUJ-1 (Green), DAPI (Blue). Media also contained mitotic inhibitors as described in Methods. Arrow marks neurite outgrowth. Double ended arrow marks direction of aligned scaffold fibres. Scale bars: 250 µm. n=3.

5.4 DISCUSSION

Trauma to the CNS often results in some level of paralysis and is common in high impact sports such as Rugby or injuries sustained from motor vehicle crashes and stab wounds. Although multiple organ systems in the adult shows some regenerative potential such as neurons in the peripheral nervous system and the liver, neurons in the CNS do not regenerate. Advances in our understanding of neural subtype, neural development and the interaction of neurons and their environment has led to the discovery that CNS neurons do have the potential to regenerate like neurons in the PNS. Differences in the composition of the local microenvironment post injury in the CNS and PNS give the neurons differing regenerative potential. Investigating the interaction between neurons and the local post injury microenvironment is important for developing novel therapeutics. This Chapter focused on using stem cell-derived CNS neural progenitors to investigate in a physiologically relevant model of CNS injury the effect of small molecules on specific signalling pathway modulators.

5.4.1 Development of a novel model to study 3D neurite outgrowth in vitro

In this study stem cell-derived neurons were combined with 3D scaffold technology to produce a highly neurogenic model of neurite outgrowth, the study utilised a two stage process to enhance reproducibility and control over the stages of differentiation. Human stem cells were differentiated into neural progenitors prior to inducing neurite outgrowth in 3D. This allowed for a controlled process at each stage, regulating the differentiation of stem cells in stage 1 and neurite outgrowth in stage 2. This two-step process allowed for manipulation of the 3D culture environment for controlled differentiation of stem cells and modulation of neurite outgrowth in 3D. Stem cells were differentiated in a 3D aggregate model and when combined with the synthetic retinoid EC23 produced highly neurogenic and reproducible differentiation. Neurite outgrowth from the aggregates could then be investigated under a number of different matrix conditions by coating Alvetex®Scaffold with different ECM proteins.

Previous studies that have used stem cell-derived neural progenitors in neurite outgrowth and differentiation studies in 3D and have completed the differentiation and neurite outgrowth process in the same 3D environment, limiting experimental control and regulation over the development of the cells. Ge, D et al (2013) [325] utilised rat neural

stem cells to investigate 3D neural differentiation for use in high throughput studies. The investigation demonstrated the differentiation of rat neural stem cells in a 3D collagen matrix. The project utilised a two-step process of cell proliferation in 3D and then differentiation, however, a mixture of cell types developed including neurons, oligodendrocytes and astrocytes. The neurons in this study could not be used to investigate neurite outgrowth due to the complexity of the culture.

Other studies have utilised collagen matrix as a biocompatible scaffold to aid neurite differentiation and neurite outgrowth studies. Even though the scaffolds are good at inducing 3D neurite differentiation the overall assay is limited in its application due to difficulties in quantification of the neural growth in 3D. Therefore, due to the inherent difficulties of neurite growth and quantification, most neurite outgrowth studies are performed in 2D.

Hydrogels that can undergo solution-gelation transitions have been investigated for their ability to support neurite formation and outgrowth. The highly porous gels are permissive of neural migration and network formation due to interconnecting pores. Again, although neurite differentiation and outgrowth can be induced in 3D using these scaffolds it is difficult to assess any changes in outgrowth under particular conditions. Furthermore, due to the migration of neural progenitors and network formation a lack of neural polarity is often demonstrated. Nisbet, D.R et al (2008) [326] developed a Xyloglucan hydrogel to investigate primary mouse cortical neural 3D differentiation. The study demonstrated an enhancement of neural network formation when P-D-L was used in conjunction with the scaffold. This study described the use of these scaffolds for CNS regeneration; however, the neurites that formed were < 150 μm in length and without any directional growth. It is possible that implantation of the scaffold replacing scar tissue may facilitate endogenous neural regeneration however, the biocompatibility and sustainability of the gel was not investigated.

3D neural differentiation and outgrowth studies have either been described as an *in vitro* assay for drug toxicity and development studies or as potential conduits to aid endogenous CNS regeneration. Matrigel™ is a commercial gel like scaffold that can be used either to coat a 2D substrate or encapsulate cells in a 3D lattice. The gel comprises of a variety of proteins secreted from Engelbreth-Holm-Swarm mouse sarcoma cells and can induce neurite differentiation and outgrowth to a greater extent than demonstrated by individual ECM proteins such as Collagen [327]. However, again as with other gel based scaffolds

control over the composition of the gel and its processing is difficult and not easily applied to investigating neurite outgrowth.

An alternative approach to gel scaffolds is the use of porous membrane that can be manipulated either by chemical functionalization of protein coating. The scaffolds are much more rigid, however, tend to be easier to process and data more reliable to quantify. It was demonstrated by Hayman, M.W et al (2005) [122] that coating a solid polystyrene scaffold with a mixture of Laminin and P-D-L proteins could induce neurite outgrowth from human stem cell-derived neurons, however, growth into the scaffold was not demonstrated and outgrowth was a measure of lateral axon development. Sectioning of the scaffold as was demonstrated in this study may have given a better understanding of the 3D nature of the neurites that developed. The Alvetex®Scaffold, is highly porous, flexible and easy to handle using all processing techniques. Furthermore, due to the interconnectivity between pores a true 3D growth of cell tissue can be achieved.

In this study a 3D model of human neurite outgrowth was developed using ECM coated Alvetex®Scaffold and well defined stem cell-derived human neural progenitor aggregates. The application of such a model allows for advancing neurobiology in understanding the key, early developmental processes that occur during human neurite outgrowth in 3D. Furthermore, the model allows for variable protein coating to determine the role of different ECM molecules on neurite outgrowth. In addition, co-culture with other cell types in possible using our aggregate model due to the sustained aggregate of cell bodies on the scaffold surface making individual cell types easier to distinguish.

As with previous neurite outgrowth models in both 2D and 3D, the use of Laminin and P-D-L coating was essential to provide a permissive environment for neurite outgrowth as has been demonstrated in previous neurite outgrowth studies [102, 234, 322]. It was demonstrated in Figure 5-2 no neurites developed into the scaffold without ECM coating. The addition of overnight Laminin/ P-D-L coating resulted in a large number of neurites developing into the 3D scaffold, leaving cell bodies on the surface. ECM coating of Alvetex® resulted in neurites being in contact with Laminin/P-D-L at multiple focal points, similar to the ECM *in vivo* previous studies using similar scaffolds to those used in this study suggest that although Laminin was required to induce high levels of neurite outgrowth, the addition of P-D-L was necessary to aid cell adhesion [122, 328].

Neurites projected through the scaffold, spanning the 200 µm distance and grew on the underside. Thicker scaffolds may be necessary to maintain the 3D culture throughout

neurite outgrowth; however, this would make quantifying axonal changes much more difficult. Individual neurites can be retrograde traced using viral proteins to determine the cell body each developing/regenerating neurite develops from and the gene profile of the individual neurite. Overall this section described a proof of concept. Human neurites could be grown in a permissive 3D environment and analysed using immunohistochemistry. This model can be used to manipulate the 3D environment to investigate molecular processes that occur during spinal cord injury.

In 2D the use of neural progenitors for investigating neural-matrix interactions and neural regeneration have elucidated multiple pathways for potential therapeutics. The translation of these finding is difficult and animal models of spinal cord injury are required to further investigate the role of many of these pathways. Due to ethical and licencing restrictions when using animal models and species differences associated with their use developing a human physiologically relevant model of the glial scar to investigate some of the key molecular events that occur in neurons after traumatic spinal cord injury will become very important for translational research in the future. In this thesis the combined use of a 3D porous scaffold and human stem cell-derived neural progenitors has provided a reproducible *in vitro* assay to investigate the cell signalling events that may be manipulated to overcome CSPG induced neurite inhibition. Furthermore, due to the composition of the scaffold ECM coating to investigate multiple protein-neural interactions is straight forward and more routine.

5.4.2 Modulation of neurite outgrowth in 3D

Studies on the 3D effect of CSPGs on neurite outgrowth have utilised *in vivo* animal models to determine the biological role in CNS regeneration inhibition. Although these systems are important at elucidating the events that occur in neurons post CNS trauma the complexity of whole animal model systems means basic biology and signalling events are difficult to identify as multiple cell systems are acting. Compensatory mechanisms, immune cell infiltration and angiogenesis are just some of the processes that may cloud the basic biology that is occurring shortly after CNS injury or as the scar is more developed. Using physiologically relevant 3D model systems of human neurite outgrowth may be a necessary bridge between 2D biology and *in vivo* studies in the future with pressure to reduce or move away from animal studies. As with what was described in Chapter IV, the modulation of key molecular signalling pathways during Aggrecan induced neurite outgrowth inhibition by synthetic small molecules is a potential therapeutic. The need for

accurate and reproducible models of human neurite outgrowth to investigate these pathways is a major challenge in neurobiology. The lack of human *in vivo* models and the species differences between mouse and human neural development mean that an *in vitro* human model of neurite outgrowth in the CNS is important for accurate predictive capability for human clinical trials and in reducing the need for unnecessary animal research. Throughout this thesis the characterisation of developing neuronal subtype and developmental stage has been a focus since many models do not take developmental stage differences into account. This model of neurite outgrowth can be sustained and functional neurites will develop, allowing for more mature neurite outgrowth and regeneration models to be developed in the future.

We have demonstrated that the CSPG-Aggrecan, in a conventional 2D neurite outgrowth model inhibits neurite outgrowth, Aggrecan has also been described as an inhibitor of neurite regeneration in published literature. This is the first model to investigate synthetically derived human neurite outgrowth into a 3D Aggrecan coated substrate. Addition of 50 µg/ml Aggrecan to the coating substrate, which contained the permissive proteins Laminin and P-D-L resulted in an almost complete loss of neurite outgrowth from the neuroprogenitor aggregate. Sectioning the scaffold and confocal microscopy revealed a much reduced level of outgrowth as would agree with 2D models. The inhibition of neurite outgrowth by Aggrecan was highly potent but did not result in the death of cell bodies within the aggregate, making regeneration of neurites feasible. Specific modulation of neurite outgrowth by Aggrecan and its high levels in the glial scar suggest an important role for the glycoprotein in neural regeneration.

It is known that the concentration of Aggrecan, or more precisely the ratio of permissive Laminin/P-D-L and Aggrecan protein in the ECM is an important factor that determines if neurites will develop [329]. Since a concentration dependent regulation of neurite outgrowth by Aggrecan was assessed in Chapter IV it would be necessary to determine if there is any difference in the potency of Aggrecan in 3D. It may be that due to the 3D coating a much lower concentration of Aggrecan would induce a significant loss of outgrowth. Kofron, C.M et al (2009) [330] performed a study to determine the choice characteristics of neurons grown at a 2D/3D interface. They determined that neurites would develop on a Laminin substrate in 2D as opposed to developing in a more complex 3D Collagen I matrix. However, if neurites were presented with the inhibitory GAG motif by CSPG coating, the neurites would develop more into the 3D collagen scaffold. In the model in this Chapter a mixture of Laminin/P-D-L and the inhibitory CSPG Aggrecan

demonstrated growth in 2D along the top surface of the scaffold as opposed to in the 3D environment. This may suggest that the 2D environment on top of the scaffold provides less inhibitory cues to neurite outgrowth than the 3D expression of the same molecules.

In this section of Chapter V the 3D manipulation of cell signalling in neurons inhibited by Aggrecan were investigated. The molecular events targeted and inhibited were – ROCK activation, PTPσ activation, GAG-receptor binding, furthermore, enhancing the RARβ2 was also investigated as a potential modulator of neurite outgrowth. Below is a discussion of each individual pathway and how it affects neurite outgrowth in an inhibitory ECM environment.

Y-27632 (ROCK inhibition)

Activation of ROCK in neurons is related to neurite retraction and death of the neuron. Inhibition of ROCK provides neural protection in normally toxic environment [165]. The ROCK effector as has been described previously is involved in the transmission of the Aggrecan signal resulting in loss of neurite outgrowth. Many studies have investigated in 2D neurite outgrowth into a normally inhibitory environment with the addition of the synthetic ROCK inhibitor Y-27632 [331]. Furthermore, *in vitro* models of spinal cord injury have also demonstrated the protective effect of Y-27632 on neurites at the injury site [239]. A 3D *in vitro* study showed that rat astrocytes could be cultured in a Collage scaffold in a relatively physiologically normal state, treatment of these astrocytes with TGF β1 resulted in the production of a number of proteins and small molecules from the astrocytes into the 3D matrix, representing reactive gliosis. The increased production consisted of CSPG, high GFAP levels, Vimentin and IL-6. This is the only other study where CSPGs are used in a 3D *in vitro* model but the study does not assess the effects of the ECM on neurite outgrowth [332].

In this Chapter the 3D coating of a scaffold with Aggrecan resulted in an inhibitory environment for neurite outgrowth. As has been described in 2D both in this thesis and multiple published models treatment with Y-27632 at 15 μM enhanced human neurite outgrowth overcoming the inhibitory environment. This is the first study to describe an *in vitro* human model of neurite outgrowth in an inhibitory 3D environment by Y-27632.

RARβ2 activation

The activation of RARβ2 has been shown to enhance neurite outgrowth in a number of neurite outgrowth models including rat DRG, cerebellar neurons, PC12 [238]and mouse *in vivo* models [252]. Some evidence also suggests that activation of RAR β2 is involved in newt limb regeneration and innervation. Although, this receptor has been demonstrated to

have potential for enhancing neurite outgrowth in an inhibitory environment it has only been shown to do so in neurites inhibited by MAG [238] or Nogo and again no *in vitro* 3D models were able to demonstrate the effect of RARβ2 on neurite regeneration.

In the current study the specific effects of RARβ2 on Aggrecan induced neurite inhibition of human CNS stem cell-derived neurons demonstrated the enhancement of neurite outgrowth, using the highly potent synthetic small molecule agonist AC261066. This model will be able to provide a screen of highly potent RARβ2 small molecules for potential therapeutics in spinal cord injury.

Protein tyrosine phosphatase IV inhibition

As has been described previously, Aggrecan acts through a protein tyrosine phosphatase σ receptor (PTPσR) on the growth cone of developing neurites [1, 333]. Activation of the receptor results in the downstream effects describe earlier, resulting in ROCK activation and growth cone collapse [334]. Multiple methods have been shown to inhibit the downstream response to PTPσR activation; however, few have focussed on inhibiting specifically receptor activation. One benefit of using inhibitors of more upstream modulators of the receptor pathway is the increased ligand specificity, which may reduce unwanted side effects in treatment.

In Chapter IV, PTP IV inhibition was shown to overcome 2D Aggrecan induced neurite inhibition. In this Chapter these data were translated into a 3D model which is more physiologically relevant. Again inhibition of this receptor enzyme resulted in enhanced neurite outgrowth. Research into highly potent PTP inhibitors that are more specific for each receptor subtype may be a potential future therapeutic, however, currently no papers use this small molecule in models of spinal cord injury.

Chondroitinase ABC treatment

Described so far is the modulation of signalling that occurs in neurites after Aggrecan has bound and activated the PTPσR. Activation of the receptor is via the GAG side chains on the CSPGs in the glial scar. In this case of this model the GAG side chains are presented to developing neurites by Aggrecan on the surface of the scaffold. GAG side chains can be cleaved by the bacterial enzyme Chondroitinase ABC.

It is known that by cleaving the GAG side chains from CSPGs such as Aggrecan, activation of PTPσR does not occur and neurites are not inhibited. Furthermore, neurite regeneration after inhibition has also been observed in animal models of spinal cord injury, indicating the potential for therapeutic application [335]. Studies have suggested that

Chondroitinase ABC treatment may only induce a recovery of axonal projections and no functional recovery is observed [336], however, more recently functional recovery was also demonstrated indicating potentially a neural specific response to Chondroitinase ABC treatment [337].

In this Chapter the treatment of Aggrecan with Chondroitinase ABC prior to neurite outgrowth resulted in a permissive environment for neurite outgrowth and development. This confirms many of the *in vivo* animal studies using human stem cell-derived neural progenitors. Furthermore, the application of this to 3D is further enhances the physiological relevance of the assay making its translation to treatments more likely to succeed.

Finally, it may be that a synergistic affect is possible with combinations of each of the small molecules investigated here as they target different molecular pathways. It is important to keep in mind the side effects for the whole organism if targeted application is not possible.

5.4.3 3D primary mouse and human neural differentiation

To enhance the physiological relevance of the 3D neurite outgrowth model two primary neuronal progenitor cultures were grown on Alvetex® as described in Methods section 5.2.12-5.2.13. Primary 3D mouse and human neural culture is important for further assessing the effect of 3D differentiation of neural structure and function.

In this section the 3D culture and differentiation of both mouse and human neural progenitors was investigated using Alvetex®Scaffold. Primary cultures of both progenitors were demonstrated to grow and differentiate well in 3D. Primary mouse cortical neural progenitors were differentiated into aggregates of TUJ-1 and GFAP positive cells and demonstrate that primary mouse embryonic neural progenitors can be grown in 3D using Alvetex® to be used as a 3D *in vitro* neural differentiation model. Furthermore, primary human neural progenitors derived from the brain mesencephalon which are likely to represent dopaminergic neurons, were induced to differentiate on Alvetex®. The 3D human cultures formed visible TUJ-1 positive neurites with GFAP positive areas of glial cells. These data represent a novel model for investigating neural function of tissue explants grown in 3D.

In addition to immuno-staining of the human neurons grown in 3D an MEA was used to measure the firing rate of neurons throughout Alvetex®. The MEA uses multiple electrodes

to measure firing from many neurons at once, giving a better representation of the neural culture compared to individual neural patch electrophysiology. It is interesting to note at this point that human neural progenitors grown on 2D did not have any action potential measurable by MEA (Dr I Smith, Reading University). The action potential from 3D differentiated nHNP was measured using MEA and could be inhibited by TTX, CNQX/DLAP5 treatment indicating a genuine action potential form the cultures.

5.4.4 Investigating the effect of Aggrecan on primary neural progenitor differentiation in 3D

Perineuronal nets (PNs) are coatings or lattices that envelope the somata, dendrites and axons of neurons in the CNS and are composed of a hyaluronic back bone containing O-glycosylated CSPGs [338].

The structures provide a polyanionic microenvironment and are found located to specific subsets of neurons [339]. PNs have been associated with synaptic plasticity, development and maintenance [340]; furthermore, they are associated with morphological maintenance and neuroprotection in the brain [341].

Aggrecan is a major component of PNs [342, 343], and is thought to be produced by neurons in an activity dependent manner. Furthermore, loss of glial cell growth in a model of PN formation demonstrated that out of the other major components of the PNs (Brevican, tenascin-R and HAPLN1) only Aggrecan and hyaluronan were produced, and condensed at the neural membrane forming the characteristic appearance of PNs. These data demonstrate that Aggrecan alone may have a role in neural development and maintenance without other structures in the PN [342]. It is known Aggrecan does not affect the axonal conduction of an action potential, unlike the CSPG NG2 [291], suggesting the effect demonstrated by MEA in this study is an effect on synaptic transmission.

To assess the effect of Aggrecan on these cultures, Alvetex® was coated in 10 µg/ml Aggrecan. Immunocytochemical staining revealed that in the mouse cortical cultures there was a decrease in the number of neural aggregates that formed, which is likely an effect of toxicity, few axons were seen in this culture making it a poor model for neurite outgrowth studies. In addition to coating Alvetex® 10 µg/ml, human neurites were also grown and differentiated on Alvetex® coated in a low concentration of Aggrecan- 1 ng/ml. Immunocytochemical staining for TUJ-1 revealed good neurite outgrowth in cultures coated with 1 ng/ml Aggrecan, however, aggregation and loss of neurite outgrowth was

seen in cultures grown on 10 µg/ml Aggrecan, indicating a toxic or compartmentalisation effect of Aggrecan at high concentration.

To investigate the structure/function relationship of Aggrecan coated and uncoated scaffolds a MEA was used to measure action potential frequency within the cultures. Data demonstrate that there was a massive decrease in action potential in cultures treated with 1 ng/ml Aggrecan, even though little/no differences were seen in neurite outgrowth. No recordings were measured from scaffolds coated with 10 µg/ml Aggrecan, suggesting the cells were dead. Furthermore, treating control cultures with TTX resulted in a lower firing rate than that measured in cultures treated with 1 ng/ml Aggrecan suggesting the neurites grown at this concentration of Aggrecan have the potential to fire, however, do not. This can be related to the role of Aggrecan in PNs in normal physiology.

Aggrecan and specifically Brevican have been shown to regulate synaptic transmission and potassium channels activation in inhibitory neuronal membranes [344]. Therefore, the decrease in action potential observed in this model may demonstrate the role of Aggrecan at the synapse in the brain. Furthermore, CSPG sulfation patterns has been shown to regulate axonal transmission by inhibiting the action potential, thus effecting plasticity, development and survival of neurons, demonstrating a tight control over CSPG PN content and axonal firing [345].

The low concentration effect of Aggrecan on measurable action potential indicates a differential role of the CSPG than inhibition of neurite outgrowth. Understanding these concentration dependent differences and how alterations in Aggrecan levels in the PNs can affect neural plasticity and neuronal firing will be essential for understanding their effect in brain pathologies such as Alzheimer's disease [341, 346].

5.4.5 Enhancing physiological relevance: co-culture of human stem cell-derived neurons and U118MG astroglioma cell to investigate neurite outgrowth

Co-culture of neurons and glia in 2D is confined to the same physiological restraints as mono-culture; the interaction between the two cell types is likely not representative of the true *in vivo* situation. The two cell types can grow over each other and often can create carpets of highly uniform closely packed cells that do not truly represent the patterning that would be typical of *in vivo* ECM. Therefore, the interaction between the two cell types will be artificial and not representative physiologically. Neurons and astroglia are often closely associated with each other *in vivo* and there can be many astroglia to each neuron,

the role of astroglia is to support neural maintenance and development. Puschmann, T.B et al (2013) [347] demonstrated that the 3D culture of astroglial cells resulted in a more physiological morphology than in 2D. Satpute, R.M et al (2006) [348] demonstrated that glioblastoma conditioned media could induce neurite outgrowth from PC12 cells. This may not be translated into CNS derived neurons since CNS neurons are not stimulated by NGF secretion and hence, inhibition of human neurite outgrowth in this thesis may underline species and neural subtype differences *in vitro*.

Chan, C.C et al (2007) [155] described that ROCK inhibition by Y-27632 increased the reactive gliosis of astrocytes increasing CSPG production and GFAP expression. This was demonstrated by immunocytochemistry in Figure 5-21, a low level of CSPG expression by U118MG cells was demonstrated and provides an explanation for the inhibition of neurite outgrowth in co-culture. Since CSPG levels are enhanced by Y-27632 treatment it may seem counter intuitive that Y-27632 treatment also results in neurite outgrowth through the cells. An explanation for this is although CSPG levels are higher in the ECM, the inhibition of ROCK in the neurite is sufficient to overcome any level of PTPσR activation and hence neurite can develop.

5.4.6 Guidance of neurite outgrowth using physical conduits

As described earlier the regeneration of functional synapses from neurites is important for ensuring correct innervation of tissue, such as muscle. Since neurite development is dependent on a specific interplay between permissive and inhibitory cues it is likely the post-trauma ECM would not correctly guide neurites using these cues and the stimulatory proteins in the ECM may not be able to correctly guide neurites to their target tissue.

The development of aligned scaffolds that act as conduits is one method for enhancing the functional regeneration and targeted innervation of tissue in the damaged CNS. Guidance molecules act to enhance and develop neurites along tracts of specific direction. In this study aligned polystyrene scaffolds were used to assess the guidance of stem cell-derived human neural progenitors. The scaffolds were coated with Laminin and it was demonstrated that U118MG co-culture resulted in loss of directional neurite outgrowth. Although directional growth was demonstrated the number of neurites and length was dependent on the diameter and density of the fibres which was not investigated. Other studies have utilised similar methods and investigated the biomaterial properties that can produce optimal outgrowth from cultures. Aligned outgrowth has been demonstrated by hydrogels [118] and electrospun nanotubes [121]. Furthermore, functionalization of the

conduits using guidance molecules such as NGF, Poly(lactide-co-glycolide) [349], or supportive cell types like Schwann cells can be used to enhance the directional growth of neurites. It is likely that transplants of conduits of this sort will be in combination with small molecule modulators of neurite outgrowth, Chondrotinase enzymes and survival factors.

5.5 CONCLUSIONS

This Chapter focussed on the translation of a 2D neurite outgrowth assay into a 3D physiologically relevant assay that can be used to screen small molecule compounds that overcome CSPG induced neurite inhibition to be used in future therapeutics.

This study built upon previous data describing the use of hEC stem cells and neurite outgrowth. As described in detail in Chapter 4, the neural-progenitors used in this Chapter were produced by differentiating human pluripotent stem cells using the well characterised synthetic retinoid EC23. Having described a well-defined 2D model of neurite outgrowth the translation of this model to a 3D substrate may provide more physiologically relevant data on neurite outgrowth. Using this mode the interaction between developing stem cell-derived neurites and the 3D extracellular matrix was described, in particular the ECM of the glial scar that forms post-spinal cord injury.

The project described for the first time a human 3D model of Aggrecan induced neurite inhibition using stem cell-derived neurons. Furthermore, the model was used to investigate molecular signalling pathways and ligand-receptor interactions between the ECM and developing human neurites. Furthermore, primary neural data produced in collaboration with Reading University demonstrated a functional inhibition of intact neurites that develop in the presence of Aggrecan. These data described a robust and well-defined model of human neurite outgrowth for use in investigating the molecular processes that inhibit neurite outgrowth in the glial scar.

In addition to neural-ECM interactions described in 3D, the model also demonstrated the cellular interaction between the astroglial cell line U118MG and human stem cell-derived neurites, in 3D. This co-culture model demonstrated loss and recovery of neurite outgrowth when neurites developed in 3D in the presence of U118MG.

Although the assay is unlikely to replace animal studies it may be used to pre-screen compounds to reduce the number of animals used. Due to the human nature of the neurons

used it would be deemed more likely that positive drug hits in this system are more likely to be physiologically relevant in human CNS injury however, due to the simplicity of the assay other interacting factors which are found in the whole animal may not be accounted for. Multiple assays investigating individual processes may help elucidate those mechanisms which are masked by the complexity of whole animal experimentation.

This study has described a novel 3D model of neurite outgrowth and used the model to investigate known and novel small molecule enhancers of neurite outgrowth in an inhibitory environment. Further use of the model may determine clear differences between the 2D and 3D environments and the effect on drug screening assays. Furthermore, the model can be adapted to be used to investigate cellular interactions as a co-culture model.

FUTURE DIRECTION

Future work should include:

- As advancements in our understanding of receptor signalling pathways are combined with development of small molecules that regulate these pathways moved forward it is necessary to investigate these new molecules in biological assays for potential therapeutic application. An aim for future work using the 3D model of human neurite outgrowth should be to investigate other small molecule modulators of neurite regeneration to aid the structure/function relationship that guides development. Furthermore, combining modulators of separate parts of the pathway (for instance combining the PTP IV inhibitor with Chondroitinase ABC) may produce a synergistic response in the developing neurites.

- Gene profiling and protein expression of neurites grown in 2D and 3D under the permissive, inhibitory or enhanced neurite outgrowth conditions. A comparison between the neurites that develop in 2D and 3D may elucidate further the advantages of 3D neurite outgrowth and demonstrate the neurites that develop represent more in *vivo* like expression profiles

- Complex “reactive astrocyte” derived ECM coated scaffold. The use ECM directly derived from the glial scar, or produced *in vitro* by reactive astrocytes can be used to coat the scaffold and investigate more generally the role of this environment in neurite outgrowth.

- Primary glial and neural co-culture would enhance the power of the co-culture model using these human stem cell-derived neurons. Other primary cells such as schwann and astrocytic cells should also be investigated in co-culture.

CHAPTER 6 DISCUSSION

6.1 INTRODUCTION

This thesis aimed to investigate the small molecule modulation of stem cell differentiation using a well described *in vitro* model of neural development. The model was used to investigate the role of metabolism in the action of small molecules; the concentration dependant role of small molecules and the induction and maintenance of developmental genes.

Using technologies described throughout this thesis a novel human neurite outgrowth model was developed. The model was used to investigate the role of inhibitory glial scar proteins on neural development. The studies determined that human neurite outgrowth is inhibited by the CSPG – Aggrecan and that inhibition can be overcome by targeting specific signalling molecules. In addition the 2D human neurite outgrowth was translated into a 3D model of the glial scar and a more physiologically relevant co-culture model with astroglioma.

The work in this thesis has built upon recent advances in the small molecule control over cellular development and 3D culture. The model described will be used in future research to further understand the molecular pathways and small molecule modulators of human neural regeneration

6.1.1Synthetic retinoids and stem cell differentiation

Synthetic retinioids are an attractive approach for specifically regulating the pleotropic effects induced by retinoic acid receptors. As has been discussed in Chapter 1, the nuclear retinoic acid receptors (RAR) are composed of a number of subtypes and isotypes. Retinoic acid receptors act to induce gene transcription by forming heterodimers with members of the retinoid X receptors (RXR). Combinations of each of the RAR-RXR subtypes and isotypes provide the many biologically different effects of retinoic acid signalling. Synthetic retinoids that act as agonists for individual retinoic acid receptor subtypes is becoming an important tool in understanding their biological effect. Furthermore, analogues of all-trans retinoic acid (ATRA) that are pan-RAR agonists demonstrate increased potency and stability which is useful in many biological assays.

Since EC23 is a stable pan-RAR agonist, investigating the concentration dependent effect of RAR activation using EC23 would provide information as to the role of retinoid acid receptor activation and biological outcome. In this thesis the concentration dependent initiation of differentiation was investigated using cell surface and genetic markers. Changes in the cell surface glycoproteins SSEA3 and TRA-1-60 were measured using flow cytometry on differentiating stem cells, furthermore, gene expression analysis of *OCT4* and *NANOG* were measured. Data demonstrated that expression of all stem cell markers assessed was decreased upon EC23 and ATRA treatment in a concentration dependent way and this correlated with previous studies. In addition the neural specific markers A2B5 and *PAX6* were increased, indicating neural commitment. Neural commitment of the stem cells was concentration dependent and resulted in neurite formation in a monolayer culture. A similar study by Christie, V.B (2008) [95] also demonstrated neural commitment by stem cells treated with EC23, however, the study did not investigate the lower limit of concentration that will induce neural commitment.

The synthetic retinoic analogue EC23 was shown to be much more potent than its natural counterpart ATRA in a model of neural differentiation and again this agrees with previous studies [93-95]. Data from this thesis built upon the reason why EC23 is more potent. It was unknown if the increased potency was a result of receptor binding affinity or an effect of metabolism. The increased potency demonstrated by this small molecule was shown to be the result of increased stability and resistance to oxidation. Multiple studies have demonstrated that metabolism of ATRA can be inhibited by the small molecule Liarozole and results in an increased biological activity [66-68]. Using a novel stem cell-based assay to investigate the metabolism of ATRA and EC23 it was shown that EC23 unlike ATRA was not metabolised and inhibiting the metabolism of ATRA in our model resulted in a more EC23 like potency. This work was taken further to determine if a single pulse of EC23 could induce neural commitment and to what exposure do the cells require to induce differentiation. Data agreed with that in the literature for ATRA, where a pulse effect did not induce human embryonal carcinoma differentiation [171]. In contrast to this EC23 was capable of inducing stem cell differentiation after just a 1 minute pulse at 1 µM. It is unknown if these cells would then go on to form functional neurons as this was not investigated, however, data from Tonge, P. et al (2010) [171] suggest that with ATRA at least, continued RAR activation for 12 days is required for maximal neural differentiation of NTERA2.cl.D1 hEC stem cells. Investigating the effect of pulse and EC23 concentration on the subtype identity of human neurons may provide insights into the role of RAR activation on neural differentiation.

Development of novel retinoic acid analogues required understanding of the structure/function relationship in different biological systems. Previous work from our group has demonstrated that small structural modifications in retinoids can have large biological effects [89, 90]. The structure activity relationship between the stable synthetic retinoid EC23 and its para-isomer EC19 were investigated. EC19 is a similar structure to EC23, however, has much lower biological activity in our human stem cell model and is thought to induce less or differential retinoic acid receptor activation. Previous results have suggested the addition of a methyl group to the compound may result in a change in biological activity or provide a hook for metabolism of the compound [222]. Results from this section demonstrated that methylation of EC23 did not change its biological potency or metabolism, however, methylation of EC19 resulted in an enhanced biological activity and previously inactive concentrations of EC19 induced neural differentiation in our model. These data suggest that methylation of EC19 provided better RAR binding and activation compared to the un-methylated version – underlining the structure/function relationship in retinoids.

6.1.2 Concentration dependent effect of retinoids on cellular development

The role of retinoid concentration and biological effect is an important topic of stem cell and developmental research. There are still many mechanisms for the action of retinoic acid on development that are to be elucidated. It is thought that retinoid signalling regulates anterior-posterior patterning of the developing embryo and does so through a concentration dependent activation of the four *HOX* gene clusters A,B,C and D [41, 48, 279]. *HOX* genes as were described in Chapter 1 are analogous to genes found in the developing drosophila. Furthermore, mouse models and cellular models have demonstrated the regulation of cell identity by *HOX* genes [21, 188]. It is thought that regulation of the *HOX* code which is the combination of *HOX* genes that are expressed in a specific tissue, can determine neural subtype/positional identity. Retinoids have been associated with the regulation of *HOX* genes that confer anterior identity and these are at the 3' end of the *HOX* cluster of genes. The 3' genes contain RARE and their expression is induced by low concentrations of retinoic acid [23, 350]. Expression of genes associated with posterior positional identity are determined by 5' *HOX* genes. It is thought that regulation of 5' genes is via a co-linear activation by 3' *HOX* genes [41, 48, 50].

In this study the stable synthetic retinoid EC23 was used to investigate the concentration dependent regulation of *HOX* genes both 3' and 5' on the clusters A, B and D. These data

build upon that described by Simeone, A et al (1991) [48] which described the direct regulation of *HOX* genes by retinoic acid in the human embryonal carcinoma stem cell line NTERA2.cl.D1. Using the synthetic retinoid EC23 and a sensitive real-time PCR technique to measure relative change in *HOX* gene expression it was demonstrated that 3' *HOX* genes are expressed earlier and at lower concentrations of retinoic acid receptor activation. Interestingly regulation of 3' and 5' *HOX* genes was dependent on the concentration of EC23, where 5' genes were expressed earlier at higher retinoid concentrations. In this study the co-linear temporal activation of *HOX* genes was not clearly demonstrated and this may be the result of the late time points used. Earlier time points may show the co-linear relationship between genes on the same cluster. Interestingly, some of the *HOX* genes investigated such as *HOXD4* showed an optimal induction at concentrations lower than the maximal concentration used indicating a negative feedback or saturation type effect on the expression.

Since retinoid and concentration was demonstrated to regulate multiple cell processes and data demonstrated EC23 had a concentration dependent effect on neural commitment, it was decided to investigate the role of retinoic acid receptor activation and neural subtype identity. To determine if the concentration of retinoic acid used influenced the neural subtype identity of ventral progenitors the sonic hedgehog agonist Purmorphamine, was added to the culture. Purmorphamine was added to induce ventral neural subtype identity [77]. Real-time PCR was then used to determine if the ventral neural subtype could be influenced by retinoic acid concentration. The motor neuron marker *ISL1* and *HB9* and the interneuron marker *NKX2.2* were assessed at 0.1, 1 and 10 µM EC23 or ATRA in the presence of Purmorphamine (from day 6). These data indicate that retinoic acid concentration influenced motor neuron and interneuron identity markers.

Overall Chapter 3 focussed on investigating retinoic acid induced differentiation by the stable synthetic retinoid EC23. Furthermore, there was a focus on retinoid concentration and the mechanism behind the increased potency demonstrated in this model by EC23. Subsequent Chapters will use EC23 as a replacement of ATRA in neural differentiation protocols.

6.1.3 Human stem cell-derived neurite outgrowth

There are multiple cell lines that are used to investigate neurite outgrowth *in vitro.* These models usually consist of a neural progenitor that can be induced to form neurites upon induction by either permissive extracellular matrix proteins or growth factors. The process

of neurite outgrowth can then be investigated and manipulated to determine both positive and negative regulation of the process.

In Chapter 4 a human model of neurite outgrowth was described, TERA2.cl.SP12 human EC cells were differentiated by treatment with the synthetic retinoid analogue EC23, the novel analogue AH61 and natural ATRA. A standard operating produce for differentiating and inducing neurite outgrowth is described in Figure 6-1.

Standard Operating Procedure (SOP) for inducing neurite outgrowth from aggregates TERA2.cl.SP12.

Prior to starting the differentiation procedure ensure:

- Good stocks of untreated 90 mm Petri Dishes (Fisher Scientific FB51504)
- At least 200 µl of 0.1 mM EC23(Reinnervate) in molecular biology grade DMSO (Sigma Aldrich D8418)
- 1 x 500 ml bottle of DMEM (Lonza BE12-614F) containing 10 % FBS(Sigma Aldrich), 5 mM L-glutamine (Lonza BE17-605F) and penicillin/streptomycin (Lonza DE17 602F) (DMEMFGP)
- Access to a class I laminar flow microbiological safety cabinet
- 0.25 % trypsin/2 mM EDTA (Sigma Aldrich T4049)

To begin the differentiation procedure a single cell suspension of TERA2.cl.SP12 EC cells is needed. A single cell suspension was achieved as described in Chapter 2. Cells were counted using a haemocytometer as described in Chapter 2.

For differentiation of cells as aggregate follow the steps blow:

9. Add 1.5 x 10^6 TERA2.cl.SP12 EC cells to 20 ml DMEMFGP and leave overnight to initiate cell aggregation
10. After 24 hours aggregation add 20 µl of a 0.1 mM EC23 stock directly to the media and gently swirl
11. After 4 days treatment with a final concentration of 0.1 µM EC23 place the media containing aggregates into a 50 ml Falcon tube for 15 minutes allowing the aggregates to settle – this must be done in a sterile environment
12. Using an aspirator, supernatant leaving the pellet of aggregates in the bottom of the Falcon tube.
13. Add 20 ml of DMEMFGP and 20 µl of 0.1 mM EC23.
14. Gently swirl and place in to a fresh 90 mm untreated bacteriological Petri dish
15. Repeat steps 3-7 every 3-4 days or when required
16. After 21 days aggregates are differentiated and capable of forming neurites

Figure 6-1 Standard Operating Procedure (SOP) for inducing neurite outgrowth from aggregates TERA2.cl.SP12.

Previous studies have demonstrated neural differentiation and neurite outgrowth from aggregates of human EC cells [111, 270]. The cells were differentiated using retinoic acid and neurite outgrowth induced on a Laminin/P-D-L substrate. This model provided a good source of human neurites for investigating neurite outgrowth. In this section it was investigated if replacing ATRA with synthetic retinoid analogues that were more stable and potent would influence neurite outgrowth. Both concentration and temporal differentiation was demonstrated to alter the neurite outgrowth potential of progenitors on a permissive Laminin/P-D-L substrate. Differentiating hEC cells with retinoic acid for 14 days was shown to induce neurite differentiation and neurite outgrowth [85, 111, 351]. The data in this thesis suggest that increasing the differentiation length to 21 days and using highly stable synthetic analogues of ATRA can enhance neurite length and number. The aggregate maintained its integrity after 21 days differentiation and made quantification of neurite outgrowth reliable and reproducible.

6.1.4 Spinal cord injury and the glial scar

Traumatic spinal cord injury results in loss of nerve tissue and loss of function. The damage causes localised death of neurons, however, the neurite begin to regenerate indicating their potential [129]. Inhibition of neurite regeneration and functional recovery as would be seen in the peripheral nervous system is inhibited by the glial scar that forms in the injured CNS [324, 352]. After traumatic spinal cord injury a number of activated cells within the developing scar begin to produce extracellular matrix proteins [134, 161]. The proteins that are produced include permissive ECM such as Laminin, Fibronectin and Collagen; however, access to these molecules by neurite receptors is hampered by the presence of other ECM such as the chondroitin sulphate proteoglycans (CSPG). CSPGs act to form a mesh of fibres with the GFAP positive filaments of reactive astrocytes, this mesh results in neurites being unable to access growth promoting molecules and permissive ECM proteins [132]. Furthermore, receptor activation by CSPGs causes growth cone collapse and neurite retraction in regenerating neurites via a rho associated protein kinase (ROCK) and collapsing response mediator protein (CRMP) mechanism.

6.1.5 Aggrecan and the development of a human model of the glial scar

The CSPG Aggrecan is found in the CNS and acts in a normal physiological role to modulate neural plasticity and development [291, 353]. Aggrecan is used to model the effect of CSPGs on neurite regeneration and neurite outgrowth [1, 160, 314]. Aggrecan

contains many of the chondroitin sulphate glycosaminoglycan chains attached to a protein back bone making it a potent inhibitor of receptor mediated neurite outgrowth inhibition [2].

The receptors responsible for inducing growth cone collapse, neurite retraction and ultimately loss of neural development/regeneration are so far known to be two protein tyrosine phosphatase receptors: LAR and PTPσ [1, 150]. In this study the mRNA of both of these receptors were shown to be expressed in the developing neural progenitors. Furthermore, other receptors and modulators of neurite outgrowth were shown to be expressed including *NGFβ*, *NGFβR* and *RARβ2/4*. The expression of these receptors is implicated in neural development of the CNS [354, 355], in addition *RARβ2* has been demonstrated to have a role in neural differentiation and regeneration making it an important target for regenerative therapy [238]. Although expression of *NGFβR* mRNA was demonstrated during differentiation only low levels of its ligand *NGFβ* mRNA was detected. It is also important to note that there is a link between NGFβ signalling and RARβ2 activity [109].

Gene expression data indicated that the neural progenitor aggregates have up-regulated *HOXC4* expression and low levels of *OTX*2 mRNA indicating they are of likely of posterior CNS origin [196]. Therefore this model of neurite outgrowth was thought to be a promising model to investigate the effect of Aggrecan mediated human neurite inhibition and enhancement via receptor modulation.

As demonstrated in other studies, in this model Aggrecan induced inhibition of neurite outgrowth in a concentration dependent manner. Furthermore, this could be overcome through the inhibition of ROCK by Y-27632 [98, 159, 160], making this a good model for investigating human neural interactions with Aggrecan in conventional 2D. Enhancing neurite outgrowth on Aggrecan using small molecules may provide knowledge on the pathways involved in inhibition or provide novel treatment strategies for overcoming inhibition.

Multiple pathways have been associated with enhancing neurite outgrowth in an inhibitory environment or inducing regeneration in damaged CNS neurons. In this thesis a selection of highly potent small molecule modulators of these pathways were investigated for their ability to enhance human neurite outgrowth on an inhibitory Aggrecan substrate. Data demonstrated that as published [4, 238], an agonist of the RARβ2 receptor – AC261066 was able to induce partial recovery of neurite outgrowth in this model. Other small

molecule modulators i.e. CHIR 99021 a GSK3β pathway inhibitor and XAV 939 a GSK3β pathway agonist were shown to influence neurite outgrowth. CHIR 99021 inhibited neurite outgrowth on a permissive substrate and XAV 939 enhanced neurite outgrowth on an inhibitory substrate, these data agree with previous studies on neurite outgrowth regulation by this pathway however, demonstrate this in a defined human model of neurite outgrowth [176, 264].

As described earlier Aggrecan induces neurite inhibition through protein tyrosine phosphatase receptors. Directly targeting the activation of this receptor was investigated as a method of overcoming inhibition of neurite outgrowth on an Aggrecan substrate. The bacterial enzyme Chondroitinase ABC is known to cleave the chondroitin sulphate glycosaminoglycan (GAG) side chain from Aggrecan [144, 161]. The GAG side chain is the major ligand for the PTPσ and LAR receptors. In this study as has been demonstrated by published data, pre-treatment of Aggrecan with Chondroitinase ABC resulted in a more permissive substrate for neurite outgrowth in our human model. The use of this enzyme as a regenerative therapy is beginning to be realised and its effect on human neurite regeneration is an important piece of evidence to suggest its use will be beneficial [293]. Finally a novel method of inhibiting activation of the PTPσ receptor was investigated. The small molecule inhibitor PTP IV was shown to partially overcome neurite inhibition by Aggrecan, its partial effect may be due to it not inhibiting the LAR receptor which would still be activated and inhibit outgrowth. Combinations of treatments will be the best approach to ensure correct regeneration of neurites in the injured spinal cord.

A method to determine the effect of the human astroglioma cell line - U118MG on human neurite outgrowth and develop a model for investigating neural-glial co-culture was demonstrated. Data showed an inhibition of neurite outgrowth by the presence of these cells and this was overcome by ROCK inhibition which was likely a receptor mediated response. Previous studies have demonstrated the presence of CSPGs on astroglioma cells and it is known that brain astrocytes express some of these glycoproteins [295]. In this study immunocytochemical staining for Brevican was demonstrated by U118MG furthermore, mRNA expression of Brevican was detected suggesting this CSPG at least in part regulates the response of the developing neurites to U118MG cells.

Translating conventional 2D neurite outgrowth into 3D

Data from this Chapter built upon the use of small molecules to aid stem cell differentiation and investigated the ability of synthetic molecules to enhance neurite

outgrowth in conventional 2D. Although this model was easy to use its physiological relevance is hampered by the 2D environment experienced by the neurites. Neurons experience a 3D extracellular matrix environment during development and regeneration; translating the 2D model of neurite outgrowth and Aggrecan induced inhibition was the primary aim of the next part of this study. Chapter 5 investigated the interaction between human developing neurites and the 3D extracellular matrix, using the porous polymer scaffold Alvetex®.

Recent studies have described the 3D neurite outgrowth potential of a number of model systems including DRG, CGN, PC12 and differentiated hEC stem cells (see Chapter 1). Neurite outgrowth can be directed using aligned scaffolds or enhanced using functionalised material [349, 356]; furthermore, more 3D studies are investigating the *in vitro* drug discovery potential of 3D models, making the models more physiologically relevant by co-culturing with relevant cell mediators of disease processes [324, 332].

This thesis demonstrated the 3D neurite outgrowth potential of human stem cell-derived neurons. As described previously the TERA2.cl.SP12 EC cells were differentiated using a defined protocol including the synthetic retinoid EC23. Neurite outgrowth into the scaffold was imaged in transverse sections; furthermore, confocal microscopy revealed aggregates on the top elevation of the scaffold and projecting neurites on the bottom elevation. Combining permissive ECM proteins with 3D scaffolds has been demonstrated previously to promote aggregate adherence and neurite outgrowth similar to this study [122]. Manipulating the 3D ECM to investigate other processes such as Aggrecan induced inhibition was next investigated. Aggrecan induced a loss of neurite outgrowth in 3D from stem cell-derived neurites. Fewer neurites were seen on the bottom elevation and little or no outgrowth was imaged in transverse sections of the scaffold. It is important to note that many aggregates were lost from the top elevation and this is likely due to a decrease in the number of ligands for both Laminin and P-D-L. Since it is know that P-D-L promotes cell adhesion increasing the concentration of this protein may facilitate retention of the aggregate without affecting the inhibitory effect of Aggrecan on neurite outgrowth [122].

Inhibition of human neurite outgrowth in 3D by Aggrecan has not been demonstrated previously, furthermore, due to the use of stem cells and EC23 to produce neural progenitors this model is ideal to be used as a more physiologically relevant system for investigating drugs or small molecules that can overcome CSPG induced neurite inhibition. As described previously in conventional 2D, enhancing neurite outgrowth was achieved by ROCK inhibition and the RARβ2 agonist AC261066. The effects of ROCK inhibition and

RARβ2 modulation has not been shown in any 3D model of CSPG induced neurite inhibition. Furthermore, this study uses human stem cell-derived neuroprogenitors making the 3D model physiologically relevant and useful for drug screening.

The model also confirmed in 3D the observation that in 2D PTP IV inhibition can enhance neurite outgrowth in the inhibitory Aggrecan environment. Small molecule inhibitors of protein tyrosine phosphatase (PTP) are an emerging treatment for many diseases. Specificity of the small molecules in inhibiting the PTP receptor subtypes is going to be key in their therapeutic activity [357]. This section used a commercially available PTPσ receptor inhibitor and showed partial neurite outgrowth into a 3D Aggrecan ECM environment. Partial recovery is likely due to the activity of LAR and the low potency and poor subtype selectivity of the small molecule PTP IV inhibitor.

For consistency and to demonstrate the application of this model for investigating methods of overcoming neurite outgrowth inhibition by glial scar ECM the Aggrecan coated scaffold was pre-treated with the enzyme Chondroitinase ABC. Pre-treatment for 1 hour at 37 °C resulted in partial recovery of neurite outgrowth in 3D. Staining the scaffold for chondroitin sulphate GAG side chains before and after Chondrotinase pre-treatment demonstrated aggregation of immune-positive staining after Chondroitinase treatment. This is likely an effect of the scaffold therefore, increasing the washing procedures may enhance recovery of outgrowth by removing the aggregates of GAG side chains. *In vivo* GAG side chains are likely to be removed by vasculature and likely regulate other processes including inflammation and angiogenesis [183].

This 3D modulation of human neurite outgrowth is a novel method for drug discovery and in the future will provide insights into the specific effects of ECM proteins in different disease states. It is important to understand that there are limitations to this method, primarily its lack of complexity. Molecules that regulate neurite outgrowth *in vitro* may not do so in the complex environment of whole system animal models. However, both systems have advantages and should be used in combination to reduce wastage and develop key small molecule modulators of neural regeneration.

To investigate the regulation of primary neurite outgrowth in 3D by Aggrecan mouse primary cerebellar cultures and primary human brain cortex neural progenitor cells were differentiated in the presence of Aggrecan coated Alvetex®. In the brain Aggrecan makes up specialised ECM structures known as peri-neuronal nets (PNN) [353]. PNNs surround synapses and dendritic processes and are implicated in synaptic plasticity and development

[358] and alterations in Aggrecan in these structures are associated with Alzheimer's disease [341]. This part of the study demonstrated good growth of both primary mouse and primary human neural progenitors, however, the coating the scaffold with a high concentration of Aggrecan resulted in a toxic like effect in the mouse cultures and caused aggregate like structures to form in the human neural progenitors. Interestingly a low concentration of Aggrecan coating the scaffold did not induce aggregation of human neural progenitors; however, electrical signals measured via MEA at Reading University showed a complete loss of activity. These data suggest that Aggrecan alone inhibits the electrical activity of human neurites without any obvious structural effect on neurite outgrowth.

Although it is possible to enhance neurite outgrowth through the glial scar, as we understand the environment which the neurites must regenerate it becomes apparent that functional recovery and synapse formation will be more difficult to achieve. Guiding neurite regeneration and outgrowth through the scar and to re-connect the complete spinal cord will require a more engineering type approach. Nerve conduits are capable of directing neurite outgrowth in a particular polarity and direction. Methods for directing neurite outgrowth in include: differential ECM coating [349], micro patterning [359] or growth factor gradients [123].

Human neurite guidance and astroglioma co-culture

To investigate neurite guidance of our stem cell-derived neurons, aligned poly(styrene) fibres were produced using electro-spinning. The fibres were hydrophobic and so would not allow for cellular adherence or promote neurite outgrowth. An ethanol wetting procedure was used to make the scaffold hydrophilic and aid the binding or ECM proteins. The scaffolds were coated with the permissive Laminin and P-D-L proteins and induced neurite outgrowth along the fibres. This model can be adapted to investigate modulation of polarised neurite outgrowth. Furthermore, it was shown that U118MG co-culture resulted in loss of directed neurite outgrowth providing a human model to investigate the interaction between the two cell types and neurite guidance.

To further investigate neural-glial co-culture the 2D assay combining U118MG and human stem cell-derived neurons was translated into 3D. This produced a more physiologically relevant system for investigating the interactions between these cell types. U118MG cells filled the Laminin/P-D-L coated scaffold and the differentiated stem cell aggregates adhered securely to the top elevation. Both cell populations remained separate as the aggregate did not migrate into the scaffold making assessment of neurite outgrowth easier.

In the presence of U118MG, as in 2D neurite outgrowth was inhibited and this could be overcome by the ROCK inhibitor Y-27632. Treating the co-cultures with Y-27632 resulted in enhancement of neurite outgrowth and recovery in the 3D co-culture model. Staining for a pan-CSPG epitope revealed large amounts of positive immunostaining within the scaffold, furthermore, staining was enhanced by Y-27632. This effect has been published previously in astrocytes [155] and suggests that U118MG cells in this model may be a potential model of reactive astrocytes in the glial scar. Further studies to determine the ECM produced by U118MG in 3D may demonstrate more similarities between the two cell types.

6.1.6 Conclusion

In conclusion this thesis has described the genetic and phenotypical effects of synthetic retinoid induced neural differentiation and described the mechanism behind the increased potency of EC23. Bringing together the known stability and potency of synthetic small molecules a highly neurogenic model of neurite outgrowth was developed in conventional 2D. This model was then used as a model of the glial scar, by Aggrecan induced neurite inhibition. Furthermore, the role of small molecule signalling and enzymatic degradation of CSPGs in enhancing neurite outgrowth was investigated and provided evidence towards the use of small molecules modulators for neural regeneration. Finally, translation of the 2D glial scar model into 3D model was achieved and used to investigating recovery of neurite outgrowth, directed neurite outgrowth and neural-glial co-culture *in vitro.*

The work in this thesis have set a good foundation for investigating 3D human neurite regeneration *in vitro* using a potent and reproducible method of human neural differentiation and combining this method with enabling Alvetex®Scaffold technology.

6.1.7 Future work

- As advancements in our understanding of receptor signalling pathways are combined with development of small molecules that regulate these pathways moved forward it is necessary to investigate these new molecules in biological assays for potential therapeutic application. An aim for future work using the 3D model of human neurite outgrowth should be to investigate other small molecule modulators of neurite regeneration to aid the structure/function relationship that guides development. Furthermore, combining modulators of separate parts of the pathway (for instance combining the PTP IV inhibitor with Chondroitinase ABC) may produce a synergistic response and further enhance neurite outgrowth.

- Primary glial and neural co-culture would enhance the power of the co-culture model using these human stem cell-derived neurons. Other primary cells such as Schwann and astrocytic cells should also be investigated in co-culture also. It would also be interesting to develop a reactive astrocyte like model using TGFβ signalling to investigate the process in a 3D system.

- Gene profiling and protein expression of neurites grown in 2D and 3D under the permissive, inhibitory or enhanced neurite outgrowth conditions. A comparison between the neurites that develop in 2D and 3D may elucidate further the advantages of 3D neurite outgrowth and demonstrate the neurites that develop represent more *in vivo* like expression profiles.

- Other mediators of the inhibitory extracellular matrix of the glial scar should be investigated. Myelin associated glycoprotein (MAG) which has been demonstrated to inhibit neurite outgrowth and regeneration binds a well described receptor NOGO-66. Targeting downstream signalling of this receptor is an important target for regenerative therapies.

CHAPTER 7 BIBLIOGRAPHY

1. Shen, Y., et al., *PTPsigma is a receptor for chondroitin sulfate proteoglycan, an inhibitor of neural regeneration.* Science, 2009. **326**(5952): p. 592-6.
2. Yamaguchi, Y., *Lecticans: organizers of the brain extracellular matrix.* Cell Mol Life Sci, 2000. **57**(2): p. 276-89.
3. Blog, N.Y.I.C., *News & updates on pain & suffering verdicts & settlements.* http://www.newyorkinjurycasesblog.com, 2013. **Accessed 05/09/13**.
4. Puttagunta, R. and S. Di Giovanni, *Retinoic acid signaling in axonal regeneration.* Front Mol Neurosci, 2011. **4**: p. 59.
5. Wilson, P.G. and S.S. Stice, *Development and differentiation of neural rosettes derived from human embryonic stem cells.* Stem Cell Rev, 2006. **2**(1): p. 67-77.
6. Yuan, Y.M. and C. He, *The glial scar in spinal cord injury and repair.* Neurosci Bull, 2013.
7. Mark, M., F.M. Rijli, and P. Chambon, *Homeobox genes in embryogenesis and pathogenesis.* Pediatr Res, 1997. **42**(4): p. 421-9.
8. Michaeau, A.a.H., D, *Spinal Cord: Topographical and functional anatomy.* Imaios, 2009. http://www.imaios.com/en/e-Anatomy/Spine/Spinal-cord-diagrams.
9. Lee, S.K. and S.L. Pfaff, *Transcriptional networks regulating neuronal identity in the developing spinal cord.* Nat Neurosci, 2001. **4 Suppl**: p. 1183-91.
10. Castro, C. and D.P. Kuffler, *Membrane-bound CSPG mediates growth cone outgrowth and substrate specificity by Schwann cell contact with the DRG neuron cell body and not via growth cone contact.* Exp Neurol, 2006. **200**(1): p. 19-25.
11. Pelvig, D.P., et al., *Neocortical glial cell numbers in human brains.* Neurobiol Aging, 2008. **29**(11): p. 1754-62.
12. Gage, F.H. and S. Temple, *Neural stem cells: generating and regenerating the brain.* Neuron, 2013. **80**(3): p. 588-601.
13. Lledo, P.M., M. Alonso, and M.S. Grubb, *Adult neurogenesis and functional plasticity in neuronal circuits.* Nat Rev Neurosci, 2006. **7**(3): p. 179-93.
14. Cirulli, F., *Role of environmental factors on brain development and nerve growth factor expression.* Physiol Behav, 2001. **73**(3): p. 321-30.
15. Kurokawa, D., et al., *Otx2 expression in anterior neuroectoderm and forebrain/midbrain is directed by more than six enhancers.* Dev Biol, 2014.
16. Di Giovannantonio, L.G., et al., *Otx2 cell-autonomously determines dorsal mesencephalon versus cerebellum fate independently of isthmic organizing activity.* Development, 2014. **141**(2): p. 377-88.
17. Trainor, P.A. and R. Krumlauf, *Patterning the cranial neural crest: hindbrain segmentation and Hox gene plasticity.* Nat Rev Neurosci, 2000. **1**(2): p. 116-24.
18. Niederreither, K., et al., *Restricted expression and retinoic acid-induced downregulation of the retinaldehyde dehydrogenase type 2 (RALDH-2) gene during mouse development.* Mech Dev, 1997. **62**(1): p. 67-78.
19. Altmann, C.R. and A.H. Brivanlou, *Neural patterning in the vertebrate embryo.* Int Rev Cytol, 2001. **203**: p. 447-82.
20. Martinez-Ceballos, E. and L.J. Gudas, *Hoxa1 is required for the retinoic acid-induced differentiation of embryonic stem cells into neurons.* Journal of Neuroscience Research, 2008. **86**(13): p. 2809-2819.
21. Keynes, R. and R. Krumlauf, *Hox genes and regionalization of the nervous system.* Annu Rev Neurosci, 1994. **17**: p. 109-32.
22. Molotkova, N., et al., *Requirement of mesodermal retinoic acid generated by Raldh2 for posterior neural transformation.* Mechanisms of Development, 2005. **122**(2): p. 145-155.
23. Huang, D., S.W. Chen, and L.J. Gudas, *Analysis of two distinct retinoic acid response elements in the homeobox geneHoxb1 in transgenic mice.* Developmental Dynamics, 2002. **223**(3): p. 353-370.

24. Okano, H., *Neural stem cells and strategies for the regeneration of the central nervous system.* Proc Jpn Acad Ser B Phys Biol Sci, 2010. **86**(4): p. 438-50.
25. Sakry, D., K. Karram, and J. Trotter, *Synapses between NG2 glia and neurons.* J Anat, 2011. **219**(1): p. 2-7.
26. Trotter, J., K. Karram, and A. Nishiyama, *NG2 cells: Properties, progeny and origin.* Brain Res Rev, 2010. **63**(1-2): p. 72-82.
27. Su, H., et al., *Neural progenitor cells generate motoneuron-like cells to form functional connections with target muscles after transplantation into the musculocutaneous nerve.* Cell Transplant, 2012. **21**(12): p. 2651-63.
28. Surmeli, G., et al., *Patterns of spinal sensory-motor connectivity prescribed by a dorsoventral positional template.* Cell, 2011. **147**(3): p. 653-65.
29. Kessaris, N., et al., *Genetic programs controlling cortical interneuron fate.* Curr Opin Neurobiol, 2014. **26C**: p. 79-87.
30. Stipursky, J., et al., *Neuron-astroglial interactions in cell-fate commitment and maturation in the central nervous system.* Neurochem Res, 2012. **37**(11): p. 2402-18.
31. Maden, M., *Retinoid signalling in the development of the central nervous system.* Nature Reviews Neuroscience, 2002. **3**(11): p. 843-853.
32. Maden, M., et al., *Vitamin A-deficient quail embryos have half a hindbrain and other neural defects.* Curr Biol, 1996. **6**(4): p. 417-26.
33. McCaffery, P., J. Zhang, and J.E. Crandall, *Retinoic acid signaling and function in the adult hippocampus.* Journal of Neurobiology, 2006. **66**(7): p. 780-791.
34. Reijntjes, S., et al., *The control of morphogen signalling: Regulation of the synthesis and catabolism of retinoic acid in the developing embryo.* Developmental Biology, 2005. **285**(1): p. 224-237.
35. Wilson, L. and M. Maden, *The mechanisms of dorsoventral patterning in the vertebrate neural tube.* Developmental Biology, 2005. **282**(1): p. 1-13.
36. Poh, A., et al., *Patterning of the vertebrate ventral spinal cord.* Int J Dev Biol, 2002. **46**(4): p. 597-608.
37. Lloret-Vilaspasa, F., et al., *Retinoid signalling is required for information transfer from mesoderm to neuroectoderm during gastrulation.* The International Journal of Developmental Biology, 2010. **54**(4): p. 599-608.
38. Koop, D., et al., *Retinoic acid signaling targets Hox genes during the amphioxus gastrula stage: Insights into early anterior–posterior patterning of the chordate body plan.* Developmental Biology, 2010. **338**(1): p. 98-106.
39. McGinnis, W., et al., *A conserved DNA sequence in homoeotic genes of the Drosophila Antennapedia and bithorax complexes.* Nature, 1984. **308**(5958): p. 428-33.
40. Acampora, D., A. Simeone, and E. Boncinelli, *Human HOX homeobox genes.* Oxf Surv Eukaryot Genes, 1991. **7**: p. 1-28.
41. Boncinelli, E., et al., *HOX gene activation by retinoic acid.* Trends Genet, 1991. **7**(10): p. 329-34.
42. Conlon, R.A., *Retinoic acid and pattern formation in vertebrates.* Trends Genet, 1995. **11**(8): p. 314-9.
43. Krumlauf, R., *Hox genes in vertebrate development.* Cell, 1994. **78**(2): p. 191-201.
44. Marshall, H., et al., *Retinoids and Hox genes.* FASEB J, 1996. **10**(9): p. 969-78.
45. Moroni, M.C., M.A. Vigano, and F. Mavilio, *Regulation of the human HOXD4 gene by retinoids.* Mech Dev, 1993. **44**(2-3): p. 139-54.
46. Serpente, P., *Direct crossregulation between retinoic acid receptor and Hox genes during hindbrain segmentation.* Development, 2005. **132**(3): p. 503-513.
47. Waxman, J.S. and D. Yelon, *Increased Hox activity mimics the teratogenic effects of excess retinoic acid signaling.* Developmental Dynamics, 2009. **238**(5): p. 1207-1213.
48. Simeone, A., et al., *Differential regulation by retinoic acid of the homeobox genes of the four HOX loci in human embryonal carcinoma cells.* Mech Dev, 1991. **33**(3): p. 215-27.

49. Mavilio, F., et al., *Activation of four homeobox gene clusters in human embryonal carcinoma cells induced to differentiate by retinoic acid.* Differentiation, 1988. **37**(1): p. 73-9.
50. Simeone, A., et al., *Sequential activation of HOX2 homeobox genes by retinoic acid in human embryonal carcinoma cells.* Nature, 1990. **346**(6286): p. 763-6.
51. Bami, M., et al., *Directed neural differentiation of mouse embryonic stem cells is a sensitive system for the identification of novel Hox gene effectors.* PLoS One, 2011. **6**(5): p. e20197.
52. Wang, X.D., et al., *Retinoic acid can be produced from excentric cleavage of beta-carotene in human intestinal mucosa.* Arch Biochem Biophys, 1992. **293**(2): p. 298-304.
53. Cocco, S., et al., *Vitamin A deficiency produces spatial learning and memory impairment in rats.* Neuroscience, 2002. **115**(2): p. 475-82.
54. Blomhoff, R., et al., *Vitamin A metabolism: new perspectives on absorption, transport, and storage.* Physiol Rev, 1991. **71**(4): p. 951-90.
55. Zolfaghari, R. and A.C. Ross, *Lecithin:retinol acyltransferase from mouse and rat liver. CDNA cloning and liver-specific regulation by dietary vitamin a and retinoic acid.* J Lipid Res, 2000. **41**(12): p. 2024-34.
56. Blomhoff, R. and H.K. Blomhoff, *Overview of retinoid metabolism and function.* Journal of Neurobiology, 2006. **66**(7): p. 606-630.
57. Quadro, L., *Understanding the physiological role of retinol-binding protein in vitamin A metabolism using transgenic and knockout mouse models.* Molecular Aspects of Medicine, 2003. **24**(6): p. 421-430.
58. Kawaguchi, R., et al., *A membrane receptor for retinol binding protein mediates cellular uptake of vitamin A.* Science, 2007. **315**(5813): p. 820-5.
59. Chambers, D., et al., *RALDH-independent generation of retinoic acid during vertebrate embryogenesis by CYP1B1.* Development, 2007. **134**(7): p. 1369-83.
60. Gaub, M.P., et al., *Nuclear detection of cellular retinoic acid binding proteins I and II with new antibodies.* J Histochem Cytochem, 1998. **46**(10): p. 1103-11.
61. Gustafson, A.L., et al., *Nuclear import of cellular retinoic acid-binding protein type I in mouse embryonic cells.* Mech Dev, 1996. **58**(1-2): p. 27-38.
62. Verfaille, C.J., M. Borgers, and M.A. van Steensel, *Retinoic acid metabolism blocking agents (RAMBAs): a new paradigm in the treatment of hyperkeratotic disorders.* J Dtsch Dermatol Ges, 2008. **6**(5): p. 355-64.
63. Maclean, G., P. Dolle, and M. Petkovich, *Genetic disruption of CYP26B1 severely affects development of neural crest derived head structures, but does not compromise hindbrain patterning.* Dev Dyn, 2009. **238**(3): p. 732-45.
64. Ricard, M.J. and L.J. Gudas, *Cytochrome P450 Cyp26a1 alters spinal motor neuron subtype identity in differentiating embryonic stem cells.* J Biol Chem, 2013.
65. Taimi, M., *A Novel Human Cytochrome P450, CYP26C1, Involved in Metabolism of 9-cis and All-trans Isomers of Retinoic Acid.* Journal of Biological Chemistry, 2003. **279**(1): p. 77-85.
66. De Coster, R., et al., *Experimental studies with liarozole (R 75,251): an antitumoral agent which inhibits retinoic acid breakdown.* J Steroid Biochem Mol Biol, 1992. **43**(1-3): p. 197-201.
67. Pignatello, M.A., F.C. Kauffman, and A.A. Levin, *Liarozole markedly increases all trans-retinoic acid toxicity in mouse limb bud cell cultures: a model to explain the potency of the aromatic retinoid (E)-4-[2-(5,6,7,8-tetrahydro-5,5,8,8-tetramethyl-2-naphthylenyl)-1-propenyl] benzoic acid.* Toxicol Appl Pharmacol, 2002. **178**(3): p. 186-94.
68. Wouters, W., et al., *Effects of liarozole, a new antitumoral compound, on retinoic acid-induced inhibition of cell growth and on retinoic acid metabolism in MCF-7 human breast cancer cells.* Cancer Res, 1992. **52**(10): p. 2841-6.
69. Bastien, J., *Nuclear retinoid receptors and the transcription of retinoid-target genes.* Gene, 2004. **328**: p. 1-16.

70. Barnard, J.H., et al., *Synthetic Retinoids: Structure-Activity Relationships.* Chemistry-a European Journal, 2009. **15**(43): p. 11430-11442.
71. Chambon, P., *A decade of molecular biology of retinoic acid receptors.* FASEB J, 1996. **10**(9): p. 940-54.
72. Zhang, X., et al., *Derivation of human embryonic stem cells from developing and arrested embryos.* Stem Cells, 2006. **24**(12): p. 2669-76.
73. Gertow, K., et al., *Isolation of human embryonic stem cell-derived teratomas for the assessment of pluripotency.* Curr Protoc Stem Cell Biol, 2007. **Chapter 1**: p. Unit1B 4.
74. Liu, C., et al., *Neural differentiation of human embryonic stem cells as an in vitro tool for the study of the expression patterns of the neuronal cytoskeleton during neurogenesis.* Biochem Biophys Res Commun, 2013.
75. Drury-Stewart, D., et al., *Highly efficient differentiation of neural precursors from human embryonic stem cells and benefits of transplantation after ischemic stroke in mice.* Stem Cell Res Ther, 2013. **4**(4): p. 93.
76. Patani, R., et al., *Retinoid-independent motor neurogenesis from human embryonic stem cells reveals a medial columnar ground state.* Nat Commun, 2011. **2**: p. 214.
77. Li, X.J., et al., *Directed differentiation of ventral spinal progenitors and motor neurons from human embryonic stem cells by small molecules.* Stem Cells, 2008. **26**(4): p. 886-93.
78. Ban, J., et al., *Embryonic stem cell-derived neurons form functional networks in vitro.* Stem Cells, 2007. **25**(3): p. 738-49.
79. Strickland, S. and V. Mahdavi, *The induction of differentiation in teratocarcinoma stem cells by retinoic acid.* Cell, 1978. **15**(2): p. 393-403.
80. Jones-Villeneuve, E.M., et al., *Retinoic acid induces embryonal carcinoma cells to differentiate into neurons and glial cells.* J Cell Biol, 1982. **94**(2): p. 253-62.
81. Cotte, C., et al., *Characterization of a new human cell line derived from a xenografted embryonal carcinoma.* In Vitro, 1982. **18**(9): p. 739-49.
82. Andrews, P.W., *Retinoic acid induces neuronal differentiation of a cloned human embryonal carcinoma cell line in vitro.* Dev Biol, 1984. **103**(2): p. 285-93.
83. Pal, R. and G. Ravindran, *Assessment of pluripotency and multilineage differentiation potential of NTERA-2 cells as a model for studying human embryonic stem cells.* Cell Prolif, 2006. **39**(6): p. 585-98.
84. Przyborski, S.A., *Isolation of human embryonal carcinoma stem cells by immunomagnetic sorting.* Stem Cells, 2001. **19**(6): p. 500-4.
85. Horrocks, G., *Formation of neurospheres from human embryonal carcinoma stem cells.* Biochemical and Biophysical Research Communications, 2003. **304**(2): p. 411-416.
86. Stewart, R., V.B. Christie, and S.A. Przyborski, *Manipulation of human pluripotent embryonal carcinoma stem cells and the development of neural subtypes.* Stem Cells, 2003. **21**(3): p. 248-56.
87. Coyne, L., et al., *Neuropharmacological properties of neurons derived from human stem cells.* Neurochem Int, 2011. **59**(3): p. 404-12.
88. Hayman, M.W., et al., *Following the differentiation of human pluripotent stem cells by proteomic identification of biomarkers.* Stem Cells Dev, 2006. **15**(2): p. 221-31.
89. Maltman, D.J., et al., *Proteomic profiling of the stem cell response to retinoic acid and synthetic retinoid analogues: identification of major retinoid-inducible proteins.* Molecular Biosystems, 2009. **5**(5): p. 458-471.
90. Christie, V.B., et al., *Synthesis and evaluation of synthetic retinoid derivatives as inducers of stem cell differentiation.* Org Biomol Chem, 2008. **6**(19): p. 3497-507.
91. Murayama, A., T. Suzuki, and M. Matsui, *Photoisomerization of retinoic acids in ethanol under room light: a warning for cell biological study of geometrical isomers of retinoids.* J Nutr Sci Vitaminol (Tokyo), 1997. **43**(2): p. 167-76.
92. Christie, V.B., et al., *Retinoid supplementation of differentiating human neural progenitors and embryonic stem cells leads to enhanced neurogenesis in vitro.* J Neurosci Methods, 2010. **193**(2): p. 239-45.

93. Gluyas, J.B.G., et al., *Disila-analogues of the synthetic retinoids EC23 and TTNN: synthesis, structure and biological evaluation.* Organic & Biomolecular Chemistry, 2012. **10**(34): p. 6914-6929.
94. Clemens, G., et al., *The action of all-trans-retinoic acid (ATRA) and synthetic retinoid analogues (EC19 and EC23) on human pluripotent stem cells differentiation investigated using single cell infrared microspectroscopy.* Mol Biosyst, 2013. **9**(4): p. 677-92.
95. Christie, V.B., et al., *Synthesis and evaluation of synthetic retinoid derivatives as inducers of stem cell differentiation.* Organic & Biomolecular Chemistry, 2008. **6**(19): p. 3497.
96. Allodi, I., et al., *In vitro comparison of motor and sensory neuron outgrowth in a 3D collagen matrix.* J Neurosci Methods, 2011. **198**(1): p. 53-61.
97. Houle, J.D., et al., *Combining peripheral nerve grafting and matrix modulation to repair the injured rat spinal cord.* J Vis Exp, 2009(33).
98. Condic, M.L., D.M. Snow, and P.C. Letourneau, *Embryonic neurons adapt to the inhibitory proteoglycan aggrecan by increasing integrin expression.* J Neurosci, 1999. **19**(22): p. 10036-43.
99. Bilimoria, P.M. and A. Bonni, *Cultures of cerebellar granule neurons.* CSH Protoc, 2008. **2008**: p. pdb prot5107.
100. Radio, N.M., et al., *Comparison of PC12 and cerebellar granule cell cultures for evaluating neurite outgrowth using high content analysis ☆.* Neurotoxicology and Teratology, 2010. **32**(1): p. 25-35.
101. Ahmed, I., et al., *Role of Cdc42 in neurite outgrowth of PC12 cells and cerebellar granule neurons.* Mol Cell Biochem, 2006. **281**(1-2): p. 17-25.
102. Fudge, N.J. and K.M. Mearow, *Extracellular matrix-associated gene expression in adult sensory neuron populations cultured on a laminin substrate.* BMC Neurosci, 2013. **14**: p. 15.
103. Saijilafu and F.Q. Zhou, *Genetic study of axon regeneration with cultured adult dorsal root ganglion neurons.* J Vis Exp, 2012(66).
104. Rana, B., et al., *Retinoid X receptors and retinoid response in neuroblastoma cells.* J Cell Biochem, 2002. **86**(1): p. 67-78.
105. Irving, H., et al., *Retinoid-induced differentiation of neuroblastoma: comparison between LG69, an RXR-selective analogue and 9-cis retinoic acid.* Eur J Cancer, 1998. **34**(1): p. 111-7.
106. Shiohira, H., et al., *Am80 induces neuronal differentiation via increased tropomyosin-related kinase B expression in a human neuroblastoma SH-SY5Y cell line.* Biomed Res, 2012. **33**(5): p. 291-7.
107. Park, S. and D.G. Jeong, *Ribosomal protein L10 interacts with the SH3 domain and regulates GDNF-induced neurite growth in SH-SY-5y cells.* J Cell Biochem, 2006. **99**(2): p. 624-34.
108. Lichvarova, L., K. Jaskova, and L. Lacinova, *NGF-induced neurite outgrowth in PC12 cells is independent of calcium entry through L-type calcium channels.* Gen Physiol Biophys, 2012. **31**(4): p. 473-8.
109. Cosgaya, J.M. and A. Aranda, *Nerve growth factor activates the RARbeta2 promoter by a Ras-dependent mechanism.* J Neurochem, 2001. **76**(3): p. 661-71.
110. Scheibe, R.J. and J.A. Wagner, *Retinoic acid regulates both expression of the nerve growth factor receptor and sensitivity to nerve growth factor.* J Biol Chem, 1992. **267**(25): p. 17611-6.
111. Tegenge, M.A., F. Roloff, and G. Bicker, *Rapid differentiation of human embryonal carcinoma stem cells (NT2) into neurons for neurite outgrowth analysis.* Cell Mol Neurobiol, 2011. **31**(4): p. 635-43.
112. Hayman, M.W., et al., *Enhanced neurite outgrowth by human neurons grown on solid three-dimensional scaffolds.* Biochem Biophys Res Commun, 2004. **314**(2): p. 483-8.
113. Ma, W., et al., *Cell-extracellular matrix interactions regulate neural differentiation of human embryonic stem cells.* BMC Dev Biol, 2008. **8**: p. 90.

114. Lin, L. and O. Isacson, *Axonal growth regulation of fetal and embryonic stem cell-derived dopaminergic neurons by Netrin-1 and Slits.* Stem Cells, 2006. **24**(11): p. 2504-13.
115. Takahashi, K. and S. Yamanaka, *Induction of pluripotent stem cells from mouse embryonic and adult fibroblast cultures by defined factors.* Cell, 2006. **126**(4): p. 663-76.
116. Chang, T., et al., *Brief report: phenotypic rescue of induced pluripotent stem cell-derived motoneurons of a spinal muscular atrophy patient.* Stem Cells, 2011. **29**(12): p. 2090-3.
117. Swindle-Reilly, K.E., et al., *The impact of laminin on 3D neurite extension in collagen gels.* J Neural Eng, 2012. **9**(4): p. 046007.
118. Prang, P., et al., *The promotion of oriented axonal regrowth in the injured spinal cord by alginate-based anisotropic capillary hydrogels.* Biomaterials, 2006. **27**(19): p. 3560-9.
119. Jin, G.Z., et al., *Neurite outgrowth of dorsal root ganglia neurons is enhanced on aligned nanofibrous biopolymer scaffold with carbon nanotube coating.* Neurosci Lett, 2011. **501**(1): p. 10-4.
120. Liu, T., et al., *Nanofibrous collagen nerve conduits for spinal cord repair.* Tissue Eng Part A, 2012. **18**(9-10): p. 1057-66.
121. Panseri, S., et al., *Electrospun micro- and nanofiber tubes for functional nervous regeneration in sciatic nerve transections.* BMC Biotechnol, 2008. **8**: p. 39.
122. Hayman, M.W., et al., *Growth of human stem cell-derived neurons on solid three-dimensional polymers.* J Biochem Biophys Methods, 2005. **62**(3): p. 231-40.
123. Labour, M.N., et al., *Thick collagen-based 3D matrices including growth factors to induce neurite outgrowth.* Acta Biomater, 2012. **8**(9): p. 3302-12.
124. Li, X., et al., *Promotion of neuronal differentiation of neural progenitor cells by using EGFR antibody functionalized collagen scaffolds for spinal cord injury repair.* Biomaterials, 2013. **34**(21): p. 5107-16.
125. Balgude, A.P., et al., *Agarose gel stiffness determines rate of DRG neurite extension in 3D cultures.* Biomaterials, 2001. **22**(10): p. 1077-84.
126. Tse, K.H., et al., *In vitro evaluation of polyester-based scaffolds seeded with adipose derived stem cells for peripheral nerve regeneration.* J Biomed Mater Res A, 2010. **95**(3): p. 701-8.
127. Centre, N.N.S.C.I.S., *Facts and Figures at a Glance.* http://www.nscisc.uab.edu, 2013.
128. Marino, R.J., et al., *International standards for neurological classification of spinal cord injury.* J Spinal Cord Med, 2003. **26 Suppl 1**: p. S50-6.
129. Hu, R., et al., *Glial scar and neuroregeneration: histological, functional, and magnetic resonance imaging analysis in chronic spinal cord injury.* J Neurosurg Spine, 2010. **13**(2): p. 169-80.
130. Goritz, C., et al., *A pericyte origin of spinal cord scar tissue.* Science, 2011. **333**(6039): p. 238-42.
131. Matthews, M.A., et al., *Axon sprouting into segments of rat spinal cord adjacent to the site of a previous transection.* Neuropathol Appl Neurobiol, 1979. **5**(3): p. 181-96.
132. Wilhelmsson, U., et al., *Redefining the concept of reactive astrocytes as cells that remain within their unique domains upon reaction to injury.* Proc Natl Acad Sci U S A, 2006. **103**(46): p. 17513-8.
133. Holley, J.E., et al., *Astrocyte characterization in the multiple sclerosis glial scar.* Neuropathol Appl Neurobiol, 2003. **29**(5): p. 434-44.
134. Pekny, M. and M. Nilsson, *Astrocyte activation and reactive gliosis.* Glia, 2005. **50**(4): p. 427-34.
135. McKeon, R.J., M.J. Jurynec, and C.R. Buck, *The chondroitin sulfate proteoglycans neurocan and phosphacan are expressed by reactive astrocytes in the chronic CNS glial scar.* J Neurosci, 1999. **19**(24): p. 10778-88.
136. Frisen, J., et al., *Rapid, widespread, and longlasting induction of nestin contributes to the generation of glial scar tissue after CNS injury.* J Cell Biol, 1995. **131**(2): p. 453-64.
137. Lytle, J.M. and J.R. Wrathall, *Glial cell loss, proliferation and replacement in the contused murine spinal cord.* Eur J Neurosci, 2007. **25**(6): p. 1711-24.

138. Sellers, D.L., D.O. Maris, and P.J. Horner, *Postinjury niches induce temporal shifts in progenitor fates to direct lesion repair after spinal cord injury.* J Neurosci, 2009. **29**(20): p. 6722-33.
139. Meletis, K., et al., *Spinal cord injury reveals multilineage differentiation of ependymal cells.* PLoS Biol, 2008. **6**(7): p. e182.
140. Hirsch, S. and M. Bahr, *Growth promoting and inhibitory effects of glial cells in the mammalian nervous system.* Adv Exp Med Biol, 1999. **468**: p. 199-205.
141. McKeon, R.J., A. Hoke, and J. Silver, *Injury-induced proteoglycans inhibit the potential for laminin-mediated axon growth on astrocytic scars.* Exp Neurol, 1995. **136**(1): p. 32-43.
142. Tang, X., J.E. Davies, and S.J. Davies, *Changes in distribution, cell associations, and protein expression levels of NG2, neurocan, phosphacan, brevican, versican V2, and tenascin-C during acute to chronic maturation of spinal cord scar tissue.* J Neurosci Res, 2003. **71**(3): p. 427-44.
143. Jones, L.L., R.U. Margolis, and M.H. Tuszynski, *The chondroitin sulfate proteoglycans neurocan, brevican, phosphacan, and versican are differentially regulated following spinal cord injury.* Exp Neurol, 2003. **182**(2): p. 399-411.
144. Yamagata, T., et al., *Purification and properties of bacterial chondroitinases and chondrosulfatases.* J Biol Chem, 1968. **243**(7): p. 1523-35.
145. Snow, D.M., et al., *Sulfated proteoglycans in astroglial barriers inhibit neurite outgrowth in vitro.* Exp Neurol, 1990. **109**(1): p. 111-30.
146. Dou, C.L. and J.M. Levine, *Inhibition of neurite growth by the NG2 chondroitin sulfate proteoglycan.* J Neurosci, 1994. **14**(12): p. 7616-28.
147. Hodgkinson, G.N., P.A. Tresco, and V. Hlady, *The role of well-defined patterned substrata on the regeneration of DRG neuron pathfinding and integrin expression dynamics using chondroitin sulfate proteoglycans.* Biomaterials, 2012. **33**(17): p. 4288-97.
148. Fisher, D., et al., *Leukocyte common antigen-related phosphatase is a functional receptor for chondroitin sulfate proteoglycan axon growth inhibitors.* J Neurosci, 2011. **31**(40): p. 14051-66.
149. Chien, P.N. and S.E. Ryu, *Protein Tyrosine Phosphatase sigma in Proteoglycan-Mediated Neural Regeneration Regulation.* Mol Neurobiol, 2012.
150. Xie, Y., et al., *The leukocyte common antigen-related protein tyrosine phosphatase receptor regulates regenerative neurite outgrowth in vivo.* J Neurosci, 2001. **21**(14): p. 5130-8.
151. Nakae, A., et al., *The animal model of spinal cord injury as an experimental pain model.* J Biomed Biotechnol, 2011. **2011**: p. 939023.
152. Byrnes, K.R., S.T. Fricke, and A.I. Faden, *Neuropathological differences between rats and mice after spinal cord injury.* J Magn Reson Imaging, 2010. **32**(4): p. 836-46.
153. Schreiber, J., et al., *Extracellular matrix alterations, accelerated leukocyte infiltration and enhanced axonal sprouting after spinal cord hemisection in tenascin-C-deficient mice.* Acta Histochem, 2013.
154. Massey, J.M., et al., *Increased chondroitin sulfate proteoglycan expression in denervated brainstem targets following spinal cord injury creates a barrier to axonal regeneration overcome by chondroitinase ABC and neurotrophin-3.* Exp Neurol, 2008. **209**(2): p. 426-45.
155. Chan, C.C., et al., *ROCK inhibition with Y27632 activates astrocytes and increases their expression of neurite growth-inhibitory chondroitin sulfate proteoglycans.* Glia, 2007. **55**(4): p. 369-84.
156. Jin, Y., et al., *Chondroitinase activity can be transduced by a lentiviral vector in vitro and in vivo.* J Neurosci Methods, 2011. **199**(2): p. 208-13.
157. Vahidi, B., et al., *Microfluidic-based strip assay for testing the effects of various surface-bound inhibitors in spinal cord injury.* J Neurosci Methods, 2008. **170**(2): p. 188-96.
158. Monnier, P.P., et al., *The Rho/ROCK pathway mediates neurite growth-inhibitory activity associated with the chondroitin sulfate proteoglycans of the CNS glial scar.* Mol Cell Neurosci, 2003. **22**(3): p. 319-30.

159. Lingor, P., et al., *Inhibition of Rho kinase (ROCK) increases neurite outgrowth on chondroitin sulphate proteoglycan in vitro and axonal regeneration in the adult optic nerve in vivo.* J Neurochem, 2007. **103**(1): p. 181-9.
160. Tan, C.L., et al., *Integrin activation promotes axon growth on inhibitory chondroitin sulfate proteoglycans by enhancing integrin signaling.* J Neurosci, 2011. **31**(17): p. 6289-95.
161. Cua, R.C., et al., *Overcoming neurite-inhibitory chondroitin sulfate proteoglycans in the astrocyte matrix.* Glia, 2013. **61**(6): p. 972-84.
162. Jain, A., et al., *Sustained delivery of activated Rho GTPases and BDNF promotes axon growth in CSPG-rich regions following spinal cord injury.* PLoS One, 2011. **6**(1): p. e16135.
163. Alabed, Y.Z., et al., *Identification of CRMP4 as a convergent regulator of axon outgrowth inhibition.* J Neurosci, 2007. **27**(7): p. 1702-11.
164. Ahmed, Z., M. Berry, and A. Logan, *ROCK inhibition promotes adult retinal ganglion cell neurite outgrowth only in the presence of growth promoting factors.* Mol Cell Neurosci, 2009. **42**(2): p. 128-33.
165. Jeon, B.T., et al., *The Rho-kinase (ROCK) inhibitor Y-27632 protects against excitotoxicity-induced neuronal death in vivo and in vitro.* Neurotox Res, 2013. **23**(3): p. 238-48.
166. Darenfed, H., et al., *Molecular characterization of the effects of Y-27632.* Cell Motil Cytoskeleton, 2007. **64**(2): p. 97-109.
167. Wang, T., et al., *CRMP-2 is involved in axon growth inhibition induced by RGMa in vitro and in vivo.* Mol Neurobiol, 2013. **47**(3): p. 903-13.
168. Dmetrichuk, J., G. Spencer, and R. Carlone, *Retinoic acid-dependent attraction of adult spinal cord axons towards regenerating newt limb blastemas in vitro.* Developmental Biology, 2005. **281**(1): p. 112-120.
169. So, P.-L., et al., *Interactions between retinoic acid, nerve growth factor and sonic hedgehog signalling pathways in neurite outgrowth.* Developmental Biology, 2006. **298**(1): p. 167-175.
170. Piu, F., et al., *Identification of novel subtype selective RAR agonists.* Biochemical Pharmacology, 2005. **71**(1-2): p. 156-162.
171. Tonge, P.D. and P.W. Andrews, *Retinoic acid directs neuronal differentiation of human pluripotent stem cell lines in a non-cell-autonomous manner.* Differentiation, 2010. **80**(1): p. 20-30.
172. Wong, L.-F., et al., *Retinoic acid receptor β2 promotes functional regeneration of sensory axons in the spinal cord.* Nature Neuroscience, 2005. **9**(2): p. 243-250.
173. Agudo, M., et al., *A retinoic acid receptor β agonist (CD2019) overcomes inhibition of axonal outgrowth via phosphoinositide 3-kinase signalling in the injured adult spinal cord.* Neurobiology of Disease, 2010. **37**(1): p. 147-155.
174. Corcoran, J., et al., *The role of retinoic acid receptors in neurite outgrowth from different populations of embryonic mouse dorsal root ganglia.* J Cell Sci, 2000. **113 (Pt 14)**: p. 2567-74.
175. Goncalves, M.B.C.V., et al., *Sequential RARβ and α signalling in vivo can induce adult forebrain neural progenitor cells to differentiate into neurons through Shh and FGF signalling pathways.* Developmental Biology, 2009. **326**(2): p. 305-313.
176. Alabed, Y.Z., et al., *GSK3 beta regulates myelin-dependent axon outgrowth inhibition through CRMP4.* J Neurosci, 2010. **30**(16): p. 5635-43.
177. Owen, R. and P.R. Gordon-Weeks, *Inhibition of glycogen synthase kinase 3beta in sensory neurons in culture alters filopodia dynamics and microtubule distribution in growth cones.* Mol Cell Neurosci, 2003. **23**(4): p. 626-37.
178. Kim, M.J., et al., *Inhibition of RhoA but not ROCK induces chondrogenesis of chick limb mesenchymal cells.* Biochem Biophys Res Commun, 2012. **418**(3): p. 500-5.
179. Wang, Y., et al., *Inhibition of gecko GSK-3beta promotes elongation of neurites and oligodendrocyte processes but decreases the proliferation of blastemal cells.* J Cell Biochem, 2012. **113**(6): p. 1842-51.
180. Smith-Thomas, L.C., et al., *An inhibitor of neurite outgrowth produced by astrocytes.* J Cell Sci, 1994. **107 (Pt 6)**: p. 1687-95.

181. Zhou, F.Q., et al., *Neurotrophins support regenerative axon assembly over CSPGs by an ECM-integrin-independent mechanism.* J Cell Sci, 2006. **119**(Pt 13): p. 2787-96.
182. Crespo, D., et al., *How does chondroitinase promote functional recovery in the damaged CNS?* Exp Neurol, 2007. **206**(2): p. 159-71.
183. Rolls, A. and M. Schwartz, *Chondroitin sulfate proteoglycan and its degradation products in CNS repair.* Adv Pharmacol, 2006. **53**: p. 357-74.
184. Thompson, S., et al., *Cloned human teratoma cells differentiate into neuron-like cells and other cell types in retinoic acid.* J Cell Sci, 1984. **72**: p. 37-64.
185. Cohen, M., J. Briscoe, and R. Blassberg, *Morphogen interpretation: the transcriptional logic of neural tube patterning.* Curr Opin Genet Dev, 2013.
186. Le Dreau, G. and E. Marti, *Dorsal-ventral patterning of the neural tube: a tale of three signals.* Dev Neurobiol, 2012. **72**(12): p. 1471-81.
187. Uehara, M., et al., *CYP26A1 and CYP26C1 cooperatively regulate anterior-posterior patterning of the developing brain and the production of migratory cranial neural crest cells in the mouse.* Dev Biol, 2007. **302**(2): p. 399-411.
188. Itasaki, N., et al., *Reprogramming Hox expression in the vertebrate hindbrain: influence of paraxial mesoderm and rhombomere transposition.* Neuron, 1996. **16**(3): p. 487-500.
189. Stornaiuolo, A., et al., *Human HOX genes are differentially activated by retinoic acid in embryonal carcinoma cells according to their position within the four loci.* Cell Differ Dev, 1990. **31**(2): p. 119-27.
190. Blumberg, B., *An essential role for retinoid signaling in anteroposterior neural specification and neuronal differentiation.* Semin Cell Dev Biol, 1997. **8**(4): p. 417-28.
191. Andrews, P.W., et al., *Pluripotent embryonal carcinoma clones derived from the human teratocarcinoma cell line Tera-2. Differentiation in vivo and in vitro.* Lab Invest, 1984. **50**(2): p. 147-62.
192. Pera, M.F., et al., *Isolation and characterization of a multipotent clone of human embryonal carcinoma cells.* Differentiation, 1989. **42**(1): p. 10-23.
193. Chaerkady, R., et al., *Comparative proteomics of human embryonic stem cells and embryonal carcinoma cells.* Proteomics, 2010. **10**(7): p. 1359-1373.
194. Przyborski, S.A., et al., *Human embryonal carcinoma stem cells: models of embryonic development in humans.* Stem Cells Dev, 2004. **13**(4): p. 400-8.
195. Levin, A.A., et al., *A new pathway for vitamin A. Understanding the pleiotropic effects of retinoids.* Ann N Y Acad Sci, 1992. **669**: p. 70-85; discussion 85-6.
196. Okada, Y., et al., *Retinoic-acid-concentration-dependent acquisition of neural cell identity during in vitro differentiation of mouse embryonic stem cells.* Dev Biol, 2004. **275**(1): p. 124-42.
197. Shan, Z.Y., et al., *Generation of dorsal spinal cord GABAergic neurons from mouse embryonic stem cells.* Cell Reprogram, 2011. **13**(1): p. 85-91.
198. Barnard, J.H., et al., *Synthetic Retinoids: Structure-Activity Relationships.* Chemistry - A European Journal, 2009. **15**(43): p. 11430-11442.
199. Hu, B.-Y. and S.-C. Zhang, *Differentiation of spinal motor neurons from pluripotent human stem cells.* Nature Protocols, 2009. **4**(9): p. 1295-1304.
200. Li, X.-J., et al., *Directed Differentiation of Ventral Spinal Progenitors and Motor Neurons from Human Embryonic Stem Cells by Small Molecules.* Stem Cells, 2008. **26**(4): p. 886-893.
201. Pignatello, M.A., F.C. Kauffman, and A.A. Levin, *Multiple factors contribute to the toxicity of the aromatic retinoid, TTNPB (Ro 13-7410): binding affinities and disposition.* Toxicol Appl Pharmacol, 1997. **142**(2): p. 319-27.
202. Buttner, M.W., et al., *Silicon analogues of the retinoid agonists TTNPB and 3-methyl-TTNPB, disila-TTNPB and disila-3-methyl-TTNPB: chemistry and biology.* Chembiochem, 2007. **8**(14): p. 1688-99.
203. Ericson, J., et al., *Pax6 controls progenitor cell identity and neuronal fate in response to graded Shh signaling.* Cell, 1997. **90**(1): p. 169-80.

204. Osumi, N., et al., *Pax-6 is involved in the specification of hindbrain motor neuron subtype.* Development, 1997. **124**(15): p. 2961-72.
205. Bradley, C.K., et al., *Derivation of three new human embryonic stem cell lines.* In Vitro Cellular & Developmental Biology - Animal, 2010. **46**(3-4): p. 294-299.
206. Priddle, H., et al., *Derivation and characterisation of the human embryonic stem cell lines, NOTT1 and NOTT2.* In Vitro Cellular & Developmental Biology - Animal, 2010. **46**(3-4): p. 367-375.
207. Fong, C.Y., et al., *Separation of SSEA-4 and TRA-1–60 Labelled Undifferentiated Human Embryonic Stem Cells from A Heterogeneous Cell Population Using Magnetic-Activated Cell Sorting (MACS) and Fluorescence-Activated Cell Sorting (FACS).* Stem Cell Reviews and Reports, 2009. **5**(1): p. 72-80.
208. Bradley, C.K., et al., *Derivation of three new human embryonic stem cell lines.* In Vitro Cell Dev Biol Anim, 2010. **46**(3-4): p. 294-9.
209. Przyborski, S.A., et al., *Developmental regulation of neurogenesis in the pluripotent human embryonal carcinoma cell line NTERA-2.* Eur J Neurosci, 2000. **12**(10): p. 3521-8.
210. Henley, B.M. and K.W. McDermott, *The expression of neuroepithelial cell fate determinants in rat spinal cord development.* J Mol Neurosci, 2010. **42**(1): p. 28-34.
211. Xu, S., et al., *The proliferation and expansion of retinal stem cells require functional Pax6.* Dev Biol, 2007. **304**(2): p. 713-21.
212. De Robertis, E.M. and H. Kuroda, *Dorsal-ventral patterning and neural induction in Xenopus embryos.* Annu Rev Cell Dev Biol, 2004. **20**: p. 285-308.
213. Hu, B.Y. and S.C. Zhang, *Directed differentiation of neural-stem cells and subtype-specific neurons from hESCs.* Methods Mol Biol, 2010. **636**: p. 123-37.
214. Sjödal, M. and L. Gunhaga, *Expression patterns of Shh, Ptc2, Raldh3, Pitx2, Isl1, Lim3 and Pax6 in the developing chick hypophyseal placode and Rathke's pouch.* Gene Expression Patterns, 2008. **8**(7-8): p. 481-485.
215. Renoncourt, Y., et al., *Neurons derived in vitro from ES cells express homeoproteins characteristic of motoneurons and interneurons.* Mech Dev, 1998. **79**(1-2): p. 185-97.
216. Genethliou, N., et al., *Spatially distinct functions of PAX6 and NKX2.2 during gliogenesis in the ventral spinal cord.* Biochem Biophys Res Commun, 2009. **382**(1): p. 69-73.
217. Pignatello, M., *Liarozole Markedly Increases all trans-Retinoic Acid Toxicity in Mouse Limb Bud Cell Cultures: A Model to Explain the Potency of the Aromatic Retinoid (E)-4-[2-(5,6,7,8-Tetrahydro-5,5,8,8-tetramethyl-2-naphthylenyl)-1-propenyl] Benzoic Acid.* Toxicology and Applied Pharmacology, 2002. **178**(3): p. 186-194.
218. Pijnappel, W.W., et al., *The retinoid ligand 4-oxo-retinoic acid is a highly active modulator of positional specification.* Nature, 1993. **366**(6453): p. 340-4.
219. Maltman, D.J., et al., *Proteomic profiling of the stem cell response to retinoic acid and synthetic retinoid analogues: identification of major retinoid-inducible proteins.* Mol Biosyst, 2009. **5**(5): p. 458-71.
220. Smith, S.C., et al., *The role of aggregation in embryonal carcinoma cell differentiation.* J Cell Physiol, 1987. **131**(1): p. 74-84.
221. Lako, M., et al., *Characterisation of Wnt gene expression during the differentiation of murine embryonic stem cells in vitro: role of Wnt3 in enhancing haematopoietic differentiation.* Mech Dev, 2001. **103**(1-2): p. 49-59.
222. Bauer, J.B., et al., *Novel silicon-containing analogues of the retinoid agonist bexarotene: syntheses and biological effects on human pluripotent stem cells.* ChemMedChem, 2011. **6**(8): p. 1509-17.
223. Christie, V.B., *Evaluation and comparison of natural and synthetic retinoids on model of neural development.* 2008. **PhD Thesis, Durham University**.
224. Amirthalingam, G.S., et al., *Regulation of Hoxb4 induction after neurulation by somite signal and neural competence.* BMC Developmental Biology, 2009. **9**(1): p. 17.
225. Gillespie, R.F. and L.J. Gudas, *Retinoic Acid Receptor Isotype Specificity in F9 Teratocarcinoma Stem Cells Results from the Differential Recruitment of Coregulators to*

Retinoic Acid Response Elements. Journal of Biological Chemistry, 2007. **282**(46): p. 33421-33434.

226. Su, H., et al., *Neural progenitor cells enhance the survival and axonal regeneration of injured motoneurons after transplantation into the avulsed ventral horn of adult rats.* J Neurotrauma, 2009. **26**(1): p. 67-80.
227. Nolte, C., et al., *Stereospecificity and PAX6 function direct Hoxd4 neural enhancer activity along the antero-posterior axis.* Developmental Biology, 2006. **299**(2): p. 582-593.
228. Chen, N. and J.L. Napoli, *All-trans-retinoic acid stimulates translation and induces spine formation in hippocampal neurons through a membrane-associated RAR* The FASEB Journal, 2007. **22**(1): p. 236-245.
229. Manohar, C.F., et al., *Up-regulation of HOXC6, HOXD1, and HOXD8 homeobox gene expression in human neuroblastoma cells following chemical induction of differentiation.* Tumour Biol, 1996. **17**(1): p. 34-47.
230. Dasen, J.S., J.P. Liu, and T.M. Jessell, *Motor neuron columnar fate imposed by sequential phases of Hox-c activity.* Nature, 2003. **425**(6961): p. 926-33.
231. Dasen, J.S., et al., *A Hox regulatory network establishes motor neuron pool identity and target-muscle connectivity.* Cell, 2005. **123**(3): p. 477-91.
232. Gouti, M. and A. Gavalas, *Hoxb1 Controls Cell Fate Specification and Proliferative Capacity of Neural Stem and Progenitor Cells.* Stem Cells, 2008. **26**(8): p. 1985-1997.
233. Wilson, L., et al., *Retinoic acid and the control of dorsoventral patterning in the avian spinal cord.* Dev Biol, 2004. **269**(2): p. 433-46.
234. Jones, L.L., D. Sajed, and M.H. Tuszynski, *Axonal regeneration through regions of chondroitin sulfate proteoglycan deposition after spinal cord injury: a balance of permissiveness and inhibition.* J Neurosci, 2003. **23**(28): p. 9276-88.
235. Rolls, A., R. Shechter, and M. Schwartz, *The bright side of the glial scar in CNS repair.* Nat Rev Neurosci, 2009. **10**(3): p. 235-41.
236. Yu, P., et al., *An in vitro model of reactive astrogliosis and its effect on neuronal growth.* Methods Mol Biol, 2012. **814**: p. 327-40.
237. Carulli, D., et al., *Chondroitin sulfate proteoglycans in neural development and regeneration.* Curr Opin Neurobiol, 2005. **15**(1): p. 116-20.
238. Agudo, M., et al., *A retinoic acid receptor beta agonist (CD2019) overcomes inhibition of axonal outgrowth via phosphoinositide 3-kinase signalling in the injured adult spinal cord.* Neurobiol Dis, 2010. **37**(1): p. 147-55.
239. Boomkamp, S.D., et al., *The development of a rat in vitro model of spinal cord injury demonstrating the additive effects of Rho and ROCK inhibitors on neurite outgrowth and myelination.* Glia, 2012. **60**(3): p. 441-56.
240. Chan, C.C., et al., *Aggrecan components differentially modulate nerve growth factor-responsive and neurotrophin-3-responsive dorsal root ganglion neurite growth.* J Neurosci Res, 2008. **86**(3): p. 581-92.
241. Thompson, K.M., et al., *Receptor protein tyrosine phosphatase sigma inhibits axonal regeneration and the rate of axon extension.* Mol Cell Neurosci, 2003. **23**(4): p. 681-92.
242. Radio, N.M., et al., *Assessment of Chemical Effects on Neurite Outgrowth in PC12 cells Using High Content Screening.* Toxicological Sciences, 2008. **105**(1): p. 106-118.
243. Feltrin, D. and O. Pertz, *Assessment of Rho GTPase signaling during neurite outgrowth.* Methods Mol Biol, 2012. **827**: p. 181-94.
244. Xiao, J., et al., *BDNF exerts contrasting effects on peripheral myelination of NGF-dependent and BDNF-dependent DRG neurons.* J Neurosci, 2009. **29**(13): p. 4016-22.
245. Auer, M., et al., *Rho-independent stimulation of axon outgrowth and activation of the ERK and Akt signaling pathways by C3 transferase in sensory neurons.* Front Cell Neurosci, 2012. **6**: p. 43.
246. Henderson, A., *Small Molecules for Controlling Stem Cell Differentiation.* 2011.
247. Beller, J.A., et al., *Comparison of sensory neuron growth cone and filopodial responses to structurally diverse aggrecan variants, in vitro.* Exp Neurol, 2013. **247C**: p. 143-157.

248. Schuldiner, M., et al., *Induced neuronal differentiation of human embryonic stem cells.* Brain Res, 2001. **913**(2): p. 201-5.
249. Inoue, F., et al., *Gbx2 directly restricts Otx2 expression to forebrain and midbrain, competing with class III POU factors.* Mol Cell Biol, 2012. **32**(13): p. 2618-27.
250. Otero, J.J., et al., *Beta-catenin signaling is required for neural differentiation of embryonic stem cells.* Development, 2004. **131**(15): p. 3545-57.
251. Goncalves, M.B.C.V., et al., *Timing of the retinoid-signalling pathway determines the expression of neuronal markers in neural progenitor cells.* Developmental Biology, 2005. **278**(1): p. 60-70.
252. Corcoran, J., *Retinoic acid receptor beta2 and neurite outgrowth in the adult mouse spinal cord in vitro.* Journal of Cell Science, 2002. **115**(19): p. 3779-3786.
253. Ibanez, C.F. and A. Simi, *p75 neurotrophin receptor signaling in nervous system injury and degeneration: paradox and opportunity.* Trends Neurosci, 2012. **35**(7): p. 431-40.
254. Price, R.D., T. Yamaji, and N. Matsuoka, *FK506 potentiates NGF-induced neurite outgrowth via the Ras/Raf/MAP kinase pathway.* Br J Pharmacol, 2003. **140**(5): p. 825-9.
255. Rossino, P., et al., *Nerve growth factor induces increased expression of a laminin-binding integrin in rat pheochromocytoma PC12 cells.* Exp Cell Res, 1990. **189**(1): p. 100-8.
256. Houle, J.D. and J.E. Johnson, *Nerve growth factor (NGF)-treated nitrocellulose enhances and directs the regeneration of adult rat dorsal root axons through intraspinal neural tissue transplants.* Neurosci Lett, 1989. **103**(1): p. 17-23.
257. Wyatt, S., E.M. Shooter, and A.M. Davies, *Expression of the NGF receptor gene in sensory neurons and their cutaneous targets prior to and during innervation.* Neuron, 1990. **4**(3): p. 421-7.
258. Ernfors, P., et al., *Expression of nerve growth factor receptor mRNA is developmentally regulated and increased after axotomy in rat spinal cord motoneurons.* Neuron, 1989. **2**(6): p. 1605-13.
259. Hsiang, J., et al., *The effects of nerve growth factor on the development of septal cholinergic neurons in reaggregate cell cultures.* Neuroscience, 1989. **29**(1): p. 209-23.
260. Hui, S.P., et al., *Expression pattern of Nogo-A, MAG, and NgR in regenerating urodele spinal cord.* Dev Dyn, 2013. **242**(7): p. 847-60.
261. Sharma, K., M.E. Selzer, and S. Li, *Scar-mediated inhibition and CSPG receptors in the CNS.* Exp Neurol, 2012. **237**(2): p. 370-8.
262. Koyanagi, M., et al., *Inhibition of the Rho/ROCK pathway reduces apoptosis during transplantation of embryonic stem cell-derived neural precursors.* J Neurosci Res, 2008. **86**(2): p. 270-80.
263. Yoneda, A., et al., *A collapsin response mediator protein 2 isoform controls myosin II-mediated cell migration and matrix assembly by trapping ROCK II.* Mol Cell Biol, 2012. **32**(10): p. 1788-804.
264. Zhao, S., et al., *Activation of Akt/GSK-3beta/beta-catenin signaling pathway is involved in survival of neurons after traumatic brain injury in rats.* Neurol Res, 2012. **34**(4): p. 400-7.
265. Faux, C., et al., *PTPsigma binds and dephosphorylates neurotrophin receptors and can suppress NGF-dependent neurite outgrowth from sensory neurons.* Biochim Biophys Acta, 2007. **1773**(11): p. 1689-700.
266. Huang, P., et al., *Structure-based design and discovery of novel inhibitors of protein tyrosine phosphatases.* Bioorg Med Chem, 2003. **11**(8): p. 1835-49.
267. Bradbury, E.J. and L.M. Carter, *Manipulating the glial scar: chondroitinase ABC as a therapy for spinal cord injury.* Brain Res Bull, 2011. **84**(4-5): p. 306-16.
268. Li, H.P., et al., *Roles of chondroitin sulfate and dermatan sulfate in the formation of a lesion scar and axonal regeneration after traumatic injury of the mouse brain.* J Neurotrauma, 2013. **30**(5): p. 413-25.
269. Morgenstern, D.A., R.A. Asher, and J.W. Fawcett, *Chondroitin sulphate proteoglycans in the CNS injury response.* Prog Brain Res, 2002. **137**: p. 313-32.
270. Horrocks, G.M., et al., *Formation of neurospheres from human embryonal carcinoma stem cells.* Biochem Biophys Res Commun, 2003. **304**(2): p. 411-6.

271. Parsons, X.H., et al., *Efficient derivation of human neuronal progenitors and neurons from pluripotent human embryonic stem cells with small molecule induction.* J Vis Exp, 2011(56): p. e3273.
272. Yin, D., et al., *Comparison of neural differentiation potential of human pluripotent stem cell lines using a quantitative neural differentiation protocol.* Methods Mol Biol, 2012. **873**: p. 247-59.
273. Chen, G., et al., *Application of human persistent fetal vasculature neural progenitors for transplantation in the inner retina.* Cell Transplant, 2012. **21**(12): p. 2621-34.
274. Chanut, F., *BMPs: conserved morphogens in neural patterning.* PLoS Biol, 2006. **4**(10): p. e346.
275. Cho, G.S., S.C. Choi, and J.K. Han, *BMP signal attenuates FGF pathway in anteroposterior neural patterning.* Biochem Biophys Res Commun, 2013. **434**(3): p. 509-15.
276. Augustine, K.A., E.T. Liu, and T.W. Sadler, *Interactions of Wnt-1 and Wnt-3a are essential for neural tube patterning.* Teratology, 1995. **51**(2): p. 107-19.
277. Balaskas, N., et al., *Gene regulatory logic for reading the Sonic Hedgehog signaling gradient in the vertebrate neural tube.* Cell, 2012. **148**(1-2): p. 273-84.
278. Takahashi, M. and N. Osumi, *Pax6 regulates specification of ventral neurone subtypes in the hindbrain by establishing progenitor domains.* Development, 2002. **129**(6): p. 1327-38.
279. Folberg, A., et al., *RARbeta mediates the response of Hoxd4 and Hoxb4 to exogenous retinoic acid.* Dev Dyn, 1999. **215**(2): p. 96-107.
280. Hébert, J.M., et al., *The Level of the Transcription Factor Pax6 Is Essential for Controlling the Balance between Neural Stem Cell Self-Renewal and Neurogenesis.* PLoS Genetics, 2009. **5**(6): p. e1000511.
281. Asher, R.A., et al., *Chondroitin sulphate proteoglycans: inhibitory components of the glial scar.* Prog Brain Res, 2001. **132**: p. 611-9.
282. McKeon, R.J., et al., *Reduction of neurite outgrowth in a model of glial scarring following CNS injury is correlated with the expression of inhibitory molecules on reactive astrocytes.* J Neurosci, 1991. **11**(11): p. 3398-411.
283. Sun, Y., et al., *ProBDNF collapses neurite outgrowth of primary neurons by activating RhoA.* PLoS One, 2012. **7**(4): p. e35883.
284. Borisoff, J.F., et al., *Suppression of Rho-kinase activity promotes axonal growth on inhibitory CNS substrates.* Mol Cell Neurosci, 2003. **22**(3): p. 405-16.
285. Snow, D.M., E.M. Brown, and P.C. Letourneau, *Growth cone behavior in the presence of soluble chondroitin sulfate proteoglycan (CSPG), compared to behavior on CSPG bound to laminin or fibronectin.* Int J Dev Neurosci, 1996. **14**(3): p. 331-49.
286. Puttagunta, R., et al., *RA-RAR-beta counteracts myelin-dependent inhibition of neurite outgrowth via Lingo-1 repression.* J Cell Biol, 2011. **193**(7): p. 1147-56.
287. Rossino, P., et al., *Up-regulation of the integrin alpha 1/beta 1 in human neuroblastoma cells differentiated by retinoic acid: correlation with increased neurite outgrowth response to laminin.* Cell Regul, 1991. **2**(12): p. 1021-33.
288. Dill, J., et al., *Inactivation of glycogen synthase kinase 3 promotes axonal growth and recovery in the CNS.* J Neurosci, 2008. **28**(36): p. 8914-28.
289. Kawakami, Y., et al., *Wnt/beta-catenin signaling regulates vertebrate limb regeneration.* Genes Dev, 2006. **20**(23): p. 3232-7.
290. Fancy, S.P., et al., *Axin2 as regulatory and therapeutic target in newborn brain injury and remyelination.* Nat Neurosci, 2011. **14**(8): p. 1009-16.
291. Hunanyan, A.S., et al., *Role of chondroitin sulfate proteoglycans in axonal conduction in Mammalian spinal cord.* J Neurosci, 2010. **30**(23): p. 7761-9.
292. Zhao, R.R. and J.W. Fawcett, *Combination treatment with chondroitinase ABC in spinal cord injury-breaking the barrier.* Neurosci Bull, 2013. **29**(4): p. 477-83.
293. Garcia-Alias, G. and J.W. Fawcett, *Training and anti-CSPG combination therapy for spinal cord injury.* Exp Neurol, 2012. **235**(1): p. 26-32.
294. Arslan, F., et al., *The role of versican isoforms V0/V1 in glioma migration mediated by transforming growth factor-beta2.* Br J Cancer, 2007. **96**(10): p. 1560-8.

295. Maurage, C.A., et al., *Endocan expression and localization in human glioblastomas.* J Neuropathol Exp Neurol, 2009. **68**(6): p. 633-41.
296. Lu, R., et al., *The role of brevican in glioma: promoting tumor cell motility in vitro and in vivo.* BMC Cancer, 2012. **12**: p. 607.
297. Clements, K.M., et al., *Matrix metalloproteinase 17 is necessary for cartilage aggrecan degradation in an inflammatory environment.* Ann Rheum Dis, 2011. **70**(4): p. 683-9.
298. Lendvai, D., et al., *Perisynaptic aggrecan-based extracellular matrix coats in the human lateral geniculate body devoid of perineuronal nets.* J Neurosci Res, 2012. **90**(2): p. 376-87.
299. Guo, Y., et al., *The effects of astrocytes on differentiation of neural stem cells are influenced by knock-down of the glutamate transporter, GLT-1.* Neurochem Int, 2013.
300. Shi, M., et al., *Glia co-culture with neurons in microfluidic platforms promotes the formation and stabilization of synaptic contacts.* Lab Chip, 2013. **13**(15): p. 3008-21.
301. Bovolenta, P., F. Wandosell, and M. Nieto-Sampedro, *CNS glial scar tissue: a source of molecules which inhibit central neurite outgrowth.* Prog Brain Res, 1992. **94**: p. 367-79.
302. Kawano, H., et al., *Role of the lesion scar in the response to damage and repair of the central nervous system.* Cell Tissue Res, 2012. **349**(1): p. 169-80.
303. Schachner, M. and U. Bartsch, *Multiple functions of the myelin-associated glycoprotein MAG (siglec-4a) in formation and maintenance of myelin.* Glia, 2000. **29**(2): p. 154-65.
304. McKerracher, L., et al., *Identification of myelin-associated glycoprotein as a major myelin-derived inhibitor of neurite growth.* Neuron, 1994. **13**(4): p. 805-11.
305. Raisman, G. and Y. Li, *Repair of neural pathways by olfactory ensheathing cells.* Nat Rev Neurosci, 2007. **8**(4): p. 312-9.
306. Richardson, P.M., U.M. McGuinness, and A.J. Aguayo, *Axons from CNS neurons regenerate into PNS grafts.* Nature, 1980. **284**(5753): p. 264-5.
307. Quadrato, G. and S. Di Giovanni, *Waking up the sleepers: shared transcriptional pathways in axonal regeneration and neurogenesis.* Cell Mol Life Sci, 2013. **70**(6): p. 993-1007.
308. Zhao, W.N., et al., *A high-throughput screen for Wnt/beta-catenin signaling pathway modulators in human iPSC-derived neural progenitors.* J Biomol Screen, 2012. **17**(9): p. 1252-63.
309. Cullen, D.K., M.C. Lessing, and M.C. LaPlaca, *Collagen-dependent neurite outgrowth and response to dynamic deformation in three-dimensional neuronal cultures.* Ann Biomed Eng, 2007. **35**(5): p. 835-46.
310. Cullen, D.K., C.M. Simon, and M.C. LaPlaca, *Strain rate-dependent induction of reactive astrogliosis and cell death in three-dimensional neuronal-astrocytic co-cultures.* Brain Res, 2007. **1158**: p. 103-15.
311. Ribeiro, A., et al., *beta1-Integrin cytoskeletal signaling regulates sensory neuron response to matrix dimensionality.* Neuroscience, 2013. **248C**: p. 67-78.
312. Lei, W.L., et al., *Laminin/beta1 integrin signal triggers axon formation by promoting microtubule assembly and stabilization.* Cell Res, 2012. **22**(6): p. 954-72.
313. Raisman, G., *Repair of spinal cord injury by transplantation of olfactory ensheathing cells.* C R Biol, 2007. **330**(6-7): p. 557-60.
314. Gilbert, R.J., et al., *CS-4,6 is differentially upregulated in glial scar and is a potent inhibitor of neurite extension.* Mol Cell Neurosci, 2005. **29**(4): p. 545-58.
315. Spejo, A.B., et al., *Neuroprotective effects of mesenchymal stem cells on spinal motoneurons following ventral root axotomy: Synapse stability and axonal regeneration.* Neuroscience, 2013.
316. Stevens, B., *Neuron-astrocyte signaling in the development and plasticity of neural circuits.* Neurosignals, 2008. **16**(4): p. 278-88.
317. Colognato, H. and I.D. Tzvetanova, *Glia unglued: how signals from the extracellular matrix regulate the development of myelinating glia.* Dev Neurobiol, 2011. **71**(11): p. 924-55.
318. Yu, Z., et al., *ROCK inhibition with Y27632 promotes the proliferation and cell cycle progression of cultured astrocyte from spinal cord.* Neurochem Int, 2012. **61**(7): p. 1114-20.

319. Kimura-Kuroda, J., et al., *An in vitro model of the inhibition of axon growth in the lesion scar formed after central nervous system injury.* Molecular and Cellular Neuroscience, 2010. **43**(2): p. 177-187.
320. Daly, W.T., et al., *Comparison and characterization of multiple biomaterial conduits for peripheral nerve repair.* Biomaterials, 2013. **34**(34): p. 8630-9.
321. Jin, G.Z., et al., *Effect of carbon nanotube coating of aligned nanofibrous polymer scaffolds on the neurite outgrowth of PC-12 cells.* Cell Biol Int, 2011. **35**(7): p. 741-5.
322. Condic, M.L. and P.C. Letourneau, *Ligand-induced changes in integrin expression regulate neuronal adhesion and neurite outgrowth.* Nature, 1997. **389**(6653): p. 852-6.
323. Georgiou, M., et al., *Engineered neural tissue for peripheral nerve repair.* Biomaterials, 2013. **34**(30): p. 7335-43.
324. Daud, M.F., et al., *An aligned 3D neuronal-glial co-culture model for peripheral nerve studies.* Biomaterials, 2012. **33**(25): p. 5901-13.
325. Ge, D., et al., *Culture and differentiation of rat neural stem/progenitor cells in a three-dimensional collagen scaffold.* Appl Biochem Biotechnol, 2013. **170**(2): p. 406-19.
326. Nisbet, D.R., et al., *Neural tissue engineering of the CNS using hydrogels.* J Biomed Mater Res B Appl Biomater, 2008. **87**(1): p. 251-63.
327. Kothapalli, C.R. and R.D. Kamm, *3D matrix microenvironment for targeted differentiation of embryonic stem cells into neural and glial lineages.* Biomaterials, 2013. **34**(25): p. 5995-6007.
328. Yamada, Y., et al., *Laminin-111-derived peptide-hyaluronate hydrogels as a synthetic basement membrane.* Biomaterials, 2013. **34**(28): p. 6539-47.
329. Snow, D.M. and P.C. Letourneau, *Neurite outgrowth on a step gradient of chondroitin sulfate proteoglycan (CS-PG).* J Neurobiol, 1992. **23**(3): p. 322-36.
330. Kofron, C.M., V.J. Fong, and D. Hoffman-Kim, *Neurite outgrowth at the interface of 2D and 3D growth environments.* J Neural Eng, 2009. **6**(1): p. 016002.
331. Gopalakrishnan, S.M., et al., *Role of Rho kinase pathway in chondroitin sulfate proteoglycan-mediated inhibition of neurite outgrowth in PC12 cells.* J Neurosci Res, 2008. **86**(10): p. 2214-26.
332. East, E., J.P. Golding, and J.B. Phillips, *A versatile 3D culture model facilitates monitoring of astrocytes undergoing reactive gliosis.* J Tissue Eng Regen Med, 2009. **3**(8): p. 634-46.
333. Ketschek, A.R., et al., *The roles of neuronal and glial precursors in overcoming chondroitin sulfate proteoglycan inhibition.* Exp Neurol, 2012. **235**(2): p. 627-37.
334. Sandvig, A., et al., *Myelin-, reactive glia-, and scar-derived CNS axon growth inhibitors: expression, receptor signaling, and correlation with axon regeneration.* Glia, 2004. **46**(3): p. 225-51.
335. Kwok, J.C., et al., *Proteoglycans in the central nervous system: plasticity, regeneration and their stimulation with chondroitinase ABC.* Restor Neurol Neurosci, 2008. **26**(2-3): p. 131-45.
336. Tom, V.J., et al., *Administration of chondroitinase ABC rostral or caudal to a spinal cord injury site promotes anatomical but not functional plasticity.* J Neurotrauma, 2009. **26**(12): p. 2323-33.
337. Starkey, M.L., et al., *Chondroitinase ABC promotes compensatory sprouting of the intact corticospinal tract and recovery of forelimb function following unilateral pyramidotomy in adult mice.* Eur J Neurosci, 2012. **36**(12): p. 3665-78.
338. Morawski, M., et al., *Aggrecan-based extracellular matrix shows unique cortical features and conserved subcortical principles of mammalian brain organization in the Madagascan lesser hedgehog tenrec (Echinops telfairi Martin, 1838).* Neuroscience, 2010. **165**(3): p. 831-49.
339. Celio, M.R., et al., *Perineuronal nets: past and present.* Trends Neurosci, 1998. **21**(12): p. 510-5.
340. Bruckner, G., et al., *Perineuronal nets provide a polyanionic, glia-associated form of microenvironment around certain neurons in many parts of the rat brain.* Glia, 1993. **8**(3): p. 183-200.

341. Morawski, M., et al., *Neurons associated with aggrecan-based perineuronal nets are protected against tau pathology in subcortical regions in Alzheimer's disease.* Neuroscience, 2010. **169**(3): p. 1347-63.
342. Giamanco, K.A. and R.T. Matthews, *Deconstructing the perineuronal net: cellular contributions and molecular composition of the neuronal extracellular matrix.* Neuroscience, 2012. **218**: p. 367-84.
343. Koppe, G., et al., *Developmental patterns of proteoglycan-containing extracellular matrix in perineuronal nets and neuropil of the postnatal rat brain.* Cell Tissue Res, 1997. **288**(1): p. 33-41.
344. Jager, C., et al., *Perineuronal and perisynaptic extracellular matrix in the human spinal cord.* Neuroscience, 2013. **238**: p. 168-84.
345. Miyata, S., et al., *Persistent cortical plasticity by upregulation of chondroitin 6-sulfation.* Nat Neurosci, 2012. **15**(3): p. 414-22, S1-2.
346. Lendvai, D., et al., *Neurochemical mapping of the human hippocampus reveals perisynaptic matrix around functional synapses in Alzheimer's disease.* Acta Neuropathol, 2013. **125**(2): p. 215-29.
347. Puschmann, T.B., et al., *Bioactive 3D cell culture system minimizes cellular stress and maintains the in vivo-like morphological complexity of astroglial cells.* Glia, 2013. **61**(3): p. 432-40.
348. Satpute, R.M., et al., *Secretory factors of human neuroblastoma (IMR-32) and human glioblastoma (U87MG) cell lines induce neurite outgrowths in PC12 cells.* Indian J Exp Biol, 2006. **44**(5): p. 367-70.
349. Yao, L., et al., *Effect of functionalized micropatterned PLGA on guided neurite growth.* Acta Biomater, 2009. **5**(2): p. 580-8.
350. Marshall, H., et al., *A conserved retinoic acid response element required for early expression of the homeobox gene Hoxb-1.* Nature, 1994. **370**(6490): p. 567-71.
351. Podrygajlo, G., et al., *Cellular phenotypes of human model neurons (NT2) after differentiation in aggregate culture.* Cell and Tissue Research, 2009. **336**(3): p. 439-452.
352. Fawcett, J.W. and R.A. Asher, *The glial scar and central nervous system repair.* Brain Res Bull, 1999. **49**(6): p. 377-91.
353. Giamanco, K.A., M. Morawski, and R.T. Matthews, *Perineuronal net formation and structure in aggrecan knockout mice.* Neuroscience, 2010. **170**(4): p. 1314-27.
354. Schatteman, G.C., et al., *Expression of NGF receptor in the developing and adult primate central nervous system.* J Neurosci, 1988. **8**(3): p. 860-73.
355. Liao, W.L., et al., *Differential expression of RARbeta isoforms in the mouse striatum during development: a gradient of RARbeta2 expression along the rostrocaudal axis.* Dev Dyn, 2005. **233**(2): p. 584-94.
356. Donoghue, P.S., et al., *The development of a epsilon-polycaprolactone scaffold for central nervous system repair.* Tissue Eng Part A, 2013. **19**(3-4): p. 497-507.
357. Heneberg, P., *Use of protein tyrosine phosphatase inhibitors as promising targeted therapeutic drugs.* Curr Med Chem, 2009. **16**(6): p. 706-33.
358. McRae, P.A., et al., *Aggrecan expression, a component of the inhibitory interneuron perineuronal net, is altered following an early-life seizure.* Neurobiol Dis, 2010. **39**(3): p. 439-48.
359. Curley, J.L. and M.J. Moore, *Facile micropatterning of dual hydrogel systems for 3D models of neurite outgrowth.* J Biomed Mater Res A, 2011. **99**(4): p. 532-43.